

# HOST-GUEST CHEMISTRY BETWEEN CUCURBIT[7]URIL AND NEUTRAL AND CATIONIC GUESTS

by

Ian William Wyman

A thesis submitted to the Department of Chemistry

In conformity with the requirements for

the degree of Doctor of Philosophy.

Queen's University

Kingston, Ontario, Canada

(January, 2010)

Copyright © Ian William Wyman, 2010

Dedicated in memory of my Grandfather, Norman Brannen, 1917-2009.

## Abstract

This thesis describes the host-guest chemistry between cucurbit[7]uril (CB[7]) and various series of guests, including neutral polar organic solvents, bis(pyridinium)alkane dications, local anaesthetics, acetylcholine analogues, as well as succinylcholine and decamethonium analogues, in aqueous solution. A focus of this thesis is the effects of varying the chemical structures within different series of guests upon the nature of the host-guest chemistry, such as the relative position and orientation of the guest relative to the CB[7] cavity, and the strengths of the binding affinities.

The binding affinities of polar organic solvents with CB[7] depend upon the hydrophobic effect and dipole-quadrupole interactions. The polar guests align themselves so that their dipole moment is perpendicular to the quadrupole moment of CB[7]. The binding strengths of acetone and acetophenone to CB[7] decrease in the presence of alkali metals.

Discrete 1:1 and 2:1 host-guest complexes are formed between CB[7] and a series of  $\alpha,\omega$ -bis(pyridinium)alkane guests. In most cases the CB[7] initially occupies the aliphatic linker when the 1:1 complex is formed and migrates to the terminal regions as the second CB[7] is added. When bulky, hydrophobic *tert*-butyl substituents are present, however, the CB[7] occupies the terminal pyridinium region and not the central linker.

Supramolecular complexes between CB[7] and a series of local anaesthetics have binding affinities 2-3 orders of magnitude greater than reported values with  $\beta$ -cyclodextrin. The first  $pK_a$  values of the guests increase by 0.5-1.9 units upon complexation. The binding positions of the guests within CB[7] differ in neutral and acidic media, with the systems thus behaving as pH-activated switches.

With supramolecular complexes between CB[7] and various cationic cholines and their phosphonium analogues, the CB[7] cavity is occupied by the charge-diffuse cationic region. The binding affinities and positions vary depending on the nature of the onium group as well as the substituents within the guest molecule.

Host-guest complexes between CB[7] and dicationic acetylcholinesterase inhibitors have 1:1 binding affinities between  $8 \times 10^6$  and  $3 \times 10^{10} \text{ M}^{-1}$ , with 2:1 binding being significantly weaker. These binding affinities are related to the nature of the cationic onium groups, and the length and hydrophobicity of the connecting linkers.

## Acknowledgements

I would like to take this opportunity, first and foremost, to thank my supervisor, Dr. Donal Macartney, for his kindness, help, guidance, and patience during my studies. It has been a pleasure studying in his research group.

I would also like to thank Dr. Francoise Sauriol for her kindness, helpful discussions, regarding NMR characterizations, and her assistance and training with the instrumentation. In addition, I would like to thank the members of the mass spectrometry facility, which have included Bernd Keller, Jie (Jessie) Sui, Lina Yuan, and Jiayi Wang for their helpful advice, and for running the high-resolution samples.

I wish to also thank the faculty members of the Department of Chemistry for their guidance, excellent teaching and research advice, and also the staff of both the department and Queen's University. I would like to take this opportunity to thank members of the chemistry office, especially Annette Keyes, for her helpfulness with scholarship and fellowship applications. I also want to thank Lyndsay Hull for loaning chemicals and equipment during the course of my studies here.

It has been a pleasure working with members of the Macartney lab, both past and present, including Ruibing Wang, Lina Yuan, Saroja Hettiarachchi, Andrew Fraser, Mona Gamal Eldin, Brendan MacGillivray, Julian Kwok, Antony St-Jacques, Priscilla Leung, and Andrew Carrier. I thank them for their friendship and helpful discussions.

I would like to especially take this opportunity to thank my parents, Bill and Diane Wyman, for their love, encouragement, and support.

In addition, I greatly appreciate the financial assistance that has been provided by the Ontario Ministry of Training, Colleges and Universities through the OGS program, as well as to the Walter C. Sumner Foundation, for its support.

## **Statement of Originality**

I hereby certify that all of the work described within this thesis is the original work of the author.

Any published (or unpublished) ideas and/or techniques from the work of others are fully acknowledged in accordance with the standard referencing practices.

Ian William Wyman

January, 2010

## Table of Contents

Abstract .....	iii
Acknowledgements .....	v
Statement of Originality .....	vii
Table of Contents .....	viii
List of Figures .....	xii
List of Abbreviations.....	xviii
Chapter 1 Introduction .....	1
1.1 Non-covalent interactions .....	1
1.1.1 Hydrogen Bonding .....	2
1.1.2 Van der Waals Interactions .....	3
1.1.3 The Hydrophobic Effect.....	4
1.1.4 $\pi$ - $\pi$ Stacking Interactions .....	6
1.1.5 Electrostatic Interactions .....	8
1.2 Concepts of Supramolecular Chemistry: Molecular Recognition and Self-Assembly, Macrocyclic Hosts, Rotaxanes, and Catenanes .....	10
1.2.1 Self-Assembly and Molecular Recognition.....	11
1.2.2 Macrocyclic Hosts.....	12
1.2.3 Supramolecular Complexes involving Macrocyclic Hosts: Rotaxanes and Catenanes.....	13
1.3 Supramolecular Characterization .....	15
1.3.1 Nuclear Magnetic Resonance (NMR) Spectroscopy.....	16
1.3.2 UV-visible Spectroscopy.....	18
1.3.3 X-ray Crystallography.....	18
1.3.4 Mass Spectrometry.....	19
1.3.5 Determination of Binding Constants.....	20
1.4 Non-Cucurbituril Macrocyclic Hosts .....	23
1.4.1 Crown Ethers.....	23
1.4.2 Calixarene Hosts .....	27
1.4.3 Porphyrin Hosts.....	35
1.4.4 Cyclodextrins .....	38



1.5 Cucurbituril Hosts .....	42
1.5.1 Cucurbit[6]uril (CB[6]) .....	46
1.5.2 Cucurbit[5]uril (CB[5]) .....	56
1.5.3 Cucurbit[7]uril (CB[7]) .....	59
1.5.4 Cucurbit[8]uril (CB[8]) .....	65
1.5.5 Cucurbit[10]uril (CB[10]) .....	71
1.5.6 Cucurbit[ <i>n</i> ]uril Derivatives .....	75
1.6 Applications of Cucurbit[ <i>n</i> ]urils .....	85
1.6.1 Catalysis and Stabilization of Guests .....	85
1.6.2 Drug Delivery Systems .....	88
1.6.3 Separations .....	92
1.6.4 Molecular Switches .....	93
1.6.5 Chemical Sensors and Imaging .....	96
1.7 Summary, Outlook, and Research Goals .....	99
1.7.1 Overview of the Field .....	99
1.7.2 Research Summary .....	100
1.7.3 Research Goals .....	103
References .....	104
Chapter 2 Host-Guest Chemistry between Cucurbit[7]uril and Small Polar Organic Guests .....	126
2.1 Introduction .....	126
2.2 Results and Discussion .....	127
2.2.1 Stability Constants for Host-Guest Complexes of CB[7] with Solvents .....	127
2.2.2 Host-Guest Complexes of CB[7] with Alkali Metal Cations .....	138
2.3 Experimental .....	144
2.3.1 Materials .....	144
2.3.2 Methods .....	146
2.4 Conclusions .....	149
References .....	150
Chapter 3 Cucurbit[7]uril Host-Guest and Pseudorotaxane Complexes with $\alpha,\omega$ - bis(pyridinium)alkane Dications .....	153
3.1 Introduction .....	153
3.2 Results and Discussion .....	155
3.2.1 Host-Guest Complexes Between CB[7] and BPE <sup>2+</sup> , BAPE <sup>2+</sup> , and BBPE <sup>2+</sup> .....	155

3.2.2 Host-Guest Complexes Between CB[7] and BPH <sup>2+</sup> , BAPE <sup>2+</sup> , B2PH <sup>2+</sup> , B3PH <sup>2+</sup> , BBPH <sup>2+</sup> , and BBPX <sup>2+</sup> .....	163
3.2.3 Host-Guest Stability Constants .....	167
3.3 Experimental .....	173
3.3.1 Materials .....	173
3.3.2 Methods .....	177
3.4 Conclusions .....	178
References .....	179
Chapter 4 Host-Guest Chemistry between CB[7] and a Series of Local Anaesthetics .....	182
4.1 Introduction .....	182
4.2 Results and Discussion .....	184
4.2.1 <sup>1</sup> H NMR Spectroscopy and ESI Mass Spectrometry .....	184
4.2.2 UV-visible Absorbance and Emission Spectroscopy .....	200
4.2.3 Complexation-Induced p <i>K</i> <sub>a</sub> Shifts .....	205
4.3 Experimental .....	207
4.3.1 Materials .....	207
4.3.2 Methods .....	208
4.4 Conclusions .....	209
References .....	211
Chapter 5 Cucurbit[7]uril Host-Guest Complexes of Cholines and Phosphonium Cholines in Aqueous Solution .....	215
5.1 Introduction .....	215
5.2 Results and Discussion .....	221
5.2.1 Binding Trends Between CB[7] and Trialkylonium-Bearing Guests .....	221
5.2.2 Host-Guest Binding Between CB[7] and Guests Bearing Benzyl, Quinuclidinium, and DABCO Units .....	239
5.2.3 Host-Guest Stability Constants .....	244
5.3 Experimental .....	258
5.3.1 Materials .....	258
5.3.2 Methods .....	264
5.4 Conclusions .....	265
References .....	267

Chapter 6 Host-Guest Complexes and Pseudorotaxanes of Cucurbit[7]uril with Acetylcholinesterase Inhibitors .....	272
6.1 Introduction .....	272
6.2 Results and Discussion.....	278
6.2.1 Host-Guest Complex Formation .....	278
6.2.2 Host-Guest Stability Constants .....	297
6.3 Experimental .....	305
6.3.1 Materials.....	305
6.3.2 Methods.....	307
6.4 Conclusions .....	308
References .....	310
Chapter 7 Conclusions and Future Work .....	314
7.1 Conclusions and Summary of Research.....	314
7.1.1 Polar Solvent Guest Complexation with CB[7] .....	314
7.1.2 $\alpha,\omega$ -Bis(pyridinium)alkane Guest Binding to CB[7].....	315
7.1.3 Binding between CB[7] and Local Anaesthetics.....	316
7.1.4 Choline and Acetylcholine Guest Complexation with CB[7].....	317
7.1.5 Encapsulation of Acetylcholinesterase Inhibitors by CB[7] .....	318
7.1.6 General Overview of the Research.....	319
7.2 Suggestions for Future Work .....	320
References .....	326

## List of Figures

Figure 1.1	Diagram of offset face-to-face and edge-to-face $\pi$ - $\pi$ stacking arrangements	7
Figure 1.2	Self-assembly of the tobacco mosaic virus	12
Figure 1.3	Diagram of a [2]-catenane, a [2]rotaxane, and a [2]pseudorotaxane	15
Figure 1.4	Structure of dibenzo-18-crown-6	24
Figure 1.5	Conformations observed for calix[4]arene	29
Figure 1.6	Calix[4]biscrown binding two Cs <sup>+</sup> guests	31
Figure 1.7	A resorc[4]arene with its aromatic rings in the cone conformation	33
Figure 1.8	Structure of Protoporphyrin IX	35
Figure 1.9	X-ray crystal structure of sapphyrin bound to a fluoride anion	37
Figure 1.10	Structures of $\alpha$ -CD, $\beta$ -CD, and $\gamma$ -CD	40
Figure 1.11	CB[6] bound to 1,6-diammoniumhexane, with its hydrophobic cavity and electron rich portals shown	43
Figure 1.12	Electrostatic potential maps of $\beta$ -CD and CB[7]	44
Figure 1.13	X-ray crystal structure of <i>p</i> -xylylenediammonium encapsulated by CB[6]	48
Figure 1.14	Structures of cystamine and cysteamine and an energy-minimized (B3LYP/3-21G) structure of the complex between CB[6] and cystamine	50
Figure 1.15	X-ray crystal structure of THF encapsulated within Na <sup>+</sup> -capped CB[6]	55
Figure 1.16	Structure of Thioflavin T	58
Figure 1.17	2,3-Diazabicyclo[2.2.2]oct-2-ene (DBO) encapsulated by CB[7]	60
Figure 1.18	Structure of <i>trans</i> -[PtCl(NH <sub>3</sub> ) <sub>2</sub> ] <sub>2</sub> $\mu$ -dzpm] <sup>2+</sup> and complexation between CB[7] and oxaliplatin	61
Figure 1.19	Schematic view of the use of CB[7] as a sensor for enzyme assays	63
Figure 1.20	Salt-induced release of Neutral Red, with subsequent binding to the hydrophobic pocket of BSA	65
Figure 1.21	Structure of a ternary host-guest system with CB[8] encapsulating the guests 2,6-dihydroxynaphthalene and methylviologen	67
Figure 1.22	Structure of 4,6-bis(4-(aminomethyl)phenylamino)-1,3,5-triazin-2(1H)-one	72
Figure 1.23	Complex of CB[10] and a porphyrin derivative	73
Figure 1.24	Structures of CB[6] and its analogue synthesized by Isaacs and coworkers	77

Figure 1.25	Structure of <i>i</i> -CB[6] .....	78
Figure 1.26	Structures of <i>ns</i> -CB[6] (top), ( $\pm$ )-bis- <i>ns</i> -CB[6], and bis- <i>ns</i> -CB[10] .....	80
Figure 1.27	Structure of ortho-xylylene bridged CB[6] derivative and its host-guest complex with alkanediammonium guest back-folded to the portal .....	81
Figure 1.28	X-ray crystal structures of a C-shaped and S-shaped glycoluril dimers .....	82
Figure 1.29	A vesicle embedded with functionalized CB[ <i>n</i> ] acting as an ion channel .....	84
Figure 1.30	Cross-sectional view of Mock's cycloaddition catalyzed CB[6] .....	86
Figure 1.31	Schematic view of Nau's catalyzed hydrolysis using CB[6] and CB[7] .....	87
Figure 1.32	Positioning of CB[7] over Pt anti-cancer drugs CT033 and CT233 .....	91
Figure 1.33	Complexation between CB[7] and a viologen-bearing guest at low and high pH .....	94
Figure 1.34	Intensity changes over time of Rhodamine 6G in a quartz cuvette, in a borosilicate vial, and in a borosilicate vial with CB[7] .....	98
Figure 2.1	<sup>1</sup> H NMR chemical shift titrations for CB[7] complexation with acetone, acetophenone, DMF, methyl acetate, DMSO, 2-butanone, and acetonitrile .....	128
Figure 2.2	<sup>1</sup> H NMR spectra from the titration of acetone with CB[7] .....	132
Figure 2.3	<sup>1</sup> H NMR spectra from the titration of acetophenone with CB[7] .....	133
Figure 2.4	<sup>1</sup> H NMR spectra from the titration of 3,3-dimethylbutan-2-one with CB[7] .....	134
Figure 2.5	Diagram of acetone encapsulated by CB[7] with respect to dipole moment and quadropole moment .....	136
Figure 2.6	Energy-minimized structures of host-guest complexes between CB[7] and acetone, butan-2-one, pentan-3-one, 3,3-dimethylbutan-2-one, acetophenone, methyl acetate, dimethylsulfoxide, dimethylformamide, and acetonitrile. ....	137
Figure 2.7	Equilibria between CB[7], organic guests, and alkali metal cations .....	139
Figure 2.8	Dependence of $-\Delta\delta_{\text{obs}}$ of acetone on the concentrations of CB[7] in the absence of Na <sup>+</sup> and K <sup>+</sup> , the presence of 0.20 M Na <sup>+</sup> , and 0.20 M K <sup>+</sup> .....	139
Figure 2.9	Dependences of $-\Delta\delta_{\text{obs}}$ of acetophenone on the concentrations of CB[7] in the absence of Na <sup>+</sup> and K <sup>+</sup> , in the presence of 0.20 M Na <sup>+</sup> , and in 0.20 M K <sup>+</sup> .....	140
Figure 2.10	Dependences $\Delta\delta_{\text{obs}}$ of guest protons on the concentration of K <sup>+</sup> in the presence of excess CB[7] .....	142
Figure 3.1	Structures of BPE <sup>2+</sup> , BAPE <sup>2+</sup> , and BBPE <sup>2+</sup> with their $\Delta\delta_{\text{im}}$ values shown .....	156
Figure 3.2	Quinoidal and pyridinium resonance structures of BAPE <sup>2+</sup> , and the energy-minimized structures of {CB[7]•BAPE} <sup>2+</sup> and {2CB[7]•BAPE} <sup>2+</sup> .....	157
Figure 3.3	<sup>1</sup> H NMR spectra from the titration of BAPE <sup>2+</sup> with CB[7] .....	158

Figure 3.4 UV-visible titration of BAPE <sup>2+</sup> with CB[7] and a plot of the absorbance at 314 nm as a function of the [CB[7]] / [BAPE] <sup>2+</sup> ratio.....	161
Figure 3.5 <sup>1</sup> H NMR spectra from the titration of BBPE <sup>2+</sup> with CB[7].....	162
Figure 3.6 Structures of BPH <sup>2+</sup> , BAPH <sup>2+</sup> , B2PH <sup>2+</sup> , B3PH <sup>2+</sup> , BBPH <sup>2+</sup> , and BBPX <sup>2+</sup> , with their $\Delta\delta_{lim}$ values shown .....	164
Figure 3.7 <sup>1</sup> H NMR spectra from the titration of BAPH <sup>2+</sup> with CB[7].....	165
Figure 3.8 Downfield regions of the <sup>1</sup> H NMR spectra of BBPE <sup>2+</sup> , BBPH <sup>2+</sup> , and BBPX <sup>2+</sup> from their titrations with CB[7].....	166
Figure 4.1 Monocationic structures of procaine, procainamide, prilocaine, tetracaine, and dibucaine with their $\Delta\delta_{lim}$ values (for both monocationic and dicationic species) shown .....	187
Figure 4.2 <sup>1</sup> H NMR spectra from the titration of procaine with CB[7] in D <sub>2</sub> O. ....	188
Figure 4.3 <sup>1</sup> H NMR spectra from the titration of procaine with CB[7] in 0.1 M DCl. ....	189
Figure 4.4 <sup>1</sup> H NMR spectra from the titration of tetracaine with CB[7] in D <sub>2</sub> O.....	190
Figure 4.5 <sup>1</sup> H NMR spectra from the titration of tetracaine with CB[7] in 0.1 M DCl. ....	191
Figure 4.6 <sup>1</sup> H NMR spectra from the titration of dibucaine with CB[7] in D <sub>2</sub> O. ....	192
Figure 4.7 <sup>1</sup> H NMR spectra from the titration of dibucaine with CB[7] in 0.1 M DCl. ....	193
Figure 4.8 <sup>1</sup> H NMR spectra from the titration of prilocaine with CB[7] in D <sub>2</sub> O. ....	194
Figure 4.9 Plot of the <sup>1</sup> H NMR upfield shift vs. concentration of CB[7] from the titration of procainamide with CB[7] in D <sub>2</sub> O.....	195
Figure 4.10 UV-visible spectra from the titration of tetracaine with CB[7] and a plot of the change of absorbance at 322 nm as a function of CB[7] concentration. ....	202
Figure 4.11 Fluorescence spectra from the titration of procaine with CB[7] and plot of dependence of F/F <sub>0</sub> at 354 nm on the concentration of CB[7] .....	203
Figure 4.12 UV-visible spectra from the titration of epinephrine bitartrate with CB[7] and plot of dependence of change in absorbance at 280 nm on the concentration of CB[7].....	204
Figure 4.13 UV pH titrations of the CB[7] host-guest complexes of procaine, tetracaine, dibucaine, and procainamide.....	207
Figure 5.1 LogK <sub>CB[7]}</sub> vs. number of carbon atoms in R groups of NR <sub>4</sub> <sup>+</sup> , superimposed with Chem3D models of the corresponding {CB[7]•NR <sub>4</sub> } <sup>+</sup> complexes.....	219
Figure 5.2 Plots of logK <sub>CB[7]}</sub> versus the number of carbon atoms in the alkyl group of the NR <sub>4</sub> <sup>+</sup> guests for CB[7] compared to binding with other hosts.....	219

Figure 5.3	General structures of the choline and acetylcholine series of guests studied .....	221
Figure 5.4	Structures and $\Delta\delta_{\text{lim}}$ values for the series of trimethylammonium and triethylammonium-bearing choline and acetylcholine derivatives.....	223
Figure 5.5	Structures and $\Delta\delta_{\text{lim}}$ values for the series of trimethylphosphonium and triethylphosphonium-bearing choline and acetylcholine derivatives .....	223
Figure 5.6	$^1\text{H}$ NMR spectra from the titration of choline with CB[7].....	224
Figure 5.7	$^1\text{H}$ NMR spectra from the titration of (2-hydroxyethyl)trimethylphosphonium with CB[7].....	225
Figure 5.8	$^1\text{H}$ NMR spectra from the titration of acetylcholine with CB[7].....	226
Figure 5.9	$^1\text{H}$ NMR spectra from the titration of (2-acetoxyethyl)trimethylphosphonium with CB[7].....	227
Figure 5.10	$^1\text{H}$ NMR spectra from the titration of triethylpentylammonium with CB[7].....	228
Figure 5.11	$^1\text{H}$ NMR spectra from the titration of trimethylpentylphosphonium with CB[7]. ...	229
Figure 5.12	$^1\text{H}$ NMR spectra from the titration of butyrylcholine with CB[7].....	230
Figure 5.13	$^1\text{H}$ NMR spectra from the titration of acetyl- $\beta$ -methylcholine with CB[7]. .....	231
Figure 5.14	$^1\text{H}$ NMR spectra from the titration of choline phosphate with CB[7]. .....	232
Figure 5.15	$^1\text{H}$ NMR spectra from the titration of ( $\pm$ )-carnitine with CB[7]. .....	233
Figure 5.16	$^1\text{H}$ NMR spectra from the titration of benzyldimethylcholine with CB[7].....	234
Figure 5.17	$^1\text{H}$ NMR spectra from the titration of quinuclidiniumcholine with CB[7]. .....	235
Figure 5.18	Structures and $\Delta\delta_{\text{lim}}$ values for the benzyl- and quinuclidinium-bearing derivatives of choline, as well as for <i>N</i> -methylquinuclidinium and dimethylDABCO.....	240
Figure 5.19	$^1\text{H}$ NMR spectra from the titration of <i>N</i> -methylquinuclidinium with CB[7]. .....	242
Figure 5.20	$^1\text{H}$ NMR spectra from the titration of dimethylDABCO with CB[7]. .....	243
Figure 5.21	$^1\text{H}$ NMR chemical shift titrations curves of ( $\pm$ )-carnitine with CB[7] in $\text{D}_2\text{O}$ solutions with no added electrolytes, at pD 2.0, and in 0.05 M NaOAc- $d_3$ .....	246
Figure 5.22	Structures of compounds described in Table 5.4 .....	255
Figure 6.1	Schematic and ribbon structures of AChE.....	274
Figure 6.2	The hydrolysis of acetylcholine by AChE.....	275
Figure 6.3	Structures of the $\text{NMe}_3$ - and $\text{NEt}_3$ -capped guests employed in this study, along with their $^1\text{H}$ NMR $\Delta\delta_{\text{lim}}$ values .....	279
Figure 6.4	Structures of the $\text{PMe}_3$ - and $\text{PEt}_3$ -capped guests employed in this study, along with their $^1\text{H}$ NMR and $^{31}\text{P}$ NMR $\Delta\delta_{\text{lim}}$ values.....	280

Figure 6.5	$^1\text{H}$ NMR spectra from the titration of $[\text{NMe}_3(\text{CH}_2)_6\text{NMe}_3]^{2+}$ with CB[7].	282
Figure 6.6	$^1\text{H}$ NMR spectra from the titration of $[\text{NMe}_3(\text{CH}_2)_8\text{NMe}_3]^{2+}$ with CB[7].	283
Figure 6.7	$^1\text{H}$ NMR spectra from the titration of $[\text{NMe}_3(\text{CH}_2)_{10}\text{NMe}_3]^{2+}$ with CB[7].	284
Figure 6.8	$^1\text{H}$ NMR spectra from the titration of $[\text{NEt}_3(\text{CH}_2)_{10}\text{NEt}_3]^{2+}$ with CB[7].	285
Figure 6.9	$^1\text{H}$ NMR spectra from the titration of $[\text{PMe}_3(\text{CH}_2)_{10}\text{PMe}_3]^{2+}$ with CB[7].	286
Figure 6.10	$^1\text{H}$ NMR spectra from the titration of $[\text{PEt}_3(\text{CH}_2)_{10}\text{PEt}_3]^{2+}$ with CB[7].	287
Figure 6.11	$^1\text{H}$ NMR spectra from the titration of succinylcholine with CB[7].	288
Figure 6.12	$^1\text{H}$ NMR spectra from the titration of $[\text{Quin}(\text{CH}_2)_{10}\text{Quin}]^{2+}$ with CB[7].	289
Figure 6.13	$^1\text{H}$ NMR spectra from the titration of BW284c51 with CB[7].	290
Figure 6.14	$^{31}\text{P}$ NMR spectra from the titration of $[\text{PMe}_3(\text{CH}_2)_{10}\text{PMe}_3]^{2+}$ with CB[7].	291
Figure 6.15	Plot of upfield shift vs. concentration of CB[7] for $[\text{PMe}_3(\text{CH}_2)_{10}\text{PMe}_3]^{2+}$ for the trimethylammonium protons ( $^1\text{H}$ NMR) and phosphorus centre ( $^{31}\text{P}$ NMR).	292
Figure 6.16	Plot of upfield shift of $\alpha$ $\text{CH}_2$ of succinylcholine vs. concentration of CB[7] from $^1\text{H}$ NMR.	292
Figure 6.17	Structures and $^1\text{H}$ NMR $\Delta\delta_{\text{lim}}$ values of $[\text{Quin}(\text{CH}_2)_{10}\text{Quin}]^{2+}$ and BW284c51	293
Figure 6.18	Formation of the 1:1 [2]Pseudorotaxane and 2:1 host-guest complexes between CB[7] and succinylcholine.	303
Figure 7.1	Structures of muscle relaxants that may form host-guest systems with CB[7].	322
Figure 7.2	Selected examples of asymmetric diacationic ammonium and pyridinium guests.	324



## List of Tables

Table 1.1	Cavity dimensions and aqueous solubilities of CB[ <i>n</i> ] and CD hosts.....	45
Table 2.1	Binding constants and <sup>1</sup> H NMR Δδ <sub>lim</sub> values for binding between CB[7] and the neutral organic guests studies.....	131
Table 2.2	Host-guest binding affinities between CB[7] and the solvents acetone and acetophenone in the presence and absence of Na <sup>+</sup> and K <sup>+</sup> .....	144
Table 3.1	Host-guest stability constants for the complexes between CB[7] and the α,ω-bis(pyridinium)alkane guests.....	168
Table 3.2	ESI-MS spectral peaks for the host-guest complexes between the dicationic α,ω-bis(pyridinium)alkane guests and CB[7]......	169
Table 4.1	Host-guest stability constants for complexes of local anaesthetics with CB[7] and β-CD, and pK <sub>a</sub> values for the guest in the absence and presence of CB[7]......	197
Table 4.2	ESI-MS data for the host-guest complexes between local anaesthetics and CB[7]....	198
Table 5.1	Binding constants and Δδ <sub>lim</sub> values for host-guest complexes between CB[7] and peralkylated onium guests.....	217
Table 5.2	Host-guest binding constants between CB[7] and the series of cholines, their phosphonium analogues, and related guests.....	236
Table 5.3	ESI-MS data for the host-guest complexes of the choline derivatives with CB[7]......	237
Table 5.4	Literature values of host-guest binding constants between various synthetic hosts and choline, acetylcholine, carnitine, trimethylammonium, and triethylammonium.....	253
Table 6.1	ESI-MS data for the host-guest complexes between CB[7] and the dicationic quaternary onium guests studied.....	296
Table 6.2	Host-guest binding constants between CB[7] and the dicationic quaternary onium guests.....	297

## List of Abbreviations

1:1	A host-guest system composed of 1 host and 1 guest (1 host: 1 guest).
2:1	Unless otherwise stated, refers to a host-guest system with 2 hosts and 1 guest (2 hosts: 1 guest).
AChE	acetylcholinesterase
AD	Alzheimer's disease
B2PH <sup>2+</sup>	[1,6-bis(2-methyl-1-pyridinium)hexane] <sup>2+</sup>
B3PH <sup>2+</sup>	[1,6-bis(3-methyl-1-pyridinium)hexane] <sup>2+</sup>
BAPE <sup>2+</sup>	[1,2-bis(4-dimethylamino-1-pyridinium)ethane] <sup>2+</sup>
BAPH <sup>2+</sup>	[1,6-bis(4-dimethylamino-1-pyridinium)hexane] <sup>2+</sup>
BBPE <sup>2+</sup>	[1,2-bis(4- <i>tert</i> -butyl-1-pyridinium)ethane] <sup>2+</sup>
BBPH <sup>2+</sup>	[1,6-bis(4- <i>tert</i> -butyl-1-pyridinium)hexane] <sup>2+</sup>
BBPX <sup>2+</sup>	[ $\alpha,\alpha'$ -bis(4- <i>tert</i> -butyl-1-pyridinium) <i>p</i> -xylene] <sup>2+</sup>
bp.	boiling point
BPE <sup>2+</sup>	[1,2-bis(1-pyridinium)ethane] <sup>2+</sup>
BPH <sup>2+</sup>	[1,6-bis(1-pyridinium)hexane] <sup>2+</sup>
bpy	4,4'-bipyridinium
BSA	bovine serum albumin
Bz	benzyl
calc.	calculated
CA[ <i>n</i> ]	calix[ <i>n</i> ]arene
CB[ <i>n</i> ]	cucurbit[ <i>n</i> ]uril
CB[5]	cucurbit[5]uril
CB[6]	cucurbit[6]uril

CB[7]	cucurbit[7]uril
CB[8]	cucurbit[8]uril
CB[10]	cucurbit[10]uril
CB*[5]	penta(cyclohexyl)cucurbit[6]uril
CB*[6]	hexa(cyclohexyl)cucurbit[6]uril
Cp	cyclopentadienyl
CD	cyclodextrin
COSY	correlation spectroscopy
$\delta$	chemical shift (ppm), also used to describe positioning within a structure
$\Delta\delta_{\text{lim}}$	limiting complexation induced shift change
$\Delta\delta_{\text{obs}}$	observed complexation induced shift change
d	doublet
D <sub>2</sub> O	deuterated water
DABCO	1,4-diazabicyclo[2.2.2]octane
DADAT <sup>2+</sup>	4,8-diamino-3,7-diazatricyclo[4.2.2.2]-dodeca-3,7,9,11-tetraene
DBO	2,3-diazabicyclo[2.2.2]oct-2-ene
dd	doublet of doublets
dec.	decomposed
DCM	dichloromethane
dd	doublet of doublets
DMF	dimethylformamide
DMSO	dimethylsulfoxide
DNA	deoxyribonucleic acid
dt	doublet of triplets
dq	doublet of quartets

EDTA	N, N',N'',N'''-ethylenediaminetetraacetate
equiv.	equivalents
ESI-MS	Electrospray Ionization Mass Spectrometry
Et	ethyl (-CH <sub>2</sub> CH <sub>3</sub> )
FAB	fast atom bombardment
Glu	glutamic acid
Gly	glycine
HILIC	hydrophilic interaction chromatography
His	histidine
HMBC	heteronuclear multiple bond coherence
HMQC	heteronuclear multiple quantum coherence
hp	heptet
HPLC	high-performance liquid chromatography
HPTS	8-hydroxypyrene-1,3,6-trisulfonate
HR-ESI-MS	High-Resolution Electrospray Ionization Mass Spectrometry
HSQC	heteronuclear single quantum coherence
Hz	hertz (s <sup>-1</sup> )
IC <sub>50</sub>	half maximal inhibitory concentration
<i>i</i> -CB[ <i>n</i> ]	inverted cucurbit[ <i>n</i> ]uril
Int	relative integral, based on area of a particular signal in <sup>1</sup> H NMR
ITC	isothermal calorimetry
IUPAC	International Union of Pure and Applied Chemistry
IR	infrared
<i>J</i>	coupling constant (in Hertz)
<i>K</i>	binding constant (M <sup>-1</sup> )

$K_{1:1}$	1:1 (host:guest) binding constant ( $M^{-1}$ )
$K_{2:1}$	2:1 (host:guest) binding constant ( $M^{-1}$ )
$K_{\beta\text{-CD}}$	binding constant between a particular guest and $\beta$ -CD
$K_{\text{CB}[6]}$	binding constant between a particular guest and CB[6] ( $M^{-1}$ )
$K_{\text{CB}[7]}$	binding constant between a particular guest and CB[7] ( $M^{-1}$ )
$K_{2\text{CB}[7]}$	2:1 (host:guest) binding constant to CB[7]
L	litre
$\lambda_{\text{max}}$	wavelength of maximum absorbance
<i>m</i>	<i>meta</i>
m	multiplet
M	Molar (concentration, in moles per Litre)
MALDI	matrix-assisted laser desorption ionization
Me	methyl ( $-\text{CH}_3$ )
mL	milliliter ( $10^{-3}$ L)
MM2	molecular mechanics 2
MMFF	Merck molecular force field
mp.	melting point
MS	mass spectrometry
<i>m/z</i>	mass to charge ratio
nm	nanometer ( $10^{-9}$ m)
NMR	nuclear magnetic resonance
NOE	nuclear Overhauser enhancement
NOESY	nuclear Overhauser effect spectroscopy
<i>ns</i>	<i>nor seco</i>
<i>o</i>	<i>ortho</i>

OAc <sup>-</sup>	acetate anion
<i>p</i>	<i>para</i>
Ph	phenyl
Phe	phenylalanine
p <i>K</i> <sub>a</sub> <sup>CB[7]</sup>	p <i>K</i> <sub>a</sub> of a particular guest in the presence of CB[7]
PNPCC	<i>p</i> -nitrophenyl choline carbonate
ppm	parts per million
pyr	pyridine, also pyridinium <sup>+</sup>
q	quartet
qd	quartet of doublets
qn	quintet
Quin	quinuclidine, also quinuclidinium <sup>+</sup>
RA[ <i>n</i> ]	resorc[ <i>n</i> ]arene
RNA	ribonucleic acid
s	singlet
SCE	saturated calomel electrode
Ser	serine
sx	sextet
<i>t</i>	<i>tert</i>
t	triplet
td	triplet of doublets
TEMPO	2,2,6,6-tetramethyl-pyridinyl-N-oxyl radicals
TFA	trifluoroacetic acid
THF	tetrahydrofuran
TOF	time of flight

Trp	tryptophan
tt	triplet of triplets
Tyr	tyrosine
UV	ultraviolet
UV-vis	UV-visible spectroscopy
v/v	volume-to-volume ratio

# Chapter 1

## Introduction

Supramolecular chemistry is defined as “chemistry beyond the molecule”<sup>1</sup> and involves non-covalent associations between different molecules.<sup>2</sup> These intermolecular associations can include electrostatic interactions, hydrogen bonding,  $\pi$ - $\pi$  stacking, associations due to the hydrophobic effect, and van der Waals interactions. Supramolecular chemistry therefore focuses mainly on intermolecular non-covalent interactions rather than intramolecular covalent interactions. Although supramolecular chemistry is a relatively new field of chemistry, it has parallels that are observed in biology and founded on the “lock and key” principle described by Emil Fischer.<sup>3</sup>

This introduction will describe the basic principles of supramolecular chemistry, will discuss the non-covalent interactions observed and the common families of host molecules used, leading to a description of the cucurbiturils.

### 1.1 Non-covalent interactions

Non-covalent interactions are the driving force of supramolecular chemistry. In fact, Lehn has also defined supramolecular chemistry as “chemistry of the intermolecular bond” due to the crucial role of these interactions in holding supramolecular systems together.<sup>1,2</sup> Non-covalent interactions are normally significantly weaker than covalent bonds, which are typically near 350 kJ/mol for a single bond.<sup>1</sup> In this section the different common types of intermolecular forces



will be briefly described. Often a successful supramolecular host will utilize a combination of the intermolecular interactions described below.

### 1.1.1 Hydrogen Bonding

Hydrogen bonding involves donor-acceptor interactions between two atoms. One atom, X-H, will act as a proton donor, while another atom, Y, will act as a proton acceptor,<sup>4,5</sup> resulting in the hydrogen bond X-H $\cdots$ Y. In general the atom X should be sufficiently electronegative to withdraw electron density from the proton so that atom Y may donate electron density to the proton. Atom Y should have a lone pair or polarizable  $\pi$  electrons in order to act as a hydrogen bond acceptor.<sup>4</sup> A recent IUPAC panel has proposed that a hydrogen bond can be described as "...an attractive interaction between a group X-H and an atom or group of atoms Y in the same or different molecule(s), where there is evidence of bond formation".<sup>6,7</sup>

The strength of hydrogen bonds can vary significantly, with stronger hydrogen bonds being almost as strong as covalent bonds and weaker hydrogen bonds having similar strength to van der Waals interactions,<sup>4,5</sup> with bond energies between approximately 0.5 and 40 kJ/mol.<sup>5</sup> As a general rule, hydrogen bonds are considered electrostatic interactions, with stronger interactions when X and Y are more electronegative.<sup>5</sup> There is, however, disagreement between chemists regarding the extent of electrostatic interaction required to define an X-H $\cdots$ Y interaction as a hydrogen bond. Earlier, only interactions involving more electronegative X and Y atoms, such as N-H $\cdots$ O, O-H $\cdots$ O, and F-H $\cdots$ F were considered as hydrogen bonds.<sup>5</sup> More recently, weaker interactions involving less electronegative atoms, such as C-H $\cdots$ O, O-H $\cdots$  $\pi$  (where  $\pi$  represents electrons such as those in an aromatic ring, double bond, or other  $\pi$ -electron containing bond) are also considered as hydrogen bond interactions.

General factors influencing the strength of a hydrogen bond interaction such as X-H...Y include the distance between atoms X and H, the distance between Y and H, and the bond angle between X, H and Y. The shorter the distance between the proton and atoms X and Y, the stronger the hydrogen bond will be. Hydrogen bonds are directional interactions, and will be stronger when the X-H...Y angle is closer to 180°, making the bond more linear.<sup>5</sup> In contrast, hydrogen bonds of moderate strength will be slightly bent with bond angles between approximately 130 and 180°, while weak hydrogen bonds can be between 90 and 150°.<sup>4,5</sup>

### **1.1.2 Van der Waals Interactions**

The van der Waals interactions involve intermolecular interactions between molecules that have an instantaneous dipole and an induced dipole.<sup>8</sup> These interactions involve Coulombic (charge based) forces, although they are due normally to partial charges within a molecule (due to the instantaneous or induced dipole moment present) rather than Coulombic interactions between ions.<sup>8</sup> Intermolecular interactions now known as van der Waals interactions were proposed as early as 1873 when it was noted that gases exerted less pressure than would be expected by the ideal gas law.<sup>9,10</sup> These interactions don't necessarily result from permanent charges, but may be observed due to polarization of the electron cloud of the molecules involved.<sup>11</sup> These interactions can be classified as permanent dipole-induced dipole interactions, and instantaneous dipole-induced dipole interactions.<sup>8,9</sup>

Instantaneous dipole-induced dipole interactions are also sometimes called London forces or dispersion forces.<sup>8</sup> Because electrons are constantly moving, the electron density is not symmetric at a given instant of time, so that at one moment the electron density may be congregated more at one side of the molecule than the other, even if the molecule is nonpolar. As a result, a molecule without a permanent dipole moment may still have an instantaneous dipole if the electrons happen to be situated more on one side of the molecule than the other at a particular

moment of time. If another molecule is nearby, it may be affected by the instantaneous dipole so that an induced dipole is created in this nearby molecule.

van der Waals forces can be either attractive or repulsive, depending on the distance between the atoms involved. These interactions are attractive from a distance and become more attractive as the molecules approach each other, but as the molecules become very close together, the interactions become repulsive due to repulsions between the electron clouds of the two molecules.<sup>12</sup> Individually, van der Waals interactions are weak, with typical bond energies of 8 kJ/mol, but they can become significant when they are observed between large numbers of molecules. In fact, the ability of geckos to climb walls is due to van der Waals interactions.<sup>13,14</sup>

The energy of interaction for van der Waals interactions is dependent on the distance,  $r$ , between the two atoms or molecules involved. In the case of dispersion interactions (instantaneous dipole-induced dipole) the interaction energy is proportional to  $r^{-6}$ .<sup>14,15</sup>

### **1.1.3 The Hydrophobic Effect**

The hydrophobic effect describes the tendency for oil and water to separate, and is seen as the driving force for a variety of phenomenon, such as the formation of micelles, protein folding, and the poor solubility of nonpolar solutes in aqueous solution.<sup>16,17</sup> A common trend of this hydrophobic effect is the formation of clusters of the hydrophobic solute within an aqueous solution. The hydrophobic effect has been attributed to the large amount of energy required to form a cavity in the aqueous solvent.<sup>18</sup> Water interacts strongly with other water molecules due to hydrogen bonding, however these interactions are interrupted by the presence of a hydrophobic solute that occupies space that becomes unavailable for water to hydrogen bond with itself. Although water can also interact with the nonpolar solute (such as through van der Waals interactions and hydrogen bonding, if the solute has appropriate functional groups present for

hydrogen bonding), these interactions are generally weaker than the hydrogen bonding interactions occurring between water molecules.<sup>1,19</sup>

A view regarding the low solubility of nonpolar solutes in water is that the water molecules tend to form a shell of more ordered water molecules that surround the nonpolar solute.<sup>18</sup> This ordering of the water molecules surrounding the solute is due to them aligning themselves in a direction so that they may form hydrogen bonds outwardly (and thus with other water molecules) rather than wasting potential hydrogen bonds by directing them inwardly toward the solute.<sup>20</sup> This is energetically unfavorable due to the loss of entropy involved in this process. However, if the nonpolar solutes are merged into a cluster this will reduce the surface area of the nonpolar solute, and therefore reduce the number of water molecules needed to solvate the solute. This view is referred to as the Frank-Evans hypothesis, and is also sometimes called the “iceberg” model.<sup>18,20,21</sup>

There is some debate about the actual origins of the hydrophobic effect, as although entropy has been mentioned above as a cause of this effect, enthalpy is also believed to play a role.<sup>22,23</sup> Some researchers have suggested that the reordering of the solvent may not play as significant a role as predicted by the Frank-Evans hypothesis.<sup>24</sup> In a similar manner as the Frank-Evans hypothesis, recent models have also described the cost of forming two or more cavities in aqueous solutions, as being greater than forming one cavity, when more than one solute molecule is present. In contrast to the entropic costs due to the ordering of the orientation of the water molecules surrounding the solute as they attempt to maximize their hydrogen bonds, a recent explanation has been the loss of translational freedom of the solvent molecules associated with having more than one cavity (due to the greater loss of volume that the solvent molecules may occupy) as contributing to the entropic advantage of forming one cavity.<sup>18</sup> In addition to this, as suggested earlier, the formation of a cavity in the water solvent needed to accommodate the nonpolar solute comes with an enthalpic energy cost due to the disruption of the hydrogen

bonding between the water molecules, and as a result the strong interactions between water molecules are considered to be a dominant cause of the hydrophobic effect.<sup>22</sup> The small size of the water molecules is also believed to be a factor in the hydrophobic effect, so that upon the addition of a given volume of solute, a large number of water molecules are affected through disruption of their hydrogen bonds, and the need to vacate a certain volume in order to accommodate the solute.<sup>18,22,25,26</sup> In summary, the higher entropic cost of forming multiple cavities in the solvent, as opposed to one consolidated cavity, in combination with the enthalpy associated with the disruption of hydrogen bonds are important factors affecting the hydrophobic effect.<sup>18,19</sup>

In terms of supramolecular chemistry, complexation of a nonpolar guest into the hydrophobic receptor site of a host molecule is favorable due to the release of water molecules from the host's receptor pocket, with a resulting increase in entropy.<sup>1</sup> Also, the complexation of a nonpolar guest into a host's hydrophobic receptor may be enthalpically favorable, as the water that is released from the hosts receptor can then more readily form hydrogen bonds with other water molecules in the solvent.<sup>1</sup>

Cyclophane and cyclodextrin hosts bind guests largely due to the hydrophobic effect.<sup>18</sup> In addition, the binding between guests and cucurbit[*n*]uril hosts involves the hydrophobic effect.

#### **1.1.4 $\pi$ - $\pi$ Stacking Interactions**

The  $\pi$ - $\pi$  stacking interactions generally involve aromatic rings, whose planar rings contain delocalized  $\pi$  electrons above and below the plane of the ring. These interactions are a combination of dispersion and electrostatic interactions.<sup>27,28</sup> The polarizable nature of the delocalized  $\pi$ -electrons present allows for dispersion interactions, which can be further enhanced by the presence of softer, more polarizable nuclei in the rings.<sup>27</sup> Also, the C-H bond is slightly

polar ( $C^{\delta-}-H^{\delta+}$ ), so that the outer edge of the aromatic group tends to be slightly electropositive while the  $\pi$  electrons near the carbon atoms have a slight negative charge.<sup>27</sup> The van der Waals component of  $\pi$ - $\pi$  interactions is considered to be a non-directional interaction, while the electrostatic component involves a directional interaction.<sup>27</sup>

Two common arrangements between  $\pi$ -stacked aromatic rings are the edge-to-face and the offset face-to-face arrangements (Figure 1.1). In the edge-to-face arrangement, the slightly negatively charged  $\pi$ -electrons in one ring are attracted to the slightly positive hydrogen atoms on the edge (in the plane) of another ring, so that the two rings are arranged perpendicular to each other. With the offset face-to-face arrangement, the rings are parallel to each other but are offset from each other in order to allow oppositely charged regions of the molecules to align with each other.<sup>27</sup>

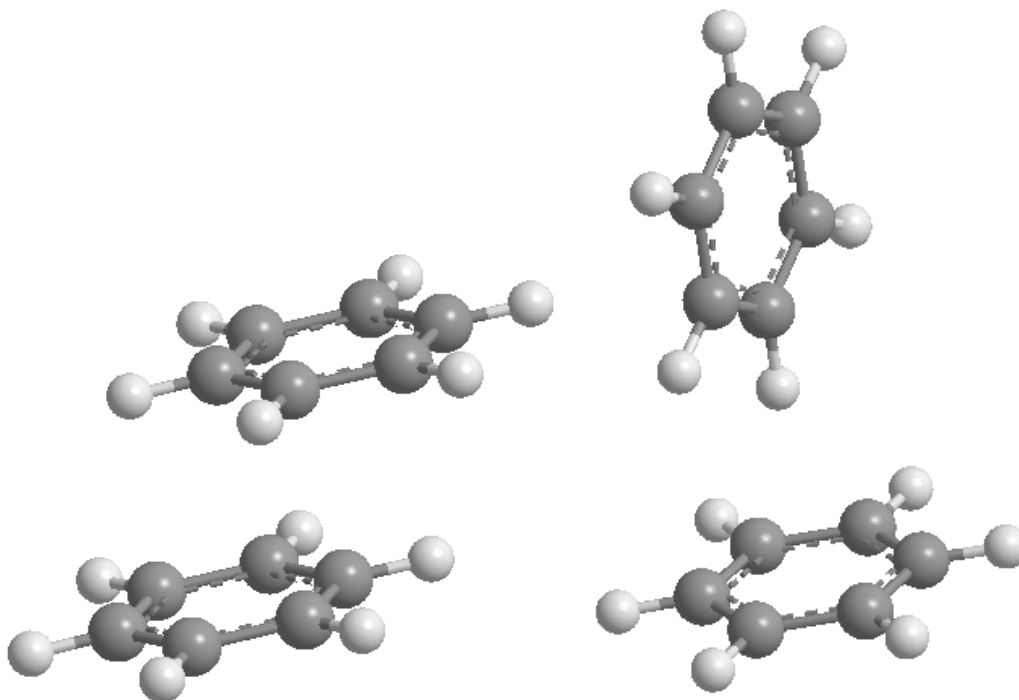


**Figure 1.1** Offset face-to-face (left) and edge-to-face (right)  $\pi$ - $\pi$  stacking arrangements.

Another, less common arrangement is the face-to-face arrangement in which two planes of rings are parallel to each other but not offset from each other. This can occur where one ring has substituents that are more electronegative than the carbons at the core of the ring ( $C^{\delta+}$ ), while the other ring has substituents that are less electronegative than the core atoms (therefore the quadrupoles of the two rings are reversed with respect to each other). In this case when the two planes of rings are parallel to each other, their oppositely charged orbitals may also be aligned without the need for the rings to be offset from each other.

If a polarizing heteroatom is incorporated into the molecule with delocalized  $\pi$  electrons, a partial charge may be introduced into the molecule that may cause donor-acceptor behavior to be observed, in addition to the  $\pi$ -stacking that can be observed.<sup>28</sup> These interactions could involve atom-atom interactions (which are electrostatic interactions between the partial charges of atoms in different molecules) and also atom- $\pi$  interactions, which are interactions between the heteroatom of one molecule and the  $\pi$ -electrons of another molecule.<sup>28</sup>

More recent studies have suggested that the traditional view of  $\pi$ - $\pi$  stacking may have placed too much importance on the electrostatic component of the binding, while a more important factor in binding between planar unsaturated systems may be due to dispersion interactions.<sup>29</sup>

### **1.1.5 Electrostatic Interactions**

Electrostatic interactions are Coulombic (charge-based) interactions that result in an attraction between two oppositely charged molecules. These can generally include ion-ion, and ion-dipole interactions, as well as permanent dipole-permanent-dipole interactions and permanent dipole-induced dipole interactions.<sup>1,19</sup>

Electrostatic interactions, especially ion-ion and, to a lesser extent, ion-dipole interactions are often among the strongest non-covalent interactions available, being estimated as up to 250 kJ/mol for an ion-ion interaction.<sup>1</sup> Ion-ion interactions are independent of direction, while ion-dipole interactions need to be arranged in a particular direction (for example the partially negative end of the dipole should be facing a positive ion and vice versa) in order to attain maximum strength.<sup>1</sup> Examples of electrostatic interactions observed in supramolecular chemistry are the binding between cations and crown ethers, and the interactions between cationic guests and the electron rich carbonyl-lined rims of cucurbit[*n*]urils. Permanent dipole-permanent dipole interactions involve interactions between molecules that have a permanent dipole, being partially negative at one end and partially positive at the other end. These molecules will interact so that the partially positive end of one molecule will attract the partially negative end of the other molecule. This will result in the molecules aligning so that their opposite partial charges are arranged toward each other.<sup>1</sup> Permanent dipole-induced dipole interactions may occur when a molecule with a permanent dipole and a nonpolar molecule approach each other. As the polar molecule approaches, the dipole moment of that molecule causes the electron density within the nonpolar molecule to migrate to the side of the molecule that is facing away from the partially negative end of the polar molecule. This migration within the nonpolar molecule results in an induced dipole moment in this molecule, so that it may align attractively with the other molecule as its partial charge is directed toward the opposite partial charge of the other molecule. Both permanent dipole-induced dipole and permanent dipole-permanent dipole interactions are sometime referred to generally as dipole-dipole interactions.<sup>8</sup>

As is the case with van der Waals interactions, the interaction energy of electrostatic interactions is related to the distance, *r*, between the two atoms or molecules. In the case of ion-dipole interactions the interaction energy decreases by  $r^2$  as the distance increases. For ion-induced dipole interactions the decrease is  $r^4$  with increasing distance, while this decrease is  $r^3$



with increasing distance for permanent dipole-permanent dipole interactions.<sup>14</sup> Meanwhile, the interaction energy of permanent dipole-induced dipole interactions decreases by  $r^6$  as distance increases.

One widespread form of noncovalent bonding that is observed is cation- $\pi$  bonding,<sup>30,31</sup> which is essentially a form of ion-dipole interactions, although these interactions sometimes involve the quadrupole moment of a  $\pi$ -system. This interaction involves the noncovalent bonding between a cation and the face of a  $\pi$  system, with the main contribution being due to electrostatic interactions. Other interactions, such as dispersion interactions and the hydrophobic effect, may sometimes contribute to a lesser extent.<sup>31</sup>

## **1.2 Concepts of Supramolecular Chemistry: Molecular Recognition and Self-Assembly, Macrocyclic Hosts, Rotaxanes, and Catenanes**

As mentioned above, noncovalent interactions are normally much weaker than covalent interactions, and in order to obtain strong binding, successful hosts often utilize more than one type of noncovalent interaction. In addition, the host and guest should ideally have corresponding geometries, as well as binding sites that are positioned in locations that maximize their effectiveness. The binding sites should be well aligned with each other, and this is referred to as complementarity.<sup>1,32</sup>

Although supramolecular systems are often held together by weaker interactions than covalent systems, in some cases the “strength” of supramolecular systems actually lies in the weakness of these intermolecular forces.<sup>13</sup> In particular, the weakness of these interactions allows host-guest binding to become a reversible process, so that a host and guest can associate and dissociate without either of the building blocks being damaged or altered. This can be useful for

systems such as molecular switches and for catalysis, and is utilized frequently in natural enzymes.

### 1.2.1 Self-Assembly and Molecular Recognition

Self-assembly is described as the spontaneous construction of ordered structures from molecular building blocks.<sup>33</sup> Strict self-assembly also involves a reversible assembly process that is thermodynamically controlled.<sup>34</sup> In particular, the host-guest complex which is formed, sometimes referred to as a *supermolecule*,<sup>32</sup> should be the thermodynamically favoured species under the existing conditions. An often-cited example of self-assembly from Nature is the tobacco mosaic virus (Figure 1.2), in which 2130 identical protein units, each containing 158 amino acid residues, encapsulate a strand of RNA through non-covalent interactions in order to form the helix-shaped protein shell of the virus.<sup>35,33,36,37</sup> This virus can dissociate due to changes in pH, temperature, or pressure but will reassemble once the optimum conditions return, and the reassembled virus is indistinguishable from the original virus.<sup>33,37</sup>

Molecular recognition involves binding and selectivity between a host and guest, and should also provide potential for a specific function.<sup>38</sup> Information processing is often associated with this concept also,<sup>38,39</sup> in that the information is stored in the substrate through its architecture and its binding sites. As a result, complexation between the host and guest occurs when the information stored in the two building blocks match each other best.<sup>38</sup>

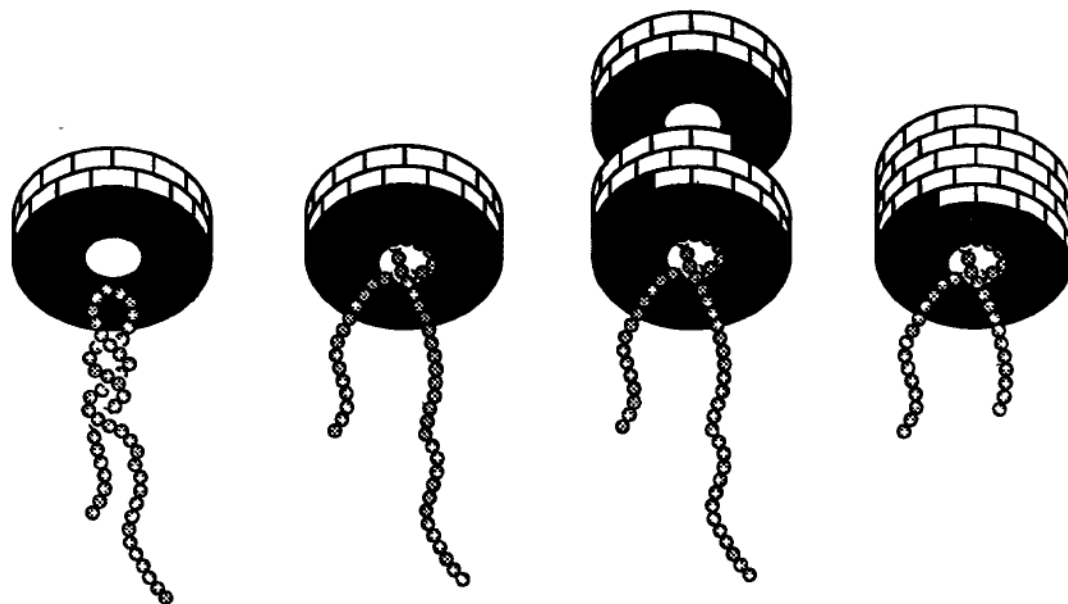


**Figure 1.2** Self-assembly of the tobacco mosaic virus. The beaded string represents the strand of RNA, which becomes encapsulated by 2130 protein units, which are represented by the blocks in the diagram.<sup>37</sup> The protein units encapsulate the RNA strand through non-covalent interactions to form the protein coating of the virus.

### 1.2.2 Macrocyclic Hosts

Macrocyclic hosts are molecular receptors that are arranged as a ring, in which the guest, or substrate, may bind in the interior. Macrocyclic hosts can be generally classified as types of *endoreceptors*, in that they bind with their guests located in the interior of the host.<sup>40</sup> *Exoreceptors*, in contrast, bind to substrates on their exterior. Some common examples of macrocyclic hosts include crown ethers, calixarenes, cyclodextrins, and cucurbiturils, and these will be described below.

Macrocyclic molecules tend to be less solvated than acyclic molecules are, so that the complexation of a macrocyclic host to a substrate requires less desolvation, thus making complexation more enthalpically favorable than it would be for an acyclic host, with more solvation. In addition, the increased rigidity of macrocyclic hosts compared to their acyclic analogues allows the macrocyclic hosts to bind to a guest with a smaller relative loss of entropy

upon complexation than an acyclic host would experience, since the rigidity of the macrocyclic host already incorporates some order into the host.<sup>1</sup> Furthermore, complexes of macrocyclic hosts tend to associate and dissociate more slowly than those with acyclic hosts, therefore macrocyclic complexes are more kinetically inert.<sup>1</sup> These enhanced capabilities of macrocyclic receptors to bind to guests, due to increased thermodynamic and kinetic stabilities of the complex, are referred to as the macrocyclic effect.<sup>1,41</sup> As a consequence of the increased binding stability provided by the macrocyclic effect, the majority of supramolecular hosts-guest systems studied involve some form of macrocyclic receptor.

In addition, hosts that are more preorganized for binding will also tend to be more selective with respect to the guests that they may bind.<sup>42</sup> A rigid, preorganized host has less freedom to rearrange itself to bind to a guest of a different size or arrangement of binding sites, and it will form a much more stable complex with a guest that complements its pre-existing conformation than with other guests that do not match the host as well. This host is then said to be selective due to its preferential binding of compatible guests (with appropriate size, shape and position and types of binding sites, for example) over those that do not match the host as well.

### **1.2.3 Supramolecular Complexes involving Macrocyclic Hosts: Rotaxanes and Catenanes**

In some of the supramolecular systems involving smaller guests, such as alkali metals, the guest is essentially encapsulated inside the macrocycle using noncovalent interactions. In some cases, however, the geometry of the host guest system can become more complex and may consist of mechanically interlocked components.

Catenanes are composed of at least two rings that are interlocked with each other. These rings are not covalently bound to each other, but they are mechanically locked together in a similar manner to links of a chain. In fact, the name catenane is derived from the Latin word

*catena*, which means chain.<sup>43</sup> As a result, the individual components form one interlocked complex. The number of interlocked rings incorporated into a catenane complex may vary and the nomenclature used for catenanes have the general format of *m*-crossing-[*n*]-catenane, where *m* indicates the number of times each ring crosses the other ring and *n* represents the number of macrocycles that are interlocked into the complex.<sup>44</sup> Normally, these interlocked rings cross each other 2 times and if this is the case, the term 2-crossing is dropped from the name. The most basic catenane system would be a 2-crossing-[2]-catenane, which would be referred to as a [2]-catenane (Figure 1.3).<sup>45</sup> There are also polymeric systems composed of many interlocked rings, which are referred to as [*n*]-polycatenanes.<sup>44</sup>

There are three general ways that catenanes can be synthesized.<sup>46</sup> In one method, one of the free rings exists as a closed macrocycle initially, while the other component is initially open. These two precursors are then bound (or “threaded”), thus forming a pseudo-rotaxane with a subsequent step that closes the open thread so that the two rings are then interlocked.<sup>46</sup> With the second approach, both of the components are initially acyclic, and they are then assembled into an appropriate complex, with a subsequent cyclization of both of the ligands to form the catenane. The third approach begins with two macrocycles, which are then opened and allowed to associate with each other, prior to the rings being closed again.<sup>46</sup> These three methods often make use of template effects in order to increase the efficiency of the synthesis.

While catenanes are made up of interlocked macrocycles, rotaxanes consist of an axle that is threaded through a macrocycle.<sup>47</sup> The name rotaxane comes from the Latin words *rota*, which means wheel, and *axis*, meaning axle.<sup>35,44</sup> The thread of a rotaxane consists of “stoppers” at both ends, often bulky organic groups or metal centres, which effectively trap the macrocycle on the thread due to the bulkiness of the stoppers. A complex that lacks stoppers at the ends of the thread is called a pseudorotaxane, and the macrocycle is therefore free to migrate on or off the thread. More than one macrocycle can be threaded onto the axle, and a numbering system is used

to indicate the total number of components of the complex, the number of axles plus the number of macrocycles. For example, a basic rotaxane made up of one thread and one macrocycle would be referred to as a [2]rotaxane (Figure 1.3), while a rotaxane containing two macrocycles threaded onto an axle would be referred to as a [3]rotaxane. One macrocycle threaded by two axles would also be called a [3]rotaxane.

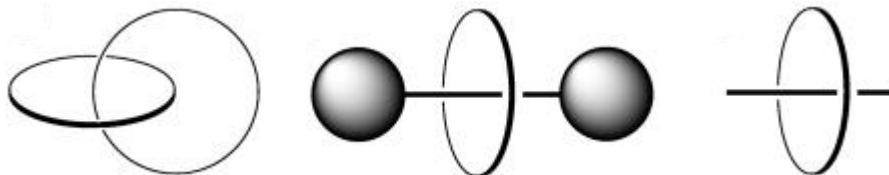


**Figure 1.3** A [2]-catenane (left), a [2]rotaxane (centre), and a [2]pseudorotaxane (right).<sup>47</sup>

### 1.3 Supramolecular Characterization

A variety of analytical techniques may be used to characterize supramolecular systems. Tools used for characterization can include (depending on the system studied) nuclear magnetic resonance (NMR) spectroscopy, UV-visible (UV-vis) spectroscopy, mass spectrometry (MS), fluorescence spectroscopy, and X-ray crystallography. Brief descriptions of these characterization techniques will be given below. Spectroscopic techniques, such as NMR and UV-visible, for example, often take advantage of changes in the spectroscopic features of either the host and/or the guest, which may be observed upon complexation. Depending on the system studied and the characterization methods used, information can be provided about the binding constant, the stoichiometry of the host-guest system studied, and the location of the binding between the host and the guest within their relative structures.

### 1.3.1 Nuclear Magnetic Resonance (NMR) Spectroscopy

NMR spectroscopy is one of the most versatile characterization tools available in chemistry, and is also very useful in studying supramolecular systems. Changes in the shielding of protons due to the proximity of hosts and guests can result in changes of chemical shifts (often called  $\Delta\delta$  values) of receptive protons.<sup>48</sup> This can therefore provide information regarding the structural location of the interaction between the host and guest. For example, it may reveal which guest protons are encapsulated by the host and which are not. Depending on the supramolecular system studied, the magnitude of the  $\Delta\delta$  shifts observed may vary. While guests encapsulated by cyclodextrin hosts reveal relatively modest shifts, guests bound with cucurbiturils hosts display up to 1 ppm upfield shifts when they are in the centre of the shielding cavity and downfield shifts when the protons are near the deshielding portals. The variation of electron density along the structure of cucurbiturils are very well defined compared to those of cyclodextrins, which have less variation of this density in different parts of their structure.

The appearances of the changes of the host and guest proton resonances can vary depending on how fast the exchange between the host and guest is with respect to the NMR timescale.<sup>49</sup> The NMR timescale is dependent on experimental conditions such as the field of the NMR instrument, as well as the Larmor frequency of a given nucleus. With regard to the interconversion between two states for a particular nucleus (such as “free” and “bound” in the case of a supramolecular system), whether an exchange on an NMR timescale is fast or slow is dependent on the frequency difference between the two states of the nucleus, and how it compares to the exchange rate of that nucleus. If a nucleus’ exchange rate between the two states is slower than the difference in frequencies between the two states, the system is said to be a *slow exchange* system compared to the NMR timescale.<sup>50,51</sup> When a guest’s nucleus within a supramolecular host-guest system exhibits slow exchange behaviour, both the “free” and “bound” peaks of a given guest nucleus (representing the unbound and bound protons, respectively) may

be seen in the spectrum. Alternatively, if a nucleus' exchange between two states is faster than the frequency difference between the two states, the system is said to exhibit *fast exchange* behaviour. When a guest proton in a supramolecular system displays fast exchange behaviour, the “free” and “bound” proton resonances are combined into one peak that represents a weighted average of the bound and unbound proton resonances.<sup>49,52</sup> A third type of situation occurs when the host-guest exchange occurs on a timescale that is similar to that of the NMR timescale.<sup>52</sup> In this case, the peaks that correspond to the free and bound nuclei will become broad, or even disappear. This broadening is observed when the ratio of host and guest is such that there is a mixture of free and bound species present. When the species are either totally unbound or completely bound, the effected peaks normally become sharp again.

Nuclear Overhauser enhancement (NOE)-based experiments, such as NOESY and ROESY are sometimes used, as NOE interactions are based on through-space interactions as opposed to through-bond interactions observed in NMR coupling. As a result, NOE experiments may be used to determine if protons from the host and guest come in close proximity, as would be the case in a host-guest interaction.<sup>53</sup>

Normally <sup>1</sup>H NMR is more useful for supramolecular studies than NMR of other nuclei, because protons are closer to the exterior of the molecule and are therefore more exposed to other molecules. As a result, they are more receptive to changes in the environment resulting from presence of another molecule.<sup>48</sup> Other nuclei, such as <sup>13</sup>C, are usually more deeply buried and their chemical shifts tend to be less responsive to intermolecular interactions due to their isolation from the external environment. Alternatively however, nuclei such as <sup>13</sup>C and <sup>31</sup>P have a wider chemical shift range available, which may help improve their responsiveness (demonstrated through changes in chemical shifts) toward noncovalent interactions. The sensitivity of the <sup>13</sup>C nucleus is relatively poor, having a natural abundance of only 1.1 %, thus providing a small proportional of nuclei that are NMR active within a given sample. Also, <sup>13</sup>C nuclei have a low



magnetogyric ratio, thus requiring longer acquisition times, although this is not as much of an issue for  $^{31}\text{P}$  NMR, which has a natural abundance of 100 % and a large magnetogyric ratio.

### 1.3.2 UV-visible Spectroscopy

The encapsulation of a guest in a host can affect its UV-visible absorption properties, which can be utilized as an indication of complexation. The sensitivity of UV-visible spectroscopy is greater than that of NMR, providing good signal to noise. Sample concentrations for UV-visible experiments are typically on the order of  $10^{-4}$  to  $10^{-5}$  M, depending on the sample's extinction coefficient. UV-visible spectroscopy generally doesn't provide as much information about the location of the host-guest binding as NMR spectroscopy does, and at least one of the samples needs to show absorption in the UV-visible region (between approximately 200 and 900 nm). As a result, compounds with conjugation in their structures will more readily be observed by UV-visible. UV-visible spectroscopy can be useful for determining binding constants by titration, in which the change of absorption at a responsive wavelength is plotted against the concentration of either the host or guest (with the other species being kept constant).

### 1.3.3 X-ray Crystallography

X-ray crystallography can be a very powerful tool for determining the solid-state structure of a compound. It can also be utilized for determining the structures of host-guest complexes. It can sometimes be difficult to determine the structures of supramolecular structures through crystallography, as the size of the systems is often larger, thus requiring more reflections.<sup>48</sup> In addition, these systems also are more likely to include solvent than smaller molecules do. Also, supramolecular systems often have more flexibility in their frameworks, which can introduce more disorder into the crystals.<sup>48,54</sup> This disorder is observed especially

when the guest is associated weakly with the host. The electron density from the guest can be difficult to locate when the system is disordered, and in some more extreme situations, the guest or solvent cannot be found.<sup>55</sup>

X-ray crystallography can show how molecules are positioned with respect to each other. It can also give detailed information about individual bond lengths and bond angles within the molecule. X-ray structures can also show likely positions within the system where intermolecular interactions are taking place. This is especially true for showing positions that are likely involved with hydrogen bonding. Caution should be exercised however, when using a crystal structure to interpret behaviour of a system in solution, as behaviour observed in the solid state may not necessarily represent that in the solution.

#### **1.3.4 Mass Spectrometry**

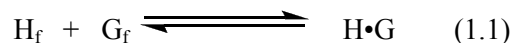
Mass spectrometry is a valuable tool that can provide information about the molecular weight and stoichiometry of a compound, as well as the identification of a particular structure due to its characteristic fragmentation patterns observed. Because supramolecular systems are held together by weak intermolecular forces, harsher ionization methods, such as electron impact (EI) and chemical ionization (CI), for example, tend to have limited application for supramolecular chemistry.<sup>56,57</sup> Softer ionization methods, such as electrospray ionization (ESI) and matrix-assisted laser desorption ionization (MALDI), on the other hand, are more useful for studying supramolecular systems, as the noncovalent bonds can often survive these milder ionizations, so that, for example, the molecular weight of the supramolecular complex may be obtained.

Data from mass spectrometry is normally obtained in the gas phase. This can have advantages and disadvantages, depending on the situation. The nature of gas phase interactions observed by mass spectrometry can be useful if one wants to study the host-guest interactions of a

system in the absence of a solvent. In addition, because calculations based on computational chemistry often assume the gas phase, mass spectrometry can in some cases be the closest experimental link with theoretical calculations.<sup>55</sup> The host-guest binding behaviour observed in gas phase and solution may differ, as the solvent may interact with the host or the guest and thus affect the binding. Also, solvation of the host or guest may affect the entropy or enthalpy of the host-guest system. Therefore, if the system of interest is normally in solution, it is important to be aware that interactions observed in the gas phase by mass spectrometry may differ from those occurring in solution.

### 1.3.5 Determination of Binding Constants

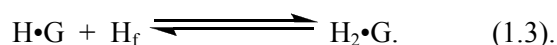
Binding constants (also called *association* or *stability constants*) are equilibrium constants that are used as a quantitative measurement of the strength of the interaction between a particular host and guest, and the more favourable the interaction between a given host and guest is, the higher the binding constant will be.<sup>58</sup> The calculation of the binding constant therefore takes into account the concentrations of the free guest (that is the unbound guest) and the free host, as well as the concentration of the host-guest complex. For a 1:1 complex the equilibrium is Equation 1.1:



where  $H_f$  and  $G_f$  represent the free host and guest, respectively, and  $H \cdot G$  is the host-guest complex.<sup>58</sup> The binding constant of this system can therefore be expressed as Equation 1.2:

$$K = [H \cdot G] / ([H_f] [G_f]) \quad (1.2).$$

The ratio of binding between the host and guest (the binding stoichiometry) may vary, such as with situations where multiple guests bind to one host, or more than one host binds to one guest.<sup>58</sup> The latter situation has been observed with some systems to be discussed in later sections. If a second host is able to bind to the guest, the equilibrium between the 1:1 complex that has already formed and the host can be expressed as Equation 1.3:



The binding constant of this expression, which is the 2:1 (H:G) binding constant, also called  $K_2$ , is expressed as Equation 1.4:

$$K_2 = [\text{H}_2\cdot\text{G}] / ([\text{H}_f] [\text{H}\cdot\text{G}]) \quad (1.4).$$

The 1:1 binding constant described initially would in turn be expressed as  $K_1$  in this case. For systems with multiple binding constants due to their higher stoichiometries, an overall binding constant, expressed as  $\beta_n$ , can also be determined as the product of the individual binding constants.<sup>58</sup> Therefore the overall binding constant,  $\beta_n$ , can be expressed as Equation 1.5:

$$\beta_n = K_1 \times K_2 \times K_3 \dots \times K_n \quad (1.5).$$

Binding constants can be obtained through a titration,<sup>59</sup> such that the guest's concentration is held constant and the concentration of the host is varied. Normally the solutions containing the host and the guest contain an equal concentration of the guest, so that the concentration of the guest does not vary. Alternatively, the host concentration may also be held

constant and the guest's concentration varied. A variety of spectroscopic methods may be used for these titrations, although the output will differ between the methods used. For example, if an NMR chemical shift titration is used, the output will be the change in the chemical shift of a particular resonance that is sensitive to variations in the ratio between the host and guest, which will normally be plotted as the independent variable (that is, on the y-axis). In the case of a UV-visible titration, the output will be a change in the absorbance at a responsive wavelength. Once a titration curve is obtained, this can then be fitted by a least-squares method, in order to obtain a binding constant.

In the case of an NMR experiment of a host-guest system that is undergoing slow exchange, it may be possible to calculate binding constants more directly based on the relative integrals of the free and bound peaks observed either for the host or guest.

One limitation in using titrations for determining binding constants, is that in some situations the binding between the host and guest will be too strong to obtain a curve that is "curved" enough to be used for calculating a binding constant. If a  $^1\text{H}$  NMR titration is used, this situation is often encountered for binding constants as they reach approximately  $10^4 \text{ M}^{-1}$ . This is also near the upper range of binding constants that can be calculated using UV-visible titrations, although with UV-visible spectroscopy this also depends on the concentration of the guest that is studied.<sup>59</sup> With very strong binding, the curve may plateau abruptly once the complex is completely bound, making it difficult or impossible to fit. If this is the case, it may be necessary to determine the binding constant indirectly, such as by using a competitive binding method. This has been used with cucurbituril host-guest complexes using  $^1\text{H}$  NMR spectroscopy,<sup>60,61</sup> where ligands that bind to the host with a known binding strength are used to compete with the guest for binding to the host. The relative binding strengths between the guest, with an unknown binding constant to the host, and the competitor, with a known binding constant, may be compared, and the binding constant of the guest can be calculated according to the binding

strength of the competitor. When possible, it is normally best to choose a competitor that has a binding constant to the host that is of similar strength (often within an order of magnitude) as that of the guest.

It should be noted that a binding constant that is measured for a given system is specific to the conditions under which the measurement was carried out (choice of solvent, temperature, salt content, etc.), and will usually vary outside of those specific conditions. Therefore the binding constant of a particular system will not necessarily be the same value if those conditions are changed. The experimental conditions should also be given when a binding constant is reported.

## **1.4 Non-Cucurbituril Macrocyclic Hosts**

In addition to cucurbiturils, which are the family of hosts utilized in this thesis, there are a variety of other macrocyclic hosts used in supramolecular chemistry. These include crown ethers, calixarenes, porphyrins, and cyclodextrins. These will be discussed in the following sections.

### **1.4.1 Crown Ethers**

Macrocyclic polyethers were reported<sup>62,63</sup> as early as 1937 and in the late 1950s various polyether macrocycles, including 12-crown-4 derivatives, were reported by Wilkinson and coworkers<sup>63-65</sup> to dissolve small amounts of potassium metal and sodium-potassium alloy to give unstable blue solutions. However, the unique inclusion properties of macrocyclic polyethers with alkali metals were not fully realized until the discovery of the crown ethers in 1967 by Charles Pedersen<sup>66-70</sup>. It was Pedersen who introduced the term “crown ether” that is widely used today.<sup>66,70</sup> In the naming format, the total number of atoms in the ring is named first with the

number of heteroatoms listed last. For example, 18-crown-6 is a crown ether macrocycle containing eighteen atoms in the macrocyclic ring, and of those six are heteroatoms (oxygen in this case). The heteroatoms of crown ethers are normally linked by two carbons, such as ethyl spacers, as is seen most frequently, but these two carbons can be more rigid, as the edge of an aromatic ring, for example.

Charles Pedersen was studying open-chained complexing agents for vanadium when he obtained dibenzo-18-crown-6 (Figure 1.4) as a by-product.<sup>71</sup> This novel compound was insoluble in methanol, but dissolved in methanol with the presence of sodium ions.<sup>63,68</sup> He realized that an inclusion complex was being formed and followed up this discovery with the synthesis of a series of crown ethers complexed with various cations.<sup>69</sup> This recognition by Pedersen in 1967 that crown ethers form inclusion complexes with alkali metals is often said to be the foundation of modern supramolecular chemistry.<sup>66</sup>

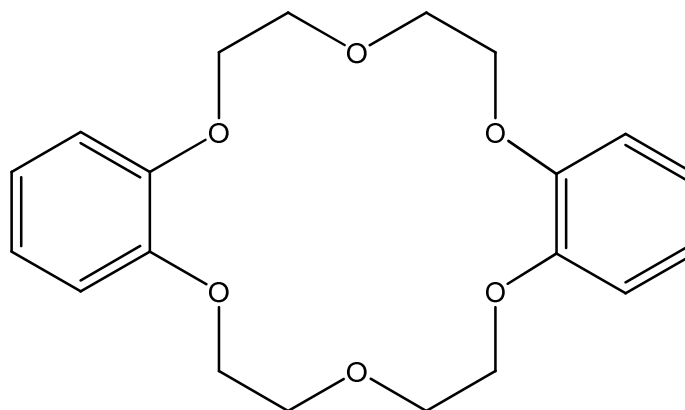


**Figure 1.4** Structure of dibenzo-18-crown-6.

Although oxygen is the most common heteroatom of crown compounds, crown compounds can often include macrocycles containing other heteroatoms such as nitrogen and sulfur.<sup>66</sup> The term “crown ether” is usually more strictly associated with those compounds

containing oxygen as the heteroatom,<sup>66</sup> while terms such as *azacrown ethers* and *thiacrown ethers* refer to those macrocycles containing nitrogen or sulfur, respectively, in addition to oxygen.<sup>66</sup> If the heteroatom present is only nitrogen or sulfur, and oxygen is absent, the macrocycle is then called an *azacrown* or a *thiacrown*, respectively.<sup>66</sup> In some definitions crown compounds consist of twelve or more members of the macrocyclic ring, and include four or more heteroatoms in the ring.<sup>71</sup> Macrocycles containing heteroatom donors, such as crown ethers, are sometimes called *corrands*.<sup>72</sup>

Factors influencing the selectivity of crown ethers include the relative size of the macrocyclic cavity with respect to the guest (with stronger binding with a closer match in sizes), the number of heteroatoms in the ring, the nature of the heteroatoms present (such as whether they are harder oxygen atoms or softer atoms such as sulfur or nitrogen), and the charge of the guest.<sup>39,66,68</sup> The oxygen atoms will generally bind to guests such as alkali metal cations, while nitrogen and sulfur are more likely to bind to softer transition metal cations.<sup>71</sup> While traditionally crown ethers were studied as hosts for cationic guests, in some cases they may also bind to neutral or anionic guests (with anionic guest binding observed with azacrowns and protonated azacrowns).<sup>71</sup>

There are various derivatives of crown compounds that have built upon the crown-ether core by additions of more substituents or rings. For example, lariat crown ethers are crown ether macrocycles that have a pendant acyclic ethylene glycol arm, in which one end of the arm is attached to the macrocycle while the other end is free. These lariat heteroatoms act as donors, in addition to the heteroatoms that exist in the macrocycle itself, and this arm can therefore also take part in binding to the guest.<sup>67</sup> The sidearm of the lariat ether is normally attached to either a carbon in the macrocycle, or nitrogen of an azacrown ether.<sup>44,73</sup> In some cases the presence of this lariat arm may add the chelate effect to the macrocyclic effect that already exists (from the crown ether ring) and thus enhance binding stability. In addition, the donor atoms may bind to



binding sites of the guest that are not bound to the macrocyclic ring itself, and can reduce competition from solvents for binding to the guest. It can also be possible to tune the length and nature of heteroatoms in the lariat arm to enhance selectivity of binding to a guest. Generally, it is also synthetically easier to incorporate a wider variety of donor atoms into the lariat arm than in the macrocyclic ring itself, so that a lariat arm may introduce donor atoms or functional groups into the crown ether host that may not have been otherwise readily available.<sup>67</sup> Like crown ethers, lariat crown ethers are relatively flexible hosts. Although they lack the thermodynamic stability of complexation that the more preorganized cryptands have (which will be described below), they are kinetically able to associate with, and dissociate from, their guests more quickly than the more rigid cryptand.<sup>72</sup> In addition to having one arm, lariat ethers may have two pendant arms containing donor atoms, and are then referred to as bibracchial lariat ethers.<sup>74</sup> The addition of this second arm generally enhances binding of the crown ether host. Depending on the structure of the host or the nature of the host-guest system involved, these arms may either bind to the guest from the same side of the ring, or from opposite sides of the ring (that is, one above the face of the macrocycle, and the other arm below).

Soon after Pedersen discovered crown ethers as intermolecular hosts, Jean-Marie Lehn synthesized the first cryptand.<sup>45,75,76</sup> These efforts were due to the realization by Lehn that a three-dimensional host would have potential to bind more strongly to spherical cation guests, such as potassium cations.<sup>45</sup> The host-guest complex composed of a cryptand host and its guest is referred to as a *cryptate*.<sup>2</sup> Like crown ethers, cryptands have heteroatoms present in their cage structure that take part in binding. While crown compounds consist of one ring, a cryptate consists of two rings and is therefore a macrobicyclic compound.<sup>2,32,72</sup> Due to the increased rigidity provided by this second ring, cryptands generally have higher binding constants and more selectivity than crown ethers have for specific guests.<sup>72</sup> Due to the increased selectivity of cryptands, the selectivity of cryptands is referred to as *peak selectivity*, while that of crown ethers

is called *plateau selectivity*.<sup>73</sup> This enhanced stability and selectivity observed by cryptates is known as the *macrobicyclic effect* (sometimes called the *macrobicyclic cryptate effect*),<sup>2</sup> which is essentially due to the increased preorganization of the cryptand host.<sup>2,72</sup> Due to this effect, the binding constants between a cryptand and a well-matched guest can be 4 to 5 orders of magnitude stronger than those between the same guest and an analogous host with only one macrocycle.<sup>2,73</sup> Another feature that Lehn has attributed to cryptates is efficient shielding of their encapsulated guests from the surrounding environment.<sup>2</sup>

The links of the cryptands are usually, but not always, connected through a nitrogen atom. For traditional ether-containing cryptands, the nomenclature system uses three numbers, with each number indicating the number of oxygens in each linking arm of the macrocycle.<sup>45</sup> For example, cryptand [2.2.2], the first cryptand which was synthesized by Lehn and coworkers,<sup>45,75,76</sup> consists of three crown ether arms, that are all linked in a cage through nitrogen heteroatoms. The number system indicates that each of these arms contains two oxygen atoms.

#### 1.4.2 Calixarene Hosts

Calixarenes are cup-like macrocyclic hosts and their name comes from the Latin word *calix*, which means cup.<sup>77</sup> They are made up of various numbers of *meta*-disubstituted phenol rings that are linked together by methylene groups to form a macrocycle. These phenol rings are usually (although not always) substituted in the position *para* to the phenol, often with a bulky substituent. This region is called the *upper rim* of the calixarene, while the phenol OH groups make up the *lower rim* of the calixarene. The upper rim is wider than the lower rim when the calixarene is in the cone conformation, and the upper rim is sometimes referred to as the *exo rim*, while the lower rim is referred to as the *endo rim*.<sup>78</sup> The number of phenol rings contained within the macrocycle is denoted by *n*, within the name calix[*n*]arene. Macrocycles with *n* = 4-8 are the

most common, although larger macrocycles, such as those with  $n$  up to 20 have also been synthesized.<sup>79,80</sup> The name of the substituent that is *para* to the phenol hydroxyl group precedes that of the calixarene, so that if a calixarene is composed of *p-tert*-butylphenol rings, the calixarene would be named *p-tert*-butylcalix[ $n$ ]arene.<sup>77</sup>

The orientation of the aromatic rings that make up the calixarene may vary. When the aromatic rings are arranged in the same direction (for example, with the upper rim component of each aromatic ring facing the same direction), the conformation is referred to as the *cone conformation*. In the case of calix[4]arene, when all of the aromatic rings are arranged in the same direction except for one, the conformation is referred to as the *partial cone conformation*. When two of the aromatic rings that are adjacent to each other are facing the same direction, the conformation is referred to as the *1,2-alternate* conformation, while if adjacent rings are facing opposite directions to each other the conformation is referred to as *1,3-alternate*.<sup>77,79</sup> Of these conformations, the *cone* conformation most closely matches the cup-like description of calixarenes (Figure 1.5).

Although modern calixarene chemistry, and the introduction of the name of calixarene, is considered to have begun in the 1970s,<sup>81</sup> work with calixarenes actually began about 130 years ago with work done by Adolf von Baeyer, who was attempting to synthesize new dyes.<sup>82-84</sup> As part of this study, he reacted phenol with formaldehyde and obtained a tar that could not be characterized at the time. He therefore abandoned this area of research in order to study other areas of chemistry. About thirty years later, Leo Baekeland found that adding base to this reaction of phenol with formaldehyde mixture yielded a potentially useful product, and he patented this reaction and referred to the product as Bakelite.<sup>85</sup> This is considered to be the first plastics industry.<sup>82</sup>

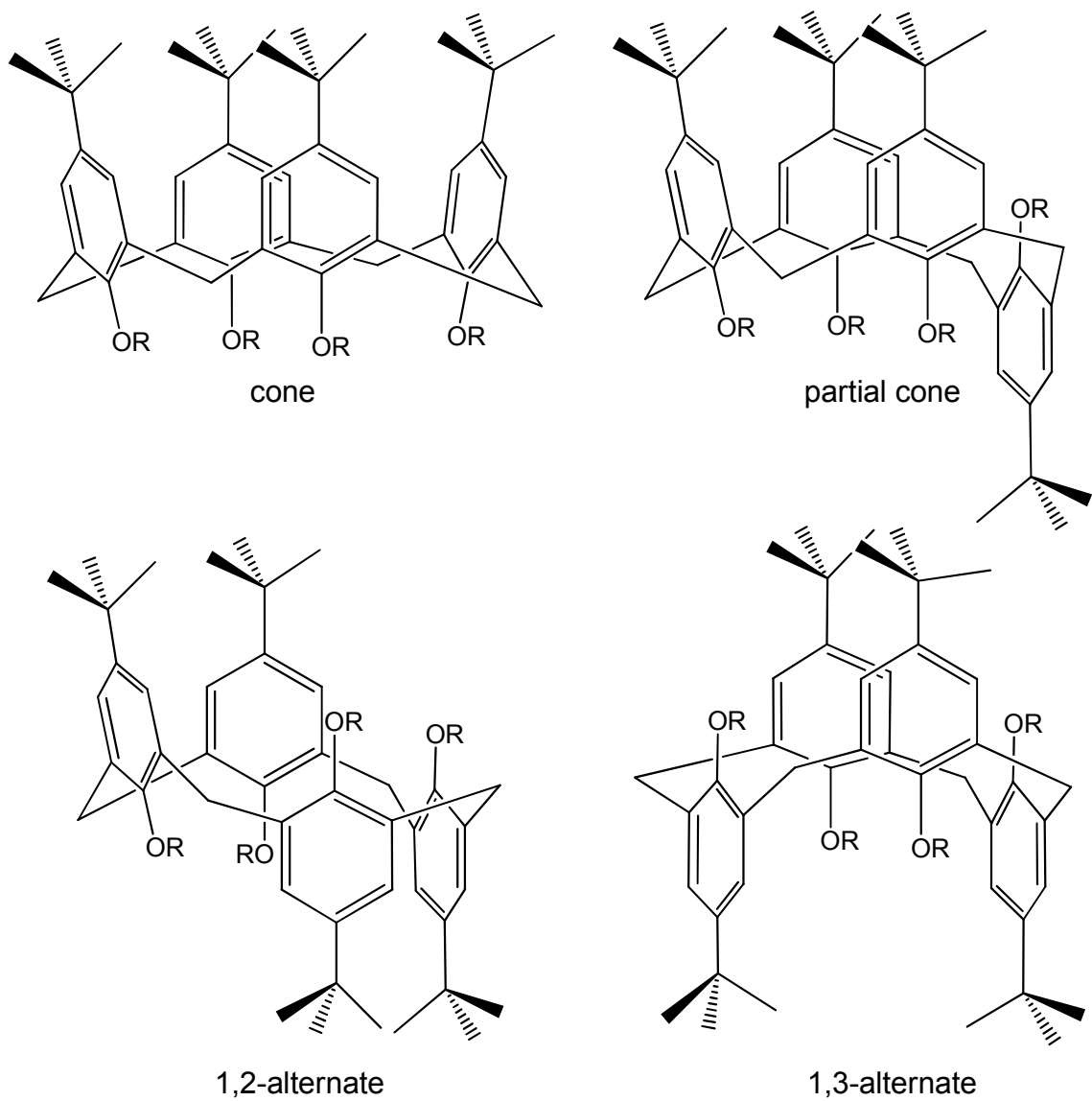


**Figure 1.5** Conformations observed for calix[4]arene, including cone, partial cone, 1,2-alternate, and 1,3-alternate.

In 1944, Erich Ziegler and Alois Zinke proposed the structure of the cyclic tetramer from the reaction of *p*-*tert*-butylphenol with formaldehyde, which would today be described as calix[4]arene.<sup>86-88</sup> They had also reported the synthetic procedure for this compound three years earlier in 1941, although they did not propose the structure at that time.<sup>88,89</sup>

The Petrolite Corporation specialized in preparing demulsifiers for separating crude oil.<sup>82</sup> One of their products, based on the condensation of *p-tert*-butylphenol with formaldehyde, followed by treatment with ethylene oxide, had been causing problems as an insoluble sludge had been reported by customers to be forming from this demulsifier. Researchers at the company, led by John Munch, found that refluxing paraformaldehyde with *p*-alkylphenols (such as *p*-octylphenol) in basic solution yielded clear, insoluble crystals.<sup>82,90</sup> C. David Gutsche, who had an interest in enzyme mimics and was then a professor at Washington University, was also a consultant with the Petrolite Corporation.<sup>78,91</sup> While early researchers believed that calixarenes existed mainly as tetramers, Gutsche had developed a reliable method to isolate the tetramer, hexamer, and octamer calixarenes.<sup>79,92</sup> In addition, Gutsche recognized the potential for calixarenes to behave as molecular containers and enzyme mimics.

The upper and lower rims of calixarenes, as well as the bridging group that connects the aromatic rings of the macrocycle can be modified, making the calixarenes one of the more versatile families of supramolecular hosts. The *tert*-butyl group normally observed on the upper rim can be replaced by treatment with aluminum trichloride and subsequently replaced with other functional groups.

In addition, the OH group of the lower rim can readily be replaced with esters or ethers.<sup>79</sup> While the solubility of calixarenes in water as well as many organic solvents is generally low,<sup>78</sup> esterification and etherification of the calixarenes, or addition of carboxylate or sulfonate groups has often improved their solubility.<sup>93</sup> Usually, the lower-rim substituents are connected to only one part of the calixarene host, but they sometimes are bridging substituents, connecting one lower-rim position with another. A good example of this is when the lower rim has been substituted with ethylene glycol moieties to some or all of the lower rim positions, so that a crown ether moiety can be fused with the calixarene.<sup>79,93,94</sup> The presence of a bridging group tends to “lock” the conformation of the calixarene, so that it becomes unable to change its conformation

once a bridging group is in place.<sup>78,93</sup> Some calixcrown complexes have shown a very high selectivity for the Cs<sup>+</sup> cation, and have attracted attention due to their potential ability to remove Cs<sup>+</sup> from radioactive waste.<sup>78,95,96</sup> These complexes have a tendency to bind more strongly in the 1,3-alternate conformation, as in this arrangement two of the aromatic rings are directed toward the cation binding positions, and could therefore enhance cation- $\pi$  interactions with the guest. In addition, when two crown linkers are present in the calix[4]crown in the 1,3-alternate conformation (so that the two crown moieties are facing opposite directions), it becomes possible for the host to bind to two Cs<sup>+</sup> cations, as shown in Figure 1.6.<sup>97</sup>

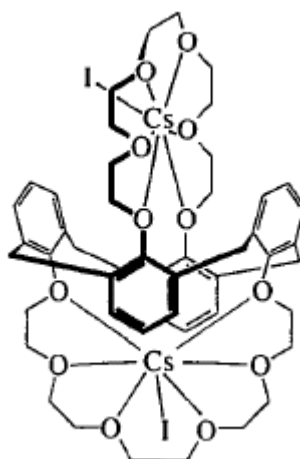


**Figure 1.6** Calix[4]biscrown in the 1,3-alternate conformation, binding two Cs<sup>+</sup> guests.<sup>97</sup> In this conformation two of the aromatic rings are also directed towards the cation.

The default linkers between the aromatic rings of calixarenes are methylene groups. However, calixarenes have been synthesized that contain a variety of linkers, including sulfur (referred to as *thiacalixarenes*), oxygen, and various other groups. Calixarenes with at least two CH<sub>2</sub> groups within one of the linker are referred to as *homocalixarenes*.<sup>98,99</sup>

Calixarenes often can bind to cations, due to the presence of the electron rich oxygen groups present in lower rim, as well as the aromatic groups in the structure, which can contribute toward cation- $\pi$  interactions.<sup>100</sup> Cation binding to unmodified calixarenes containing OH groups

mainly occurs due to deprotonation of the OH groups, so that the cations may bind through ion pairing.<sup>101,102</sup> Selective binding of calixarenes to cations was first observed by Izatt and coworkers, when they found that *p-tert*-butylcalix[*n*]arene (*n* = 4, 6, and 8) bound Cs<sup>+</sup> selectively over other alkali metals.<sup>101,103</sup> Of these, they found that the tetramer was the most selective for Cs<sup>+</sup>. They observed complexation primarily in basic solution, where the OH groups were readily deprotonated, rather than at lower pH.<sup>101</sup> The lower rim may be readily functionalized with functional groups including, but not limited to, esters, amides, ketones, and ethers, which can also be used to enhance cation binding.<sup>102</sup>

In addition, the hydrophobic pocket present in calixarenes can lend itself to binding of neutral guests, particularly when water-soluble derivatives of calixarenes are used.<sup>104,105</sup> In nonpolar solvents, binding to neutral guests is generally weak, and quite often the cavity is too small and too flexible (due to the various conformations) to bind strongly to a neutral guest.<sup>100</sup> In addition, the solvent molecules may compete with the guest for binding to the hydrophobic pocket.<sup>106</sup> If the cavity is rigid, it is possible to choose a solvent that is too large to fit into the cavity. If the cavity is not sufficiently rigid, it may change its conformation so that it will become capable of binding the solvent, thus losing capability to discriminate between the solvent and the guest.<sup>106</sup> A neutral guest tends to bind more favorably with the calixarene host if it has an acidic CH group that may allow it to be involved with CH- $\pi$  interactions with the host.<sup>107</sup> Cases have been observed where amines have been bound to calixarenes in acetonitrile solution.<sup>108,109</sup> It was proposed that this involved a two-step process, where a proton was transferred from one of the hydroxyl groups of the calixarene to the amine, thus forming an ammonium cation and an anionic calixarene. This ammonium guest is then able to bind through ion pairing.<sup>77,108,109</sup> Although calixarenes aren't readily soluble in water, some have been derivatized with ionic or hydrophilic functional groups to facilitate their solubility in water, and are able to bind guests due to the hydrophobic effect.<sup>100,106</sup>

An important member of the calixarene family are the *resorcarennes*, which are sometimes called *resorcinarenes* or *calixresorcarennes*.<sup>110</sup> In contrast to calixarenes, which are composed of phenol rings, the aromatic ring of resorcarennes contain two OH groups, which are on the upper rim when the resorcarene is in the cone conformation. In a similar manner to that of the calixarenes, the number of monomer units contained within the resorc[*n*]arene is represented by *n*. In the cone conformation, resorcarennes have wider and shallower cavities than calixarenes.<sup>100</sup> Both calix[4]arenes and resorc[4]arenes are most stable in the cone conformation due to intramolecular hydrogen bonding between the OH groups.<sup>100</sup>

Resorcarennes are synthesized by condensing resorcinol with aldehydes.<sup>78,91,111</sup> In contrast with calixarenes, which are condensed from phenols and formaldehyde, when formaldehyde is condensed with resorcinol, polymers are obtained in place of the macrocycle.<sup>91</sup> As a consequence of their condensation from aldehydes, the methylene groups bridging the aromatic rings are normally substituted with an R group whose composition is dependent on the type of aldehyde precursor used (Figure 1.7).<sup>91</sup> The presence of these substituents provides more variation in the conformations observed.

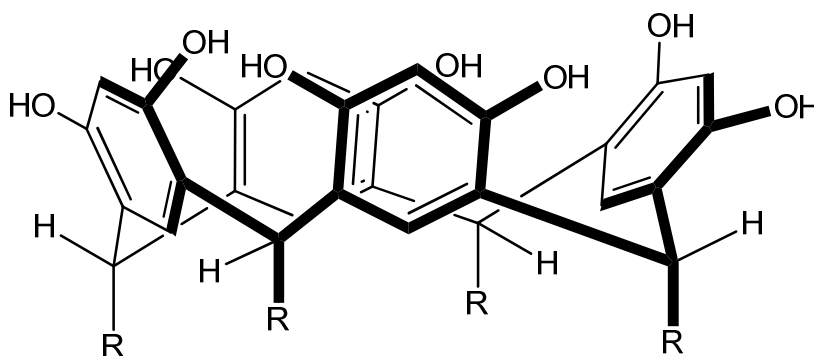


**Figure 1.7** A resorc[4]arene with its aromatic rings in the cone conformation.

The history of resorcarennes, like that of calixarenes, can also be linked with Baeyer's research in 1872,<sup>83</sup> as in his work he reported that condensation of benzaldehyde with resorcinol



provided a red product, that when heated gave crystals in addition to a red resin.<sup>83,112</sup> Twelve years later, Michael conducted further studies of the condensation between aldehydes and resorcinol, and proposed a macrocyclic product.<sup>113</sup> Decades later, Niederl and Vogel proposed a tetrameric macrocycle as the product, on the basis of elemental analysis.<sup>114</sup> The X-ray crystal structure was subsequently determined by Nilsson and coworkers.<sup>115,116</sup>

The main conformations observed for resorc[4]arenes based on the orientations of the aromatic rings in the macrocycle include cone, flattened cone (or boat), 1,2-alternate, 1,3-alternate, chair, and partial cone.<sup>117</sup> In addition, the orientation of the substituent on the bridging carbon may also vary, by either being in the axial (facing downward, or parallel to the cavity) or equatorial (facing outward from, and perpendicular to the cavity) positions, and this variation can also produce combinations of equatorial and axial substituents for a given macrocycle.<sup>91,117</sup>

As is the case for calixarenes, resorcarenes may also be readily derivatized. The OH groups on the aromatic groups of the resorcarenes can be alkylated in order to create additional bridges between the aromatic rings, making these macrocycles more rigid (enhancing the preorganization of the host).<sup>118</sup> In addition, the upper rim can be derivatized in order to provide a deeper pocket for the resorcarene. This is often done by adding more aromatic groups at the upper rim, thus providing another aromatic “layer” to the host.<sup>119,120</sup>

*Carcerands* are a cage-like family of molecules with an empty internal cavity capable of holding a guest.<sup>121,122</sup> When a guest is enclosed in the cavity these complexes are referred to as *carceplexes*, and it is not possible for a guest to escape a carceplex without breaking bonds of the host. A carcerand from which a guest may enter or escape without breaking bonds of the host is referred to as a *hemicarcerand*, while the resulting host-guest complex is called a *hemicarceplex*.<sup>121,122</sup> These are often, although not always, derivatives of resorcarenes, in which two resorcarenes are linked together through their upper rim, forming the cage. Carcerands were first proposed<sup>123</sup> and synthesized<sup>124,125</sup> by Donald J. Cram and coworkers. Cram was also very

active in studying highly preorganized spherand hosts and shared a Nobel prize with Charles Pedersen and Jean-Marie Lehn for their contributions to the field of supramolecular chemistry.

### 1.4.3 Porphyrin Hosts

Porphyrins and metalloporphyrins are widespread in biological systems, with iron porphyrin systems (called *haems*) present in heme proteins, and cytochrome P-450.<sup>126</sup> Porphyrins are a family of tetrapyrrole macrocycles whose parent compound is porphine, which has eleven double bonds.<sup>126,127</sup> A metalloporphyrin is obtained by replacing two pyrrole protons with a metal. Meanwhile, two protons can also be added to porphine to obtain the doubly charged diacid species. Porphyrins are often present in Nature in the form of protoporphyrin IX (Figure 1.8).

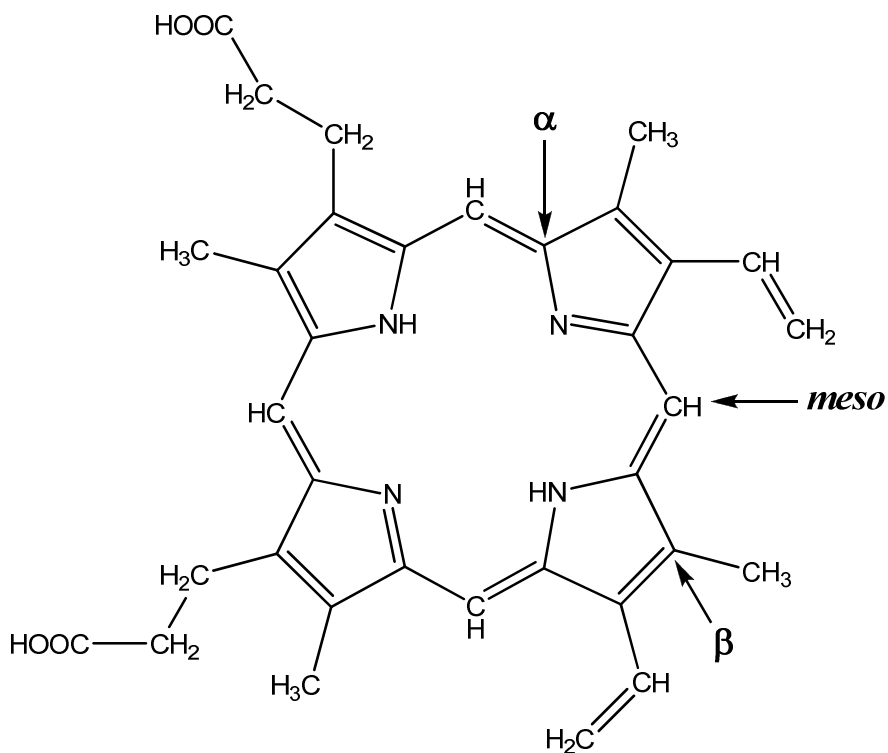


**Figure 1.8** Protoporphyrin IX, a form of porphyrin present in natural systems.<sup>127</sup>

The pyrroles are linked by a conjugated carbon, called the *meso* carbon, while the two  $\alpha$  carbons of each pyrrole rings are those closer to the interior of the macrocycle and directly attached to the *meso* carbons. The  $\beta$  carbons of the pyrrole are the two carbons facing the exterior of the cavity.

The tetrapyrrole structure of porphyrins was proposed as early as 1912 by Kuster,<sup>128</sup> and was synthesized in 1929 by Fischer and Zeile.<sup>126,129</sup> A significant amount of interest has been focused on the syntheses of expanded porphyrins, which are porphyrin analogues that contain more than four pyrrole rings.<sup>130-133</sup> The first example of which is called sapphyrin, due to its brilliant blue colour, which contains five pyrrole rings in the macrocycle.<sup>130-132</sup> Expanded porphyrins have been synthesized, with the number of pyrrole rings in the macrocycle ranging from less than four up to twenty four.<sup>132,134</sup>

Porphyrin analogues may have different arrangements of the pyrrole rings. The heteroatoms normally face the interior of the macrocycle, particularly if the porphyrin is substituted at the  $\beta$  carbons. However some expanded porphyrins, particularly those substituted at the *meso* carbons, can have a variety of arrangements of their pyrrole rings. Some expanded porphyrins contain one or more pyrrole rings that are inverted, with their heteroatom facing the exterior of the cavity. Other analogues also contain one or more groups of two pyrrole rings that are connected directly, lacking a *meso* carbon between them.

While porphyrins and their derivatives are often associated with binding to metals, owing to their roles in Nature, they have also have been observed to bind to other cations. An example of anion binding, such as fluoride, chloride, or bromide; has been observed for sapphyrin. The binding was found to be selectively in favour of fluoride over chloride and bromide anions, with binding constants of  $(9.6 \pm 2.0) \times 10^4 \text{ M}^{-1}$  for fluoride, approximately  $10^2 \text{ M}^{-1}$  for chloride, and less than  $10^2 \text{ M}^{-1}$  for bromide in methanol solution, showing approximately 1000-fold selectivity toward the fluoride anion.<sup>135</sup> While the fluoride anion was observed by X-ray crystallography to

sit in the plane of the sapphyrin host (Figure 1.9), an X-ray crystal structure of sapphyrin bound to two chloride anions showed them to be out of the plane of the cavity, suggesting that chloride and larger anions were too large to fit directly in the cavity. In addition to halides, binding has also been studied between sapphyrin and carboxylates and phosphates.<sup>136</sup> Compared to porphyrin, sapphyrin is more basic and more readily protonated, and thus available over a wider pH range as a host for anions.<sup>136</sup>

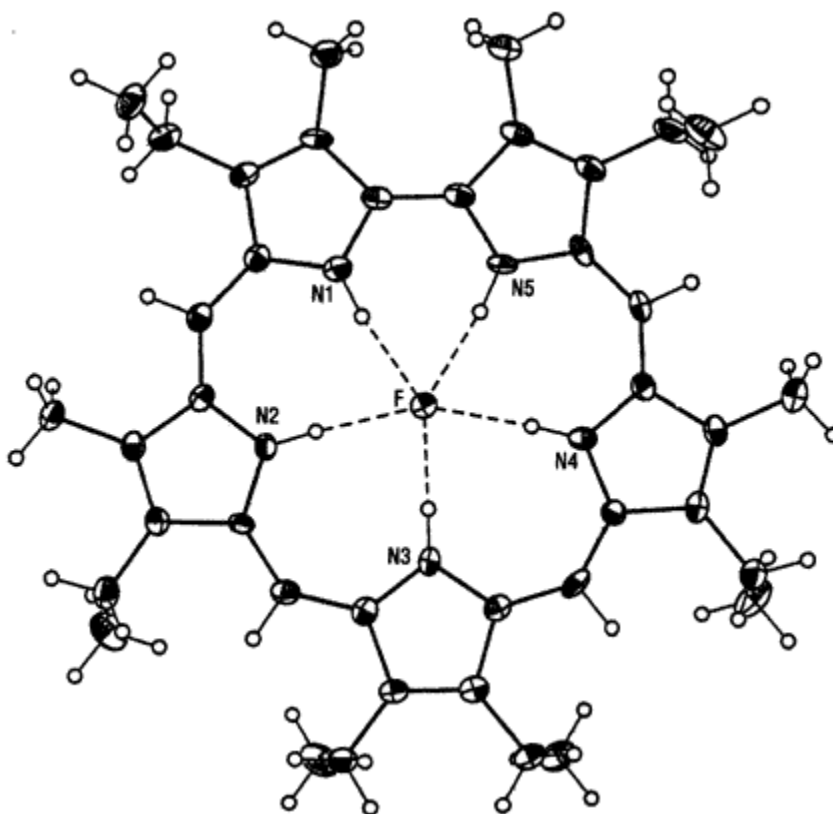


**Figure 1.9** X-ray crystal structure of sapphyrin bound to a fluoride anion. The anion is in the plane of the sapphyrin host.<sup>136</sup>

Significant interest lies in the study of synthetic porphyrin systems as heme models and enzyme mimics.<sup>137,138</sup> In addition, because these highly conjugated macrocycles readily absorb ultraviolet and visible light, and are fluorescent, which has attracted interest in porphyrins and their analogues for use as photosensitizers.<sup>139,140</sup>

#### 1.4.4 Cyclodextrins

Cyclodextrins (CDs) are a family of hosts made up of glucopyranose units, normally having six, seven, and eight units.<sup>141,142</sup> The name “cyclodextrin” comes from the word dextrose, which was an early name for glucose.<sup>143</sup> These cyclodextrins are abbreviated  $\alpha$ -,  $\beta$ -, and  $\gamma$ -CDs if they have six, seven, or eight carbohydrate units, respectively (Figure 1.10). Some examples of other, less common cyclodextrin homologues include  $\delta$ -CD (nine units),  $\epsilon$ -CD (ten units), and pre- $\alpha$ -CD (with five units), and cyclodextrins have been purified containing up to 35 glucopyranose units.<sup>141,143</sup> The overall shape of these hosts is a truncated cone, with their wider rim lined with secondary alcohols and their narrow rim lined with primary alcohols.<sup>142</sup> The cavity is lined with the oxygens that bridge the carbohydrates, and also hydrogen atoms. The oxygen atom, with its lone pairs, increases the electron density of the cavity and provides some Lewis base character to exist in the cavity.<sup>142</sup> The exterior and upper (wider) rim of the CD host is hydrophilic, while the interior and the lower (narrower) rim is hydrophobic in nature.<sup>144,145</sup>

The cavity sizes vary, with  $\alpha$ -CD having an interior diameter of 4.7 Å at the smaller portal and 5.3 Å at the larger portal, while for  $\beta$ -CD these values are 6.0 and 6.5 Å at the smaller and larger portals, respectively. With  $\gamma$ -CD, the portals are 7.5 and 8.3 Å, respectively, at the smaller and larger portals.<sup>142</sup> The heights of the  $\alpha$ -,  $\beta$ -, and  $\gamma$ -CDs are similar at 7.9 Å. These dimensions provide  $\alpha$ -,  $\beta$ -, and  $\gamma$ -CD with internal volumes of 174, 262, and 427 Å<sup>3</sup>, respectively.<sup>142</sup>

Hydrogen bonding plays a role with CDs, both in terms of its intramolecular structure, and with respect to intermolecular bonding. Within the macrocycle, the C2 OH group from one glucopyranose ring and the C3 OH group from the adjacent ring can form a hydrogen bond.<sup>142</sup> This intramolecular hydrogen bonding is more extensive for  $\beta$ -CD than for  $\alpha$ - and  $\gamma$ -CDs. One of

the units of  $\alpha$ -CD is distorted from the others, which reduces the hydrogen bonding, while the  $\gamma$ -CD is less rigid. This increased rigidity of  $\beta$ -CD is believed to be the reason why its solubility in water (1.85 g/100 mL) is significantly less than those of  $\alpha$ - or  $\gamma$ -CD (14.5 and 23.2 g/100 mL, respectively).<sup>142</sup> In addition to this intramolecular hydrogen bonding within the CD structure, there is also intermolecular hydrogen bonding between different cyclodextrins in the solid state,<sup>146</sup> with binding between the wider rims of two CDs, the wider rim of one CD and the narrow rim of another CD, or between the narrow rims of two CDs.<sup>143</sup> This intermolecular attraction between CDs contrasts with the intermolecular repulsion of the portal rims observed with cucurbiturils, as will be mentioned later in this chapter.

Cyclodextrins were first isolated in 1891 by Villiers, when he noted formation of a crystalline substance from a *Bacillus amylobacter* culture (although this culture likely also contained *Bacillus macerans* as impurities) grown on starch.<sup>144,147-149</sup> He found the elemental composition to be  $(C_6H_{10}O_5)_2 \cdot 3H_2O$ , and named this compound “cellulostine”, as it resisted acid hydrolysis, and did not have reducing properties. Interestingly, Villiers noted formation of two different crystalline species of this compound, which were likely  $\alpha$ - and  $\beta$ -CD.<sup>144</sup> The first inclusion chemistry involving these “cellulostines” was observed by Schardinger, when he noted that they formed complexes with iodine.<sup>144,150</sup> Schardinger was able to distinguish between what he called “ $\alpha$ -dextrin” and “ $\beta$ -dextrin”, by their complexation with iodine. The  $\alpha$ -dextrin/iodine complex was blue when wet and grey-green when dry, while the  $\beta$ -dextrin/iodine complex was red-brown, both when it was damp and dry.<sup>144,150</sup> In addition, Schardinger isolated *Bacillus macerans*, the bacteria that gives rise to formation of cyclodextrins, when it acts on starch.<sup>149,151</sup>

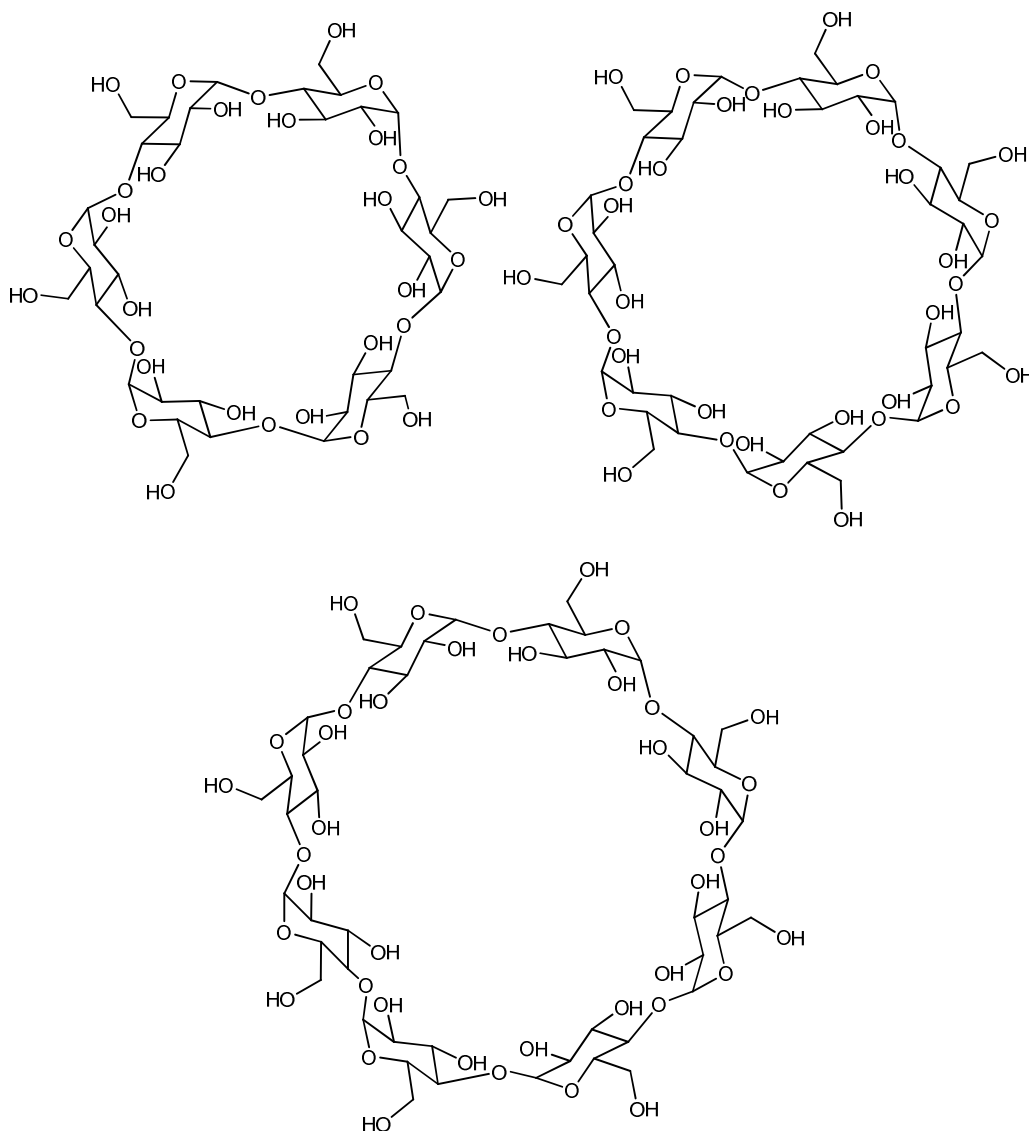


**Figure 1.10** Structures of  $\alpha$ -CD (top left),  $\beta$ -CD (top right), and  $\gamma$ -CD (bottom centre).

The hydrophobic effect is considered a major factor in the host-guest chemistry of CDs. When in aqueous solution, water molecules (with high enthalpy) present in the cavity are readily displaced by an appropriate nonpolar guest.<sup>143,144</sup> This is favorable enthalpically, as the water rejoins the aqueous solvent (with which it can interact more favourably), and also entropically (particularly when multiple water molecules are released in exchange for one guest).<sup>143</sup> In addition to this, other factors affecting the host-guest properties of CDs include hydrogen bonding

and electrostatic interactions due to the presence of OH groups. These OH groups may also be able to facilitate CD binding with more polar guests, through hydrogen bonds and electrostatic interactions.<sup>1,152</sup> Furthermore, the size of the cavity also is an important factor with host-guest chemistry of CDs.

One consequence of guest encapsulation that is often utilized, for example, with drug delivery systems, is that the solubility of the nonpolar guest is effectively increased in aqueous solution once it is complexed with CD.<sup>142,144</sup> Other effects of guest encapsulation are that the spectral features of the guest are changed, and also the reactivity of the guest is affected.<sup>142</sup> Often the reactivity of the guest decreases, but in some cases the guest's reactivity actually increases, so that the CD can act as an artificial enzyme.<sup>142</sup>

Because of the presence of OH groups within their structure, CDs are readily derivatized. In addition, the differences between these OH groups can be used to vary the derivatization so that specific OH groups are derivatized and not others. One motivation for derivatizing CDs is to improve their solubility. This is especially true for  $\beta$ -CD, which is the most popular CD homologue but is at the same time limited by relatively poor solubility.<sup>142</sup> Derivatization can enhance solubility of  $\beta$ -CD from 18 g/L to 500 g/L.<sup>142</sup> Another reason for synthesizing derivatives of CDs is to enhance their binding, so that binding to a particular guest may be improved. Methylated  $\beta$ -CD has enhanced binding to hydrophobic guests, such as cholesterol, which can be extracted from blood cell membranes through this binding.<sup>142</sup> Functional groups may also be attached, or the CDs may be attached to solid surfaces in order to improve their utility.<sup>142</sup>

Cyclodextrins are among the most commercially successful supramolecular hosts, and have a wide variety of applications involving drug delivery systems, foods, cosmetics, deodorizers, and catalysis.<sup>144,153</sup> Another factor that has helped their popularity is their relatively low cost. In 1970,  $\beta$ -CD was available as a fine chemical and cost \$2000 US per kilogram.<sup>144</sup>



Now, however, over 1000 tons are produced per year, and the cost has been reduced to several dollars per kilogram.<sup>144</sup>

## 1.5 Cucurbituril Hosts

The cucurbit[*n*]urils (CB[*n*]) are a family of macrocyclic hosts composed of *n* glycoluril units, where *n* can be = 5, 6, 7, 8, and 10. The name of these pumpkin-shaped hosts is derived from the Latin word, *cucurbitaceae*, which is the name of the plant family that includes pumpkins.<sup>154</sup> The cavity of the cucurbiturils hosts is nonpolar and is ideal for binding to hydrophobic guests. At the same time, the carbonyl-lined portals are electron rich and are suitable for binding to positively charged guests through electrostatic interactions (Figure 1.11).

The first synthesis of a cucurbituril was as early as 1905, when Behrend reported the formation of an insoluble polymer upon the condensation of glycoluril with formaldehyde in concentrated HCl.<sup>155</sup> The structure of this residue was unknown. Referred to as “Behrend’s polymer”, it was noted to be amorphous and had poor solubility in common solvents.<sup>154-156</sup> Behrend was able to obtain crystals of this compound after it was dissolved in hot (110 °C) concentrated sulfuric acid and subsequently diluted with cold water. The molecular formula was calculated to be C<sub>10</sub>H<sub>11</sub>N<sub>7</sub>O<sub>4</sub>•2H<sub>2</sub>O.<sup>155,156</sup> Interestingly, even at this early stage, Behrend had noted that this substance had an affinity toward a variety of compounds, such as KMnO<sub>4</sub>, AgNO<sub>3</sub>, H<sub>2</sub>PtCl<sub>6</sub>, NaAuCl<sub>4</sub>, Congo red, and methylene blue.<sup>154,155</sup>

It wasn’t until 1981 that the structure of Behrend’s polymer became known, when Mock and coworkers were able to fully characterize this compound, and obtain its crystal structure.<sup>156</sup> They found it to be a macrocycle, composed of glycoluril units held together with aminal linkages. Due to the general shape of this molecule, Mock named this compound cucurbituril, which is derived from the Latin word *cucurbitaceae*, for the pumpkin family.<sup>155,156</sup> As early as

his first characterization of cucurbituril, Mock immediately recognized its potential as a supramolecular host and, in his paper regarding cucurbituril, noted complexation with alkylammonium cations, based on NMR evidence such as the upfield shift of the guest's proton resonances observed when guests were in the cavity of the host.<sup>156</sup> He also suggested that the alkylammonium cations were involved in electrostatic interactions with the electron rich carbonyl-lined portals of cucurbituril.

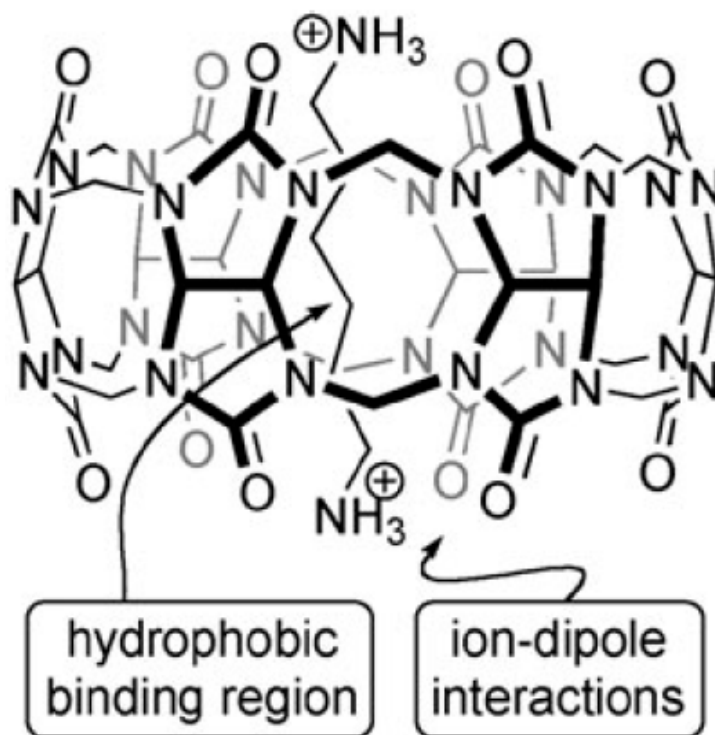


**Figure 1.11** CB[6] bound to 1,6-diammoniumhexane, with its hydrophobic cavity and electron rich portals shown.<sup>164</sup>

The cucurbituril characterized initially by Mock, and synthesized earlier by Behrend, was what is today called cucurbit[6]uril (CB[6]). When the synthetic methods of Behrend and Mock were utilized to synthesize CB[6], no other CB[*n*] homologues had been reported.<sup>157,158</sup> This situation differed from that encountered with calixarenes and cyclodextrins, where different homologues were available at an early stage of their discovery. More recently, however, Kimoon

Kim<sup>159</sup> and Anthony Day<sup>160</sup> have independently developed methods to separate different homologues of cucurbit[n]uril from the reaction mixture, so that currently homologues of cucurbituril exist with  $n = 5, 6, 7, 8,$  and  $10$ . Both Kim and Day used milder reaction conditions in their synthesis of the CB[n] homologues than those which were used by Mock and Behrend, such as lower temperatures and milder acid concentrations. Kim reported the use of 9 M sulfuric acid and reaction temperatures of 75-90 °C,<sup>159</sup> while Day used concentrated HCl and temperatures of 100 °C.<sup>160</sup> The isolation of these homologues has dramatically increased the popularity of cucurbiturils as hosts, as there is now a wider variety of cucurbituril cavity sizes available, so that a host may be chosen with a size that more appropriately matches that of a given guest. In addition, the cucurbiturils containing an odd number of glycoluril units, CB[5] and CB[7], have better solubility in water than those composed of even numbers of the monomer.<sup>161</sup> This improved solubility may be due to the decreased symmetry of the macrocycles bearing odd numbers of glycoluril monomers.

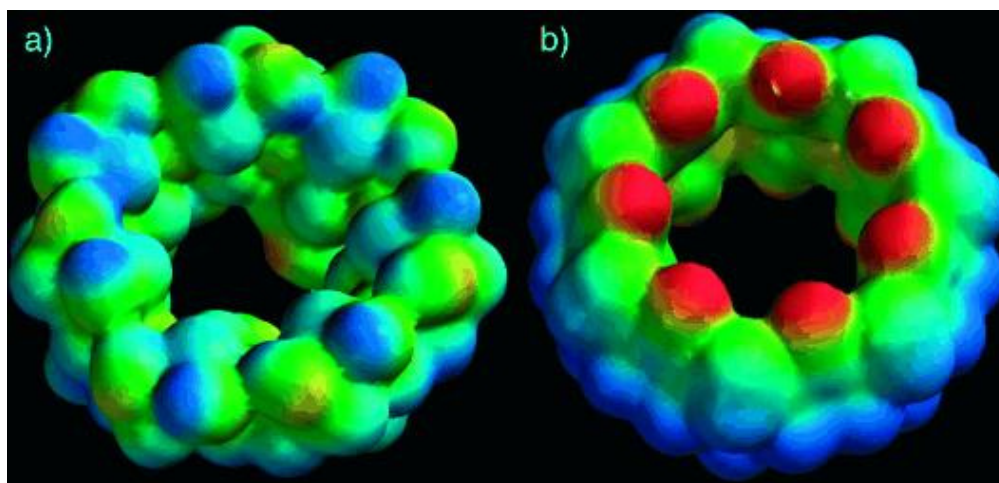


**Figure 1.12** Electrostatic potential maps of  $\beta$ -CD (a), and CB[7] (b). The red to blue range is -80 kcal/mol for red and 40 kcal/mol for blue.<sup>154</sup>

The cucurbiturils are often compared to cyclodextrins (Table 1.1), which are considered to be their closest relatives in terms of size and shape, and the fact that both are often studied in aqueous solution. While CDs have the shape of a tapered cylinder, with one opening being wider than the other, CB[*n*] are symmetrical, with both of their portals being the same size on each end of the host. Compared with  $\beta$ -CD, the electrostatic potential of the portals of CB[7] are more negative (Figure 1.12), so that CB[*n*] hosts tend to bind more readily to cationic guests, while  $\beta$ -CD favours binding to neutral and anionic guests.<sup>154</sup> CB[*n*] hosts are less readily soluble in water than the CD hosts. This is particularly true of CB[6] and CB[8], as their solubilities in water are 0.018 mM<sup>162</sup> and <0.01 mM,<sup>161</sup> respectively. On the other hand, as mentioned earlier, the solubilities of CB[5] and CB[7] are both in the range of 20 to 30 mM (with some variation depending on how hydrated the samples were),<sup>161</sup> which rivals that of  $\beta$ -CD, having a solubility of approximately 16 mM.<sup>144</sup> The CB[*n*] hosts are relatively rigid, and also thermally stable, resisting decomposition at temperatures reaching 420 °C for most members of the CB[*n*] family, while CB[7] decomposes at a slightly lower temperature of 370 °C.<sup>154,161</sup>

**Table 1.1** Cavity dimensions and aqueous solubilities of CB[*n*] and CD hosts.<sup>144,154,161,164</sup>

Host	Portal Diameter (Å)	Interior Cavity Diameter (Å)	Height (Å)	Cavity Volume (Å <sup>3</sup> )	Solubility in Water (mM)
CB[5]	2.4	4.4	9.1	82	20-30
CB[6]	3.9	5.8	9.1	164	0.018
CB[7]	5.4	7.3	9.1	279	20-30
CB[8]	6.9	8.8	9.1	479	<0.01
CB[10]	9.5-10.6	11.3-12.4	9.1	870	Not reported
$\alpha$ -CD	4.7	5.3	7.9	174	297
$\beta$ -CD	6.0	6.5	7.9	262	16
$\gamma$ -CD	7.5	8.3	7.9	427	293

As is the case for CD hosts, the height of the CB[*n*] hosts is the same, with all homologues having a height of 9.1 Å (Table 1.1).<sup>154,161</sup> The interior volumes of CB[6], CB[7],

and CB[8], being 164, 279, and 479 Å<sup>3</sup>, respectively,<sup>154,161</sup> are comparable to those of α-, β-, and γ-CD, which are 174, 262, and 427 Å<sup>3</sup>, respectively.<sup>144</sup> The interior cavities of CB[5], CB[6], CB[7], CB[8], and CB[10] are 4.4, 5.8, 7.3, 8.8, and 11.3-12.4 Å, respectively, at their widest points (the latter value was determined from the structure of CB[5]@CB[10]).<sup>154,161,163,164</sup> The portals are normally about 2 Å narrower than the cavity, with portal diameters of 2.4, 3.9, 5.4, 6.9, and 9.5-10.6 Å for CB[5], CB[6], CB[7], CB[8], and CB[10], respectively.<sup>154,161,164</sup> This smaller portal size relative to the cavity can provide steric barriers towards complexation and decomplexation with guests, resulting in constrictive binding.<sup>154,165</sup>

As described above, a variety of CB[*n*] homologues have been synthesized, with *n* = 5-8 and 10. The following pages will briefly describe these homologues, their supramolecular properties, and their derivatives.

### 1.5.1 Cucurbit[6]uril (CB[6])

The cavity size of CB[6] is approximately the same as that of α-CD, and both hosts have hydrophobic cavities. However, CB[6] differs from α-CD and many other hosts, such as crown ethers, for example, in that it is more rigid.<sup>166</sup> As a result, binding involving CB[6] can be more selective compared to binding involving the more flexible α-CD host.

Since CB[6] was the first member of the CB[*n*] family to be discovered, it was therefore the first to be studied as a supramolecular host, and has been studied since the 1980s. The earliest series of organic guests bound with CB[6] have included alkylammonium and alkanediammonium salts, which were studied by Mock and Shih.<sup>167,168</sup> The chain lengths of these guests were varied, and in the case of the alkylammonium guests, the binding constant was the highest (10<sup>5</sup> M<sup>-1</sup>) when the guest was *n*-butylammonium, while for the alkanediammonium guests [NH<sub>3</sub>(CH<sub>2</sub>)<sub>*n*</sub>NH<sub>3</sub>]<sup>2+</sup>, the binding was strongest for guests with *n* = 6 (2.8 x 10<sup>6</sup> M<sup>-1</sup>), followed

closely by those with  $n = 5$  ( $2.4 \times 10^6 \text{ M}^{-1}$ ).<sup>167,168</sup> These particular chain lengths provided a complementary fit between CB[6] and the guests, as they allowed the two ammonium groups to be aligned with the electron rich portals, while the aliphatic linker fit into the CB[6] cavity. Because of the low solubility of CB[6] in water, these binding constants were obtained in a 1:1 (v/v) solution of water and 85% formic acid.

The hydrophobic alkyl groups of these ammonium guests tend to favour the CB[6] cavity, and display upfield shifts in their proton NMR resonances upon complexation. Meanwhile, the protonated ammonium component of the guests are situated at the electron rich portals of the CB[6] host, where they can bind through electrostatic interactions. Further evidence of this was observed by Freeman via X-ray crystallography for the binding between CB[6] and *p*-xylylenediammonium chloride (Figure 1.13), showing the ammonium groups located at the portals, and the hydrophobic linker in the cavity.<sup>169,170</sup>

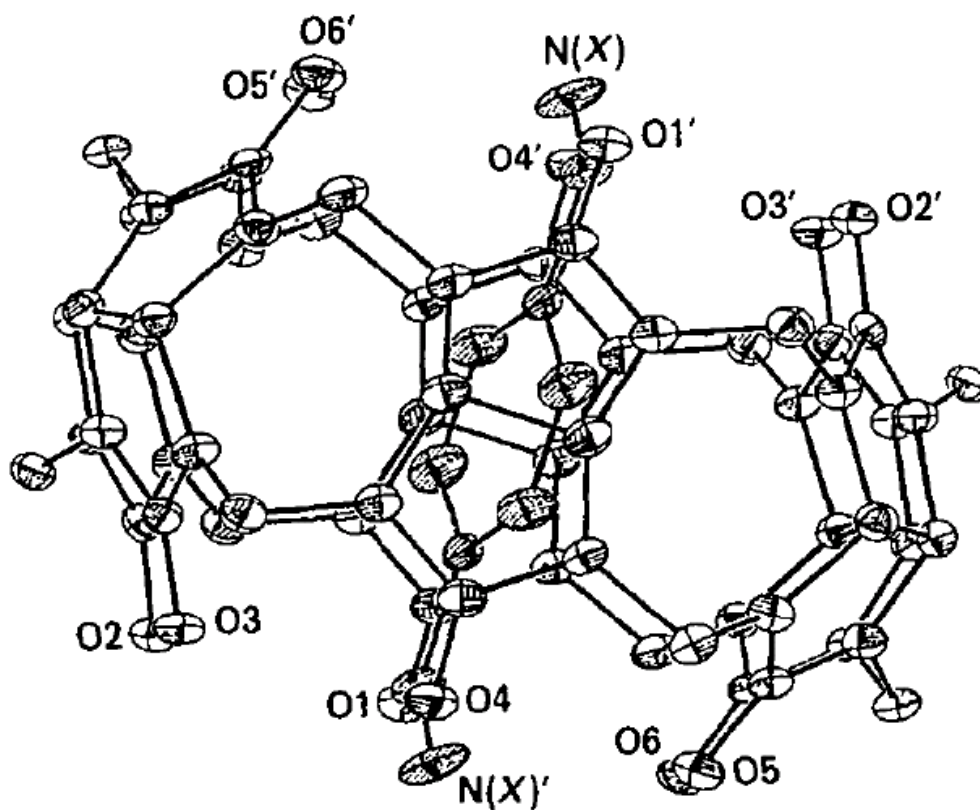


**Figure 1.13** X-ray crystal structure of *p*-xylylenediammonium chloride encapsulated by CB[6].<sup>169</sup> The ammonium cations are near the portals, while the hydrophobic linker is in the cavity.

Although the van der Waals dimensions of benzene are larger than the interior of CB[6], it is possible to form host-guest complexes between CB[6] and aromatic guests, although if the ring is disubstituted, the substituents must be in the *para* arrangement, while *ortho* or *meta* disubstituted aromatic rings are unable to bind to CB[6].<sup>166</sup> Benzene-containing amines are near the maximum size of guests that bind to CB[6]. Meanwhile, the more bulky cyclohexane cannot fit into the CB[6] cavity.<sup>166</sup> Also, the binding constants are generally lower for CB[6] with aromatic amines than those between CB[6] with aliphatic amines.<sup>158</sup> The crystal structure of CB[6] bound to the *p*-xylylenediammonium dication reveals a distortion of the CB[6] host, in that its diameter is reduced by 40 pm compared to the unbound CB[6] host in directions perpendicular

to the benzene ring, while the diameter is increased in the plane of the ring in order to accommodate the ring.<sup>158,169</sup> These distortions were observed despite the relative rigidity of the CB[6] host. The weaker CB[6] binding to aromatic guests has been attributed to an energy compensation between the favourable binding between the host and guest against the energy required to distort the CB[6] host in order to encapsulate the guest.<sup>158,168</sup>

In accordance with the apolar cavity present in CB[6], the polarity of the guests affects their binding strength, as demonstrated by Mock and coworkers. As a result, guests containing a thioether in their structure generally bind more strongly to CB[6] than their more polar ether analogues do.<sup>166</sup> At the same time, these thioether guests also bind more weakly than their analogues that contain a methylene group in place of the sulfur. As an example, 1,5-diammoniumpentane binds to CB[6] with a binding constant of  $2.4 \times 10^6 \text{ M}^{-1}$ , but when the central methylene group is replaced with a sulfur atom, the binding constant drops to  $4.2 \times 10^5 \text{ M}^{-1}$ , which subsequently decreases to  $5.3 \times 10^3 \text{ M}^{-1}$  when the sulfur is replaced by oxygen.<sup>168</sup>

The complexation of CB[6] with organic dyes has also been of interest, as studied by Buschmann and Schollmeyer.<sup>171,172</sup> They found that CB[6] binds to the dye phenol blue with a binding constant of  $92.8 \text{ M}^{-1}$ , while the same dye is complexed to  $\beta$ -CD with a binding constant of  $1.3 \text{ M}^{-1}$ , in water at 25 °C.<sup>171</sup> Once encapsulated in a supramolecular host, the guests are relatively isolated from the surrounding media, and can be protected from decomposition. This was the case for phenol blue, as it was observed that the rate of decomposition of phenol blue to *p*-benzoquinone was reduced by approximately 100-fold in the presence of CB[6] (from a rate constant of  $3.51 \times 10^{-3} \text{ M}^{-1}\text{s}^{-1}$  to  $2.66 \times 10^{-5} \text{ M}^{-1}\text{s}^{-1}$ ), while it was reduced 2-fold in the presence of  $\beta$ -CD ( $1.60 \times 10^{-3} \text{ M}^{-1}\text{s}^{-1}$ ).<sup>166</sup> No significant change was observed in the presence of  $\alpha$ - or  $\gamma$ -CD.



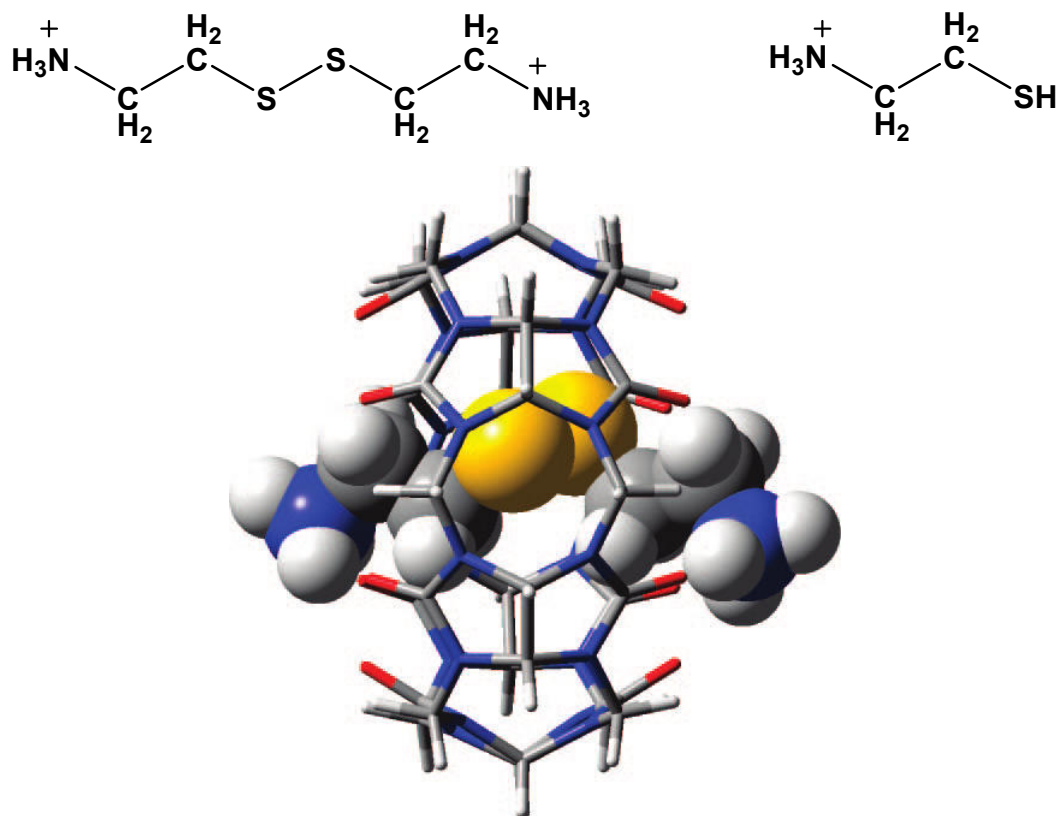


**Figure 1.14** Cystamine (top left) and cysteamine (top right) and an energy-minimized (B3LYP/3-21G) structure of the complex between CB[6] and cystamine (above), determined by Kaifer and coworkers.<sup>173</sup>

More recently, Kaifer and coworkers have studied the binding of guests with thiol and disulfide moieties, and have also looked at the effect of complexation on their reactivity.<sup>173</sup> In the case of cystamine, based on  $^1\text{H}$  NMR titrations and a DFT model (B3LYP/3-21G), they found that CB[6] binds to cystamine such that the central disulfide bridge is encapsulated in the middle of the CB[6] cavity (Figure 1.14).<sup>173</sup> When they explored the stability of cystamine in the absence of CB[6], they observed that complete reductive cleavage of the disulfide bridge in the presence of excess dithiothreitol, to produce cysteamine, occurred in aqueous solution at 25 °C within one hour. When one equivalent of CB[6] was also present, no formation of cysteamine was observed after fifty hours.<sup>173</sup> As the thiol-containing cysteamine can also be oxidized to produce cystamine, Kaifer and coworkers looked at the effect of the presence of CB[6] on the

oxidation of cysteamine. It was found that without the presence of CB[6], the oxidation of cysteamine to produce cystamine was complete in seven hours when FeCl<sub>3</sub> was used as the oxidizing agent. Under the same conditions, but with presence of CB[6], no oxidation was detected for twenty four hours, suggesting that the thiol group of cysteamine was protected by CB[6].<sup>173</sup>

Rotaxanes containing CB[6] were reported by Kim and coworkers in 1996.<sup>174</sup> Spermine was threaded through CB[6] and both ends of the guest were subsequently capped with 2,4-dinitrophenyl groups, which are sufficiently bulky to trap the CB[6], thus forming the rotaxane of CB[6]. The 2,4-dinitrophenyl groups could be replaced with carbamate groups, in which case a pseudorotaxane was observed. In this example, the CB[6] did not move along the spermine thread because its carbonyl portals interacted strongly with the protonated amines of the guest.

In some rotaxanes and pseudorotaxanes, however, the CB[6] is capable of migrating between different positions within the thread, and its binding position may be controlled by external factors, such as pH. As early as 1990, Mock and Pierpont<sup>175</sup> observed that when CB[6] formed a [2]pseudorotaxane with [PhNH<sub>2</sub>(CH<sub>2</sub>)<sub>6</sub>NH<sub>2</sub>(CH<sub>2</sub>)<sub>4</sub>NH<sub>3</sub>]<sup>3+</sup>, that when all of the guest's nitrogens were fully protonated, the CB[6] host would preferentially bind so that the hexyl linker was encapsulated within its hydrophobic cavity. This behaviour is consistent with what Mock had discovered earlier, that CB[6] tended to favour dialkylammonium guests containing a hexyl linker.<sup>167,168</sup> However, once the aniline nitrogen became deprotonated, the upfield shifts of the guest proton resonances revealed that the CB[6] had migrated so that the butyl group had then become encapsulated by the cavity. They also noted that the pK<sub>a</sub> value of that aniline nitrogen had shifted from 4.69 to 6.73 in the presence of CB[6].<sup>175</sup> This migration of CB[6] from the hexyl to the butyl linker, depending on pH, allowed the system to act as a pH-activated molecular switch.

While most of the research involving CB[6] has involved binding in solution, more recently Dearden and coworkers have explored binding between CB[6] and ammonium-containing guests in the gas phase through mass spectrometry.<sup>176-178</sup> While the optimum chain length of a dialkylammonium guest in solution is the hexyl linker, Dearden and coworkers found that the optimum length of the guest in the gas phase is the butyl linker.<sup>177</sup> They postulated that in solution phase, the charge of the ammonium centre may be stabilized by the solvent so that it is favourable for the ammonium guests to extend beyond the portals of the CB[6] host. However, in the gas phase, since solvent is not present, the optimum length of the dialkylammonium guests is reduced to the butyl spacer. When they carried out computational studies (based on HF/6-31G\* level of theory, and generally representative of solvent-free conditions) of the binding between dialkylammonium guests with various chain lengths and CB[6], they found that the optimum geometry match between the dialkylammonium guests and the CB[6] cage occurred when the guests had butyl and pentyl linkers.<sup>177</sup> Dearden and coworkers also calculated the energies of the dissociation process  $[H_3N^+(CH_2)_nNH_3^+]@CB[6] \rightarrow H_2N(CH_2)_nNH_3^+ + CB[6]H^+$ , and found that these dissociation energies were highest when  $n = 5$ , suggesting that optimum binding between the CB[6] and guest occurred with this chain length.

Very recently, Dearden's group has explored the binding of CB[6] with *ortho*-, *meta*-, and *para*-phenylenediamine isomers in the gas phase, using computational studies and mass spectrometry.<sup>178</sup> Through computational studies of the doubly charged complex  $[(1,4\text{-phenylenediamine} + 2H)@CB[6]]^{2+}$  using HF/6-31G\* models, Dearden and coworkers compared external and internal binding with CB[6] for the three isomers of phenylenediamine. They found that for internal binding, the complex between CB[6] and 1,4-phenylenediamine was of the lowest energy (indicating that binding was more favourable with this isomer), while that of 1,2-phenylenediamine was of highest energy (thus being the least favoured). Meanwhile, with the computational model for external binding between CB[6] and these isomers, the external complex

with 1,3-phenylenediamine was of the lowest energy and the complex between 1,4-phenylenediamine was of the highest energy. The apparent observation of internal binding of the *para* isomer and external binding of the *ortho* and *meta* isomers parallels observations made earlier by Mock and Shih<sup>158,168</sup> in the solution phase, where only disubstituted aromatics in the *para* arrangement were observed to form complexes with CB[6].

In addition to binding to organic guests, CB[6] has also been noted to bind to various alkali, and alkaline earth metals.<sup>179-182</sup> The metal ions Na<sup>+</sup>, K<sup>+</sup>, Rb<sup>+</sup>, Cs<sup>+</sup>, Ca<sup>2+</sup>, in addition to the H<sup>+</sup> and NH<sub>4</sub><sup>+</sup> cations, were found to bind to CB[6] with binding constants that were two to three orders of magnitude greater than to 18-crown-6,<sup>179</sup> and, with the exception of H<sup>+</sup>, comparable in order of magnitude to their binding to cryptand [2.2.2].<sup>179</sup> Despite the closer size match between these cations and 18-crown-6, CB[6] is more rigid and preorganized for binding. In addition, the donor oxygens of CB[6] are stronger electron donors than those of 18-crown-6.<sup>179,183</sup>

Although the solubility of CB[6] is poor in aqueous solutions, the presence of alkali metals in solution tends to improve its solubility significantly.<sup>179,180</sup> Kim and coworkers have found that it is possible to bind CB[6] with an organic guest, and also cap either one or both portals with alkali cations such as sodium<sup>181</sup> or cesium.<sup>182</sup> Neutral organic guests such as diethyl ether were encapsulated in the cavity in the presence of 0.2 M Na<sub>2</sub>SO<sub>4</sub>, and in both cases X-ray crystal structures were obtained. For these complexes, the organic guest was visible in the cavity of the CB[6], while each portal had two sodium ions coordinated to it. In addition, the sodium cations were bridged by water molecules, thus further covering the lids of the portals. Kim and coworkers observed that when guests such as THF, furan, benzene, and cyclopentanone were bound to sodium-capped CB[6], the signals for the bound organic guest would disappear when they lowered the pH, suggesting that as the portals became protonated, the sodium cations and organic guests were released from the CB[6]. However, this process was apparently reversible, as when the pH was raised again, the signals for the bound organic guest returned.<sup>181</sup> When

cesium cations were used as caps in place of sodium, the behaviour differed somewhat. When Kim obtained an X-ray crystal structure of the CB[6] complex containing an ethanol guest and capped by  $\text{Cs}^+$ , they found that only one cesium cation was present for each portal, and the larger cation was bound closer to the CB[6] than the sodium cations were in their other crystal structure, so that it effectively reduced the size of the cavity. When the slightly larger THF guest was bound in the cavity in place of ethanol, a cesium cation was bound to only one of the portals, effectively forming a “bowl” in place of a “lidded barrel”.<sup>182</sup> In the case of the sodium-capped system, the THF guest that was located near the centre of the cavity had its oxygen atom pointed toward the sodium cations (Figure 1.15), but was too far away from the sodiums to coordinate with them.<sup>181</sup> With the cesium-capped system, however, the oxygen of the THF guest was coordinated to the cesium cation.<sup>182</sup> As reported by Nau and coworkers, the presence and concentration of alkali ions can have important effects on the binding constants of organic guests with CB[6], as well as their complexation rate.<sup>184</sup>

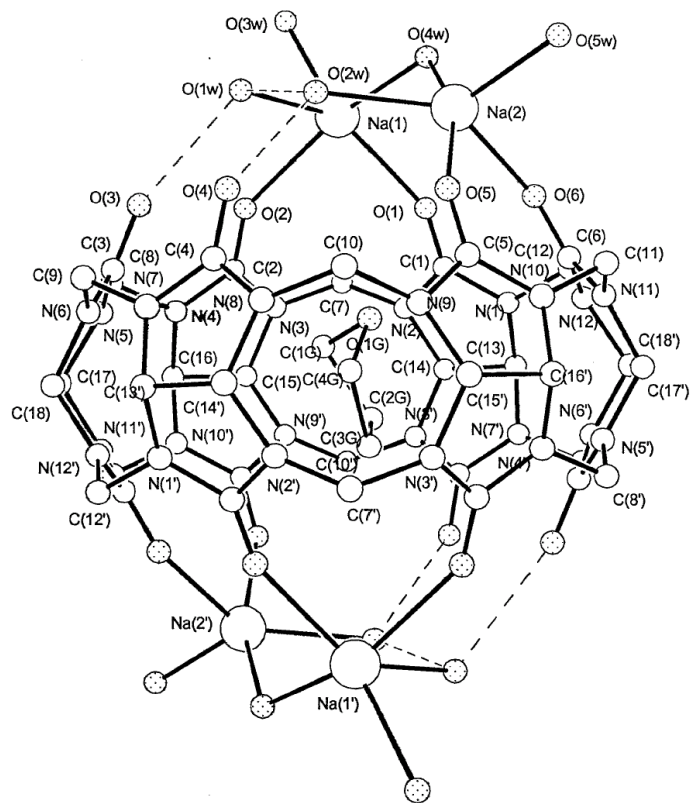


**Figure 1.15** X-ray crystal structure of THF encapsulated within CB[6], whose portals are capped by two sodium atoms.<sup>181</sup>

Complexes have also been reported between CB[6] and guests composed of main group elements,<sup>185</sup> transition metals,<sup>186-192</sup> and lanthanides,<sup>193-195</sup> with leading research in this area being carried out by Fedin, Gerasko, and their coworkers.<sup>170</sup> While alkali metals have been observed to coordinate directly with the portals of CB[6], often the heavier metal-containing complexes, particularly those with aqua ligands, tend to associate with the CB[6] portals indirectly through hydrogen bonding between their aqua ligands and the CB[6] carbonyls, as opposed to interacting through the core metal itself, so that the CB[6] acts as an outer sphere ligand.<sup>170</sup> The water ligands of these metal complexes have increased acidity, due to the positive charge of their coordinated metal centre, so that they can act more readily as proton donors for hydrogen bonding, with the carbonyl portals of CB[6] acting as the hydrogen acceptor.<sup>170</sup> When metal

cluster complexes are utilized, they have been observed to become sandwiched between two CB[6] hosts, and this has also been extended so that metal-CB[6] networks can be prepared.<sup>170,187,195</sup> Although direct coordination to heavy metals is unusual for CB[6], monodentate coordination has been observed between uranyl ions and CB[6] (as well as CB[7] and CB[8]), where the cation is bound directly to one CB portal, and its remaining coordination sphere is filled by oxo and aqua ligands.<sup>194</sup> Complexation of CB[6] has also been observed with inert gases, particularly xenon.<sup>196,197</sup> The hydrophobic xenon guest is believed to become encapsulated primarily in the CB[6] cavity, in contrast to the charged metals, which primarily bind externally.

### 1.5.2 Cucurbit[5]uril (CB[5])

CB[5] is the smallest member of the CB[*n*] family, and was isolated independently by Kim<sup>159</sup> and Day.<sup>160</sup> Prior to this, a derivative of CB[5], decamethylcucurbit[5]uril, was synthesized and characterized in 1992 by Stoddart and coworkers.<sup>198</sup> Similar to CB[7], CB[5] has improved solubility in water over its homologues with even numbers of glycoluril units.<sup>161</sup>

A significant amount of attention has been given to binding of metals by CB[5].<sup>199,200</sup> In contrast to heavier metal binding observed for CB[6], where the metal was often bound via hydrogen bonds through the metal's ligands, the smaller CB[5] has a greater tendency to coordinate directly to heavier metals such as cadmium, lanthanides and uranium ions through its carbonyl portals,<sup>199-202</sup> although the formation of outer-sphere systems between metal complexes have also been observed.<sup>200,201</sup> A recent example of this was observed by Thuery, with his work involving complexation of uranyl-organic frameworks with CB[*n*] employing X-ray crystallography.<sup>194,200</sup> While he observed up to one direct coordination between each uranyl cation and one portal carbonyl for systems involving CB[6], CB[7], and CB[8], Thuery observed

systems in which all five carbonyl groups on a rim of CB[5] were coordinated to a uranyl cation. The uranyl cation was perpendicular to the plane of the CB[5] portal, so that the binding was internal (although in the plane in the portal, and not in the hydrophobic cavity itself),<sup>200</sup> while only external binding was observed for the other CB[*n*] homologues.<sup>194</sup> Binding between CB[5] and the uranyl cation was to one portal, although addition of potassium or cesium cations to the system provided complexes in which one portal was bound to the uranyl cation, and the other portal was bound to potassium or cesium.<sup>200</sup>

Although common guests of cucurbiturils are usually cationic or neutral, CB[5] has been observed to bind to anionic guests, most notably the chloride anion.<sup>199,202-206</sup> This was initially observed by Day and coworkers in the CB[5] cavity, which itself was encapsulated by the larger CB[10] macrocycle (this system being referred to as CB[5]@CB[10]), by X-ray crystallography.<sup>203</sup> Chloride binding has also been observed for CB[5] in the absence of CB[10].<sup>202-205</sup> Normally, the chloride binding to CB[5] also involves the presence of metal cations, with the metals coordinated to one or both portals and the chloride anion located in the cavity and coordinated to the metal. The presence of a cationic metal coordinated to one or both of the portals appears to be a major driving force for chloride encapsulation, as the chloride anion becomes attracted to the CB[5] cavity due to the availability of electrostatic interactions with the coordinated cations.<sup>202,204,205</sup> It has been observed that in the absence of lanthanide ions, CB[5] will selectively bind to the nitrate anion over the chloride anion, with this preference being reversed in the presence of the La(III) cations.<sup>199</sup> It has been speculated that since the nitrate anion has a lower charge density, it can fit more readily into the hydrophobic cavity of the CB[5] cavity than can the chloride anion. Meanwhile, when the portals are blocked by the cations, the smaller chloride could more readily enter the cavity than the nitrate anion, which is more hindered by the blocked portals.<sup>199</sup>



CB[5] can also bind to organic aliphatic (but not aromatic) guests.<sup>207</sup> When compared to decamethylcucurbit[5]uril, which has a similar cavity size as CB[5], but is more rigid, it was found that while CB[5] could bind guests such as 1,6-diammoniumhexane<sup>207</sup> and spermine<sup>208</sup> to form an inclusion guest (with the aliphatic group in the cavity), the more rigid decamethylcucurbit[5]uril was unable to form an inclusion complex with these aliphatic guests. A crystal structure of the *exclusion* complex (in which the guest was bound externally to the host) between 1,6-diammoniumhexane and CB[5] was obtained, where the alkyldiammonium guest was bound to the portals of the two CB[5] derivatives (one ammonium centre for each host), with the hexyl group bridging the two hosts.<sup>207</sup> Buschmann and coworkers noted that it was necessary to heat the solution in order to allow formation of aliphatic inclusion complexes between CB[5] and guests such as spermine,<sup>208</sup> and suggested that this may indicate that it was necessary for the relatively small portals of CB[5] to be distorted in order to allow the guest to become threaded through the macrocycle. Meanwhile, the more rigid decamethylcucurbit[5]uril derivative was unable to become distorted sufficiently allow threading of the aliphatic guests.<sup>208</sup> Very recently, binding of Thioflavin T (Figure 1.16) with CB[5] and CB[7] has been compared.<sup>209</sup> While CB[7] was observed to bind with Thioflavin T to form an inclusion complex, external binding was observed with the smaller CB[5] macrocycle.<sup>209</sup>

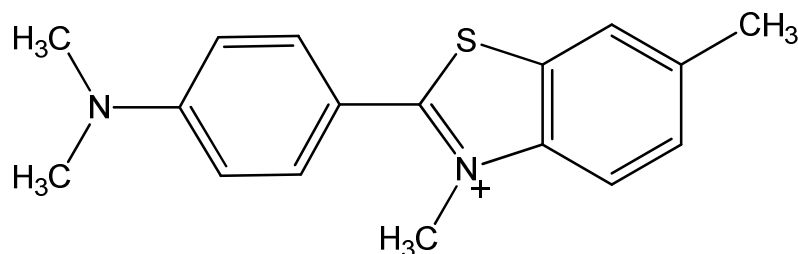


**Figure 1.16** Structure of Thioflavin T.

Neutral gas and solvent molecules have been observed to bind to decamethylcucurbit[5]uril.<sup>210,211,212</sup> Gases encapsulated by this host have included N<sub>2</sub>, O<sub>2</sub>, He,

Ne, Ar, H<sub>2</sub>, N<sub>2</sub>O, NO, CO, CO<sub>2</sub>, and acetylene, as well as solvent molecules such as acetonitrile, methanol, and water. Larger gases such as CH<sub>4</sub>, Kr, and Xe could not be absorbed by a solution of decamethylcucurbit[5]uril host at room temperature, although they did become absorbed upon heating at 80 °C. Decamethylcucurbit[5]uril readily binds with ammonium cations, with two ammonium ions at the portals<sup>211</sup> and peaks corresponding to complexes containing guests such as N<sub>2</sub>, O<sub>2</sub>, acetonitrile and methanol encapsulated by the macrocycle with both of its portals capped by ammonium ions were observed using electrospray mass spectrometry.<sup>210</sup> Miyahara and coworkers noted that while decamethylcucurbit[5]uril could absorb gas molecules with its portals capped by ammonium cations in aqueous solution, it was necessary to remove these ammonium cations in order to allow the host to absorb gases while it was in the solid state.<sup>211</sup> Once this was done, the macrocycle could readily absorb gas molecules such as N<sub>2</sub>O, NO, CO<sub>2</sub>, O<sub>2</sub>, and N<sub>2</sub>, which could in turn be released upon heating of the decamethylcucurbit[5]uril, suggesting potential for use of this host as a molecular sieve.<sup>211</sup>

### 1.5.3 Cucurbit[7]uril (CB[7])

Since its discovery, CB[7] has become the most popular CB[*n*] homologue, owing to its improved solubility over CB[6], as well as its cavity size, which can accommodate a wider variety of guests. Like the prototypical CB[6], CB[7] is capable of binding to both cationic guests through electrostatic interactions near its portals, as well as neutral guests due to its hydrophobic cavity. CB[7] has been independently observed by Kim<sup>213</sup> and Kaifer<sup>214</sup> to bind to the dicationic methylviologen guest with a binding constant of  $2.0 \times 10^5 \text{ M}^{-1}$ , while  $\beta$ -CD, which has a similar sized cavity that is only slightly smaller than that of CB[7], does not bind to the methylviologen dication appreciably.<sup>213</sup> After reduction of the methylviologen species from the doubly charged species to the singly charged guest, the binding constant is approximately halved

to  $8.5 \times 10^4 \text{ M}^{-1}$ . Further reduction of the methylviologen to its neutral form lead to a more dramatic decrease in the binding constant, to  $2.5 \times 10^2 \text{ M}^{-1}$ , with the neutral species having a *weaker* binding constant to CB[7] than to  $\beta$ -CD ( $1.4 \times 10^3 \text{ M}^{-1}$ ).<sup>213,215</sup> This decrease in binding affinity as the methylviologen is reduced reflects the importance of electrostatic interactions in strengthening the binding of the guest with the electron rich portals. This trend was the opposite of that observed for  $\beta$ -CD, which saw an increase in its binding affinity to methylviologen as its cationic charge was decreased.<sup>213,215</sup> In addition to studies involving methylviologen and its derivatives,<sup>213,214,216-218</sup> host-guest studies with CB[7] have been carried out with guests such as *cis*-stilbene,<sup>219</sup> *o*-carborane,<sup>220</sup> imidazole derivatives,<sup>221,222</sup> 2,3-diazabicyclo[2.2.2]oct-2-ene (DBO),<sup>223,224</sup> pyridinium and its substituted derivatives,<sup>225,226</sup> as well as adamantane and its derivatives.<sup>60</sup> Nau and coworkers have noted that complexation of DBO with CB[7] causes significant changes of the polarizability of DBO.<sup>224</sup> In fact the polarizability of DBO, while in the CB[7] cavity (Figure 1.17), was found to be even less than it is in the solvent perfluorohexane, and the photophysical properties of encapsulated DBO were more similar to those observed in the gas phase than in solution.<sup>224</sup> This reflects the significant differences in the environment of a host's cavity, such as CB[7], compared to the surrounding bulk solution.

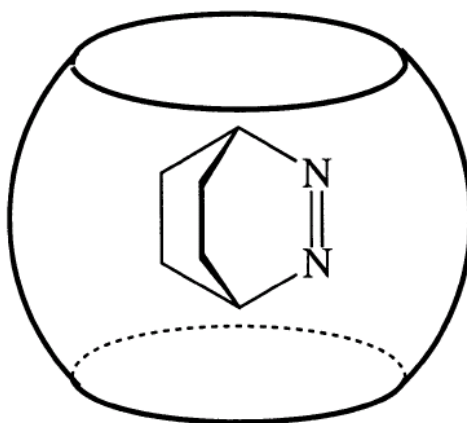


**Figure 1.17** 2,3-Diazabicyclo[2.2.2]oct-2-ene (DBO) encapsulated by CB[7].<sup>224</sup>

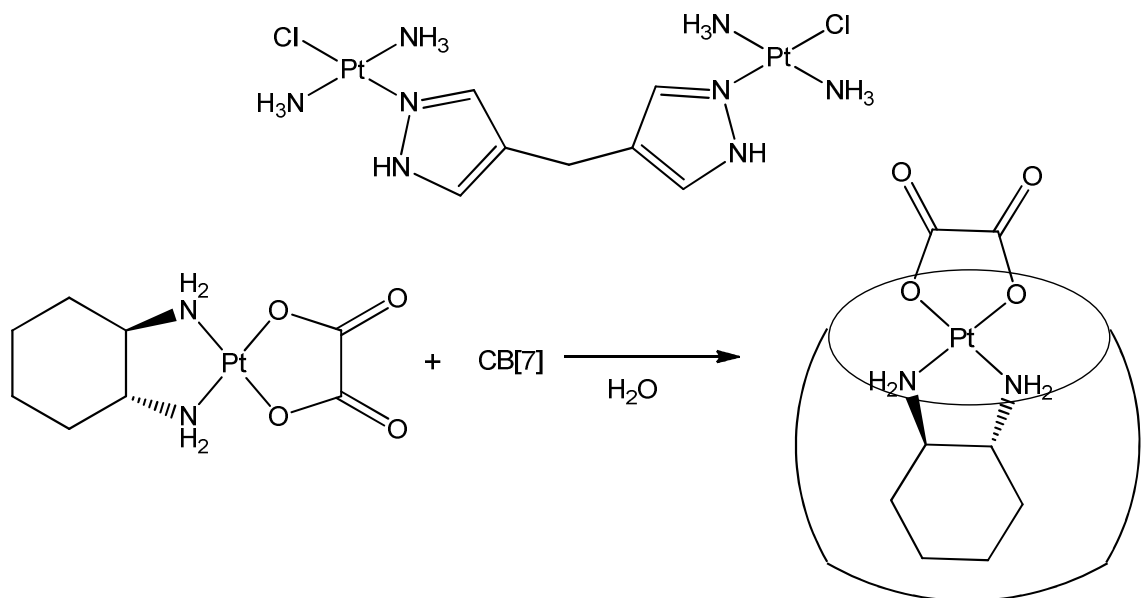


**Figure 1.18** *trans*-[PtCl(NH<sub>3</sub>)<sub>2</sub>]<sub>2</sub>μ-dzpm]<sup>2+</sup> (above),<sup>227</sup> and complexation between CB[7] and oxaliplatin (below).<sup>230</sup>

CB[7] has been observed to bind with a variety of platinum-based anti-cancer drugs (Figure 1.18), by Day and coworkers,<sup>227-229</sup> as well as Kim's group.<sup>230</sup> This attention has also been extended to metallocene-based anti-cancer drugs (containing titanocene and molybdocene),<sup>231</sup> as well as organic anti-tumor drugs such as albendazole<sup>232</sup> and camptothecin.<sup>233</sup> Complexation of camptothecin with CB[7] increased that drug's solubility by up to 70 times (and 8 times when bound to CB[8]),<sup>233</sup> while the aqueous solubility of albendazole was enhanced 2000-fold upon complexation with CB[7].<sup>232</sup> When CB[7] was complexed with the dinuclear platinum-containing drugs, the drug's stability was improved, in that they were more resistant to decomposition due to undesired side reactions, such as binding to thiol-containing proteins (such as glutathione, as well as the amino acids cysteine and methionine) which can cause the drug to decompose to non-active metabolites.<sup>227,228,234</sup> Kim and coworkers also observed that when the drug oxaliplatin was bound to CB[7], it was more resistant to decomposition by guanosine and methionine.<sup>230</sup> The stabilization of these drugs is believed to be at least partially due to the steric bulk introduced by the presence of the host,<sup>234</sup> preventing nucleophiles from approaching the

encapsulated drug. Day and coworkers observed that encapsulation of the dinuclear platinum drug *trans*-[PtCl(NH<sub>3</sub>)<sub>2</sub>]<sub>2</sub>μ-dzpm]<sup>2+</sup> by CB[7] was able to protect it from decomposition by guanosine, while not affecting its cytotoxicity or ability to bind to DNA.<sup>227,235</sup> However, Kim's group noted that complexation of oxaliplatin reduced its cytotoxicity.<sup>230,235</sup>

In addition to anti-cancer drugs, CB[7] has been observed to complex with other biologically relevant guests, such as the histamine H<sub>2</sub>-receptor antagonist ranitidine,<sup>236</sup> and also to the α-axial 5,6-dimethylbenzimidazole nucleotide base that binds to the cobalt(III) centre of vitamin B<sub>12</sub> and coenzyme B<sub>12</sub>. Encapsulation of this base by CB[7] has been found to have the capability to stabilize the base-off forms of vitamin B<sub>12</sub> and coenzyme B<sub>12</sub>.<sup>237</sup> CB[7] has been shown to discriminate between dipeptide sequences, by binding to one sequence over another with a very high selectivity.<sup>238</sup> For example, CB[7] binds to the dipeptide sequence Phe-Gly with an affinity constant of 3.0 x 10<sup>7</sup> M<sup>-1</sup>, while binding to the sequence Gly-Phe with a binding constant of 1300 M<sup>-1</sup> (relative affinity of 23 000). Also, there were relative affinities of 18 000 for the Tyr-Gly sequence (with a binding constant to CB[7] of 3.6 x 10<sup>6</sup> M<sup>-1</sup>) over the Gly-Tyr sequence (200 M<sup>-1</sup>), and of 2000 for the Trp-Gly (5.6 x 10<sup>5</sup> M<sup>-1</sup>) over the Gly-Trp dipeptide (280 M<sup>-1</sup>).<sup>238</sup>

Recently Nau and coworkers have developed a method for using CB[7] as part of a sensor in enzyme assays used to monitor amino acid decarboxylases, which can play important roles in tumor growth and inflammation.<sup>239,240</sup> A fluorescent dye, Dapoxyl, was used as a competitor. This dye was chosen because it had a stronger binding affinity for the CB[7] than the amino acid substrates, but a lower binding constant than their products after cleavage of their carboxylates. Thus, once the amino acid, which was initially unable to displace the dye from the CB[7] cavity, had its carboxylate group cleaved by the enzyme (such as the conversion of lysine to cadaverine), the product was then able to displace the dye from the CB[7] cavity (Figure 1.19). Because Dapoxyl's fluorescence signal differed significantly between its free form and its CB[7]-

bound species, a change in the dye's fluorescence signal could be used to indicate that it was being displaced by the decarboxylated amino acid.<sup>239,240</sup>

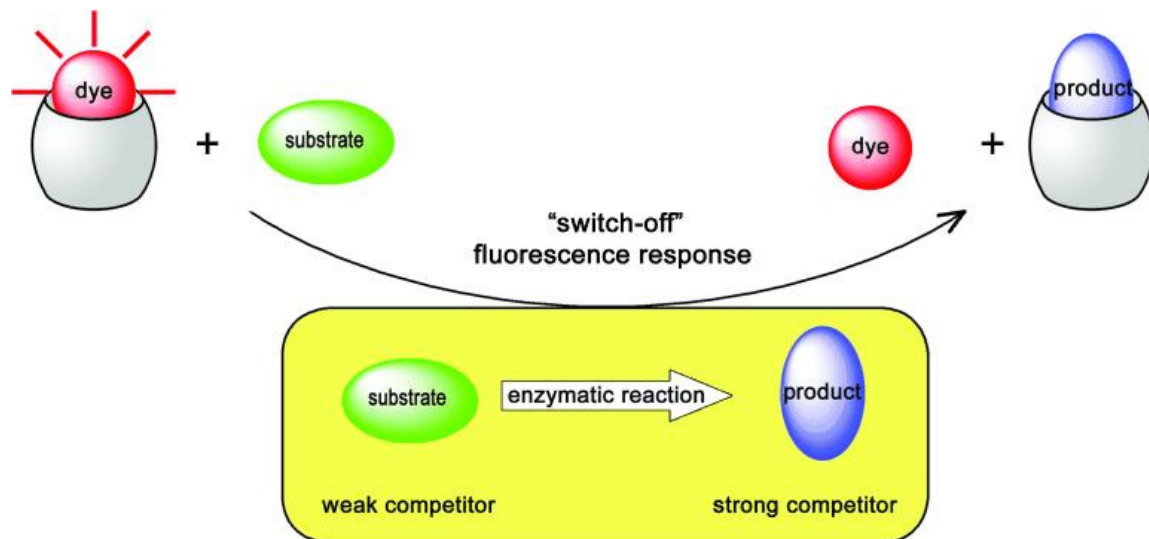


**Figure 1.19** Schematic view of the use of CB[7] as a sensor for enzyme assays. The fluorescent dye has stronger affinity for CB[7] than the amino acid (the substrate). However, after enzymatic cleavage of the amino acid's carboxylate, the decarboxylated product displaces the dye with a change in the dye's fluorescent signal.<sup>240</sup>

Exceptionally high binding affinities have been observed between CB[7] and ammonium-containing derivatives of both ferrocene<sup>241-243</sup> and adamantane,<sup>60,242,244</sup> having binding constants in the range of  $10^{11}$  to  $10^{12} \text{ M}^{-1}$ .<sup>60</sup> This binding is almost as high as that observed for the biotin-avidin system, which has the strongest naturally-occurring noncovalent interaction, with a binding constant of up to  $10^{15} \text{ M}^{-1}$ .<sup>243,245</sup> Work has been done by Kim and coworkers to attach CB[7] to a self-assembled monolayer bound to a solid gold electrode, while also attaching ferrocenylammonium groups to the protein glucose oxidase. The glucose oxidase could then bind to the surface through the pendant ferrocene derivative on the protein and CB[7], which is immobilized on the surface.<sup>243</sup> They were able to observe different levels of current that would

change with the concentration of glucose, suggesting that this system may have application as a glucose sensor.<sup>243</sup>

Kaifer has observed that the presence of salt in solution can compete with a guest, such as methylviologen, for binding to CB[7], and reduce its binding constant as the salt's concentration is increased.<sup>216</sup> This was observed when both NaCl and CaCl<sub>2</sub> were added to solution, with the effect being more pronounced for CaCl<sub>2</sub>. In Tris buffer at pH 7.2, Kaifer found the binding constant between CB[7] and methylviologen to be  $2.24 \times 10^5 \text{ M}^{-1}$  when no salt was added. When either the NaCl or CaCl<sub>2</sub> concentrations were increased, the binding constant between CB[7] and methylviologen would decrease. The binding constant between CB[7] and methylviologen was reduced to  $2.49 \times 10^4 \text{ M}^{-1}$  in the presence of 0.20 M NaCl and to  $5.60 \times 10^3 \text{ M}^{-1}$  in the presence of 0.20 M CaCl<sub>2</sub>.<sup>216</sup> The Na<sup>+</sup> and Ca<sup>2+</sup> cations competed with the guest for complexation with CB[7], thus reducing the observed host-guest binding affinities. This reinforces the concept that reported binding constants are often accurate for the specific conditions used in a study, but can vary significantly if the matrix is changed.

More recently Pal and Nau<sup>246</sup> have proposed that salt addition may be a useful method to induce the release of a guest, such as a drug, from the CB[7] cavity. When the dye Neutral Red (3-amino-7-dimethylamino-2-methyl phenazine) is bound with CB[7], it experiences a pK<sub>a</sub> shift, with its pK<sub>a</sub> increasing by two units, therefore it becomes more basic and favours its protonated form while in the cavity.<sup>246,247</sup> With the addition of NaCl, they observed both a decrease in the binding constant between CB[7] and Neutral Red, and also a decrease in the pK<sub>a</sub> shift that is observed with complexation to CB[7], so that the unprotonated species of the dye becomes more favourable when salt is added. As a test, they studied Neutral Red in the presence of both bovine serum albumin (BSA) and CB[7]. While CB[7] preferentially binds the protonated form of Neutral Red, BSA has a hydrophobic pocket which prefers to bind the unprotonated form of Neutral Red.<sup>246</sup> As NaCl was added and the pK<sub>a</sub> shift of Neutral Red decreased, the dye moved

from the CB[7] cavity and into the BSA cavity (Figure 1.20), as could be observed by a shift in the UV-visible signal from a wavelength that was characteristic of the dye encapsulated by CB[7] to a wavelength that was characteristic of the dye bound to BSA.<sup>246</sup>

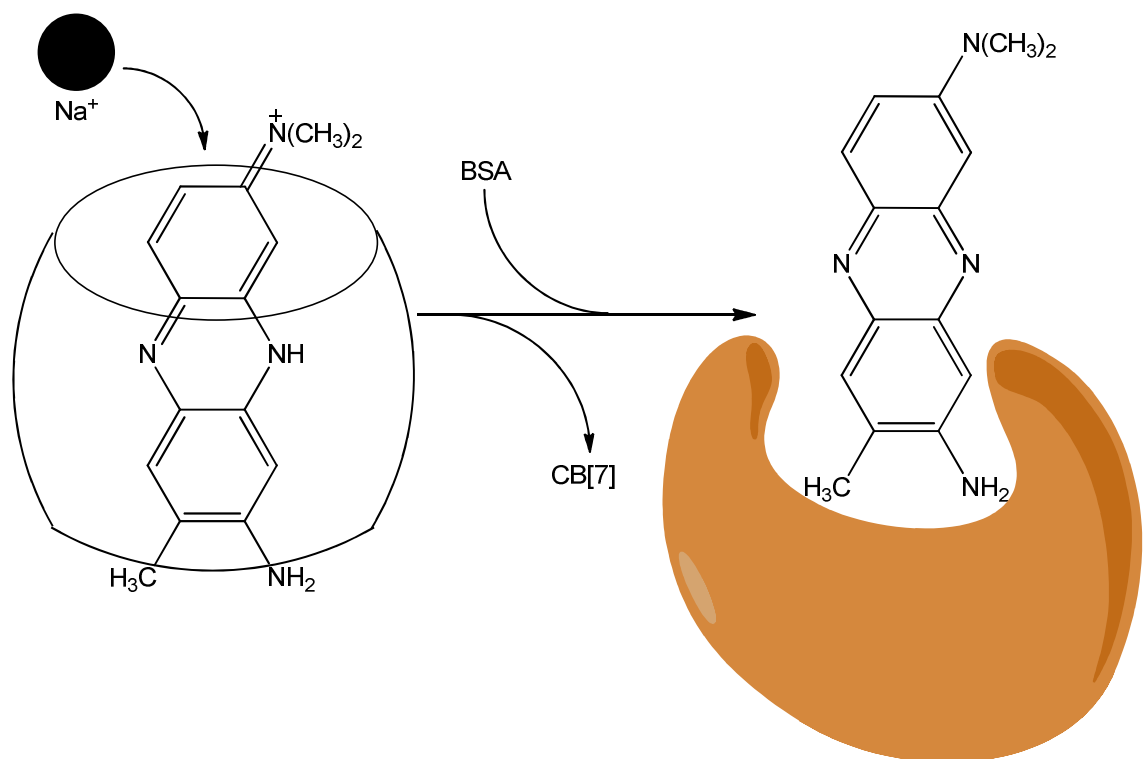


**Figure 1.20** Salt-induced release of Neutral Red from CB[7], with subsequent binding to the hydrophobic pocket of BSA.<sup>246</sup>

#### 1.5.4 Cucurbit[8]uril (CB[8])

While the main supramolecular features of CB[8], which has a similar cavity volume as  $\gamma$ -CD, are generally similar to those of other CB[*n*] homologues,<sup>154</sup> and its cavity is large enough to bind to individual guests, one feature that makes CB[8] stand out from its smaller homologues is that the CB[8] cavity can readily accommodate two guests simultaneously.<sup>248-261</sup> Although CB[7] also has the capability of simultaneously binding to two guests, such as protonated 2-



aminopyridine,<sup>262</sup> the larger CB[8] is able to encapsulate a wider variety of guests in this manner. In addition, the larger cavities of CB[8] allow them to bind to larger guests, such as cyclen (1,4,7,10-tetraazacyclododecane) and cyclam (1,4,8,11-tetraazacyclotetradecane), thus allowing formation of a “macrocycle within macrocycle” complex.<sup>263</sup> Kim and coworkers were able to subsequently metalate the tetraaza macrocycles with copper(II) and zinc(II) within the CB[8] cavity in order to create supramolecular complexes of CB[8] encapsulating the cyclen and cyclam macrocycles, which were in turn bound to transition metals.<sup>263</sup> CB[8] has even shown an ability to bind to larger guests such as fullerene (C<sub>60</sub>), with two fullerene guests being externally bound to CB[8], with one being bound to each portal.<sup>264</sup>

When two guests are simultaneously bound to CB[8], the guests can either be identical to each other (homo-guest pairs), as was observed with guests such as naphthalene derivatives,<sup>159</sup> stilbene derivatives,<sup>248</sup> cinnamic acids,<sup>242,255</sup> coumarins,<sup>265</sup> viologen derivatives,<sup>249,266</sup> tetrathiafulvalenes,<sup>251</sup> and acridines,<sup>267</sup> or the guests can be different from each other (hetero-guest pairs), such as guests combinations of viologen derivatives with either naphthalene derivatives<sup>250,268,269</sup> (Figure 1.21) or 1,4-dihydroxybenzene,<sup>268</sup> methylviologen and tryptophan derivatives,<sup>269</sup> dimethyldiazapyrenium and catechol or dopamine,<sup>270</sup> as well as methylviologen (paraquat) and diquat.<sup>271</sup>

The complexation of two guests can allow the CB[8] host to essentially act as a reaction vessel, and reactions that may occur can vary depending on whether the two encapsulated guests are identical to one another or different. Photodimerizations have been reported when a similar pair of olefin guests were bound.<sup>248,253-255</sup> In addition to catalyzing photodimerization, the presence of CB[8] has also been found to facilitate stereoselective dimerization of the guests. In the case of diaminstilbene, for example, the dimerization occurs for the *E* isomer but not the *Z* isomer, whereas the photodimerization of the *Z* isomer is preferred in the absence of CB[8].<sup>248</sup> In addition, a 95:5 selectivity for forming the *syn* dimer over the *anti* dimer is observed in the

presence of CB[8], while in the presence of  $\gamma$ -CD the *syn-anti* ratio is 4:1. Only half an hour of UV irradiation is required to allow the photodimerization to proceed when CB[8] is used as the host, while 72 hours is needed when  $\gamma$ -CD is used.<sup>248</sup> When the two similar guests are asymmetrical, such as cinnamic acid derivatives,<sup>254,255</sup> the photodimerization product shows a selectivity for whether the guests are *head-to-head* or *tail-to-tail*, depending on the geometry and functional groups present in the guest and which arrangement of the guests provides the best fit within the CB[8] cavity. While the *syn-head-to-head* product was favoured over the *syn-head-to-tail*, *anti-head-to-head*, and *anti-head-to-tail* dimers in the case of cinnamic acid guests,<sup>254,255</sup> when coumarin derivatives<sup>258</sup> were studied, their photodimerization product favoured the *head-to-tail* conformation. When CB[8] binds to two guests, the system is a ternary complex. Tetrathiafulvalene has been shown to form a  $\pi$ -dimer when it is encapsulated into the CB[8] cavity as a 1:2 host-guest complex, as evidenced by a loss of the tetrathiafulvalene's EPR signal upon addition of CB[8]. The quenching of the EPR signal is believed to be due to the coupling of the two cation radical guests in the CB[8] cavity.<sup>251</sup>

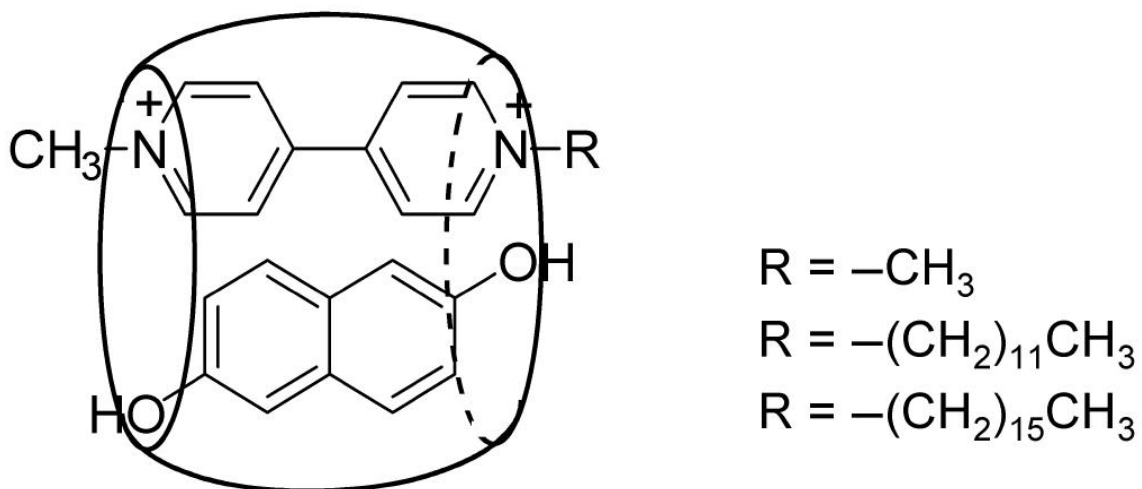


**Figure 1.21** A ternary host-guest system with CB[8] encapsulating the guests 2,6-dihydroxynaphthalene and methylviologen, as well as its analogues.<sup>250</sup>

Kim and coworkers have noted that the binding stoichiometry between methylviologen and CB[8] can be controlled through their redox chemistry.<sup>249</sup> When the methylviologen guest is in its dicationic form, the CB[8] favours formation of a 1:1 complex, even though there is sufficient room to accommodate two methylviologen guests.<sup>249,268</sup> However, when the methylviologen guests are reduced to give the singly charged species, the stoichiometry changes in favour of the 1:2 complex (containing two guests).<sup>249</sup> While the single electron reduction of methylviologen was observed at -0.704 V (vs. SCE) in the absence of CB[8], when CB[8] is present, this occurs at -0.546 V, suggesting that the 1:2 complex containing the monocationic methylviologen is readily formed.<sup>249</sup> The tendency of CB[8] to bind to one doubly charged viologen species, with a 1:1 stoichiometry, instead of two guests, likely arises from electrostatic repulsion between two viologens, which becomes less of an issue as the viologen is reduced.<sup>272</sup>

Encapsulation of hetero-guest pairs into the CB[8] cavity potentially allows a charge-transfer complex to be formed, especially when one of the guests is electron rich and the other guest is electron poor.<sup>268</sup> Although the 1:1 complex is observed when the electron poor, dicationic methylviologen guest is bound to the cavity, CB[8] readily forms a ternary complex with both methylviologen and electron rich guests such as 2,6-dihydroxynaphthalene or 1,4-dihydroxybenzene.<sup>250,268</sup> This ternary complex forms despite the fact that the electron rich guest, does not readily bind to CB[8] in the absence of the electron poor guest.<sup>268,273</sup>

When long-chain alkyltrimethylammonium guests were encapsulated by CB[8], the alkyl chain (lengths of which were octyl, decyl, or dodecyl) was observed to bend, forming a “U-shaped” guest in preference to remaining relatively linear.<sup>274</sup> When these guests were bound with the smaller CB[7] host, they observed <sup>1</sup>H NMR upfield shifts for the methylene protons located near the ammonium group, while the protons of the terminal end of the guest further away from the ammonium group were not significantly shifted, suggesting that the CB[7] cavity was bound near the ammonium with the other end of the alkyl chain sticking out of the CB[7] cavity.<sup>274</sup> On

the other hand, when CB[8] was used as a host, all of the methylene protons displayed upfield shifts, with the terminal end of the guest showing the largest shift, suggesting that this end was located deep in the CB[8] cavity. This suggests that the greater width of the CB[8] cavity allowed the aliphatic chain to form a U-shape so that the terminal end could also be encapsulated. In addition to X-ray crystal structures showing the U-shape conformation of the guests in the CB[8] while in the solid state, further evidence of the U-shape conformation of the aliphatic chain in the solution phase was observed with ROESY NMR, as crosspeaks between the terminal methyl protons and the trimethylammonium protons could be observed, indicating that these protons from opposite ends of the molecule were in close proximity. Similar behaviour is observed during complexation between fatty acid binding proteins and palmitic acid and oleic acid, where the fatty acids attain a U-shaped conformation upon binding with the protein.<sup>274-276</sup>

In a similar manner to the aliphatic guests adopting a U-shaped conformation, guests have also been synthesized with two or more functional groups that have a binding affinity for CB[8] (such as viologen) embedded into their backbone, so that the backbone of the molecule forms a loop in order to allow the functional groups to bind.<sup>277-279</sup> The binding is therefore similar to the 2:1 or ternary structures observed when two guests are encapsulated, except in this case the two guests are actually part of the same molecule. When the guest had in its backbone both an electron-poor viologen and an electron rich naphthalene unit, the system readily formed a loop, so that both the viologen and naphthalene were encapsulated by CB[8].<sup>277</sup> It was possible to open and close this loop through the redox chemistry. Addition of a dicationic methylviologen was unable to displace the naphthalene functional group from the cavity, and the CB[8] complex maintained its 1:1 stoichiometry, with the both functional groups from the same molecule bound to CB[8]. However, when Na<sub>2</sub>S<sub>2</sub>O<sub>4</sub> was added to the solution and the methylviologen was reduced to its monocationic species, the naphthalene site was then displaced by the methylviologen guest and a ternary guest was formed, with the larger guest now in the “open”

form (and bound to CB[8] through one site). Subsequently, when oxygen was bubbled into the solution, the larger guest retained its closed loop, displacing the smaller methylviologen guest.<sup>277</sup> In a similar manner, when a guest has three binding sites embedded in its backbone, with two electron-deficient viologen sites at the ends and one electron rich naphthalene site near the middle, the binding positions of the guest could be controlled through the redox chemistry. When the methylviologens were reduced, the loop was in the “end to end” conformation, with both of its terminal viologen groups encapsulated in the CB[8] cavity.<sup>278</sup> Upon oxidation, only one viologen group remained in the cavity, and the other was displaced by the electron rich naphthalene-based group, thus switching to “end to interior” loop.<sup>278</sup> Kaifer and coworkers have utilized this redox control of binding to CB[8] by appending viologen to dendrimers so that one can control the stoichiometry of their self-assembly through electrochemistry,<sup>252</sup> and can also tune the size of the dendrimer assembly complex by attaching a large dendrimer to an electron rich alkoxyethoxybenzene group, and a smaller dendrimer to a viologen group.<sup>280</sup> Therefore when the viologen is in its dicationic form, the ternary complex containing both the electron rich and poor guests will form, and thus both the large and small dendrimers will be assembled. When the viologen is reduced, the CB[8] binds to the viologens, so that a complex is formed with the viologens and their smaller pendant dendrimers.<sup>280</sup> More recently, Rauwald and Scherman<sup>281</sup> have used this method to noncovalently graft two polymers together through the CB[8], with these polymers having either a viologen group, or 2-naphthol as their terminal groups.<sup>281</sup> Another application of this binding has been used by Urbach and coworkers in order to link peptides noncovalently through CB[8].<sup>282</sup> They grafted viologen onto a peptide backbone, and complexed it with CB[8]. Upon addition of peptides containing tryptophan residues, the tryptophan-bearing peptide would also bind to the CB[8] with its tryptophan residue, thus forming a ternary complex with the CB[8] and the two peptides.<sup>282</sup> This work was carried out with peptides having between one and three viologens grafted to their backbone, and these would in turn bind to peptides with

tryptophan residues in the corresponding placements, so that up to three noncovalent CB[8] linkages could connect the proteins.<sup>282</sup>

### 1.5.5 Cucurbit[10]uril (CB[10])

CB[10] is the largest of the CB[*n*] homologues, and is also the most recent member of the series to be isolated.<sup>203,283</sup> As mentioned in the CB[5] description, CB[10] was characterized by Day and coworkers in 2002 as a complex encapsulating the smaller CB[5] macrocycle, and this system is often called CB[5]@CB[10].<sup>203</sup> In the X-ray crystal structure of CB[5]@CB[10], the CB[5] guest was not aligned in the same direction as the CB[10] host, as the CB[5] guest had a 64° incline with respect to the surrounding CB[10].<sup>203</sup> In solution phase the authors noted the ability of CB[5] to rotate inside the CB[10] cavity, in a similar manner to a gyroscope, and referred to this system as a *gyroscane*.<sup>203</sup> They did not isolate CB[10] from CB[5] at that time.<sup>203</sup>

More recently, Isaacs and coworkers have isolated CB[10] from CB[5] by treating the CB[5]@CB[10] complex with a five-fold excess of the triflate salt of 4,6-bis(4-(aminomethyl)phenylamino)-1,3,5-triazin-2(1H)-one (Figure 1.22), which bound to CB[10] with sufficient affinity to displace CB[5], so that CB[10] could be isolated as a precipitate.<sup>283</sup> The CB[10] was found to contain two equivalents of this guest, arranged head-to-tail. Meanwhile, CB[5] was also separately bound with this guest, albeit externally. The second equivalent in CB[10] was bound relatively weakly, and could be displaced from CB[10] by washing it with methanol. The 1:1 complex was heated in acetic anhydride and subsequently washed to yield free CB[10].<sup>283</sup>

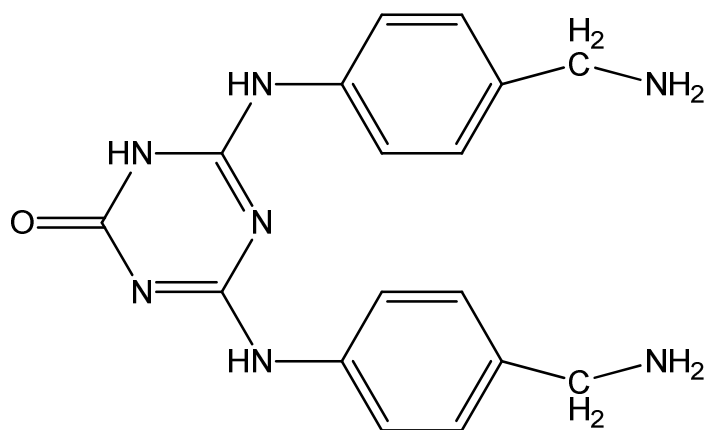


**Figure 1.22** 4,6-bis(4-(aminomethyl)phenylamino)-1,3,5-triazin-2(1H)-one. The triflate salt of this compound has been used by Isaacs to isolate CB[10] from the CB[5]@CB[10] complex.<sup>283</sup>

After isolation of CB[10], Isaacs and coworkers tested a variety of potential guests in order to survey its capabilities as a host. They found that CB[10] formed 1:2 host-guest complexes with guests such as (*R*)-1,1'-binaphthyl-2,2'-diamine. When a racemic ( $\pm$ )-1,1'-binaphthyl-2,2'-diamine was mixed with CB[10], the host was found to form a racemic mixture of the complexes and bound to homochiral pairs (that is, two *R* guests and two *S* guests in separate CB[10] cavities) with a three to one preference for binding homochiral pairs of the guests over binding both *R* and *S* guests in the same CB[10] host.<sup>283</sup> They also found that CB[10] exhibits an ability to form supramolecular complexes with tetracycline, the peptide tetralysine, coumarin 138, and Nile Blue in solution. When 3,5-dimethyl-1-aminoadamantane was added to a solution of CB[5]@CB[10], the adamantane derivative was able to displace the CB[5] from the CB[10] cavity and the insoluble complex of 3,5-dimethyl-1-aminoadamantane precipitated from the solution. Similar insoluble CB[10]:guest precipitations were observed when the solution of CB[5]@CB[10] was treated with ligands such as pyrenemethylamine hydrochloride, Disperse Blue 1, and biphenyl-3,3',4,4'-tetraamine.<sup>283</sup>

Since CB[10] had a large cavity, and had shown a strong tendency to bind to CB[5], Isaacs and coworkers explored the affinity of CB[10] for small hosts such as  $\alpha$ -CD, CB[6], and calix[4]arenes. While CB[10] retained its ability to form a complex with CB[5], it was unable to form a complex with CB[6] or  $\alpha$ -CD. However, it did form a complex with *p*-methyldimethylaminocalix[4]arene, and was found to form a solution complex with the calixarene in its *1,3-alternate* form, in addition to a rapidly equilibrating mixture of the *cone*, *1,2-alternate*, and *partial cone* conformations within the CB[10] cavity.<sup>283</sup> Addition of adamantanecarboxylic acid to the CB[10]•calixarene complex caused the calixarene to favour the *cone* conformation when the ternary complex was formed, even though the calixarene does not bind to the adamantane in the absence of CB[10].<sup>283</sup> When the adamantanecarboxylic acid was removed from CB[10] by sequestering it with CB[7] (to which it has a higher affinity), the calixarenes bound in the CB[10]•calixarene system returned to the conformation equilibrium that existed prior to the formation of the ternary complex with the adamantane derivative.<sup>283</sup>

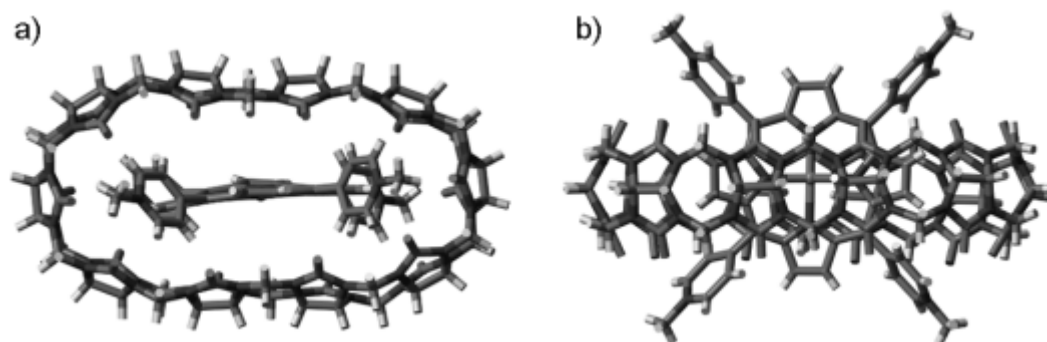


**Figure 1.23** Complex of CB[10] and a porphyrin derivative, based on molecular mechanics calculations (MMFF-minimized geometry) top view (a), and side view (b).<sup>284</sup>

More recently the supramolecular chemistry of CB[10] has been extended to porphyrin derivatives, as well as their ternary complexes with various aromatic amines.<sup>284</sup> The porphyrin



guest was encapsulated in the CB[10] both in its *apo* form and also when it was coordinated to transition metals such as zinc(II), iron(III), and manganese(III). Molecular modeling has suggested that the CB[10] macrocycle flattens somewhat in order to facilitate binding to the porphyrin (Figure 1.23), indicating that CB[10] is more flexible than its smaller homologues. Despite the distortion of CB[10], and the fact that the photophysical properties of chromophoric guests are often changed upon complexation with CB[*n*], no significant changes were observed to the  $\lambda_{\text{max}}$  in the UV-visible spectra of the porphyrin guests upon encapsulation by CB[10].<sup>284</sup> In the same manner, only minor changes were observed in the iron(III/II) and manganese(III/II) electrochemistry of porphyrins containing these metals when they were bound to CB[10].

With the zinc-coordinated porphyrin encapsulated by CB[10], Isaacs and coworkers used a series of aromatic amines to form a ternary complex with the CB[10] and the porphyrin, noting that the amine would be likely to coordinate to the zinc centre.<sup>284</sup> However, the Q band in the absorbance spectrum of the porphyrin experienced only a minor change in its intensity and  $\lambda_{\text{max}}$  (from 566 to 562 nm), suggesting that the amine was not coordinated to the zinc metal. They noted that aromatic amines exhibited significant upfield shifts in their proton NMR, however, and determined that the interaction between the aromatic guests and the porphyrin inside the porphyrin cavity was due to  $\pi$ - $\pi$  stacking with the conjugated porphyrin, instead of coordination to the zinc centre. Also, the presence of upfield shifts of aromatic resonances of guests such as benzene, toluene, and ethylbenzene, when a ternary complex was formed, further suggested that  $\pi$ - $\pi$  stacking with the porphyrin ring was driving the aromatic guest's complexation with the porphyrin inside the CB[10] cavity.

### 1.5.6 Cucurbit[*n*]uril Derivatives

CB[*n*] derivatives have received significant attention,<sup>164,285</sup> with notable classes of derivatives including functionalized, inverted,<sup>286,287</sup> and *nor-seco*-CB[*n*].<sup>288-290</sup> Motivation for derivatization of cucurbiturils includes the desire to improve their solubility, and adjustment of their supramolecular host properties (such as by changing the size and/or shape of the cavity). Furthermore, additions of reactive groups to the macrocycle can also expand its host properties, and in turn, have been shown to allow the host to be attached onto solid surfaces, thus increasing the utility of CB[*n*]s.<sup>164,285</sup>

From early on, attention has been devoted toward adding functional groups to CBs, either through direct functionalization of the CB,<sup>291</sup> or derivatization of its precursors, such as the glycoluril monomer<sup>292,293</sup> or the formaldehyde.<sup>285</sup> Among the earliest examples of functionalized cucurbiturils was decamethylcucurbit[5]uril,<sup>198</sup> which was discussed earlier, and whose synthesis actually predated that of CB[5]. In addition to the methyl substituents at the equatorial position of decamethylcucurbit[5]uril (with methyl groups replacing the methine protons), other CB[*n*] derivatives have been synthesized containing methyl,<sup>294,295</sup> cyclohexyl,<sup>296</sup> phenyl,<sup>297</sup> and carbohydrate<sup>298</sup> substituents at the equatorial positions of the cucurbituril. These substitutions have produced both fully and partially substituted CB[*n*] derivatives, with either all of the methine protons replaced by the substituent, or only those on certain glycoluril units within the CB[*n*] macrocycle being replaced. Although substitution of the methine protons of cucurbiturils with methyl groups has not been found to alter their solubilities, when they were replaced with bridging cyclohexane groups, the derivatized macrocycles solubility was improved in both water and organic solvents.<sup>296</sup> Substitution of the methine protons of CB[*n*] has traditionally been accomplished through use of glycoluril precursors containing substituents at the desired positions. One drawback of this method is that the yields of the substituted derivatives tend to be low, with

the smaller CB[n] analogues (such as CB[5] derivatives) being favoured over the larger homologues.<sup>285</sup>

Analogues of cucurbiturils have been synthesized by Isaacs and coworkers containing bis(phthalhydrazide) walls.<sup>299-301</sup> In these cases the backbone of the macrocycle is made up of glycoluril units as well as bis(phthalhydrazide) units. These were obtained from condensation of bis(phthalhydrazide) with glycoluril units (depending on the analogue synthesized, the glycoluril units existed as monomers, dimers, or trimers) containing bicyclic ethers at their ends. Analogues of CB[6] were formed that contained two glycoluril dimer units and two bis(phthalhydrazide) units, while the CB[7] analogue contained two glycoluril trimer units and one bis(phthalhydrazide) unit as the macrocycle's backbone (Figure 1.24). The glycoluril units in these macrocycles contained esters, imide, or carboxylic acid functional groups in place of their methine protons.<sup>299</sup> An analogue of CB[5] was also synthesized, in lower yield, by Isaacs and coworkers that contained two bis(phthalhydrazide) units that were linked by a glycoluril monomer unit and a glycoluril dimer unit. The presence of the bis(phthalhydrazide) units in the ring allow for  $\pi$ - $\pi$  stacking interactions with aromatic guests, in addition to the ion-dipole interactions and hydrophobic effect observed with conventional CB[n] hosts.<sup>301</sup> The CB[6] analogue has been found to bind to guests such as *para*-xylylene in a comparable manner as CB[6], showing slow exchange with the guest on the NMR timescale.<sup>299</sup> In addition, the bis(phthalhydrazide) units provide UV-visible, fluorescence, and electrochemical activity to the macrocycles. While these hosts are stable in acidic solution, they are unstable in basic solutions above pH 7.<sup>300</sup>

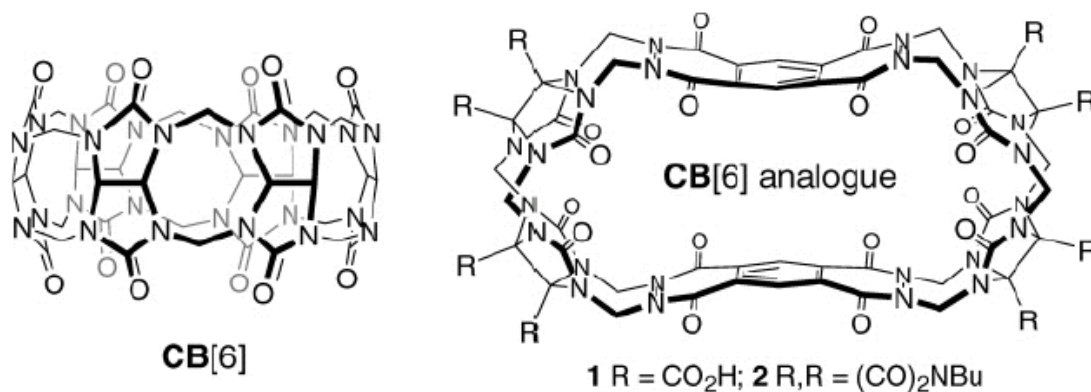


**Figure 1.24** CB[6] (left), and its analogue (right), synthesized by Isaacs and coworkers.<sup>301</sup>

Inverted cucurbiturils, such as inverted CB[6] and CB[7] (*i*-CB[6] and *i*-CB[7], respectively) have been isolated by both Kim and Isaacs, in collaboration.<sup>164,285,302,303</sup> These structures differ from conventional CB[*n*] in that one of the glycoluril monomers of *i*-CB[*n*] faces the opposite direction of the other glycoluril units, with its carbonyl groups pointed outwards and away from the cavity instead of towards the cavity (Figure 1.25). At the same time, the methine protons of this inverted glycoluril unit are projected inside the cavity.

Because the methine protons of the inverted glycoluril unit are inside the cavity, the cavity volumes of the *i*-CB[*n*] are smaller than those of their corresponding CB[*n*] analogues.<sup>302</sup> Furthermore, the cavities of the *i*-CB[*n*] hosts tend to be somewhat flatter than those of the corresponding CB[*n*], but the portals are less constrained than those of traditional CB[*n*] hosts. As a result of these structural changes, Isaacs and Kim have observed that these inverted hosts have a preference for flatter guests. The *i*-CB[*n*] hosts have been observed to bind similar guests as their conventional analogues do, but tend to have weaker binding constants and also the complexation is generally more labile.<sup>302</sup> A good example of the preference for flatter guests exhibited by the inverted hosts was shown for *i*-CB[7], as it shows a higher binding affinity for *p*-xylylenediamine over (ferrocenyl)trimethylammonium guests,<sup>302</sup> to which CB[7] has an extremely high affinity.<sup>60</sup>

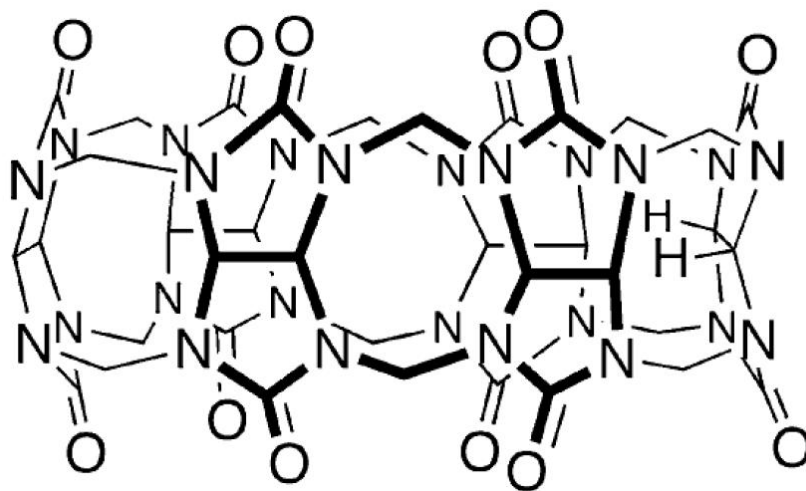


**Figure 1.25** *i*-CB[6]. The inverted glycoluril unit is shown at the right side of the diagram, with its methine protons inside the cavity.<sup>303</sup>

The *i*-CB[*n*] were isolated from the reaction mixture of glycoluril and formaldehyde, which is used to synthesize CB[*n*], by gel permeation chromatography.<sup>285,302</sup> By the use of product resubmission experiments, they found that the *i*-CB[*n*] were converted to CB[*n*], suggesting that the inverted products were a kinetic product, and less stable than conventional cucurbiturils.<sup>303</sup> Recent computational studies have also predicted that both *i*-CB[6] and *i*-CB[7] are less stable than their conventional CB[*n*] analogues.<sup>304</sup> On the other hand, the larger *i*-CB[8] macrocycle (which hasn't been isolated yet) is predicted by Pinjari and Geiji to be more stable than CB[8].<sup>304</sup> Isaacs and Kim have also predicted improved stability of *i*-CB[8] due to reduced ring strain.<sup>303</sup>

Another derivative of CB[*n*] that is a kinetic product from the synthesis of cucurbiturils are *nor-seco*-CB[*n*] (*ns*-CB[*n*]), which have been isolated by Isaacs and coworkers.<sup>288-290</sup> In the bis-*ns*-CB[*n*] macrocycles, two bridging CH<sub>2</sub> units are missing from the macrocycle as compared to conventional CB[*n*],<sup>288,289</sup> while for *ns*-CB[*n*], one CH<sub>2</sub> group is missing (Figure 1.26).<sup>290</sup> These macrocycles were prepared by using a deficiency of formaldehyde compared to the

synthesis of CB[*n*], so that instead of using a 2:1 ratio of formaldehyde:glycoluril (which is the optimum ratio for CB[*n*] synthesis), the *ns*-CB[*n*] macrocycles are more readily isolated when the ratio of formaldehyde:glycoluril is slightly less than 2:1.<sup>288,289</sup> Initially, Isaacs and coworkers isolated bis-*ns*-CB[10] and (±)-bis-*ns*-CB[6], while more recently they have also isolated *ns*-CB[6]. An exciting feature of bis-*ns*-CB[10] is that it consists of two symmetric cavities, and therefore has the capability of forming 1:2 host-guest complexes. Each of the cavities can bind guests that normally bind with CB[6] and CB[7], such as alkyl, aromatic, and adamantyl amines.<sup>288</sup> Meanwhile, larger guests can fill both cavities and form a 1:1 complex with the host.<sup>288</sup> In the case of (±)-bis-*ns*-CB[6], this host binds to aromatic, aliphatic, and cycloalkyl amines, but not to adamantane-bearing amines, which is also observed for CB[6].<sup>305</sup> However, bis-*ns*-CB[6] binds to methyl viologen, which is too large to bind to CB[6], suggesting that the effective cavity volume of (±)-bis-*ns*-CB[6] is between that of CB[6] and CB[7].<sup>305</sup> This host also displays moderate chiral recognition, as when a guest such as (+)-1-phenylethylamine is in excess with a solution of (±)-bis-*ns*-CB[6], the ratio of the diastereomers is 72:28.<sup>305</sup> This diastereoselectivity is highest for (±)-2-amino-3-phenylpropanoic acid, which has a ratio of 88:12.<sup>305</sup>

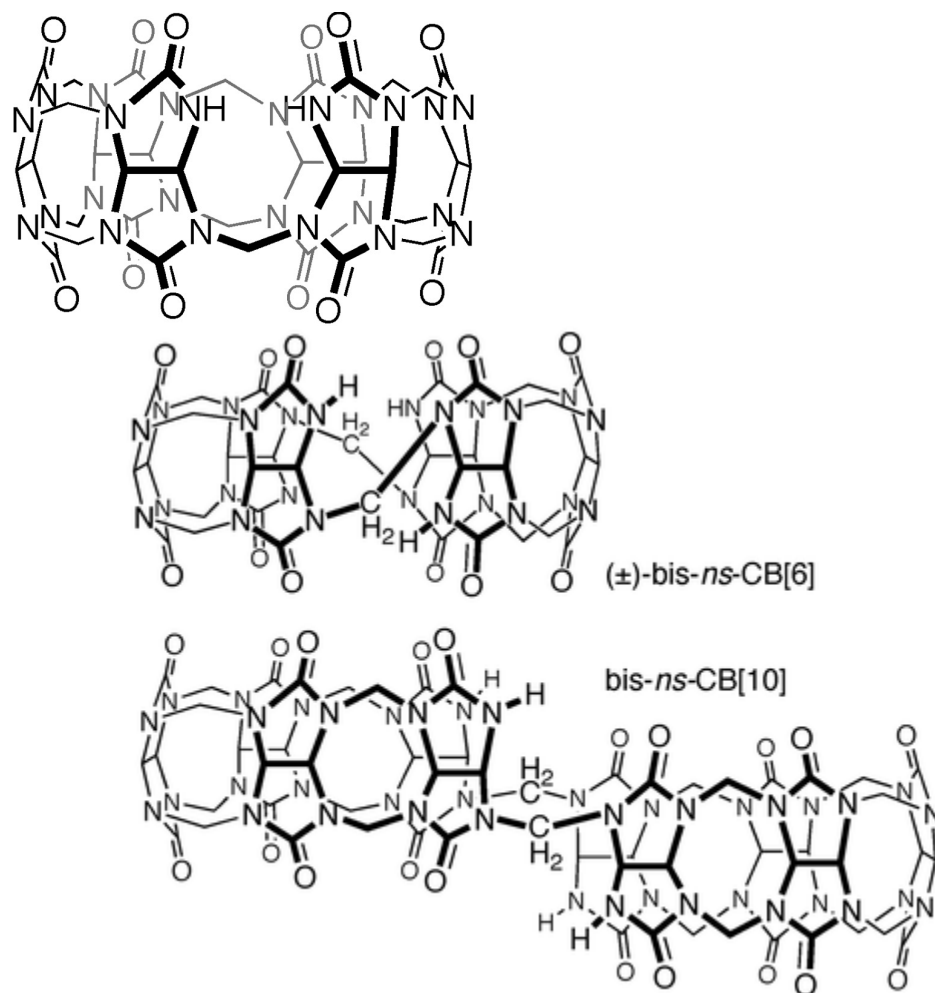


**Figure 1.26** *ns*-CB[6] (top),<sup>290</sup> (±)-bis-*ns*-CB[6] (middle),<sup>289</sup> and bis-*ns*-CB[10] (bottom).<sup>289</sup>

Isaacs and coworkers took *ns*-CB[6], which was missing one CH<sub>2</sub> linker as compared to CB[6], and subsequently reacted it with *ortho*-phthalaldehyde, and obtained a novel derivative that contained an *ortho*-xylylene (with the CH<sub>2</sub> groups of the xylylene also being bridged by an oxo bridge) bridging two glycoluril units, now being bridged by a N-CH-O-CN-N, at the site which formerly lacked the CH<sub>2</sub> bridge (Figure 1.27). The incorporation of this *ortho*-xylylene bridge into the portal caused a widening of that portal, while the other portal, which was linked completely with CH<sub>2</sub> linkers, was contracted to give a smaller portal.<sup>290</sup> As a result of this, it was observed that this smaller portal had enhanced complexation with the potassium cation in the solid state. The portal at the top, containing the *ortho*-xylylene bridge, was found to be have a

more positive electrostatic potential than the lower rim, while on the other hand, the upper rim of *ns*-CB[6] that contained the missing CH<sub>2</sub> group, has a more negative electrostatic potential than the lower, fully bridged rim.<sup>290</sup> Isaacs observed that when a series of alkanediammonium guests were encapsulated by the *ortho*-xylylene bridged CB[6] analogue, the guests with longer alkyl backbones, such as those with nonyl and dodecyl linkers, had a tendency to fold back so that both of the cationic ammoniums could be located near the electron rich portals (Figure 1.27).<sup>290</sup> This capability was attributed to the larger diameter of the *ortho*-xylylene-containing portal, as it was wide enough for the ammonium to become back-folded and still be influenced by the electron density from that portal.<sup>290</sup> This back-folding parallels that observed with alkanediammonium guests bound to CB[8] by Kim and coworkers,<sup>274</sup> except in this case the folding occurs outside of the cavity.<sup>290</sup> This *ns*-CB[6] represented the first CB[*n*] based macrocycle that was reactive towards aldehydes, and may open possibilities for further functionalization of cucurbiturils.<sup>290</sup>

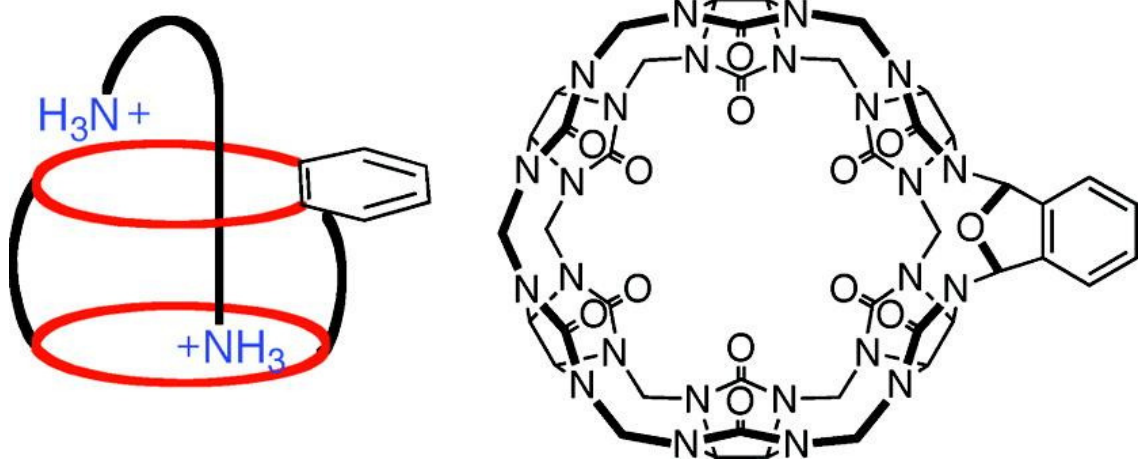


**Figure 1.27** Longer chain alkanediammonium guest back-folded to the portal (left), and structure of *ortho*-xylylene bridged CB[6] derivative (right).<sup>290</sup>

CB[*n*] derivatives have included both their cyclic derivatives,<sup>306,307</sup> as well as their acyclic analogues.<sup>289,308,309</sup> Isaacs and coworkers have synthesized acyclic dimers of glycoluril that are



linked by methylene groups, and have *ortho*-xylylene groups at their ends.<sup>309, 310</sup> These dimers were found to exist as diastereomers, having either a C-shaped  $C_{2v}$  symmetry or an S-shaped  $C_{2h}$  symmetry (Figure 1.28). While both the C- and S-shaped dimers were kinetic products, the C-shaped diastereomer was the preferred thermodynamic product. The shape of the  $C_{2v}$  product is also consistent with the C-shaped arrangement of glycoluril units within the cucurbituril macrocycle, and the preference for the C-shaped dimers is believed by Isaacs to be a contributing factor to the relatively high yield (82 %) of CB[6].<sup>309</sup>

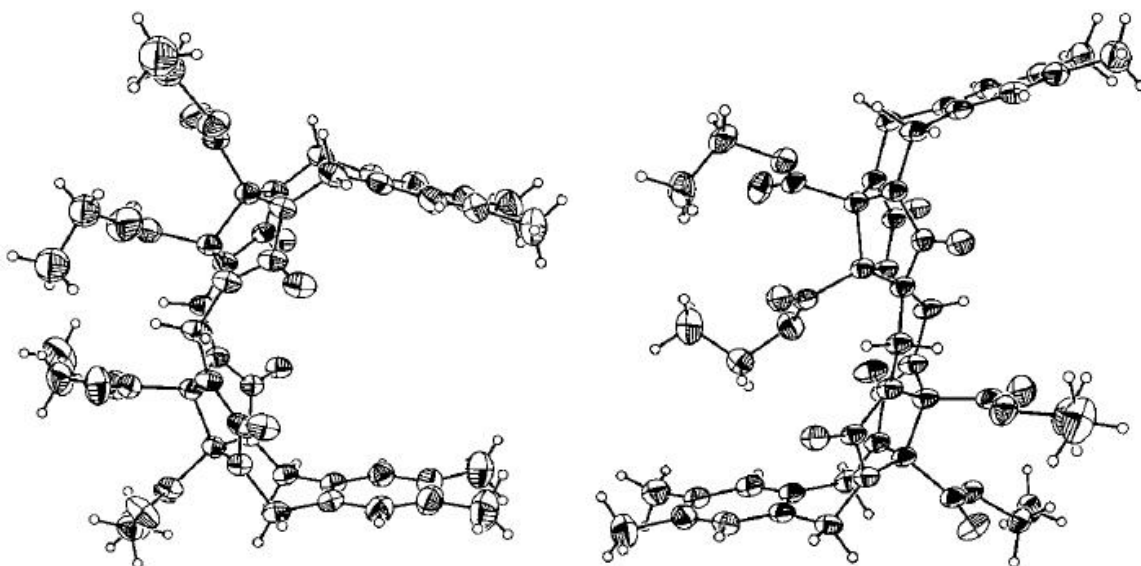


**Figure 1.28** X-ray crystal structures of a C-shaped glycoluril-based dimer (left), and an S-shaped dimer (right).<sup>154</sup>

Oligomers of glycoluril units (in this case the glycolurils are not derivatized other than being acyclic as opposed to cyclic), made up of five or six glycolurils, have been found to retain some of the supramolecular properties of cyclic cucurbiturils.<sup>289</sup> The acyclic glycoluril pentamer and hexamer have both been observed to show slow exchange binding with *para*-xylylene. While slow exchange complexation is common for cucurbiturils, it is less common for other hosts such as cyclodextrins and calixarenes.<sup>289</sup> The hexamer is further able to complex with larger guests, such as adamantane and ferrocene-based guests, which are more commonly associated

with complexation with the larger CB[7] and CB[8] macrocycles. This suggests that the acyclic glycoluril hexamer has a reasonable degree of flexibility so that it may rearrange itself to accommodate these larger guests.<sup>289</sup> These oligomers exist in the C-shaped, as opposed to the S-shaped form, and are found to have similar curvature to that of CB[6].<sup>289</sup>

Isaacs and coworkers<sup>289</sup> have recently concluded that acyclic glycoluril oligomers, with the number of monomer units ranging between two and six, are intermediates in the step growth oligomerization towards the formation of cucurbiturils.<sup>289</sup> Once the precursor oligomer contains five or six glycolurils, it can then undergo cyclization through condensation with two equivalents of formaldehyde. The *ns*-CB[*n*] macrocycles also apparently represent intermediates in this cyclization process.<sup>164,289</sup>

Kim and coworkers have discovered that cucurbiturils can be derivatized directly by oxidation with  $K_2S_2O_8$ , to produce their perhydroxycucurbituril derivatives, with the methine protons being replaced by hydroxyl groups.<sup>291</sup> The yield for the CB[5] and CB[6] derivatives was between 40 and 45%, but significantly lower for the CB[7] and CB[8] derivatives, at 5%. These derivatives are soluble in solvents such as DMSO and DMF, and they can in turn be derivatized further by acylation and alkylation.<sup>285,291</sup> Of particular interest has been the derivative perallyloxyCB[6], as it has both a reactive functional group and good solubility in organic solvents.<sup>291</sup> From this derivative, through a photo-addition reaction with alkylthiols, thioether-substituted CB[6] derivatives have been produced.<sup>291</sup> These thioether-substituted derivatives have subsequently been immobilized on surfaces such as glass chips<sup>291</sup> and gold surfaces<sup>243</sup> for potential use as sensors,<sup>291</sup> as well as to silica gel for separations.<sup>311</sup>

When the functionalized CB[6] has a long chain, such as  $[CH_3(CH_2)_7S(CH_2)_3O]_{12}CB[6]$ , it can form nanospheres, with diameters between 50 and 150 nm, upon emulsification, which may have potential application in drug delivery.<sup>291</sup> Functionalized CB[6] derivatives have also been shown to act as artificial ion channels<sup>312</sup> when derivatized CB[6] was embedded into a vesicle

made up of L- $\alpha$ -phosphatidylcholine (EYPC), cholesterol, and dicetyl phosphate. A pH sensitive dye, 8-hydroxypyrene-1,3,6-trisulfonate (HPTS), was encapsulated inside the vesicle and it was observed that when acid was added to the surrounding solution, the fluorescence of the dye was quenched for the dye encapsulated in vesicles embedded with the CB[6] derivative, but no change in the fluorescence of the dye occurred when it was encapsulated in vesicles that did not have the CB[6] derivative embedded into the membrane. This suggested that the CB[6] was aiding the transport of protons across the membrane (Figure 1.29).<sup>312</sup> Interestingly, when excess acetylcholine was added to the matrix, the quenching was no longer observed for the dye encapsulated inside the CB[6]-embedded membrane, indicating that the acetylcholine was blocking transport of the protons through the CB[6] channels in the membrane.<sup>312</sup> In the case of alkali metals, activity of  $[\text{CH}_3(\text{CH}_2)_7\text{S}(\text{CH}_2)_3\text{O}]_{12}\text{CB}[6]$  towards the transport of alkali cations has been found to follow the order of  $\text{Li}^+ > \text{Cs}^+ \sim \text{Rb}^+ > \text{K}^+ > \text{Na}^+$ , which is the opposite of the binding affinity of CB[6] towards these cations. Planar bilayer conductance measurements have shown that when a +80 mV potential was applied to the membrane separating two 0.3 M  $\text{Cs}^+$  solutions, an ion flux of  $\text{Cs}^+$  was measured as 5 pA (approximately  $3 \times 10^7$  ions/s), which rivals that of gramicidin.<sup>312</sup>

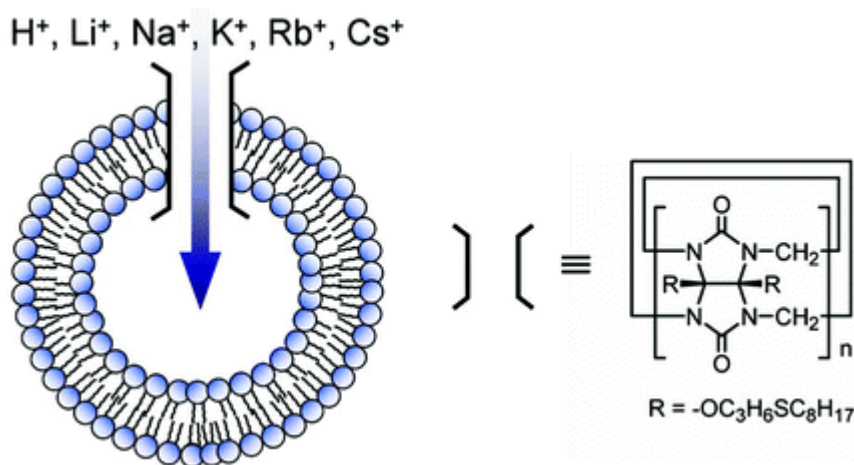


**Figure 1.29** A vesicle embedded with a functionalized CB[ $n$ ] ( $n = 5$  and  $6$ ), which is able to act as an ion channel, aiding the transport of ions into the vesicle.<sup>312</sup>

## 1.6 Applications of Cucurbit[*n*]urils

Cucurbiturils have been shown to have a variety of potential applications, some of which have been discussed earlier in this chapter. Applications include the catalysis and inhibition of reactions, molecular sensors, molecular switches and machines, applications towards drug delivery and the controlled release of drugs, environmental remediation, and also separations.

### 1.6.1 Catalysis and Stabilization of Guests

The ability of CB[*n*] to act as a catalyst for a chemical reaction was recognized by Mock relatively soon after his characterization of CB[6].<sup>313,314</sup> He realized that, since CB[6] has two electron rich portals, it had the potential to bring two cationic reactants in close proximity, as well as in specific orientations, so that the two reactants could undergo an accelerated reaction if they were simultaneously bound with the macrocycle.<sup>313</sup> These early reactions catalyzed by CB[6] were cycloaddition reactions, with the initial observation in 1983 being the acceleration of the 1,3-cycloaddition reaction between alkynes and alkyl azides by a factor of  $5.5 \times 10^4$ .<sup>313,314</sup> Both of these reactants had cationic ammonium groups attached to them, which were attracted to opposing portals of the CB[6], while the alkyne and azide moieties of the two guests were in close proximity within the cavity (Figure 1.30). This reaction was apparently a rare example of catalysis that demonstrates the Pauling principle of catalysis, which states that complementarity between the transition state of a reaction and an enzyme should be greater than that between the enzyme and the reactants.<sup>154,314,315</sup> Other features of this catalysis that were similar to that observed with enzymes were that the release of the product from CB[6] was the rate limiting step, the reaction rate reached a limit with high concentrations of the reactants, and the substrate was inhibited through the formation of non-reactive ternary complexes (such as CB[6] forming a

complex with two alkynes instead of the alkyne and the azide).<sup>154,314</sup> Mock noted also that if the reactants were sufficiently bulky, the product may not be able to dissociate from the CB[6], and will instead form a rotaxane.<sup>314</sup> Mock's CB[6]-catalyzed 1,3-cycloaddition between alkynes and azides has later been utilized by Steinke and coworkers for the formation of rotaxanes.<sup>316-318</sup> In addition, Steinke has used this methodology for the preparation of oligotriazoles.<sup>319</sup>

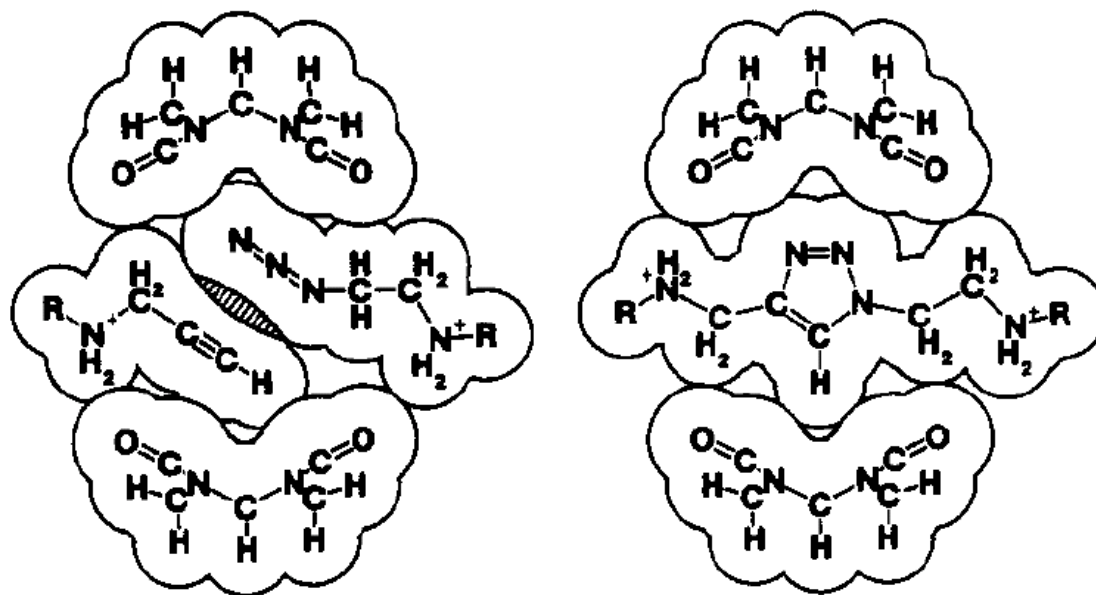


**Figure 1.30** Cross-sectional views of cycloaddition catalyzed by simultaneous complexation of the reactants with CB[6], as proposed by Mock.<sup>314</sup>

Very recently, Nau and coworkers have used CB[6], as well as CB[7], to catalyze the acid hydrolysis of guests such as N-benzoyl-cadaverine, mono-N-(*tert*-butoxy) carbonyl cadaverine, and benzaldoxime (Figure 1.31).<sup>320</sup> In this paper, Nau used CB[6] and CB[7] macrocycles as acid catalysts due to the  $pK_a$  shifts experienced by the guest upon binding. In these systems, Nau used acid-labile substrates attached to anchoring groups that bind strongly to the CB[6] or CB[7] host. The reactive group was positioned close to the portal of the cucurbituril, and the protonation of the guest was induced, which in turn catalyzed the hydrolysis reaction.<sup>320</sup> Depending on the guests, the reactive substrates included amide, carbamate, and

oxime functional groups, while the anchoring group was cadaverine for the former two groups, and a benzyl group for the oxime substrate.

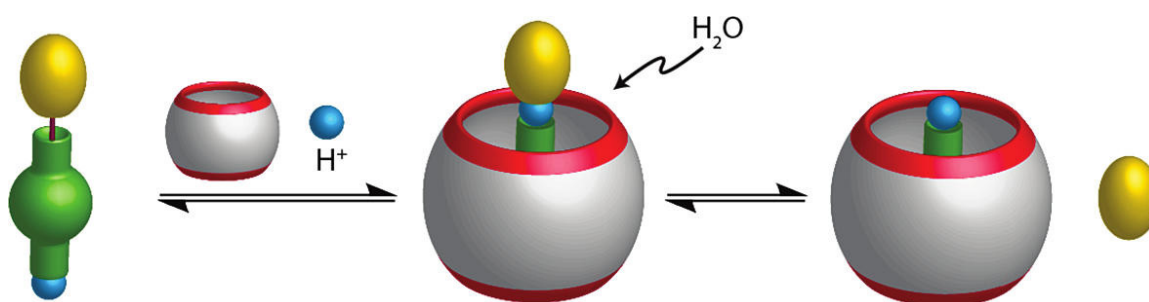


**Figure 1.31** Schematic view of the strategy used by Nau and coworkers for the catalysis of hydrolysis with CB[6] and CB[7]. The acid-labile reactive group (amide, carbamate, or oxime) is shown in yellow, with the anchoring group in green (cadaverine, or phenyl group).<sup>320</sup>

The larger macrocycles, such as CB[7] and especially CB[8], have seen further use for catalyzing and inhibiting reactions, as their larger cavity size allow them to form complexes, including ternary complexes, with a greater variety of guests. As an example, CB[7] has been observed by Macartney and coworkers to mediate the [4+4] photodimerization of 2-aminopyridine to give 4,8-diamino-,3,7-diazatricyclo[4.2.2.2<sup>2,5</sup>]-dodeca-3,7,9,11-tetraene (DADAT<sup>2+</sup>).<sup>262</sup> This photodimerization was stereoselective, as only the *anti-trans*-DADAT<sup>2+</sup> was formed, while in the absence of CB[7] a 4:1 ratio between the *anti-trans* and *syn-trans* products was observed. This formation of only the *anti-trans*-DADAT<sup>2+</sup> species is apparently due to the arrangement of the monomers upon complexation with CB[7], as they form a 1:2 complex with CB[7] in an *anti-trans* manner in order to enhance their individual electrostatic and hydrogen binding interactions with the portals.<sup>262</sup> The reaction was also observed to require less time to proceed in the presence of CB[7] than without the CB[7].<sup>262</sup> Furthermore, while the dimer has been noted to revert back to the aromatic monomer in the absence of CB[7], this was not observed in the presence of CB[7], with the product being stabilized by the CB[7] host.<sup>262</sup>

Stabilization of guests have also been observed by Kim and coworkers<sup>219</sup> as when diprotonated *trans*-diaminostilbene was bound to the macrocycle, and subsequently irradiated with UV light, it was converted to the *cis* isomer. This isomer was relatively stable in the presence of CB[7] due to the better alignment between the cationic ammonium centres and the electron rich portals, and lasted thirty days at room temperature in CB[7], while it would more readily revert to the *trans* isomer in the absence of CB[7].<sup>219</sup>

Of the CB[*n*] homologues, CB[8] appears to have drawn the most widespread interest in its use as a catalyst, owing to its larger cavity size, which can readily accommodate two aromatic guests. As has been mentioned earlier in this chapter, photodimerization reactions are readily observed in the CB[8] cavity.<sup>248,253-255</sup> As was observed with CB[7] catalysis, selectivity is often observed for one stereoisomer over another, depending on the geometrical arrangement of the guests that best fits into the cavity.<sup>254,255,258</sup>

This stabilization of guests that might otherwise readily undergo decomposition or isomerization, could, in some situations, further enhance the cucurbituril's application as a drug delivery vehicle, particularly if the drug happens to be prone to decomposition.<sup>321</sup> The host could be used to extend the lifetime of an unstable drug so that it will be still active, or retains the required stereochemistry, when it reaches the target. In effect, in addition to acting as molecular containers, cucurbiturils may act as "molecular gloveboxes".

### 1.6.2 Drug Delivery Systems

Considerable interest has been devoted to the use of cucurbiturils as drug delivery vehicles. As mentioned in the discussion of CB[7], Day<sup>227-229</sup> as well as Kim<sup>230</sup> have studied complexation between CB[7] and platinum-based anti-cancer drugs (Day had also explored binding of these drugs with CB[6] and CB[8]).<sup>227-229</sup>

Recently Nau and coworkers<sup>321</sup> have bound the drug thiabendazole to CB[7] and found that complexation with the macrocycle serves to both catalyze the formation of the active form of the drug (the sulfenamide form), and also to enhance the stability of this active form. Traditional limitations to the use of thiabendazole as a drug is the slow conversion to its active cyclic sulfenamide form, while at the same time the active form of the drug is unstable and readily undergoes dimerization and decomposition in acidic environments.<sup>321</sup> Because this drug is used to reduce gastric acid production in the stomach, stability in an acidic environment is necessary for its effectiveness. Nau and coworkers have found that the half-life of the formation of the active form of the drug decreased from five minutes without CB[7] to twenty seconds in the presence of CB[7]. Meanwhile, the active form of the drug had a half-life of sixty minutes at pH 2.9 in the absence of CB[7], which increased to three weeks in the presence of CB[7].<sup>321</sup> A driving force of this stabilization of the sulfenamide form of the drug is a complexation-induced  $pK_a$  shift, as complexation of a guest with CB[7] will stabilize its protonated form.<sup>321</sup>

Kim and coworkers have recently explored the use of nanoparticles based on functionalized CB[6] as drug delivery vehicles.<sup>322,323</sup> The preparation of these CB[6] containing nanoparticles utilize direct functionalization of the CB[6], to yield (3-(6-hydroxyhexanethio)propan-1-oxy)<sub>n</sub>CB[6], from the photoreaction between (allyloxy)<sub>12</sub>CB[6] and 6-mercaptohexanol.<sup>322</sup> The nanoparticles, with diameters of approximately 160 to 190 nm, were formed by sonicating (3-(6-hydroxyhexanethio)propan-1-oxy)<sub>n</sub>CB[6] for half an hour in a mixture of water and a minimal amount of ethanol. They found that hydrophobic guests, such as Nile Red, or the anti-cancer drug paclitaxel, could readily be loaded into the nanoparticle. At the same time, the surface of the nanoparticle could be modified noncovalently by using a spermidine anchor which had high affinity for the CB[6] macrocycle, and appending groups such as fluorescein isothiocyanate or folate. Because human ovarian carcinoma HeLa cells require large amounts of folic acid, and have over-expressed folate receptors on the cancer cell, the authors



hoped to use the spermidine-folate conjugate to enhance the uptake of the nanoparticles by the cancer cells. When they used nanoparticles containing Nile Red in their interior (they used this fluorescent dye as a marker for the nanoparticles), they found that the nanoparticles that were also bound to the spermidine-folate conjugate through the CB[6] macrocycles on the exterior of the nanoparticle were readily taken into the cells after one hour of incubation at 37 °C, with little to no uptake under similar conditions for nanoparticles that were not bound to the spermidine-folate conjugate.<sup>322</sup> This suggests that the nanoparticles bearing the external folate ligands had improved uptake due to folate receptor-mediated endocytosis.<sup>322</sup> When HeLa cells were incubated with paclitaxel in the absence of the nanoparticles, paclitaxel encapsulated by the CB[6] nanoparticles (in the interior), as well as paclitaxel encapsulated by the CB[6] nanoparticles which were bound to the spermidine-folate conjugate on their surface, they found that the respective IC<sub>50</sub> values were 1.24, 0.33, and 0.08 μg mL<sup>-1</sup>.<sup>322</sup> These results indicated an enhancement of the drug activity was observed upon encapsulation by the CB[6] nanoparticles, with further improvement being obtained when these nanoparticles were bound to the spermidine-folate conjugate. In summary, these CB[6]-based nanoparticles provided a platform with a high drug loading capacity, and with surfaces that could be adjusted noncovalently and utilized to enhance the uptake of the nanoparticles into the cells.

A recent paper by Day and coworkers<sup>324</sup> reported complexation between CB[7] and CB[8] with novel tricationic compounds containing two platinum centres and three amine ligands. The compounds, *trans*-[PtCl(NH<sub>3</sub>)<sub>2</sub>]<sub>2</sub>(μ-NH<sub>2</sub>(CH<sub>2</sub>)<sub>3</sub>NH<sub>2</sub>(CH<sub>2</sub>)<sub>3</sub>NH<sub>2</sub>)<sup>3+</sup> (CT033), and *trans*-[PtCl(NH<sub>3</sub>)<sub>2</sub>]<sub>2</sub>(μ-NH<sub>2</sub>(CH<sub>2</sub>)<sub>3</sub>N(CH<sub>3</sub>)<sub>2</sub>(CH<sub>2</sub>)<sub>3</sub>NH<sub>2</sub>)<sup>3+</sup> (CT233), shown in Figure 1.32, have activity against the murine leukemia line L1210 and the cisplatin resistant L1210/DDP subline. Upon complexation of CT033 by CB[7] and CB[8] (in separate experiments for each macrocycle), the macrocycles were found to form a pseudorotaxane with their cavity encapsulating the linkers between the terminal platinum end and the central ammonium, with the

macrocycle shuttling between the two linkers. The compound CT233 differs from CT033 in that the central secondary ammonium nitrogen has been methylated to give a quaternary ammonium group. When CT233 was bound to CB[7] and CB[8], the cucurbiturils were observed to become localized over the quaternary ammonium centre. The greatest upfield shifts were observed for the methyl ammonium protons, suggesting the central quaternary ammonium cation was buried deep in the cucurbituril cavity. This behaviour, although unusual, is consistent with our observations with tetraalkylammonium guests,<sup>61</sup> as well as with choline derivatives, which will be discussed in greater detail in this thesis.

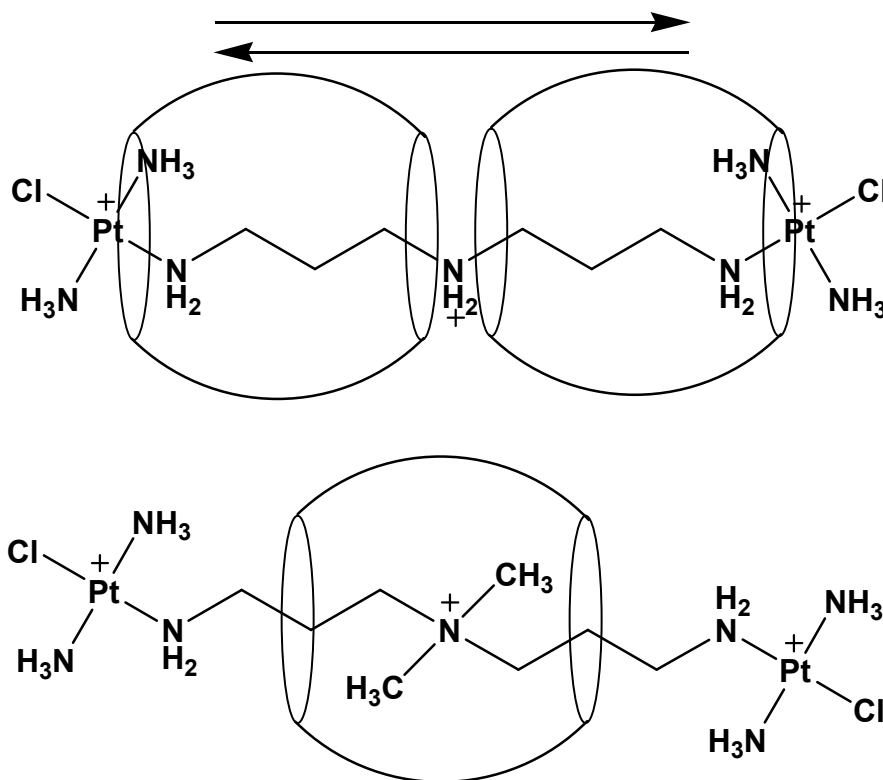


**Figure 1.32** Positioning of CB[7] over CT033, with the delocalized CB[7] shuttling between the two binding positions (above), and CT233, with CB[7] encapsulating the quaternary ammonium centre (below).<sup>324</sup>

There are a variety of benefits that may potentially arise from the use of cucurbiturils as hosts for drugs. In addition to delivery of the drug, the hosts may also be useful for slow or controlled release of a drug. Also, depending on the situation, they may also improve the solubility of a drug,<sup>232</sup> reduce its undesired toxicity,<sup>227</sup> improve its stability,<sup>321</sup> or activate the drug.<sup>321</sup>

### 1.6.3 Separations

Karcher and coworkers have explored the use of CB[6] for water treatment, specifically the removal of reactive dyes from textile wastewater.<sup>325-327</sup> The authors precipitated CB[6] onto silica that was placed in a glass column, in order to prepare CB[6] in the more useful solid state. While the CB[6] did successfully complex with the dyes as insoluble aggregates, dissolution of the CB[6] was unfortunately a problem. This became an issue especially when they tested the CB[6] with actual textile wastewaters, which tend to have a high sodium concentration.<sup>325</sup>

It should be noted that when these papers were published, methods to covalently bind cucurbiturils were not available. More recently, this has been addressed by Kim and coworkers<sup>243,291</sup> through the use of direct functionalization of the cucurbituril, as described earlier in this chapter, and it has been successfully immobilized onto silica stationary phases.<sup>311,328</sup> With perhydroxy-CB[6] immobilized onto silica gel, Liu and coworkers<sup>311</sup> have found that the derivatized CB[6]-bearing silica could be used as a stationary phase for hydrophilic-interaction chromatography (HILIC). HILIC chromatography is somewhat similar to normal phase chromatography, in that the mobile phase is generally nonpolar, except that while in normal phase chromatography the mobile phase contains no water, in HILIC chromatography the mobile phase contains mostly organic solvents mixed with a small amount of water. In both HILIC and normal phase chromatography the stationary phase is hydrophilic. Liu and coworkers have found that HILIC chromatography utilizing CB[6]-immobilized stationary phase could be successfully used

to separate alkaloids, particularly when the mobile phase had a high organic content, such as an 80:20 mixture of acetonitrile and 5 mM Na<sub>2</sub>HPO<sub>4</sub> aqueous buffer solution. This was consistent with hydrophilic interactions, which include interactions between polar molecules such as electrostatic interactions and hydrogen bonding, being the major driving force of the separation.<sup>329,330</sup> Separation was achieved when the aqueous phase was at pH 3.48. Meanwhile, the alkaloids were retained for longer times as the pH of the aqueous buffer component in the mobile phase was increased, while at lower pH, particularly below pH 2.5, when both the alkaloids and CB[6] became protonated, they began to experience electrostatic repulsions. While hydrophilic interactions with the exterior of the perhydroxy-CB[6] bearing stationary phase and the alkaloids were the primary driving forces, when a more polar mobile phase with lower organic solvent content was used, separation was also observed. Although this separation was not as well defined as when the less polar mobile phase was used, it suggested that the hydrophobic effect may also be a secondary driving force in the separation due to the hydrophobic cavity of the perhydroxy-CB[6] attached to the stationary phase.<sup>311</sup>

Cucurbiturils tend to have higher selectivity compared to other hosts such as cyclodextrins and calixarenes, which facilitates their potential use in separations as well as self-sorting systems.

#### **1.6.4 Molecular Switches**

Molecular switches are systems whose properties can be changed by external stimuli such as pH, electrochemical potential, temperature, or solvent polarity. Some examples mentioned earlier have included the complexation between CB[8] and methylviologen, where the stoichiometry of the host-guest system is affected electrochemically. When methylviologen is doubly charged, it binds as a 1:1 system<sup>249</sup> (or alternatively with one methylviologen guest and

another electron rich guest),<sup>250,268</sup> as a result of electrostatic repulsion between doubly cationic methylviologen guests. Meanwhile, when the methylviologen guest is reduced, a 1:2 complex, with one CB[8] host and two monocationic methylviolgens, is readily observed.<sup>249</sup>

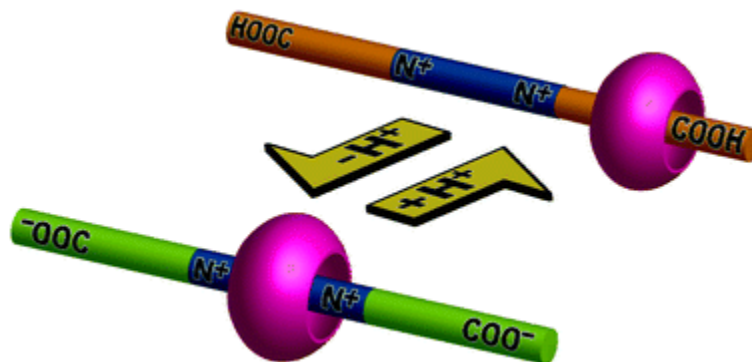


**Figure 1.33** Complexation between CB[7] and a viologen-bearing guest at lower pH (above) and at higher pH, with the CB[7] driven to the central viologen unit away from the carboxylates (below).<sup>331</sup>

The first report, by Mock and Pierpont, of a host-guest system with cucurbiturils acting as a molecular switch, was for the complex between CB[6] and  $\text{PhNH}(\text{CH}_2)_6\text{NH}(\text{CH}_2)_4\text{NH}_2$ , mentioned earlier, with the position of CB[6] being controlled by pH.<sup>175</sup> Kaifer and coworkers have reported pseudorotaxanes between CB[7] and guests containing central viologen units, with the position of the CB[7] being controlled by pH.<sup>331</sup> The viologen has aliphatic linkers with terminal carboxylic acids at either end of the molecule. While the viologen was dicationic throughout the experiment, the terminal carboxylic acids could be deprotonated at higher pH to give anionic carboxylates, giving a zwitterionic guest. At lower pH, Kaifer observed the guest to bind to the terminal aliphatic linkers between the carboxylic acid and the viologen unit. However, when the carboxylic acids became deprotonated, above approximately pH 5, the CB[7] migrated to bind directly over the viologen (Figure 1.33). The CB[7] was driven away from the terminal carboxylates, with their negative charges at higher pH, due to electrostatic repulsion.

While this system was a pseudorotaxane and not a rotaxane in terms of steric bulk, at higher pH it acted as a rotaxane because the anionic carboxylates acted as a barrier to the dissociation of the CB[7].<sup>331</sup>

Also, as seen earlier, Nau<sup>246</sup> has proposed the addition of NaCl may be used to induce the release of guests, such as Neutral Red, from CB[7]. When NaCl was added, they observed that the guest became displaced from the CB[7] cavity, and also its complexation-induced  $pK_a$  shift was decreased.<sup>246</sup>

Kim and coworkers have found that CB[7] can form a hydrogel, with its formation being triggered by pH, as well as temperature.<sup>332</sup> When a heated solution containing CB[7] and dilute sulfuric acid was allowed to cool, a sol-to-gel transition occurred near 42 °C. When the system was heated, on the other hand, a gel-to-sol transition occurred between 43 and 57 °C. Kim and coworkers believe, based on a crystal structure of CB[7] obtained from conditions similar to those used to obtain the hydrogel, but with a lower CB[7] concentration, that the driving force for the hydrogel formation is hydrogen bonding between the CB[7] portals and water molecules or hydronium ions, as well as between the CB[7] molecules themselves. The optimum pH range for formation of the CB[7]-based hydrogel is between pH 0 and 2. Above pH 2 the CB[7] formed a solid precipitate upon cooling, while the solution remained clear upon cooling below pH 0.<sup>332</sup> The presence of alkali cations suppressed the formation of the CB[7] hydrogels, likely by binding to the portals and thus disrupting the formation of the hydrogel.

When 0.1 equivalents of 4,4'-diaminostilbene, which forms a stable guest with CB[7] as the *cis* isomer,<sup>219</sup> was included in the acidic CB[7] solution, a gel also formed upon cooling.<sup>332</sup> In this case the white gel turned into a yellow sol after two hours of UV irradiation at 365 nm. Twelve hours of heating, followed by gradual cooling to room temperature provided a pale yellow gel. This was reversible, with alternate UV treatment and heating creating the sol and gel, respectively, and could be repeated many times. The inclusion complex formed between *trans*-

4,4'-diaminostilbene and CB[7] involves interaction between one ammonium terminus of the guest, but when the guest is the *cis* isomer, both of the ammonium termini are bound to the CB[7] portals.<sup>219,332</sup> The interaction with both portals by the *cis* isomer of the guest apparently disrupts formation of the gel more than the *trans* isomer of the guest, which only interacts with one portal. This was the first report of the configuration of the guest in a host-guest complex affecting the formation of a hydrogel.<sup>332</sup>

### 1.6.5 Chemical Sensors and Imaging

In many cases the complexation between cucurbituril and a guest causes a change in the guest's spectroscopic properties. While this is useful for measuring the complexation between the host and guest, it can also have applications towards detecting the presence of a particular compound that the cucurbituril has an affinity for.

As discussed earlier, recent developments in the use of cucurbiturils as biosensors has been shown by Nau and coworkers, to detect enzymes such as amino acid decarboxylases.<sup>239,240</sup> Kim and coworkers have also shown the ability of CB[7] to be used as glucose sensors.<sup>243</sup>

Nau and coworkers have found that CB[7] binds to the dye rhodamine 6G and also serves to stabilize the dye.<sup>333</sup> In the absence of CB[7] the fluorescence lifetime of the dye was 4.08 ns in aqueous solution, while it was 4.76 ns when bound to CB[7], the longest reported lifetime for that dye.<sup>333</sup> Nau and coworkers proposed that the enhancement of the dye's fluorescent lifetime by binding with CB[7] could have applications toward fluorescence lifetime imaging microscopy. This enhancement of the fluorescence lifetime of the dye was apparently due to the low polarizability of the CB[7] cavity. A small reduction of the dye's radiationless decay rate was also noted, with a reduction from  $2.7 \times 10^7 \text{ s}^{-1}$  to  $2.3 \times 10^7 \text{ s}^{-1}$  in the absence and presence of CB[7], respectively. This was attributed to protection of the dye from quenching by the

surrounding water when it was bound to CB[7]. In addition, Nau noted that CB[7] could reduce photobleaching of rhodamine 6G (which results from photo-induced chemical damage of the dye). They found that the photostability of the dye was improved by a factor of 1.5 when irradiation levels of below  $1 \text{ kW cm}^{-2}$  were used, and was improved further, by a factor of 30, when high levels of irradiation were applied, at  $10 \text{ MW cm}^{-2}$ . This improvement in the photostability of the dye suggested an application of CB[7] as a stabilizer for scanning confocal microscopy.<sup>333</sup> Unlike other stabilizers used, CB[7] does not act as a quencher and does not undergo autofluorescence. Another potential benefit of the use of CB[7] for stabilizing dyes such as rhodamine 6G, is that it was found to reduce the adsorption of the dye onto glass and plastic surfaces. The fluorescence intensity of a  $1 \text{ }\mu\text{M}$  rhodamine 6G solution, stored for several weeks in a borosilicate vial showed no loss after several weeks of storage when it was encapsulated by CB[7] (Figure 1.34). However, in the absence of CB[7], the dye showed a dramatic reduction of its fluorescence intensity over a period of eight days. A final application of CB[7] with regards to dyes such as rhodamine 6G is that it can reduce the aggregation of dyes at higher concentrations (above  $0.1 \text{ mM}$ ), such as those used for dye lasers.<sup>333,334</sup>



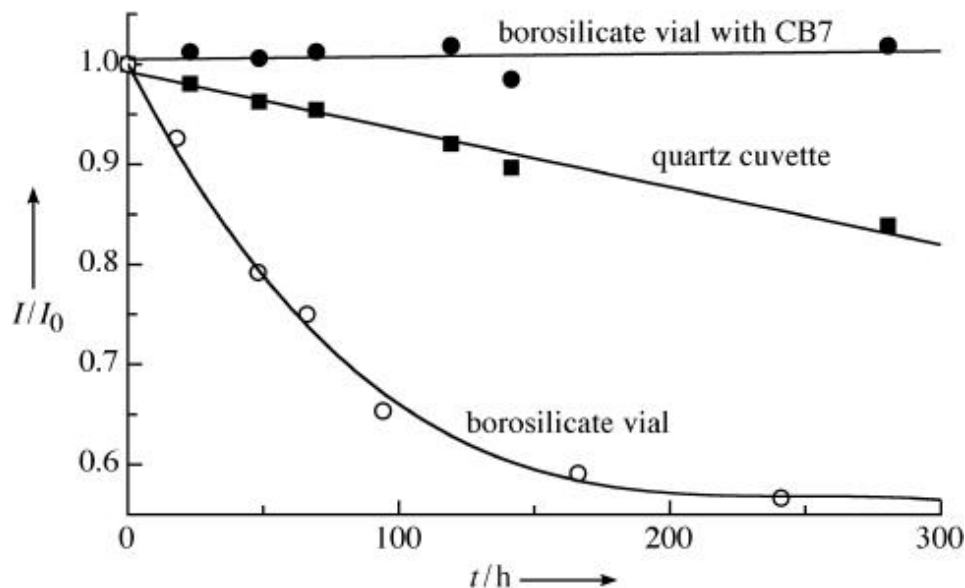


**Figure 1.34** Intensity changes over time of Rhodamine 6G at 1 mM concentration in a borosilicate vial with CB[7], in a quartz cuvette, and in a borosilicate vial.<sup>333</sup>

Li and coworkers have found that complexation with CB[7] enhanced the fluorescence of alkaloids such as palmatine and dehydrocorydaline.<sup>335</sup> Both of these alkaloids are biologically relevant, as palmatine has been shown to have anti-microbial, anti-malarial, anti-inflammatory, and anti-tumor activities, while dehydrocorydaline can inhibit acetylcholinesterase.<sup>335</sup> While there is interest in using isoquinoline alkaloids for photodynamic therapy, their application towards this has been limited by low quantum yields.<sup>335</sup> Li and coworkers observed a dramatic enhancement of the fluorescence quantum yield in the presence of CB[7], with factors of 8.2 and 5.8 for palmatine and dehydrocorydaline, respectively, compared to their quantum yields in the absence of CB[7]. In fact, the improvement was sufficient that fluorescence of the solutions were visible to the naked eye when held under a UV lamp, with the CB[7]-containing solutions of palmatine and dehydrocorydaline showing yellow and cyan fluorescence, respectively. In contrast, similar solutions of each alkaloid that lacked CB[7] did not show observable fluorescence.<sup>335</sup> This demonstrated the potential of CB[7] towards detecting the presence of these

alkaloids, as well as improving their photophysical properties so that they may be used for photodynamic therapy.<sup>335</sup>

## 1.7 Summary, Outlook, and Research Goals

### 1.7.1 Overview of the Field

Cucurbituril research has grown greatly in the over one hundred years since Behrend's initial synthesis of CB[6],<sup>155</sup> and Mock's characterization of CB[6] thirty years ago.<sup>156</sup> While the growth of the field was quite slow when only CB[6], with its poor solubility, was available, the development of methods by Kim<sup>159</sup> and Day<sup>160</sup> to synthesize the other CB[*n*] homologues has opened up significant opportunities for research. Interest in the field has grown rapidly in the nine years since these newer homologues have been made available.

The improved solubility of CB[7] in water, which is comparable to that of  $\beta$ -CD, makes it an attractive host for supramolecular chemistry, as well as for drug delivery systems and biosensors. One challenge that remains is the relatively high cost of CB[7], mostly due to its isolation from the other CB[*n*] homologues. Hopefully, as interest grows in the field, methods for its synthesis and purification will be refined and may in turn reduce its cost. In the meantime, its higher cost is often at least partially compensated for with its higher affinity for guests (for example CB[7] often binds to guests with 2 to 3 orders of magnitude higher affinity than  $\beta$ -CD), as well as its good selectivity.

An ultimate test for the utility of CB[*n*] as hosts for drug delivery systems will be whether they are sufficiently safe for human consumption. Preliminary results seem somewhat promising in this regard,<sup>336</sup> and even if this does become an issue, there seems to be strong potential application for these hosts for sensors in assays, as well as for separations, catalysis, and molecular switches.

Although not a major focus of this thesis, the derivatization of cucurbiturils has been a challenge, and many early attempts were met with limited success. This has traditionally been a disadvantage of cucurbiturils compared to cyclodextrins and calixarenes, which have been more readily derivatized. However, the direct functionalization method<sup>291</sup> developed by Kim's group appears to have mitigated this problem. Perhaps the greatest benefit of this method is that it has provided a methodology for covalently immobilizing cucurbiturils onto surfaces, which greatly expands the utility of these hosts.

The future of CB[*n*] chemistry appears promising, and growth has been quite rapid in the last nine years, with an exponential growth in the number of publications, especially in the past five years. While there is always a risk of a field becoming mature, the inherent affinity of CB[*n*] towards many biologically relevant guests, as well as the recent establishment of methods to immobilize CB[*n*] to surfaces, should provide room and interest for the field to continue growing into the future also.

### **1.7.2 Research Summary**

The research that was pursued in the thesis, which will be discussed in the following chapters, involved a number of parallel studies, most of which were focused on complexation of different guests with CB[7]. The families of guests which were studied in this work include a) polar organic solvents, b) dicationic  $\alpha,\omega$ -bis(pyridinium)alkane guests, c) local anaesthetics, d) choline and acetylcholine, and their derivatives, as well as acetylcholinesterase inhibitors such as succinylcholine, decamethonium, and its analogues. A common feature in the work with the acetylcholinesterase inhibitors and local anesthetics is that both of these are medically relevant, specifically towards surgery. While local anaesthetics are used to reduce pain during surgery, the succinylcholine and other acetylcholinesterase inhibitors are used as muscle relaxants for

procedures such as endotracheal intubation.<sup>337</sup> A brief summary of the work conducted in this thesis is given below.

a) Polar Organic Solvents. This project involved the complexation between CB[7] and small, polar organic solvents such as acetone and other ketones, and solvents such as DMSO, acetonitrile, and methyl acetate. Because these guests were not cationic, their binding was not driven by the combination of electrostatic interactions and the hydrophobic effect that was seen in the other projects, as well as many other studies involving cucurbiturils. Instead, the factors in these complexations were a combination of the hydrophobic effect and dipole-quadrupole interactions. In addition, the effect of the alkali cations sodium and potassium on the complexation between CB[7] and the guests acetone and acetophenone were studied. These cations cap the CB[7] portals and reduce the binding constants between CB[7] and acetone and acetophenone. The greatest reduction in binding affinity due to the presence of the alkali cations was observed by acetophenone, as this larger guest protruded from the CB[7] cavity somewhat, and its binding was disrupted by the presence of the capping cations.

b)  $\alpha,\omega$ -Bis(pyridinium)alkane guests. A series of dicationic  $\alpha,\omega$ -bis(pyridinium)alkane ligands were synthesized and their formation of pseudorotaxanes with CB[7] was explored. Two main structural features of the pyridinium guests that were varied were the nature and length of the linker, as well as the nature of the terminal substituents of the pyridinium ring that were *para* to the linkers. Depending on the length of the linker and the nature of the substituents present on the guest ligand, most of these guests had the capacity to bind to more than one host. The nature of the terminal substituent could either block, or allow the passage of, the CB[7] towards the centre of the molecule. The properties of the binding between the bis(pyridinium)alkane guests and the CB[7] host were studied, and their binding constants measured.

c) Local Anaesthetics. The host-guest chemistry between the local anaesthetics procaine, procainamide, tetracaine, dibucaine, and prilocaine and CB[7] were explored. With the exception

of prilocaine, these guests had two protonation sites with widely separated  $pK_a$  values. Therefore, one aspect of this project was to study the effect of pH on the binding between CB[7] and the anaesthetic. In some cases protonation of the second site changed the preferred binding position of the CB[7], so that they behaved as pH-activated switches. The effects of CB[7] inclusion on the  $pK_a$  values of the guests were also explored.

d) Choline, Acetylcholine, Succinylcholine and derivatives. The host-guest chemistry between CB[7] and choline, acetylcholine and succinylcholine and their derivatives was studied. Derivatives were synthesized that contained triethylammonium, trimethylphosphonium, and triethylphosphonium head groups in place of the native trimethylammonium cation. In addition, the guests studied in this family were compared to their aliphatic analogues, most notably with the use of dicationic guests containing peralkylated head groups connected by aliphatic (usually decyl) linkers. One unusual result that was observed in the course of this research was that for the pseudorotaxanes formed between CB[7] and these onium cationic guests, the cationic centres of these guests were often located deep in the CB[7] cavity, instead of near the electron rich portals, where cations normally bind. This was attributed to the alkyl groups bound to the ammonium nitrogen, which effectively diffused the charge, making the cation more hydrophobic. The work involving the binding between CB[7] and the monocationic choline acetylcholine guests is the focus of Chapter 5 in this thesis, while the dicationic acetylcholinesterase inhibitors, as well as their derivatives is discussed in Chapter 6. The study of the choline and acetylcholine guests, as well as the dicationic acetylcholinesterase inhibitors are essentially two projects, but they are closely related in that the guest contain quaternary ammonium and phosphonium centres, and they both have relevance to the enzyme acetylcholinesterase. While the neurotransmitter acetylcholine is a substrate of the enzyme acetylcholinesterase (with choline being the enzyme product), succinylcholine and other acetylcholinesterase inhibitors act by binding to acetylcholinesterase, and thus blocking access of acetylcholine to the enzyme.<sup>337</sup>

### 1.7.3 Research Goals

A goal of these studies is to further understanding of the host-guest binding between CB[7] between various cationic and neutral guests. In order to do this, the potential role of quadrupole-dipole interactions was explored through the use of the carbonyl-bearing nonpolar solvents. In addition, the somewhat unusual encapsulation of the cationic regions of guests, within the CB[7] cavity, as opposed to them being bound to the electron rich portal, was observed when the cations were made up of charge diffuse cations, such as the quaternary ammonium- and phosphonium-bearing guests. Throughout these studies, the effects of different structures of the guests within a given series were explored, either by incorporating different functional groups into a structure, or incorporating similar substituents of different sized and/or positions within the guest.

While the studies involving the binding between CB[7] and the solvent guests, as well as the series of  $\alpha,\omega$ -bis(pyridinium)alkanes, were essentially fundamental in nature, binding between CB[7] and medically relevant guests, such as local anaesthetics, acetylcholine and choline derivatives, as well as succinylcholine, and other acetylcholinesterase inhibitors, were also explored. The host-guest binding systems between CB[7] and these guests may have potential medical applications, either through the use of CB[7] as a vehicle for drug delivery systems, or for controlled release. In addition, as adverse side-effects have occasionally been reported with succinylcholine and other muscle relaxants when they are administered to patients,<sup>337,338</sup> CB[7] may be useful as a drug-reversal agent, if it is administered to a patient who is experiencing complications with succinylcholine.

## References

1. P.D. Beer, P.A. Gale, and David K. Smith, *Supramolecular Chemistry*, Oxford Chemistry Primers, 74, Oxford University Press: Oxford, 2003; pp. 1-14.
2. J. M. Lehn, *Angew. Chem., Int. Ed. Engl.*, **1988**, 27, 89.
3. J.M. Lehn, *Science*, **1985**, 227, 849.
4. Jeffrey, G.A., *An Introduction to Hydrogen Bonding*, Oxford University Press: New York, 1997; pp. 11-32.
5. G.R. Desirau, *Hydrogen Bonding*, In *Encyclopedia of Supramolecular Chemistry*, Marcel Dekker: New York, 2004; pp. 658-665.
6. A.D. Buckingham, J.E. Del Bene, and S.A.C. McDowell, *Chem. Phys. Lett.*, **2008**, 463, 1.
7. E. Arunan, *Current Science*, **2007**, 92, 17.
8. C. Prior, *Chemistry Review*, **2003**, 13, 12.
9. R.H.S. Winterton, *Contemp. Phys.*, **1970**, 11, 559.
10. T. Zeegers-Huyskens and P. Huyskens, *Chapter 1: Intermolecular Forces, Intermolecular Forces An Introduction to Modern Methods and Results*, P.L. Huyskens, W.A.P. Luck, and T. Zeegers-Huyskens (eds.), Springer-Verlag: Berlin, 1991; pp. 1-30.
11. H.-J. Schneider, *van der Waals Forces*, In *Encyclopedia of Supramolecular Chemistry*, Marcel Dekker, Inc.: New York, 2004; pp. 1550-1556.
12. D.H. Kim, *Chapter 14: Supramolecular Aspects of Enzymes*, In *Comprehensive Supramolecular Chemistry, Vol. 4*, J.L. Atwood, J.E.D. Davies, D.D. MacNicol, F. Vogtle, (eds.), Pergamon: New York, 1996; pp. 503-526.
13. G.R. Desirau, *Nature*, **2001**, 412, 397.
14. P.S. Murthy, *J. Chem. Ed.*, **2006**, 83, 1010.
15. D. Leckband and J. Israelachvili, *Q. R. Biophys.*, **2001**, 34, 105.
16. D. Chandler, *Nature*, **2005**, 437, 29.

17. E.E. Meyer, K.J. Rosenberg, and J. Israelachvili, *Proc. Nat. Acad. Sci. U.S.A.*, **2006**, *103*, 15739.
18. H.-J. Schneider, *Hydrophobic Effects*, In *Encyclopedia of Supramolecular Chemistry*, J.L. Atwood, J.W. Steed (eds.), Marcel Dekker: Inc., New York, 2004; pp.673-678.
19. J.W. Steed, D.R. Turner, and K.J. Wallace, *Core Concepts in Supramolecular Chemistry*, John Wiley & Sons, Ltd., Chichester, 2007; pp. 17-26.
20. N.T. Southall, K.A. Dill, and A.D.J. Haymet, *J. Phys. Chem. B.*, **2002**, *106*, 521.
21. H.S. Frank and M.W. Evans, *J. Chem. Phys.*, **1945**, *13*, 507.
22. B. Kronberg, M. Costas, and Rebecca Silveston, *J. Dispersion Sci. Technol.*, **1994**, *15*, 333.
23. K.A. Sharp, *Curr. Opin. Struct. Biol.*, **1991**, *1*, 171.
24. G. Graziano, *J. Chem. Soc., Faraday Trans.*, **1998**, *94*, 3345.
25. K. Shinoda, *J. Phys. Chem.*, **1977**, *81*, 1300.
26. K. Shinoda and M. Fujihara, *Bull. Chem. Soc. Jpn.*, **1968**, *41*, 2612.
27. I. Dance,  *$\pi$ - $\pi$  Interactions: Theory and Scope*, In *Encyclopedia of Supramolecular Chemistry*, J.L. Atwood, J.W. Steed (eds.), Marcel Dekker, Inc.: New York, 2004; pp. 1076-1092.
28. C.A. Hunter, *Chem. Soc. Rev.*, **1994**, 101.
29. S. Grimme, *Angew. Chem., Int. Ed.*, **2008**, *47*, 3430.
30. H.-J. Schneider and A.K. Yatsimirsky, *Principles and Methods in Supramolecular Chemistry*, John Wiley and Sons, Ltd.: Chichester, 2000; pp. 89-95.
31. D.A. Dougherty, *Cation- $\pi$  Interactions*, In *Encyclopedia of Supramolecular Chemistry*, J.L. Atwood, J.W. Steed (eds.), Marcel Dekker, Inc.: New York, 2004; pp. 214-218.
32. J.M. Lehn, *Pure & Appl. Chem.*, **1978**, *50*, 871.



33. J.A. Thomas, *Self-Assembly: Definition and Kinetic and Thermodynamic Considerations*, In *Encyclopedia of Supramolecular Chemistry*, J.L. Atwood, J.W. Steed (eds.), Marcel Dekker, Inc.: New York, 2004; pp. 1248-1256.
34. J.W. Steed, *Supramolecular Chemistry: Definition*, In *Encyclopedia of Supramolecular Chemistry*, J.L. Atwood, J.W. Steed (eds.), Marcel Dekker, Inc.: New York, 2004; pp. 1401-1411.
35. P.D. Beer, P.A. Gale, and David K. Smith, *Supramolecular Chemistry*, Oxford Chemistry Primers, 74, Oxford University Press: Oxford, 2003; pp. 61-80.
36. B. Konig, *J. Prakt. Chem.*, **1995**, 337, 339.
37. G.M. Whitesides, J.P. Mathias, C.T. Seto, *Science*, **1991**, 254, 1312.
38. J.M. Lehn, *Angew. Chem., Int. Ed. Engl.*, **1988**, 27, 89.
39. J.M. Lehn, *Pharm. Acta Helv.*, **1995**, 69, 205.
40. K. Ariga and T. Kunitake, *Supramolecular Chemistry – Fundamentals and Applications*, Springer-Verlag: Berlin, 2006; pp. 30-31.
41. L.F. Lindoy, *The Chemistry of Macrocyclic Complexes*, Cambridge University Press: Cambridge, 1989; pp. 176-185.
42. D.J. Cram, *Angew. Chem., Int. Ed. Engl.*, **1986**, 25, 1039.
43. A. Rang and C.A. Schalley, *Catenanes and Other Interlocked Molecules*, In *Encyclopedia of Supramolecular Chemistry*, J.L. Atwood, J.W. Steed (eds.), Marcel Dekker, Inc.: New York, 2004; pp. 206-213.
44. J.W. Steed, D.R. Turner, and K.J. Wallace, *Core Concepts in Supramolecular Chemistry and Nanochemistry*, John Wiley & Sons, Ltd.: Chichester, 2007; pp. 133-155
45. B. Dietrich, *Cryptands*, In *Encyclopedia of Supramolecular Chemistry*, J.L. Atwood, J.W. Steed (eds.), Marcel Dekker, Inc.: New York, 2004; pp. 334-339.

46. A. Rang and C.A. Schalley, *Catenanes and Other Interlocked Molecules*, In *Encyclopedia of Supramolecular Chemistry*, J.L. Atwood, J.W. Steed (eds.), Marcel Dekker, Inc.: New York, 2004; pp. 206-213.
47. P. Linnartz and C.A. Schalley, *Rotaxanes and Pseudorotaxanes*, In *Encyclopedia of Supramolecular Chemistry*, J.L. Atwood, J.W. Steed (eds.), Marcel Dekker, Inc.: New York, 2004; pp. 1194-1201.
48. H.-J. Schneider and A.K. Yatsimirsky, *Principles and Methods in Supramolecular Chemistry*, John Wiley & Sons Ltd.: Chichester, 2000; pp. 227-258.
49. J.W. Steed and J.L. Atwood, *Supramolecular Chemistry*, John Wiley & Sons, Ltd.: Chichester, 2000; pp. 15-19.
50. J.K.M. Sanders and B.K. Hunter, *Modern NMR Spectroscopy. A Guide for Chemists*; Oxford University Press: Oxford, 1988; pp. 208-211.
51. K.A. Connors, *Binding Constants. The Measurement of Complex Stability*, John Wiley & Sons: New York, 1987; pp. 189-193.
52. K. Hirose, *J. Incl. Phenom. Macrocycl. Chem.*, **2001**, 39, 193.
53. A. Moser and C. Detellier, *Nuclear Magnetic Resonance Spectroscopy*, In *Encyclopedia of Supramolecular Chemistry*, J.L. Atwood, J.W. Steed (eds.), Marcel Dekker, Inc.: New York, 2004; pp. 981-988.
54. Z. Dauter and K.S. Wilson, *Chapter 1: Diffraction Techniques*, In *Comprehensive Supramolecular Chemistry, Volume 8*, J.E.D. Davies and J.A. Ripmeester (volume eds.), J.L. Atwood, J.E.D. Davies, D.D. MacNicol, F. Vogle and J.M. Lehn (eds.), Pergamon: New York, 1996; pp. 1-31.
55. K. Rissanen, *X-Ray Crystallography*, In *Encyclopedia of Supramolecular Chemistry*, J.L. Atwood, J.W. Steed (eds.), Marcel Dekker, Inc.: New York, 2004; pp. 1586-1591.
56. C.A. Schalley, *Mass Spectrom. Rev.*, **2001**, 20, 253.

57. C.A. Schalley, *Int. J. Mass Spectrom.*, **2000**, *194*, 11.
58. J.W. Steed, D.R. Turner, and K.J. Wallace, *Core Concepts in Supramolecular Chemistry and Nanochemistry*, John Wiley & Sons, Ltd.: Chichester, 2007; pp. 14-15.
59. H.-J. Schneider and A. Yatsimirsky, *Principles and Methods in Supramolecular Chemistry*, John Wiley & Sons Ltd.: Chichester, 2000; pp. 137-226.
60. S. Liu, C. Ruspic, P. Mukhopadhyay, S. Chakrabarti, P.Y. Zavalij, and L. Isaacs, *J. Am. Chem. Soc.*, **2005**, *127*, 15959.
61. A.D. St-Jacques, I.W. Wyman, and D.H. Macartney, *Chem. Commun.*, **2008**, 4936.
62. A. Lustringhaus, *Ann. Chem.*, **1937**, *181*, 528.
63. D.A. Laidler and F.J. Stoddart, *Chapter 1: Synthesis of crown ethers and analogs*, In *Crown Ethers and Analogous Compounds*, S. Patai and Z. Rappoport (eds.), John Wiley & Sons: Chichester, 1989; pp. 1-57.
64. J.L. Down, J. Lewis, B. Moore, and G.W. Wilkinson, *Proc. Chem. Soc.*, **1957**, 209.
65. J.L. Down, J. Lewis, B. Moore, and G. Wilkinson, *J. Chem. Soc.*, **1959**, 3767.
66. M. Hiraoka, *Studies in Organic Chemistry, Vol. 45, Chapter 1: Introductory Remarks*, In *Crown Ethers and Analogous Compounds*, M. Hiraoka (ed.), 1992, Elsevier Science Publishers B.V.: Amsterdam, 1992; pp. 1-16.
67. J.S. Bradshaw, R.M. Izatt, A.V. Bordunov, C.Y. Zhu, and J.K. Hathaway, *Chapter 2: Crown Ethers*, In *Comprehensive Supramolecular Chemistry, Vol. 1*, J.L. Atwood, J.E.D. Davies, D.D. MacNicol, F. Vogle and J.M. Lehn (eds.), G.W. Gokel (volume ed.), Pergamon: New York, 1996; pp. 35-95.
68. C.J. Pedersen, *J. Am. Chem. Soc.*, **1967**, *89*, 2495.
69. C.J. Pedersen, *J. Am. Chem. Soc.*, **1967**, *89*, 7017.
70. C.J. Pedersen, *Science*, **1988**, *241*, 536.

71. G.W. Gokel, *Crown Ethers*, In *Encyclopedia of Supramolecular Chemistry*, J.L. Atwood, J.W. Steed (eds.), Marcel Dekker, Inc.: New York, 2004; pp. 326-333.
72. J.W. Steed, D.R. Turner, and K.J. Wallace, *Core Concepts in Supramolecular Chemistry and Nanochemistry*, John Wiley & Sons, Ltd.: Chichester, 2007; pp. 36-51.
73. J.M. Lehn and J.P. Sauvage, *J. Am. Chem. Soc.*, **1975**, *97*, 6700.
74. E. Weber, *Chapter 5: New Developments in Crown Ether Chemistry: Lariat, spherand and second-sphere complexes*, In *Crown Ethers and Analogs*, S. Patai and Z. Rappoport (eds.), John Wiley & Sons Ltd.: Chichester, 1989; pp. 305-357.
75. B. Dietrich, J.-M. Lehn, and J.-P. Sauvage, *Tetrahedron Lett.*, **1969**, *10*, 2885.
76. B. Dietrich, J.-M. Lehn, and J.-P. Sauvage, *Tetrahedron Lett.*, **1969**, *10*, 2889.
77. A. Pochini and R. Ungaro, *Chapter 4: Calixarenes and Related Hosts*, In *Comprehensive Supramolecular Chemistry, Volume 2*, J.L. Atwood, J.E.D. Davies, D.D. MacNicol, F. Vogtle and J.M. Lehn (eds.), F. Vogtle (volume ed.), Pergamon: New York, 1996; pp. 103-142.
78. C.D. Gutsche, *Monographs in Supramolecular Chemistry, Calixarenes An Introduction 2nd Edition*, J.F. Stoddart (series ed.), The Royal Society of Chemistry: Cambridge, 2008; pp. 1-37.
79. C.D. Gutsche, *Calixarenes: Synthesis and Historical Perspectives*, In *Encyclopedia of Supramolecular Chemistry*, J.L. Atwood, J.W. Steed (eds.), Marcel Dekker, Inc.: New York, 2004; pp. 153-160.
80. D.R. Stewart and C.D. Gutsche, *J. Am. Chem. Soc.*, **1999**, *121*, 4136.
81. C.D. Gutsche and R. Muthukrishnan, *J. Org. Chem.*, **1978**, *43*, 4905.
82. C.D. Gutsche, J.S. Rogers, D. Stewart, and K.-A. See, *Pure & Appl. Chem.*, **1990**, *62*, 485.
83. A. Baeyer, *Ber.*, **1872**, *5*, 25, 280, 1094.

84. D. Gutsche, *Chapter 1: Calixarenes: A Personal History*, In *Calixarenes in the Nanoworld*, J. Vicens, J. Harrowfield (eds.), L. Bklouti (assistant ed.), Springer: Dordrecht, 2007; pp. 1-19.
85. L.H. Baekeland, U.S. Patent 942, 699 (October 1908).
86. A. Zinke and E. Ziegler, *Ber. Dtsch. Chem. Ges.*, **1944**, 77, 264.
87. A. Zinke and E. Ziegler, *Wiener Chem. Ztg.*, **1944**, 47 (13/14), 151.
88. T. Kappe, *J. Incl. Phenom. Mol. Recognit. Chem.*, **1994**, 19, 3.
89. A. Zinke and E. Ziegler, *Ber. Dtsch. Chem. Ges.*, **1941**, 74, 1729.
90. R.S. Buriks, A.R. Fauke, and J.H. Munch, U.S. Patents 4,032,514, 4,0998,717, and 4,259,464.
91. C.D. Gutsche, *Monographs in Supramolecular Chemistry, Calixarenes*, J.F. Stoddart (series ed.), The Royal Society of Chemistry: Cambridge, 1989; pp. 16-35.
92. C.D. Gutsche, B. Dhawan, K.H. No, and R. Muthukrishan, *J. Am. Chem. Soc.*, **1981**, 103, 3782.
93. C.D. Gutsche, *Monographs in Supramolecular Chemistry, Calixarenes*, J.F. Stoddart (series ed.), The Royal Society of Chemistry: Cambridge, 1989; pp. 106-134.
94. R. Ungaro, A. Pochini, and G.D. Andreotti, *J. Incl. Phenom. Mol. Recognit. Chem.*, **1984**, 2, 199.
95. R. Ungaro, A. Casnati, F. Ugozzoli, A. Pochini, J.-F. Dozol, C. Hill, and H. Rouquette, *Angew. Chem., Int. Ed. Engl.*, **1994**, 33, 1506.
96. A. Casnati, A. Pochini, R. Ungaro, F. Ugozzoli, F. Arnaud, S. Fanni, M.-J. Schwing, R.J.M. Egberink, F. de Jong, and D.N. Reinhoudt, *J. Am. Chem. Soc.*, **1995**, 117, 2767.
97. P. Thuery, M. Nierlich, V. Lamare, J.-F. Dozol, Z. Asfari, and J.Vicens, *Acta Cryst.*, **1996**, C52, 2729.

98. P.J. Cragg, *Homocalixarenes*, In *Encyclopedia of Supramolecular Chemistry*, J.L. Atwood, J.W. Steed (eds.), Marcel Dekker, Inc.: New York, 2004; pp. 649-657.
99. G. Brodesser, F. Vogtle, *J. Incl. Phenom. Mol. Recognit. Chem.*, **1994**, *19*, 111.
100. J.W. Steed and J.L. Atwood, *Supramolecular Chemistry*, John Wiley & Sons, Ltd.: Chichester, 2000; pp. 169-182.
101. R.M. Izatt, J.D. Lamb, R.T. Hawkins, P.R. Brown, S.R. Izatt, and J.J. Christensen, *J. Am. Chem. Soc.*, **1984**, *105*, 1782.
102. A.W. Coleman, A.N. Lazar, E. Da Silva, *Calixarenes and their Analogues: Cation Complexation*, In *Encyclopedia of Supramolecular Chemistry*, J.L. Atwood, J.W. Steed (eds.), Marcel Dekker, Inc.: New York, 2004; pp. 137-144.
103. M.A. McKervey, M.-J. Schwing-Weill, and F. Arnaud-Neu, *Chapter 15: Cation Binding by Calixarenes*, In *Comprehensive Supramolecular Chemistry, Volume 1*, J.L. Atwood, J.E.D. Davies, D.D. MacNicol, F. Vogtle and J.M. Lehn (eds.), Pergamon: New York, 1996; pp. 537-603.
104. A. Pochini and A. Arduini, *Chapter 3: Recognition of Neutral Molecules by Calixarenes in Solution and in Gas Phase*, In *Calixarenes in Action*, L. Mandolini and R. Ungaro (eds.), Imperial College Press: London, 2000; pp. 37-61.
105. V. Bohmer, *Angew. Chem., Int. Ed. Engl.*, **1995**, *34*, 713.
106. I. Stibor and P. Lhotak, *Calixarenes and their analogues: Molecular Complexation*, In *Encyclopedia of Supramolecular Chemistry*, J.L. Atwood, J.W. Steed (eds.), Marcel Dekker, Inc.: New York, 2004; pp. 145-152.
107. A. Arduini, A. Pochini, A. Secchi, and D. Ugozzoli, *Chapter 25: Recognition of Neutral Molecules*, In *Calixarenes 2001*, Kluwer Academic Publishers: Dordrecht, 2001; pp. 457-475.
108. L.J. Bauer and C.D. Gutsche, *J. Am. Chem. Soc.*, **1985**, *107*, 6063.

109. C.D. Gutsche, M. Iqbal, and I. Alam, *J. Am. Chem. Soc.*, **1987**, *109*, 4314.
110. J.W. Steed, D.R. Turner, and K.J. Wallace, *Core Concepts in Supramolecular Chemistry and Nanochemistry*, John Wiley & Sons, Ltd.: Chichester, 2007; pp. 85-90.
111. J.B. Niederl and H.J. Vogel, *J. Am. Chem. Soc.*, **1940**, *62*, 2512.
112. P. Timmerman, W. Verboom, and D.N. Reinhoudt, *Tetrahedron*, **1996**, *52*, 2663.
113. A. Michael, *Ber. Dtsch. Chem. Ges.* **1883**, *17*, 20.
114. J.B. Niederl and H.J. Vogel, *J. Am. Chem. Soc.*, **1940**, *62*, 2512.
115. H. Erdtman, S. Hogsberg, S. Abrahamsom, and B. Nilsson, *Tetrahedron Lett.*, **1968**, *9*, 1679.
116. B. Nilsson, *Acta Chim. Scand.*, **1968**, *22*, 732.
117. B. Botta, M. Cassani, I. D'Acquarica, D. Misiti, D. Subissati, and G. Delle Monache, *Curr. Org. Chem.*, **2005**, *9*, 337.
118. K. Rissanen, *Angew. Chem., Int. Ed.*, **2005**, *44*, 3652.
119. B. Botta, M. Cassani, I. D'Acquarica, D. Subissati, G. Zappia, and G.D. Monache, *Curr. Org. Chem.*, **2005**, *9*, 1167.
120. B.C. Gibb, *Cavitands*, In *Encyclopedia of Supramolecular Chemistry*, J.L. Atwood, J.W. Steed (eds.), Marcel Dekker, Inc.: New York, 2004; pp. 219-222.
121. B.C. Gibb, *Carcerands and Hemicarcerands*, In *Encyclopedia of Supramolecular Chemistry*, J.L. Atwood, J.W. Steed (eds.), Marcel Dekker, Inc.: New York, 2004; pp. 189-192.
122. C. Naumann and J.C. Sherman, *Chapter 10: Carcerands*, In *Calixarenes 2001*, Z. Asfari, V. Bohmer, J. Harrowfield, J. Vicens, and M. Saadioui (eds.), Kluwer Academic Publishers: New York, 2002; pp. 199-218.
123. D.J. Cram, *Science*, **1983**, *219*, 1177.

124. D.J. Cram, S. Karbach, Y.H. Kim, L. Baczynskyj, and G. Kallemeyn, *J. Am. Chem. Soc.*, **1985**, *107*, 2575.
125. D.J. Cram, S. Karbach, Y.H. Kim, L. Baczynskyj, K. Marti, R.M. Sampson, and G.M. Kallemeyn, *J. Am. Chem. Soc.*, **1988**, *110*, 2554.
126. J.E. Falk, *Porphyrins and Metalloporphyrins*, Elsevier Publishing Company: Amsterdam, 1964; pp. 1-29.
127. E.B. Fleischer, *Acc. Chem. Res.*, **1970**, *3*, 105.
128. W. Kuster, *Z. Physiol. Chem.*, **1912**, *82*, 463.
129. H. Fischer and K. Zeile, *Ann. Chem.*, **1929**, *468*, 98.
130. R. Mishra and T.K. Chandrashekar, *Acc. Chem. Res.*, **2008**, *41*, 265.
131. R.B. Woodward, Presented at the Aromaticity Conference, Sheffield, UK, 1966.
132. J.L. Sessler and D. Seidel, *Angew. Chem., Int. Ed.*, **2003**, *42*, 5134.
133. A. Jasat and D. Dolphin, *Chem. Rev.*, **1997**, *97*, 2267.
134. J. Setsune and S. Maeda, *J. Am. Chem. Soc.*, **2000**, *122*, 12405.
135. M. Shionoya, H. Furuta, V. Lynch, A. Harriman, and J.L. Sessler, *J. Am. Chem. Soc.*, **1992**, *114*, 5714.
136. J.L. Sessler and J.M. Davis, *Acc. Chem. Res.*, **2001**, *34*, 989.
137. J.W. Steed and J.L. Atwood, *Supramolecular Chemistry*, John Wiley & Sons, Ltd.: Chichester, 2000; pp. 669-683.
138. S. Van Doorslaer, *Vitamin B12 and Heme Models*, In *Encyclopedia of Supramolecular Chemistry*, J.L. Atwood, J.W. Steed (eds.), Marcel Dekker, Inc.: New York, 2004; pp. 1569-1575.
139. K. Berg, P.K. Selbo, A. Weyergang, A. Dietze, L. Prasmickaite, A. Bronsted, B.O. Engesaeter, E. Angell-Petersen, T. Warloe, N. Frandsen, and A. Hogset, *J. Microsc.*, **2005**, *218*, 133.



140. E.D. Sternberg, D. Dolphin, and C. Bruckner, *Tetrahedron*, **1998**, *54*, 4151.
141. H. Dodziuk, *Molecules with Holes – Cyclodextrins*, In *Cyclodextrins and Their Complexes*, H. Dodziuk (ed.), Wiley-VCH Verlag GmbH & Co. KGaA: Weinheim, 2006; pp. 1-30.
142. J. Szejtli, *Cyclodextrins*, In *Encyclopedia of Supramolecular Chemistry*, J.L. Atwood, J.W. Steed (eds.), Marcel Dekker, Inc.: New York, 2004; pp. 398-404.
143. J.W. Steed and J.L. Atwood, *Supramolecular Chemistry*, John Wiley & Sons, Ltd.: Chichester, 2000; pp. 321-334.
144. J. Szejtli, *Chem. Rev.*, **1998**, *98*, 1743.
145. F.W. Lichtenthaler and S. Immel, *Tetrahedron: Asymmetry*, **1994**, *5*, 2045.
146. A. Harada, *Acc. Chem. Res.*, **2001**, *34*, 456.
147. J.F. Stoddart, *Carbohydrate Res.*, **1989**, *192*, xii-xv.
148. A. Villiers, *Compt. Rend.*, **1891**, *112*, 536.
149. D. French, *Adv. Carbohydr. Chem.*, **1957**, *12*, 189.
150. F. Schardinger, *Zentralb. Bakteriol. Parasitenk. Abt. 2*, **1911**, *29*, 188.
151. F. Schardinger, *Wien. klin. Wochschr.*, **1904**, *17*, 204.
152. J. Szejtli, *Chapter 5: Inclusion of Guest Molecules, Selectivity and Molecular Recognition by Cyclodextrins*, In *Comprehensive Supramolecular Chemistry, Volume 3*, J. Szejtli and T. Osa (volume eds.), J.L. Atwood, J.E.D. Davies, D.D. MacNicol, F. Vogle and J.M. Lehn (eds.), Pergamon: New York, 1996; pp. 189-203.
153. H. Dodziuk, *Chapter 16: Applications other than in the pharmaceutical industry*, In *Cyclodextrins and Their Complexes*, H. Dodziuk (ed.), Wiley-VCH Verlag GmbH & Co. KGaA: Weinheim, 2006; pp. 450-473.
154. J. Lagona, P. Mukhopadhyay, S. Chakrabarti, and L. Isaacs, *Angew. Chem., Int. Ed.*, **2005**, *44*, 4844.
155. R. Behrend, E. Meyer, F. Rusche, *Justus Liebigs Ann. Chem.*, **1905**, *339*, 1-37.

156. W.A. Freeman, W.L. Mock, and N.Y. Shih, *J. Am. Chem. Soc.*, **1981**, *103*, 7367.
157. W.L. Mock, *Top. Curr. Chem.*, **1995**, *175*, 1.
158. W.L. Mock, *Chapter 15: Cucurbituril*, In *Comprehensive Supramolecular Chemistry, Volume 2*, J.L. Atwood, J.E.D. Davies, D.D. MacNicol, F. Vogle and J.M. Lehn (eds.), F. Vogtle (volume ed.), Pergamon: New York, 1996; pp. 477-493.
159. J. Kim, I.-S. Jung, S.-Y. Kim, E. Lee, J.-K. Kang, S. Sakamoto, K. Yamaguchi, and K. Kim, *J. Am. Chem. Soc.*, **2000**, *122*, 540.
160. A. Day, A.P. Arnold, R.J. Blanch, and B. Snushall, *J. Org. Chem.*, **2001**, *66*, 8094.
161. J.W. Lee, S. Samal, N. Selvapalam, H.-J. Kim, and K. Kim, *Acc. Chem. Res.*, **2003**, *36*, 621.
162. H.-J. Buschmann, E. Cleve, K. Jansen, A. Wego, E. Schollmeyer, *Mater. Sci. Eng. C*, **2001**, *14*, 35.
163. A.I. Day, R.J. Blanch, A.P. Arnold, S. Lorenzo, G.R. Lewis, I. Dance, *Angew. Chem., Int. Ed.*, **2002**, *41*, 275.
164. L. Isaacs, *Chem. Commun.*, **2009**, 619.
165. C. Marquez, R.R. Hudgins, and W.M. Nau, *J. Am. Chem. Soc.*, **2004**, *126*, 5806.
166. P. Cintas, *J. Incl. Phenom. Mol. Recognit. Chem.*, **1994**, *17*, 205.
167. W.L. Mock and N.-Y. Shih, *J. Org. Chem.*, **1983**, *48*, 3618.
168. W.L. Mock and N.-Y. Shih, *J. Org. Chem.*, **1986**, *51*, 4440.
169. W.A. Freeman, *Acta Cryst.*, **1984**, *B40*, 382.
170. O.A. Gerasko, D.G. Samsonenko, and V.P. Fedin, *Russ. Chem. Rev.*, **2002**, *71*, 741.
171. H.-J. Buschmann and E. Schollmeyer, *J. Incl. Phenom. Mol. Recognit. Chem.*, **1992**, *14*, 91.
172. H.-J. Buschmann and E. Schollmeyer, *J. Incl. Phenom. Mol. Recognit. Chem.*, **1997**, *29*, 167.
173. L.S. Berbeci, W. Wang, and A.E. Kaifer, *Org. Lett.*, **2008**, *10*, 3721.
174. Y.-M. Jeon, D. Whang, J. Kim, and K. Kim, *Chem. Lett.*, **1996**, 503.

175. W.L. Mock and J. Pierpont, *J. Chem. Soc., Chem. Commun.*, **1990**, 1509.
176. H. Zhang, E.S. Paulsen, K.A. Walker, K.E. Krakowiak, and D.V. Dearden, *J. Am. Chem. Soc.*, **2003**, *125*, 9284.
177. H. Zhang, T.A. Ferrel, M.C. Asplund, and D.V. Dearden, *Int. J. Mass Spectrom.*, **2007**, *265*, 187.
178. D.V. Dearden, T.A. Ferrell, M.C. Asplund, L.W. Zilch, R.R. Julian, and M.F. Jarrold, *J. Phys. Chem. A.*, **2009**, *113*, 989.
179. H.-J. Buschmann, E. Cleve, and E. Schollmeyer, *Inorg. Chim. Acta*, **1992**, *193*, 93.
180. H.-J. Buschmann, E. Cleve, K. Jansen, A. Wego, and E. Schollmeyer, *J. Incl. Phenom. Macrocycl. Chem.*, **2001**, *40*, 117.
181. Y.-M. Jeon, J. Kim, D. Whang, and K. Kim, *J. Am. Chem. Soc.*, **1996**, *118*, 9790.
182. D. Whang, J. Heo, J.H. Park, and K. Kim, *Angew. Chem., Int. Ed.*, **1998**, *37*, 78.
183. Y. Marcus, *Ion Solvation*, Wiley: Chichester, 1985; pp. 130-183.
184. C. Marquez, R.R. Hudgins, and W.M. Nau, *J. Am. Chem. Soc.*, **2004**, *126*, 5806.
185. D.G. Samsonenko, M.N. Sokolov, A.V. Virovets, N.V. Pervukhina, and V.P. Fedin, *Eur. J. Inorg. Chem.*, **2001**, 167.
186. M.N. Sokolov, A.V. Virovets, D.N. Dybtsev, E.V. Chubarova, V.P. Fedin, and D. Fenske, *Inorg. Chem.*, **2001**, *40*, 4816.
187. V.P. Fedin, V. Gramlich, M. Worle, and T. Weber, *Inorg. Chem.*, **2001**, *40*, 1074.
188. D.N. Dybtsev, O.A. Gerasko, A.V. Virovets, M.N. Sokolov, and V.P. Fedin, *Inorg. Chem. Commun.*, **2000**, *3*, 345.
189. V.P. Fedin, M.N. Sokolov, D.N. Dybtsev, O.A. Gerasko, A.V. Virovets, and D. Fenske, *Inorg. Chim. Acta*, **2002**, *331*, 31.
190. V.P. Fedin, A.V. Virovets, D.N. Dybtsev, O.A. Gerasko, K. Hegetschweiler, M.J. Elsegood, and W. Clegg, *Inorg. Chim. Acta*, **2000**, *304*, 301.

191. M.N. Sokolov, A.V. Virovets, D.N. Dybtsev, O.A. Gerasko, V.P. Fedin, R. Hernandez-Molina, W. Clegg, and A.G. Sykes, *Angew. Chem., Int. Ed.*, **2000**, *39*, 1659.
192. V.P. Fedin, A.V. Virovets, M.N. Sokolov, D.N. Dybtsev, O.A. Gerasko, and W. Clegg, *Inorg. Chem.*, **2000**, *39*, 2227.
193. D.G. Samsonenko, J. Lipkowski, O.A. Gerasko, A.V. Virovets, M.N. Sokolov, V.P. Fedin, J.G. Platas, R. Hernandez-Molina, and A. Mederos, *Eur. J. Inorg. Chem.*, **2002**, 2380.
194. P. Thuery, *Cryst. Growth Des.*, **2008**, *8*, 4132.
195. O.A. Gerasko, E.A. Mainicheva, M.I. Naumova, M. Neumaier, M.M. Kappes, S. Lebedkin, D. Fenske, and V.P. Fedin, *Inorg. Chem.*, **2008**, *47*, 8869.
196. M.E. Haouaj, M. Luhmer, Y.H. Ko, K. Kim, and K. Martik, *J. Chem. Soc., Perkin Trans. 2*, **2001**, 804.
197. M.E. Haouaj, Y.H. Ko, M. Luhmer, K. Kim, and K. Bartik, *J. Chem. Soc., Perkin Trans. 2*, **2001**, 2104.
198. A. Flinn, G.C. Hough, J.F. Stoddart, and D.J. Williams, *Angew. Chem., Int. Ed. Engl.*, **1992**, *31*, 1475.
199. J.-X. Liu, L.-S. Long, R.-B. Huang, and L.-S. Zheng, *Inorg. Chem.*, **2007**, *46*, 10168
200. P. Thuery, *Cryst. Growth Des.*, **2009**, *9*, 1208.
201. D.G. Samsonenko, O.A. Gerasko, A.V. Virovets, and V.P. Fedin, *Russ. Chem. Bull., Int. Ed.*, **2005**, *54*, 1557.
202. J.-X. Liu, L.-S. Long, R.-B. Huang, and L.-S. Zheng, *Cryst. Growth Des.*, **2006**, *6*, 2611.
203. A.I. Day, R.J. Blanch, A.P. Arnold, S. Lorenzo, G.R. Lewis, and I. Dance, *Angew. Chem., Int. Ed.*, **2002**, *41*, 275.
204. Y.-Q. Zhang, Q.-J. Zhu, S.-F. Xue, and Z. Tao, *Molecules*, **2007**, *12*, 1325.
205. D. Bardeland, K.A. Udachin, R. Anedda, I. Moudrakovski, D.M. Leek, J.A. Ripmeester, and C.I. Ratcliffe, *Chem. Commun.*, **2008**, 4927.

206. D.G. Samsonenko, O.A. Gerasko, A.V. Virovets, and V.P. Fedin, *Russ. Chem. Bull., Int. Ed.*, **2005**, *54*, 1557.
207. K. Jansen, H.-J. Buschmann, A. Wego, D. Dopp, C. Mayer, H.-J. Drexler, H.-J. Holdt, and E. Schollmeyer, *J. Incl. Phenom. Macrocycl. Chem.*, **2001**, *39*, 357.
208. A. Wego, K. Jansen, H.-J. Buschmann, E. Schollmeyer, and D. Dopp, *J. Incl. Phenom. Macrocycl. Chem.*, **2002**, *43*, 201.
209. S.D. Choudhury, J. Mohanty, H.P. Upadhyaya, A.C. Bhasikuttan, and H. Pal, *J. Phys. Chem. B.*, **2009**, *113*, 1891.
210. K.A. Kellersberger, J.D. Anderson, S.M. Ward, K.E. Krakowiak, and D.V. Dearden, *J. Am. Chem. Soc.*, **2001**, *123*, 11316
211. Y. Miyahara, K. Abe, and T. Inazu, *Angew. Chem., Int. Ed.*, **2002**, *41*, 3020.
212. D.M. Rudkevich, *Angew. Chem., Int. Ed.*, **2004**, *43*, 558.
213. H.-J. Kim, W.S. Jeon, Y.H. Ko, and K. Kim, *Proc. Nat. Acad. Sci. U.S.A.*, **2002**, *99*, 5007.
214. W. Ong, M. Gomez-Kaifer, and A.E. Kaifer, *Org. Lett.*, **2002**, *4*, 1791.
215. T. Matsue, T. Kato, U. Akiba, and T. Osa, *Chem. Lett.*, **1985**, 1825.
216. W. Ong and A.E. Kaifer, *J. Org. Chem.*, **2004**, *69*, 1383.
217. K. Moon and A.E. Kaifer, *Org. Lett.*, **2004**, *6*, 185.
218. L. Yuan, R. Wang, and D.H. Macartney, *J. Org. Chem.*, **2007**, *72*, 4539.
219. S. Choi, S.H. Park, A.Y. Ziganshina, Y.H. Ko, J.W. Lee, and K. Kim, *Chem. Commun.*, **2003**, 2176.
220. R.J. Blanch, A.J. Sleeman, T.J. White, A.P. Arnold, and A.I. Day, *Nano Lett.*, **2002**, *2*, 147.
221. D.S. N. Hettiarachchi and D.H. Macartney, *Can. J. Chem.*, **2006**, *84*, 905.
222. R. Wang, L. Yuan, and D.H. Macartney, *Chem. Commun.*, **2006**, 2908.
223. J. Mohanty and W.M. Nau, *Photochem. Photobiol. Sci.*, **2004**, *3*, 1026.
224. C. Marquez and W.M. Mau, *Angew. Chem., Int. Ed.*, **2001**, *40*, 4387.

225. W. Ong and A.E. Kaifer, *Angew. Chem., Int. Ed.*, **2003**, *42*, 2164.
226. A. Thangavel, A.M.M. Rawashdeh, C. Sotiriou-Leventis, and N. Leventis, *Org. Lett.*, **2009**, *11*, 1595.
227. N.J. Wheate, A.I. Day, R.J. Blanch, A.P. Arnold, C. Cullinane, and J.G. Collins, *Chem. Commun.*, **2004**, 1424.
228. M.S. Bali, D.P. Buck, A.J. Coe, A.I. Day, and J.G. Collins, *Dalton Trans.*, **2006**, 5337.
229. S. Kemp, N.J. Wheate, S. Wang, J.G. Collins, S.F. Ralph, A.I. Day, V.J. Hughs, J.R. Aldrich-Wright, *J. Biol. Inorg. Chem.*, **2007**, *12*, 969.
230. Y.J. Jeon, S.-Y. Kim, Y.H. Ko, S. Sakamoto, K. Yamaguchi, and K. Kim, *Org. Biomol. Chem.*, **2005**, *3*, 2122.
231. D.P. Buck, P.M. Abeysinghe, C. Cullinane, A.I. Day, J.G. Collins, and M.M. Harding, *Dalton Trans.*, **2008**, 2328.
232. Y. Zhao, D.P. Buck, D.L. Morris, M.H. Pourgholami, A.I. Day, and J.G. Collins, *Org. Biomol. Chem.*, **2008**, *6*, 4509.
233. N. Dong, S.-F. Xue, Q.-J. Zhu, Z. Tao, Y. Zhao, and L.-X. Yang, *Supramol. Chem.*, **2008**, *20*, 659.
234. N.J. Wheate, *Aust. J. Chem.*, **2006**, *59*, 354.
235. N.J. Wheate, D.P. Buck, A.I. Day, and J.G. Collins, *Dalton Trans.*, **2006**, 451.
236. R. Wang and D.H. Macartney, *Org. Biomol. Chem.*, **2008**, *6*, 1955.
237. R. Wang, B.C. MacGillivray, and D.H. Macartney, *Dalton Trans.*, **2009**, 3584.
238. M.V. Rekharsky, H. Yamamura, Y.H. Ko, N. Selvapalam, K. Kim, and Y. Inoue, *Chem. Commun.*, **2008**, 2236.
239. A. Hennig, H. Bakirci, and W.M. Nau, *Nat. Methods*, **2007**, *4*, 629.
240. D.M. Bailey, A. Hennig, V.D. Uzunova, and W.M. Nau, *Chem. Eur. J.*, **2008**, *14*, 6069.

241. W.S. Jeon, K. Moon, S.H. Park, H. Chun, Y.H. Ko, J.Y. Lee, E.S. Lee, S. Samal, N. Selvapalam, M.V. Rekharsky, V. Sindelar, D. Sobransingh, Y. Inoue, A.E. Kaifer, and K. Kim, *J. Am. Chem. Soc.*, **2005**, *127*, 12984.
242. S. Moghaddam, Y. Inoue, and M.K. Gilson, *J. Am. Chem. Soc.*, **2009**, *131*, 4012.
243. I. Hwang, K. Baek, M. Jung, Y. Kim, K.M. Park, D.-W. Lee, N. Selvapalam, and K. Kim, *J. Am. Chem. Sci.*, **2007**, *129*, 4170.
244. S. Gadde, E.K. Batchelor, J.P. Weiss, Y. Ling, and A.E. Kaifer, *J. Am. Chem. Soc.*, **2008**, *130*, 17114.
245. N.M. Green, *Methods Enzymol.*, **1990**, *184*, 51.
246. M. Shaikh, J. Mohanty, A.C. Bhasikuttan, V.D. Uzunova, W.M. Nau, and H. Pal, *Chem. Comm.*, **2008**, 3681.
247. J. Mohanty, A.C. Bhasikuttan, W.M. Nau, and H. Pal, *J. Phys. Chem. B*, **2006**, *110*, 5132.
248. S.Y. Jon, Y.H. Ko, S.H. Park, H.-J. Kim, and K. Kim, *Chem. Commun.*, **2001**, 1938.
249. W.S. Jeon, H.-J. Kim, C. Lee, and K. Kim, *Chem. Commun.*, **2002**, 1828.
250. Y.J. Jeon, P.K. Bharadwaj, S.W. Choi, J.W. Lee, and K. Kim, *Angew. Chem., Int. Ed.*, **2002**, *41*, 4474.
251. A.Y. Ziganshina, Y.H. Ko, W.S. Jeon, and K. Kim, *Chem. Commun.*, **2004**, 806.
252. K. Moon, J. Grindstaff, D. Sobransingh, and A.E. Kaifer, *Angew. Chem., Int. Ed.*, **2004**, *43*, 5496.
253. M. Pattabiraman, A. Natarajan, R. Kaliappan, J.T. Mague, and V. Ramamurthy, *Chem. Commun.*, **2005**, 4542.
254. M. Pattabiraman, A. Natarajan, L.S. Kaanumalle, and V. Ramamurthy, *Org. Lett.*, **2005**, *7*, 529.
255. M. Pattabiraman, L.S. Kaanumalle, A. Natarajan, and V. Ramamurthy, *Langmuir*, **2006**, *22*, 7605.

256. N. Baroah, B.C. Pemberton, A.C. Johnson, and J. Sivaguru, *Photochem. Photobiol. Sci.*, **2008**, *7*, 1473.
257. U. Rauwald and O.A. Scherman, *Angew. Chem., Int. Ed.*, **2008**, *47*, 3950.
258. N. Baroah, B.C. Pemberton, and J. Sivaguru, *Org. Lett.*, **2008**, *10*, 3339.
259. J.J. Reczek, A.A. Kennedy, B.T. Halbert, and A.R. Urbach, *J. Am. Chem. Soc.*, **2009**, *131*, 2408.
260. I. Hwang, A.Y. Ziganshina, Y.H. Ko, G. Yun, and K. Kim, *Chem. Commun.*, **2009**, 416.
261. S. Deroo, U. Rauwald, C.V. Robinson, and O.A. Scherman, *Chem. Commun.*, **2009**, 644.
262. R. Wang, L. Yuan, and D.H. Macartney, *J. Org. Chem.*, **2006**, *71*, 1237.
263. S.-Y. Kim, I.-S. Jung, E. Lee, J. Kim, S. Sakamoto, K. Yamaguchi, and K. Kim, *Angew. Chem., Int. Ed.*, **2001**, *40*, 2119.
264. G. Jiang, G. Li, *Photochem. Photobiol. B: Biol.*, **2006**, *85*, 223.
265. N. Baroah, B.C. Pemberton, A.C. Johnson, and J. Sivaguru, *Photochem. Photobiol. Sci.*, **2008**, *7*, 1473.
266. X. Xiao, Z. Tao, S.-F. Xue, Q.-J. Zhu, J.-X. Zhang, G.A. Lawrence, B. Raguse, and G. Wei, *J. Incl. Phenom. Macrocycl. Chem.*, **2008**, *61*, 131.
267. R. Wang, L. Yuan, H. Ihmels, and D.H. Macartney, *Chem. Eur. J.*, **2007**, *13*, 6468.
268. H.-J. Kim, J. Heo, W.S. Jeon, E. Lee, J. Kim, S. Sakamoto, K. Yamaguchi, and K. Kim, *Angew. Chem., Int. Ed.*, **2001**, *40*, 1526.
269. M.E. Bush, N.D. Bouley, and A.R. Urbach, *J. Am. Chem. Soc.*, **2005**, *127*, 14511.
270. V. Sindelar, M.A. Cejas, F.M. Raymo, W. Chen, S.E. Parker, and A.E. Kaifer, *Chem. Eur. J.*, **2005**, *11*, 7054.
271. Y. Ling, J.T. Mague, and A.E. Kaifer, *Chem. Eur. J.*, **2007**, *13*, 7908.



272. A. Trabolsi, M. Hmadeh, N.M. Khashab, D.C. Friedman, M.E. Belovich, N. Humbert, M. Elhabiri, H.A. Khatib, A.-M. Albrecht-Gary, and J.F. Stoddart, *New. J. Chem.*, **2009**, *33*, 254.
273. Y.H. Ko, E. Kim, I. Hwang, and K. Kim, *Chem. Commun.*, **2007**, 1305.
274. Y.H. Ko, H. Kim, Y. Kim, and K. Kim, *Angew. Chem., Int. Ed.*, **2008**, *47*, 4106.
275. G.K. Balendiran, F. Schnutgen, G. Scapin, T. Borchers, N. Xhong, K. Lim, R. Godbout, F. Spener, and J.C. Sacchettini, *J. Biol. Chem.*, **2000**, *275*, 27045.
276. G. Zanotti, G. Scapin, P. Spadona, J.H. Veerkamp, and J.C. Sacchettini, *J. Biol. Chem.*, **1992**, *267*, 18541.
277. W.S. Jeon, E. Kim, Y.H. Ko, I. Hwang, J.W. Lee, S.-Y. Kim, H.-J. Kim, and K. Kim, *Angew. Chem., Int. Ed.*, **2005**, *44*, 87.
278. J.W. Lee, I. Hwang, W.S. Jeon, Y.H. Ko, S. Sakamoto, K. Yamaguchi, and K. Kim, *Chem. Asian. J.*, **2008**, *3*, 1277.
279. D. Zou, S. Anderson, R. Zhang, S. Sun, B. Akermark, and L. Sun, *J. Org. Chem.*, **2008**, *73*, 3775.
280. W. Wang and A.E. Kaifer, *Angew. Chem., Int. Ed.*, **2006**, *45*, 7042.
281. U. Rauwald and O.A. Scherman, *Angew. Chem., Int. Ed.*, **2008**, *47*, 3950.
282. J.J. Reczek, A.A. Kennedy, B.T. Halbert, and A.R. Urbach, *J. Am. Chem. Soc.*, **2009**, *131*, 2408.
283. S. Liu, P.Y. Zavalij, and L. Isaacs, *J. Am. Chem. Soc.*, **2005**, *127*, 16798.
284. S. Liu, A.D. Shukla, S. Gadde, B.D. Wagner, A.E. Kaifer, and L. Isaacs, *Angew. Chem., Int. Ed.*, **2008**, *47*, 2657.
285. K. Kim, N. Selvapalam, Y.H. Ko, K.M. Park, D. Kim, and J. Kim, *Chem. Soc. Rev.*, **2007**, *36*, 267.

286. L. Isaacs, S.-K. Park, S. Liu, Y.H. Ko, N. Selvapalam, Y. Kim, H. Kim, P.Y. Zavalij, G.-H. Kim, H.-S. Lee, and K. Kim, *J. Am. Chem. Soc.*, **2005**, *127*, 18000.
287. S. Liu, K. Kim, and L. Isaacs, *J. Org. Chem.*, **2007**, *72*, 6840.
288. W.-H. Huang, S. Liu, P.Y. Zavalij, and L. Isaacs, *J. Am. Chem. Soc.*, **2006**, *128*, 14744.
289. W.-H. Huang, P.Y. Zavalij, and L. Isaacs, *J. Am. Chem. Soc.*, **2008**, *130*, 8446.
290. W.-H. Huang, P.Y. Zavalij, and L. Isaacs, *Org. Lett.*, **2008**, *10*, 2577.
291. S.Y. Jon, N. Selvapalam, D.H. Oh, J.-K. Kang, S.-Y. Kim, Y.J. Jeon, J.W. Lee, and K. Kim, *J. Am. Chem. Soc.*, **2003**, *125*, 10186.
292. R.P. Sijbesma, R.J.M. Nolte, *Top. Curr. Chem.*, **1995**, *175*, 25.
293. A.E. Rowan, J.A.A.W. Elemans, and R.J.M. Nolte, *Acc. Chem. Res.*, **1999**, *32*, 995.
294. A.I. Day, A.P. Arnold, and R.J. Blanch, *Molecules*, **2003**, *8*, 74.
295. J. Lin, Y. Zhang, J. Zhang, S. Xue, Q. Zhu, *J. Mol. Struct.*, **2008**, *875*, 442.
296. J. Zhao, H.-J. Kim, J. Oh, S.-Y. Kim, J.W. Lee, S. Sakamoto, K. Yamaguchi, and K. Kim, *Angew. Chem., Int. Ed.*, **2001**, *40*, 4233.
297. H. Isobe, S. Sato, and E. Nakamura, *Org. Lett.*, **2002**, *4*, 1287.
298. J. Kim, Y. Ahn, K.M. Park, Y. Kim, Y.H. Ko, D.H. Oh, and K. Kim, *Angew. Chem., Int. Ed.*, **2007**, *46*, 7393.
299. J. Lagona, J.C. Fettinger, and L. Isaacs, *Org. Lett.*, **2003**, *5*, 3745.
300. J. Lagona, J.C. Fettinger, and L. Isaacs, *J. Org. Chem.*, **2005**, *70*, 10381.
301. B.D. Wagner, P.G. Boland, J. Lagona, and L. Isaacs, *J. Phys. Chem. B*, **2005**, *109*, 7686.
302. L. Isaacs, S.-K. Park, S. Liu, Y.H. Ko, N. Selvapalam, Y. Kim, H. Kim, P.Y. Zavalij, G.-H. Kim, H.-S. Lee, and K. Kim, *J. Am. Chem. Soc.*, **2005**, *127*, 18000.
303. S. Liu, K. Kim, and L. Isaacs, *J. Org. Chem.*, **2007**, *72*, 6840.
304. R.V. Pinjari and S.P. Gejji, *J. Phys. Chem. A.*, **2009**, *113*, 1368.
305. W.-H. Huang, P.Y. Zavalij, and L. Isaacs, *Angew. Chem., Int. Ed.*, **2007**, *46*, 7425.

306. B.D. Wagner, P.G. Boland, J. Lagona, and L. Isaacs, *J. Phys. Chem. B*, **2005**, *109*, 7686.
307. J. Lagona, J.C. Fettinger, and L. Isaacs, *Org. Lett.*, **2003**, *5*, 3745.
308. C.A. Burnett, D. Witt, J.C. Fettinger, and L. Isaacs, *J. Org. Chem.*, **2003**, *68*, 6184.
309. D. Witt, J. Lagona, F. Damkaci, J.C. Fettinger, and L. Isaacs, *Org. Lett.*, **2000**, *2*, 755.
310. A. Chakraborty, A. Wu, D. Witt, J. Lagona, J.C. Fettinger, and L. Isaacs, *J. Am. Chem. Soc.*, **2002**, *124*, 8297.
311. S.-M. Liu, L. Xu, C.-T. Wu, and Y.-Q. Feng, *Talanta*, **2004**, *64*, 929.
312. Y.J. Jeon, H. Kim, S. Jon, N. Selvapalam, D.H. Oh, I. Seo, C.-S. Park, S.R. Jung, D.-S. Koh, and K. Kim, *J. Am. Chem. Soc.*, **2004**, *126*, 15944.
313. W.L. Mock, T.A. Irra, J.P. Wepsiec, and T.L. Manimaran, *J. Org. Chem.*, **1983**, *48*, 3619.
314. W.L. Mock, T.A. Irra, J.P. Wepsiec, and M. Adhya, *J. Org. Chem.*, **1989**, *54*, 5302.
315. L. Pauling, *Am. Sci.*, **1948**, *36*, 51.
316. D. Tuncel and J.H.G. Steinke, *Chem. Commun.*, **1999**, 1509.
317. D. Tuncel and J.H.G. Steinke, *Chem. Commun.*, **2002**, 496.
318. D. Tuncel and J.H.G. Steinke, *Macromolecules*, **2004**, *37*, 288.
319. T.C. Krasia and J.H.G. Steinke, *Chem. Commun.*, **2002**, 23.
320. C. Klock, R.N. Dsouza, and W.M. Nau, *Org. Lett.*, **2009**, *11*, 2595.
321. N. Saleh, A.L. Koner, and W.M. Nau, *Angew. Chem., Int. Ed.*, **2008**, *47*, 5398.
322. K.M. Park, K. Suh, H. Jung, D.-W. Lee, Y. Ahn, J. Kim, K. Baek, and K. Kim., *Chem. Commun.*, **2009**, 71.
323. D. Kim, E. Kim, J. Kim, K.M. Park, K. Baek, M. Jung, Y.H. Ko, W. Sung, H.S. Kim, J.H. Suh, C.G. Park, O.S. Na, D. Li, K.E. Lee, S.S. Han, and K. Kim, *Angew. Chem., Int. Ed.*, **2007**, *46*, 3471.
324. Y. Zhao, M.S. Bali, C. Cullinane, A.I. Day, and J.G. Collins, *Dalton Trans.*, **2009**, 5190.
325. S. Karcher, A. Kornmuller, and M. Jekel, *Water Res.*, **2001**, *35*, 3309.

326. A. Kornmuller, S. Karcher, and M. Jekel, *Water Res.*, **2001**, *35*, 3317.
327. S. Karcher, A. Kornmuller, and M. Jekel, *Water Sci. Tech.*, **1999**, *40*, 425.
328. E.R. Nagarajan, D.H. Oh, N. Selvapalam, Y.H. Ko, K.M. Park, and K. Kim, *Tetrahedron Lett.*, **2006**, *47*, 2073.
329. H.P. Nguyen and K.A. Schug, *J. Sep. Sci.*, **2008**, *31*, 1465.
330. T. Yoshida, *J. Biochem. Biophys. Methods*, **2004**, *60*, 265.
331. V. Sindelar, S. Silvi, and A.E. Kaifer, *Chem. Commun.*, **2006**, 2185.
332. I. Hwang, W.S. Jeon, H.-J. Kim, D. Kim, H. Kim, N. Selvapalam, N. Fujita, S. Shinkai, and K. Kim, *Angew. Chem., Int. Ed.*, **2007**, *46*, 210.
333. J. Mohanty, W.M. Nau, *Angew. Chem., Int. Ed.*, **2005**, *44*, 3750.
334. J. Mohanty, H. Pal, A.K. Ray, S. Kumar, and W.M. Nau, *ChemPhysChem*, **2007**, *8*, 54.
335. C. Li, J. Li, and X. Jia, *Org. Biomol. Chem.*, **2009**, *7*, 2699.
336. A.I. Day, "Cucurbit[n]uril as a Drug Delivery Vehicle", *NSF Workshop on Cucurbit[n]uril Molecular Containers*, College Park, MD, USA, Aug. 4-5, 2007, oral presentation.
337. R.K. Stoelting and R.D. Miller, *Basics of Anesthesia, Fourth Edition*, Churchill Livingstone: New York, 2000; pp. 89-106.
338. A.L.W. Po and T. Girard, *J. Clin. Pharm. Ther.*, **2005**, *30*, 497.

## Chapter 2

# Host-Guest Chemistry between Cucurbit[7]uril and Small Polar Organic Guests

### 2.1 Introduction

The most common examples of host-guest complexes formed with cucurbiturils have involved cationic guests. These are often organic cations,<sup>1-3</sup> as well as transition metal complexes, with particularly high affinities having been observed between CB[7] and ferrocene-containing guests,<sup>2,4-6</sup> and adamantane-containing guests.<sup>2,6</sup> Complexation between cucurbiturils and neutral, as well as anionic, guests have also been reported. Decamethylcucurbit[5]uril, with its small cavity, has been shown to bind to small neutral gas molecules, such as H<sub>2</sub>, He, Ne, Ar, N<sub>2</sub>, O<sub>2</sub>, N<sub>2</sub>O, NO, CO, CO<sub>2</sub>, methane, and acetylene.<sup>7,8</sup> In addition, CB[5], which has also been shown to bind to Xe gas,<sup>9</sup> was found to bind to anions, such as the chloride<sup>9-12</sup> and nitrate<sup>13</sup> anions. Meanwhile, CB[6] has been reported to bind to neutral solvent molecules such as tetrahydrofuran (THF) and trifluoroacetic acid (TFA), as well as xenon gas.<sup>14,15</sup>

When Buschmann and coworkers<sup>16</sup> studied the complexation between CB[6] and a series of aliphatic alcohols CH<sub>3</sub>(CH<sub>2</sub>)<sub>*n*</sub>OH, *n* = 1-6), they saw little change in the binding constant as the chain length was varied, with log*K* ranging between 2.53 and 2.73. The solvent used was 50% aqueous formic acid by volume, due to the low solubility of CB[6]. On the other hand, when complexation between CB[6] and aliphatic alcohols was studied in aqueous solution containing 0.05 M NaCl, with both portals capped by sodium cations, the selectivity was greater, with binding constants of 90, 710, 1220, and 410 M<sup>-1</sup> for *n* = 1, 2, 3, and 4, respectively.<sup>17</sup> In this case,

butanol ( $n = 3$ ) had the highest affinity and was able to fit within the hydrophobic CB[6] cavity best, while as the chain length was increased further, the guest began to interfere with the sodium-bound portal, as shown by the lower binding constant of pentanol ( $n = 4$ ) to CB[6].

Compared with the smaller homologues, even fewer examples of complexation between neutral guests<sup>18</sup> and CB[7] or CB[8] have been reported, with most of the guests of these macrocycles either being cations, or neutral molecules that become protonated to give cations due to complexation-induced increases in their  $pK_a$  values.<sup>19-23</sup> In this chapter, the complexation between CB[7] and a series of small polar organic guests will be discussed. While most of the guests were ketones, solvents such as acetonitrile, dimethylformamide (DMF), and dimethyl sulfoxide (DMSO) were also studied. Their binding constants were measured by a  $^1\text{H}$  NMR chemical shift titration, and the effect of the presence of  $\text{Na}^+$  and  $\text{K}^+$  on the affinity between CB[7] and acetone or acetophenone was also explored.<sup>24</sup> The contents of this chapter describe work that has been published.<sup>24</sup>

## 2.2 Results and Discussion

### 2.2.1 Stability Constants for Host-Guest Complexes of CB[7] with Solvents

$^1\text{H}$  NMR chemical shift titrations were used to measure the binding constants for the host-guest complexes formed between the small neutral organic guests and the CB[7] host. Most of the guests discussed in this chapter displayed fast exchange behaviour upon complexation with CB[7], and the chemical shift changes of the proton resonances could be measured throughout the course of the titration. Subsequently, the binding constant could be determined by plotting and fitting their titration curve to a 1:1 binding isotherm through the use of a least-squares program (Figure 2.1). In contrast, the bulkier ketones pentan-3-one and 3,3-dimethylbutan-2-one exhibited slow exchange behaviour with respect to the NMR timescale, in which case the relative

integrations of the free and bound guest proton resonances could be used to determine the stability constants. In a previous study, Mezzina and coworkers found that 1-phenylbutan-2-one and 3,3-dimethyl-1-phenylbutan-2-one exhibit slow and intermediate exchange, respectively, upon complexation with CB[7].<sup>18</sup>

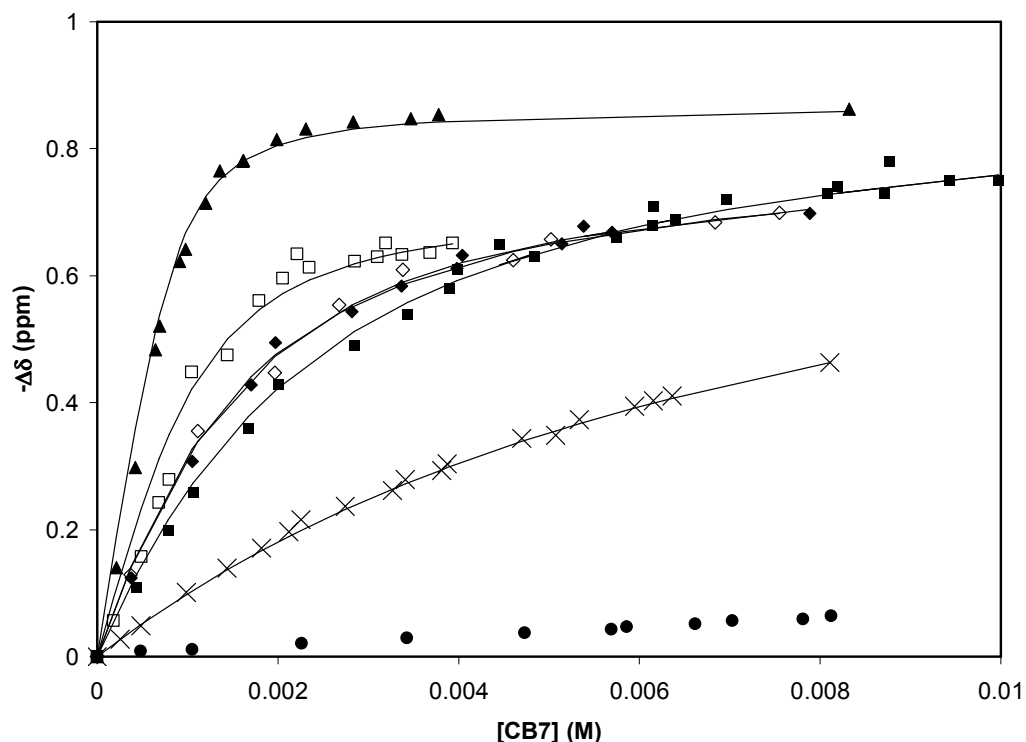


**Figure 2.1** <sup>1</sup>H NMR chemical shift titrations for CB[7] with (■) acetone, (▲) acetophenone, (◆) DMF, (◇) methyl acetate, (X) DMSO, (□) 2-butanone, and (●) acetonitrile. The guest concentrations were between 0.9 and 1.0 mM in D<sub>2</sub>O at 25 °C.

In addition to determining the binding affinity, <sup>1</sup>H NMR spectroscopy (examples shown in Figures 2.2-2.4) can also be used to determine the positioning and orientation of the guest with respect to the CB[7]. These can be determined from the limiting chemical shift shown by the guest's proton resonances upon binding to CB[7] ( $\Delta\delta_{\text{lim}} = \delta_{\text{bound}} - \delta_{\text{free}}$ ). It has been noted by various researchers that upfield shifts,<sup>1,3</sup> with negative  $\Delta\delta_{\text{lim}}$  values, indicate that the corresponding protons are located inside the hydrophobic cucurbituril cavity. A resonance

showing a  $\Delta\delta_{\text{lim}}$  value of approximately -1 ppm suggests that the corresponding guest proton is located near the centre of the cucurbituril cavity, with more moderate upfield shifts indicating that the proton is not positioned as far into the cavity and closer to the portal. In contrast, positive  $\Delta\delta_{\text{lim}}$  values indicate that the proton is located on the exterior, near the electron rich portals.

The binding constants for the complexes formed between CB[7] and the guests measured in this study, as well as those reported by Mezzina,<sup>18</sup> may be compared with those determined for interactions with the similarly-sized  $\beta$ -CD host,<sup>25-27</sup> as shown in Table 2.1. The binding constants for the complexes formed between  $\beta$ -CD and the solvents DMSO, DMF, and acetonitrile have not been reported, and they were therefore compared to reported values for complexation with  $\alpha$ -CD instead.<sup>28,29</sup> The reported binding between  $\alpha$ -CD and these guests is very weak, with binding constants of less than 1, 3.1, and 4.6  $\text{M}^{-1}$  for DMSO, DMF, and acetonitrile, respectively.<sup>28</sup> The stability constant for the binding between acetone and  $\alpha$ -CD, reported to be 2.94  $\text{M}^{-1}$  (while Matsui<sup>28</sup> reported a binding constant of 2.0  $\text{M}^{-1}$ ), is similar to that between acetone and  $\beta$ -CD, which has a value of 2.72  $\text{M}^{-1}$ , as reported by Tee and coworkers.<sup>25</sup> They also noted that butan-2-one has similar binding constants of 9.80  $\text{M}^{-1}$  and 9.35  $\text{M}^{-1}$  to  $\alpha$ - and  $\beta$ -CD, respectively.<sup>25</sup> Therefore, it is likely that the binding constants for DMSO, DMF, and acetonitrile with  $\alpha$ -CD will show similar small binding constants with  $\beta$ -CD. The ketones exhibited an increase in their binding constants with both CB[7] and  $\beta$ -CD<sup>25,26</sup> as the hydrophobicity of their alkyl groups increased. Methanol was titrated with CB[7] in this study also, but no shift in its methyl protons was observed, even with a 10-fold excess of CB[7], indicating that no significant complexation had occurred between CB[7] and this more hydrophilic guest.

Cucurbiturils have a quadrupolar moment, due to the presence of two electron rich portals at opposing ends of their structure. When small carbonyl-bearing molecules, such as acetone, are



encapsulated by CB[7], they should ideally position themselves so that their carbonyl oxygen would be directed toward the interior wall of the cavity. The molecule should be positioned at the centre of the molecule, in order to achieve the maximum possible quadrupole-dipole interaction and separation from either of the two carbonyl-lined portals (Figure 2.5). The methyl groups would also be positioned deep inside the hydrophobic cavity, and should show large upfield shifts in  $^1\text{H}$  NMR, with a  $\Delta\delta$  of near 1 ppm. Compared to other intermolecular forces, quadrupole-dipole interactions would be a relatively minor contribution to the binding affinity, but could affect the orientation and positioning of small guests in the cavity. In their study of complexation of ammonium guests with CB[6], Mock and Shih<sup>3</sup> observed that replacement of the central methylene group of 1,5-pentanediammonium ( $K_{\text{CB}[6]} = 2.4 \times 10^6 \text{ M}^{-1}$ ) with sulfur ( $K_{\text{CB}[6]} = 4.2 \times 10^5 \text{ M}^{-1}$ ) and oxygen ( $K_{\text{CB}[6]} = 5.3 \times 10^3 \text{ M}^{-1}$ ) resulted in decreases of the binding affinity by factors of 6 and 450, respectively. This was attributed to the continuing decrease in the hydrophobicity of the molecule as the central  $\text{CH}_2$  unit was replaced by sulfur and oxygen.

**Table 2.1** Binding constants ( $K_{CB[7]}$ ) and limiting complexation-induced chemical shifts ( $\Delta\delta_{lim}$ ) for binding between CB[7] and various neutral organic guests, based on  $^1H$  NMR titration in  $D_2O$  at 25 °C. The binding constants for  $\beta$ -CD ( $K_{\beta-CD}$ ) are from literature.

Guest	$\Delta\delta_{lim}$ (ppm)	$K_{CB[7]}$ ( $M^{-1}$ )	$K_{\beta-CD}$ ( $M^{-1}$ )
Acetone	-0.92 (CH <sub>3</sub> )	$580 \pm 50^a$	$2.7 \pm 0.4^b$
Butan-2-one	-0.91 (CH <sub>3</sub> ) -1.05 (CH <sub>2</sub> ) -0.70 (CH <sub>2</sub> CH <sub>3</sub> )	$3100 \pm 500^a$	$9.3 \pm 0.2^b$
Pentan-3-one	-0.53 (CH <sub>3</sub> ) -0.97 (CH <sub>2</sub> )	$2060 \pm 550^c$	$18 \pm 1^b$
3,3-Dimethylbutan-2-one	-0.83 (CH <sub>3</sub> ) -0.76 (C(CH <sub>3</sub> ) <sub>3</sub> )	$6740 \pm 20^c$	$585 \pm 55^b$ $64 - 343^d$
Acetophenone	-0.29 (CH <sub>3</sub> ) -0.82 ( <i>o</i> -CH) -0.86 ( <i>m</i> -CH) -0.65 ( <i>p</i> -CH)	$9600 \pm 700^a$	$123 \pm 9^b$
1-Phenylbutan-2-one <sup>e</sup>	-0.73 (CH <sub>2</sub> Ph) -0.68 (CH <sub>2</sub> CH <sub>3</sub> ) -0.34 (CH <sub>2</sub> CH <sub>3</sub> ) -0.62 ( <i>o</i> -CH) -0.81 ( <i>m</i> -CH) -0.83 ( <i>p</i> -CH)	$4600^e$	–
3,3-Dimethyl-1-phenylbutan-2-one <sup>e</sup>	-0.75 (CH <sub>2</sub> Ph) -0.79 (C(CH <sub>3</sub> ) <sub>3</sub> ) +0.29 ( <i>o</i> -CH) +0.01 ( <i>m</i> -CH) -0.05 ( <i>p</i> -CH)	$27340^e$	$6238 - 18300^d$
Methyl acetate	-0.85 (CH <sub>3</sub> ) -0.80 (OCH <sub>3</sub> )	$1020 \pm 100^a$	$11.8 \pm 1.2^f$
Dimethylsulfoxide	-0.91 (CH <sub>3</sub> )	$140 \pm 20^a$	$<1^g$ $0.41 \pm 0.04^h$
Dimethylformamide	-0.78 (CH <sub>3</sub> ) -0.80 (CH <sub>3</sub> ) -0.80 (COH)	$1000 \pm 80^a$	$3.1^g$
Acetonitrile	-0.67 (CH <sub>3</sub> )	$11 \pm 1^a$	$4.6^g$ $5.6 \pm 0.1^h$

<sup>a</sup>Based on  $^1H$  NMR chemical shift titrations (fast exchange), <sup>b</sup>From Tee *et al.* (Ref. 25), <sup>c</sup>Determined from relative integration of bound and free proton resonances (slow exchange), <sup>d</sup>From Zubiaur and Jaime (Ref. 26).  $K_{\beta-CD}$  values were dependent on host or guest proton measured, <sup>e</sup>From Mezzina *et al.* (Ref. 18), <sup>f</sup>From Feliciano and coworkers, recorded at 22 °C (Ref. 27), <sup>g</sup>From Matsui and Tokunaga for  $\alpha$ -CD (Ref. 28), <sup>h</sup>From Gelb *et al.*, for  $\alpha$ -CD (Ref. 29).

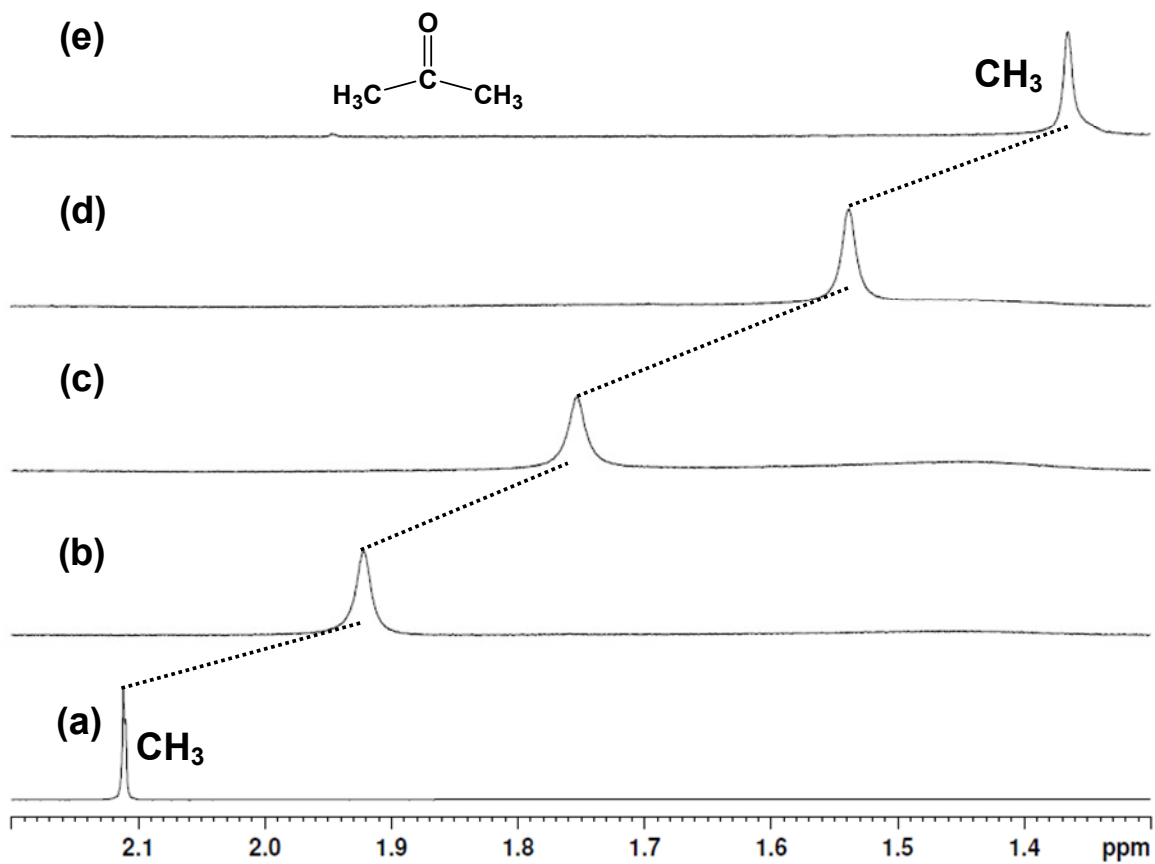


**Figure 2.2** Selected spectra from the  $^1\text{H}$  NMR titration of acetone (1.00 mM) in the presence of (a) 0.00, (b) 0.78, (c) 1.66, (d) 3.89, and (e) 10.07 equiv. CB[7].

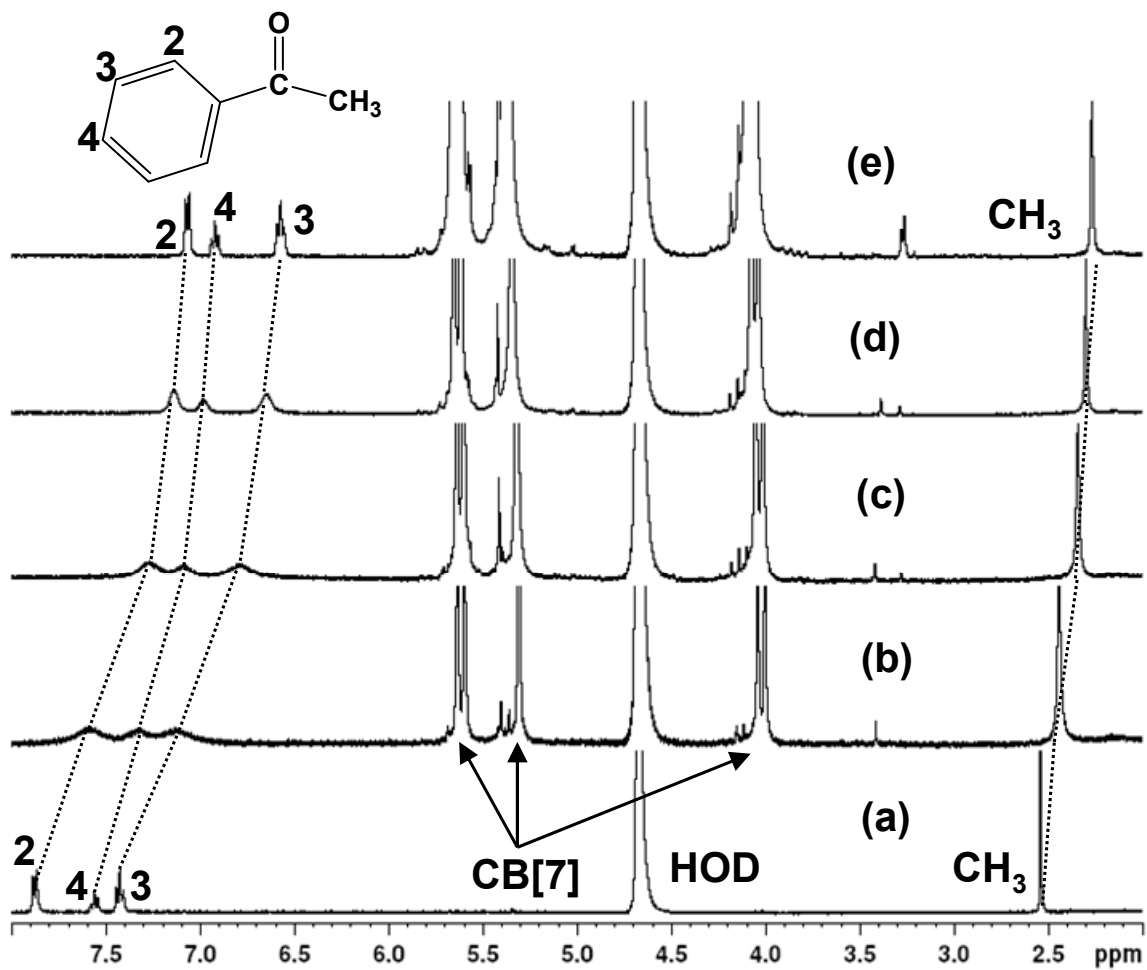


**Figure 2.3** Selected spectra from the  $^1\text{H}$  NMR titration of acetophenone (0.87 mM) in the presence of (a) 0.00, (b) 0.49, (c) 1.13, (d) 1.86, and (e) 4.36 equiv. of CB[7]. This system exhibited intermediate to fast exchange on the NMR timescale, with an average of the free and bound signals being observed.

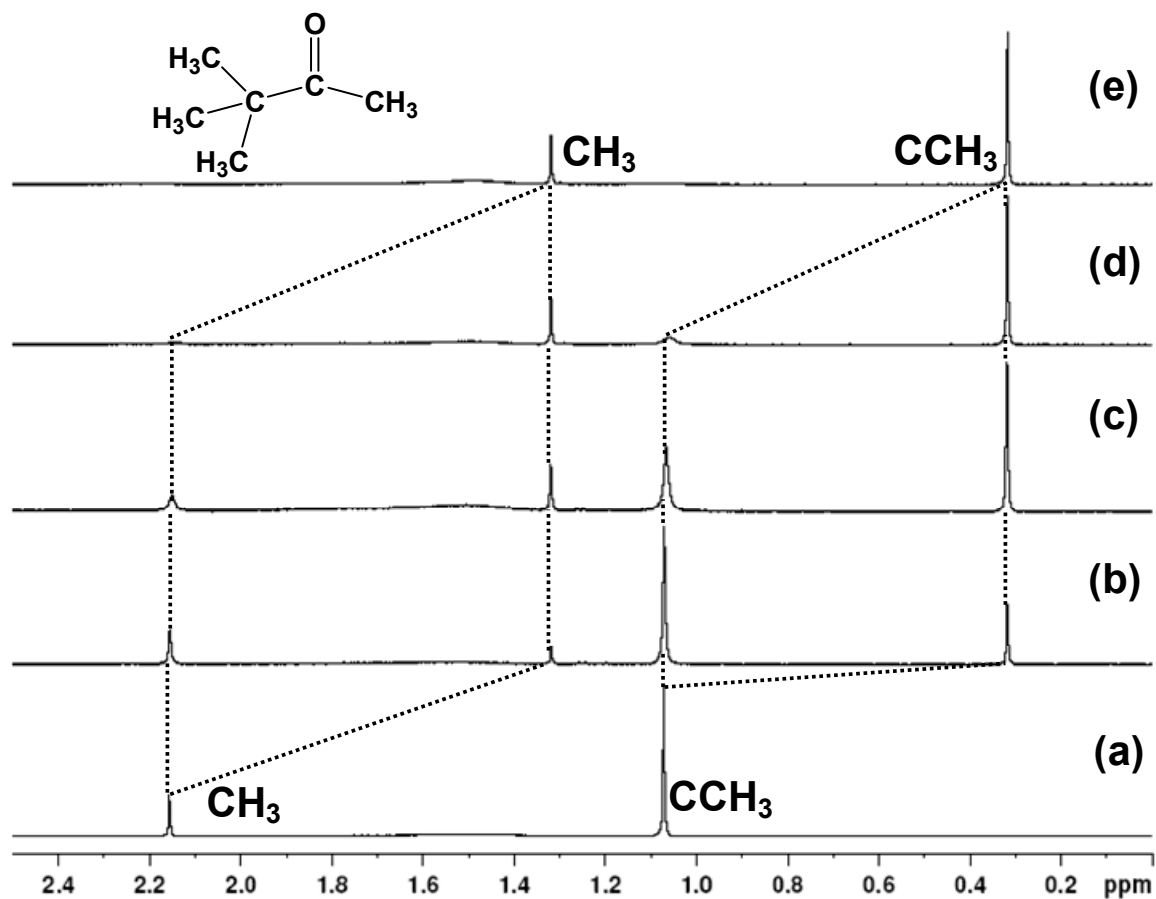


**Figure 2.4** Selected spectra from the  $^1\text{H}$  NMR titration of 3,3-dimethylbutan-2-one (1.02 mM) in the presence of (a) 0.00, (b) 0.35, (c) 0.65, (d) 0.97, and (e) 1.49 equiv. CB[7]. This host-guest system exhibited slow exchange behaviour, with both the free and bound signals being visible.

As a model for the binding between these guests and CB[7], Molecular Mechanics 2 (MM2) energy-minimized structures of their host-guest complexes were obtained, and are shown in Figure 2.6.<sup>30</sup> The MM2 models are consistent with the limiting  $\Delta\delta$  values obtained from the  $^1\text{H}$  NMR titrations. The guests which show fast exchange with respect to the NMR timescale, have their carbonyl groups aligned toward the interior wall of the CB[7] cavity, specifically toward the

centre of the linkage between two glycoluril units within the macrocycle. For these molecules, the plane of the O=CRR' molecule is nearly perpendicular to the major axis of the CB[7] cavity, which passes through the portals. In other words, the plane of these guests are aligned with the equatorial plane of the CB[7] host. The limiting upfield shifts of the alkyl protons of these guests were quite large, with  $\Delta\delta_{\text{lim}}$  values between -0.70 and -1.05 ppm, indicating that they were buried deep in the cavity. The S=O bond of DMSO is also aligned perpendicular to the channel of the CB[7] cavity, with the oxygen facing the interior wall of the host. The guests pentan-3-one, 3,3-dimethylbutan-2-one (Figure 2.4) and 3,3-dimethyl-1-phenylbutane-2-one<sup>18</sup> exhibited slow exchange binding with CB[7]. These guests also have their carbonyl oxygen directed toward the centre of the linkage between two glycoluril units. However, according to their <sup>1</sup>H NMR  $\Delta\delta_{\text{lim}}$  values, the O=CRR' plane of these bulkier molecules is parallel to the major axis of the CB[7], so that their aliphatic or aromatic groups are directed towards the portals. The upfield shifts observed for the corresponding protons of these guests were more modest, particularly with a decreasing upfield shift, as the distance from the carbonyl group increased. For example, the methylene protons of pentan-3-one, adjacent to the carbonyl group, had a  $\Delta\delta_{\text{lim}}$  value of -0.97 ppm, while the methyl protons, which were positioned closer to the portals had a more modest  $\Delta\delta_{\text{lim}}$  value of -0.53 ppm. The energy-minimized structures of 3-pentanone and 3,3-dimethylbutan-2-one suggested that their molecular planes were perpendicular to the CB[7] channel, in contrast to the <sup>1</sup>H NMR  $\Delta\delta_{\text{lim}}$  values. However, the experimental  $\Delta\delta_{\text{lim}}$  values most likely represents the actual situation more accurately than the positioning predicted by the energy-minimized structures.

Acetophenone displayed fast exchange behaviour when it was titrated with CB[7] (Figure 2.3), and based on the molecular model and the limiting  $\Delta\delta$  values, the phenyl ring appears to be completely encapsulated by the CB[7] cavity, while the methyl group is located near the portal.

The more hydrophobic aromatic group apparently is the preferred binding site for the CB[7] host. Mezzina and coworkers<sup>18</sup> reported the complexation of benzyl *tert*-butyl nitroxide and 2,2,6,6-tetramethyl-pyridinyl-N-oxyl (TEMPO) radicals with CB[7] and also reported binding constants between CB[7] and the corresponding ketones of these radicals, as diamagnetic analogues. The guest 1-phenylbutan-2-one showed fast exchange behaviour upon complexation with CB[7], and both the aliphatic and aromatic regions of the guest had large upfield shifts, suggesting that the position of the CB[7] was averaged over the entire length of the molecule, by moving back and forth. Meanwhile, 3,3-dimethyl-1-phenylbutan-2-one exhibited slow exchange complexation with CB[7], and the observed upfield shifts in the *tert*-butyl methyl proton resonance indicated that the CB[7] cavity was localized over the region containing this hydrophobic group.<sup>18</sup>

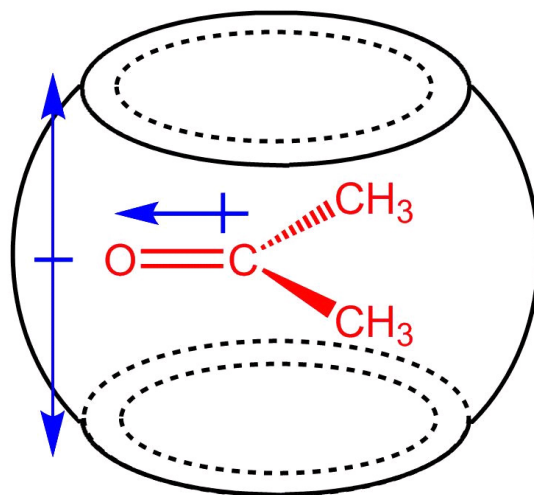


**Figure 2.5** Acetone encapsulated by CB[7]. Due to the quadrupole moment, the dipole of the carbonyl group is directed toward the interior wall of the CB[7]. The guest is deep inside the hydrophobic cavity with its  $\text{O}=\text{C}(\text{CH}_3)_2$  plane perpendicular to the major axis of the CB[7] host.

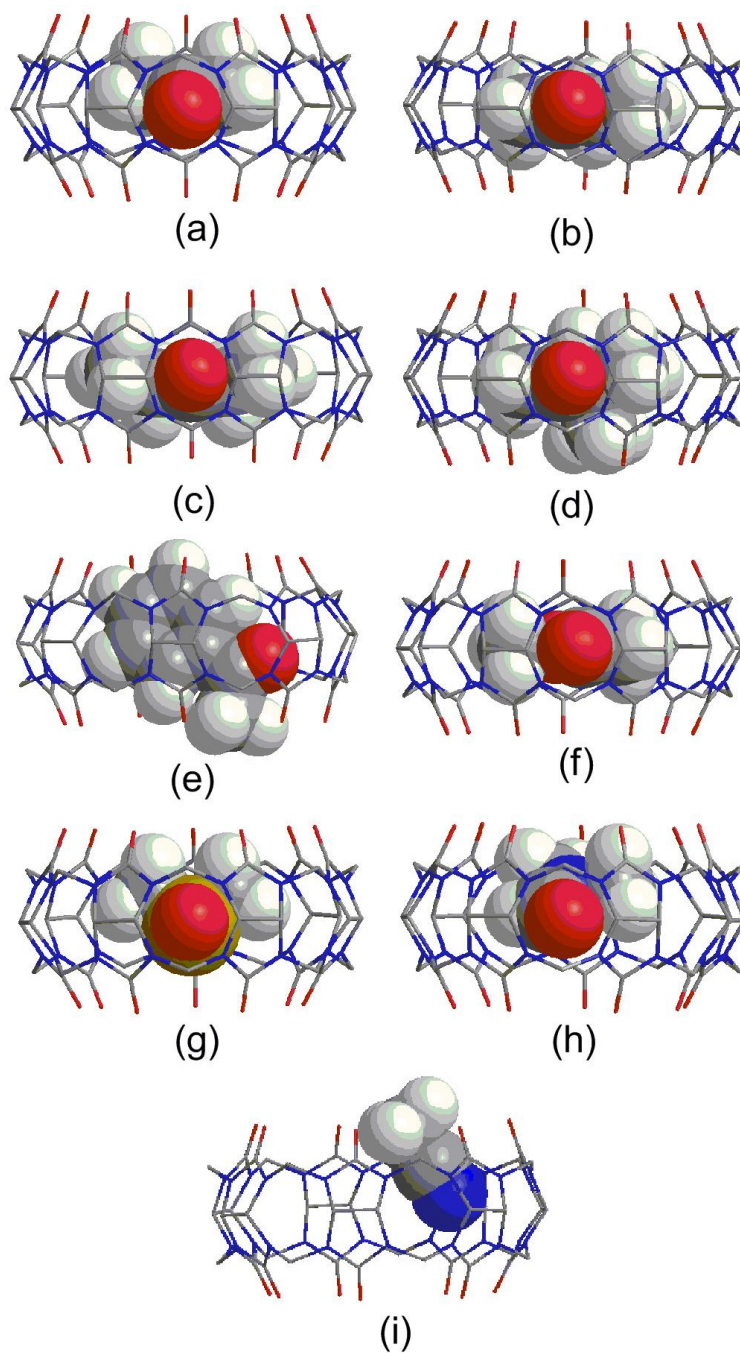


**Figure 2.6** Energy-minimized MM2 structures of host-guest complexes between CB[7] and (a) acetone, (b) butan-2-one, (c) pentan-3-one, (d) 3,3-dimethylbutan-2-one, (e) acetophenone, (f) methyl acetate, (g) dimethylsulfoxide, (h) dimethylformamide, and (i) acetonitrile. The hydrogens of CB[7] have been removed for clarity.



### 2.2.2 Host-Guest Complexes of CB[7] with Alkali Metal Cations

Various researchers<sup>17,18,31-37</sup> have observed that the type and concentration of cations present within the solvent matrix can have a significant effect on the magnitude of host-guest binding constants of cucurbiturils. In fact, the use of salt in solution has recently been proposed as a method to induce the release of a guest, such as a drug, from cucurbiturils.<sup>37</sup> This effect of the cations in the solvent upon the binding strength between guests and cucurbiturils is due to the affinity of cations for the cucurbituril portals, thus affecting the rates of guest association and dissociation, as well as the overall binding strength of guests with CB[7]. The cations compete with the guest for complexation to CB[7], and weaken the host-guest binding constants. The binding constants for alkali metal cations with cucurbiturils have been reported by Buschmann *et al.*<sup>32</sup> who determined the binding constants between Na<sup>+</sup> and CB[6] to have values of 1450 M<sup>-1</sup> ( $K_1$ ) for the {CB[6]•Na}<sup>+</sup> complex and 60 M<sup>-1</sup> ( $K_2$ ) for the {CB[6]•2Na}<sup>2+</sup> complex. Meanwhile, for binding between CB[6] and K<sup>+</sup>, they calculated values of 560 M<sup>-1</sup> and <20 M<sup>-1</sup> for the {CB[6]•K}<sup>+</sup> and {CB[6]•2K<sup>+</sup>}<sup>2+</sup> complexes, respectively.<sup>32</sup> In a study involving CB[7], Mezzina and coworkers<sup>18</sup> noted that the binding constant between CB[7] and 1-phenylbutan-2-one decreased from 4.6 x 10<sup>3</sup> M<sup>-1</sup> to 4.7 x 10<sup>2</sup> M<sup>-1</sup> when K<sup>+</sup> cations were present. They also found that the binding constant between CB[7] and TEMPO decreased from 2.50 x 10<sup>4</sup> M<sup>-1</sup> to 6.15 x 10<sup>3</sup> M<sup>-1</sup> when the portals of CB[7] were capped by K<sup>+</sup> cations. Based on effect of the concentration of K<sup>+</sup> on the binding constant for the CB[7]:TEMPO complex, they determined the binding constants between CB[7] and K<sup>+</sup> to be  $K_{M1} = 600 \text{ M}^{-1}$  and  $K_{M2} = 53 \text{ M}^{-1}$  for the {CB[7]•K}<sup>+</sup> and {CB[7]•2K}<sup>2+</sup> complexes, respectively. A representation of the equilibria between CB[7], the guest, and the alkali metal cations is shown in Figure 2.7. The work by Mezzina *et al.*<sup>18</sup> represented the first reported calculation of the binding constant between K<sup>+</sup> and CB[7].<sup>18</sup>

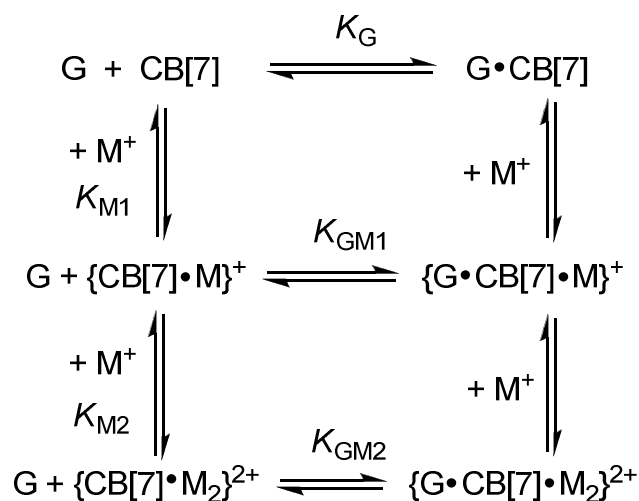


**Figure 2.7** The equilibria between CB[7], organic guests (G), and alkali metal cations ( $M^+$ ).

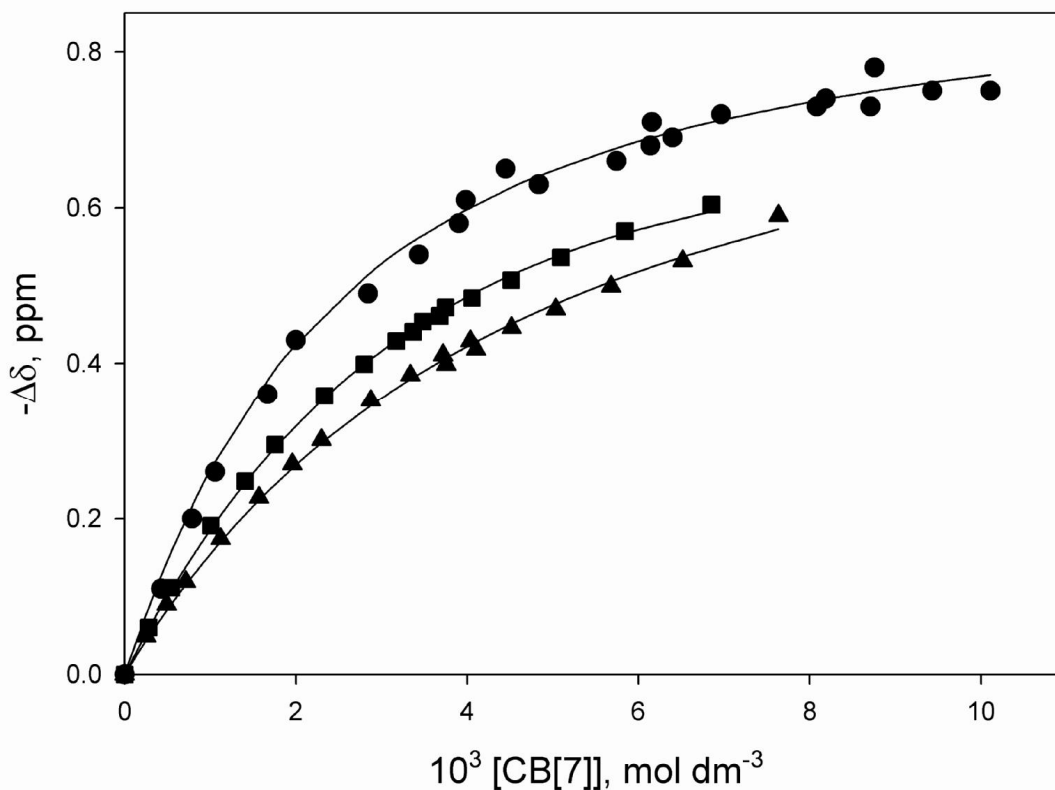


**Figure 2.8** The dependence of the complexation-induced chemical shift ( $-\Delta\delta_{\text{obs}}$ ) for the methyl resonances of acetone (0.7-0.8 mM) on the concentrations of CB[7] in  $\text{D}_2\text{O}$  solution in the (●) absence of  $\text{Na}^+$  and  $\text{K}^+$ , and the presence of 0.20 M (■) NaCl and (▲) KCl.

In our laboratory,  $^1\text{H}$  NMR titrations of acetone with CB[7] in the absence of alkali metal cations and in the presence of 0.20 M concentrations of  $\text{Na}^+$  and  $\text{K}^+$  cations were carried out (Figure 2.8). When either cation was present, a reduction in the binding affinity with CB[7] was observed for both the acetone and acetophenone guests. In the case of acetone complexation with CB[7], the binding constant decreased from  $580\text{ M}^{-1}$  in  $\text{D}_2\text{O}$  (no cations) to 370 and  $250\text{ M}^{-1}$  in the presence of 0.20 M  $\text{Na}^+$  and  $\text{K}^+$ , respectively (Table 2.2).

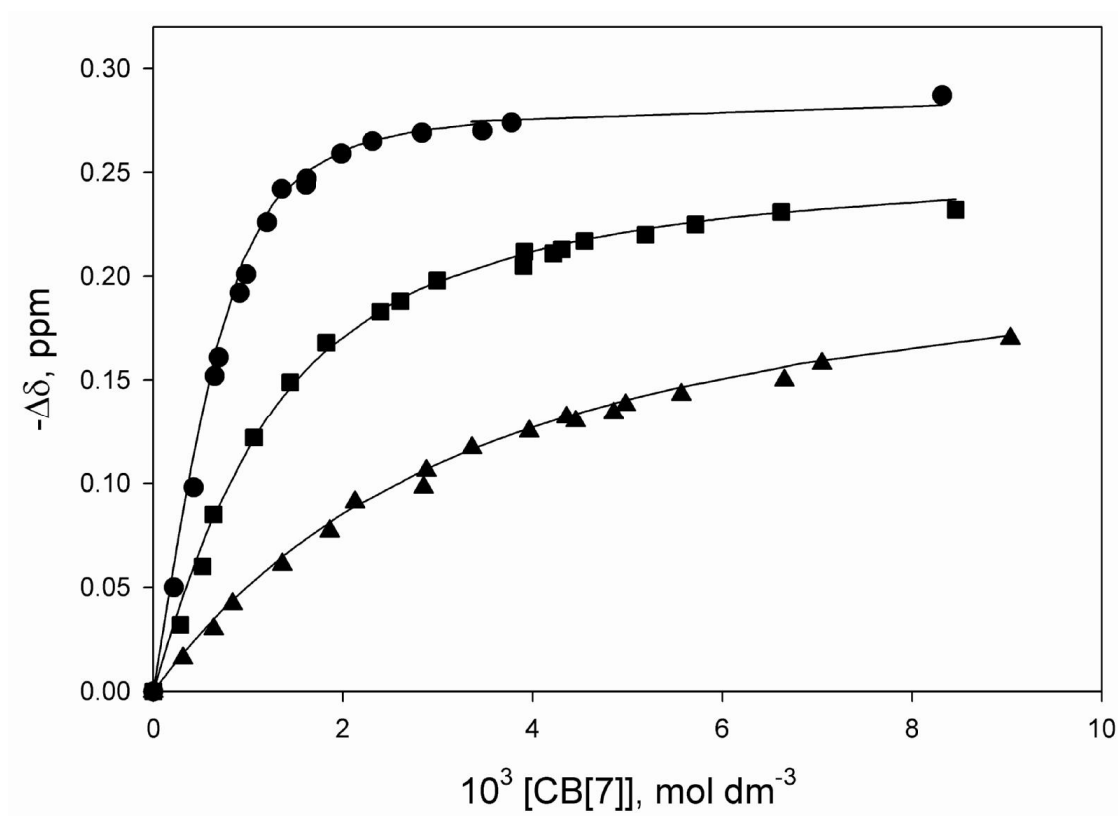


**Figure 2.9** The dependences of the complexation-induced chemical shift ( $-\Delta\delta_{\text{obs}}$ ) for the methyl resonances of acetophenone (0.7-0.8 mM) on the concentrations of CB[7] in  $\text{D}_2\text{O}$  solution in the (●) absence of  $\text{Na}^+$  and  $\text{K}^+$ , and in the presence of 0.20 M (■) NaCl and (▲) KCl.

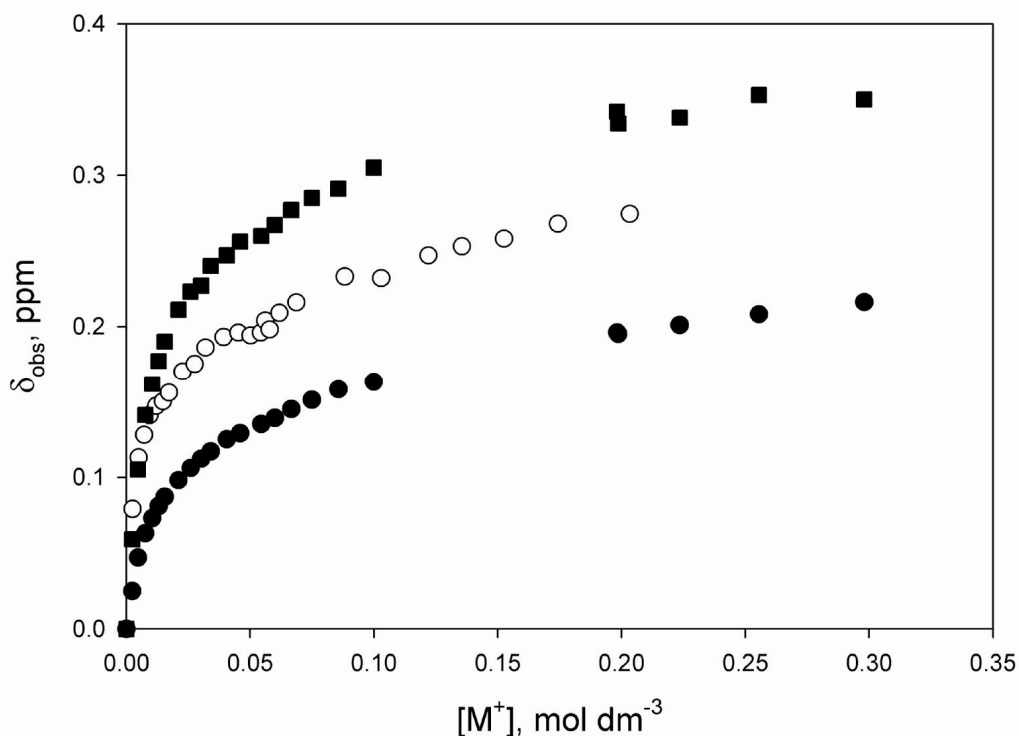
Acetophenone has a stability constant for binding to CB[7] of  $9600\text{ M}^{-1}$ , which was reduced to 1350 and  $350\text{ M}^{-1}$  in the presence of 0.20 M  $\text{Na}^+$  and  $\text{K}^+$ , respectively (Figure 2.9 and

Table 2.2). The reduction of the binding constants in the presence of these alkali metal cations for this guest was much more dramatic than that encountered with acetone as the guest. The larger methyl and phenyl groups of acetophenone extended to the portal region, and therefore the presence of alkali metal cations capping the portals had a greater tendency to disrupt binding between acetophenone and CB[7] by blocking the portals. Meanwhile, the smaller acetone guest, which was able to bind more completely inside the CB[7] cavity without extending to the portals, experienced smaller reductions in its binding affinity to CB[7] when the portals were capped by alkali metal cations.

The limiting  $\Delta\delta$  values observed for both the acetone and acetophenone guests help demonstrate the difference in the effect of the capped portals on the binding of the smaller and larger guests. For example, while the methyl protons of acetone showed no significant change from their limiting  $\Delta\delta$  value of -0.92 ppm in the presence of either  $\text{Na}^+$  or  $\text{K}^+$ , the methyl protons of acetophenone showed a change in their  $\Delta\delta$  values from -0.29 ppm in the absence of alkali cations, to -0.23 and -0.26 ppm in the presence of 0.20 M  $\text{Na}^+$  and  $\text{K}^+$ , respectively. This suggests that the acetophenone methyl protons, which bind near the portals, are not able to bind in the same position they normally occupy once the portals are blocked by the cations.

With a four to five-fold excess of CB[7] present, the acetone and acetophenone guests were each titrated with increasing amounts of  $\text{K}^+$  (Figure 2.10) and  $\text{Na}^+$ , and the changes in their chemical shifts were measured. If it can be assumed that the limiting change in the chemical shifts of the guest protons in the host-guest complexes are not affected by the binding of alkali metal cations ( $\text{M}^+$ ) to the portal(s) of the CB[7], then the change in the observed chemical shifts should be due to a decrease in the binding affinity of the  $\{\text{G}\cdot\text{CB}[7]\cdot\text{M}\}^+$  and  $\{\text{G}\cdot\text{CB}[7]\cdot\text{M}_2\}^{2+}$  complexes. This assumption would be more accurate for the inner protons, which are closer to the carbonyl groups of the guests. However, the  $\Delta\delta_{\text{lim}}$  values of the outer protons that are further away from the carbonyl group would be more likely to be perturbed by the cations bound to the

portals. The outer protons would be closer to the portals upon complexation with CB[7], and thus more likely to be disturbed by the presence of the cations, which are also near the portals. Therefore during these titrations, the protons closer to the carbonyl region, and more deeply positioned inside the cavity, were chosen in attempts to minimize potential deviation due to changes in the  $\Delta\delta_{\text{lim}}$  values. These protons included the methyl protons of acetone and acetophenone, as well as the *ortho* aromatic protons of acetophenone. As can be seen from the titration curve of the change in the observed chemical shift change as a function of the concentration of the alkali metal cations, the first cation apparently shows strong binding to CB[7], while the second cation subsequently shows weaker binding. The binding of these cations to the CB[7] in turn causes a reduction in the binding affinity between the CB[7] and the organic guests.



**Figure 2.10** The dependences of the change in chemical shift ( $\Delta\delta_{\text{obs}}$ ) of guest protons on the concentration of  $\text{K}^+$  in the presence of excess CB[7] (4-5-fold excess). The guest protons plotted are: (○) acetone methyl, (●) acetophenone methyl, and (■) acetophenone *ortho*-phenyl protons.

If it can be assumed that the presence of the cations does not significantly affect the limiting chemical shift changes of the guest protons, and that the concentrations of the free alkali metal cations approximately equal their total concentrations (because the concentration of CB[7] and the neutral guests are much lower than the cation concentrations), then the value of the observed binding constant ( $K_{\text{obs}}$ ), which may be calculated using the  $\Delta\delta_{\text{obs}}$  and  $\Delta\delta_{\text{lim}}$  values (in these calculations of  $K_{\text{obs}}$ , the small variations in the free acetone and free acetophenone chemical shifts with differing concentrations of  $\text{Na}^+$  and  $\text{K}^+$  were neglected), and can be related to the binding constants of the cations and organic guests, using Equation 2.1:

$$K_{\text{obs}} = \frac{K_G + K_{\text{GM1}}K_{\text{M1}}[\text{M}^+] + K_{\text{GM2}}K_{\text{M1}}K_{\text{M2}}[\text{M}^+]^2}{1 + K_{\text{M1}}[\text{M}^+] + K_{\text{M1}}K_{\text{M2}}[\text{M}^+]^2} \quad (2.1)$$

where  $K_G$  represents the binding constant between the organic guest and CB[7] in the absence of the alkali metal cations,  $K_{\text{M1}}$  represents the binding constant between CB[7] and one alkali metal cation, and  $K_{\text{M2}}$  is the binding constant between CB[7] and two alkali metal cations. Meanwhile,  $K_{\text{GM1}}$  corresponds to the stability constant of the complex between CB[7] and the organic guest and one alkali metal cation, while  $K_{\text{GM2}}$  is the binding strength of the complex formed between CB[7], one organic guest and two alkali metal cations. In the case of acetone, where  $K_G$  was found to be  $580 \text{ M}^{-1}$ , and using the binding constants between CB[7] and  $\text{K}^+$  reported by Mezzina *et al.*<sup>18</sup> ( $K_{\text{M1}} = 600 \text{ M}^{-1}$  and  $K_{\text{M2}} = 53 \text{ M}^{-1}$ ), values of  $K_{\text{GM1}} \approx 400 \text{ M}^{-1}$  and  $K_{\text{GM2}} \approx 150$  were obtained from fitting the experimental data to Equation 2.1. Meanwhile, for acetophenone, which was determined to have a  $K_G$  value of  $9600 \text{ M}^{-1}$ , values of  $K_{\text{GM1}} \approx 2000 \text{ M}^{-1}$  and  $K_{\text{GM2}} \approx 500 \text{ M}^{-1}$  were determined from fitting the titration data for the *ortho*-phenyl proton resonance to equation 2.1. A similar trend was observed by Mezzina and coworkers,<sup>18</sup> with binding affinities for the

guest 1-phenylbutan-2-one of  $K_G = 4600 \text{ M}^{-1}$  and  $K_{GM1} = 470 \text{ M}^{-1}$ . If, upon complexation with CB[7], a guest extends from the cavity into the portal region, the binding of the cations will have a greater effect on the guest's binding affinity with CB[7]. This was exhibited by the large decrease in binding strength of the host-guest complex between CB[7] with acetophenone, while the host-guest complex with the acetone guest experienced a smaller decrease in its binding constant in the presence of alkali metal cations.

**Table 2.2** Host-guest binding affinities between CB[7] and the solvents acetone and acetophenone in the presence and absence of alkali cations. The solvent and salt conditions are described below each binding constant heading.

Guest	$K_{CB[7]} (\text{M}^{-1})$	$K_{CB[7]} (\text{M}^{-1})$	$K_{CB[7]} (\text{M}^{-1})$
	D <sub>2</sub> O, no electrolyte	D <sub>2</sub> O, 0.2 M NaCl	D <sub>2</sub> O, 0.2 M KCl
Acetone	580	370	250
Acetophenone	9600	1350	350

Acetonitrile and DMSO showed the weakest binding affinities with CB[7], with values of 11 and 140  $\text{M}^{-1}$ , respectively. The CB[7] is reasonably soluble in DMSO,<sup>38,39</sup> and considering the relatively low binding constant between this guest and CB[7], it should permit the formation of fairly strong host-guest complexes with other guests. In the presence of a guest, the solubility of CB[7] in DMSO has been reported to reach 10 mM.<sup>39</sup>

## 2.3 Experimental

### 2.3.1 Materials

CB[7] was prepared and characterized using the method developed by Day.<sup>40</sup> In particular, 30.0 g (211 mmol) of glycoluril and 12.7 g (423 mmol) of paraformaldehyde were stirred in 42.6 mL of cold concentrated HCl. This mixture was stirred until it set as a gel, and was then allowed to stand for approximately one hour. This mixture was then refluxed at 100 °C

for approximately 18 hours. Shortly after the start of the reflux the gel melted to give an orange solution. At the end of the reflux the cloudy solution was allowed to cool to room temperature, and was then cooled further in an ice bath. This solution was then filtered, to give an orange, viscous filtrate and a pasty white solid. The filtrate was allowed to stand for approximately one hour at room temperature, and a grey-white, semi-crystalline, precipitate was observed, which was then removed by gravity filtration. The filtrate was then placed in a rotary evaporator, and its volume was reduced to between one half and one quarter of its original volume. After the rotary evaporation, 15 mL of water was added to the remaining solution, and it was subsequently filtered to remove white crystals that had formed. 105 mL of methanol was added to this filtrate, and it was allowed to stand for approximately 18 hours at room temperature, and the solid precipitate was collected by filtration. This solid was placed in 300 mL of a 20 % (by volume) solution of aqueous glycerol, and the solution was heated to almost boiling, with stirring for half an hour, in an attempt to dissolve the solid. Often, this solution was still cloudy after this step, and it was subsequently filtered until a clear filtrate was obtained, with repetition of filtration if necessary. Methanol was subsequently added to this filtrate until a white precipitate began to form. This cloudy solution was allowed to stand for 15 to 30 minutes, with more precipitate forming during this time. This was then filtered, and washed with methanol, in order to remove the glycerol, to give a flaky yellow solid, which in most cases was composed mainly of CB[6]. The filtrate was collected, and methanol was then added to it, with a cloudy white precipitate being formed. This cloudy solution was allowed to stand, and was subsequently filtered to give a white solid, which was often composed mainly of CB[7]. The filtrate from this was also collected, and methanol was added, and after standing for between 15 and 30 minutes, it was filtered, to give a white, powdery, solid composed of CB[7] and a clear filtrate. This process of addition of methanol to the filtrate, and subsequent filtration, was normally repeated several times, in order to obtain as many fractions of the product as possible. The yield of CB[7] was



1.92 g (1.65 mmol), or 5.47 %. The purity of the fractions was determined by  $^1\text{H}$  NMR, while confirmation of the correct CB[ $n$ ] homologue was determined by ESI-MS. The solid fractions of CB[7] were normally washed with methanol in order to remove residual glycerol, and subsequently dried. The use of acetone was avoided, due to the affinity between CB[7] and this solvent, which made it difficult to remove.

The guests compounds were purchased commercially and used as received (anhydrous, Aldrich). The salts sodium chloride and potassium chloride were also purchased from Aldrich and used as received.

### 2.3.2 Methods

The  $^1\text{H}$  NMR experiments were recorded on a Bruker Avance 400 MHz NMR instrument, with  $\text{D}_2\text{O}$  as the solvent. The binding constants for the host-guest complexes that exhibited fast exchange were calculated using least squares fitting of the  $\Delta\delta_{\text{obs}}$  parameter for the guest protons, as a function of the concentration of CB[7], to a 1:1 binding isotherm, using a formula utilized previously by Macartney and coworkers.<sup>41</sup> This formula can be expressed as shown for Equations 2.2 and 2.3:

$$[\text{H}\cdot\text{G}] = \{b - (b^2 - 4[\text{G}]_{\text{total}}[\text{H}]_{\text{total}})^{1/2}\} / 2 \quad (2.2)$$

$$\text{where } b = [\text{G}]_{\text{total}} + [\text{H}]_{\text{total}} + K^{-1} \quad (2.3)$$

and  $[\text{G}]_{\text{total}}$  is the total guest concentration (M),  $[\text{H}]_{\text{total}}$  is the total host concentration (M, host is CB[7] in this case),  $[\text{H}\cdot\text{G}]$  is the concentration of the 1:1 host-guest complex (M), and  $K$  is the binding constant ( $\text{M}^{-1}$ ). The observed shift was plotted against the concentration of CB[7], while

the predicted shift (based on the estimated values of  $K$  and the limiting chemical shift change) was also plotted. The predicted shift was calculated as (Equation 2.4):

$$\Delta\delta_{\text{predicted}} = \Delta\delta_{\text{lim}} \times ([\text{H}\cdot\text{G}]/[\text{G}]_{\text{total}}) \quad (2.4)$$

where  $\Delta\delta_{\text{lim}}$  is the limiting change in the chemical shift,  $[\text{H}\cdot\text{G}]$  is the concentration of the host-guest complex, and  $[\text{G}]_{\text{total}}$  is the total guest concentration. When an accurate value for the binding constant ( $K$ ) is entered into this formula, the plots of observed chemical shift change against the concentration of the host will overlap with the plot of the predicted chemical shift change against the concentration of the host. When the binding is reasonably strong, the limiting chemical shift change ( $\Delta\delta_{\text{lim}}$ ) can often be observed directly, as the maximum change in chemical shift, which occurs when there is an excess of the CB[7] and the guest is fully bound in the host. At this point the change of chemical shift no longer increases as more CB[7] is added. In cases where the host-guest binding is quite weak, it may become necessary to estimate the limiting chemical shift change, as it may not be possible to reach a large enough excess of CB[7] to reach the point where the true limiting chemical shift change occurs.

For host-guest systems exhibiting slow exchange with respect to the NMR timescale, the relative integrals (that is, the area occupied by each NMR signal) of the free and bound species were used to calculate the stability constants,<sup>42</sup> as shown in Equation 2.5:

$$K = (\text{Int H}\cdot\text{G})/(\text{Int H}_f \times \text{Int G}_f) \quad (2.5)$$

where Int H•G refers to the integral of the NMR signal representing the host-guest complex, Int H<sub>f</sub> refers to the integral of the NMR signal of the free host (CB[7] in this case), and Int G<sub>f</sub> refers to the integral of the NMR signal of the free guest, and  $K$  is the binding constant. Because the

integrals are proportional to the respective concentrations, the formula for calculating binding constants based on slow exchange systems can also be expressed as Equation 2.6:

$$K = [\text{H}\cdot\text{G}]/([\text{H}]_f \times [\text{G}]_f) \quad (2.6)$$

where  $[\text{H}\cdot\text{G}]$  is the concentration of the host-guest system,  $[\text{H}]_f$  is the concentration of the free host, and  $[\text{G}]_f$  is the concentration of the free guest.

For the weakly binding acetonitrile guest, the values of  $\Delta\delta_{\text{lim}}$  and  $K_{\text{CB}[7]}$  were calculated from the inverse of the intercept and from the intercept/slope ratio, respectively, of a double reciprocal plot of  $\Delta\delta_{\text{obs}}^{-1}$  against  $[\text{CB}[7]]^{-1}$ .<sup>43</sup> The  $\Delta\delta_{\text{lim}}$  value can therefore be determined from the y-intercept, which occurs when the value of  $[\text{CB}[7]]^{-1}$  is equal to zero, which could be expressed as  $\Delta\delta_0$ . This would give Equation 2.7:

$$\Delta\delta_{\text{lim}} = \Delta\delta_0 \quad (2.7)$$

where  $\Delta\delta_0$  is inverse of the  $\Delta\delta_{\text{obs}}^{-1}$  value that corresponds with the point where  $[\text{CB}[7]]^{-1} = 0$  in the  $\Delta\delta_{\text{obs}}^{-1}$  vs.  $[\text{CB}[7]]^{-1}$  plot. In other words,  $\Delta\delta_0^{-1}$  (and also  $\Delta\delta_{\text{lim}}$ ) corresponds to the inverse of the y-intercept in the double reciprocal plot.

Meanwhile, the value of the binding constant,  $K$ , is determined from the ratio of the intercept / slope in the plot of  $\Delta\delta_{\text{obs}}^{-1}$  against  $[\text{CB}[7]]^{-1}$  and can be expressed as Equation 2.8:

$$K = \Delta\delta_0^{-1} / \{(\Delta\delta_2 - \Delta\delta_1)^{-1}([\text{CB}[7]_2 - \text{CB}[7]_1])\} = \Delta\delta_0^{-1} / (\Delta\Delta\delta^{-1} \times \Delta[\text{CB}[7]]) \quad (2.8)$$

where  $\Delta\delta_0^{-1}$  is the  $y$ -intercept,  $\Delta\delta_2$  and  $\Delta\delta_1$  are the values of  $\Delta\delta_{\text{obs}}$  at points 2 and 1, respectively, and  $[\text{CB}[7]]_2$  and  $[\text{CB}[7]]_1$  are the concentrations of CB[7] at points 2 and 1, respectively.

The energy-minimized structures of the host-guest systems were obtained from the MM2 program from Chem3D software (ChemBioDraw 11.0 and Chem3D Pro 11.0), developed by CambridgeSoft.<sup>30</sup>

## 2.4 Conclusions

The formation of host-guest complexes between CB[7] and a series of small neutral organic molecules have been observed using  $^1\text{H}$  NMR spectroscopy. The driving force for the formation of these complexes is believed to be a combination of the hydrophobic effect and quadrupole-dipole interactions between the CB[7] host and carbonyl and related polar groups on the guest. The ketone-bearing guests displayed an increase in their CB[7] stability constants with an increase in their hydrophobicity. The binding affinity of the neutral guests was reduced in the presence of the alkali metal cations  $\text{Na}^+$  and  $\text{K}^+$ . The reduction in the stability constants was more dramatic when the portions of the guest molecule extended to the portal region(s) of the host, as a result of a competition between the cation(s) and the neutral guest for binding to these portal sites. The binding affinities of the solvent guests were determined, and since CB[7] has some degree of solubility in DMSO, this study may help others to determine more accurate binding constants for guests in this particular solvent, since the level of competition contributed by that solvent has now been determined. The research described in this chapter has been published in *Organic and Biomolecular Chemistry*.<sup>24</sup>

## References

1. J. Lagona, P. Mukhopadhyay, S. Chakrabarti, and L. Isaacs, *Angew. Chem., Int. Ed.*, **2005**, *44*, 4844.
2. S. Liu, C. Ruspic, P. Mukhopadhyay, S. Chakrabarti, P.Y. Zavalij, and L. Isaacs, *J. Am. Chem. Soc.*, **2005**, *127*, 15959.
3. W.L. Mock and N.-Y. Shih, *J. Org. Chem.*, **1986**, *51*, 4440.
4. I. Hwang, K. Baek, M. Jung, Y. Kim, K.M. Park, D.-W. Lee, N. Selvapalam, and K. Kim, *J. Am. Chem. Soc.*, **2007**, *129*, 4170.
5. W.S. Jeon, K. Moon, S.H. Park, H. Chun, Y.H. Ko, J.Y. Lee, E.S. Lee, S. Samal, N. Selvapalam, M.V. Rekharsky, V. Sindelar, D. Sobransingh, Y. Inoue, A.E. Kaifer, and K. Kim, *J. Am. Chem. Soc.*, **2005**, *127*, 12984.
6. S. Moghaddam, Y. Inoue, and M.K. Gilson, *J. Am. Chem. Soc.*, **2009**, *131*, 4012.
7. Y. Miyahara, K. Abe, and T. Inazu, *Angew. Chem., Int. Ed.*, **2002**, *41*, 3020.
8. D.M. Rudkevich, *Angew. Chem., Int. Ed.*, **2004**, *43*, 558.
9. D. Bardelang, K.A. Udachin, R. Anedda, I. Moudrakovski, D.M. Leek, J.A. Ripmeester, and C.I. Ratcliffe, *Chem. Commun.*, **2008**, 4927.
10. J.-X. Liu, L.-S. Long, R.-B. Huang, and L.S. Zheng, *Cryst. Growth Des.*, **2006**, *6*, 2611.
11. D.G. Samsonenko, O.A. Gerasko, A.V. Virovets, and V.P. Fedin, *Russ. Chem. Bull.*, **2005**, *54*, 1557.
12. Y.-Q. Zhang, Q.-J. Zhu, S.-F. Xue, and Z. Tao, *Molecules*, **2007**, *12*, 1325.
13. J.-X. Liu, L.-S. Long, R.-B. Huang, and L.-S. Zheng, *Inorg. Chem.*, **2007**, *46*, 10168.
14. M. El Haouaj, Y.H. Ko, M. Luhmer, K. Kim, and K. Kim, and K. Bartik, *Perkin Trans. 2*, **2001**, 2104.
15. M. El Haouaj, M. Luhmer, Y.H. Ko, K. Kim, and K. Bartik, *Perkin Trans. 2*, **2001**, 804.
16. H.-J. Buschmann, K. Jansen, and E. Schollmeyer, *Thermochim. Acta*, **2000**, *346*, 33.

17. M.V. Rekharsky, Y.H. Ko, N. Selvapalam, K. Kim, and Y. Inoue, *Supramol. Chem.*, **2007**, *19*, 39.
18. E. Mezzina, F. Cruciani, G.F. Pedulli, and M. Lucarini, *Chem. Eur. J.*, **2007**, *13*, 7223.
19. R. Wang, L. Yuan, and D.H. Macartney, *Chem. Commun.*, **2005**, 5867.
20. J. Mohanty, A.C. Bhasikuttan, W.M. Nau, and H. Pal, *J. Phys. Chem. B*, **2006**, *110*, 5132.
21. M. Shaikh, J. Mohanty, P.K. Singh, W.M. Nau, and H. Pal, *Photochem. Photobiol. Sci.*, **2008**, *7*, 408.
22. R. Wang, L. Yuan, and D.H. Macartney, *Chem. Commun.*, **2006**, 2908.
23. A. Praetorius, D.M. Bailey, T. Schwarzlose, and W.M. Nau, *Org. Lett.*, **2008**, *10*, 4098.
24. I.W. Wyman and D.H. Macartney, *Org. Biomol. Chem.*, **2008**, *6*, 1796.
25. O.S. Tee, A.A. Fedortchenko, P.G. Loncke, and T.A. Gadosy, *Perkin Trans. 2*, **1996**, 1243.
26. M. Zubiaur and C. Jaime, *J. Org. Chem.*, **2000**, *65*, 8139.
27. C.E. Feliciano, M. Garcia, H. Rivera, Y. Pedrego, and E. Quinones, *Biol. J. Armenia*, **2001**, *53*, 200.
28. Y. Matsui and S. Tokunaga, *Bull. Chem. Soc. Jpn.*, **1996**, *69*, 2477.
29. R.I. Gelb, L.M. Schwartz, M. Radeos, R.B. Edmonds, and D.A. Lauger, *J. Am. Chem. Soc.*, **1982**, *104*, 6283.
30. *Chem 3D Pro 11.0*, CambridgeSoft, Cambridge, MA, 2007.
31. C. Marquez, R.R. Hudgins, and W.M. Nau, *J. Am. Chem. Soc.*, **2004**, *126*, 5806.
32. R. Hoffman, W. Knoche, C. Fenn, and H.-J. Buschmann, *J. Chem. Soc., Faraday Trans.*, **1994**, *90*, 1507.
33. W. Ong and A.E. Kaifer, *J. Org. Chem.*, **2004**, *69*, 1383.
34. V. Sindelar, S.E. Parker, and A.E. Kaifer, *New J. Chem.*, **2007**, *31*, 725.
35. H.-J. Buschmann, E. Cleve, L. Mutihac, E. Schollmeyer, *J. Incl. Phenom. Macrocycl. Chem.*, **2009**, *65*, 293.

36. Y.-M. Jeon, J. Kim, D. Whang, and K. Kim, *J. Am. Chem. Soc.*, **1996**, *118*, 9790
37. M. Shaikh, J. Mohanty, A.C. Bhasikuttan, V.D. Uzunova, W.M. Nau, and H. Pal, *Chem. Commun.*, **2008**, 3681.
38. The use of non-aqueous solvents for cucurbituril host-guest chemistry was discussed in an oral presentation by A.E. Kaifer at the NSF Workshop on Cucurbituril Molecular Containers, College Park, MD, August 4, 2007.
39. A. Thangavel, A.M.M. Rawashdeh, C. Sotiru-Leventis, and N. Leventis, *Org. Lett.*, **2009**, *11*, 1595.
40. A. Day, A.P. Arnold, R.J. Blanch, and B. Snushall, *J. Org. Chem.*, **2001**, *66*, 8094.
41. R.S. Wylie and D.H. Macartney, *Inorg. Chem.*, **1993**, *32*, 1830.
42. J.W. Steed and J.L. Atwood, *Supramolecular Chemistry*, John Wiley & Sons Ltd.: Chichester, 2000; p. 16.
43. K.A. Connors, *Binding Constants*, John Wiley & Sons: New York, 1987; p. 152.

## Chapter 3

# Cucurbit[7]uril Host-Guest and Pseudorotaxane Complexes with $\alpha,\omega$ -bis(pyridinium)alkane Dications

### 3.1 Introduction

Rotaxanes and pseudorotaxanes using CB[5],<sup>1</sup> CB[6],<sup>2-7</sup> CB[7],<sup>8-17</sup> and CB[8]<sup>18-20</sup> as the cyclic component have been reported by various research groups. While some of these rotaxanes and pseudorotaxanes consist of one cucurbituril and one guest as the linear thread (to give a [2]rotaxane/[2]pseudorotaxane), examples have also been prepared with multiple cucurbiturils bound to the thread,<sup>4-6,21,22</sup> and even combinations of cucurbiturils and other cyclic hosts, such as cyclodextrins.<sup>11,13,23,24</sup> In addition, in some examples there are multiple potential binding sites that a given cucurbituril may occupy, and the cucurbituril ring may shuttle between these sites along the thread,<sup>4,9,25</sup> depending on external stimuli, or on the presence of other macrocycles nearby on the thread.

In the case of cyclodextrins binding guests along with cucurbiturils, it has been demonstrated that positive cooperativity may occur. A ternary complex composed of CB[6],  $\beta$ -CD, and dihexylammonium has a stability constant 33 times higher than that of the complex between  $\beta$ -CD and dihexylammonium.<sup>23</sup> In the NOESY NMR spectrum of the ternary complex, NOE cross-peaks between the CB[6] and  $\beta$ -CD were visible, indicating close proximity of the two macrocycles, and leading the authors to conclude that hydrogen bonding was occurring between a rim of CB[6] and a rim of  $\beta$ -CD, thus contributing to the enhanced stability of the



ternary complex. Although the 1:1 complexes formed between the  $\alpha$ -,  $\beta$ -, and  $\gamma$ -CDs and CB[6] have binding constants below  $40 \text{ M}^{-1}$ ,<sup>26</sup> the complexation of the two macrocycles to the dihexylammonium guest may act as a template to further enhance these weak interactions between the macrocycles, and thus improve the stability of the ternary complex. Schmitzer *et al.* have reported that the ternary complexes between diimidazolium salts and both CB[7] and cyclodextrins ( $\alpha$ - and  $\beta$ -CD were studied) resulted in the CB[7] encapsulating the dicationic diimidazolium cation, while in binary complexes between the guest and either the CB[7] or CD, the macrocycles were positioned over the aromatic rings at the end of the molecule.<sup>13</sup>

When complexation of the tetracationic guest  $[\text{CH}_3\text{bpy}(\text{CH}_2)_6\text{bpyCH}_3]^{4+}$  (bpy = 4,4'-bipyridinium) with CB[7] was studied, it was found that when one equivalent of CB[7] was present, a [2]pseudorotaxane was formed with the CB[7] located over the central hexamethylene linker.<sup>27</sup> However, upon addition of a second CB[7] to the molecule to form the [3]pseudorotaxane, the first CB[7] that was originally located over the hexamethylene linker migrated to one of the viologens at the end of the molecule, with the second CB[7] occupying the viologen moiety at the opposite end of the guest. The electron rich portals of the cucurbiturils can repel each other so that the presence of a second CB[7] will cause the first CB[7] to relocate to another binding site further along the guest. Two well-separated CB[7] macrocycles may thus bind to the tetracationic thread to form the [3]pseudorotaxane.

In this chapter, the host-guest chemistry between CB[7] and a series of dicationic bis(pyridinium) guests, whose pyridinium centres were linked with ethylene, hexamethylene, or *p*-xylylene linkers, was explored.<sup>28</sup> In addition to the three types of linkers, the substitutions of the pyridinium guests were varied to include 4-*tert*-butyl-, 4-dimethylamino-, 2-methyl-, and 3-methylpyridinium units. [2]Pseudorotaxane complexes of these bis(pyridinium) guests with CB[7] have been formed, with the bis(pyridinium) guest acting as the thread and the CB[7] hosts acting as the rings, or beads. These [2]pseudorotaxanes, made up of a 1:1 complex between

CB[7] and the bis(pyridinium) guest, as well as [3]pseudorotaxanes, as 2:1 complexes (with two CB[7] beads and one bis(pyridinium) thread) have been prepared in aqueous solution. The host-guest interactions of these complexes were characterized using  $^1\text{H}$  NMR and UV-visible spectroscopies, as well as electrospray mass spectrometry (ESI-MS). The work described in this chapter has been published.<sup>28</sup>

## 3.2 Results and Discussion

As  $^1\text{H}$  NMR spectroscopy is sensitive to whether guest protons are encapsulated within the CB[7] cavity (and thus display an upfield shift), or outside the cavity and near the electron rich portals (giving a downfield shift),  $^1\text{H}$  NMR titrations can provide useful information regarding the location of the CB[7] macrocycle(s) along the bis(pyridinium) thread at different host-guest stoichiometries, based on the limiting complexation-induced shifts (Figures 3.1 and 3.6). Within this series of dicationic bis(pyridinium) guests, the exchange rates of their host-guest complexes were found to vary considerably, from showing slow exchange with respect to the NMR timescale (with both the free and bound guest peaks being visible), to fast exchange with respect to the NMR timescale (in which case the only the average of the free and bound peaks was visible). In addition, intermediate exchange, with significant broadening of the average resonance peak that was seen in fast exchange, also occurred, and was observed for the 1,6-bis(4-tert-butylpyridinium)*p*-xylylene (BBPX<sup>2+</sup>) guest.

### 3.2.1 Host-Guest Complexes Between CB[7] and BPE<sup>2+</sup>, BAPE<sup>2+</sup>, and BBPE<sup>2+</sup>

The smallest dication in this series, 1,2-bis(pyridinium)ethane (BPE<sup>2+</sup>), upon complexation with CB[7], showed upfield shifts of both its pyridinium and ethylene spacer proton resonances. This suggested that the CB[7] was moving back and forth over the pyridinium and

ethylene groups through fast exchange behaviour on the NMR timescale. This guest formed a 1:1 complex with CB[7] without any spectroscopic evidence of two CB[7] macrocycles being bound to this dication. When the CB[7] ratio was increased beyond the 1:1 host-guest ratio, there was no further change in the NMR spectra, which would otherwise be expected if a second CB[7] was beginning to complex with the guest. Also, there was no evidence of formation of a [3]pseudorotaxane between CB[7] and BPE<sup>2+</sup> from the ESI-MS data (Table 3.2). Meanwhile, the other guests, which were all larger than BPE<sup>2+</sup> (to varying degrees), showed evidence of forming 2:1 host-guest complexes when excess CB[7] was present.

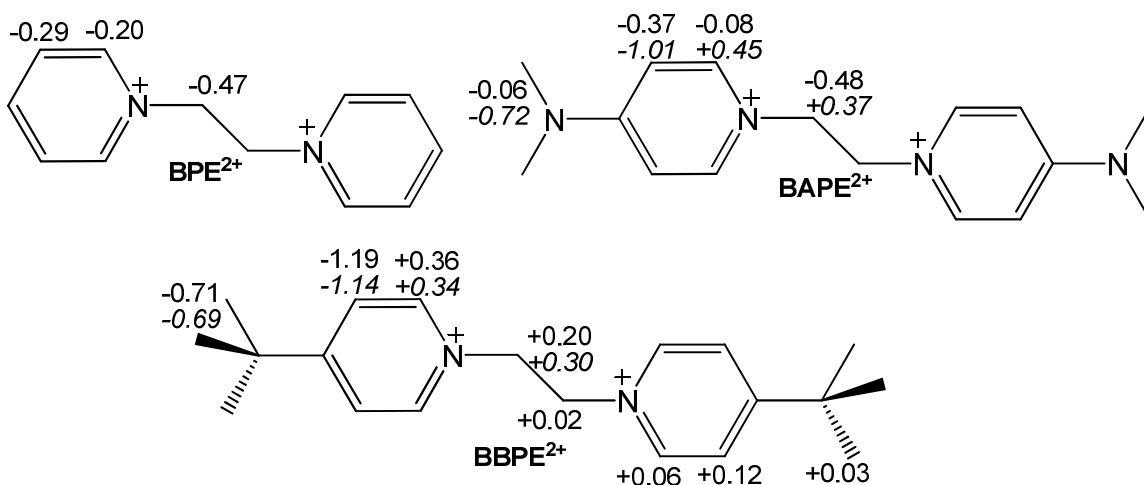


**Figure 3.1** Structures of the guests and complexation-induced chemical shifts ( $\Delta\delta_{\text{lim}}$ , ppm) for the 1:1 (top numbers) and 2:1 (bottom number, in italics) host-guest complexes with CB[7]. The numbers at the bottom and right of BBPE<sup>2+</sup> represent the  $\Delta\delta$  values for the unbound end of the 1:1 complex.

The 1,2-bis(4-dimethylaminopyridinium)ethane (BAPE<sup>2+</sup>) dication exists in two possible resonance structures (Figure 3.2), either with the positive charges positioned at the pyridinium nitrogens (the pyridinium form), or alternatively, at the nitrogens of the dimethylamines (the quinoidal form). In the quinoidal form, the carbon-nitrogen bond between the pyridine ring and the amine exists as a double bond (and the amine becomes an iminium group in this species). In

fact, Kalatzis and Kiriazis<sup>29</sup> have observed that the carbon-nitrogen bond connecting the pyridine ring and the amine of 1-methyl-4-alkylaminopyridinium cations have significant double bond character, on the basis of <sup>13</sup>C NMR measurements recorded in aqueous solution at room temperature. When the BAPE<sup>2+</sup> dication exists in the quinoidal form, the encapsulation of the guest, with the CB[7] cavity centred over the ethylene spacer, would place the cations at the portals of the CB[7], thus stabilizing this form further, as is shown from the energy minimized structure (Figure 3.2) as well as the observed complexation-induced shifts with one equivalent of CB[7] (with the upfield shifts of the ethylene proton resonances in Figure 3.1).

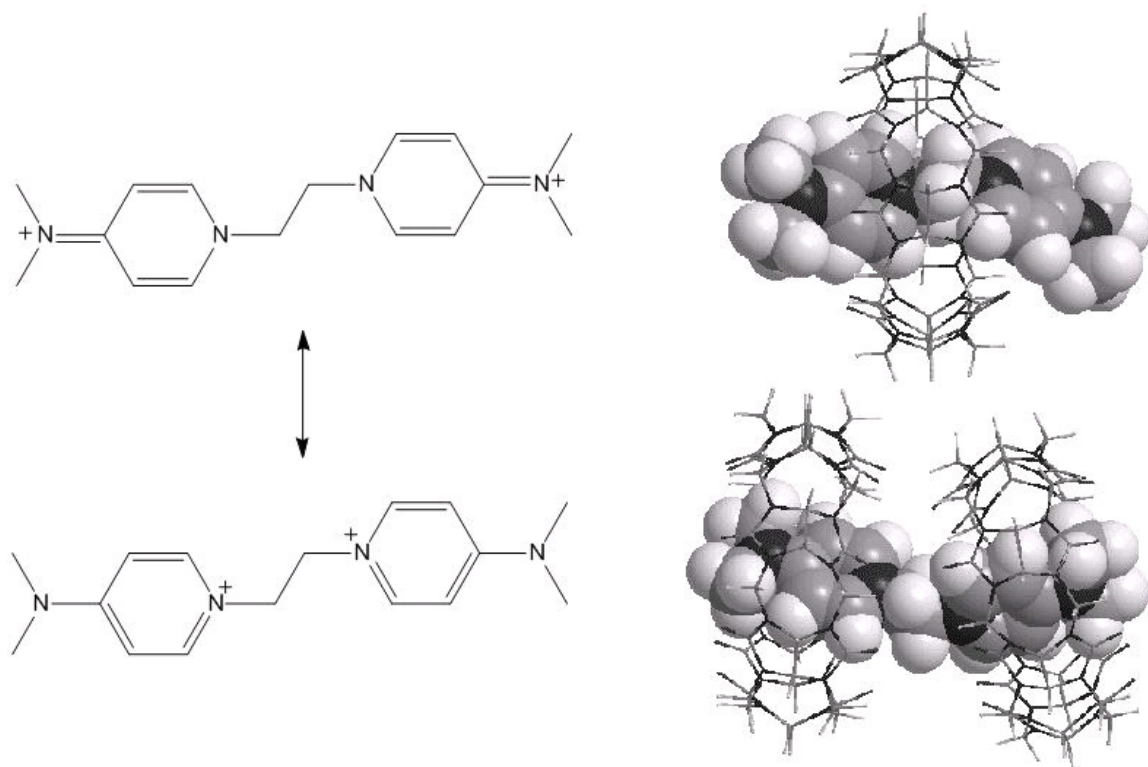


**Figure 3.2** The quinoidal (top left) and pyridinium (bottom left) resonance structures of BAPE<sup>2+</sup>, and the energy-minimized structures of {CB[7]•BAPE}<sup>2+</sup> (top right) and {2CB[7]•BAPE}<sup>2+</sup> (bottom right).

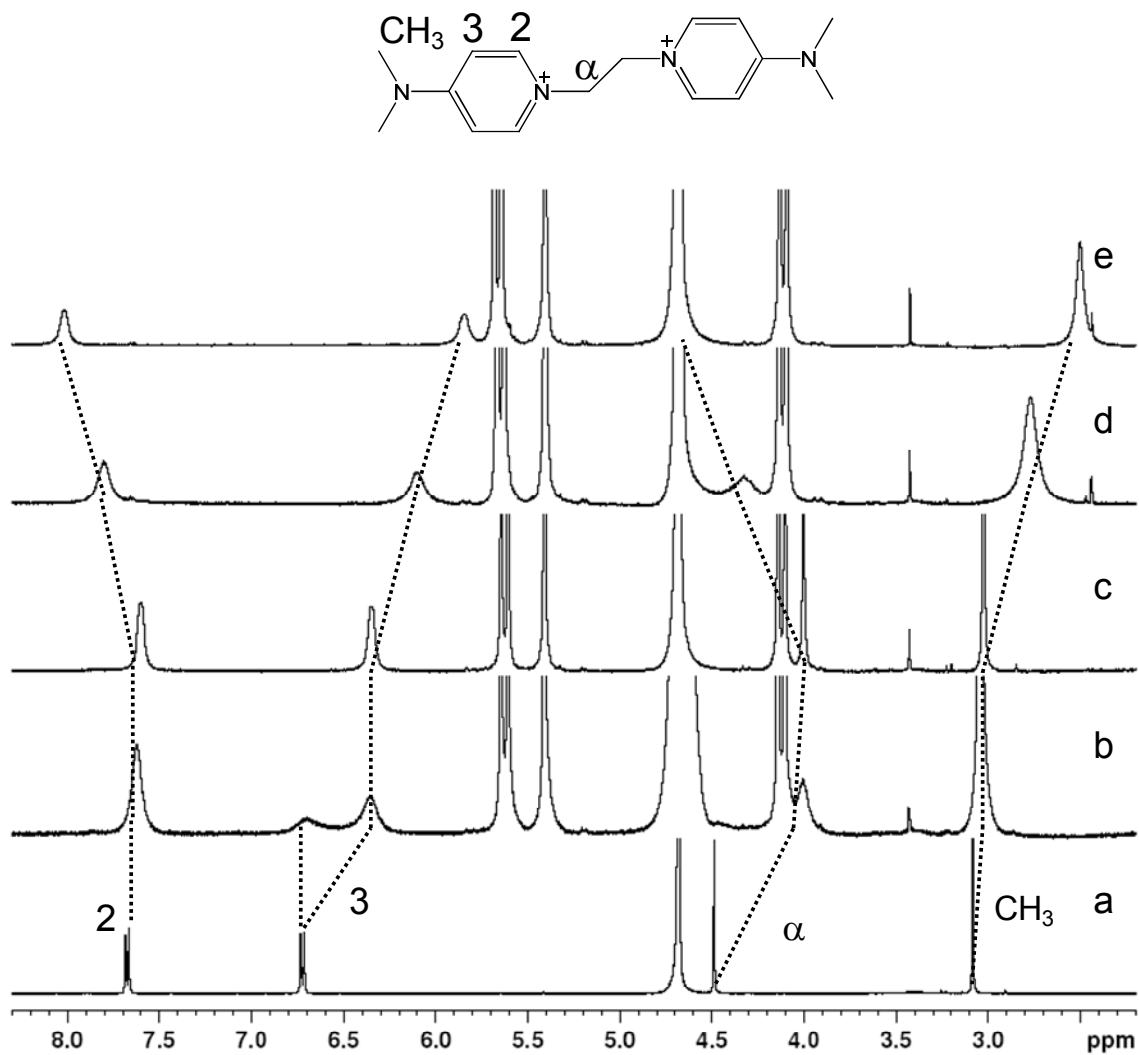


**Figure 3.3**  $^1\text{H}$  NMR titration of  $\text{BAPE}^{2+}$  (1.08 mM in  $\text{D}_2\text{O}$ ) in the presence of: (a) 0.00, (b) 0.73, (c) 1.14, (d) 1.86, and (e) 2.34 equivalents of  $\text{CB}[7]$ .

Since the  $\text{BAPE}^{2+}$  dication can undergo a change between its two resonance structures, the changes in the chemical shifts of the guest upon complexation would represent a combination

of the complexation-induced shifts as well as changes due to the shift in the equilibrium between the pyridinium resonance structure of the guest and the quinoidal resonance form. The quinoidal resonance structure should have proton chemical shifts that are all upfield compared to those of the pyridinium form of the  $\text{BAPE}^{2+}$  cation. Therefore, the small upfield shifts shown for the methyl protons of  $\text{BAPE}^{2+}$  represent a combination of the upfield shift due to the change of the equilibrium in favour of the quinoidal resonance form, and a downfield shift due to the proximity of the carbonyl-lined portals of CB[7], when the 1:1 complex is formed. The formation of the 1:1 complex occurs by slow exchange on the NMR timescale, while formation of the 2:1 complex occurs by fast exchange (Figure 3.3). This difference in the exchange rates would be consistent with the positioning of the CB[7] macrocycles along the  $\text{BAPE}^{2+}$  guest, as when the 1:1 complex is formed, the CB[7] is located in the middle of the molecule, and it would therefore be slower to associate and dissociate from the complex. On the other hand, when the CB[7] is located over the pyridinium region of the guest, near the ends of the  $\text{BAPE}^{2+}$  ligand, the guest can more quickly associate with, and dissociate from, the CB[7]. Upfield shifts of the aliphatic linker of  $\text{BAPE}^{2+}$  were observed while CB[7] encapsulated that region, while this trend was reversed as the equivalence point was exceeded and the CB[7] migrated to the ends of the molecule, to give downfield shifts for the aliphatic linker of the guest.

The titration of  $\text{BAPE}^{2+}$  with CB[7] was also monitored by UV-visible spectroscopy (Figure 3.4), and it was observed that as CB[7] was added, the  $\lambda_{\text{max}}$  shifted from 286 nm for the free solution of  $\text{BAPE}^{2+}$ , to 298 nm for the 1:1 host-guest complex, with an isosbestic point present at 292 nm. When the concentration of CB[7] was greater than that of  $\text{BAPE}^{2+}$ , the  $\lambda_{\text{max}}$  moved to 294 nm, with an isosbestic point at 296 nm. The bathochromic shift observed during the formation of the 1:1 complex is likely due to the stabilization of the quinoidal resonance structure of the guest. This preference for the quinoidal form is reduced slightly upon addition of the second CB[7], as observed by the slight hypsochromic shift as the equilibrium shifts in favour

of the pyridinium resonance of the dication. In their study of complexation between the tetracationic 1,2-bis(4-*N,N*'-dimethylamino)bipyridinium)ethane guest with the dibenzo-24-crown-6 host, Loeb *et al.*<sup>30</sup> observed the opposite behaviour. In this system, the crown ether formed a complex with the guest only when it was in its pyridinium form, and not when it was in the pseudo-quinoidal form. The central  $^+NCH_2CH_2N^+$  linker of the guest formed ion-dipole interactions with the crown ether, while in our complex, the pseudo-quinoidal structure provides a good match between the positive charges at the iminium nitrogens and the electron rich portals of the CB[7] in the 1:1 host-guest complex.

The 1,2-bis(4-*tert*-butylpyridinium)ethane (BBPE<sup>2+</sup>) guest, with its hydrophobic *tert*-butyl substituents, forms a stable 1:1 complex with CB[7], with the CB[7] encapsulating the *tert*-butyl group on one end of the molecule but not the other. Unlike the other pyridinium substituents in this study, the bulky *tert*-butyl groups prevent the CB[7] from migrating to the middle of the linker, but also provides a very hydrophobic environment for the CB[7] to bind. While the complexation-induced shifts are larger at the end that is encapsulated by the CB[7], the guest protons at the other end of this asymmetric host-guest complex also display small downfield complexation-induced shifts (Figures 3.1 and 3.5). Unlike BPE<sup>2+</sup> or BAPE<sup>2+</sup>, the aliphatic linker displayed only downfield shifts upon complexation with CB[7], and no upfield shifts were observed over this region. This behaviour was a result of the CB[7] cavity remaining at the outer regions of the guest. The bis(pyridinium) guests containing bulky *tert*-butyl groups display slow exchange host-guest complex formation, and resonances of the free guest, both the “free” and encapsulated ends of the guest for the 1:1 complex, as well as protons corresponding to the 2:1 (CB[7]:guest) complex are visible. The addition of the second CB[7] had little effect on the chemical shifts of the pyridinium protons already encapsulated by the first CB[7].

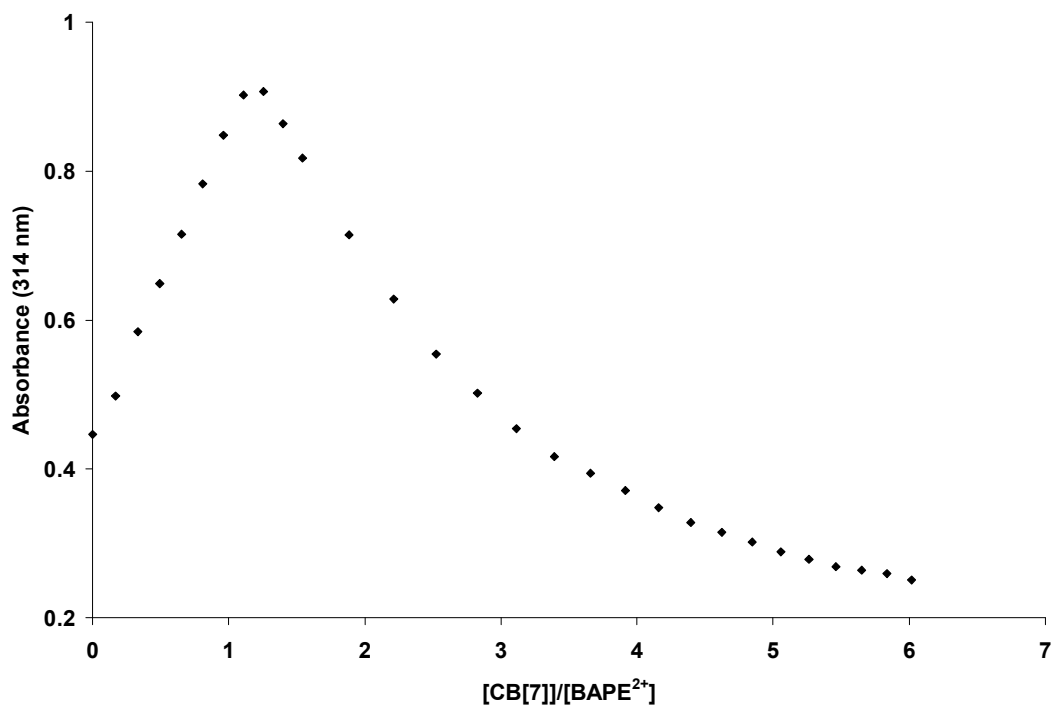
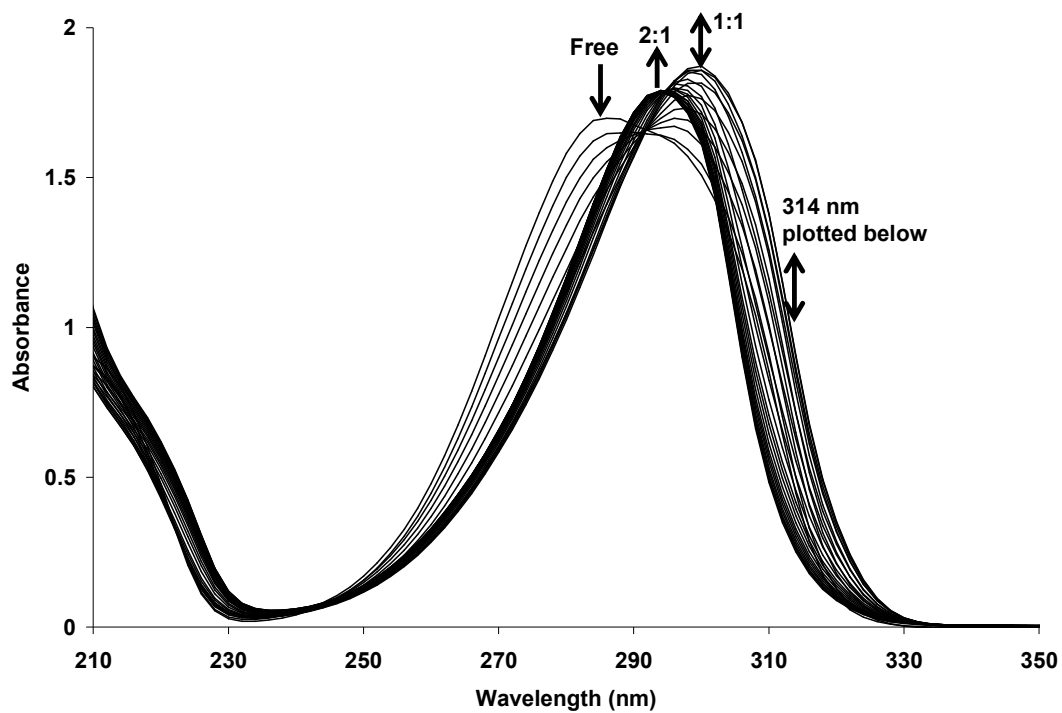


**Figure 3.4** UV-visible titration of BAPE<sup>2+</sup> ( $5.1 \times 10^{-5}$  M in aqueous solution) with CB[7] (above) and a plot of the absorbance at 314 nm as a function of the [CB[7]] / [BAPE<sup>2+</sup>] ratio (below). Absorbance at 314 nm was plotted, as it was receptive to changes in the complexation behaviour.



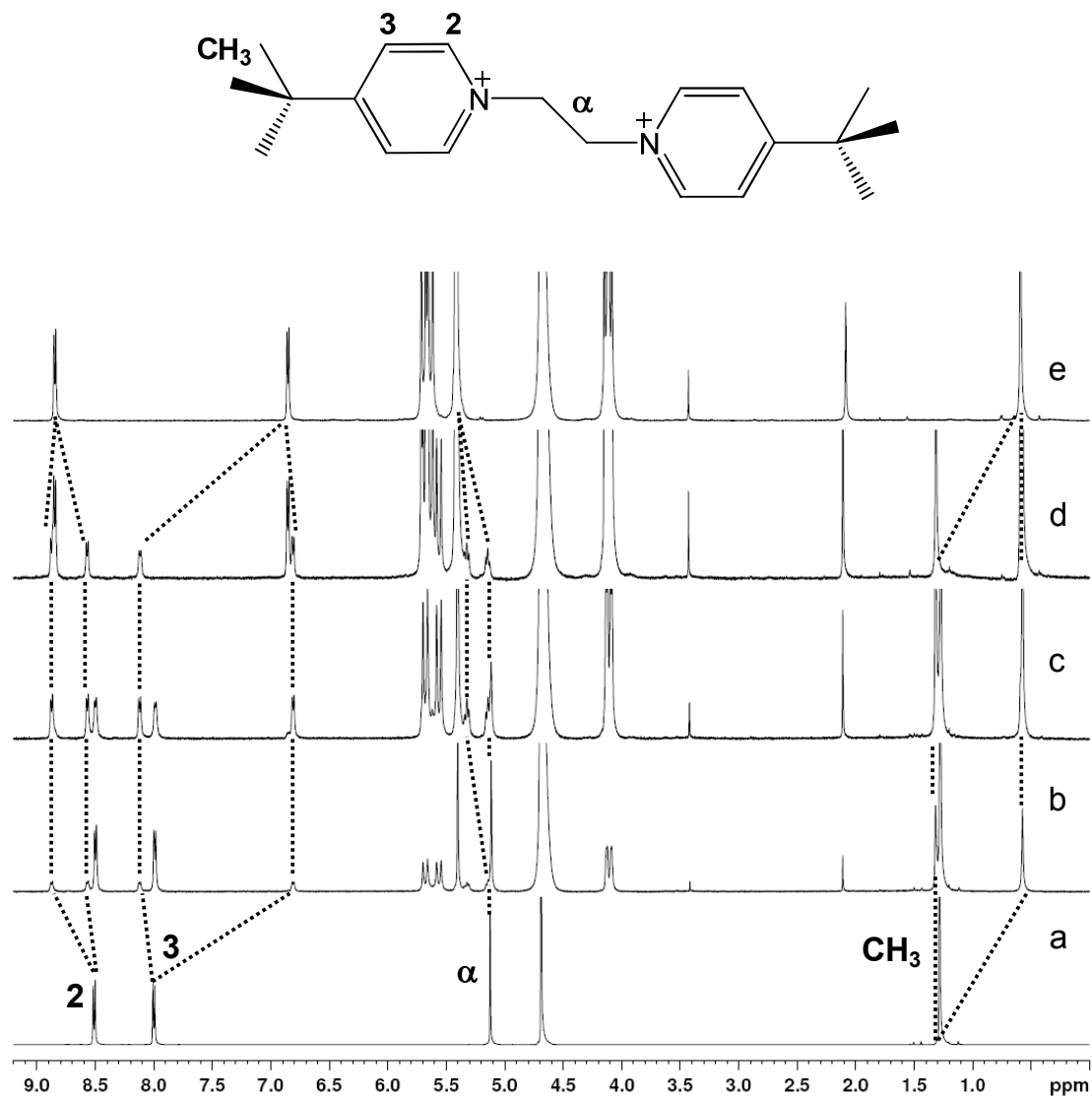


**Figure 3.5** <sup>1</sup>H NMR spectra of the titration of BBPE<sup>2+</sup> (1.00 mM in D<sub>2</sub>O) in the presence of: (a) 0.00, (b) 0.30, (c) 0.73, (d) 1.57, and (e) 2.19 equivalents of CB[7].

### 3.2.2 Host-Guest Complexes Between CB[7] and BPH<sup>2+</sup>, BAPH<sup>2+</sup>, B2PH<sup>2+</sup>, B3PH<sup>2+</sup>, BBPH<sup>2+</sup>, and BBPX<sup>2+</sup>

For the dicationic guests having longer linkers between the pyridinium groups (Figure 3.6), the CB[7] is able to form a 1:1 complex with the macrocycle positioned centrally over the linker. An X-ray crystal structure of a complex formed between 1,6-bis(pyridinium)hexane (BPH)<sup>2+</sup> and CB[6] was reported by Xiao and coworkers, with the CB[6] cavity located over the hexamethylene linker of the guest, while the cationic pyridinium rings are positioned near the portals.<sup>3</sup> For the host-guest complex between BPH<sup>2+</sup> and the slightly larger CB[7] macrocycle, a stability constant of  $4.8 \times 10^8 \text{ M}^{-1}$  was determined, followed by a much weaker 2:1 binding affinity of near  $80 \text{ M}^{-1}$  when larger excess of CB[7] was present. Formation of the 1:1 complex resulted in upfield shifts of the hexamethylene linker protons that were encapsulated by the hydrophobic CB[7] cavity, while the *meta* and *para* pyridinium protons yielded modest downfield shifts due to their proximity to the portal region. As the amount of CB[7] was increased and the 2:1 complex formed, the pyridinium protons began to exhibit modest upfield shifts, while the protons of the hexamethylene chain showed a downfield shift. Although it wasn't possible to obtain accurate  $\Delta\delta$  values for the 2:1 complex due to its weak binding, the trend observed was consistent with localization of the CB[7] cavities over one or (probably) both of the pyridinium regions upon formation of the 2:1 complex.

As was the case with the BPH<sup>2+</sup> complex, it was observed with the 1,6-bis(2-picoline)hexane (B2PH<sup>2+</sup>) and 1,6-bis(3-picoline)hexane (B3PH<sup>2+</sup>) complexes that the CB[7] was located initially over the hexamethylene regions, with upfield shifts of those protons, upon formation of the 1:1 complex. When the second CB[7] was added to form the 2:1 complex, the CB[7] that bound first migrated to the pyridinium region, while the second CB[7] became bound to the pyridinium at the opposite end of the molecule. The first CB[7] was more stable in the hexamethylene region, where both portals could be near cationic pyridinium centres. However,

electrostatic repulsions between the cucurbiturils drove the first CB[7] to one end, with the other CB[7] then binding at the opposite end of the molecule. Similar behaviour was also observed for the 1,6-bis(4-dimethylaminopyridinium)hexane ( $\text{BAPH}^{2+}$ ) dication (Figure 3.7).

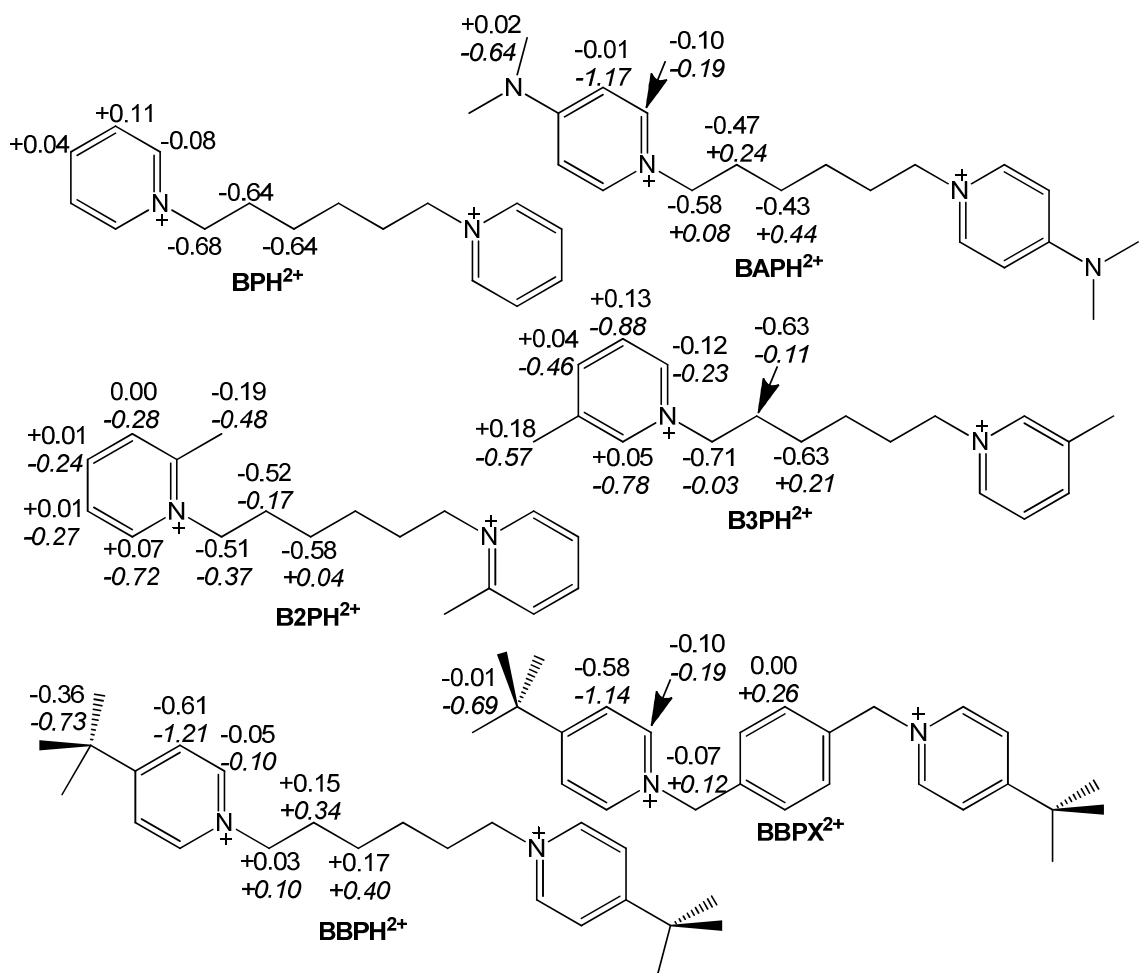


**Figure 3.6** Structures and limiting complexation-induced shifts ( $\Delta\delta_{\text{lim}}$ , ppm) of the bis(pyridinium)guests bearing the hexamethylene and *p*-xylylene linkers. The upper numbers represent the  $\Delta\delta_{\text{lim}}$  values of the 1:1 host-guest complex with CB[7], while the lower numbers (in italics) represent the  $\Delta\delta_{\text{lim}}$  values of the 2:1 host-guest complexes with CB[7].

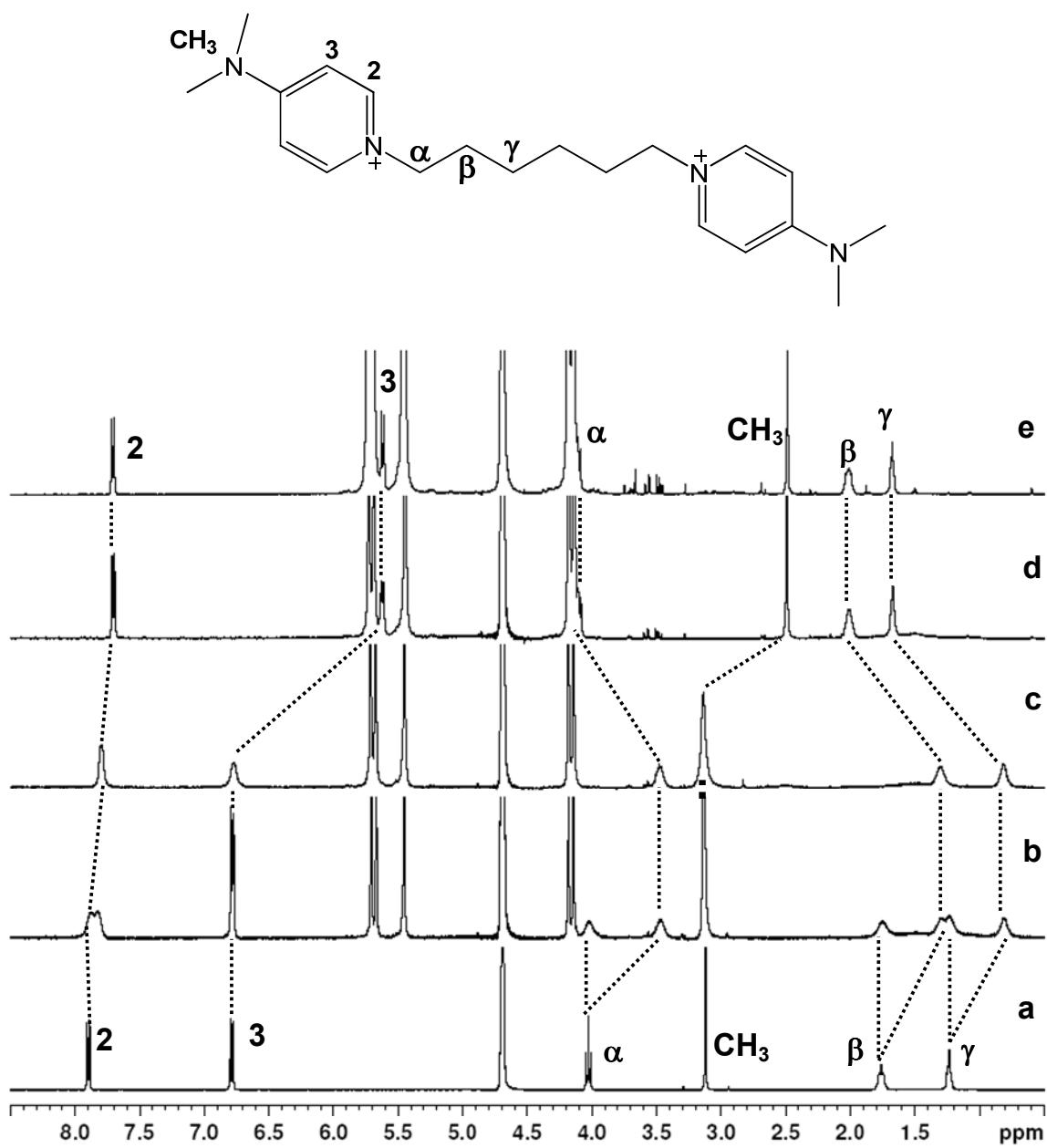


**Figure 3.7** Titration of BAPH<sup>2+</sup> (1.13 mM in D<sub>2</sub>O) in the presence of: (a) 0.00, (b) 0.54, (c) 1.17, (d) 2.37, and (e) 5.47 equivalents of CB[7].

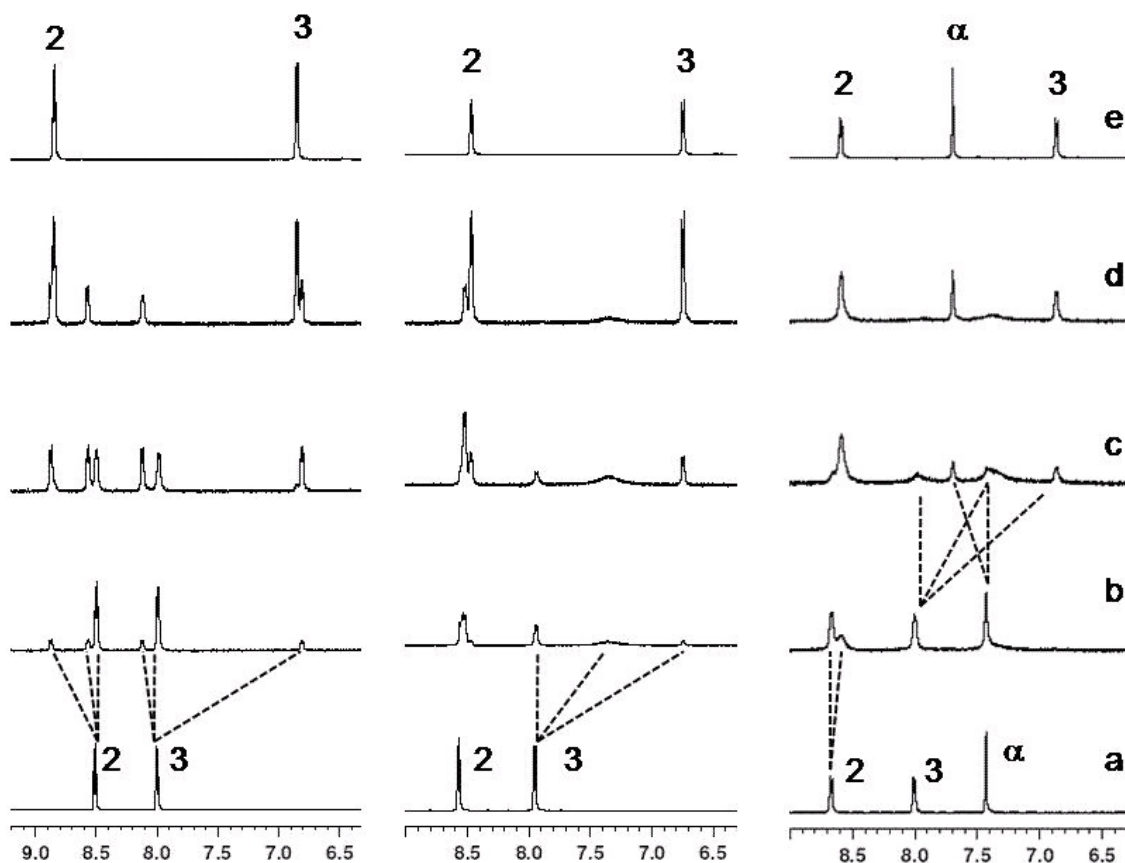


**Figure 3.8** Downfield regions of the  $^1\text{H}$  NMR spectra of  $\text{BBPE}^{2+}$  (left, with (a) 0.00, (b) 0.30, (c) 0.73, (d) 1.57, and (e) 2.19 equiv. of  $\text{CB}[7]$ ),  $\text{BBPH}^{2+}$  (middle, with (a) 0.00, (b) 0.34, (c) 0.90, (d) 1.57, and (e) 2.48 equiv. of  $\text{CB}[7]$ ), and  $\text{BBPX}^{2+}$  (right, with (a) 0.00, (b) 0.56, (c) 1.13, (d) 1.36, and (e) 2.53 equiv. of  $\text{CB}[7]$ ) in  $\text{D}_2\text{O}$ . Protons 2 and 3 represent protons of the pyridinium ring that are *ortho* and *meta* to the pyridinium nitrogen, respectively. Meanwhile, in the stackplot to the right,  $\alpha$  represents the aromatic protons of the xylyl linker of  $\text{BBPX}^{2+}$ .

On the other hand, when  $\text{CB}[7]$  forms 1:1 complexes with bis(4-*tert*-butylpyridinium)hexane ( $\text{BBPH}^{2+}$ ) and bis(4-*tert*-butylpyridinium)*p*-xylylene ( $\text{BBPX}^{2+}$ ), the bulky *tert*-butyl substituents of these guests prevents the  $\text{CB}[7]$  from crossing to the central linker region. Therefore, the 1:1 complexes between  $\text{CB}[7]$  and either  $\text{BBPH}^{2+}$  or  $\text{BBPX}^{2+}$  result in an asymmetric complex, with the  $\text{CB}[7]$  encapsulating the *tert*-butylpyridinium region at one end of the molecule (Figure 3.8). This behaviour differs from that between  $\text{CB}[7]$  and the guests that

lack *tert*-butyl units, where the CB[7] initially occupies the central linker between the pyridinium units in those cases. When the second CB[7] is added to give the 2:1 complex, the second CB[7] binds to the other *tert*-butylpyridinium region at the opposite end of the guest. This binding behaviour is also reflected in the proton NMR limiting  $\Delta\delta$  values, as formation of the 1:1 complex results in upfield shifts of the pyridinium and methyl protons, followed by a doubling of this upfield shift upon formation of the 2:1 complex.

### 3.2.3 Host-Guest Stability Constants

For most of these complexes, except for BPE<sup>2+</sup> and BPH<sup>2+</sup>, both the 1:1 and 2:1 binding constants were too large to measure directly by NMR or UV-visible titrations. Therefore, the <sup>1</sup>H NMR competition experiments at pD = 4.75 with a buffer of 50 mM sodium acetate and 25 mM DCl, using a series of competitors developed by Isaacs and coworkers,<sup>31</sup> as well as a series developed later in our lab,<sup>32</sup> were undertaken. The 2:1 binding affinity between CB[7] and BPH<sup>2+</sup> was determined using a Benesi-Hildebrand double reciprocal plot,<sup>33</sup> of  $\Delta\delta^{-1}$  versus  $[\text{CB}[7]]^{-1}$ , to give a binding constant from the ratio of intercept/slope. The binding constants obtained suggest that both the pyridinium substituents and the linker between the pyridinium rings influence the binding affinities. These binding constants are listed in Table 3.1.

The largest 1:1 binding affinities are observed for the dicationic guests with the hydrophobic *tert*-butyl substituents, with the strongest binding occurring between CB[7] and BBPE<sup>2+</sup> at  $1.0 \times 10^{11} \text{ M}^{-1}$ , followed fairly closely by BBPH<sup>2+</sup> ( $5.2 \times 10^{10} \text{ M}^{-1}$ ) and BBPX<sup>2+</sup> ( $1.2 \times 10^{10} \text{ M}^{-1}$ ). The smaller CB[7]•BBPE<sup>2+</sup> complex seems to be stabilized by the relatively close proximity of the two positive charges, so that in addition to the cationic centre at the end encapsulated by CB[7], the second positive charge at the other end of the molecule is close enough to also undergo ion-dipole interactions with CB[7]. Also, the ethylene linker should be

sufficiently flexible to allow the “free” pyridinium end to come near the portal, which is consistent with the small downfield shifts observed in the  $^1\text{H}$  NMR of the unbound *tert*-butylpyridinium protons of the 1:1 complex.

**Table 3.1** The 1:1 and 2:1 host-guest stability constants for the CB[7] complexes in  $\text{D}_2\text{O}$  (competitive binding at pD 4.75 with 0.05 M sodium acetate, 0.025 M DCl).

Guest	$K_{1:1}$ ( $\text{M}^{-1}$ )	$K_{2:1}$ ( $\text{M}^{-1}$ )	$K_{1:1}/K_{2:1}$
BPE $^{2+}$	$(3.1 \pm 0.6) \times 10^6$ <sup>a</sup>	not observed	-
BAPE $^{2+}$	$(7.4 \pm 1.3) \times 10^7$ <sup>a</sup>	$(1.6 \pm 0.7) \times 10^5$ <sup>b,c</sup>	460
BBPE $^{2+}$	$(1.0 \pm 0.2) \times 10^{11}$ <sup>d,e</sup>	$(8.1 \pm 2.3) \times 10^9$ <sup>d,e</sup>	12
BPH $^{2+}$	$(4.8 \pm 1.1) \times 10^8$ <sup>d</sup>	$(8 \pm 2) \times 10^{1f}$	$6 \times 10^6$
B2PH $^{2+}$	$(2.4 \pm 0.4) \times 10^7$ <sup>a</sup>	$(3.2 \pm 1.5) \times 10^4$ <sup>b</sup>	750
B3PH $^{2+}$	$(1.6 \pm 0.3) \times 10^8$ <sup>a</sup>	$(2.3 \pm 1.2) \times 10^4$ <sup>b</sup>	7000
BAPH $^{2+}$	$(1.5 \pm 0.5) \times 10^8$ <sup>a,g</sup>	$(6.8 \pm 2.6) \times 10^5$ <sup>a,b,c</sup>	220
BBPH $^{2+}$	$(5.2 \pm 1.2) \times 10^{10}$ <sup>d,e</sup>	$(2.1 \pm 0.4) \times 10^9$ <sup>d</sup>	25
BBPX $^{2+}$	$(1.2 \pm 0.3) \times 10^{10}$ <sup>g</sup>	$(7.9 \pm 1.9) \times 10^8$ <sup>d</sup>	15

<sup>a</sup>With 3-(trimethylsilyl)propionic acid as competitor (Ref. 31). <sup>b</sup>With  $[\text{N}(\text{CH}_3)_4]^+$  as competitor (Ref. 32). <sup>c</sup>With  $[\text{N}(\text{CH}_2\text{CH}_3)_4]^+$  as competitor (Ref. 32). <sup>d</sup>With *p*-xylylenediamine as competitor (Ref. 31). <sup>e</sup>With  $[\text{CpFe}(\text{CpCH}_2\text{N}(\text{CH}_3)_3)^+]$  as competitor (Ref. 31). <sup>f</sup>From Benesi-Hildebrand double reciprocal plot. <sup>g</sup>With  $[\text{PhCH}_2\text{N}(\text{CH}_3)_3]^+$  as competitor (Ref. 32).

**Table 3.2** High resolution ESI-MS spectral peaks for the 1:1 and 2:1 CB[7] host-guest complexes with the dicationic bis(pyridinium)alkane guests. (The values in parentheses represent the calculated  $m/z$  value of the peak for the corresponding formula mass).

Guest	[Guest•CB[7]-2Br] <sup>2+</sup> ( $m/z$ )	[Guest•2CB[7]-2Br] <sup>2+</sup> ( $m/z$ )
BPE <sup>2+</sup>	674.2286 (674.2291 for C <sub>54</sub> H <sub>56</sub> N <sub>30</sub> O <sub>14</sub> <sup>2+</sup> )	not observed
BAPE <sup>2+</sup>	717.2748 (717.2723 for C <sub>58</sub> H <sub>66</sub> N <sub>32</sub> O <sub>14</sub> <sup>2+</sup> )	1298.4761 (1298.4431 for C <sub>104</sub> H <sub>116</sub> N <sub>60</sub> O <sub>28</sub> <sup>2+</sup> )
BBPE <sup>2+</sup>	730.2947 (730.2927 for C <sub>62</sub> H <sub>72</sub> N <sub>30</sub> O <sub>14</sub> <sup>2+</sup> )	1311.4967 (1311.4635 for C <sub>104</sub> H <sub>114</sub> N <sub>58</sub> O <sub>28</sub> <sup>2+</sup> ) <sup>a</sup>
BPH <sup>2+</sup>	702.2599 (702.2603 for C <sub>58</sub> H <sub>64</sub> N <sub>30</sub> O <sub>14</sub> <sup>2+</sup> )	1283.4428 (1283.4321 for C <sub>100</sub> H <sub>106</sub> N <sub>58</sub> O <sub>28</sub> <sup>2+</sup> )
B2PH <sup>2+</sup>	716.40959 (716.2760 for (C <sub>60</sub> H <sub>68</sub> N <sub>30</sub> O <sub>14</sub> ) <sup>2+</sup> )	1298.2939 (1297.4478 for C <sub>102</sub> H <sub>110</sub> N <sub>58</sub> O <sub>28</sub> <sup>2+</sup> )
B3PH <sup>2+</sup>	716.2784 (716.2760 for C <sub>60</sub> H <sub>68</sub> N <sub>30</sub> O <sub>14</sub> <sup>2+</sup> )	1297.4906 (1297.4478 for C <sub>102</sub> H <sub>110</sub> N <sub>58</sub> O <sub>28</sub> <sup>2+</sup> )
BAPH <sup>2+</sup>	745.3032 (745.3025 for C <sub>62</sub> H <sub>74</sub> N <sub>32</sub> O <sub>14</sub> <sup>2+</sup> )	1326.5051 (1326.4743 for C <sub>104</sub> H <sub>116</sub> N <sub>60</sub> O <sub>28</sub> <sup>2+</sup> )
BBPH <sup>2+</sup>	758.3227 (758.3229 for C <sub>66</sub> H <sub>80</sub> N <sub>30</sub> O <sub>14</sub> <sup>2+</sup> )	1339.5195 (1339.4947 for C <sub>108</sub> H <sub>122</sub> N <sub>58</sub> O <sub>28</sub> <sup>2+</sup> )
BBPX <sup>2+</sup>	768.3064 (768.3131 for C <sub>68</sub> H <sub>76</sub> N <sub>30</sub> O <sub>14</sub> <sup>2+</sup> )	1349.5275 (1349.4792 for C <sub>110</sub> H <sub>118</sub> N <sub>58</sub> O <sub>28</sub> <sup>2+</sup> )

<sup>a</sup>For BBPE<sup>2+</sup>, the addition of sodium ions was also observed, with a peak at  $m/z = 881.9857$  (calculated  $m/z = 881.9721$  for [BBPE•2CB[7]-2Br+Na]<sup>3+</sup>).

When [2]pseudorotaxanes are formed with the CB[7] bound over the hexamethylene linker between the pyridinium centres, the stability constants varied between  $2 \times 10^7$  and  $5 \times 10^8$  M<sup>-1</sup>. These values are somewhat lower than the 1:1 binding constant between CB[7] and the 1,6-bis(trimethylammonium)hexane dication,  $3.9 \times 10^9$  M<sup>-1</sup>, but which formed no 2:1 complex.<sup>34</sup> The



1:1 complex between CB[7] and the  $\alpha,\alpha$ -bis(pyridinium)-*p*-xylylene dication displayed a weaker binding with  $K = 1.0 \times 10^6 \text{ M}^{-1}$  (in a  $\text{D}_2\text{O}$  solution with 0.20 M NaCl), as reported by Kaifer and coworkers.<sup>15</sup> As also observed for the present bis(pyridinium) guests lacking the *tert*-butyl substituent, Kaifer observed that the 1:1 complex between CB[7] and  $\alpha,\alpha$ -bis(pyridinium)-*p*-xylylene existed with CB[7] encapsulating the *p*-xylylene linker. This was also true when the terminal pyridinium groups were replaced with viologen groups, and Kaifer was able to cap the viologens to trap the CB[7] onto the guest, thus forming a [2]rotaxane.<sup>15</sup>

The 2:1 host-guest stability constants were also determined using  $^1\text{H}$  NMR competition experiments, using a CB[7]:guest ratio of 1.5:1 and assuming strong 1:1 binding of the host-guest complex. If the presence of the first CB[7] did not hinder the binding of the second CB[7], and thus a statistical binding situation was in effect, the 2:1 binding constants should have been one quarter of the strength of the 1:1 binding constants ( $K_{1:1}/K_{2:1} = 4$ ), assuming that both CB[7] macrocycles occupied similar binding sites. In all of the host-guest systems measured in this study, the 2:1 stability constants were significantly less than those predicted by statistical binding, indicating that the presence of the first CB[7] was, in fact, reducing the ability of the second CB[7] to bind to the guest. This may be partially explained by the electrostatic repulsions that would exist between two adjacent CB[7] hosts, due to their carbonyl-lined portals.

In addition, the extent to which the 2:1 binding constant was reduced compared to the 1:1 binding affinity varied throughout the series of guests. The smallest differences between the  $K_{1:1}$  and  $K_{2:1}$  values were observed for the *tert*-butylpyridinium-bearing guests, such as BBPE<sup>2+</sup>, BBPH<sup>2+</sup>, and BBPX<sup>2+</sup>, which had  $K_{2:1}/K_{1:1}$  ratios ranging between 12 and 25. In the course of the host-guest complexation with these guests, the CB[7] macrocycles bound to the *tert*-butylpyridinium regions without any migration occurring between the central and terminal regions during the transition from 1:1 to 2:1 host-guest complexation. These smaller values suggest that the absence of the requirement of the first CB[7] to migrate upon addition of the

second CB[7] reduces the barrier for 2:1 binding compared to systems that require relocation of the first CB[7] in order to facilitate the binding of the second CB[7]. In this sense, these host-guest systems, with the first CB[7] occupying one end of the guest, require less reorganization of the host-guest binding positions in order to accommodate the second CB[7] than those systems in which the first CB[7] binds to the central linker, and then subsequently migrate to one end as the second CB[7] is added. Kaifer and coworkers<sup>9</sup> note that with the complexation between CB[7] and the series  $[\text{HO}_2\text{C}(\text{CH}_2)_n\text{bpy}(\text{CH}_2)_n\text{CO}_2\text{H}]^{2+}$  ( $n = 5-7$ , and  $10$ ), the ratio of  $K_{1:1}/K_{2:1}$  varies between 25 and 102, which also indicates that the initial binding of CB[7] tends to inhibit the ability of the second CB[7] to bind.

Sun *et al.*<sup>35</sup> studied the host-guest chemistry between CB[8] and guests made up of one N,N-dimethyl-3,3'-dimethyl-4,4'-bipyridinium (dimethylviologen) end group and a N,N-dimethyl-4,4'-bipyridinium (methylviologen) end group at the other end of either propylene or hexamethylene linkers. They found that the CB[8] bound only to the end groups and not over the linker, upon formation of both the 1:1 and 2:1 complexes, with preference for initial binding at the dimethylviologen end group. When the end groups were separated by a hexamethylene linker, the binding of the second CB[8] to the viologen was reasonably stable and localized, with upfield shifts of the viologen protons and downfield shifts of the nearby linker protons. Meanwhile, when the end groups were separated by the shorter propyl linker, the binding of the second CB[8] was relatively weak and dynamic, likely due to electrostatic repulsions between the CB[8] portals.

When the first CB[7] must migrate from the central to the terminal region in order to accommodate the addition of the second CB[7], the extent to which 1:1 binding will be favoured over 2:1 binding will depend on factors such as the nature of the terminal pyridinium substituents, as well as the length of the linker separating the two pyridinium regions. As mentioned earlier, the larger ratios of  $K_{1:1}/K_{2:1}$  ( $2 \times 10^2$  to  $6 \times 10^6$ ) were observed for the host-guest systems that

involved movement of the first CB[7] from the central region to the terminal pyridinium region upon addition of the second CB[7]. It therefore appears that the displacement of the first CB[7] from its initial central position along the hexamethylene linker, where a cationic charge is near each portal, to the terminal pyridinium regions, with only one cationic charge nearby, can act as a barrier to addition of the second CB[7]. On the other hand, it was noted earlier by Macartney and coworkers<sup>27</sup> that when host-guest complexes between CB[7] and the tetracationic guest  $[\text{CH}_3\text{bpy}(\text{CH}_2)_6\text{bpyCH}_3]^{4+}$ , the ratio of  $K_{1:1}/K_{2:1}$  was relatively modest, at approximately 9. This system, like many of the pyridinium guests in this study, involved the migration of the first CB[7] from the central region to the terminal region upon formation of the 2:1 complex. However, the end groups of this tetracationic guest consisted of dicationic viologen groups, unlike the monocationic pyridinium guests explored in this study. Therefore, the first CB[7], which was initially positioned on the hexamethylene linker, was able to migrate to the terminal dicationic viologen groups and still have positive charges located near each of its portals. In the present systems, however, the first CB[7], in order to accommodate the addition of the second CB[7], had to migrate from the hexamethylene linker, where both portals were involved with ion-dipole interactions from each pyridinium, to the terminal monocationic pyridinium regions, where only one portal could employ ion-dipole interactions. Since the CB[7] is localized over the pyridinium region during 2:1 complexation, the binding constant of the 2:1 host-guest species is also influenced by the hydrophobicity of the substituents of the pyridinium ring. The apparent effect of this, as suggested from the 2:1 binding constants, is that the CB[7] affinity for the pyridinium groups follows the order: pyridinium < 2-picolinium  $\approx$  3-picolinium < 4-dimethylaminopyridinium  $\ll$  4-*tert*-butylpyridinium.

The length of the linker between the pyridinium moieties also affects the 2:1 binding affinity. It would normally be expected that guests with shorter linkers would form host-guest complexes with lower 2:1 binding constants, as was observed by Sun and coworkers.<sup>35</sup> In our

systems, this seems to be the case for BPE<sup>2+</sup> (with no CB[7]-BPE<sup>2+</sup> 2:1 complex observed) vs. BPH<sup>2+</sup> and BAPE<sup>2+</sup> vs. BAPH<sup>2+</sup>. However, the guests bearing *tert*-butylpyridinium groups appear to show the opposite effect, as the 2:1 binding affinity of BBPE<sup>2+</sup> is greater than that of either BBPH<sup>2+</sup> or BBPX<sup>2+</sup>. This may be due to the more hydrophobic substituent, positioned at the opposite end of the pyridinium ring from the spacer, that places the CB[7] units of the 2:1 further away from each other than with other substituted pyridinium end groups. The bulkiness of the *tert*-butyl groups also prevents the CB[7] macrocycles from approaching the linker region and becoming repulsed by each other's portals. While the *tert*-butyl group may reduce the ability of the CB[7] units to repel each other (even with the shorter linker), the cationic pyridinium centre of the opposite pyridinium ring may be close enough with the shorter ethylene linker to weakly enhance the binding of the second CB[7] and thus give rise to the higher stability of the 2:1 complexes of BBPE<sup>2+</sup>. The stability constant for the 1:1 host-guest complex between CB[7] and BBPE<sup>2+</sup> is also slightly greater than that of either BBPH<sup>2+</sup> or BBPX<sup>2+</sup>, possibly due to a higher effect of the charges on the shorter linker with more closely spaced positive charges.

### 3.3 Experimental

#### 3.3.1 Materials

The CB[7] was prepared and characterized using the method of Day and coworkers, as described in Chapter 2.<sup>36</sup> The bis(pyridinium)alkane complexes were prepared as dibromide salts by heating 15-30 mmol of the appropriately substituted pyridine (pyridine, 4-dimethylpyridine, 2-picoline, 3-picoline, or 4-*tert*-butylpyridine (Sigma-Aldrich) with 4-5 mmol of 1,2-dibromoethane, 1,6-dibromohexane, or  $\alpha,\alpha$ -dibromo-*p*-xylylene (Sigma-Aldrich), in 50 mL acetonitrile (15 mL of DMF was used for the reaction with 2-picoline) at 70 °C for 24 hours. The

resulting precipitate was filtered, washed with methanol, followed by ether, and then recrystallised from methanol/ether mixtures.

### **1,2-bis(1-pyridinium)ethane dibromide ([BPE]Br<sub>2</sub>)**

Yield: 26%. Melting point: 240-245 °C, <sup>1</sup>H NMR (D<sub>2</sub>O, 400 MHz): δ 8.82 (d, 4H, H2 (*ortho*), *J* = 6.2 Hz), 8.66 (t, 2H, H4, *J* = 7.8 Hz), 8.13 (dd, 4H, H3, *J* = 7.8, 6.2 Hz), 5.32 (s, 4H, Hα) ppm. <sup>13</sup>C NMR (D<sub>2</sub>O, 400 MHz): δ 147.59 (C4), 144.76 (C2), 129.23 (C3), 60.16 (Cα) ppm. HR-ESI-MS: calc. for C<sub>12</sub>H<sub>14</sub>N<sub>2</sub><sup>2+</sup> ([M-2Br]<sup>2+</sup>) *m/z* = 93.0573, found *m/z* = 93.0571.

### **1,2-bis(4-dimethylamino-1-pyridinium)ethane dibromide ([BAPE]Br<sub>2</sub>)**

Yield: 38%. Melting point > 300 °C (literature values 301 °C, dec.,<sup>37</sup> and > 300 °C, dec.<sup>38</sup>), <sup>1</sup>H NMR (D<sub>2</sub>O, 400 MHz): δ 7.74 (d, 2H, H2, *J* = 7.2 Hz), 6.79 (d, 2H, H3, *J* = 7.2 Hz), 4.56 (s, 4H, Hα), 3.15 (s, 12H, CH<sub>3</sub>) ppm. <sup>13</sup>C NMR (100 MHz, D<sub>2</sub>O): δ 156.46 (C2), 141.05 (C3), 56.72 (Cα), 39.60 (CH<sub>3</sub>) ppm. HR-ESI-MS: calc. for C<sub>16</sub>H<sub>24</sub>N<sub>2</sub><sup>2+</sup> ([M-2Br]<sup>2+</sup>) *m/z* = 136.0994, found *m/z* = 136.0995.

### **1,2-bis(4-*tert*-butyl-1-pyridinium)ethane dibromide ([BBPE]Br<sub>2</sub>)**

Yield: 29%. Melting point: > 300 °C (literature value > 300 °C),<sup>39</sup> <sup>1</sup>H NMR (D<sub>2</sub>O, 400 MHz): δ 8.51 (d, 4H, H2 (*ortho*), *J* = 6.5 Hz), 8.00 (d, 4H, H3 (*meta*), *J* = 6.5 Hz), 5.12 (s, 4H, Hα), 1.38 (s, 18H, CH<sub>3</sub>) ppm. <sup>13</sup>C NMR (D<sub>2</sub>O, 125 MHz): δ 174.37 (C4, *para*), 144.05 (C2, *ortho*), 126.66 (C3, *meta*), 59.70 (Cα), 36.76 (C<sub>*tert*</sub>), 29.39 (CH<sub>3</sub>) ppm. HR-ESI-MS: calc. for C<sub>20</sub>H<sub>30</sub>N<sub>2</sub><sup>2+</sup> ([M-2Br]<sup>2+</sup>) *m/z* = 149.1199, found *m/z* = 149.1199.

### **1,6-bis(1-pyridinium)hexane dibromide ([BPH]Br<sub>2</sub>)**

Yield: 93%. Melting point: 140 - 143 °C. <sup>1</sup>H NMR (D<sub>2</sub>O, 400 MHz): δ 8.80 (d, 4H, H<sub>2</sub>, *J* = 6.4 Hz), 8.52 (t, 2H, H<sub>4</sub>, *J* = 7.7 Hz), 8.03 (dd, 4H, H<sub>3</sub>, *J* = 7.7, 6.4 Hz), 4.57 (t, 4H, H<sub>α</sub>, *J* = 7.4 Hz), 1.99 (m, 4H, H<sub>β</sub>), 1.37 (m, 4H, H<sub>γ</sub>) ppm. <sup>13</sup>C NMR (D<sub>2</sub>O, 100 MHz): δ 145.62 (C<sub>4</sub>, *para*), 144.20 (C<sub>2</sub>, *ortho*), 128.26 (C<sub>3</sub>, *meta*), 61.73 (C<sub>α</sub>), 30.29 (C<sub>β</sub>), 24.81 (C<sub>γ</sub>) ppm. HR-ESI-MS: calc. for C<sub>16</sub>H<sub>22</sub>N<sub>2</sub><sup>2+</sup> ([M-2Br]<sup>2+</sup>) *m/z* = 121.0886, found *m/z* = 121.0881.

### **1,6-bis(2-methyl-1-pyridinium)hexane dibromide ([B2PH]Br<sub>2</sub>)**

Yield: 15%. Melting point: 230-235 °C, <sup>1</sup>H NMR (D<sub>2</sub>O, 400 MHz): δ 8.66 (d, 2H, H<sub>6</sub> (*ortho*), *J* = 6.4 Hz), 8.33 (t, 2H, H<sub>4</sub> (*para*), *J* = 8.0 Hz), 7.87 (d, 2H, H<sub>3</sub> (*meta*), *J* = 8.0 Hz), 7.81 (t, 2H, H<sub>5</sub> (*meta*), *J* = 6.4 Hz), 4.49 (t, 4H, H<sub>α</sub>, *J* = 7.9 Hz), 2.80 (s, 6H, CH<sub>3</sub>), 1.93 (m, 4H, H<sub>β</sub>), 1.46 (m, 4H, H<sub>γ</sub>) ppm. <sup>13</sup>C NMR (D<sub>2</sub>O, 125 MHz): δ 155.63 (C<sub>2</sub>, *ortho*), 145.42 (C<sub>4</sub>, *para*), 145.07 (C<sub>6</sub>, *ortho*), 130.61 (C<sub>3</sub>, *meta*), 125.98 (C<sub>5</sub>, *meta*), 58.19 (C<sub>α</sub>), 29.54 (C<sub>β</sub>), 25.50 (C<sub>γ</sub>), 19.89 (CH<sub>3</sub>) ppm. HR-ESI-MS: calc. for C<sub>18</sub>H<sub>26</sub>N<sub>2</sub><sup>2+</sup> ([M-2Br]<sup>2+</sup>) *m/z* = 135.1042, found *m/z* = 135.1043.

### **1,6-bis(3-methyl-1-pyridinium)hexane dibromide ([B3PH]Br<sub>2</sub>)**

Yield: 55%. Melting point: 157-162 °C. <sup>1</sup>H NMR (D<sub>2</sub>O, 400 MHz): δ 8.62 (s, 2H, H<sub>2</sub> (*ortho*)), 8.57 (d, 2H, H<sub>6</sub> (*ortho*), *J* = 6.1 Hz), 8.30 (d, 2H, H<sub>4</sub> (*para*), *J* = 8.0 Hz), 7.87 (dd, 2H, H<sub>5</sub> (*meta*), *J* = 8.0, 6.1 Hz), 4.49 (t, 4H, H<sub>α</sub>, *J* = 7.9 Hz), 2.48 (s, 6H, CH<sub>3</sub>), 1.94 (m, 4H, H<sub>β</sub>), 1.32 (m, 4H, H<sub>γ</sub>) ppm. <sup>13</sup>C NMR: (D<sub>2</sub>O, 100 MHz) δ 145.98 (C<sub>4</sub>, *para*), 143.66 (C<sub>2</sub>, *ortho*), 141.23 (C<sub>6</sub>, *ortho*), 139.91 (C<sub>3</sub>, *meta*), 127.39 (C<sub>5</sub>, *meta*), 61.45 (C<sub>α</sub>), 30.24 (C<sub>β</sub>), 24.78 (C<sub>γ</sub>), 17.60 (CH<sub>3</sub>) ppm. HR-ESI-MS: calc. for C<sub>18</sub>H<sub>26</sub>N<sub>2</sub><sup>2+</sup> ([M-2Br]<sup>2+</sup>) *m/z* = 135.1042, found *m/z* = 135.1043.

### **1,6-bis(4-dimethylamino-1-pyridinium)hexane dibromide ([BAPH]Br<sub>2</sub>)**

Yield: 80%. Melting point: 275-276 °C. <sup>1</sup>H NMR (D<sub>2</sub>O, 400 MHz): δ 7.92 (d, 2H, H<sub>2</sub> (*ortho*), *J* = 7.6 Hz), 6.80 (d, 2H, H<sub>5</sub> (*meta*), *J* = 7.6 Hz), 4.05 (t, 4H, H<sub>α</sub>, *J* = 7.0 Hz), 3.14 (s, 12H, CH<sub>3</sub>), 1.78 (m, 4H, H<sub>β</sub>), 1.25 (m, 4H, H<sub>γ</sub>) ppm. <sup>13</sup>C NMR (D<sub>2</sub>O, 100 MHz): δ 156.29 (C<sub>4</sub>, *para*), 141.25 (C<sub>2</sub>, *ortho*), 107.47 (C<sub>3</sub>, *meta*), 57.46 (C<sub>α</sub>), 39.33 (CH<sub>3</sub>), 29.68 (C<sub>β</sub>), 24.83 (C<sub>γ</sub>) ppm. HR-ESI-MS: calc. for C<sub>20</sub>H<sub>32</sub>N<sub>2</sub><sup>2+</sup> ([M-2Br]<sup>2+</sup>) *m/z* = 164.1308, found *m/z* = 164.1309.

### **1,6-bis(4-*tert*-butyl-1-pyridinium)hexane dibromide ([BBPH]Br<sub>2</sub>)**

Yield: 74%. Melting point: 274-277 °C (Literature value 299-300 °C).<sup>40</sup> <sup>1</sup>H NMR (D<sub>2</sub>O, 500 MHz): δ 8.63 (d, 4H, H<sub>2</sub> (*ortho*), *J* = 7.0 Hz), 8.01 (d, 4H, H<sub>3</sub> (*meta*), *J* = 7.0 Hz), 4.49 (t, 4H, H<sub>α</sub>, *J* = 7.2 Hz), 1.95 (m, 4H, H<sub>β</sub>), 1.36 (s, 18H, CH<sub>3</sub>), 1.34 (m, 4H, H<sub>γ</sub>) ppm. <sup>13</sup>C NMR (D<sub>2</sub>O, 125 MHz): δ 171.96 (C<sub>4</sub>, *para*), 143.67 (C<sub>2</sub>, *ortho*), 125.74 (C<sub>3</sub>, *meta*), 61.00 (C<sub>α</sub>), 36.32 (C<sub>*tert*</sub>), 30.59 (C<sub>β</sub>), 29.49 (CH<sub>3</sub>), 25.18 (C<sub>γ</sub>) ppm. HR-ESI-MS: calc. for C<sub>24</sub>H<sub>38</sub>N<sub>2</sub><sup>2+</sup> ([M-2Br]<sup>2+</sup>) *m/z* = 177.1512, found *m/z* = 177.1514.

### **α,α'-bis(4-*tert*-butyl-1-pyridinium)-*p*-xylylene dibromide ([BBPX]Br<sub>2</sub>)**

Yield: 89%. Melting point: > 300 °C. <sup>1</sup>H NMR (D<sub>2</sub>O, 500 MHz): δ 8.66 (d, 4H, H<sub>2</sub> (*ortho*), *J* = 6.8 Hz), 8.01 (d, 4H, H<sub>3</sub> (*meta*), *J* = 6.8 Hz), 7.44 (s, 4H, H<sub>2'</sub> (xylyl)), 5.72 (s, 4H, H<sub>α</sub>), 1.33 (s, 18H, CH<sub>3</sub>) ppm. <sup>13</sup>C NMR (D<sub>2</sub>O, 125 MHz): δ 172.72 (C<sub>4</sub>, *para*), 143.93 (C<sub>2</sub>, *ortho*), 134.98 (C<sub>1'</sub>, xylyl, *ipso* to CH<sub>2</sub>), 130.11 (C<sub>2'</sub>, xylyl, *ortho* to CH<sub>2</sub>), 126.03 (C<sub>3</sub>, *meta*), 63.30 (CH<sub>2</sub>), 36.33 (C<sub>*tert*</sub>), 29.45 (CH<sub>3</sub>) ppm. HR-ESI-MS: calc. for C<sub>26</sub>H<sub>34</sub>N<sub>2</sub><sup>2+</sup> ([M-2Br]<sup>2+</sup>) *m/z* = 187.1355, found *m/z* = 167.1356.

### 3.3.2 Methods

$^1\text{H}$  NMR and  $^{13}\text{C}$  NMR spectra were recorded on Bruker Avance 400 MHz and Bruker Avance 500 MHz instruments at 25 °C in  $\text{D}_2\text{O}$ . The  $^1\text{H}$  and  $^{13}\text{C}$  resonances were confirmed using 2D COSY, HSQC, and HMBC techniques. The stability constants for the 1:1 and 2:1 host-guest complexes were determined using  $^1\text{H}$  NMR competitive binding experiments, in  $\text{D}_2\text{O}$  solvent with 0.05 M deuterated sodium acetate (Aldrich) and 0.025 M DCl (Sigma-Aldrich), to give a pH of 4.75. During the determination of the 1:1 binding constant, the ratio of CB[7]:guest:competitor was normally kept at near 3:4:4, with the concentration of CB[7] ranging between 3 and 4 mM. During the determination of the 2:1 binding constants, the ratio between CB[7]:guest:competitor was normally kept at 6:4:3, with the CB[7] concentration ranging between 6 and 8 mM, normally using a competitor that had a lower binding constant with CB[7] than the guest. It was assumed at this ratio and under these conditions that the 1:1 complex was fully formed. Competitors used in this study were 3-(trimethylsilyl)propionic-2,2,3,3- $d_4$  acid ( $K_{\text{CB}[7]} = (1.82 \pm 0.22) \times 10^7 \text{ M}^{-1}$ ),<sup>31</sup> benzyltrimethylammonium bromide ( $(2.5 \pm 0.6) \times 10^8 \text{ M}^{-1}$ ),<sup>32</sup> *p*-xylylenediamine ( $(1.84 \pm 0.34) \times 10^9 \text{ M}^{-1}$ ),<sup>31</sup> 1-(trimethylammonio)methylferrocene iodide ( $(3.31 \pm 0.62) \times 10^{11} \text{ M}^{-1}$ ),<sup>31</sup> tetramethylammonium bromide ( $(1.2 \pm 0.4) \times 10^5 \text{ M}^{-1}$ ),<sup>32</sup> and tetraethylammonium bromide ( $(1.0 \pm 0.2) \times 10^6 \text{ M}^{-1}$ ).<sup>32</sup>

UV-visible spectra were recorded on a Hewlett-Packard 8452A diode-array spectrometer with a 1.00 cm pathlength quartz cuvette. The electrospray mass spectra were obtained using a QstarXL Qq TOF MS/MS system with an ESI source, and samples were prepared in distilled water. The energy-minimized gas-phase structural calculations were carried out with the MM2 program in the Chem 3D Pro (Version 11.0.1, CambridgeSoft) software.



### 3.4 Conclusions

A series of 1:1 and 2:1 host-guest systems were formed between CB[7] and various  $\alpha,\omega$ -bis(pyridinium)alkane salts, and their binding constants were determined. With the presence of the longer hexamethylene linker, and the absence of the bulkier *tert*-butyl substituents of the pyridine, the CB[7] bound to the central linker between the pyridinium centres, to form a [2]pseudorotaxane. Upon addition of the second CB[7], the first CB[7] migrated to the terminal pyridinium region, to form 2:1 complexes, with one CB[7] on each terminal pyridinium region, giving a dumbbell shaped host-guest system. Electrostatic repulsions between the portals of different CB[7] hosts acted to drive the CB[7] hosts away from each other, towards the ends of the molecules, and also reduced the 2:1 binding affinities in most cases. When the bulkier *tert*-butylpyridinium groups were present, the first CB[7] was unable to cross over into the central pyridinium region, thus forming an asymmetric complex with the CB[7] bound to one *tert*-butylpyridinium substituent but not the other. The second CB[7] occupied the other *tert*-butylpyridinium group, with little or no movement of the first CB[7]. The research described in this chapter has been published in *Organic and Biomolecular Chemistry*.<sup>28</sup>

## References

1. A. Wego, K. Jansen, H. Buschmann, E. Schollmeyer, and D. Doepp, *J. Incl. Phenom. Macrocycl. Chem.*, **2002**, *43*, 201.
2. K. Kim, *Chem. Soc. Rev.*, **2002**, *31*, 96.
3. X. Xiao, Y.-Q. Zhang, Z. Tao, S.-F. Xue, and Q.-J. Zhu, *Acta Cryst.*, **2007**, *E63*, o389.
4. D. Tuncel, O. Ozsar, H.B. Tiftik, and B. Salih, *Chem. Commun.*, **2007**, 1369.
5. D. Tuncel and M. Katterle, *Chem. Eur. J.*, **2008**, *14*, 4110.
6. S.W. Choi and H. Ritter, *Macromol. Rapid Commun.*, **2007**, *28*, 101.
7. H. Lu, L. Mei, G. Zhang, and X. Zhou, *J. Incl. Phenom. Macrocycl. Chem.*, **2007**, *59*, 81.
8. V. Sindelar, S. Silvi, and A.E. Kaifer, *Chem. Commun.*, **2006**, 2185.
9. V. Sindelar, S. Silvi, S.E. Parker, D. Sobransingh, and A.E. Kaifer, *Adv. Funct. Mater.*, **2007**, *17*, 694.
10. J.W. Lee, S.W. Choi, Y.H. Ko, S.-Y. Kim, and K. Kim, *Bull. Korean Chem. Soc.*, **2002**, *23*, 1347.
11. Y. Liu, X.-Y. Li, H.-Y. Zhang, C.-J. Li, and F. Ding, *J. Org. Chem.*, **2007**, *72*, 3640.
12. I.B. Shir, S. Sasmal, T. Mejuch, M.K. Sinha, M. Kapon, and E. Keinan, *J. Org. Chem.*, **2008**, *73*, 8772.
13. L. Leclercq, N. Noujeim, S.H. Sanon, and A.R. Schmitzer, *J. Phys. Chem. B*, **2008**, *112*, 14176.
14. K. Moon and A.E. Kaifer, *Org. Lett.*, **2004**, *6*, 185.
15. V. Sindelar, K. Moon, and A.E. Kaifer, *Org. Lett.*, **2004**, *6*, 2665.
16. A. Thangavel, A.M.M. Rawashdeh, C. Sotirou-Leventis, and N. Leventis, *Org. Lett.*, **2009**, *11*, 1595.
17. D.S.N. Hettiarachchi and D.H. Macartney, *Can. J. Chem.*, **2006**, *84*, 905.

18. S. Andersson, D. Zou, R. Zhang, S. Sun, B. Akermark, and L. Sun, *Eur. J. Org. Chem.*, **2009**, 1163.
19. W. Wang and A.E. Kaifer, *Angew. Chem., Int. Ed.*, **2006**, *45*, 7042.
20. S.-Y. Kim, J.W. Lee, S.C. Han, and K. Kim, *Bull Korean Chem. Soc.*, **2005**, *26*, 1265.
21. D. Tuncel and J.H.G. Steinke, *Chem. Commun.*, **2002**, 496.
22. D. Tuncel and J.H.G. Steinke, *Chem. Commun.*, **2001**, 253.
23. M.V. Rekharsky, H. Yamamura, M. Kawai, I. Osaka, R. Arawaka, A. Sato, Y.H. Ko, N. Selvapalam, K. Kim, and Y. Inoue, *Org. Lett.*, **2006**, *8*, 815.
24. T. Ooya, D. Inoue, H.S. Choi, Y. Kobayashi, S. Loethen, D.H. Thompson, Y.H. Ko, K. Kim, and N. Yui, *Org. Lett.*, **2006**, *8*, 3159.
25. V. Sindelar, S. Silvi, and A.E. Kaifer, *Chem. Commun.*, **2006**, 2185.
26. H.-J. Buschmann, E. Cleve, K. Jansen, A. Wego, E. Schollmeyer, *Mat. Sci. Eng. C*, **2001**, *14*, 35.
27. L. Yuan, R. Wang, and D.H. Macartney, *J. Org. Chem.*, **2007**, *72*, 4539.
28. I.W. Wyman and D.H. Macartney, *Org. Biomol. Chem.*, **2009**, *7*, 4045.
29. E. Kalatzis and L. Kiriazis, *J. Chem. Soc. Perkin Trans. 2*, **1989**, 179.
30. S.J. Vella, J. Tiburcio, J.W. Gauld, and S.J. Loeb, *Org. Lett.*, **2006**, *8*, 3421.
31. S. Liu, C. Ruspic, P. Mukhopadhyay, S. Chakrabarti, P.Y. Zavalij, and L. Isaacs, *J. Am. Chem. Soc.*, **2005**, *127*, 15959.
32. A.D. St-Jacques, I.W. Wyman, and D.H. Macartney, *Chem. Commun.*, **2008**, 4936.
33. K.A. Connors, *Binding Constants*, John Wiley & Sons: New York, 1987; p. 152.
34. I.W. Wyman and D.H. Macartney, *J. Org. Chem.*, **2009**, *74*, 8031.
35. S. Andersson, D. Zou, R. Zhang, S. Sun, B. Akermark, and L. Sun, *Eur. J. Org. Chem.*, **2009**, 1163.
36. A. Day, A.P. Arnold, R.J. Blanch, and B. Snushall, *J. Org. Chem.*, **2001**, *66*, 8094.

37. J.W. Bunting, A. Toth, and J.P. Kanter, *Can. J. Chem.*, **1992**, *70*, 1195.
38. A.R. Katritsky and M.J. Mokrosz, *Heterocycles*, **1984**, *22*, 505.
39. J. Ikegami, T. Murematsu, and K. Hanaya, *J. Am. Chem. Soc.*, **1989**, *111*, 5782.
40. K. Schoene, J. Steinhanses, and H. Oldiges, *Biochem. Biopharm.*, **1976**, *25*, 1955.

## Chapter 4

# Host-Guest Chemistry between CB[7] and a Series of Local Anaesthetics

### 4.1 Introduction

The development of long-acting local anaesthetics has been a goal of pharmaceutical research, and has even been compared to the search for the Holy Grail.<sup>1</sup> Two common families of local anaesthetics include ester (including procaine and tetracaine) and amide (including procainamide, prilocaine, and dibucaine) groups of anaesthetics.<sup>2</sup> These local anaesthetics can block nerve impulses by interrupting the movement of sodium through the sodium channels of the cell membrane, and thus preventing depolarization of the nerve cell. These drugs have both hydrophilic and hydrophobic units within their structure, with an aromatic ring corresponding to the hydrophobic region and an aliphatic region that houses an amine (normally secondary or tertiary) that represents the more hydrophilic region, and these regions are separated by either an ester or amide linker.<sup>2</sup> Often, these anaesthetics contain two protonation sites, with well-separated  $pK_a$  values, having one  $pK_a$  value between 2 and 3, and the other protonation site having a  $pK_a$  above 7.4.<sup>2,3</sup> These drugs can therefore exist in dicationic, monocationic, or neutral forms, depending on the pH of the solution. When the latter  $pK_a$  is of a higher value, the onset of the drug will tend to be slower, as a greater proportion of the drug becomes ionized when it has a higher  $pK_a$ , and the ionized form of the drug tends to penetrate nerve membranes slower than the neutral form.<sup>2</sup>

The use of host-guest drug delivery systems in order to facilitate the slow, controlled release of the local anaesthetics have been studied using hosts such as liposomes,<sup>1,5,6,7</sup> lipid-

protein-sugar particles,<sup>8</sup> biodegradable polymers,<sup>9</sup> cationic gel formulations (made up of mixtures of cationic and anionic surfactants),<sup>10</sup> bentonite clays,<sup>11</sup> and macrocyclic hosts.<sup>12-23</sup> Of these macrocyclic hosts, the majority of the attention has been devoted to the use of cyclodextrins (CDs) as hosts for local anaesthetics, most notably  $\beta$ -CD and its derivatives. The host-guest complexes containing  $\beta$ -CD and procaine (also called novocaine) have been studied by a variety of spectroscopic methods, and it has been generally observed that  $\beta$ -CD has a higher affinity for the neutral form of the guest over the cationic species. Iglesias<sup>20</sup> has observed that the host-guest complex between procaine and  $\beta$ -CD has a stability constant of just under  $300 \text{ M}^{-1}$  when the guest is in the monocationic form, and a value of approximately  $1500 \text{ M}^{-1}$  when the procaine guest is in the neutral form. Meanwhile, the dicationic procaine species was found to have a negligible binding affinity with  $\beta$ -CD.<sup>20</sup> While some evidence of weak binding was observed between  $\beta$ -CD and procaine when the pH was below 2, at which point the procaine should exist primarily as the dicationic species, this binding was attributed to the decrease in the  $\text{p}K_{\text{a}}$  of the procaine in the presence of  $\beta$ -CD to give a small amount of the monocationic species.<sup>20</sup> This *decrease* in the guest's  $\text{p}K_{\text{a}}$  upon complexation with  $\beta$ -CD contrasts with behaviour observed with CB[7], where the protonation sites of guests that bind to CB[7] often display an *increase* in their  $\text{p}K_{\text{a}}$  values upon complexation by CB[7], particularly for the sites that bind adjacent to the electron rich CB[7] portals.<sup>24-29</sup>

While cyclodextrins have had widespread applications in drug delivery systems for some time,<sup>30,31</sup> cucurbiturils have recently been shown to act as hosts for a variety of medically relevant guests, with examples including complexes with platinum-containing anti-cancer drugs,<sup>32-37</sup> the organic anti-cancer drugs albendazole<sup>38</sup> and camptothecin,<sup>39</sup> as well as the  $\text{H}_2$ -receptor antagonist ranitidine.<sup>40</sup> Often, organic guests have binding affinities with CB[7] that are orders of magnitude greater than they are to  $\beta$ -CD. The binding constant of ranitidine with CB[7] was

found to be approximately five orders of magnitude greater than its binding constant was to  $\beta$ -CD.<sup>40</sup> Although the interior dimensions of CB[7] and  $\beta$ -CD are comparable, CB[7] has more constricted and electron rich carbonyl-lined portals which may engage in ion-dipole electrostatic interactions to enhance the host-guest complex binding affinities.

This chapter will describe the complexation between CB[7] and five local anaesthetics; procaine, tetracaine, procainamide, dibucaine, and prilocaine. The former two are members of the ester family of local anaesthetics, while the latter three are amide local anaesthetics. The host-guest complexes between CB[7] and these local anaesthetics were studied by <sup>1</sup>H NMR spectroscopy, UV-visible absorbance and emission spectroscopies, as well as electrospray ionization mass spectrometry. The host-guest binding constants were calculated and the complexation-induced shifts of the lower p*K*<sub>a</sub> were also determined.

In addition to local anaesthetics, the binding between CB[7] and epinephrine will also be discussed. Although epinephrine (also called adrenaline) is not a local anaesthetic itself, it is often administered in combination with anaesthetics, where it can serve to reduce blood flow and thus allow more of the accompanying anaesthetic to remain at the injection site.<sup>41</sup> Another medical application of epinephrine, although not directly related to anaesthetics, is in emergency situations such as cardiac arrest, as a patient's chances of recovery are often improved if epinephrine is administered quickly once cardiac arrest occurs.<sup>42</sup>

The work with the local anaesthetics described in this chapter has been published.<sup>43</sup>

## 4.2 Results and Discussion

### 4.2.1 <sup>1</sup>H NMR Spectroscopy and ESI Mass Spectrometry

The complexation-induced  $\Delta\delta_{\text{lim}}$  shifts observed by <sup>1</sup>H NMR spectroscopy (Figures 4.1-4.9) were useful in determining the location of the local anaesthetic guests with respect to the

CB[7] cavity, with the protons displaying upfield shifts (negative  $\Delta\delta_{\text{lim}}$ ) corresponding to those encapsulated by the CB[7] cavity, and those displaying downfield shifts (positive  $\Delta\delta_{\text{lim}}$ ) representing protons that were outside of the cavity, near the portals. This therefore allowed one to determine which part of the guest was encapsulated by the CB[7] cavity under given conditions. The local anaesthetics in this study primarily displayed fast exchange complexation with CB[7] with respect to the NMR timescale, so that the average of the free and bound resonances were observed, as opposed to both the free and bound resonances being visible in the spectra in slow exchange behaviour.

Recently in the Macartney laboratory it has been demonstrated that tetraalkylammonium cations may actually become encapsulated within the hydrophobic cavity of CB[7],<sup>44</sup> as opposed to at the portals, where less hydrophobic cations normally bind with cucurbiturils.<sup>45-47</sup> Of the tetraalkylammonium series explored in that study, the highest binding was observed for the tetraethylammonium guest, with a stability constant of  $(1.0 \pm 0.2) \times 10^6 \text{ M}^{-1}$  with CB[7].<sup>44</sup> With the local anaesthetic guests, encapsulation of the tertiary diethylamine ( $\text{RNHEt}_2^+$ ) was observed for the procaine, procainamide, and dibucaine guests, particularly when the anaesthetics were in their monocationic form, and the aromatic portion of the guest is outside of the cavity and near the portal. This behaviour differs from that proposed by Eglesias for the host-guest complex formed between  $\beta$ -CD and procaine, who noted that when procaine was in its neutral and monocationic form, the aromatic region of the guest is encapsulated by the cyclodextrin's cavity, and the triethylamine group is outside the cavity.<sup>20</sup> Upon encapsulation with CB[7], the  $\text{CH}_2$  protons of the triethylamine were observed to split into two different resonances (Figures 4.1-4.3), suggesting that these magnetically nonequivalent prochiral protons were placed in chemically non-equivalent positions within the CB[7] cavity. Similar behaviour has been observed for methylene protons of more rigid guests, such as substituted adamantanes.<sup>46</sup>



The complexation of CB[7] with tetracaine displayed interesting behaviour that was also unexpected (Figures 4.4 and 4.5). The tertiary amine of free tetracaine is protonated in neutral solution, and it would therefore be anticipated that CB[7] may bind to the tetracaine at that site. However, the  $^1\text{H}$  NMR spectra of the 1:1 complex between CB[7] and tetracaine indicate that the CB[7] has instead bound to the butylamine group at the opposite, more hydrophobic end of the guest, with large upfield shifts observed for the butyl protons and smaller upfield shifts observed for the nearby aromatic ring protons. Since the binding affinity of CB[7] with the tetramethylammonium cation ( $(1.2 \pm 0.4) \times 10^5 \text{ M}^{-1}$ ) is smaller than that of CB[7] with the tetraethylammonium cation ( $(1.0 \pm 0.2) \times 10^6 \text{ M}^{-1}$ ),<sup>44</sup> it may be postulated, by analogy, that the tertiary dimethylammonium group ( $\text{RNHMe}_2^+$ ) of tetracaine would present a less attractive binding site than the corresponding triethylammonium sites of procaine, procainamide, and dibucaine. Another, albeit less thermodynamically reasonable, possibility is that the complexation of CB[7] to the secondary amine causes it to become protonated preferentially over the tertiary amine, despite the much lower  $\text{p}K_a$  value of the secondary amine (2.24) compared to the tertiary amine (8.48).<sup>3</sup> Meanwhile, CB[7] appears to bind with prilocaine primarily at the aromatic region, with large upfield shifts of the prilocaine's aromatic ring and methyl proton resonances, and only a small upfield shift of the central  $\text{CH}_2$  resonance of the propyl group of prilocaine. This lack of binding by CB[7] at the propylammonium group of prilocaine is unusual, particularly when compared to the preference of CB[7] to bind to the butylamine group of tetracaine.

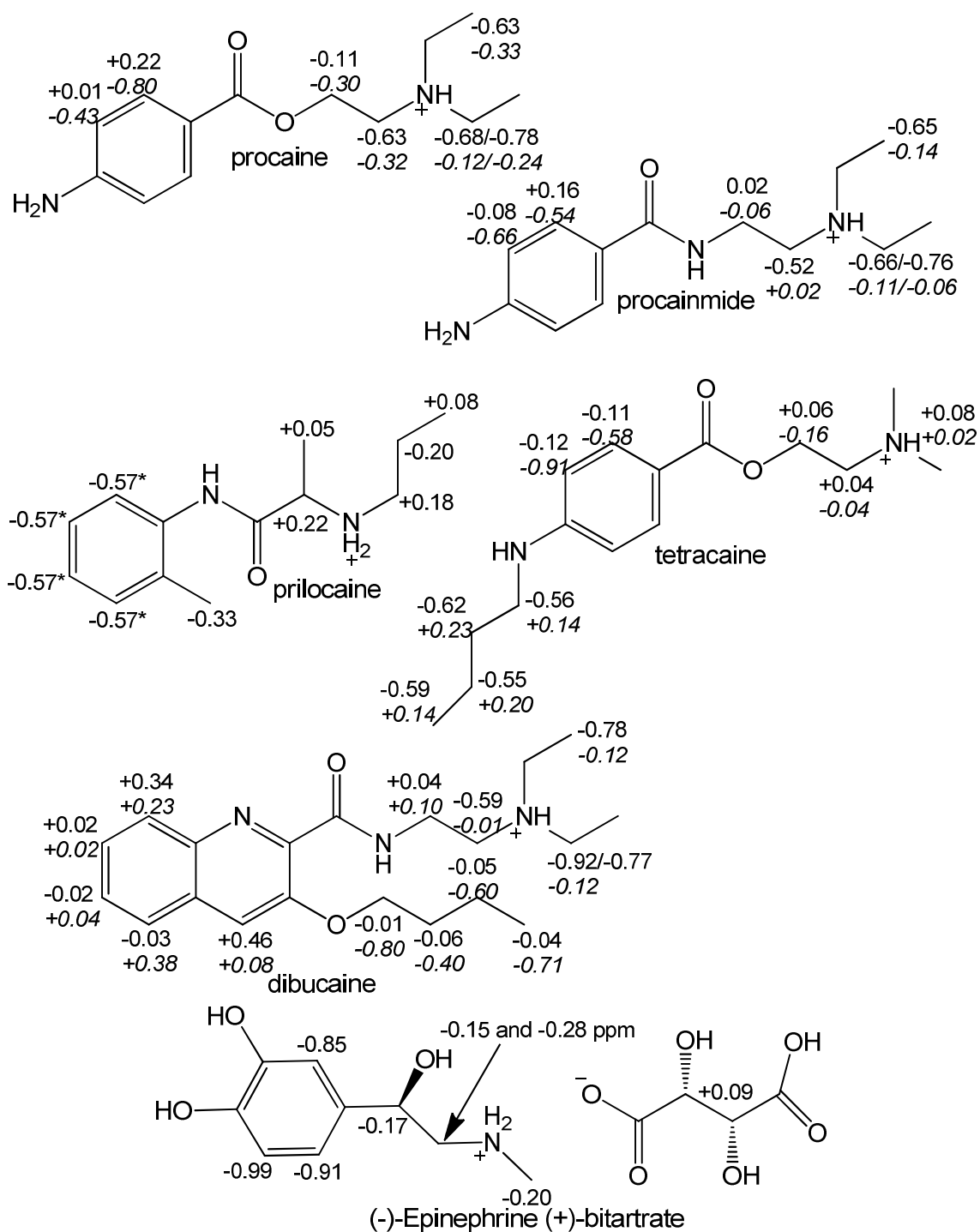


**Figure 4.1** The monocationic structures of procaine, procainamide, prilocaine, tetracaine, dibucaine, and epinephrine bitartrate. The  $^1\text{H}$  NMR  $\Delta\delta_{\text{im}}$  values are shown, with the top numbers representing the values in neutral solution, and the bottom numbers (*in italics*) representing values observed in 0.10 M DCl.

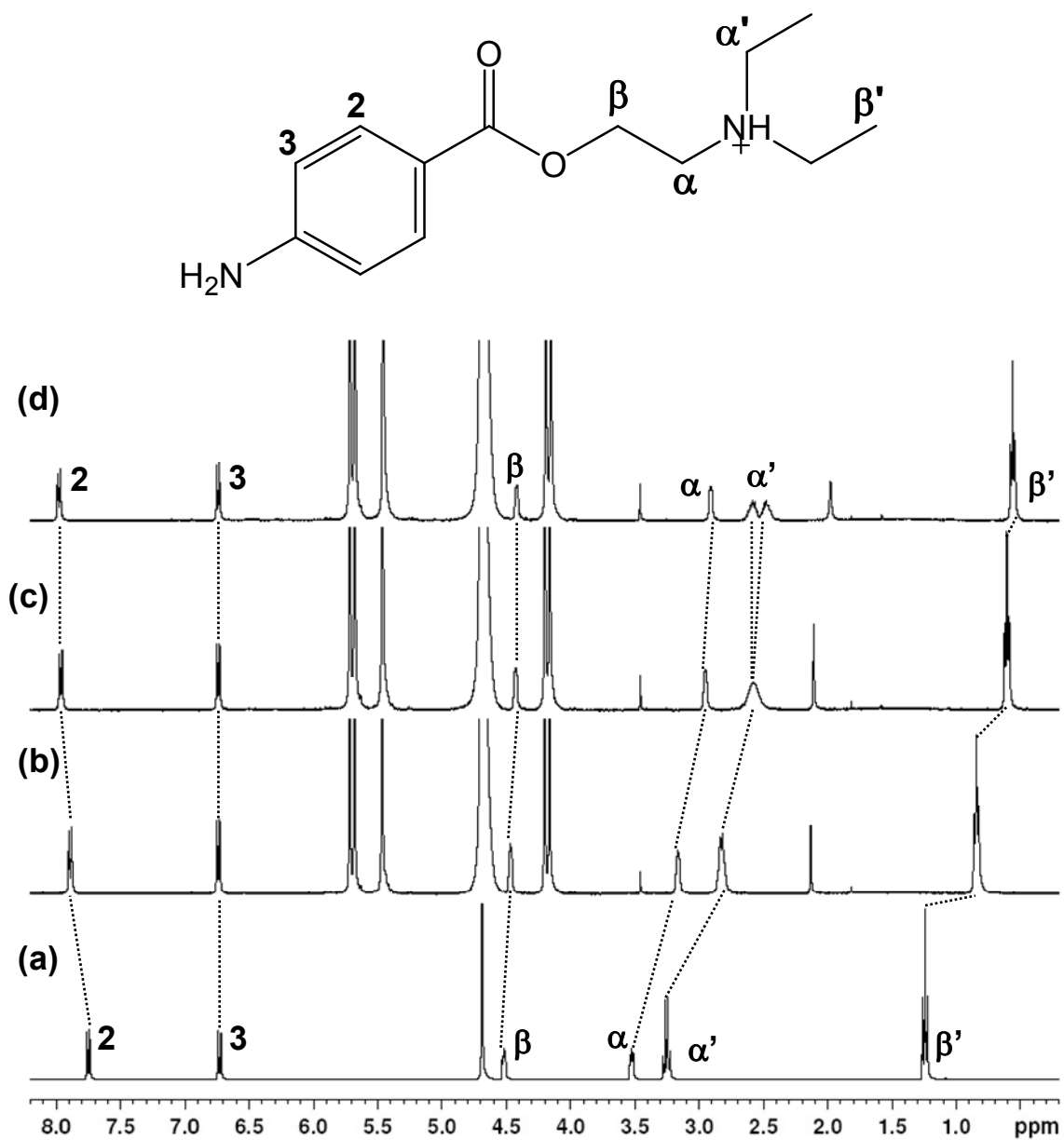


**Figure 4.2**  $^1\text{H}$  NMR spectra of procaine (1.02 mM) in the presence of (a) 0.00, (b) 0.57, (c) 0.96, and (d) 1.18 equivalents of CB[7], titrated in  $\text{D}_2\text{O}$ . The resonance at 3.5 ppm corresponds to residual glycerol from the preparation of CB[7].

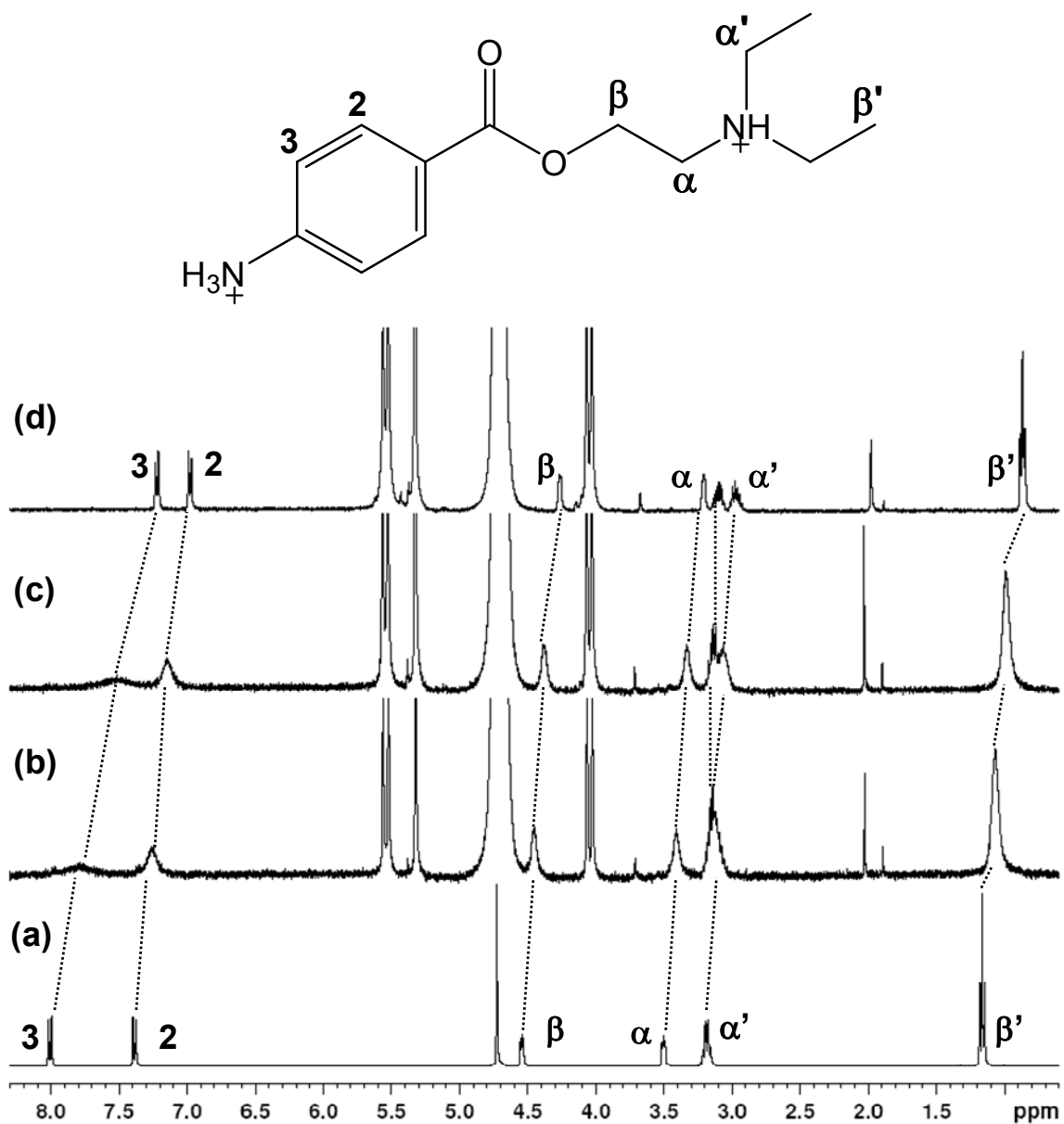


**Figure 4.3** <sup>1</sup>H NMR spectra of procaine (1.02 mM) in the presence of (a) 0.00, (b) 0.33, (c) 0.72, and (d) 1.28 equivalents of CB[7], titrated in 0.1 M DCl.

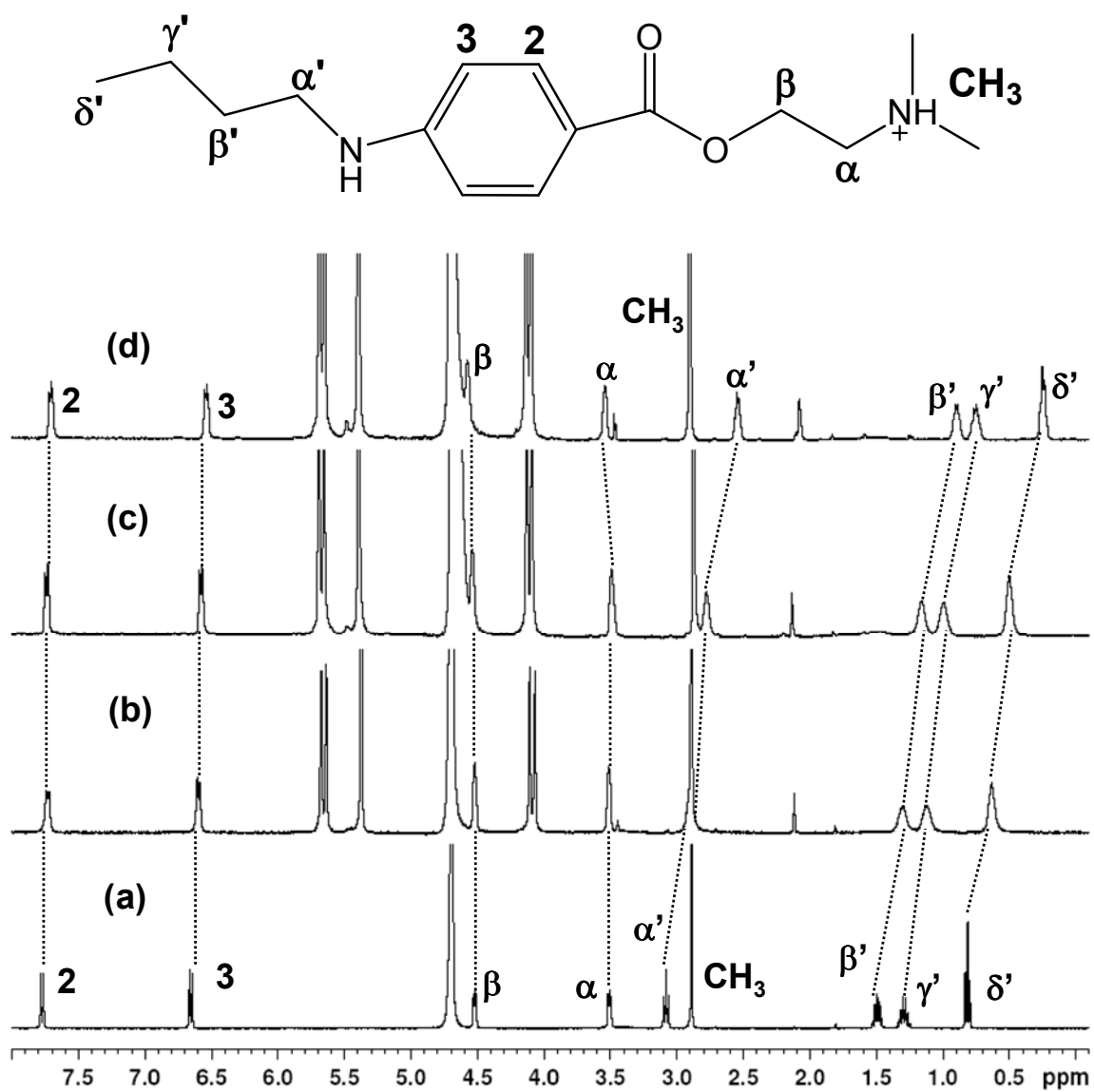


**Figure 4.4** <sup>1</sup>H NMR spectra of tetracaine (1.33 mM) in the presence of (a) 0.00, (b) 0.40, (c) 0.62, and (d) 1.11 equivalents of CB[7], titrated in D<sub>2</sub>O.

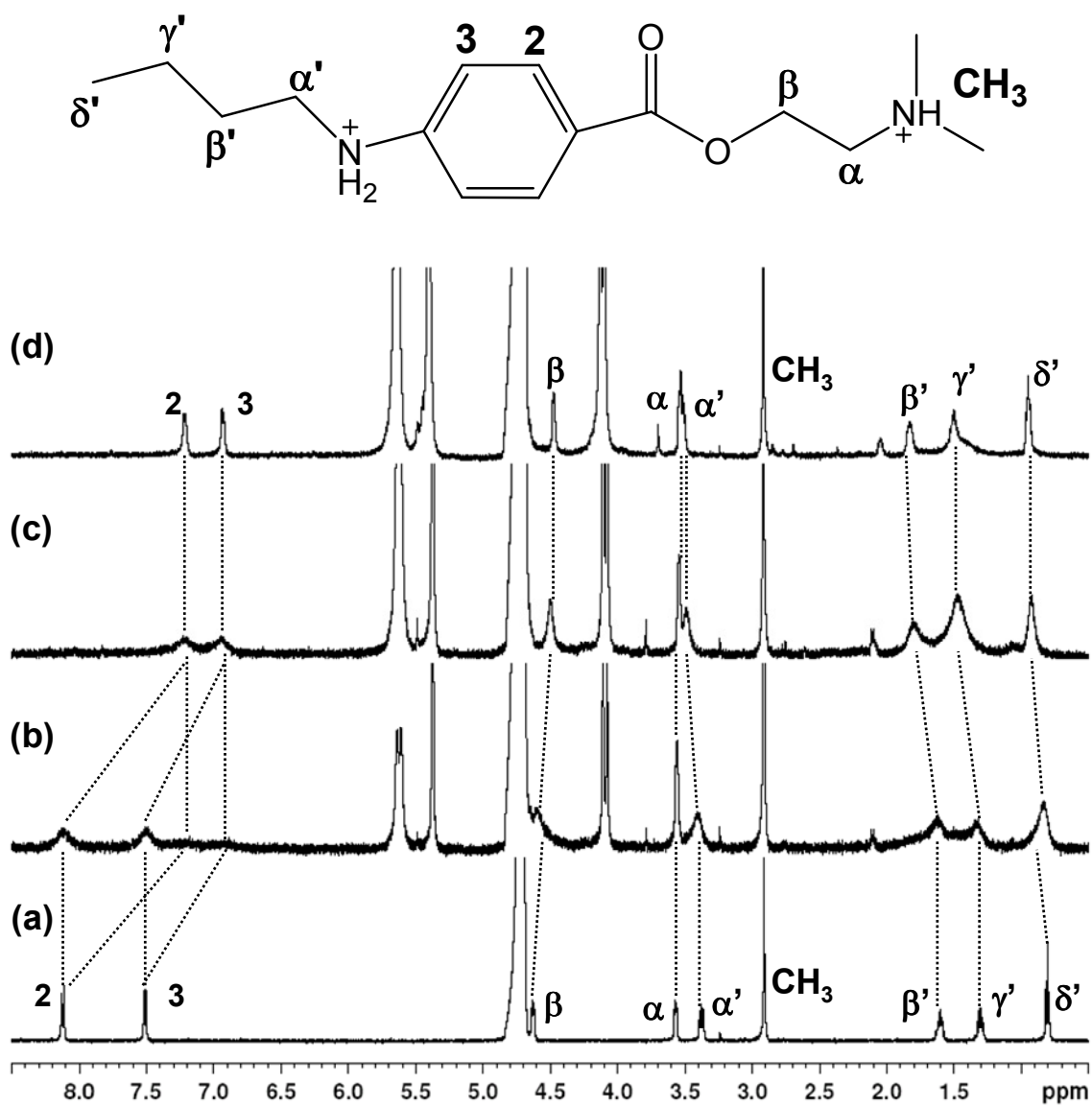


**Figure 4.5** <sup>1</sup>H NMR spectra of tetracaine (1.03 mM) in the presence of (a) 0.00, (b) 0.29, (c) 0.78, and (d) 1.59 equivalents of CB[7], titrated in 0.1 M DCl.

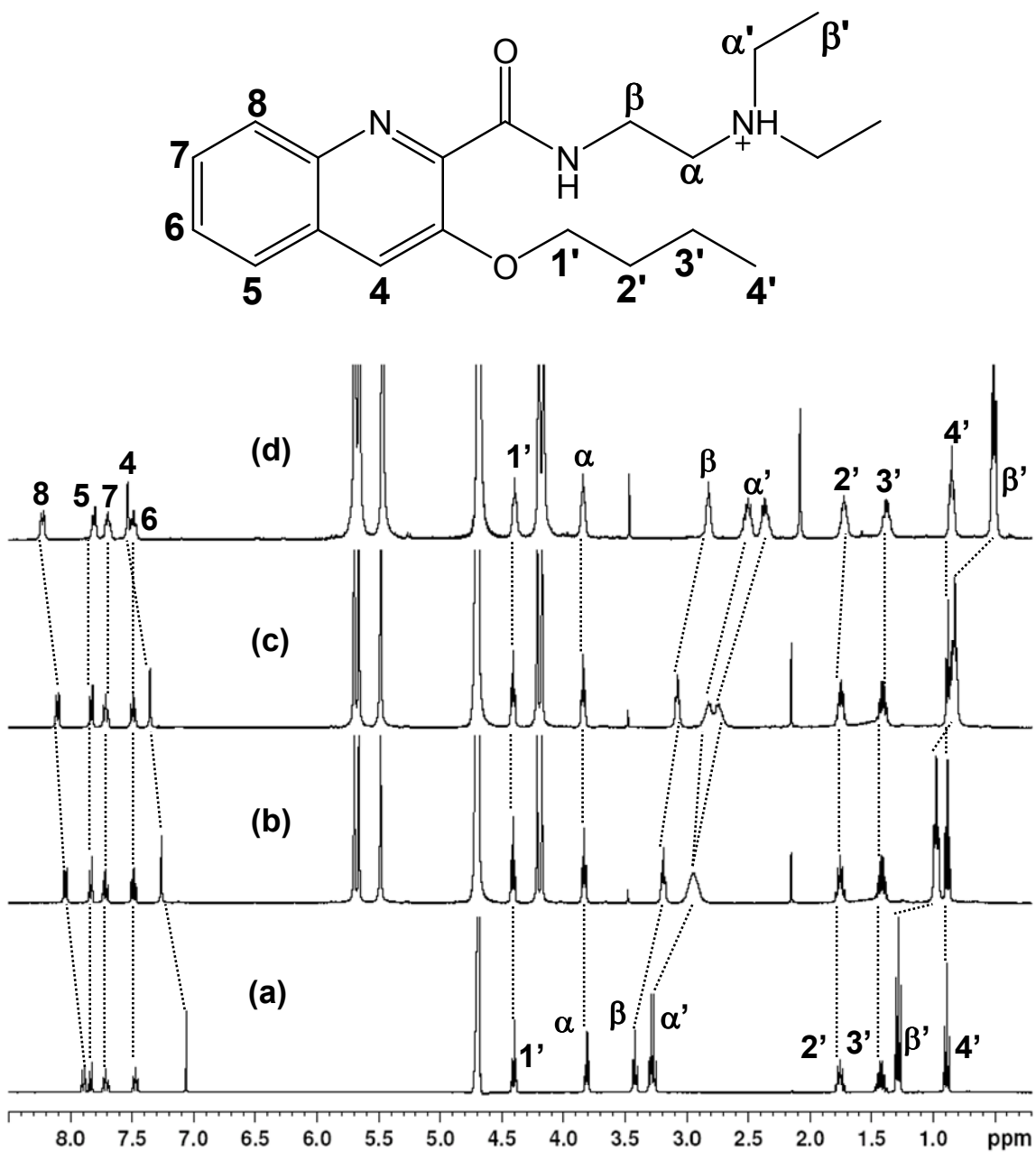


**Figure 4.6** <sup>1</sup>H NMR spectra of dibucaine (1.01 mM) in the presence of (a) 0.00, (b) 0.44, (c) 0.67 and (d) 1.36 equivalents of CB[7], titrated in D<sub>2</sub>O.

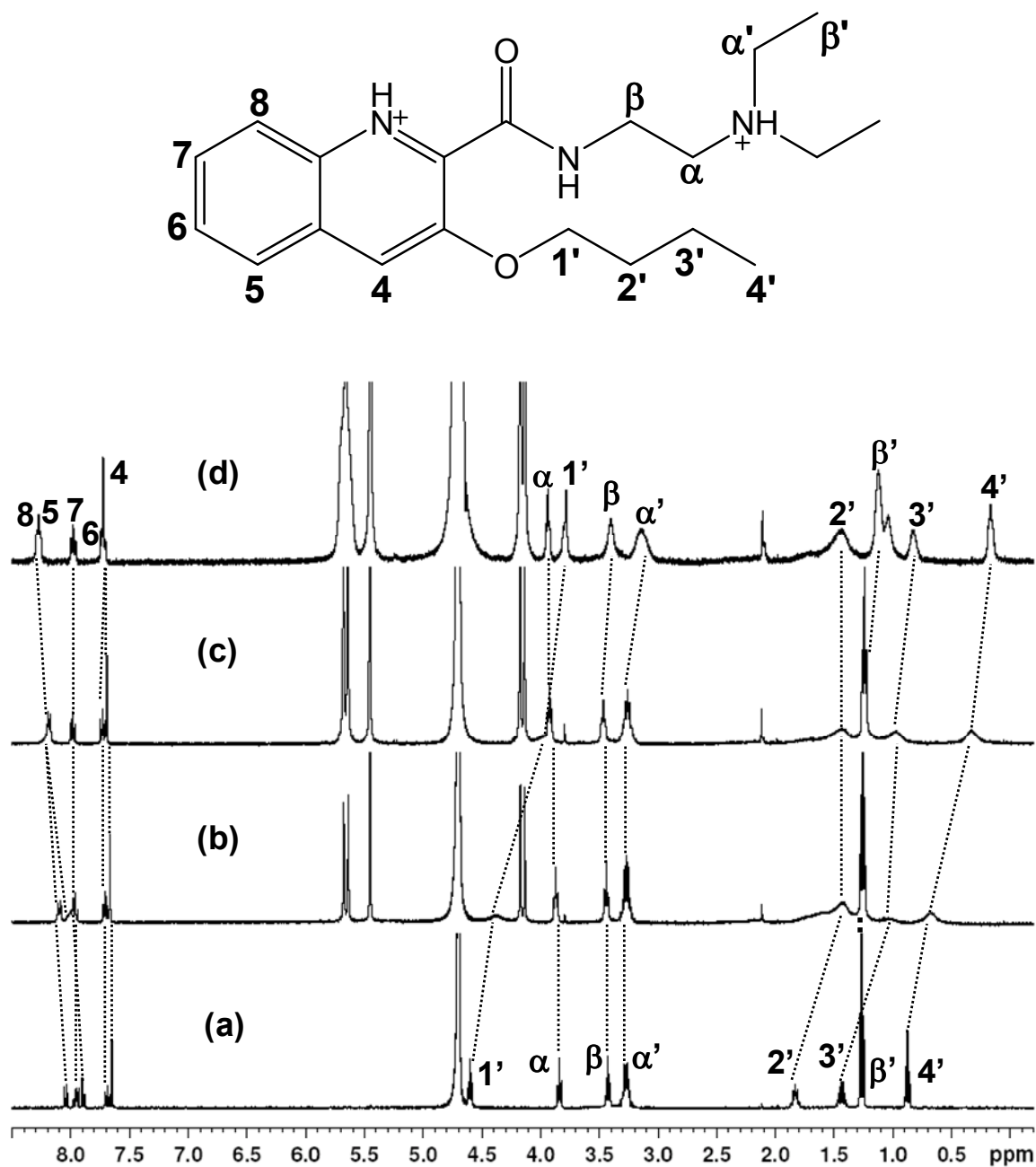


**Figure 4.7** <sup>1</sup>H NMR spectra of dibucaine (1.02 mM) in the presence of (a) 0.00, (b) 0.31, (c) 0.78, and (d) 1.16 equivalents of CB[7] in 0.1 M DCl.



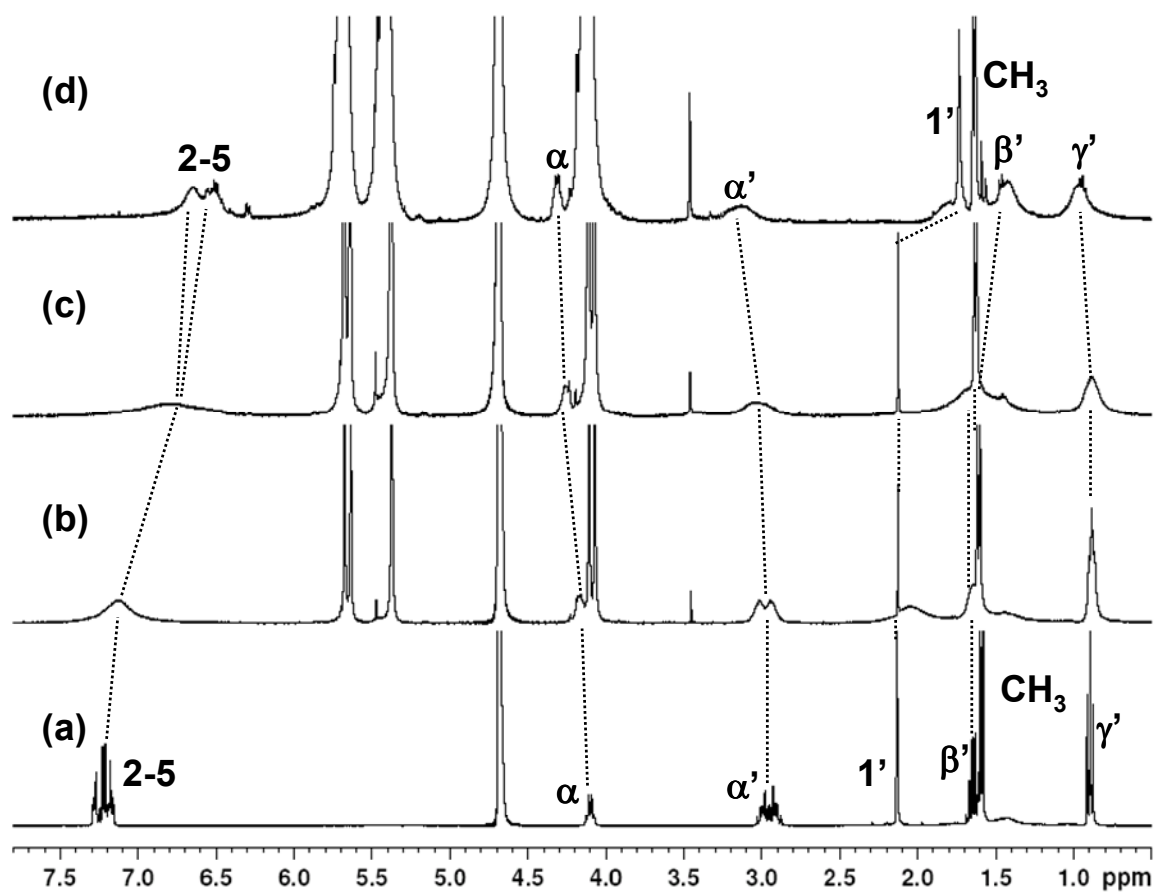
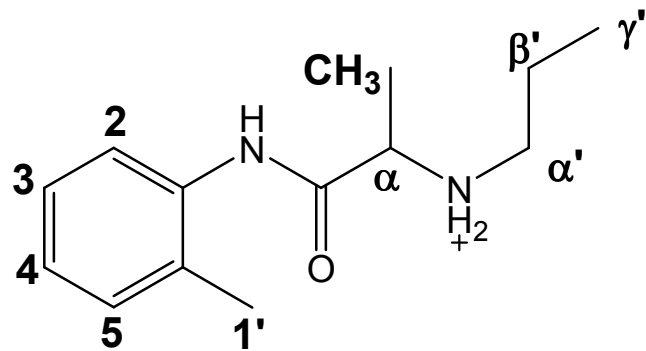


**Figure 4.8**  $^1\text{H}$  NMR spectra of prilocaine (1.27 mM) in the presence of (a) 0.00, (b) 0.31, (c) 0.68, and (d) 1.80 equivalents of CB[7], titrated in  $\text{D}_2\text{O}$ .

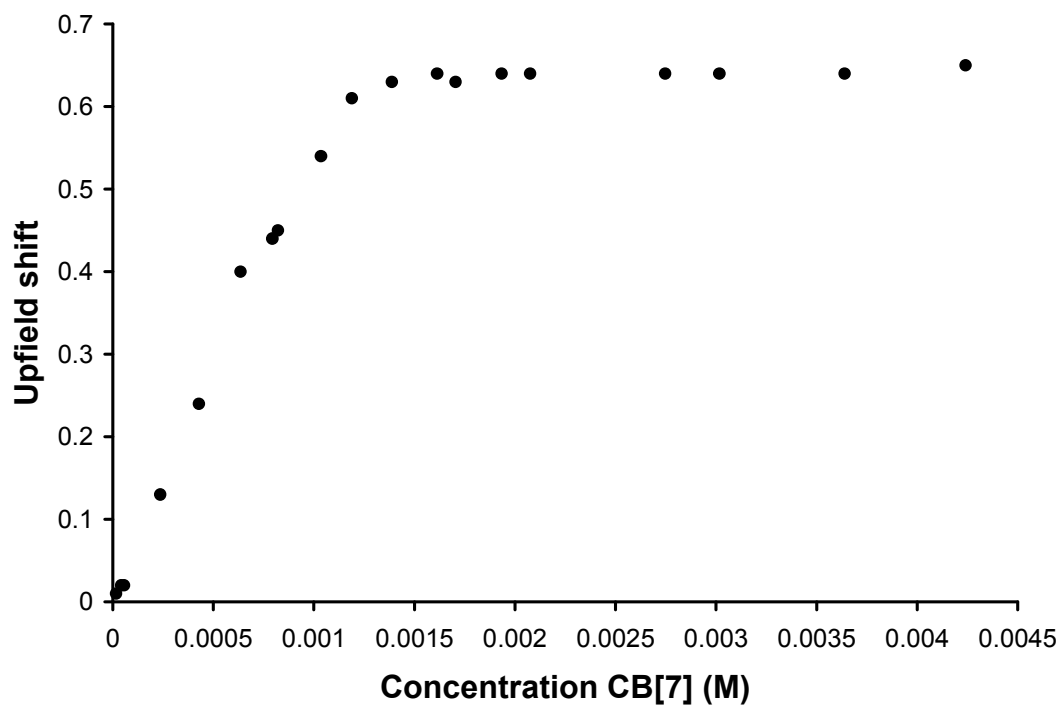


**Figure 4.9** Plot of upfield shift vs. concentration of CB[7] from the  $^1\text{H}$  NMR titration of procainamide (1.10 mM in  $\text{D}_2\text{O}$ ) for its methyl protons of its diethylammonium unit.

When complexation between CB[7] and the anaesthetics is conducted in  $\text{D}_2\text{O}$  in the presence of 0.1 M DCl, the favoured binding site of CB[7] to the guest differed from that observed in the absence of DCl. In the 0.1 M DCl solutions, the local anaesthetics (with the exception of prilocaine) exist in the dicationic form, with both of their amines protonated. The procaine, procainamide, and tetracaine guests, show significant upfield shift of their aromatic protons, suggesting that the aromatic region, with the newly protonated amine nearby, has become the favoured binding site for the CB[7] in the acidic media. In the case of procaine (Figure 4.3), and to a lesser extent procainamide, the diethylammonium protons are also shifted upfield somewhat, suggesting that either the CB[7] is spending some time at this site, or, possibly, that a second CB[7] may be binding weakly to this site. Upon titration with tetracaine in acidic media (Figure 4.5), the CB[7] appears to be binding at the same ammonium site (the

secondary ammonium) but the position of the CB[7] cavity has changed, and it now encapsulates the aromatic ring adjacent to the secondary ammonium instead of the butyl group. With dibucaine (Figure 4.7) the binding site of CB[7] migrates from the diethylammonium group that was the primary binding site in neutral solution to the butyloxy group in the presence of 0.10 M DCl, with no evidence of complexation to the aromatic region of this molecule in either the neutral or acidic media.

Since the 1:1 binding constants between the local anaesthetics and CB[7] were too large to measure directly by either  $^1\text{H}$  NMR or UV-visible titrations, competitive binding experiments, through the use of  $^1\text{H}$  NMR were used instead. Isaacs and coworkers<sup>50</sup> have reported the binding constants of a series of guests with binding constants to CB[7] ranging between  $10^4$  and  $10^{12} \text{ M}^{-1}$  that may be used to determine the binding constant between CB[7] and a given guest. With this series of local anaesthetics, diprotonated 1,2-phenylenediamine, with a binding constant of  $(8.04 \pm 1.28) \times 10^4 \text{ M}^{-1}$  with CB[7], was used as a competitive binding guest in media with pD = 4.75 (0.05 M NaOAc- $d_3$  and 0.025 M DCl).

The host-guest binding constants of the anaesthetics with CB[7] were found to fall between  $1.5 \times 10^4 \text{ M}^{-1}$  and  $1.8 \times 10^5 \text{ M}^{-1}$  at pD 4.75, as listed in Table 4.1. Meanwhile, at pD 1.0, the corresponding binding constants of these guests with CB[7] range between  $2.1 \times 10^4$  and  $1.1 \times 10^7 \text{ M}^{-1}$ . Both of the ester local anaesthetics, procaine and tetracaine, in addition to the amide anaesthetic dibucaine, experienced significant increases in their binding constant to CB[7] in the more acidic solution (1 to 2 orders of magnitude), while the remaining two amide anaesthetics, procainamide and prilocaine, displayed slight decreases of their binding constants to CB[7] in the more acidic solution. The literature values<sup>12,14,20</sup> of binding constants between these local anaesthetics and  $\beta$ -CD are listed in Table 4.1, and are between 2 and 3 orders of magnitude lower than the corresponding binding constants with CB[7] at pD 4.75. Despite the comparable cavity size between  $\beta$ -CD and CB[7], the portals of CB[7] are more constrained, which may facilitate

tighter, more selective binding with the guests. In addition, the electron rich portals of CB[7] more readily facilitate non-covalent interactions (such as ion-dipole, dipole-dipole, or hydrogen bonding) with a cationic guest more readily than the less polar rims of  $\beta$ -CD. Recently, CB[6] has been reported to bind with the amide local anaesthetic bupivacaine, with a stability constant of  $3 \times 10^3 \text{ M}^{-1}$  in aqueous solution,<sup>51</sup> while it has been found to have weaker binding constants of  $102 \pm 10$  and  $63.2 \pm 5.2 \text{ M}^{-1}$  to  $\alpha$ -CD and  $\beta$ -CD, respectively.<sup>52</sup>

**Table 4.1** Host-guest stability constants for complexes of local anaesthetics with CB[7] and  $\beta$ -CD, and  $\text{p}K_{\text{a}}$  values for the guest in the absence and presence of CB[7] ( $\text{p}K_{\text{a}}^{\text{CB}[7]}$ ). At pD 4.75 0.05 M NaOAc-d3 and 0.025 M DCl were present, while at pD 1.0, 0.05 M NaCl and 0.1 M DCl were present.

Guest	$K_{\text{CB}[7]}$ (pD 4.75, $\text{M}^{-1}$ )	$K_{\text{CB}[7]}$ (pD 1.0, $\text{M}^{-1}$ )	$K_{\beta\text{-CD}}$ ( $\text{M}^{-1}$ )	$\text{p}K_{\text{a}}$	$\text{p}K_{\text{a}}^{\text{CB}[7]}$
procaine	$(3.5 \pm 0.7) \times 10^4$	$(4.4 \pm 1.6) \times 10^5$	$3.3 \times 10^{2a,c}$ $1.4^c$	$2.28^b$	$3.50 \pm 0.05$
tetracaine	$(1.5 \pm 0.4) \times 10^4$	$(1.1 \pm 0.3) \times 10^6$	$1.1 \times 10^{3a}$	$2.24^b$	$4.15 \pm 0.05$
procainamide	$(7.8 \pm 1.6) \times 10^4$	$(5.5 \pm 1.1) \times 10^4$		$2.83^b$	$3.38 \pm 0.05$
dibucaine	$(1.8 \pm 0.4) \times 10^5$	$(1.1 \pm 0.2) \times 10^7$	$6.6 \times 10^{2a}$	$1.77^d$	$3.55 \pm 0.05$
prilocaine	$(2.6 \pm 0.6) \times 10^4$	$(2.1 \pm 0.4) \times 10^4$	$9.6 \times 10^{1e}$		
epinephrine	$(3.2 \pm 0.7) \times 10^4$				

<sup>a</sup>Reference 12. <sup>b</sup>Reference 2. <sup>c</sup>For diprotonated form, reference 20. <sup>d</sup>Reference 49. <sup>e</sup>Reference 14.

**Table 4.2** High resolution ESI-MS data for the formation of host-guest complexes between local anaesthetics and CB[7]. The numbers in bold represent the observed values, while the numbers in parenthesis represent the predicted values based on the isotopic mass of the corresponding species.

Guest	1:1 Complex ( <i>m/z</i> )	2:1 Complex ( <i>m/z</i> )
<b>Procaine</b>	<b>[1:1-Cl+H]<sup>2+</sup>: 700.2551</b> (calc. C <sub>55</sub> H <sub>64</sub> N <sub>30</sub> O <sub>16</sub> <sup>2+</sup> = 700.2553); <b>[1:1+Na-Cl]<sup>2+</sup>: 711.2382</b> (calc. C <sub>55</sub> H <sub>63</sub> N <sub>30</sub> O <sub>16</sub> Na <sup>2+</sup> = 711.2463); <b>[1:1-Cl]<sup>+</sup>: 1399.5323</b> (calc. C <sub>55</sub> H <sub>63</sub> N <sub>30</sub> O <sub>16</sub> <sup>+</sup> = 1399.5033)	<b>[2:1+H-Cl]<sup>2+</sup>: 1281.4674</b> (calc. C <sub>97</sub> H <sub>106</sub> N <sub>58</sub> O <sub>30</sub> <sup>2+</sup> = 1281.4271); <b>[2:1+Na-Cl]<sup>2+</sup>: 1292.4687</b> (calc. C <sub>97</sub> H <sub>105</sub> N <sub>58</sub> O <sub>30</sub> Na <sup>2+</sup> = 1292.4181)
<b>Tetracaine</b>	<b>[1:1-Cl+H]<sup>2+</sup>: 714.2447</b> (calc. C <sub>57</sub> H <sub>68</sub> N <sub>30</sub> O <sub>16</sub> <sup>2+</sup> = 714.2709); <b>[1:1-Cl+Na]<sup>2+</sup>: 725.254</b> (calc. C <sub>57</sub> H <sub>67</sub> N <sub>30</sub> O <sub>16</sub> Na <sup>2+</sup> = 725.2619); <b>[1:1-Cl]<sup>+</sup>: 1427.5585</b> (calc. C <sub>57</sub> H <sub>67</sub> N <sub>30</sub> O <sub>16</sub> <sup>+</sup> = 1427.5346)	<b>[2:1+H-Cl]<sup>2+</sup>: 1295.4767</b> (calc. C <sub>99</sub> H <sub>110</sub> N <sub>58</sub> O <sub>30</sub> <sup>2+</sup> = 1295.4428)
<b>Procainamide</b>	<b>[1:1-Cl+H]<sup>2+</sup>: 699.7661</b> (calc. C <sub>55</sub> H <sub>65</sub> O <sub>15</sub> N <sub>31</sub> <sup>2+</sup> = 699.7633); <b>[1:1-Cl]<sup>+</sup>: 1398.5446</b> (calc. C <sub>55</sub> H <sub>64</sub> N <sub>31</sub> O <sub>15</sub> <sup>+</sup> = 1398.5193)	<b>[2:1-Cl+H]<sup>2+</sup>: 1280.9546</b> (calc. C <sub>97</sub> H <sub>107</sub> N <sub>59</sub> O <sub>29</sub> <sup>2+</sup> = 1280.9351); <b>[2:1-Cl+Na]<sup>2+</sup>: 1291.9526</b> (calc. C <sub>97</sub> H <sub>106</sub> N <sub>59</sub> O <sub>29</sub> Na <sup>2+</sup> = 1291.9261)
<b>Dibucaine</b>	<b>[1:1-Cl+H]<sup>2+</sup>: 753.8056</b> (calc. C <sub>62</sub> H <sub>73</sub> N <sub>31</sub> O <sub>16</sub> <sup>2+</sup> = 753.7920); <b>[1:1-Cl]<sup>+</sup>: 1506.6074</b> (calc. C <sub>62</sub> H <sub>72</sub> N <sub>31</sub> O <sub>16</sub> <sup>+</sup> = 1506.5768)	<b>[2:1-Cl+H]<sup>2+</sup>: 1334.9858</b> (calc. C <sub>104</sub> H <sub>115</sub> N <sub>59</sub> O <sub>30</sub> <sup>2+</sup> = 1334.9639); <b>[2:1-Cl+Na]<sup>2+</sup>: 1345.9803</b> (calc. C <sub>104</sub> H <sub>114</sub> N <sub>59</sub> O <sub>30</sub> Na <sup>2+</sup> = 1345.9549)
<b>Prilocaine</b>	<b>[1:1-Cl]<sup>+</sup>: 1383.5430</b> (calc. C <sub>55</sub> H <sub>63</sub> N <sub>30</sub> O <sub>15</sub> <sup>+</sup> = 1383.5084)	<b>[2:1-Cl+H]<sup>2+</sup>: 1273.4501</b> (calc. C <sub>97</sub> H <sub>106</sub> N <sub>58</sub> O <sub>29</sub> <sup>2+</sup> = 1273.4296); <b>[2:1-Cl+Na]<sup>2+</sup>: 1284.4416</b> (calc. C <sub>97</sub> H <sub>105</sub> N <sub>58</sub> O <sub>29</sub> Na <sup>2+</sup> = 1284.4206)

It has been noted that the binding affinity between procaine and  $\beta$ -CD decreases from approximately  $300 \text{ M}^{-1}$  on going from the anaesthetic's monocationic form,<sup>12,20</sup> to approximately  $1.4 \text{ M}^{-1}$  when it exists as the dicationic species.<sup>20</sup> Meanwhile, Iglesias observed that this binding constant increases to  $1.1 \times 10^3$  when the drug is in its neutral form.<sup>20</sup> Similarly, it has also reported that the binding affinity between  $\beta$ -CD and tetracaine increases from  $1.36 \times 10^3$  to  $6.60 \times 10^3 \text{ M}^{-1}$ , respectively, as the anaesthetic is changed from its monocationic to its neutral species.<sup>19</sup> When the binding between the smaller  $\alpha$ -CD macrocycle and procaine was studied,<sup>21</sup> only the neutral form of procaine would bind, with a host-guest stability constant of  $120 \text{ M}^{-1}$ . Ludwig and coworkers<sup>15</sup> have reported that hydroxypropyl- $\beta$ -CD binds to monocationic tetracaine with a binding affinity of  $1.31 \times 10^3 \text{ M}^{-1}$ , while de Paula and coworkers<sup>19</sup> noted that this species binds to *p*-sulfonated calix[6]arene with a binding constant of  $3.89 \times 10^3 \text{ M}^{-1}$ . This binding constant is larger than that observed between the monocationic tetracaine and  $\beta$ -CD by the same authors, and they attributed this increased binding affinity with the calixarene complex to be a result of the negatively charged sulfonate groups attached to this calixarene.<sup>19</sup> While prilocaine has been reported to bind to  $\beta$ -CD<sup>14</sup> with a stability constant of  $96 \text{ M}^{-1}$ , a smaller value of  $< 5 \text{ M}^{-1}$  was determined for the complexation this drug by  $\alpha$ -CD.<sup>22</sup> Similar weak binding ( $< 5 \text{ M}^{-1}$ ) was also reported between  $\alpha$ -CD and lidocaine.<sup>22</sup>

The results of the  $^1\text{H}$  NMR and UV-visible spectroscopic titrations, as well as an examination of the ESI-MS data (Table 4.2) seem to indicate that very weak 2:1 host-guest binding between some of the anaesthetics and CB[7] occurs when the CB[7] is present in excess of the guest. For example, in the case of procaine, the UV-visible titration curve suggests an initial formation of a strongly bound 1:1 host-guest complex, followed by a much weaker 2:1 complex as the CB[7] ratio is increased beyond the equivalence point. The anaesthetics explored in this study are large enough to potentially bind with two CB[7] hosts, especially the drugs

procaine, procainamide, and tetracaine, with amine moieties located at opposite ends of the molecule. However, the electron rich CB[7] portals can cause the CB[7] units to undergo electrostatic repulsions with one another, so that any 2:1 complexes formed would have significantly weaker binding affinities than those of the preceding 1:1 complexes. The ESI-MS data suggested that the smaller prilocaine anaesthetic was also involved in 2:1 host-guest binding with CB[7], although these peaks were much weaker than the corresponding 1:1 peaks, and may represent external binding between the prilocaine and CB[7] in the gas-phase rather than encapsulation of part of the guest with a second CB[7] host.

#### **4.2.2 UV-visible Absorbance and Emission Spectroscopy**

During the UV-visible titration of tetracaine with increasing amounts of CB[7] (Figure 4.10), the formation of the host-guest complex results in a bathometric shift of the peak's maximum from 310 to 322 nm, with an isosbestic point at 314 nm. The isosbestic point drifted somewhat, which was likely a result of the formation of the 2:1 complex as the concentration of CB[7] was increased. Procaine, in contrast to tetracaine, shows a slight hypsochromic shift upon complexation with CB[7], from 290 nm to 286 nm. Similarly, in the fluorescence titration of procaine with CB[7] (Figure 4.11), the emission maximum exhibits a hypsochromic shift from 354 to 346 nm with a 2.5-fold increase in the fluorescence upon formation of the host-guest complex. Previous reports have established that encapsulation of guests inside cucurbituril cavities cause significant changes in the fluorescence intensity of the included guest. Often, inclusion of a guest in cucurbiturils causes enhancement of the guest's fluorescence intensity, as observed with the stabilization of fluorescent dyes,<sup>53-56</sup> while occasionally quenching of the guest's fluorescence upon encapsulation may also be observed, such as when two guests included in close proximity to each other in the cavity of CB[8] quench each other's emission.<sup>57</sup> Upon

complexation of procaine with  $\beta$ -CD, Iglesias also noted that the emission wavelength decreases, while its fluorescence intensity is enhanced.<sup>20</sup> They attributed the former change to the decrease in polarity of the cyclodextrin cavity compared to the bulk media, and the latter to the more rigid structure of the guest that is bound to  $\beta$ -CD.

An increase of procaine's fluorescence intensity was also observed when it was titrated with CB[7] (Figure 4.11). When the plot of the change of fluorescence intensity ( $F/F_0$ ) against the concentration of CB[7] was fit by a least squares method, a stability constant of  $(1.0 \pm 0.3) \times 10^5 \text{ M}^{-1}$  was determined in water (with no electrolyte). This stability constant between CB[7] and procaine was significantly stronger than the corresponding value determined by  $^1\text{H}$  NMR through competitive binding experiments  $((3.5 \pm 0.7) \times 10^4 \text{ M}^{-1})$ , and this discrepancy likely arises from the presence of sodium cations in the buffer used for the  $^1\text{H}$  NMR competitive studies, which can compete with the guest for binding to cucurbiturils, and thus reduce the value of the binding constant in that media. Various research groups have reported that alkali cations bind to cucurbiturils,<sup>57-63</sup> and it has been reported that cucurbituril-guest binding affinities decrease in the presence of alkali cations.<sup>64-66</sup> We have previously reported (see Chapter 2) that the binding constant between CB[7] and small polar solvent guests such as acetophenone decrease by seven-fold when the solution is changed from  $\text{D}_2\text{O}$  (with no sodium cations added) to 0.20 M NaCl in  $\text{D}_2\text{O}$ .<sup>66</sup>



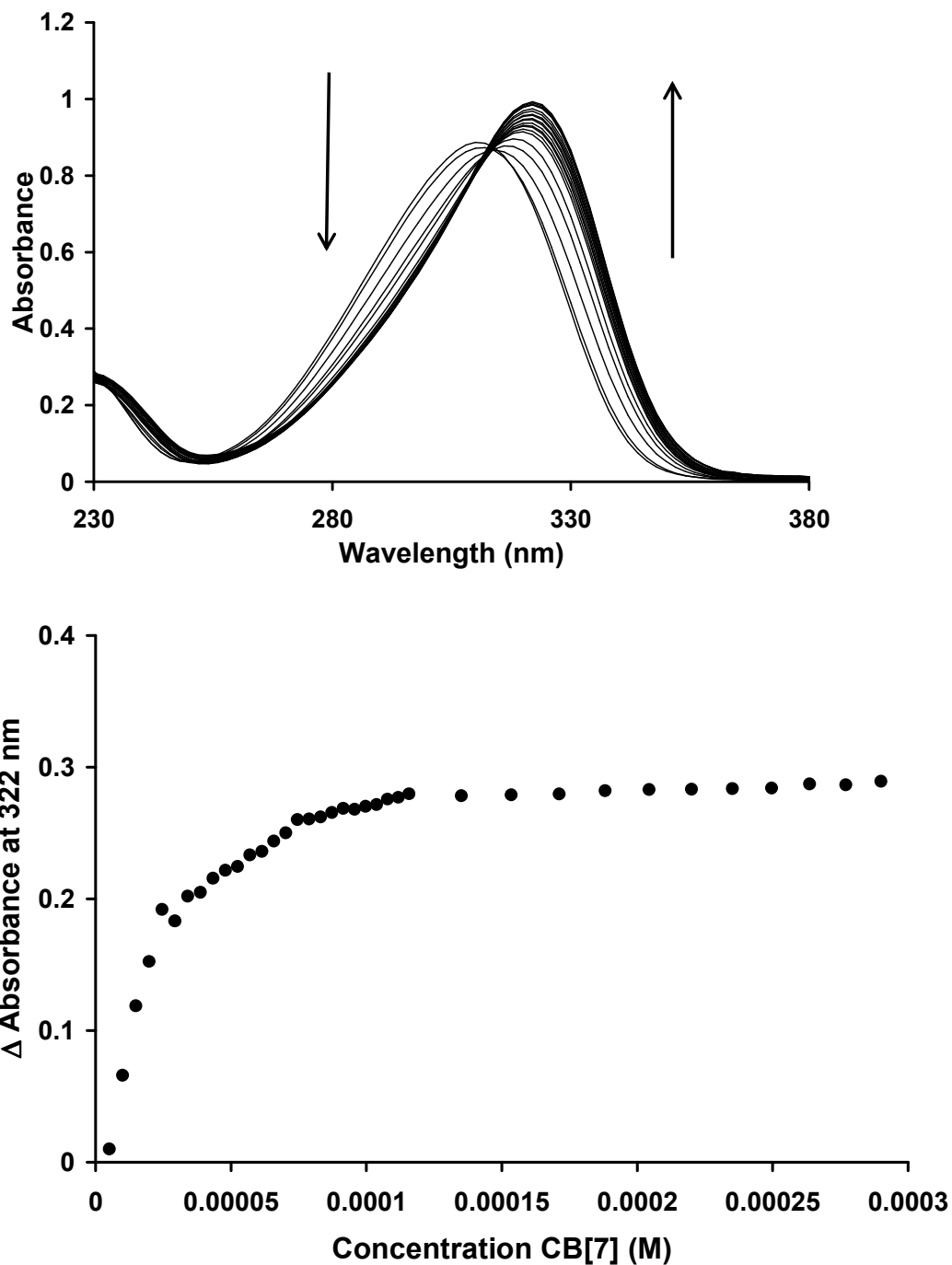


**Figure 4.10** Titration of tetracaine ( $5 \times 10^{-5}$  M) with CB[7] (top) with an isosbestic point observed at 314 nm. Arrows indicate direction of changes in absorbance with increasing CB[7] concentration. The drifting of the isosbestic point likely resulted from formation of the 2:1 complex at higher CB[7] concentrations. A plot of the change of absorbance at 322 nm as a function of CB[7] concentration (bottom). The titration was conducted in aqueous solution.

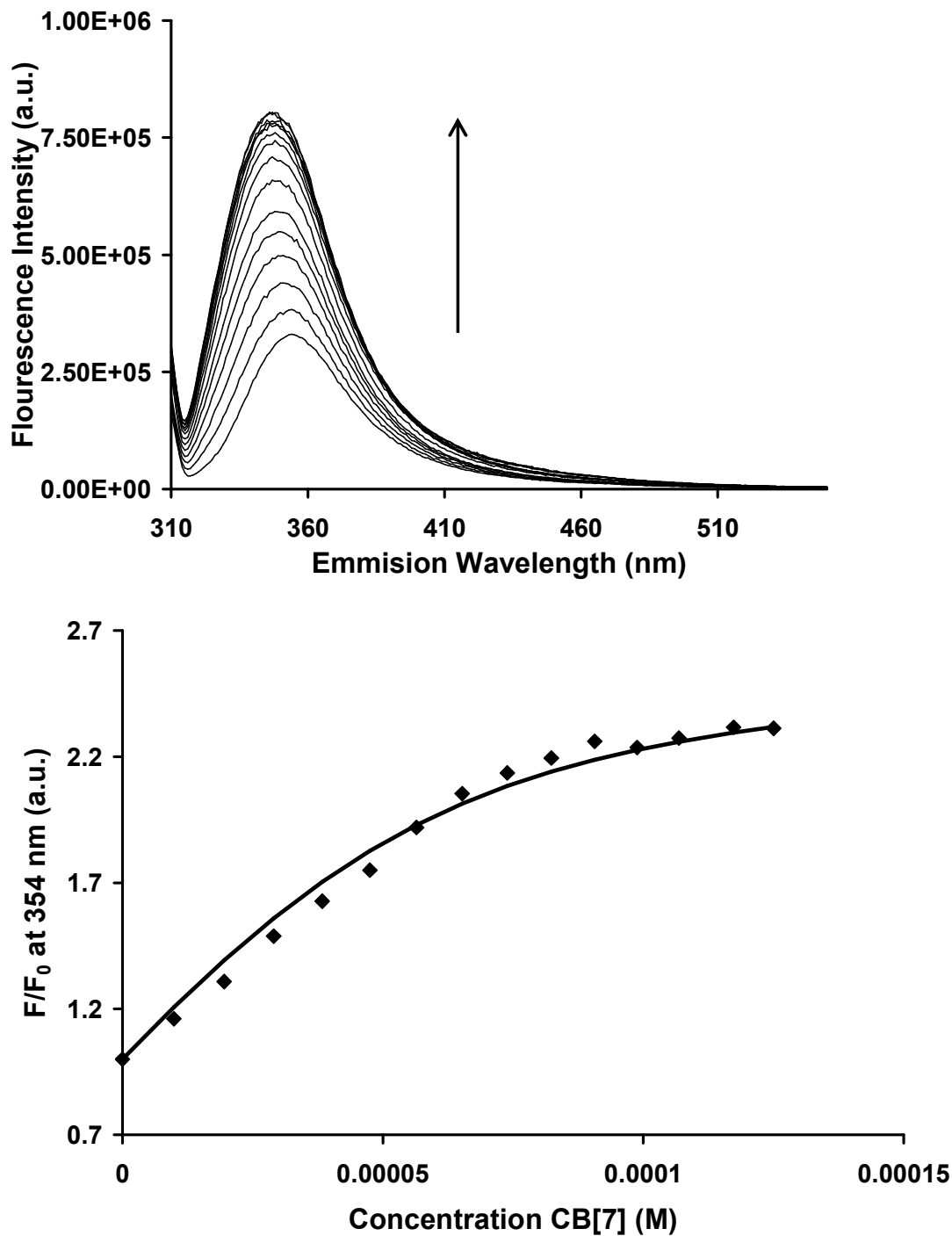


**Figure 4.11** Fluorescence spectra of procaine ( $5.0 \times 10^{-5}$  M) in aqueous solution in the presence of increasing concentrations of CB[7] (top). Dependence of  $F/F_0$  at 354 nm on the concentration of CB[7] (bottom). The deviation from the curve fitting likely arises from formation of the 2:1 complex at higher CB[7] concentrations.

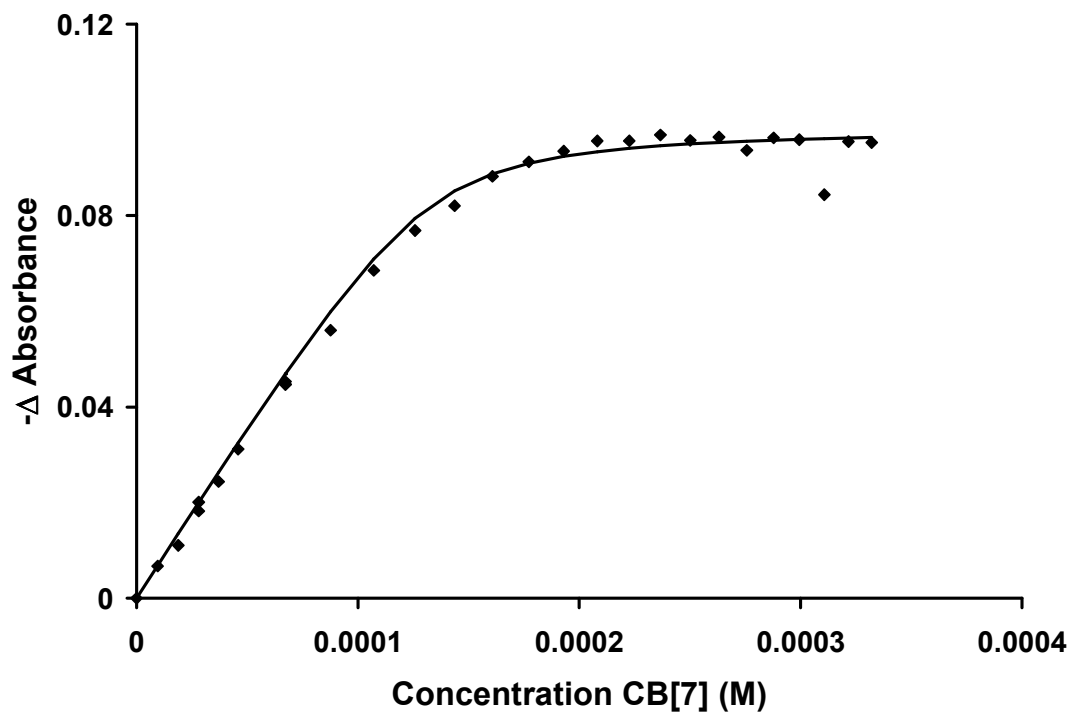
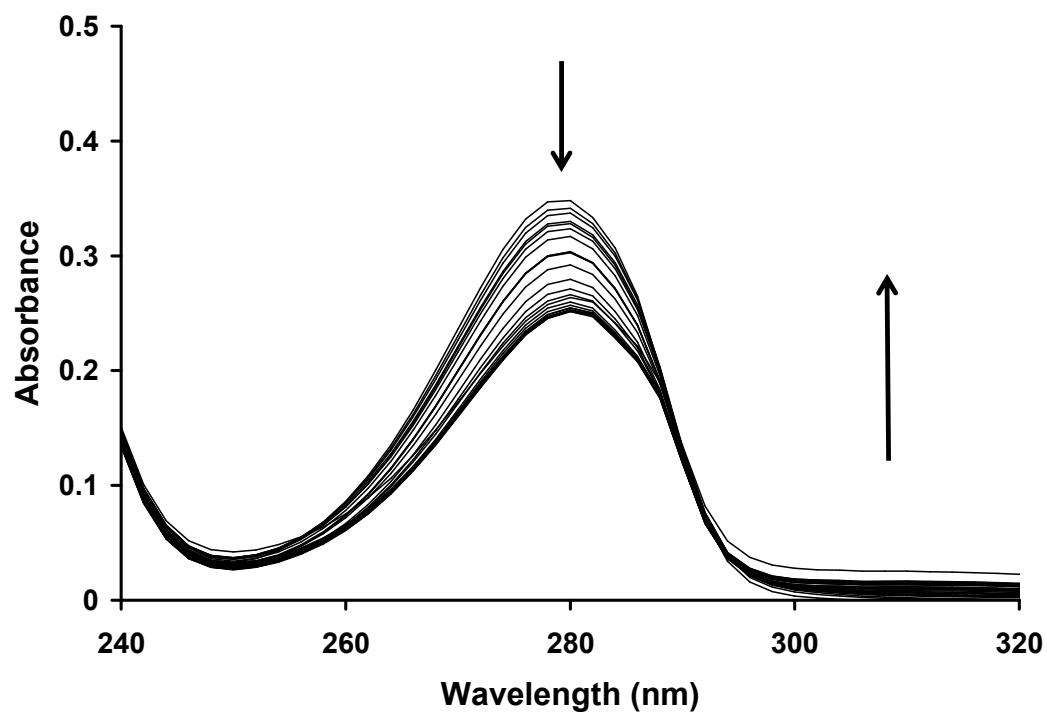


**Figure 4.12** UV titration of epinephrine bitartrate (1.3 mM) with CB[7] in aqueous solution (top). The dependence of the change in absorbance at 280 nm on the concentration of CB[7] (bottom).

When the binding constant between CB[7] and epinephrine bitartrate was determined by UV-visible titration, a value of  $(2.2 \pm 0.7) \times 10^5 \text{ M}^{-1}$  was obtained (Figure 4.12). This stability constant is almost an order of magnitude greater than the value calculated by  $^1\text{H}$  NMR using the competitive binding method. While the majority of the local anaesthetics had binding constants too large to measure directly by UV-visible titration, it was possible to determine a binding constant of  $(2.5 \pm 0.6) \times 10^5 \text{ M}^{-1}$  from the titration of tetracaine with CB[7] (Figure 4.10), which is also approximately an order of magnitude stronger than the value determined from the competitive binding method. These differences may be partially attributed to the influence of different media, with the UV titration being conducted in water with no added electrolyte, while the media used in the competitive binding experiment contains 0.05 M NaOAc- $d_3$  and 0.025 M DCl. The presence of sodium cations in solution has been observed to reduce binding constants between CB[7] and its guests, both by other researchers,<sup>64</sup> and also in Chapter 2 of this thesis.

#### 4.2.3 Complexation-Induced $pK_a$ Shifts

The pH of the patient's tissue surrounding the injection site has a significant effect on the pharmacokinetics of the local anaesthetic, as the non-ionized species of the drug can more readily cross neural membranes and block sodium channels.<sup>2</sup> Therefore, the greater the proportion of the non-ionized form that is present, the faster the onset of the anaesthetic. When a patient experiences inflammation (acidosis), the pH of the surrounding media is decreased, so that the drug more readily becomes protonated, and thus the onset of the drug slows down. It has been reported that the  $pK_a$  values of local anaesthetics in the presence of micelles and membranes differ from those of the anaesthetics in bulk solution.<sup>67</sup> Fernandez and coworkers noted that the  $pK_a$  values of the tertiary amine of tetracaine was decreased by 1.38 and 0.68 pK units, respectively, in the presence of cationic (cetyltrimethylammonium bromide as surfactant) and

neutral micelles (Triton X-100 surfactant), while the  $pK_a$  was increased by 1.66  $pK$  units in the presence of anionic micelles (sodium dodecyl sulfate as surfactant).<sup>67</sup> Zhang *et al.* have reported that when the monocationic tetracaine was adsorbed onto neutral bilayers of phosphatidylcholine membranes, with its tertiary amine positioned near the phosphate of the head group, its  $pK_a$  value was reduced by between 0.3 and 0.4  $pK$  units compared to its corresponding value in bulk solution.<sup>68</sup>

As mentioned earlier, CB[7] has been reported to increase the  $pK_a$  values of certain guests.<sup>24-29</sup> Since the anaesthetics in this study exist as the monoprotonated form at near-neutral pH, we were interested in the drug's protonation site with the lower  $pK_a$  ( $pK_{a1}$ ), having values typically between 2 and 3. If the complexation-induced  $pK_a$  shifts are sufficiently large, the formation of the diprotonated species of the anaesthetic would be promoted by the presence of CB[7]. UV titrations were used to determine the  $pK_{a1}$  values of the local anaesthetics in the presence of a three-fold excess of CB[7] (Figure 4.13). The  $pK_a$  values were found to increase between 0.5 and 1.8 pH units compared to literature values of the free guests in aqueous solution. These increases were relatively modest compared to some of the larger  $pK_a$  shifts reported for guests encapsulated by CB[7]. For example, Nau and coworkers have reported that thiabendazole experiences a  $pK_a$  increase of up to 4 units in the presence of CB[7],<sup>29</sup> while Wang *et al.* reported an increase of 3.7  $pK$  units in the  $pK_a$  of the conjugate acid of 5,6-dimethylbenzimidazole, as a result of the complexation with CB[7].<sup>28</sup> The increase of a guest's  $pK_a$  value as a result of complexation with CB[7] has been attributed to the greater stabilization of the diprotonated forms of the guest, which may then experience stronger cation-dipole interactions with the electron rich cucurbituril portals.

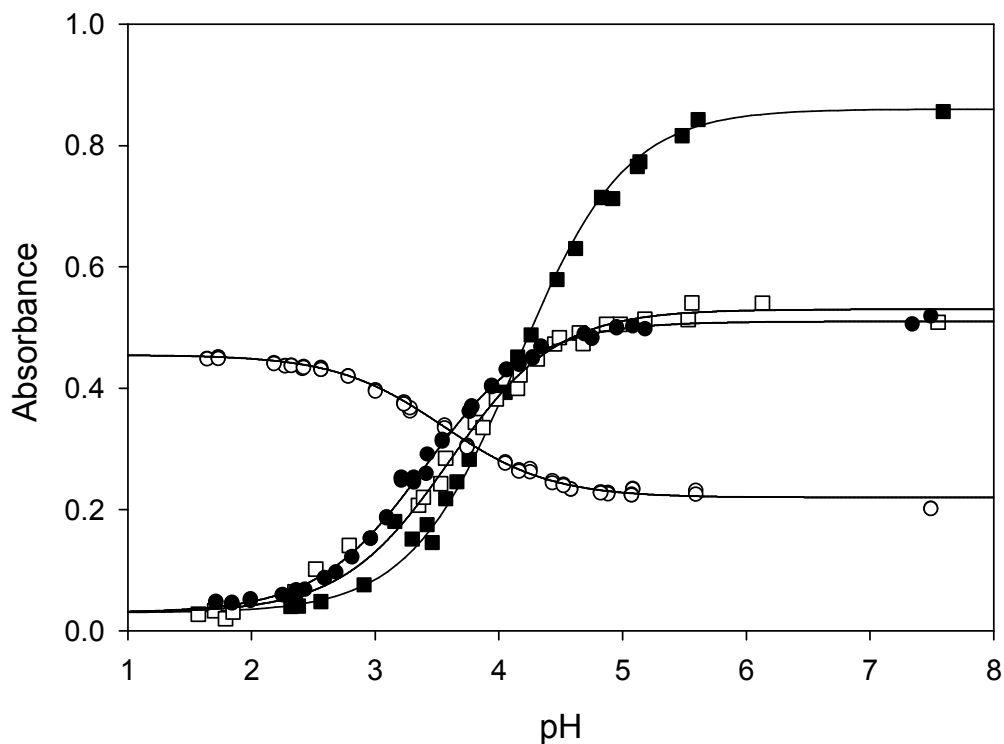


**Figure 4.13** UV pH titrations of the CB[7] host-guest complexes of (□) procaine (at 288 nm), (■) tetracaine (at 312 nm), (○) dibucaine (at 318 nm), and (●) procainamide (at 378 nm) at 25 °C.

## 4.3 Experimental

### 4.3.1 Materials

The CB[7] host was prepared and characterized as described in Chapter 2, using the method of Day and coworkers.<sup>69</sup> Epinephrine bitartrate, and the hydrochloride salts of procaine, tetracaine, procainamide, dibucaine, and prilocaine were purchased from Sigma-Aldrich, and used as received.

### 4.3.2 Methods

The  $^1\text{H}$  NMR spectra were recorded at 25 °C, using Bruker Avance 400 and 500 MHz instruments, in  $\text{D}_2\text{O}$  using the HOD signal as an internal reference. UV-visible spectra were recorded using a Hewlett-Packard 8452A diode array spectrometer, while fluorescence data was recorded on a Photon Technologies International QuantaMaster C-60 spectrometer. The high-resolution mass spectra were collected on a QStar XL MS/MS system with an electrospray ionization source. The host-guest binding constants were determined using competitive binding studies employing diprotonated 1,2-phenylenediamine ( $K_{\text{CB}[7]} = (8.04 \pm 1.28) \times 10^4 \text{ M}^{-1}$ ) and 3-(trimethylsilyl)propionic acid ( $K_{\text{CB}[7]} = (1.82 \pm 0.22) \times 10^7 \text{ M}^{-1}$ ) as the competitors. These competitive binding studies were carried out in  $\text{D}_2\text{O}$  solutions with 0.05 M NaOAc- $d_3$  and 0.025 M DCl (pD = 4.75) and with 0.05M NaCl and 0.10 M DCl (pD = 1). The stability constants and error limits from the competitive binding experiments were calculated using the method developed by Isaacs and coworkers.<sup>50</sup> The binding constants of epinephrine bitartrate and procaine that were obtained by UV-visible and fluorescence spectroscopy, were determined by a least-squares analysis, using equations 2.2, 2.3, and 2.4 from Chapter 2, except that instead of being based on a plot of  $\Delta\delta_{\text{obs}}$  against the concentration of CB[7] (which is specific to an NMR titration), the titrations were based on plots of changes in absorbance against the concentration of CB[7] in the case of the titration of epinephrine bitartrate by UV-visible absorbance spectroscopy. In this UV-visible titration equation 2.4 would be expressed as Equation 3.1:

$$\Delta \text{Absorbance}_{\text{predicted}} = \Delta \text{Absorbance}_{\text{limiting}} \times ([\text{H}\cdot\text{G}]/[\text{G}]_{\text{total}}) \quad (3.1)$$

In a similar manner, for the fluorescence titration of procaine with CB[7], which was plotted as  $F/F_0$  against the concentration of CB[7], equation 2.4 would be expressed as equation 3.2:

$$F/F_{0 \text{ predicted}} = F/F_{0 \text{ limiting}} \times ([H \cdot G]/[G]_{\text{total}}) \quad (3.2)$$

where  $[H \cdot G]$  is the concentration of the host-guest complex, and  $[G]_{\text{total}}$  is the total guest concentration.

The pH titrations were conducted using UV-visible spectroscopy, in which the guest had a three-fold excess of CB[7] present. UV-spectra were then recorded at various pH values, and plots were prepared as Absorbance versus pH. The  $pK_a$  was determined as the inflection points in the sigmoidal curves observed in the plots.

#### 4.4 Conclusions

The local anaesthetics procaine, procainamide, tetracaine, dibucaine, and prilocaine form stable host-guest systems with CB[7], and their stability constants were determined to be between one and three orders of magnitudes greater than the binding constants determined for the complexes formed between the corresponding anaesthetics and  $\beta$ -CD.

The binding position of CB[7] can be altered depending upon the pH, with the CB[7] migrating to the protonated amine in the acidic solutions of most of the anaesthetic guests, particularly those containing a diethylamine at their hydrophilic side. This behaviour is not observed for the host-guest complex with tetracaine, as the CB[7] instead encapsulates the amine with the lower  $pK_a$ , and remains at that same amine in the more acidic solution, although it does migrate from the butyl neighbour of this amine in the neutral solution to the adjacent aromatic ring in the acidic solution. Although the cause of this behaviour with tetracaine is uncertain, possibilities may include the relatively weaker binding of CB[7] to methylammonium guests compared with their ethyl analogues (as observed with tetraalkylammonium salts),<sup>44</sup> so that the



CB[7] may then prefer the more hydrophobic end of the molecule if a higher affinity ethyl-substituted ammonium site is not available. Modest increases of the first  $pK_a$  values of the anaesthetics (for the amine at the hydrophobic end of the guest) are observed upon complexation with CB[7], with tetracaine showing the largest increase within the series. It may also be possible that the complexation-induced  $pK_a$  shift of the tetracaine is partially protonating the hydrophobic amine of tetracaine, and thus making it a more favourable binding site for CB[7]. A third possibility may be that the order of the protonations of the amines are becoming *reversed* by the presence of CB[7], with the hydrophobic butyl amine becoming protonated *before* the tertiary amine. If this is the case, it could explain the migration of the CB[7] from the butyl group adjacent to the hydrophobic amine to the aromatic group adjacent to the same amine once the solution becomes more acidic. If the tertiary amine was becoming protonated *after* the hydrophobic amine, the cationic charge of this new ammonium centre could act to “pull” the CB[7] to the aromatic ring through cation-dipole interactions, where one of its portals could then be closer to this ammonium center, while the other portal would remain close to the more hydrophobic ammonium group. The research involving binding between CB[7] and the local anaesthetics has been published in *Organic and Biomolecular Chemistry*.<sup>43</sup>

## References

1. S.A. Grant, *Best Pract. Res. Clin. Anaesth.*, **2002**, *16*, 1521.
2. C.C. Buckenmaier III, and L.L. Bleckner, *Drugs*, **2005**, *65*, 745.
3. G. Volgyi, R. Ruiz, K. Box, J. Comer, E. Bosch, K. Takacs-Novak, *Anal. Chim. Acta*, **2007**, *583*, 418.
4. K. Box, C. Bevan, J. Comer, A. Hill, R. Allen, and D. Reynolds, *Anal. Chem.*, **2003**, *75*, 883
5. G.J. Grant, Y. Barenholz, E.M. Bolotin, M. Bansinath, H. Turndorf, B. Piskoun, and E.M. Davidson, *Anesthesiology*, **2004**, *101*, 133.
6. G.J. Grant and M. Bansinath, *Reg. Anesth. Pain Med.*, **2001**, *26*, 61.
7. J.J. Mowat, M.J. Mok, B.A. MacLeod, T.D. Madden, *Anesthesiology*, **1996**, *85*, 635.
8. G. Colombo, R. Padera, R. Langer, and D.S. Kohane, *J. Biomed. Mater. Res.*, **2005**, *75A*, 458.
9. A. Shikanov, A.J. Domb, C.F. Weiniger, *J. Controlled Release*, **2007**, *117*, 97.
10. T. Bramer, N. Dew, K. Edsman, *J. Pharm. Sci.*, **2006**, *95*, 769.
11. S.N. Zhumagalieva, B.M. Kudaibergenova, M.K. Beisebekov, and Z.A. Abilov, *J. Appl. Polym. Sci.*, **2007**, *106*, 1601.
12. N. Takisawa, K. Shirahama, and I. Tanaka, *Colloid Polym. Sci.*, **1993**, *271*, 499.
13. S.-M. Shuang, S.-Y. Guo, J.-H. Pan, L. Li, and M.-Y. Cai, *Anal. Lett.*, **1998**, *31*, 879.
14. G. Dollo, P. Le Corre, F. Chevanne, and R. Le Verge, *Int. J. Pharm.*, **1996**, *136*, 165.
15. L. Van Santvliet, K. Caljon, L. Pieters, and A. Ludwig, *Int. J. Pharm.*, **1998**, *171*, 147.
16. C. Merino, E. Junquera, J. Jimenez-Barbero, and E. Aicart, *Langmuir*, **2000**, *16*, 1557.
17. N. Li, J. Duan, H. Chen, and G. Chen, *Talanta*, **2003**, *59*, 493.
18. D.R. de Araujo, L.M.A. Pinto, A.F.A. Braga, E. de Paula, *Rev. Brasil Anest.*, **2003**, *53*, 663.
19. S.A. Fernandes, L.F. Cabeça, A.J. Marsaioli, and E. de Paula, *J. Incl. Phenom. Macrocycl. Chem.*, **2007**, *57*, 395.
20. E. Iglesias, *J. Org. Chem.*, **2006**, *71*, 4383.

21. E. Iglesias-Martinez, I. Brandariz, and F. Penedo, *J. Incl. Phenom. Macrocycl. Chem.*, **2007**, 57, 573.
22. M.A. Deryabina, S.H. Hansen, J. Ostergaard, and H. Jensen, *J. Phys. Chem. B*, **2009**, 113, 7263.
23. I. Brandariz and E. Iglesias-Martinez, *J. Chem. Eng. Data*, **2009**, 54, 2103.
24. R. Wang, L. Yuan, and D.H. Macartney, *Chem. Commun.*, **2005**, 5867.
25. J. Mohanty, A.C. Bhasikuttan, W.M. Nau, and H. Pal, *J. Phys. Chem. B*, **2006**, 110, 5132.
26. R. Wang, L. Yuan, D.H. Macartney, *Chem. Commun.*, **2006**, 2908.
27. M. Shaikh, J. Mohanty, P.K. Singh, W.M. Nau, and H. Pal, *Photochem. Photobiol. Sci.*, **2008**, 7, 408.
28. R. Wang, B.C. MacGillivray, and D.H. Macartney, *Dalton Trans.*, **2009**, 3584.
29. N. Saleh, A.L. Koner, and W.M. Nau, *Angew. Chem., Int. Ed.*, **2008**, 47, 5398.
30. K. Uekama, F. Hirayama, and T. Irie, *Chem. Rev.*, **1998**, 98, 2045.
31. K. Uekama, F. Hirayama, and H. Arima, *Chapter 14: Pharmaceutical Applications of Cyclodextrins and Their Derivatives*, In *Cyclodextrins and Their Complexes*, H. Dodziuk (ed.), Wiley-VCH: Weinheim, 2006; pp. 381-422.
32. N.J. Wheate, A.I. Day, R.J. Blanch, A.P. Arnold, C. Cullinane, and J.G. Collins, *Chem. Commun.*, **2004**, 1424.
33. Y.J. Jeon, S.-Y. Kim, Y.H. Ko, S. Sakamoto, K. Yamaguchi, and K. Kim, *Org. Biomol. Chem.*, **2005**, 3, 2122.
34. M.S. Bali, D.P. Buck, A.J. Coe, A.I. Day, and J.G. Collins, *Dalton Trans.*, **2006**, 5337.
35. S. Kemp, N.J. Wheate, S. Whang, J.G. Collins, S.F. Ralph, A.I. Day, V.J. Higgins, and J.R. Aldrich-Wright, *J. Biol. Inorg. Chem.*, **2007**, 12, 969.
36. N.J. Wheate, *Aust. J. Chem.*, **2006**, 59, 354.
37. Y. Zhao, M.S. Bali, C. Cullinane, A.I. Day, and J.G. Collins, *Dalton Trans.*, **2009**, 5190.

38. Y. Zhao, D.P. Buck, D.L. Morris, M.H. Pourgholami, A.I. Day, and J.G. Collins, *Org. Biomol. Chem.*, **2008**, *6*, 4509.
39. N. Dong, S.-F. Xue, Q.-J. Zhu, Z. Tao, Y. Zhao, and L.-X. Yang, *Supramol. Chem.*, **2008**, *20*, 659.
40. R. Wang and D.H. Macartney, *Org. Biomol. Chem.*, **2008**, *6*, 1955.
41. R.H. de Jong, *Local Anesthetics*, Mosby-Year Book, Inc., St. Louis, 1994, pp. 157 – 161.
42. R.K. Stoelting and R.D. Miller, *Basics of Anesthesia, Fourth Edition*, Churchill Livingstone: New York, 2000; pp. 464 - 465.
43. I.W. Wyman and D.H. Macartney, *Org. Biomol. Chem.*, **2010**, *8*, 247.
44. A.D. St-Jacques, I.W. Wyman, and D.H. Macartney, *Chem. Commun.*, **2008**, 4936.
45. J. Lagona, P. Mukhopadhyay, S. Chakrabarti, and L. Isaacs, *Angew. Chem., Int. Ed.*, **2005**, *44*, 4844.
46. J.W. Lee, S. Samal, N. Selvapalam, H.-J. Kim, and K. Kim, *Acc. Chem. Res.*, **2003**, *36*, 621.
47. W.L. Mock and N.-Y. Shih, *J. Org. Chem.*, **1986**, *51*, 4440.
48. D.S.N. Hettiarachchi and D.H. Macartney, *Can. J. Chem.*, **2006**, *84*, 905.
49. S.R.W. Loro, O.R. Nascimento, and M. Tabak, *Biochim. Biophys. Acta*, **1994**, *1190*, 319.
50. S. Liu, C. Ruspic, P. Mukhopadhyay, S. Chakrabarti, P.Y. Zavalij, and L. Isaacs, *J. Am. Chem. Soc.*, **2005**, *127*, 15959.
51. R. Glassenberg, R. Eckenhoff, and J. Xi, *Abstracts of the Annual Meeting of the American Society of Anaesthesiologists Anesthesiology*, October 19, 2008, Abstract 651  
[www.asaabstracts.com/strands/asaabstracts/abstract.htm?year=2008&index=2&absnum=200](http://www.asaabstracts.com/strands/asaabstracts/abstract.htm?year=2008&index=2&absnum=200)  
(Accessed October 7, 2009).
52. F. Kopecky, M. Vojtekova, P. Kaclik, M. Demko, and Z. Bielikova, *J. Pharm. Pharmacol.*, **2004**, *56*, 581.
53. M.A. Rankin and B.D. Wagner, *Supramol. Chem.*, **2004**, *16*, 513.

54. A.L. Koner and W.M. Nau, *Supramol. Chem.*, **2007**, *19*, 55.
55. J. Mohanty and W.M. Nau, *Angew. Chem., Int. Ed.*, **2005**, *44*, 3750.
56. W.M. Nau and J. Mohanty, *Int. J. Photoenergy*, **2005**, *7*, 133.
57. R. Wang, L. Yuan, H. Ihmels, and D.H. Macartney, *Chem. Eur. J.*, **2007**, *13*, 6468.
58. H.-J. Buschmann, E. Cleve, and E. Schollmeyer, *Inorg. Chim. Acta*, **1992**, *193*, 93.
59. H.-J. Buschmann, E. Cleve, K. Jansen, A. Wego, and E. Schollmeyer, *J. Incl. Phenom. Macrocycl. Chem.*, **2001**, *40*, 117.
60. H.-J. Buschman, K. Jansen, C. Meschke, and E. Schollmeyer, *J. Solution Chem.*, **1998**, *27*, 135.
61. C. Marquez, R.R. Hudgins, and W.M. Nau, *J. Am. Chem. Soc.*, **2004**, *126*, 5806.
62. Y.-M. Jeon, J. Kim, D. Whang, and K. Kim, *J. Am. Chem. Soc.*, **1996**, *118*, 9790.
63. D. Whang, J. Heo, J.H. Park, and K. Kim, *Angew. Chem., Int. Ed.*, **1998**, *37*, 78.
64. W. Ong and A.E. Kaifer, *J. Org. Chem.*, **2004**, *69*, 1383.
65. E. Mezzina, F. Cruciani, G.F. Pedulli, and M. Lucarini, *Chem. Eur. J.*, **2007**, *13*, 7223.
66. I.W. Wyman and D.H. Macartney, *Org. Biomol. Chem.*, **2008**, *6*, 1796.
67. J. Garcia-Soto and M.S. Fernandez, *Biochim. Biophys. Acta*, **1983**, *731*, 275.
68. J. Zhang, T. Hadlock, A. Gent, and G.R. Strichartz, *Biophys. J.*, **2007**, *92*, 3988.
69. A. Day, A.P. Arnold, R.J. Blanch, and B. Snushall, *J. Org. Chem.*, **2001**, *66*, 8094.

## Chapter 5

# Cucurbit[7]uril Host-Guest Complexes of Cholines and Phosponium Cholines in Aqueous Solution

### 5.1 Introduction

The choline family ( $((\text{CH}_3)_3\text{NCH}_2\text{CH}_2\text{OR}^+)$ ) of biologically relevant compounds have in common the trimethylammonium head group, which in the case of acetylcholine (with  $\text{R} = \text{COCH}_3$ ), allows it to bind as a substrate to the acetylcholinesterase enzyme.<sup>1</sup> This binding site is composed of aromatic amino acid residues such as tryptophan and tyrosine, which interact with the acetylcholine through cation- $\pi$  interactions.<sup>2,3,4</sup> A variety of synthetic hosts have been used to bind to choline guests, and many (although not all) of these hosts have contained aromatic units within their walls and also have had anionic charge, so that they could utilize both cation- $\pi$  and electrostatic interactions to assist their binding.<sup>5-54</sup> These hosts have included acyclic receptors,<sup>5,6</sup> cryptands,<sup>7-11</sup> cyclophanes,<sup>12-15</sup> molecular clefts,<sup>16</sup> *p-tert*-butylcalix[*n*]arene dianions (with  $n = 4$  and 6),<sup>17</sup> *p*-sulfonated calix[*n*]arenes,<sup>18-28</sup> as well as other calixarenes.<sup>29-32</sup> In addition, tetracyanoresorcin[4]arene,<sup>33,34</sup> along with other resorcin[*n*]arenes,<sup>35-41</sup> pyrogallol[4]arenes,<sup>42</sup> cyclodextrins,<sup>43,44</sup> and other macrocycles<sup>45-46</sup> have been used to bind to cholines, or their relatives containing quaternary ammonium-bearing guests. Kim *et al.*<sup>47</sup> have reported complexation between acetylcholine and a water-soluble CB[6] derivative, hexa(cyclohexyl)cucurbit[6]uril, with a binding affinity of  $1.3 \times 10^3 \text{ M}^{-1}$ . In this system, the trimethylammonium group is positioned outside of the cavity, while the remainder of the acetylcholine is encapsulated by the

cavity, according to their  $^1\text{H}$  NMR complexation-induced upfield shifts.<sup>47</sup> While this host formed a complex with acetylcholine, it did not, in contrast, readily bind with choline.

Resorcarene-based deep cavitands have been employed by Rebek and coworkers for binding with choline cations,<sup>48-51</sup> and they have carried out catalytic formations of acetylcholine from choline and acetic anhydride with the use of a deep cavitand as a template.<sup>52</sup> In the presence of their cavitand, the rate of the acylation of choline to give acetylcholine was up to 1900 times faster than in the absence of catalyst.<sup>52</sup> Meanwhile, this catalysis was approximately six times slower when a similar reaction was carried out with the triethylammonium analogue of choline, suggesting that the cavitand was selective for the smaller trimethylammonium-containing guests. Rebek's group have also used cavitands to carry out the aminolysis of the acetylcholine analogue *p*-nitrophenyl choline carbonate (PNPCC).<sup>53,54</sup>

Prior to this work by Rebek with cavitands, Cuevas and coworkers<sup>55</sup> had prepared an artificial acetylcholinesterase mimic based on a ditopic calix[6]arene host that was connected to a bicyclic guanidinium moiety, which could catalyze the methanolysis of PNPCC. While the trimethylammonium group of the guest bound to the calixarene moiety through cation- $\pi$  binding, the guanidinium unit was believed to stabilize the anionic intermediate through electrostatic interactions and hydrogen bonding.<sup>55</sup>

The phosphonium analogues of choline, acetylcholine, choline phosphate, and related compounds have been studied for some time, and the presence of the phosphorus centre has been utilized as a probe for  $^{31}\text{P}$  NMR spectroscopy.<sup>56-59</sup> These compounds have also been explored in efforts to compare their activities to those of the trimethylammonium analogues.

Although cations, such as alkali and transition metal ions, as well as organic cations (such as primary ammoniums, for example) normally bind to cucurbiturils outside of the cavity, near the electron rich portals,<sup>60,61</sup> we have recently observed that more charge diffuse hydrophobic cations such as  $\text{NR}_4^+$ ,  $\text{PR}_4^+$ , and  $\text{SR}_3^+$  (with R = methyl and ethyl), are readily encapsulated in the

cavity of CB[7] (binding constants and  $\Delta\delta_{\text{lim}}$  values shown in Table 5.1).<sup>62</sup> Within the tetraalkylammonium series ( $\text{NR}_4^+$ ), when the larger *n*-propyl and *n*-butyl substituents are attached, complexation-induced shifts from  $^1\text{H}$  NMR experiments and energy-minimized calculations suggested that at least one alkyl “arm” is left outside of the CB[7] cavity, while the remaining “arms” are encapsulated inside the cavity.

**Table 5.1** Limiting complexation-induced chemical shift changes ( $\Delta\delta_{\text{lim}}$ ) and association constants for host-guest complexes between CB[7] and peralkylated onium guests measured at 25 °C in  $\text{D}_2\text{O}$ .<sup>62</sup>

Guest	$\Delta\delta_{\text{lim}}$ (ppm)	$K_{\text{CB[7]}}$ ( $\text{M}^{-1}$ )
$\text{N}(\text{CH}_3)_4^{+b}$	-0.72	$(1.2 \pm 0.4) \times 10^5{}^c$
$\text{N}(\text{CH}_2\text{CH}_3)_4^{+b}$	-0.87, -0.44	$(1.0 \pm 0.2) \times 10^6{}^d$
$\text{N}(\text{CH}_2\text{CH}_2\text{CH}_3)_4^{+e}$	-0.70, -0.40, -0.22	$(9.0 \pm 2.4) \times 10^3{}^c$
$\text{N}(\text{CH}_2\text{CH}_2\text{CH}_2\text{CH}_3)_4^{+f}$	-0.28, -0.4, -0.2, -0.2	$(2.8 \pm 0.7) \times 10^3{}^g$
$\text{N}(\text{CH}_3)_3(\text{CH}_2\text{Ph})^{+b}$	-0.25 (CH <sub>3</sub> ), 0.70 (CH <sub>2</sub> ), Ph: -1.07 ( <i>o</i> ), -0.78 ( <i>m</i> ), -0.47 ( <i>p</i> )	$(2.5 \pm 0.6) \times 10^8{}^{d,h}$
$\text{P}(\text{CH}_3)_4^{+b}$	-0.78, -0.38 <sup>i</sup>	$(2.2 \pm 0.4) \times 10^6{}^d$
$\text{P}(\text{CH}_2\text{CH}_3)_4^{+e}$	-0.72, -0.31, -5.77 <sup>i</sup>	$(1.3 \pm 0.3) \times 10^5{}^d$
$\text{S}(\text{CH}_3)_3^{+f}$	-0.66	$(3.4 \pm 0.6) \times 10^4{}^c$
$\text{S}(\text{CH}_2\text{CH}_3)_3^{+f}$	-0.74, -0.47	$(5.2 \pm 0.9) \times 10^6{}^d$
$\text{Si}(\text{CH}_3)_3\text{CH}_2\text{NH}_3^{+j}$	-0.72 (CH <sub>3</sub> )	$(8.88 \pm 1.41) \times 10^8{}^j$

<sup>a</sup>Protons listed in order from central onium atom outwards. <sup>b</sup>Bromide salt. <sup>c</sup>From a competitive binding experiment with 1,2-phenylenediamine as the competitor.<sup>63</sup> <sup>d</sup>From a competitive binding experiment with 1,4-phenylenediamine as the competitor.<sup>63</sup> <sup>e</sup>Chloride salt. <sup>f</sup>Iodide salt. <sup>g</sup>From a  $^1\text{H}$  NMR chemical shift titration and least-squares fit. <sup>h</sup>From a competitive binding experiment using 3-(trimethylsilyl)propionic acid as the competitor.<sup>63</sup> <sup>i</sup>Central P atom. <sup>j</sup>Ref. 63.

As can be seen in Table 5.1, the limiting upfield shifts are larger for the protons that are closer to the centre of the molecule, consistent with the cation being encapsulated inside the cavity. The upfield shifts subsequently become smaller for the outer protons of the guests with longer alkyl arms as the outer portions of the arms are positioned closer to the portals. The tetra(*n*-butyl)ammonium cations show relatively small upfield shifts compared to the other guests.



These smaller shifts, as well as the broadness of the  $^1\text{H}$  NMR resonances at higher concentrations of CB[7], suggest that at least one arm is positioned outside of the CB[7] cavity. In agreement with this, energy-minimized calculations predicted that the tetra(*n*-propyl)ammonium and tetra(*n*-butyl)ammonium cations would have two of their alkane “arms” outside of the cavity upon complexation with CB[7].<sup>63</sup>

The values of the association constants between CB[7] and the onium cations vary according to the nature of the central onium atom, as well as the length and nature of the alkyl (or in one case aryl) substituents present. In the case of the ammonium (Figure 5.1) and sulfonium guests, the binding constant is higher when the alkyl chains were ethyl groups. In contrast, the phosphonium cations show stronger binding to CB[7] when methyl substituents are present rather than ethyl substituents. Within the alkyl-substituted onium guest series with equal alkyl arm lengths, the order of the binding affinities for the methyl-substituted guests is  $\text{P}(\text{CH}_3)_4^+ > \text{N}(\text{CH}_3)_4^+ > \text{S}(\text{CH}_3)_3^+$ , while the order for the ethyl-substituted cations is  $\text{S}(\text{CH}_2\text{CH}_3)_3^+ > \text{N}(\text{CH}_2\text{CH}_3)_4^+ > \text{P}(\text{CH}_2\text{CH}_3)_4^+$ . These trends, in addition to the wide range of binding constants observed within this series, demonstrate the tendency of CB[7] to have good size selectivity for a given set of guests (Figure 5.2).

In a related study (discussed in Chapter 6) it has been observed that the dicationic depolarizing muscle relaxants succinylcholine and 1,10-bis(trimethylammonium)decane (and its phosphonium analogues) bind with CB[7] to form a [2]pseudorotaxane when the concentration of CB[7] is less than or equal to that of the guest. Once the concentration of CB[7] exceeds that of the guest, the CB[7] migrates to the end of the end of the molecule, encapsulating the quaternary ammonium or phosphonium head group, with a second CB[7] encapsulating the head group at the other end of the molecule to form a 2:1 (host-guest) system.<sup>71</sup>

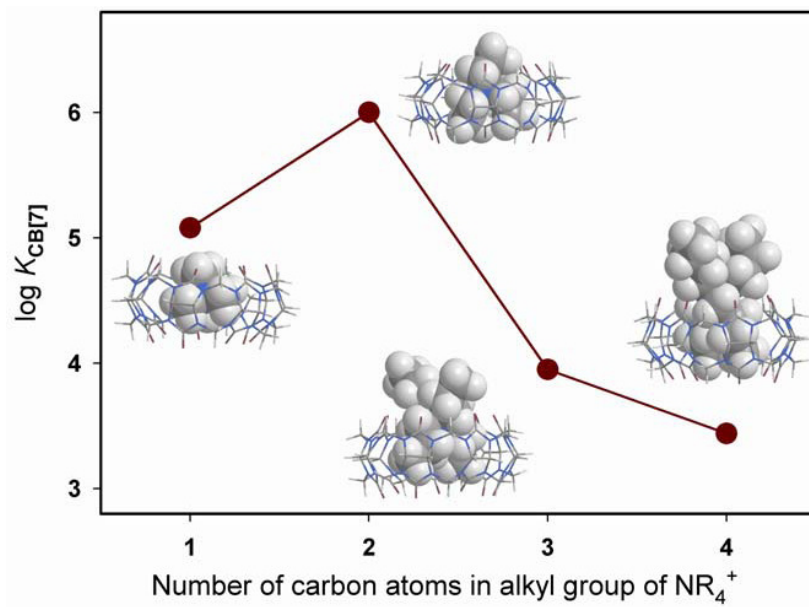


**Figure 5.1**  $\log K_{\text{CB}[7]}$  vs. number of carbon atoms in R groups of  $\text{NR}_4^+$ , superimposed with Chem3D models of the corresponding  $\{\text{CB}[7] \cdot \text{NR}_4\}^+$  complexes.<sup>62</sup> When R = ethyl, the guest fills the cavity and has the strongest binding, whereas for larger alkyl groups the arms begin to protrude from the cavity.

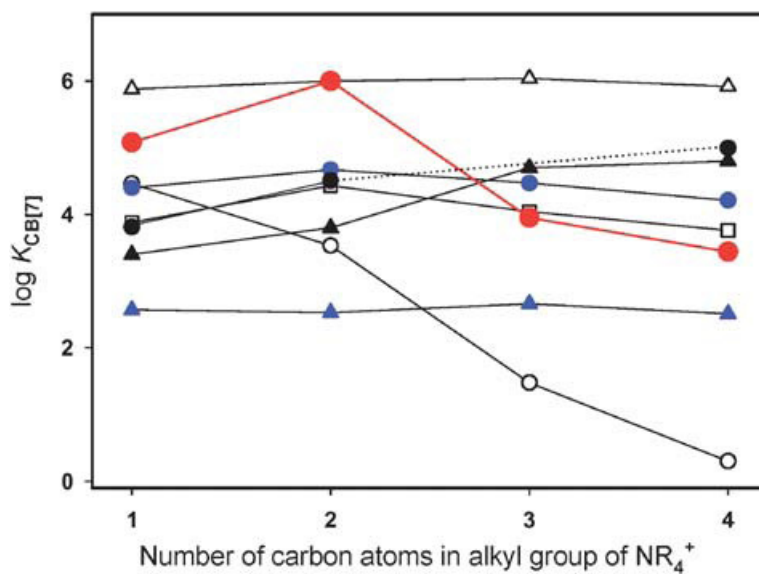


**Figure 5.2** Plots of  $\log K_{\text{CB}[7]}$  versus the number of carbon atoms in the alkyl group of the  $\text{NR}_4^+$  guests for  $\text{CB}[7]$ <sup>62</sup> (●), *p*-sulfonated-calix[4]arene (*p*- $\text{SO}_3\text{CA}[4]$ ) (●, pH 2),<sup>64</sup> *p*-sulfonated-calix[6]arene (*p*- $\text{SO}_3\text{CA}[6]$ ) (▲, pH 2),<sup>64</sup> resorcin[4]arene (RA[4]) (○, 0.5 M NaOD),<sup>65</sup> tetracyano-resorcin[4]arene (CNRA[4]) (Δ),<sup>66</sup> sulfonated cyclotetrachromotroprylene (□),<sup>67</sup> Otto's disulfide-linked pentacarboxylated cyclophane (●),<sup>68</sup> and Lehn's macrotricyclic hexacarboxylated cyclophane (▲).<sup>69</sup>

In this study, the focus was on a series of cholines, acetylcholines, and related compounds, as well as their phosphonium analogues (Figures 5.3-5.5), which contained quaternary ammonium or phosphonium head groups. Analogues of acetylcholine containing a pentyl arm, which had a similar length to that of the ester-bearing arm of acetylcholine, were also studied. While most guests within this series were monocationic, zwitterionic guests such as ( $\pm$ )-carnitine and choline phosphate (phosphocholine) were also explored, in addition to the dicationic 1,4-dimethyl-1,4-diazoniabicyclo[2.2.2]octane diiodide (DimethylDABCO) guest. These systems were investigated by  $^1\text{H}$  and  $^{31}\text{P}$  NMR spectroscopy in order to determine the nature of the binding (such as the positioning of the CB[7] relative to the guest) as well as their host-guest binding constants (Table 5.2), which were determined primarily by  $^1\text{H}$  NMR competition experiments. The work described in this chapter has been published.<sup>72</sup>

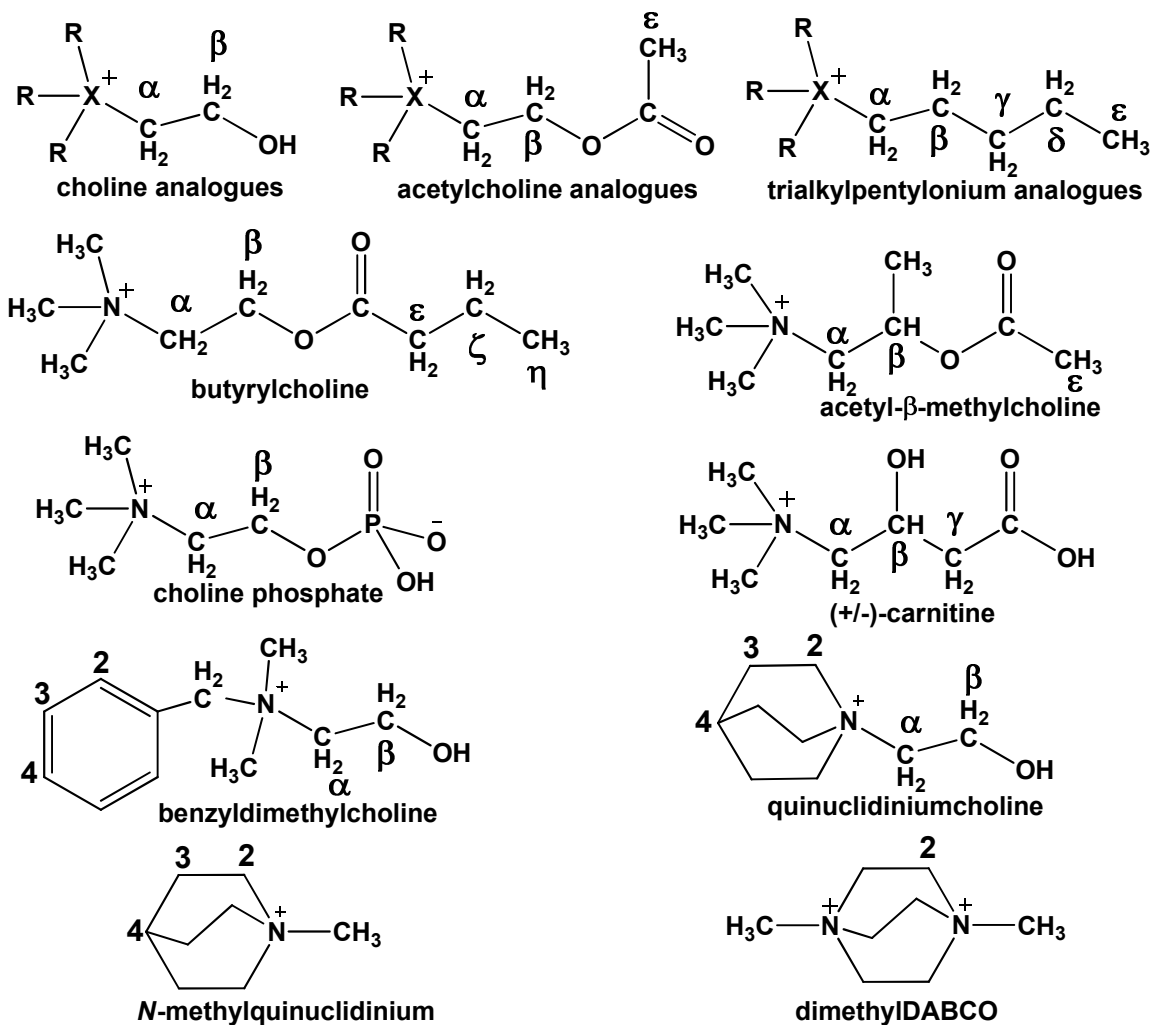


**Figure 5.3** General structures of the guests studied in this chapter, where X = N or P, and R = methyl or ethyl.

## 5.2 Results and Discussion

### 5.2.1 Binding Trends Between CB[7] and Trialkylonium-Bearing Guests

The formation of host-guest complexes between cucurbit[7]uril and the choline guests and their phosphonium analogues have been determined by  $^1\text{H}$  and  $^{31}\text{P}$  NMR spectroscopy (Figures 5.4-5.17), as well as ESI mass spectrometry (Table 5.3). During  $^1\text{H}$  NMR titrations of the choline guests with varying amounts of CB[7], the guest protons were observed to shift, with

the alkyl protons of the quaternary ammonium or phosphonium head groups normally displaying upfield shifts. Most of the guests in this series displayed fast exchange behaviour with respect to the NMR timescale, with the  $^1\text{H}$  NMR signals of the guest representing the weighted average between the free and bound resonances. In some cases, such as that of the trimethylphosphonium analogue of choline (Figure 5.7), slow exchange behaviour was observed, with both the free and bound resonances being visible.

Because guest protons that are encapsulated within the cucurbituril cavity tend to display upfield shifts (with negative  $\Delta\delta_{\text{lim}}$  values), while those near the portals undergo downfield shifts (with positive  $\Delta\delta_{\text{lim}}$  values), the complexation-induced shifts from  $^1\text{H}$  NMR titrations can be useful for determining the positioning of the CB[7] cavity relative to the guest. With all of the analogues of choline (containing the different peralkylonium head groups), upfield shifts were observed for all of the protons of the guest molecule upon binding with CB[7], indicating that the entire molecule was encapsulated within the CB[7] cavity (Figures 5.4 and 5.5). In the case of acetylcholine, which also displays upfield shifts throughout the molecule (Figure 5.8), the binding position changes for its phosphonium analogues, which display a more pronounced upfield shift of the protons near the phosphonium centre (Figure 5.9). The phosphonium methyl protons of the trimethylphosphonium analogue of acetylcholine have a  $\Delta\delta_{\text{lim}}$  value of -0.67 ppm, while the trimethylammonium protons of acetylcholine display a more modest upfield shift, with a  $\Delta\delta_{\text{lim}}$  of -0.28 ppm. Meanwhile, the acetyl methyl protons of both of the phosphonium analogues of acetylcholine show a negligible shift, in contrast to the considerable upfield shift of the acetyl methyl group of acetylcholine ( $\Delta\delta = -0.68$  ppm). These trends in the shifts suggest that while all protons of acetylcholine spend time within the CB[7] cavity, in the case of its phosphonium analogues, the cavity becomes more localized over the more charge-diffuse phosphonium head group, without encapsulating the acetyl methyl group at the other end of the guest.

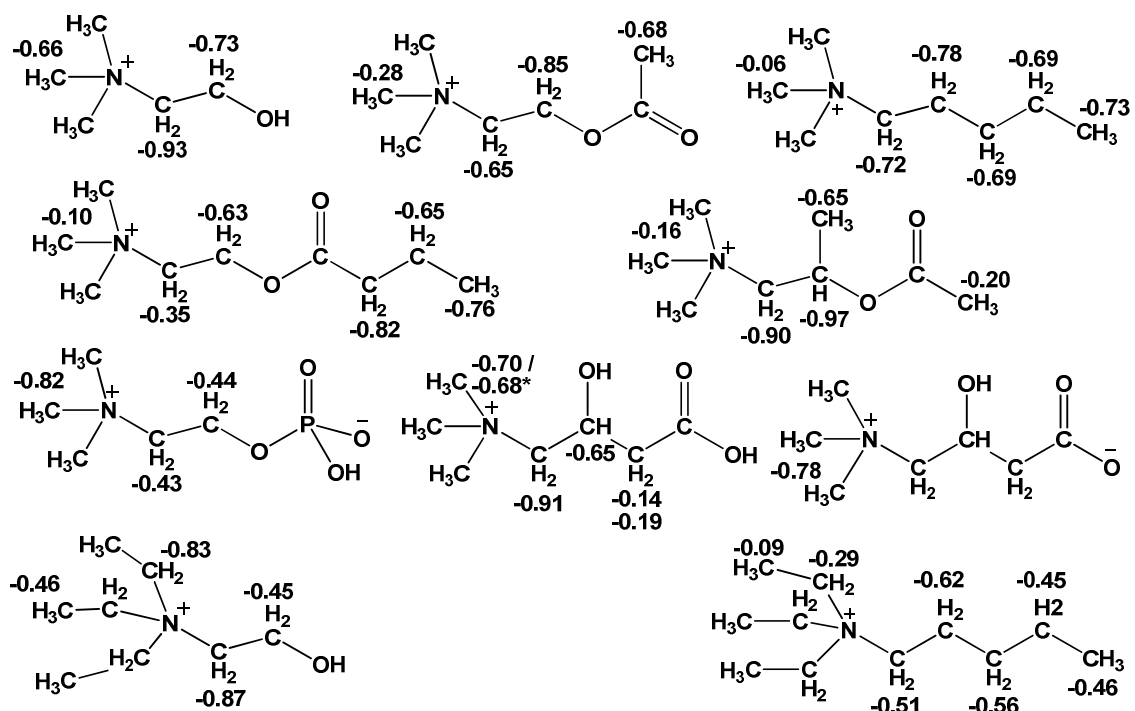


**Figure 5.4** Structures and  $\Delta\delta_{\text{lim}}$  values for the series of trimethylammonium and triethylammonium-bearing choline and acetylcholine derivatives from  $^1\text{H}$  titrations. Negative values represent upfield limiting shifts, while positive values represent downfield shifts. \* $\Delta\delta_{\text{lim}}$  values for  $\text{N}(\text{CH}_3)_3$  of ( $\pm$ )-carnitine: -0.70 ppm in  $\text{D}_2\text{O}$ , -0.68 ppm in 0.01 M DCl.

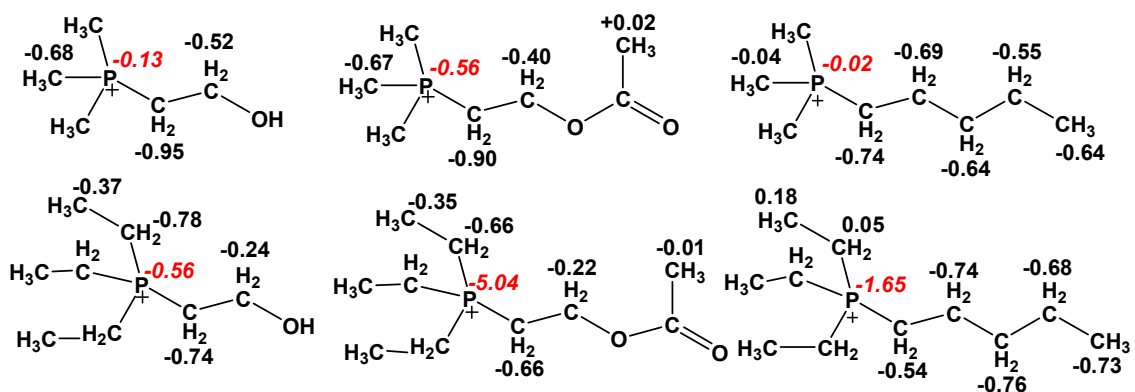


**Figure 5.5** Structures and  $\Delta\delta_{\text{lim}}$  values for the series of trimethylphosphonium and triethylphosphonium-bearing choline and acetylcholine derivatives, from  $^1\text{H}$  NMR titrations. Negative values represent upfield limiting shifts, while positive values represent downfield shifts. Values in *red italics* represent  $\Delta\delta_{\text{lim}}$  values determined from  $^{31}\text{P}$  NMR.

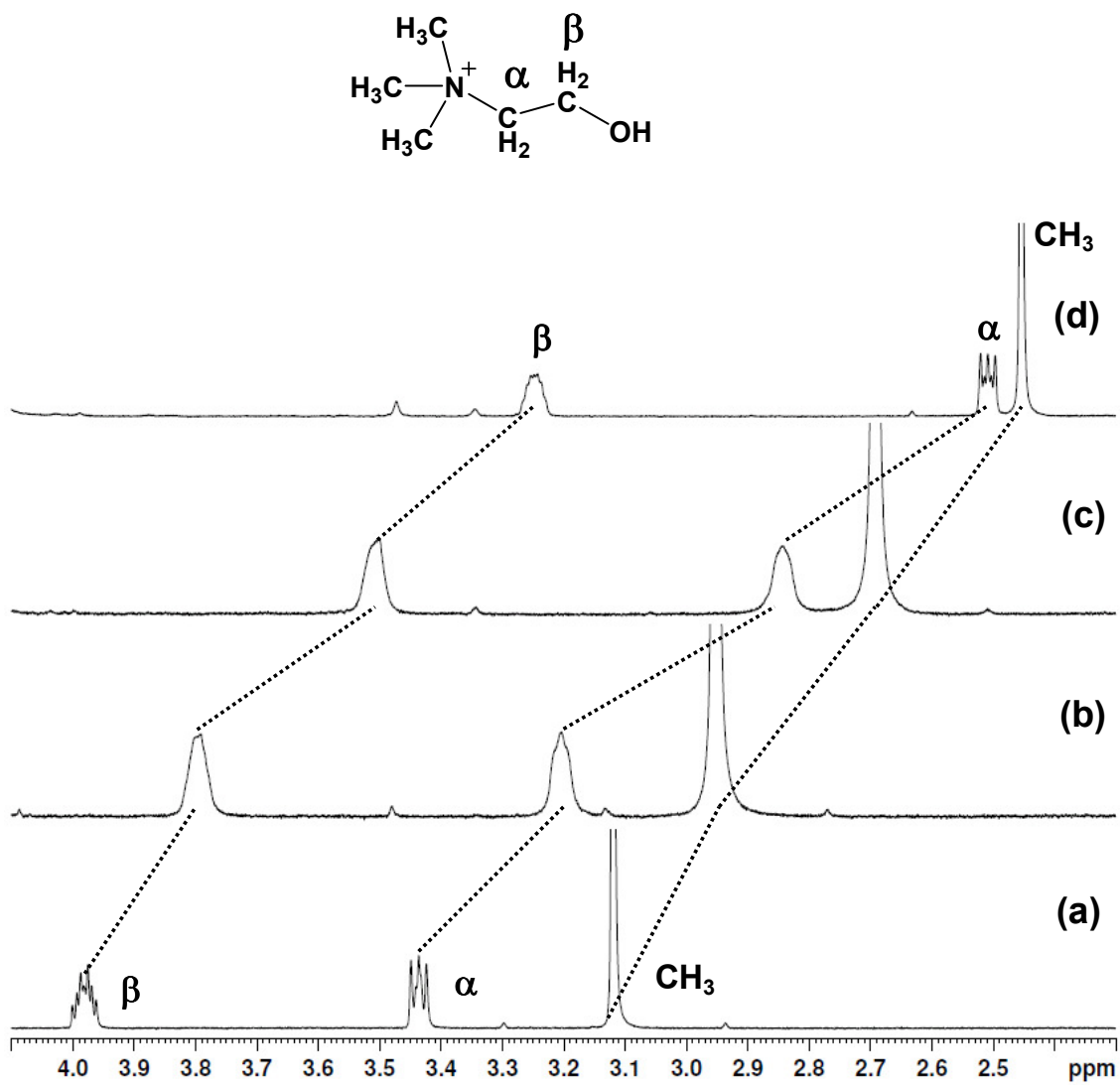


**Figure 5.6** Selected spectra from the <sup>1</sup>H NMR titration of choline chloride (1.44 mM) in the presence of (a) 0.00, (b) 0.25, (c) 0.65, and (d) 1.41 equiv. of CB[7].

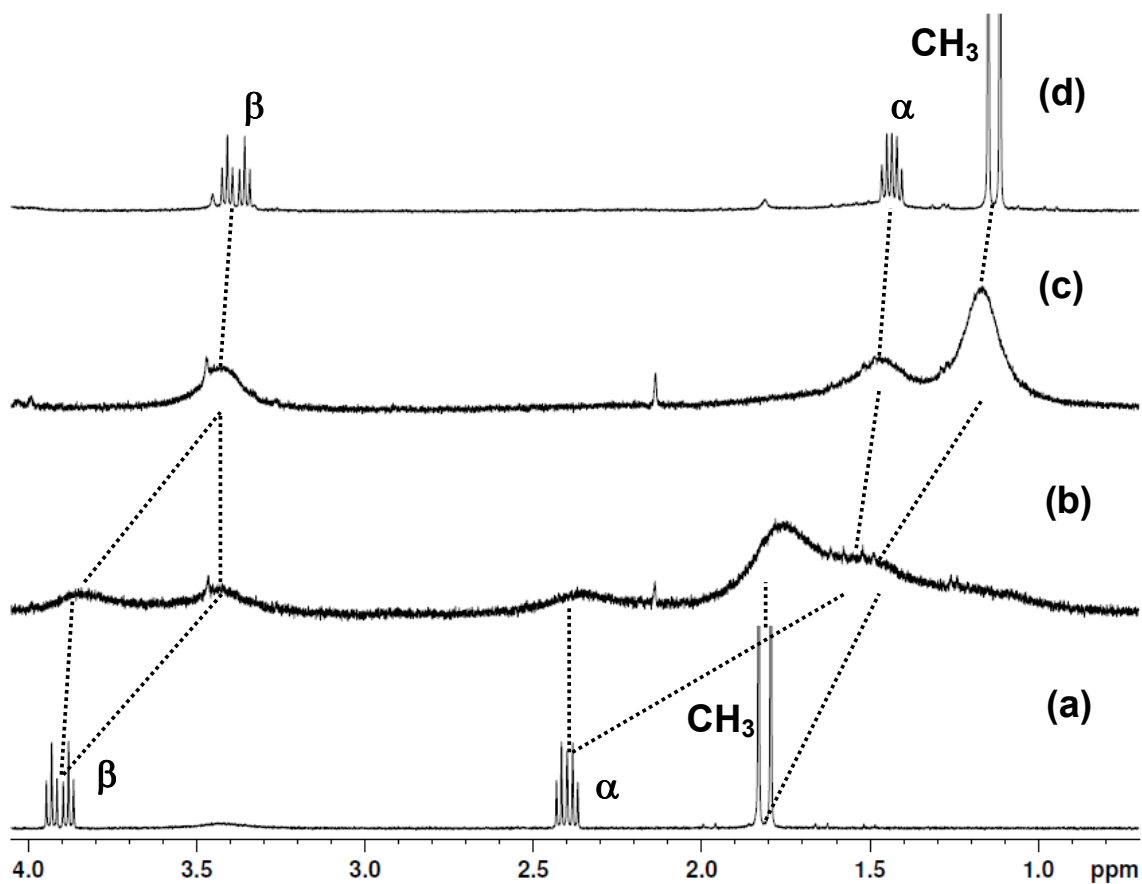
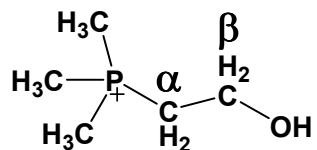


**Figure 5.7** Selected spectra from the  $^1\text{H}$  NMR titration (2-hydroxyethyl)trimethylphosphonium bromide (1.50 mM in  $\text{D}_2\text{O}$ ) in the presence of (a) 0.00, (b) 0.29, (c) 0.74, and (d) 1.30 equiv. of CB[7].



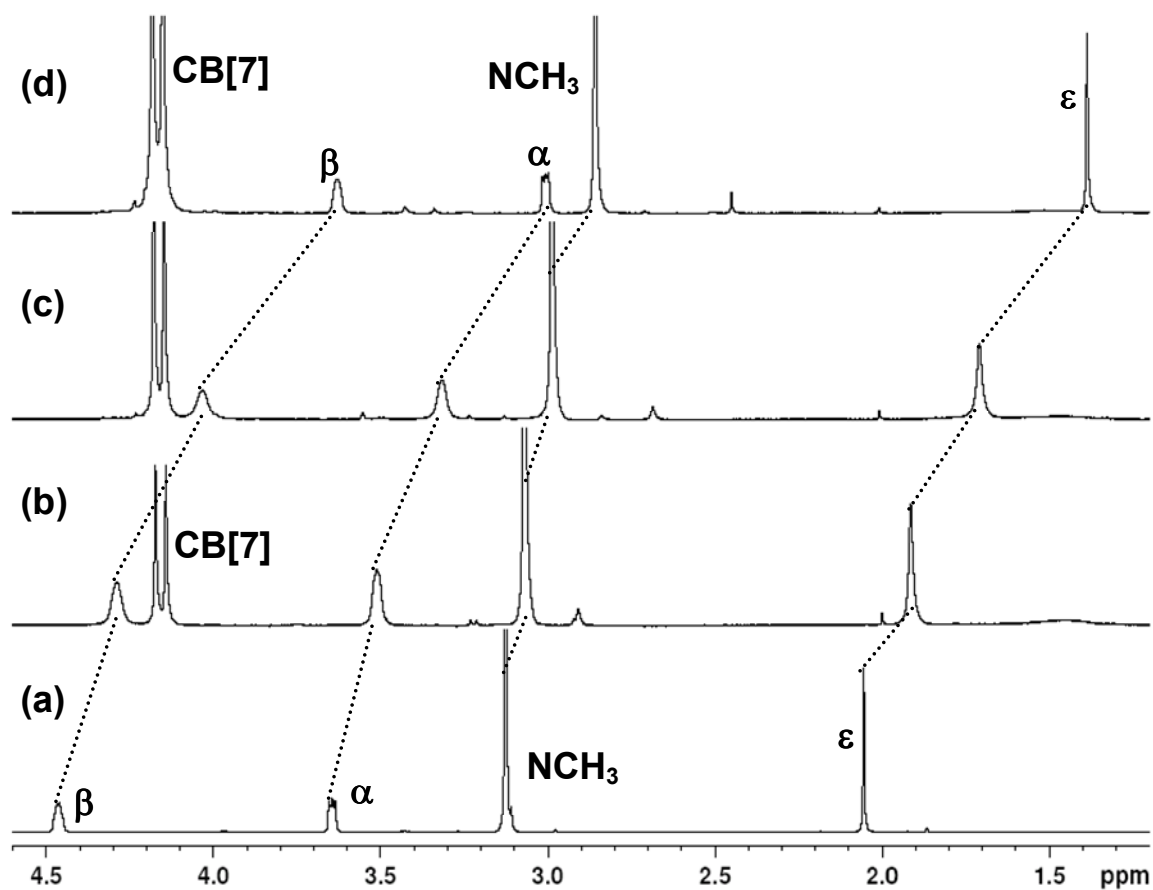
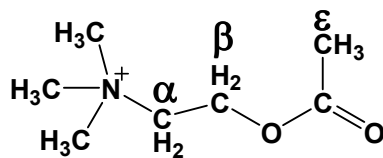


**Figure 5.8** Selected spectra from the  $^1\text{H}$  NMR titration of acetylcholine chloride (2.46 mM in  $\text{D}_2\text{O}$ ) in the presence of (a) 0.00, (b) 0.23, (c) 0.56, and (d) 1.43 equiv. of CB[7].

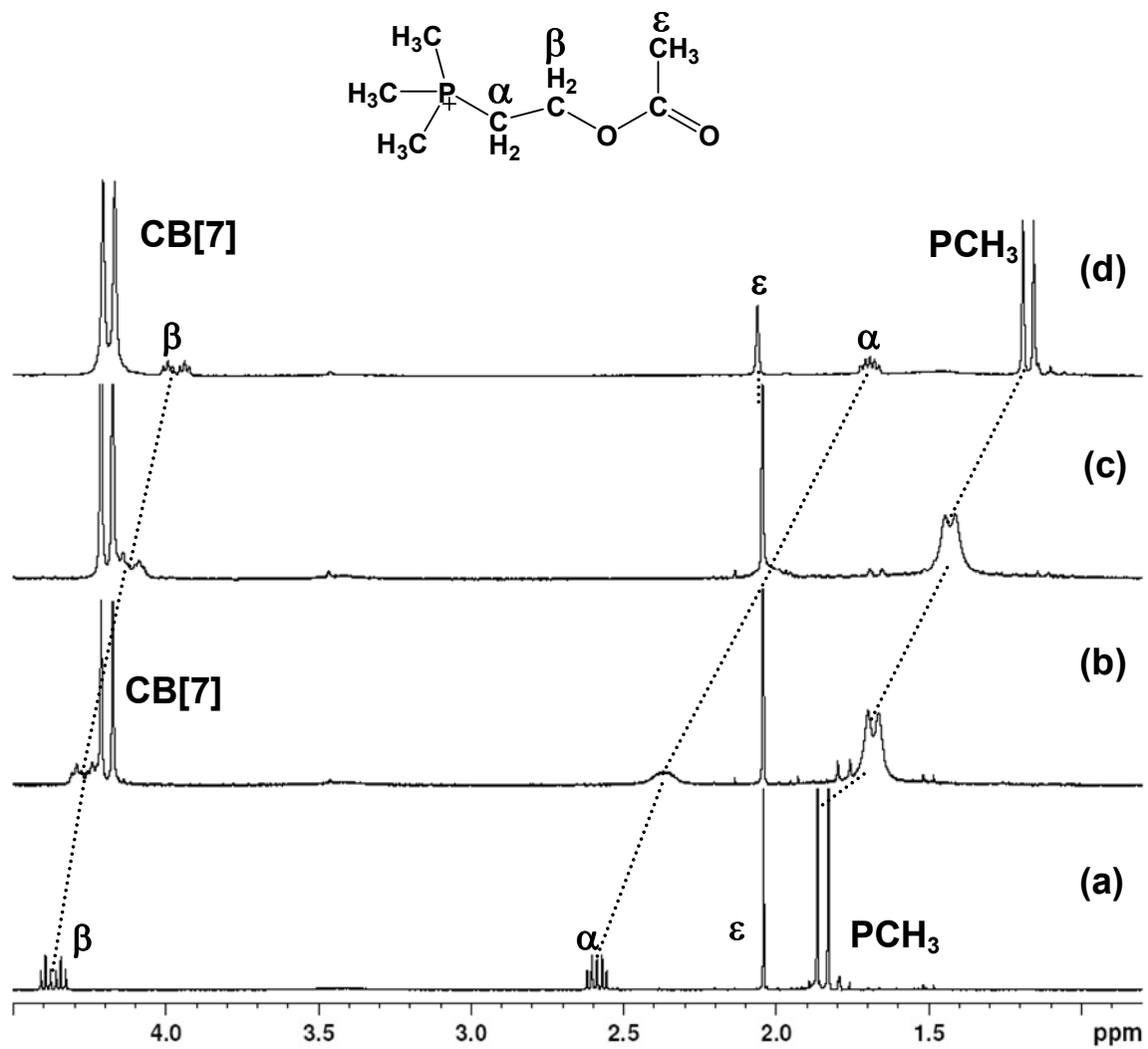


**Figure 5.9** Selected spectra from the <sup>1</sup>H NMR titration of (2-acetoxyethyl)trimethylphosphonium bromide (1.52 mM in D<sub>2</sub>O) in the presence of (a) 0.00, (b) 0.41, (c) 0.80, and (d) 1.74 equiv. of CB[7].

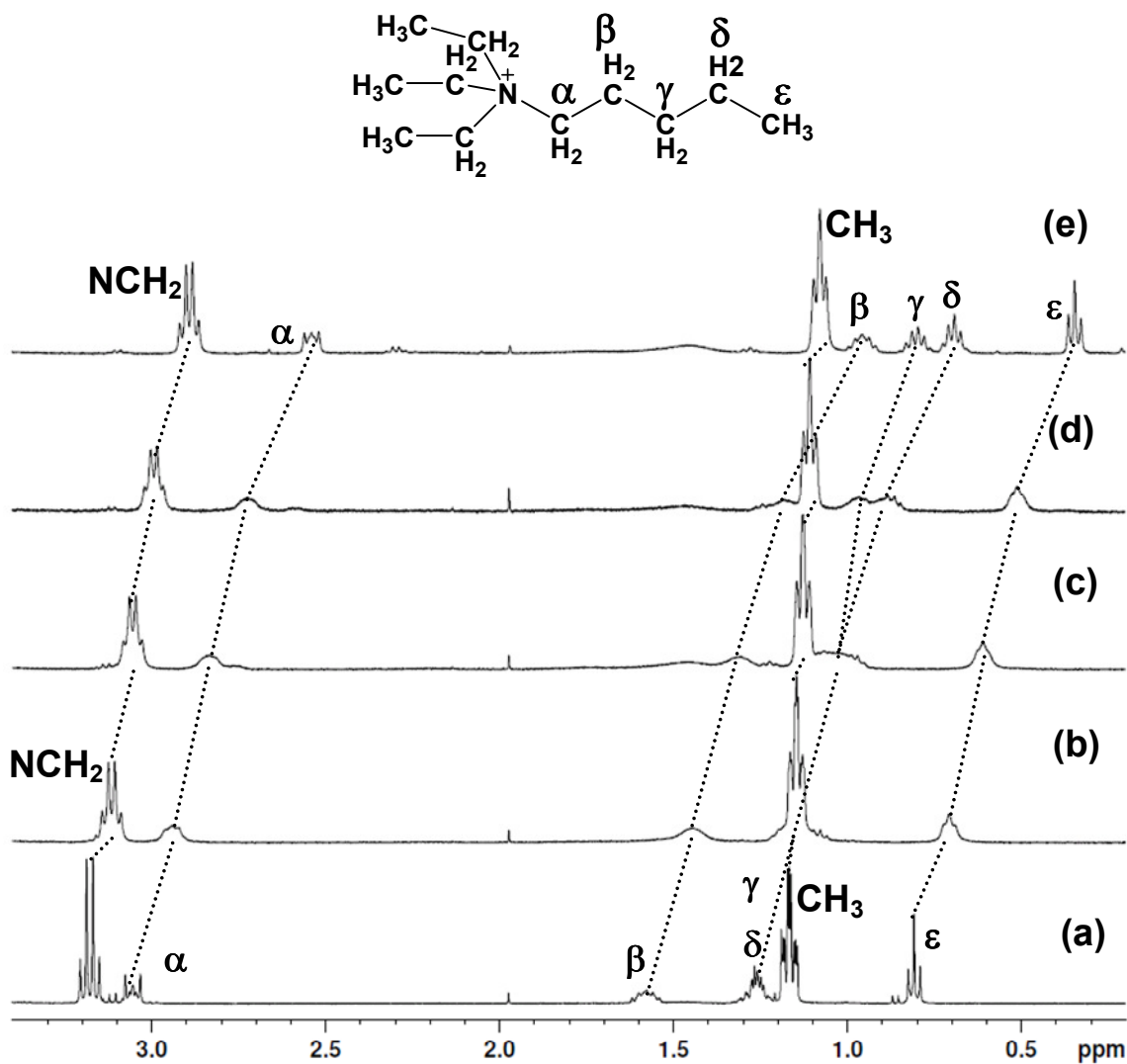


**Figure 5.10** Selected spectra from the  $^1\text{H}$  NMR titration of triethylpentylammonium bromide (1.90 mM in  $\text{D}_2\text{O}$ ) in the presence of (a) 0.00, (b) 0.26, (c) 0.52, (d) 0.76, and (e) 1.44 equiv. of CB[7].

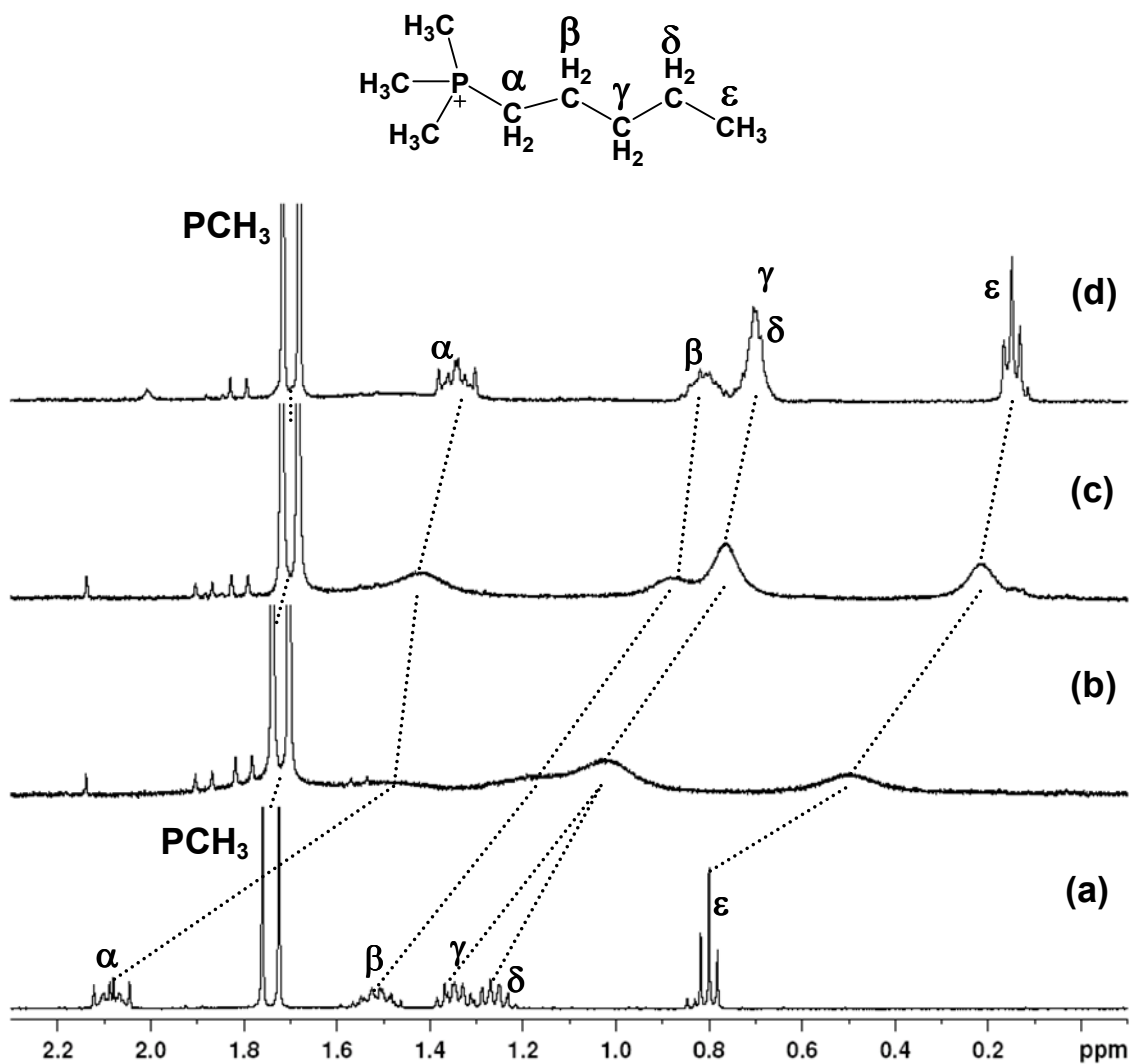


**Figure 5.11** Selected spectra from the  $^1\text{H}$  NMR titration of trimethylpentylphosphonium bromide (1.52 mM in  $\text{D}_2\text{O}$ ) in the presence of (a) 0.00, (b) 0.54, (c) 0.99, and (d) 1.37 equiv. of CB[7].

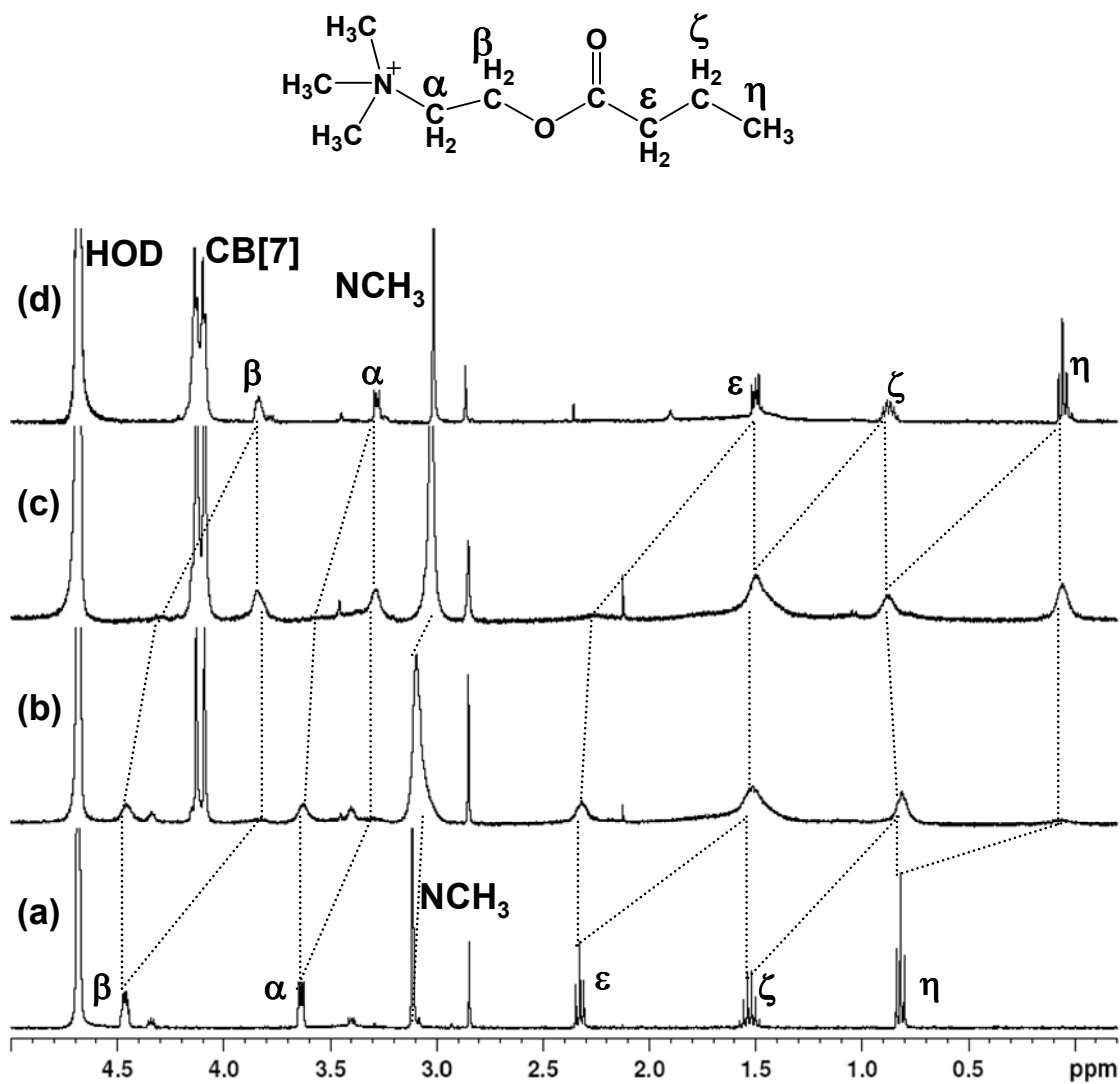


**Figure 5.12** Selected spectra from the <sup>1</sup>H NMR titration of butyrylcholine chloride (1.51 mM in D<sub>2</sub>O) in the presence of (a) 0.00, (b) 0.32, (c) 0.91, and (d) 1.68 equiv. of CB[7].

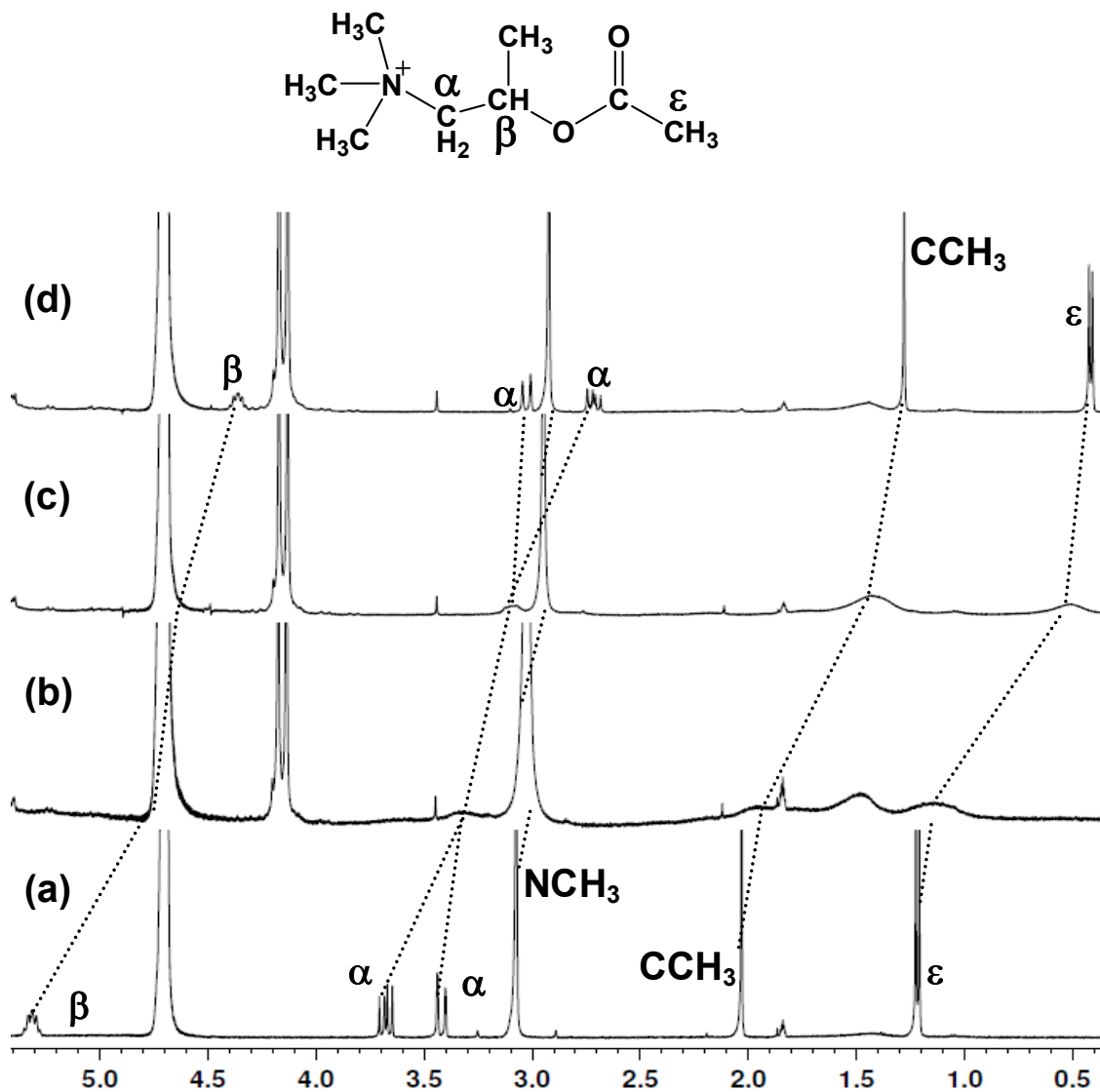


**Figure 5.13** Selected spectra from the <sup>1</sup>H NMR titration of acetyl-β-methylcholine chloride (2.06 mM in D<sub>2</sub>O) in the presence of (a) 0.00, (b) 0.40, (c) 0.95, and (d) 1.30 equiv. of CB[7].

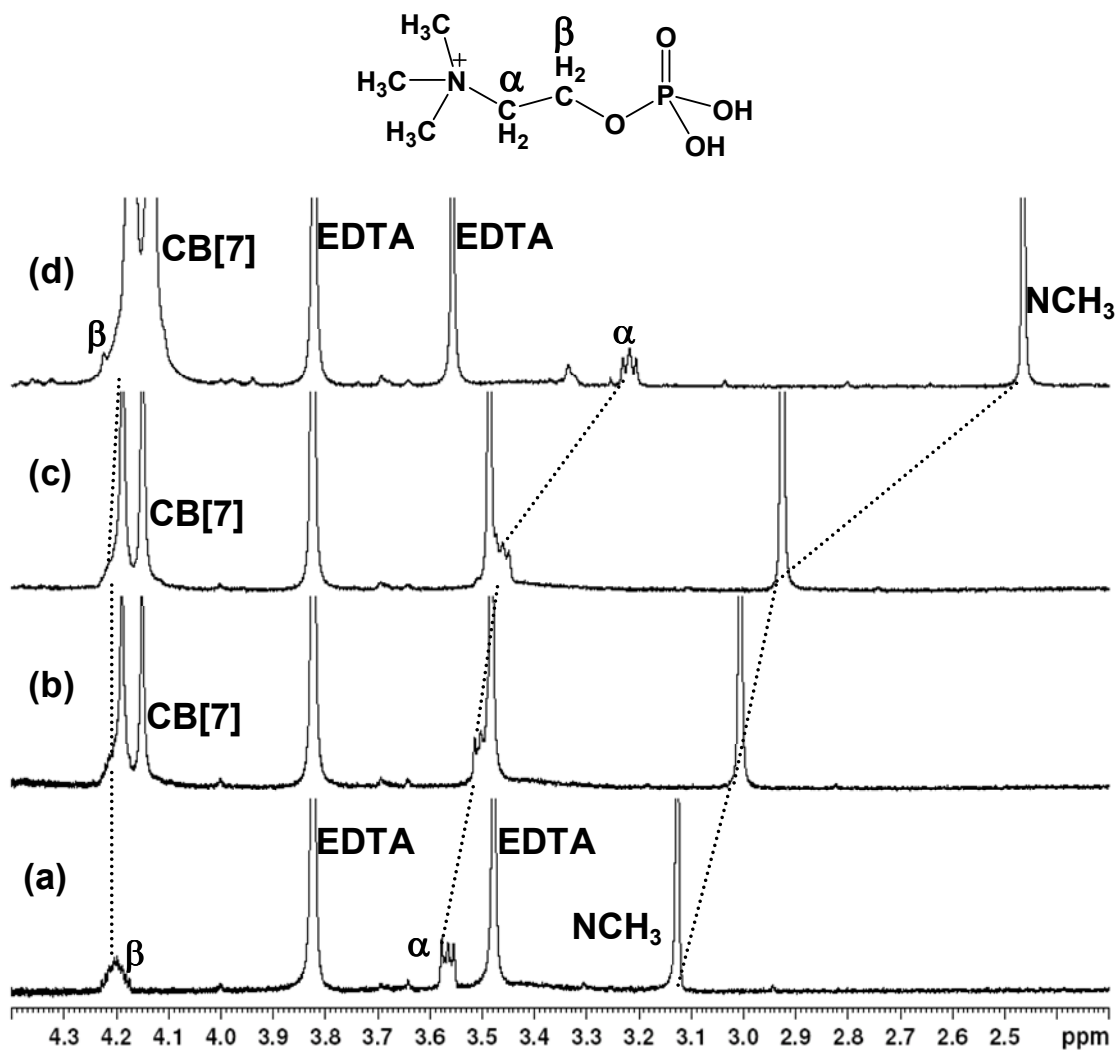


**Figure 5.14** Selected spectra from the <sup>1</sup>H NMR titration of choline phosphate (0.54 mM in D<sub>2</sub>O) in the presence of 1.12 mM EDTA and (a) 0.00, (b) 0.65, (c) 1.05, and (d) 6.80 equiv. of CB[7].

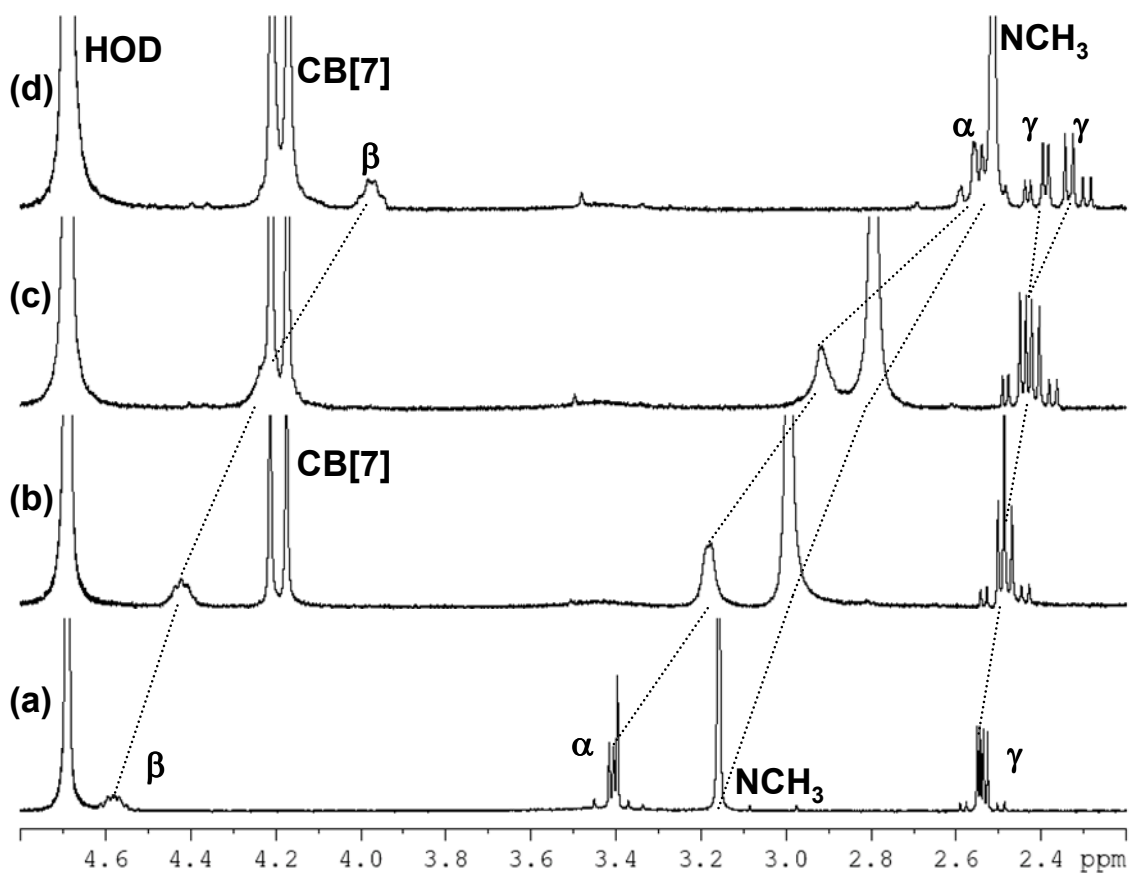
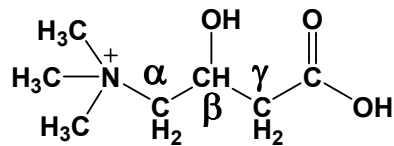


**Figure 5.15** Selected spectra from the  $^1\text{H}$  NMR titration of ( $\pm$ )-carnitine (1.53 mM in  $\text{D}_2\text{O}$ , no electrolyte) in the presence of (a) 0.00, (b) 0.25, (c) 0.56, and (d) 1.06 equiv. of CB[7].



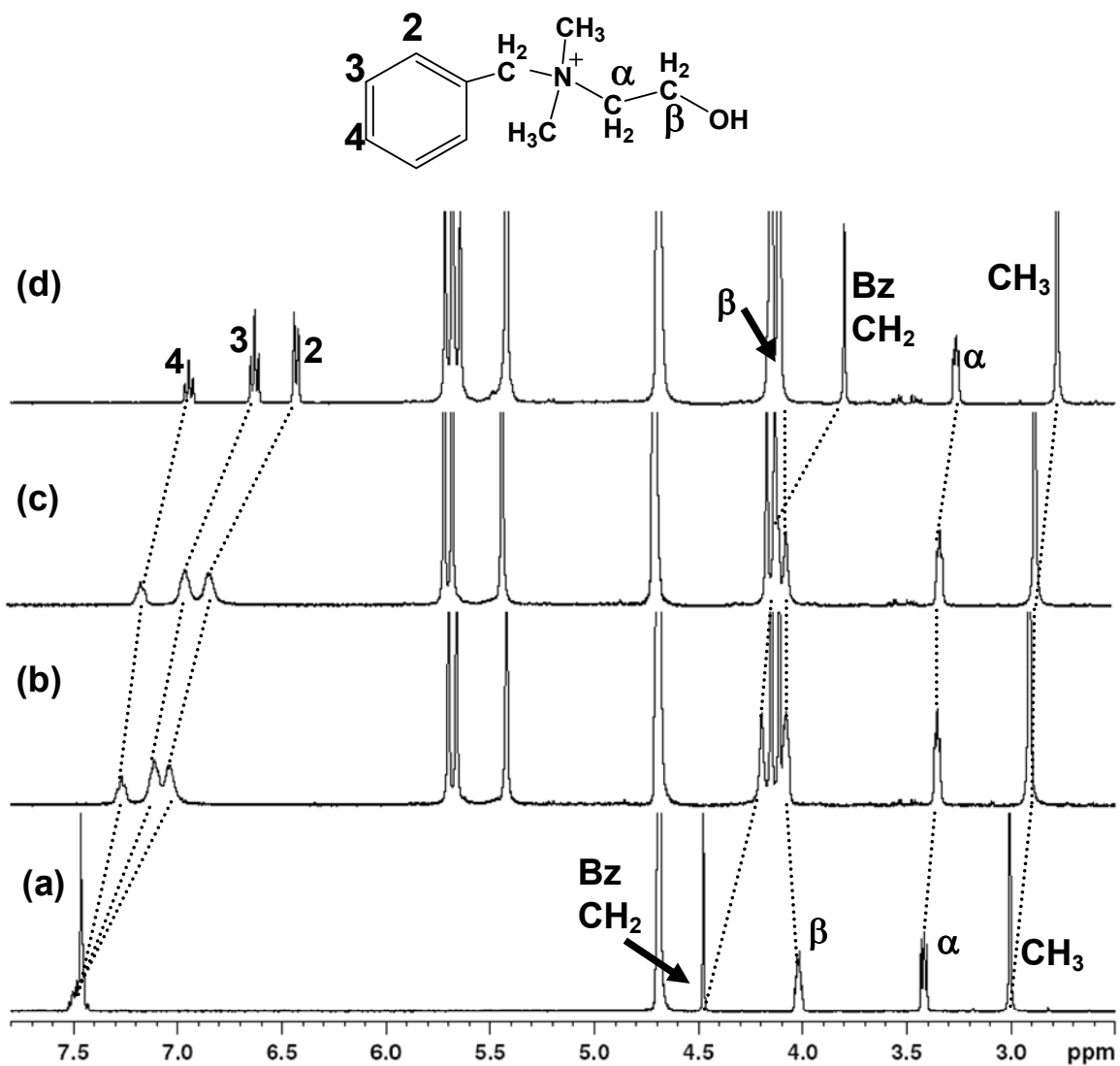


**Figure 5.16** Selected spectra from the  $^1\text{H}$  NMR titration of benzyldimethylcholine (1.90 mM in  $\text{D}_2\text{O}$ ) in the presence of (a) 0.00, (b) 0.44, (c) 0.65, and (d) 1.11 equiv. of CB[7].

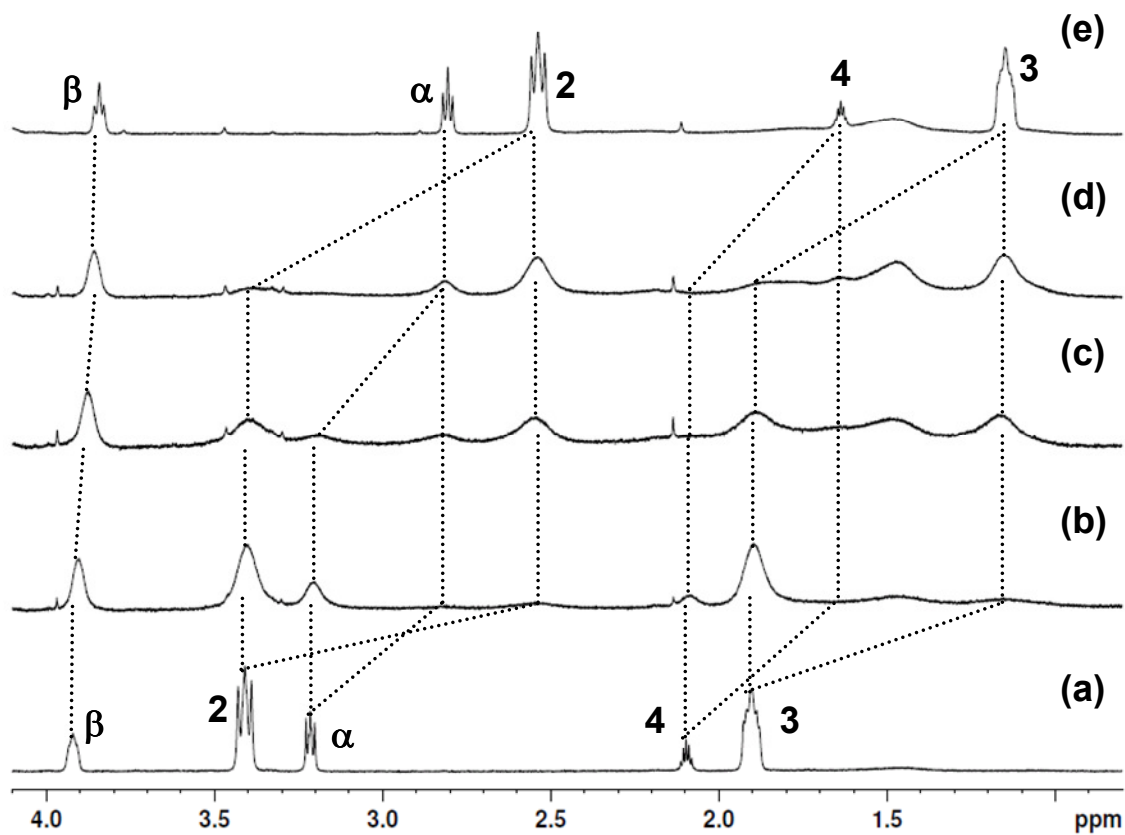
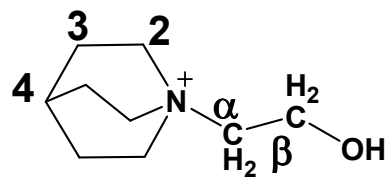


**Figure 5.17** Selected spectra from the <sup>1</sup>H NMR titration of quinuclidiniumcholine (1.08 mM in D<sub>2</sub>O) in the presence of (a) 0.00, (b) 0.22, (c) 0.53, (d) 0.71, and (e) 1.13 equiv. of CB[7].

**Table 5.2** Host-guest binding constants between CB[7] and the series of cholines, their phosphonium analogues, and related guests in D<sub>2</sub>O at 25 °C. (Competitive binding experiments determined in NaOAc (0.050 M) and DCl (0.025 M) at pD 4.75.).

Guest	$K_{CB[7]} (M^{-1})$
$(CH_3)_3N(CH_2)_2OH^+$	$(6.5 \pm 1.2) \times 10^5$ <sup>a,b</sup>
$(CH_3)_3N(CH_2)_4CH_3^+$	Not determined
$(CH_3)_3N(CH_2)_2O_2CCH_3^+$	$(7.0 \pm 1.3) \times 10^5$ <sup>a,c</sup>
$(CH_3)_3NCH_2CH(CH_3)O_2CCH_3^+$	$(4.9 \pm 0.9) \times 10^6$ <sup>d</sup>
$(CH_3)_3N(CH_2)_2O_2C(CH_2)_2CH_3^+$	$(1.7 \pm 0.3) \times 10^7$ <sup>a</sup> $(2.2 \pm 0.3) \times 10^7$ <sup>d</sup>
$(CH_3)_3N(CH_2)_{11}CH_3^+$ <sup>e</sup>	$(5.8 \pm 0.1) \times 10^4$
$(CH_3)_3N^+CH_2CH(OH)CH_2CO_2^-$	$(3.8 \pm 0.5) \times 10^7$ <sup>f</sup>
$(CH_3)_3NCH_2CH(OH)CH_2CO_2H^+$	$(8.0 \pm 1.1) \times 10^4$ <sup>g</sup> $(2.8 \pm 0.4) \times 10^3$ <sup>h</sup>
$(CH_3)_3N^+(CH_2)_2OP(O)(OH)O^-$	$(1.2 \pm 0.2) \times 10^3$ <sup>i</sup>
$(PhCH_2)(CH_3)_2N(CH_2)_2OH^+$	$(4.1 \pm 1.2) \times 10^8$ <sup>d</sup>
$(CH_3CH_2)_3N(CH_2)_2OH^+$	$(1.8 \pm 0.3) \times 10^6$ <sup>d</sup>
$(CH_3CH_2)_3N(CH_2)_4CH_3^+$	$(8.3 \pm 1.9) \times 10^5$ <sup>j</sup>
Quin(CH <sub>2</sub> ) <sub>2</sub> OH <sup>+</sup>	$(1.3 \pm 0.3) \times 10^9$ <sup>k</sup>
$(CH_3)_3P(CH_2)_4CH_3^+$	$(1.4 \pm 0.3) \times 10^7$ <sup>a</sup>
$(CH_3)_3P(CH_2)_2OH^+$	$(6.9 \pm 1.8) \times 10^6$ <sup>j,l</sup>
$(CH_3)_3P(CH_2)_2O_2CCH_3^+$	$(8.9 \pm 1.7) \times 10^5$ <sup>a</sup>
$(CH_3CH_2)_3P(CH_2)_4CH_3^+$	$(1.6 \pm 0.3) \times 10^6$ <sup>d,m</sup>
$(CH_3CH_2)_3P(CH_2)_2OH^+$	$(1.3 \pm 0.3) \times 10^5$ <sup>j</sup>
$(CH_3CH_2)_3P(CH_2)_2O_2CCH_3^+$	$(8.6 \pm 1.6) \times 10^5$ <sup>a,n</sup>
N-methylquinuclidinium <sup>+</sup>	$(5.7 \pm 1.4) \times 10^9$ <sup>k</sup>
DimethylDABCO <sup>2+</sup>	$(5.4 \pm 1.3) \times 10^5$ <sup>o</sup>

<sup>a</sup>Using 1,4-phenylenediamine as competitor. <sup>b</sup>Values  $(7.0 \pm 1.6) \times 10^5$  and  $(1.1 \pm 0.3) \times 10^6 M^{-1}$ , determined with  $PMe_4^+$  and  $PEt_4^+$  as competitors, respectively. <sup>c</sup>Values of  $(5.7 \pm 1.5) \times 10^5$  and  $(1.3 \pm 0.4) \times 10^6 M^{-1}$  determined with  $PMe_4^+$  and  $PEt_4^+$  as competitors, respectively. <sup>d</sup>Using TMSP as the competitor. <sup>e</sup>Data from ref. 73. <sup>f</sup>At pD 8.1. <sup>g</sup>In D<sub>2</sub>O with no added electrolyte. <sup>h</sup>At pD 2.0. <sup>i</sup>In D<sub>2</sub>O with 2.1 equiv. EDTA to complex Ca<sup>2+</sup>. <sup>j</sup>Using  $NEt_4^+$  as the competitor. <sup>k</sup>Using *p*-xylylenediamine as the competitor. <sup>l</sup>Value of  $(1.7 \pm 0.2) \times 10^6 M^{-1}$  determined using 1,4-phenylenediamine as the competitor. <sup>m</sup>Value of  $(5.6 \pm 1.3) \times 10^5 M^{-1}$  determined using TMSP as the competitor. <sup>n</sup>Values of  $(1.6 \pm 0.4) \times 10^6$  and  $(3.0 \pm 0.5) \times 10^6 M^{-1}$  determined using 1,4-phenylenediamine and  $NEt_4^+$ , respectively, as competitors. <sup>o</sup>Values of  $(5.8 \pm 1.3) \times 10^5$ ,  $(4.7 \pm 1.1) \times 10^5$ , and  $(1.4 \pm 0.2) \times 10^6 M^{-1}$  determined using  $PMe_4^+$ ,  $NEt_4^+$ , and TMSP as competitors, respectively.

**Table 5.3** High resolution ESI-MS data for the host-guest complexes of the various choline derivatives with CB[7].

Guest	Observed 1:1 (CB[7]:guest) ( <i>m/z</i> )	Calculated 1:1 ( <i>m/z</i> )
[(CH <sub>3</sub> ) <sub>3</sub> N(CH <sub>2</sub> ) <sub>2</sub> OH]Cl	1266.4643 [M-Cl] <sup>+</sup>	[M-Cl] <sup>+</sup> ([C <sub>47</sub> H <sub>56</sub> N <sub>29</sub> O <sub>15</sub> ) <sup>+</sup> ) 1266.4505
[(CH <sub>3</sub> CH <sub>2</sub> ) <sub>3</sub> N(CH <sub>2</sub> ) <sub>2</sub> OH]Br	1308.4904 [M-Br] <sup>+</sup>	[M-Br] <sup>+</sup> ([C <sub>50</sub> H <sub>62</sub> N <sub>29</sub> O <sub>15</sub> ) <sup>+</sup> ) 1308.4975
[(CH <sub>3</sub> ) <sub>3</sub> P(CH <sub>2</sub> ) <sub>2</sub> OH]Br	1283.4482 [M-Br] <sup>+</sup>	[M-Br] <sup>+</sup> ([C <sub>47</sub> H <sub>56</sub> N <sub>28</sub> O <sub>15</sub> P) <sup>+</sup> ) 1283.4212
[(CH <sub>3</sub> CH <sub>2</sub> ) <sub>3</sub> P(CH <sub>2</sub> ) <sub>2</sub> OH]Br	1325.4724 [M-Br] <sup>+</sup>	[M-Br] <sup>+</sup> ([C <sub>50</sub> H <sub>62</sub> N <sub>28</sub> O <sub>15</sub> P) <sup>+</sup> ) 1325.4682
[Quin(CH <sub>2</sub> ) <sub>2</sub> OH]Br	1318.4766 [M-Br] <sup>+</sup>	[M-Br] <sup>+</sup> ([C <sub>51</sub> H <sub>60</sub> N <sub>29</sub> O <sub>15</sub> ) <sup>+</sup> ) 1318.4818
[(PhCH <sub>2</sub> )(CH <sub>3</sub> ) <sub>2</sub> N(CH <sub>2</sub> ) <sub>2</sub> OH]Cl	1342.5034 [M-Cl] <sup>+</sup>	[M-Cl] <sup>+</sup> ([C <sub>53</sub> H <sub>60</sub> N <sub>29</sub> O <sub>15</sub> ) <sup>+</sup> ) 1342.4818
[(CH <sub>3</sub> ) <sub>3</sub> N(CH <sub>2</sub> ) <sub>2</sub> O <sub>2</sub> CCH <sub>3</sub> ]Cl	1308.4684 [M-Cl] <sup>+</sup>	[M-Cl] <sup>+</sup> ([C <sub>49</sub> H <sub>58</sub> N <sub>29</sub> O <sub>16</sub> ) <sup>+</sup> ) 1308.4611
[(CH <sub>3</sub> ) <sub>3</sub> P(CH <sub>2</sub> ) <sub>2</sub> O <sub>2</sub> CCH <sub>3</sub> ]Br	1325.4339 [M-Br] <sup>+</sup>	[M-Br] <sup>+</sup> ([C <sub>49</sub> H <sub>58</sub> N <sub>28</sub> PO <sub>16</sub> ) <sup>+</sup> ) 1325.4318
[(CH <sub>3</sub> CH <sub>2</sub> ) <sub>3</sub> P(CH <sub>2</sub> ) <sub>2</sub> O <sub>2</sub> CCH <sub>3</sub> ]Br	1367.4851 [M-Br] <sup>+</sup>	[M-Br] <sup>+</sup> ([C <sub>52</sub> H <sub>64</sub> N <sub>28</sub> O <sub>16</sub> P) <sup>+</sup> ) 1367.4787
[(CH <sub>3</sub> ) <sub>3</sub> NCH <sub>2</sub> CH(CH <sub>3</sub> )O <sub>2</sub> CCH <sub>3</sub> ]Cl	1322.4855 [M-Cl] <sup>+</sup>	[M-Cl] <sup>+</sup> ([C <sub>50</sub> H <sub>60</sub> N <sub>29</sub> O <sub>16</sub> ) <sup>+</sup> ) 1322.4767
[(±)-Carnitine]Cl	1324.4600 [M-Cl] <sup>+</sup>	[M-Cl] <sup>+</sup> ([C <sub>49</sub> H <sub>58</sub> N <sub>29</sub> O <sub>17</sub> ) <sup>+</sup> ) 1324.4560
[(CH <sub>3</sub> ) <sub>3</sub> N(CH <sub>2</sub> ) <sub>2</sub> O <sub>2</sub> C(CH <sub>2</sub> ) <sub>2</sub> CH <sub>3</sub> ]Cl	1336.4994 [M-Cl] <sup>+</sup>	[M-Cl] <sup>+</sup> ([C <sub>51</sub> H <sub>62</sub> N <sub>29</sub> O <sub>16</sub> ) <sup>+</sup> ) 1336.4924
[(CH <sub>3</sub> CH <sub>2</sub> ) <sub>3</sub> N(CH <sub>2</sub> ) <sub>4</sub> CH <sub>3</sub> ]Br	1334.5619 [M-Br] <sup>+</sup>	[M-Br] <sup>+</sup> ([C <sub>53</sub> H <sub>68</sub> N <sub>29</sub> O <sub>14</sub> ) <sup>+</sup> ) 1334.5495
[(CH <sub>3</sub> ) <sub>3</sub> P(CH <sub>2</sub> ) <sub>4</sub> CH <sub>3</sub> ]Br	1309.4706 [M-Br] <sup>+</sup>	[M-Br] <sup>+</sup> ([C <sub>50</sub> H <sub>62</sub> N <sub>28</sub> O <sub>14</sub> P) <sup>+</sup> ) 1309.4732
[(CH <sub>3</sub> CH <sub>2</sub> ) <sub>3</sub> P(CH <sub>2</sub> ) <sub>4</sub> CH <sub>3</sub> ]Br	1351.5148 [M-Br] <sup>+</sup>	[M-Br] <sup>+</sup> ([C <sub>53</sub> H <sub>68</sub> N <sub>28</sub> O <sub>14</sub> P) <sup>+</sup> ) 1351.5202
[N-Methylquinuclidinium]I	1288.4799 [M-I] <sup>+</sup>	[M-I] <sup>+</sup> ([C <sub>50</sub> H <sub>58</sub> N <sub>29</sub> O <sub>14</sub> ) <sup>+</sup> ) 1288.4713
[DimethylDABCO]I <sub>2</sub>	652.2453 [M-2I] <sup>2+</sup>	[M-2I] <sup>2+</sup> ([C <sub>50</sub> H <sub>60</sub> N <sub>30</sub> O <sub>14</sub> ) <sup>2+</sup> ) 652.2447

The upfield shifts of the protons adjacent to the ester group of acetylcholine are reasonably large, indicating that the ester group is encapsulated by the CB[7] cavity. While complexation between guests and cucurbiturils are largely driven by electrostatic interactions with the electron rich portals of the hosts, as well as the hydrophobic effect, another, weaker

interaction between a cucurbituril and a polar guest may arise from the quadrupole-dipole effect. This was studied in a parallel project involving a series of polar organic solvents and is discussed in Chapter 2 of this thesis. Due to the quadrupole moment of cucurbiturils, solvents such as acetone were positioned deeply into the cavity, with their carbonyl group facing the interior wall, so that the carbonyl group may be as far away as possible from either of the portals. This appears to be occurring with the acetylcholine and butyrylcholine guests, with the ester carbonyl being positioned near the middle of the cavity and the trimethylammonium group positioned closer to the portals, as the upfield shifts were significant on either side of the esters, suggesting that the ester region is encapsulated deep within the CB[7] cavity. Within the acetylcholine series, this phenomenon appears to be occurring primarily for acetylcholine, and not for its phosphonium analogues, whose more hydrophobic head groups become encapsulated in the cavity at the expense of their acetylcholine backbones.

For the guests containing trimethylammonium head groups, the trimethylammonium protons exhibit upfield shifts, with their  $\Delta\delta_{\text{lim}}$  values ranging between -0.06 and -0.82 ppm, suggesting that, albeit to varying degrees, this region is encapsulated within the CB[7] cavity. The upfield shifts of the trimethylammonium protons tend to be smaller in magnitude when the fourth branch of the quaternary ammonium is somewhat extended, such as the ester-containing arms of acetylcholine and butyrylcholine ( $\Delta\delta_{\text{lim}} = -0.28$  and  $-0.10$  ppm, respectively), or the pentyl branch of trimethylpentylammonium ( $\Delta\delta_{\text{lim}} = -0.06$  ppm). This seems to suggest that when this branch of the guest is longer, the CB[7] cavity begins to reside for more time over this branch, at the expense of the trimethylammonium region. The effect is more pronounced for the pentyl branch of trimethylpentylammonium, than the approximately equal-length ester-containing branch of acetylcholine. This trend is also observed among the phosphonium analogues, with the upfield shifts of the phosphonium protons being greatest for the choline analogue and least for their pentyl-branched analogues. As indicated earlier, the phosphonium protons of the

acetylcholine analogues experience only small decreases in their upfield shifts, compared to the corresponding upfield shifts of the phosphonium choline analogues, while the trimethylammonium protons display a greater decrease in the limiting upfield shift on going from choline to acetylcholine. This suggests that among the phosphonium analogues of acetylcholine, the CB[7] cavity is more localized over the cationic head group than it is for native acetylcholine. Among the trimethylammonium guests, the limiting upfield shifts tend to be larger for the zwitterionic guests such as phosphocholine and ( $\pm$ )-carnitine, suggesting that the CB[7] becomes more localized over the ammonium region. This may be due to repulsions between the carbonyl oxygens of the cucurbituril portal and the anionic region at the opposite end of the guest.

### **5.2.2 Host-Guest Binding Between CB[7] and Guests Bearing Benzyl, Quinuclidinium, and DABCO Units**

CB[7] has a higher affinity for benzyl and quinuclidinium groups than for the aliphatic guests. When choline derivatives contain these substituents, the limiting upfield shifts are primarily located on this region of the guest, at the expense of the choline backbone (Figure 5.18). This suggests that complexations of the CB[7] to quinuclidiniumcholine and benzyldimethylcholine are largely driven by the affinity of the CB[7] cavity to these hydrophobic substituents, rather than electrostatic attractions to the quaternary ammonium centres. For all of the analogues containing the pentyl chain, the upfield shifts are also distributed primarily over the pentyl branch, suggesting that this extended hydrophobic branch is the primary binding site for CB[7] with these guests.

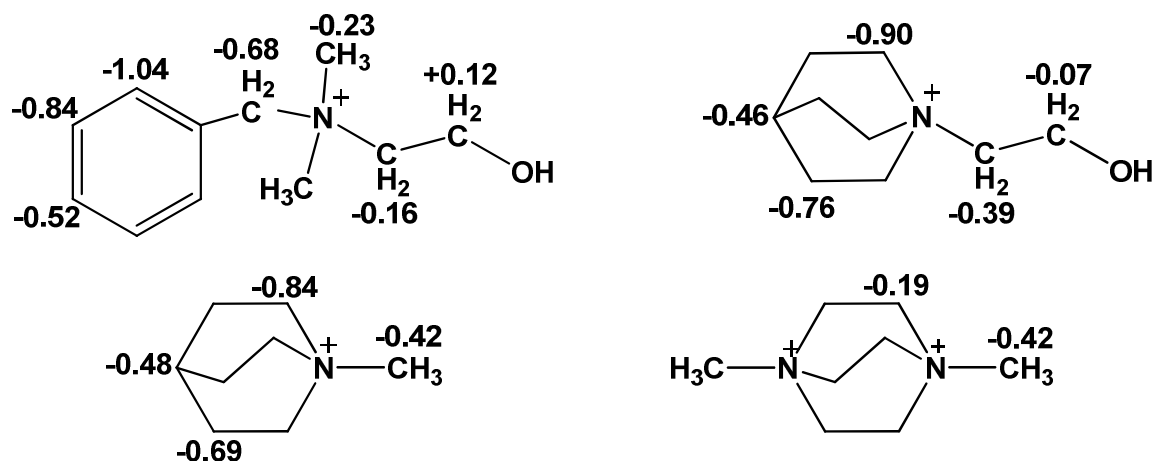


**Figure 5.18** Structures and  $\Delta\delta_{\text{lim}}$  values for the benzyl- and quinuclidinium-bearing derivatives of choline, as well as for *N*-methylquinuclidinium and dimethylDABCO, determined from  $^1\text{H}$  titrations. Negative values represent upfield limiting shifts, while positive values represent downfield shifts.

As part of this study, the binding between CB[7] and guests such as *N*-methylquinuclidinium iodide, and 1,4-dimethyl-1,4-diazoniabicyclo[2.2.2]octane diiodide (dimethylDABCO) was investigated. The stability constant for binding between CB[7] and the monocationic *N*-methylquinuclidinium guest ( $K_{\text{CB}[7]} = (5.7 \pm 1.4) \times 10^9 \text{ M}^{-1}$ ) is just over four orders of magnitude greater than that with dicationic dimethylDABCO ( $K_{\text{CB}[7]} = (5.4 \pm 1.3) \times 10^5 \text{ M}^{-1}$ ). The structural differences between these two compounds are relatively minor, except that dimethylDABCO contains a  $^+\text{N-CH}_3$  group in place of the terminal quinuclidinium C-H of the *N*-methylquinuclidinium. The more significant difference between these two guests would appear to be the additional positive charge of dimethylDABCO. In terms of electrostatics, it may seem that CB[7], with its electron rich portals, should have a higher binding affinity to the dicationic guest, as opposed to the monocationic guest. On the other hand, the charge density of the singly charged *N*-methylquinuclidinium guest is more charge-diffuse, and thus may be more readily encapsulated in the hydrophobic CB[7] cavity. While a higher positive charge density would be expected to enhance the binding of a guest when its binding site is at the cucurbituril portals, a

lower charge density should more readily facilitate a guest's encapsulation when the binding site is in the host's hydrophobic cavity. Furthermore, the positive charges on the dimethylDABCO guest are too close together for optimum simultaneous electrostatic attraction to the two portals. All of the protons of both of these guests show upfield shifts in the presence of CB[7], indicating that they become encapsulated within the cavity, as opposed to being positioned near the portals, with these guests thus displaying similar behaviour to the other quaternary ammonium guests in this study. The magnitudes of the upfield shifts of the *N*-methylquinuclidinium protons are generally greater (Figures 5.18 and 5.19), suggesting that this guest becomes more deeply encapsulated within the CB[7] cavity than dimethylDABCO (Figures 5.18 and 5.20).



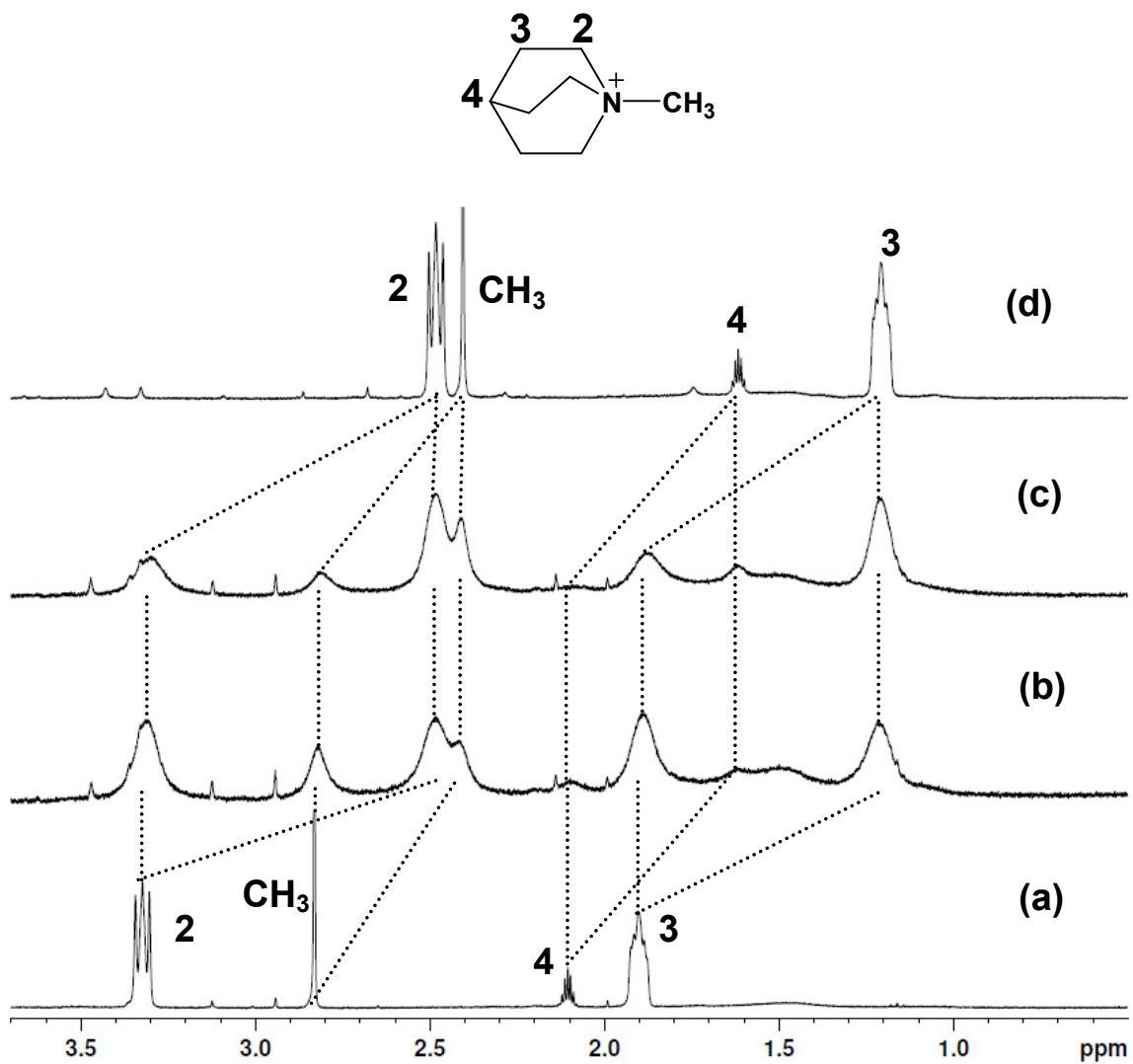


**Figure 5.19** Selected spectra from the  $^1\text{H}$  NMR titration of *N*-methylquinuclidinium iodide (1.32 mM in  $\text{D}_2\text{O}$ ) in the presence of (a) 0.00, (b) 0.57, (c) 0.74, and (d) 2.09 equiv. of CB[7].



encapsulated by the CB[7] cavity. The magnitude of the upfield shift of the trimethylphosphonium guests was smaller than that observed for the corresponding triethylphosphonium analogue. This behaviour was also observed earlier for the corresponding tetraalkylphosphonium salts.<sup>62</sup> Within the trimethylphosphonium series, the limiting upfield shift was the least for trimethylpentylphosphonium, and greatest for its acetylcholine analogue (as opposed to the choline analogue), suggesting that the CB[7] cavity was residing over the pentyl arm of trimethylpentylphosphonium, while the cavity resided primarily over the more hydrophobic phosphonium region of the choline and acetylcholine analogues. A similar trend was also observed among the triethylphosphonium series, albeit with a larger magnitude of the limiting upfield shifts. While this behaviour parallels that observed from the  $\Delta\delta_{\text{lim}}$  values of the protons adjacent to the phosphonium centres, there was a slight discrepancy in the trends of the  $\Delta\delta_{\text{lim}}$  values of the protons near the phosphonium centres and the  $^{31}\text{P}$   $\Delta\delta_{\text{lim}}$  values with regards to the choline and acetylcholine guests. The limiting upfield shifts of the phosphonium centres represented by the  $^{31}\text{P}$  NMR spectra were greater for both the trimethyl- and triethylphosphonium analogues of acetylcholine than for the corresponding analogues of choline, while the opposite trend was observed from the limiting upfield shifts of the protons adjacent to the phosphonium centres.

### 5.2.3 Host-Guest Stability Constants

The strength of the binding affinity between CB[7] and the series of choline and acetylcholine-related guests explored in this study may be affected by a variety of factors, such as the nature of core atom of the onium head group (whether N or P), as well as the head group's alkyl substituents (whether they are methyl or ethyl groups), in addition to the nature of any

functional groups that may be attached to the guest molecule, such as its hydrophobicity, length or size, as well as charge. The CB[7] host-guest stability constants are presented in Table 5.2

The smallest binding affinities were observed for the zwitterionic guests, such as choline phosphate and ( $\pm$ )-carnitine, and their 1:1 binding affinities could be determined from  $^1\text{H}$  NMR titration curves by least-squares fitting. The  $\text{p}K_{\text{a}}$  of the carboxylic acid group of ( $\pm$ )-carnitine is 3.78.<sup>74</sup> Titrations were carried out at both above and below this  $\text{p}K_{\text{a}}$  value, such as at pD 2.0 in a solution of 0.01 M DCl and 0.05 M NaCl, as well as at pD 8.1 in a solution of 0.05 M NaOAc- $d_3$ , while another titration was conducted in  $\text{D}_2\text{O}$  solution without electrolyte (Figure 5.21). At pD 2.0, the binding constant between CB[7] and cationic ( $\pm$ )-carnitine was determined to be  $(2.8 \pm 0.4) \times 10^3 \text{ M}^{-1}$ , while this binding strength decreased to  $(3.8 \pm 0.5) \times 10^2 \text{ M}^{-1}$  at pD 8.1, for the zwitterionic species. In the acidic solution, the limiting upfield shift of the trimethylammonium protons of ( $\pm$ )-carnitine was 0.68 ppm, and the magnitude increased to 0.78 ppm in the basic solution. This seems to suggest that the trimethylammonium protons become more deeply encapsulated by the CB[7] cavity in the more basic solution. This is likely driven by the predominance of the zwitterionic species of the guest, whose anionic carboxylate group (in basic solution) at the opposite end of the molecule would repel the CB[7] somewhat and cause it to become more localized over the trimethylammonium centre.

When the titration was conducted in  $\text{D}_2\text{O}$ , with the absence of electrolyte, the apparent binding constant is higher, having a value of  $(8.0 \pm 1.1) \times 10^4 \text{ M}^{-1}$ . The higher binding affinity observed from this titration is surprising, in that the binding constant is almost 29 times higher in  $\text{D}_2\text{O}$  than in the acidic solution. This increase in the binding constant in the absence of electrolyte over that of the other titrations may arise from the lack of sodium (both of the other titrations had 0.05 M  $\text{Na}^+$  present), which acts as a competitor for binding to cucurbiturils, thus resulting in a reduction of the apparent binding constant between a given guest and the cucurbituril.<sup>75-78</sup> It may also be possible that the titration in  $\text{D}_2\text{O}$ , lacking buffer, may have experienced a change in pH

during the course of the titration. If this was the case, and also considering the possibility of a complexation-induced  $pK_a$  shift of the ( $\pm$ )-carnitine guest in the presence of CB[7], it may be possible that this higher binding constant represented binding between CB[7] and ( $\pm$ )-carnitine where a significant proportion of the guest existed as the cation, instead of the expected zwitterionic species.

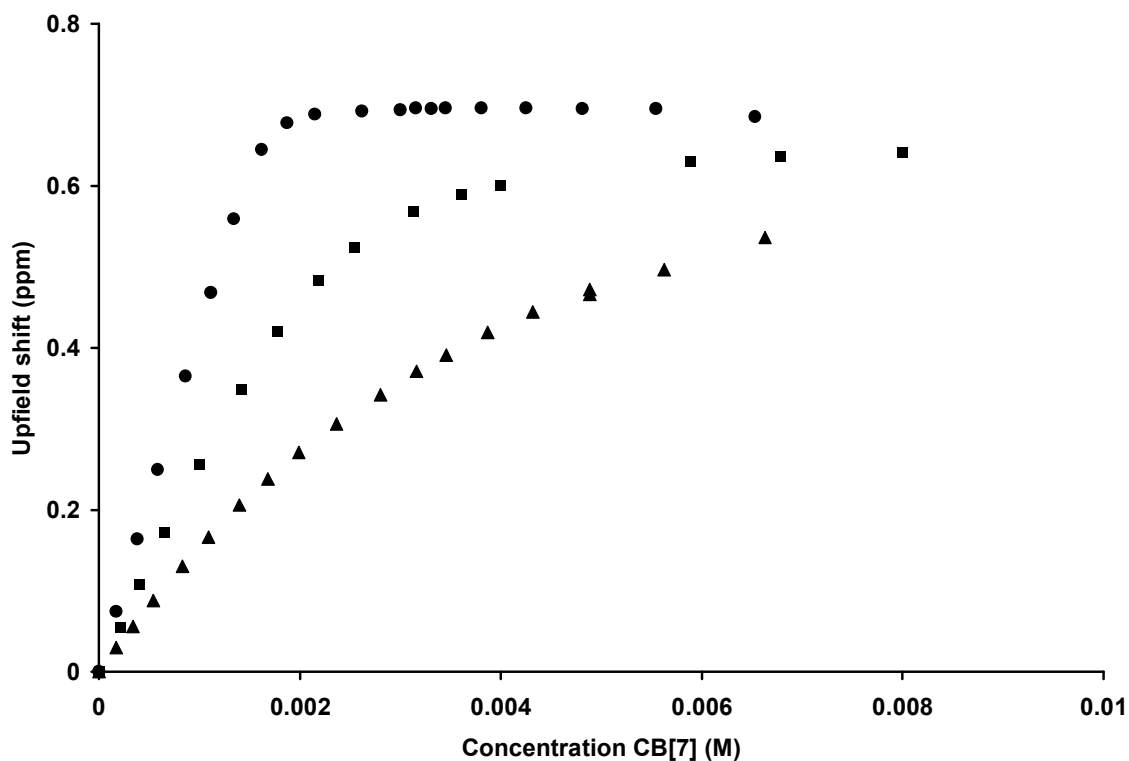


**Figure 5.21**  $^1\text{H}$  NMR chemical shift titrations of ( $\pm$ )-carnitine (1.5 mM) with CB[7] in  $\text{D}_2\text{O}$  solutions (●) with no added electrolytes, (■) at pD 2.0 (in 0.01 M DCl with 0.05 M NaCl), and (▲) in 0.05 M NaOAc- $d_3$ . These titrations represent the trimethylammonium protons of carnitine.

The choline phosphate guest was purchased commercially as a calcium salt. As a result, in the  $^1\text{H}$  NMR titration of the guest with CB[7], the  $\text{Ca}^{2+}$  cation competed with the guest for binding to the host, with a sigmoidal-shaped titration curve being observed. In order to rectify

this issue, the metal ion complexing agent EDTA (EDTA = N, N', N'', N'''-ethylenediaminetetraacetate) was added to the solution. This sigmoidal appearance of the binding curve was still an issue when one equivalent of EDTA was added per choline phosphate, however when a two-fold excess of EDTA was present, a normal shape of the binding curve was observed, indicating that the EDTA was binding with the  $\text{Ca}^{2+}$  sufficiently enough to prevent it from competing with the binding between CB[7] and the choline phosphate guest. When the zwitterionic form of the choline phosphate guest, whose  $\text{p}K_a$  is 5.5,<sup>59</sup> was titrated with CB[7] at a pD of 3.7, a binding constant of  $(1.2 \pm 0.2) \times 10^3 \text{ M}^{-1}$  was observed. Meanwhile, when the titration was conducted in more basic solution at pD 7.8 (with 0.045 M NaOAc- $d_3$  and 0.0012 M  $\text{Na}_4\text{EDTA}$ ), the phosphate group was in its dianionic form (giving the molecule an overall charge of -1) and only very small chemical shift changes of the guest were observed in the presence of CB[7], suggesting that the binding affinity between CB[7] and the overall anionic choline phosphate guest is very weak.

The host-guest binding constants between CB[7] and the remaining choline-related guests in this series were too large to be measured directly by titration, and instead competitive  $^1\text{H}$  NMR binding experiments were employed, with the resulting binding constants listed in Table 5.2. These competitive binding experiments were conducted at a pD of 4.75 using 0.05 M NaOAc- $d_3$  and 0.025 M DCl as the media, and a series of competitors with known binding constants under these conditions were used.<sup>62,63</sup> These binding constants of the choline and acetylcholine guests and their analogues were often affected by the nature of the cationic head group of the guest, as well as any functional or hydrophobic groups that were present in the backbone of the molecule, and their binding constants may be compared to those determined for the series of tetraalkylammonium and -phosphonium guests,<sup>62</sup> which are also listed in Table 5.2. Among the choline series of guests, the order of the binding affinities follows a similar trend to that observed with the peralkylated onium guests, with the order of the binding affinity (according to their head

group) being  $\text{PMe}_3^+ > \text{NEt}_3^+ > \text{PEt}_3^+ > \text{NMe}_3^+$ . For the choline analogues, the upfield shifts indicate that the quaternary head groups, in addition to the choline backbone, become encapsulated by the CB[7] cavity, and this encapsulation of the cationic head group throughout the series would be consistent with the tendency of the binding constants throughout the choline analogue series to follow the general trend of the tetraalkylated quaternary cationic salts.

Among the acetylcholine analogues, the variation in their binding constants is relatively small, with a range of  $7\text{-}9 \times 10^5 \text{ M}^{-1}$ , and the positioning of the cucurbituril's cavity is less uniform than is the case of the choline analogues. While all of the guest protons of acetylcholine are shifted upfield upon complexation with CB[7], the cavity is more localized over the cationic head group of the phosphonium analogues of acetylcholine. This may suggest that the strength of the binding affinity is less dependent on the nature of the head group in this series than in the choline series, although the CB[7] cavity does appear to become more localized over the more charge-diffuse phosphonium head groups than it does over the trimethylammonium head group of native acetylcholine. Because of the differing placements of the CB[7] cavity throughout the acetylcholine series, the similarities of their binding constants may therefore be coincidental. When the binding constants between CB[7] and the trialkylphosphonium analogues of acetylcholine are compared with the corresponding binding constants between CB[7] and the trialkylpentylphosphonium guests, the binding affinity is approximately equal (with the  $\text{PEt}_3$  head group) or greater (with the  $\text{PMe}_3$  head group) when it is bound to the trialkylpentylphosphonium guests. For all of the quaternary cations containing the pentyl chain, the upfield shifts are largest along that hydrophobic chain, and the upfield shifts of the trialkylphosphonium protons are less than they are among the corresponding trialkylphosphonium protons of the acetylcholine analogues. These trends may suggest that a significant contribution to the host-guest binding affinities and positioning of the CB[7] cavity upon complexation with the pentane-bearing series of guests is due to the hydrophobic nature of the pentyl chain. It would appear that the greater

hydrophobicity of the pentyl chain may have a greater effect on the binding to CB[7] than any quadrupole-dipole interactions between the cavity and the carbonyl group of the similar-length ester-containing chain of acetylcholine.

For the guests containing the trimethylammonium head group, the order of the binding affinities to CB[7] is: butyrylcholine > acetyl- $\beta$ -methylcholine > acetylcholine > choline > tetramethylammonium. This trend appears to be driven by the hydrophobicity of the substituents at the neutral end of the molecule, with stronger binding occurring between CB[7] and the guests with greater hydrophobicity. The order of the magnitudes of the  $\Delta\delta_{\text{lim}}$  values of the trimethylammonium protons are: butyrylcholine (-0.10 ppm) < acetyl- $\beta$ -methylcholine (-0.16 ppm) < acetylcholine < (-0.28 ppm) < choline (-0.66 ppm) < tetramethylammonium bromide (-0.72 ppm). The trend of the binding constants is reflected in the magnitude of the  $\Delta\delta_{\text{lim}}$  values of the trimethylammonium protons, although the trend is in reverse, with a *decreasing* magnitude in the upfield shift of the trimethylammonium protons as the binding constant *increases*. This trend suggests that as the guest becomes more extended, containing a more hydrophobic group at the neutral end of the molecule (and the host-guest binding constant accordingly increases), the CB[7] cavity becomes more effectively drawn away from the trimethylammonium region of the guest as it encapsulated the hydrophobic region of the guest. In the literature, there are examples of host-guest systems between CB[7] and guests containing trimethylammonium moieties, where the hydrophobic substituent attached to the trimethylammonium group determines the binding affinity, with these substituents including adamantane,<sup>63</sup> ferrocene,<sup>79</sup> and methyl viologen moieties.<sup>80</sup>

When the methyl or ethyl substituents of the trialkylammonium choline analogues are replaced with quinuclidinium or benzyl moieties, the binding constants increase significantly, falling in the  $10^8 - 10^9 \text{ M}^{-1}$  range. At the same time, the upfield shifts, which had been distributed throughout the molecule in the case of the trialkylammonium and -phosphonium analogues of



choline, become localized over the quinuclidinium or benzyl region of the guest, at the expense of the “ethanol” backbone (that is, the H $\alpha$  and H $\beta$  protons). The binding constants of these choline analogues are comparable to the binding affinities obtained for other quinuclidinium and benzyl guests, such as *N*-methylquinuclidinium ( $K_{CB[7]} = (5.7 \pm 1.4) \times 10^9 \text{ M}^{-1}$ ), and benzyltrimethylammonium ( $K_{CB[7]} = (2.5 \pm 0.2) \times 10^8 \text{ M}^{-1}$ ). The high binding affinities observed for these choline analogues appear to be therefore dependent on the hydrophobic quinuclidinium and benzyl substituents, as opposed to the choline backbone itself.

As mentioned earlier in this chapter, there are a number of reports on binding studies conducted between guests such as choline, acetylcholine, and carnitine, with a variety of synthetic hosts (Table 5.4 and Figure 5.22).<sup>5-54</sup> Many of these hosts contained aromatic units within their framework (such as, for example, calixarene, and resorcarene-based hosts and their derivatives), or anionic substituents in their structures, and thus employed cation- $\pi$ , as well as electrostatic interactions, respectively, with the trimethylammonium-bearing guests. Among these studies, there have been reports of comparisons of the binding affinities of a particular host for guests such as choline, acetylcholine, and carnitine, with a summary of these binding constants shown in Table 5.4. Nau and coworkers<sup>26</sup> have found that *p*-sulfonated calix[4]arene binds to guests such as choline, acetylcholine, and L-carnitine with binding constants of  $7 \times 10^4$ ,  $1.0 \times 10^5$ , and  $1.7 \times 10^3 \text{ M}^{-1}$ , respectively. These binding affinities decreased when the experiment was conducted at pD 2.4, with binding constants to choline, acetylcholine, and L-carnitine becoming  $1.3 \times 10^4$ ,  $1.8 \times 10^4$ , and  $6.3 \times 10^3 \text{ M}^{-1}$ , respectively. Rebek and coworkers observed binding constants of  $2.6 \times 10^4$ ,  $1.2 \times 10^4$ , and  $1.4 \times 10^2 \text{ M}^{-1}$  upon complexation between a deep cavitand host and choline, acetylcholine, and L-carnitine, respectively, based on isothermal calorimetry (ITC) experiments.<sup>50</sup> Also using ITC data, Inoue and coworkers<sup>42</sup> have determined that the binding constants between pyrogallol[4]arene and the guests choline, acetylcholine, and L-carnitine were  $3.4 \times 10^3$ ,  $6.1 \times 10^3$ , and  $4.4 \times 10^3 \text{ M}^{-1}$  ( $1.8 \times 10^4 \text{ M}^{-1}$  for the zwitterion), respectively, in ethanol. The water

soluble analogue of CB[6], CB\*[6], bearing equatorial cyclohexane units externally at the equatorial positions, bound to acetylcholine with a binding affinity of  $1.3 \times 10^3 \text{ M}^{-1}$  in aqueous media, while showing negligible interaction with choline.

From comparing the complexation between guests such as choline, acetylcholine, and carnitine, some general trends appear to emerge. The majority of the host-guest systems showed stronger binding to the cationic guests such as choline and acetylcholine than with the zwitterionic carnitine guest. One exception to this trend was observed when pyrogallol[4]arene was used as a host, which exhibited a higher binding affinity to carnitine than to either choline or acetylcholine, when carnitine was in its zwitterionic species.<sup>42</sup> Among many of the host-guest systems involving choline and acetylcholine as guests, the receptor often showed relatively small differences in their binding affinities between these two guests, suggesting that relatively low selectivity was observed. This was also the case with our host-guest binding between CB[7] and these guests, as we observed reasonably similar binding affinities of  $(6.5 \pm 1.2) \times 10^5$  and  $(7.0 \pm 1.3) \times 10^5 \text{ M}^{-1}$ , to choline and acetylcholine, respectively. An exception to this behaviour was observed by Kim and coworkers with their cyclohexane-bearing derivative of CB[6], CB\*[6], which bound to acetylcholine with a binding affinity of  $1.3 \times 10^3 \text{ M}^{-1}$  in aqueous solution, while showing insignificant binding affinity to choline under similar conditions.<sup>47</sup> Mandolini and coworkers have observed that the magnitudes of the binding constant between their calix[*n*]arene and resorcin[*n*]arene hosts and the cationic guests were dependent on the guest's counterion, with higher binding affinities being observed when the counterion was larger and more charge-diffuse, with the more charge-diffuse counterions apparently providing less competition against the host-guest system. The host-guest binding constants that this phenomenon was observed for were relatively weak ( $\leq 10^3 \text{ M}^{-1}$ ) and this trend would likely diminish for host-guest systems with higher binding affinities, where the guest's counterion would be less effective at competing with the host for complexation to the guest. Among the various hosts employed for binding to these

quaternary ammonium guests, the binding affinities between these guests and CB[7] compare favourably, falling within the upper range of the binding constants observed. This is particularly compelling when it is considered that CB[7] lacks aromatic units within its framework, and does not possess anionic units in its structure, unlike many of the other hosts that have been studied. In addition, unlike some of the host-guest systems described, the CB[7] host was studied in aqueous solution, which often tends to be a competitive solvent that can diminish a guest's binding affinity. Furthermore, aqueous media provides a platform for the study of these host-guest systems, in an environment that more closely resembles that which surrounds acetylcholine (compared to solvents such as chloroform) in biological systems.

**Table 5.4** Literature values of host-guest binding constants between a variety of synthetic hosts and choline, acetylcholine, carnitine, trimethylammonium, and triethylammonium cations and zwitterions (Continued on next page).

Host	Choline (M <sup>-1</sup> )	Acetylcholine (M <sup>-1</sup> )	Carnitine (M <sup>-1</sup> )	NMe <sub>4</sub> <sup>+</sup> (M <sup>-1</sup> )	NEt <sub>4</sub> <sup>+</sup> (M <sup>-1</sup> )
[CA[4]] <sup>-</sup> (1) <sup>a</sup>	5 x 10 <sup>2</sup>	2.6 x 10 <sup>2</sup>	-	-	-
<i>t</i> -butyl-CA[4] (2) <sup>b</sup>	-	< 5 <sup>c</sup>	-	-	-
<i>p</i> -sulfonated-CA[4] (3) <sup>d</sup>	7 x 10 <sup>4,d</sup> , 1.3 x 10 <sup>4,e</sup> , 5.0 x 10 <sup>4,f</sup>	1.0 x 10 <sup>5,d</sup> , 1.8 x 10 <sup>4,e</sup> , 5.0 x 10 <sup>4,f</sup>	1.7 x 10 <sup>3,d,g</sup> , 6.3 x 10 <sup>3,g,e</sup>	1.2 x 10 <sup>5,d</sup> , 2.6 x 10 <sup>4,e</sup> , 7.9 x 10 <sup>4,f</sup>	4.2 x 10 <sup>5,d</sup> , 1.4 x 10 <sup>5,e</sup> , 4.0 x 10 <sup>5,f</sup>
<i>p</i> -sulfonated CA[6] (4) <sup>f</sup>	6.3 x 10 <sup>4,f</sup>	7.9 x 10 <sup>4,f</sup>	-	7.9 x 10 <sup>4,f</sup>	1.0 x 10 <sup>5,f</sup>
[ <i>p</i> - <i>t</i> -butyl-CA[6]] <sup>3-</sup> (5) <sup>h</sup>	-	3.3 x 10 <sup>5,h</sup>	-	3.2 x 10 <sup>5,h</sup>	-
(Mandolini) (6) <sup>i,c</sup>	-	47 <sup>b</sup> < 5 <sup>j</sup> , 22 <sup>k</sup> , 310 <sup>l</sup> < 5 <sup>m</sup>	-	30 <sup>j</sup> , 100 <sup>n</sup> , 390 <sup>o</sup> , 2200 <sup>p</sup>	-
(7) <sup>c</sup>	-	52 <sup>b</sup>	-	-	-
(8) <sup>c</sup>	-	210 <sup>b</sup>	-	-	-
[ <i>p</i> - <i>t</i> -butyl-dihomo-CA[4]] <sup>-</sup> (9) <sup>a</sup>	2.5 x 10 <sup>3</sup>	8 x 10 <sup>2</sup>	-	-	-
Guanidinium-appended -CA (10) <sup>d</sup>	-	730 <sup>q</sup> , 130 <sup>r</sup>	-	-	-
RA[4] (Schneider) (11) <sup>s</sup>	50 <sup>t</sup>	-	6.5 <sup>t</sup>	29 <sup>u</sup>	3.4 <sup>u</sup>
RA[4] (12) <sup>v</sup>	-	2.5 x 10 <sup>4</sup> (pH 5.0) to 5 x 10 <sup>4</sup> (pH 8.5) <sup>v</sup>	-	-	-
Tetracyano-RA[4] (13) <sup>v,w</sup>	5.8 x 10 <sup>5</sup>	7 x 10 <sup>4</sup> (pH 5.0) to 1.1 x 10 <sup>6</sup> (pH 8.5) <sup>v</sup> , 6.2 x 10 <sup>5</sup> at pH 7.0 <sup>v</sup>	-	7.6 x 10 <sup>5</sup>	1.0 x 10 <sup>6</sup>
Pyrogallo[4]arene (14)	3.4 x 10 <sup>3,x</sup>	6.1 x 10 <sup>3,x</sup>	4.4 x 10 <sup>3,y</sup> , 1.8 x 10 <sup>4,z</sup>	-	-
RA[4] derivative (15) <sup>aa</sup>	-	1.2 x 10 <sup>3</sup>	-	-	-
Deep Cavitand (Rebek) (16) <sup>ab</sup>	2.60 x 10 <sup>4,ab</sup> , > 10 <sup>4,ac</sup>	1.50 x 10 <sup>4,ab</sup> , > 10 <sup>4,ac</sup>	1.5 x 10 <sup>2,ab</sup> , 1.4 x 10 <sup>2,ac</sup>	3.8 x 10 <sup>3,ab</sup> , 4.3 x 10 <sup>3,ac</sup>	1.20 x 10 <sup>4,ab</sup> , > 10 <sup>3,ac</sup>
Cyclotrimerethylene derivative (17)	-	76 <sup>ad</sup> , 63 <sup>ae</sup> , 23 <sup>af</sup>	-	-	-

Host	Choline (M <sup>-1</sup> )	Acetylcholine (M <sup>-1</sup> )	Carnitine (M <sup>-1</sup> )	NMe <sub>4</sub> <sup>+</sup> (M <sup>-1</sup> )	NEt <sub>4</sub> <sup>+</sup> (M <sup>-1</sup> )
Roelens Cyclophane (ether) (18) <sup>ag</sup>	-	92.5, <sup>f</sup> 443, <sup>ah</sup> 362 <sup>ai</sup>	-	165, <sup>f</sup> 1004, <sup>ah</sup> 458 <sup>ai</sup>	-
Roelens ester cyclophane (19) <sup>aj</sup>	-	3.68, <sup>f</sup> 13.1, <sup>ai</sup> 4.83, <sup>u</sup> 11.4 <sup>ak</sup>	-	6.6, <sup>f</sup> 29.7 <sup>ai</sup>	-
Macrocyclic (Lehn) (20) <sup>al</sup>	-	5.0 x 10 <sup>2 al</sup>	-	2.5 x 10 <sup>2 al</sup>	~ 10 <sup>2 al</sup>
Macrobicyclic (Lehn) (21) <sup>am</sup>	-	1.3 x 10 <sup>3 am</sup>	-	1.0 x 10 <sup>3 am</sup>	1.6 x 10 <sup>3 am</sup>
Dougherty's Receptor (22) <sup>an</sup>	-	2.0 x 10 <sup>4 an</sup>	-	-	-
Otto's receptor (23) <sup>ao</sup>	-	3.9 x 10 <sup>3 ao, t</sup>	-	8.5 x 10 <sup>2 ah, ao</sup>	5.6 x 10 <sup>4 ah, ao</sup>
Otto's receptor (24) <sup>ao</sup>	-	6.5 x 10 <sup>3 ao, t</sup>	-	6.5 x 10 <sup>3 ah, ao</sup>	3.2 x 10 <sup>4 ah, ao</sup>
Costa's Molecular Cleft (25) <sup>ap</sup>	1.45 x 10 <sup>4</sup>	8.6 x 10 <sup>3</sup>	-	-	-
CB*[6] (26)	~ 0 <sup>t</sup>	1.3 x 10 <sup>3 t</sup>	-	-	-
CB[7] <sup>ar</sup>	6.5 x 10 <sup>5</sup>	7.0 x 10 <sup>5</sup>	3.8 x 10 <sup>2</sup>	1.2 x 10 <sup>5</sup>	1.0 x 10 <sup>6</sup>

<sup>a</sup>Ref. 17, determined by <sup>1</sup>H NMR titration in acetone at 30 °C. <sup>b</sup>Ref. 81, I<sup>-</sup> counterion, CDCl<sub>3</sub> solution. <sup>c</sup>Ref. 81, by <sup>1</sup>H NMR titration. <sup>d</sup>Ref. 26, at pD 7.4, based on a fluorescence displacement study, aqueous solution. <sup>e</sup>Ref. 26, at pD 2.4, based on a fluorescence displacement study, aqueous solution. <sup>f</sup>Ref. 18, based on <sup>1</sup>H NMR titration at pH 7.3. <sup>g</sup>For L-carnitine. <sup>h</sup>Ref. 17, determined by spectrophotometric titration in acetonitrile at 25 °C. <sup>i</sup>Ref. 29, <sup>1</sup>H NMR titration conducted in CDCl<sub>3</sub>. <sup>j</sup>Ref. 29, *p*-toluenesulfonate counterion, CDCl<sub>3</sub> solvent. <sup>k</sup>Ref. 81, Cl<sup>-</sup> counterion, CDCl<sub>3</sub> solvent, CDCl<sub>3</sub> solvent. <sup>l</sup>Ref. 81, I<sup>-</sup> counterion, (CDCl<sub>2</sub>)<sub>2</sub> solvent. <sup>m</sup>Ref. 81, I<sup>-</sup> counterion, acetone-*d*<sub>6</sub> solvent. <sup>n</sup>Cl<sup>-</sup> counterion in CDCl<sub>3</sub> solvent, reference 29. <sup>o</sup>Trifluoroacetate (TFA) counterion, CDCl<sub>3</sub> solution, Ref. 29. <sup>p</sup>Picrate counterion, CDCl<sub>3</sub> solvent, ref. 29. <sup>q</sup>Ref. 82, in CHCl<sub>3</sub>. <sup>r</sup>Ref. 55, in CDCl<sub>3</sub>/CD<sub>3</sub>OD 99/1 (v/v), determined by <sup>1</sup>H NMR titration. <sup>s</sup>Ref. 37, in aqueous solution by <sup>1</sup>H NMR titration. <sup>t</sup>Cl<sup>-</sup> counterion. <sup>u</sup>Br<sup>-</sup> counterion. <sup>v</sup>Ref. 33, at varying pH (pH between 5.0 and 8.5), binding constant increased with increasing pH. <sup>w</sup>Ref. 34, determined by <sup>1</sup>H NMR titration in CD<sub>3</sub>OD at room temperature. <sup>x</sup>Ref. 42, ITC experiments in ethanol. <sup>y</sup>Ref. 42, by ITC data, for L-carnitine as cation. <sup>z</sup>Ref. 42, ITC experiments in ethanol, for L-carnitine as zwitterion. <sup>aa</sup>Ref. 40, from <sup>1</sup>H NMR titration in D<sub>2</sub>O at 27 °C, all counterions are I<sup>-</sup>. <sup>ab</sup>Ref. 50, based on ITC data. <sup>ac</sup>Ref. 50, based on <sup>1</sup>H NMR titration. <sup>ad</sup>Ref. 46, <sup>1</sup>H NMR titration in water. <sup>ae</sup>Ref. 46, fluorescence titration in water. <sup>af</sup>Ref. 46, fluorescence titration in physiological media (neuroal culture). <sup>ag</sup>Ref. 14, from <sup>1</sup>H NMR titration in CDCl<sub>3</sub>. <sup>ah</sup>Me<sub>2</sub>SnCl<sub>3</sub> counterion. <sup>ai</sup>Picrate counterion. <sup>aj</sup>Ref. 13, from <sup>1</sup>H NMR titration in CDCl<sub>3</sub>. <sup>ak</sup>I<sup>-</sup> counterion. <sup>al</sup>Ref. 7. <sup>am</sup>Ref. 9, aqueous solution, <sup>1</sup>H NMR titration. <sup>an</sup>Ref. 2, in aqueous solution. <sup>ao</sup>Ref. 15, determined by ITC in aqueous borate buffer, pH 9.0 at 25 °C. <sup>ap</sup>Ref. 16, in CDCl<sub>3</sub> at 21 °C by <sup>1</sup>H NMR titration, choline and acetylcholine were I<sup>-</sup> salts. <sup>aq</sup>Ref. 47, in aqueous solution by <sup>1</sup>H NMR titration. <sup>ar</sup>More detail, along with values for full series, provided in Table 5.2.

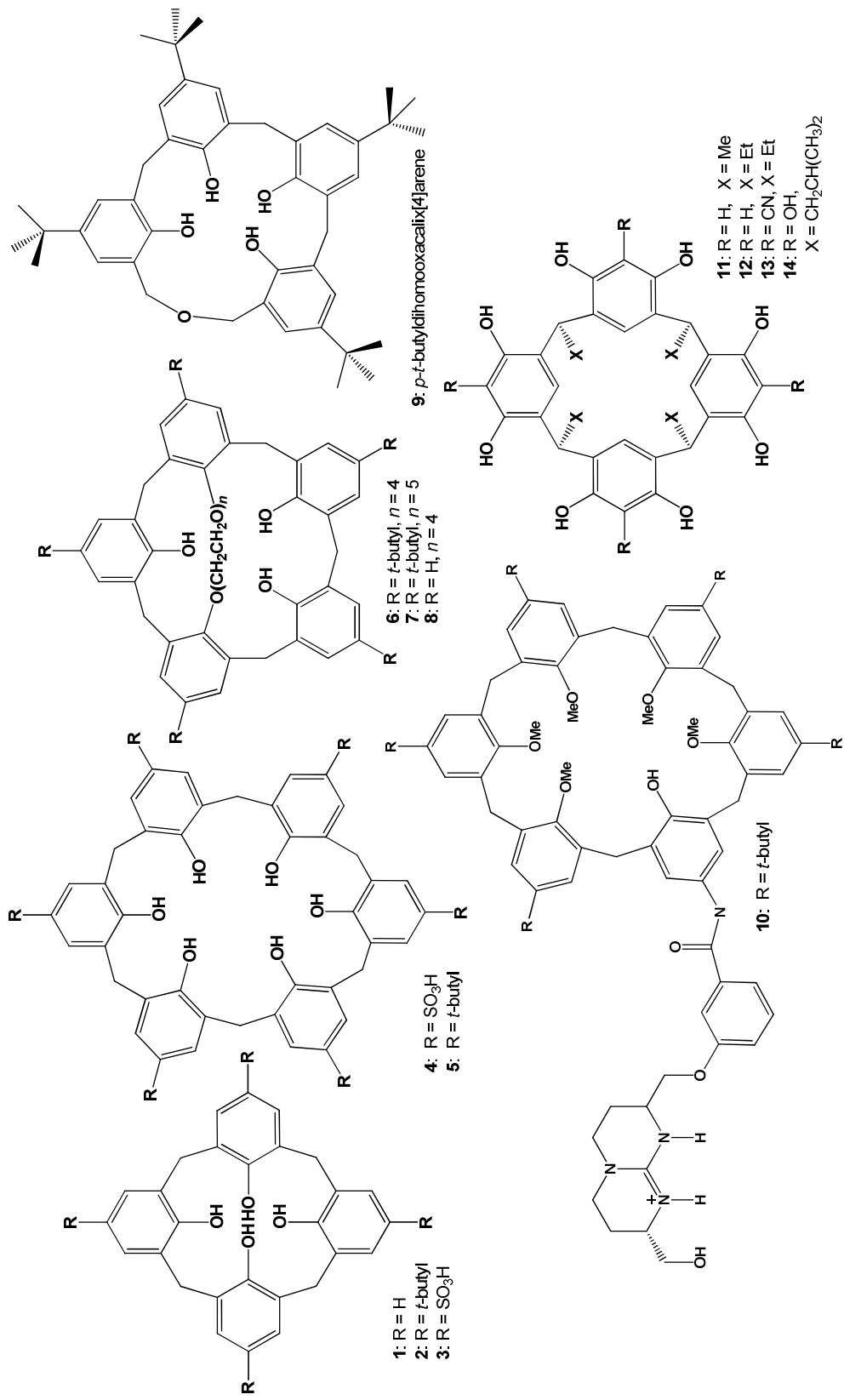


**Figure 5.22** Structures of compounds described in Table 5.4. The numbers in bold correspond to the entries in the table.

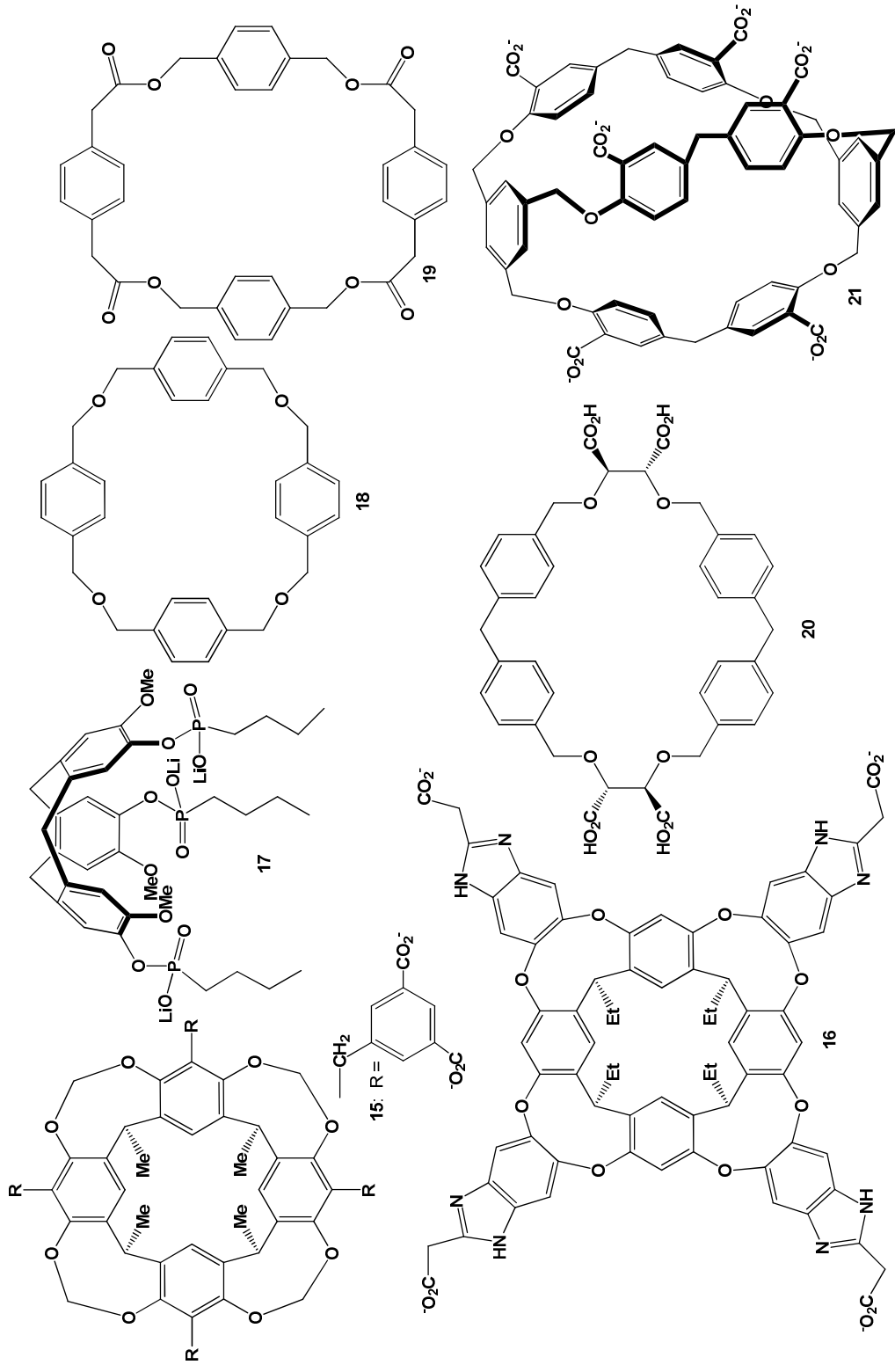


**Figure 5.22** Structures of compounds described in Table 5.4. The numbers in bold correspond to the entries in the table.

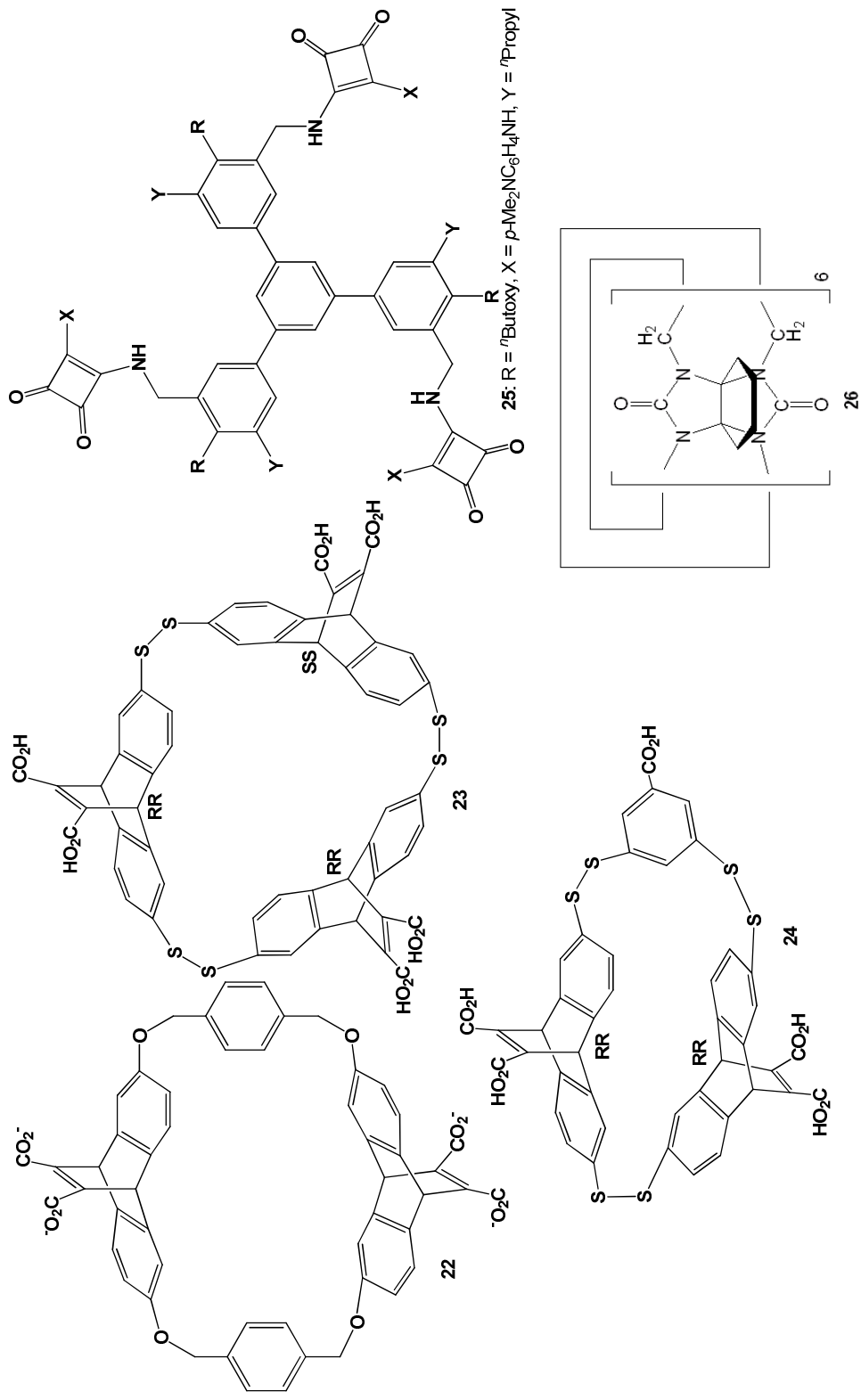


**Figure 5.22** Structures of compounds described in Table 5.4. The numbers in bold correspond to the entries in the table.



## 5.3 Experimental

### 5.3.1 Materials

Cucurbit[7]uril (CB[7]) was synthesized as described in Chapter 2 using the method developed by Day and coworkers.<sup>83</sup> Choline chloride, acetylcholine chloride, trimethylphosphine (1.0 M in THF), triethylphosphine (1.0 M in THF), triethylamine, 2-bromoethanol, 2-bromoethylacetate, quinuclidine hydrochloride (Sigma-Aldrich), 1-bromopentane (Eastman Kodak), and benzyldimethylcholine chloride (Fluka) were available commercially and used as received. The remaining compounds were prepared as described below, and their yields have not been optimized. Most of these products were hygroscopic, and were stored under argon in a desiccator.

#### Triethylpentylammonium bromide

A solution of 7.82 g (51.8 mmol) of 1-bromopentane and 5.79 g (57.2 mmol) triethylamine in 8 mL of acetonitrile was refluxed for 48 hr. Removal of the solvent yielded a hygroscopic reddish-brown solid, with a yield of 4.76 g (18.9 mmol, 36%). Melting point: 155-159 °C (literature value: 145-147 °C,<sup>84</sup> 147 °C<sup>85</sup>). <sup>1</sup>H NMR (D<sub>2</sub>O, 400 MHz): δ 3.24 (q, 6H, *J* = 7.2 Hz, N<sup>+</sup>-CH<sub>2</sub>CH<sub>3</sub>), 3.12 (t, 2H, *J* = 7.8 Hz, H<sub>α</sub>), 1.54 (qn, 2H, *J* = 7.8 Hz, H<sub>β</sub>), 1.32 (m, 4H, H<sub>γ</sub> and H<sub>δ</sub> overlapped), 1.23 (tt, 9H, *J* = 7.2 Hz, <sup>3</sup>*J*<sub>H-N</sub> = 1.9 Hz, N<sup>+</sup>-CH<sub>2</sub>CH<sub>3</sub>), 0.87 (t, 3H, *J* = 7.0 Hz, H<sub>ε</sub>) ppm. <sup>13</sup>C NMR (D<sub>2</sub>O, 100 MHz): δ 55.82 (t, *J* = 2.7 Hz, C<sub>α</sub>), 51.96 (t, *J* = 2.7 Hz, N<sup>+</sup>-CH<sub>2</sub>CH<sub>3</sub>), 26.88 (C<sub>δ</sub>), 20.66 (C<sub>δ</sub>), 19.71 (C<sub>β</sub>), 12.19 (C<sub>ε</sub>), and 5.76 (N<sup>+</sup>-CH<sub>2</sub>CH<sub>3</sub>) ppm. HR-ESI-MS: calc. for C<sub>11</sub>H<sub>26</sub>N<sup>+</sup> ([M-Br]<sup>+</sup>) *m/z* = 172.2060; found *m/z* = 172.2059.

### **(2-Hydroxyethyl)triethylammonium bromide**

A mixture of 0.724 g (5.79 mmol) of 2-bromoethanol and 0.665 g (6.57 mmol) of triethylamine in 3 mL of anhydrous ethanol was stirred at room temperature for four days. The precipitate was washed with ether and dried, to give 0.224 g (0.990 mmol) of product (Yield 17 %). Melting point: 250-253 °C (literature value: 256-257 °C<sup>86</sup>). <sup>1</sup>H NMR (D<sub>2</sub>O, 400 MHz): δ 3.92 (broad t, 2H, H $\beta$ ), 3.32 (q, 6H,  $J = 7.2$  Hz, N<sup>+</sup>-CH<sub>2</sub>CH<sub>3</sub>), 3.31 (t, overlapped with N<sup>+</sup>-CH<sub>2</sub>CH<sub>3</sub>, 2H, H $\alpha$ ), 1.22 (t, 9H,  $J = 7.2$  Hz, N<sup>+</sup>-CH<sub>2</sub>CH<sub>3</sub>) ppm. <sup>13</sup>C NMR (D<sub>2</sub>O, 100 MHz): δ 57.43 (C $\alpha$ ), 54.44 (C $\beta$ ), 53.38 (N<sup>+</sup>-CH<sub>2</sub>CH<sub>3</sub>), 6.69 (N<sup>+</sup>-CH<sub>2</sub>CH<sub>3</sub>) ppm. HR-ESI-MS: calc. for C<sub>8</sub>H<sub>20</sub>O<sub>2</sub>N<sup>+</sup> ([M-Br]<sup>+</sup>)  $m/z = 146.1534$ , found  $m/z = 146.1534$ .

### **(2-Hydroxyethyl)quinuclidinium bromide**

The quinuclidine precursor was prepared by placing 1.989 g (13.5 mmol) of quinuclidine hydrochloride in 270 mL of 0.10 M NaOH (27 mmol). The neutralized quinuclidine was isolated by extracting it from this solution with chloroform in a separatory funnel, and removing the chloroform under reduced pressure, to obtain 0.981 g (8.82 mmol) of quinuclidine (Yield 65 %). Subsequently, a solution of 0.517 g (5.79 mmol) of 2-bromoethanol and 0.391 g (3.52 mmol) of quinuclidine in 5 mL of THF was heated under argon at 50 °C for 4 hours. The product was washed with ether and dried, to provide a yield of 0.476 g (2.02 mmol, 57 % Yield). Melting Point: 231-233 °C. <sup>1</sup>H NMR (D<sub>2</sub>O, 400 MHz): δ 3.95 (broad t, 2H, H $\beta$ ), 3.44 (t, 6H, H<sub>2</sub>,  $J = 8.0$  Hz), 3.24 (t, 2H, H $\alpha$ ,  $J = 5.2$  Hz), 2.12 (hp, 1H, H<sub>4</sub>,  $J = 3.2$  Hz), 1.93 (m, 6H, H<sub>3</sub>) ppm. <sup>13</sup>C NMR: (D<sub>2</sub>O, 100 MHz) δ 65.31 (C $\alpha$ ), 55.50 (C<sub>2</sub>), 54.80 (C $\beta$ ), 23.61 (C<sub>3</sub>), 19.01 (C<sub>4</sub>) ppm. HR-ESI-MS: calc. for C<sub>9</sub>H<sub>18</sub>NO<sup>+</sup> ([M-Br]<sup>+</sup>)  $m/z = 156.1382$ , found  $m/z = 156.1382$ .

### ***N*-Methylquinuclidinium iodide**

A solution of 0.507 g (4.56 mmol) of quinuclidine in 8-10 mL of ethyl acetate was cooled in an ice bath. To this cooled solution 649 g (4.57 mmol) of iodomethane was added dropwise, to give a white precipitate. The precipitate was collected and washed with ether to give 0.746 g (2.95 mmol) of product (65 % yield). Melting Point: 275 °C (dec.) (Literature values > 300 °C<sup>87</sup>, 230 °C (dec.)<sup>88</sup>). <sup>1</sup>H NMR (D<sub>2</sub>O, 400 MHz): δ 3.41 (t, 6H, H<sub>2</sub>, *J* = 6.0 Hz), 2.91 (s, 3H, CH<sub>3</sub>), 2.18 (hp, 1H, H<sub>4</sub>, *J* = 3.2 Hz), 1.98 (broad m, 6H, H<sub>3</sub>) ppm. <sup>13</sup>C NMR (D<sub>2</sub>O, 100 MHz): δ 57.00 (t, C<sub>2</sub>, *J* = 3.0 Hz), 51.92 (t, CH<sub>3</sub>, *J* = 4.6 Hz), 23.50 (C<sub>3</sub>), 18.67 (t, C<sub>4</sub>, *J* = 4.8) ppm. HR-ESI-MS: calc. for C<sub>8</sub>H<sub>16</sub>N<sup>+</sup> ([M-I]<sup>+</sup>) *m/z* = 126.1277, found *m/z* = 126.1277.

### **1,4-Dimethyl-1,4-diazoniabicyclo[2.2.2]octane diiodide**

A solution of 0.498 g (4.44 mmol) of 1,4-diazabicyclo[2.2.2]octane (DABCO) in 5 mL of methanol was added dropwise to a solution of 1.895 g (13.4 mmol) iodomethane in 15 mL of methanol. The solution was refluxed for 2 hours, and the precipitate was collected and washed with petroleum ether. Yield 1.255 g (3.17 mmol, 71 %). Melting point: 261-265 °C (dec.) (literature value 253-258 °C<sup>89</sup>). <sup>1</sup>H NMR (D<sub>2</sub>O, 400 MHz): δ 4.06 (s, 12H, CH<sub>2</sub>), 3.39 (s, 6H, CH<sub>3</sub>) ppm. <sup>13</sup>C NMR (D<sub>2</sub>O, 100 MHz): δ 53.62 (d, CH<sub>2</sub>, *J*<sub>C-N</sub> = 3.2 Hz), 52.90 (d, CH<sub>3</sub>, *J*<sub>C-N</sub> = 3.9 Hz) ppm. HR-ESI-MS: calc. for C<sub>8</sub>H<sub>18</sub>N<sub>2</sub><sup>2+</sup> ([M-2I]<sup>2+</sup>) *m/z* = 71.0729, found *m/z* = 71.0731.

### **Trimethylpentylphosphonium bromide**

A solution of 0.755 g (5.00 mmol) of 1-bromopentane and 5.00 mL of 1.0 M trimethylphosphine (5.00 mmol) in THF was heated under argon at 70 °C for 12 hours. The precipitate was washed with ether and dried. Yield 0.0754 g (0.33 mmol, 7 %). Melting point:

174-176 °C.  $^1\text{H}$  NMR ( $\text{D}_2\text{O}$ , 400 MHz):  $\delta$  2.18 (m, 2H,  $\text{H}\alpha$ ), 1.84 (d, 9H,  $\text{P}^+\text{-CH}_3$ ,  $J_{\text{P-H}} = 15.6$  Hz), 1.61 (m, 2H,  $\text{H}\beta$ ,  $J = 7.2$  Hz), 1.44 (qn, 2H,  $\text{H}\gamma$ ,  $J = 7.2$  Hz), 1.35 (sx, 2H,  $\text{H}\delta$ ,  $J = 7.2$  Hz), 0.89 (td, 3H,  $\text{H}\epsilon$ ,  $J = 7.2$  Hz,  $J_{\text{P-H}} = 1.6$  Hz) ppm.  $^{13}\text{C}$  NMR  $\delta$  ( $\text{D}_2\text{O}$ , 100 MHz): 32.14 (d,  $\text{C}\gamma$ ,  $J_{\text{P-C}} = 15.5$  Hz), 22.95 (d,  $\text{C}\alpha$ ,  $J_{\text{P-C}} = 52.3$  Hz), 21.55 (s,  $\text{C}\delta$ ), 20.66 (d,  $\text{C}\beta$ ,  $J_{\text{P-C}} = 4.2$  Hz), 13.26 (s,  $\text{H}\epsilon$ ), 7.53 (d,  $\text{P}^+\text{-CH}_3$ ,  $J_{\text{P-C}} = 54.9$  Hz) ppm.  $^{31}\text{P}$  NMR ( $\text{D}_2\text{O}$ , 133 MHz):  $\delta$  25.93 ppm. HR-ESI-MS: calc. for  $\text{C}_8\text{H}_{20}\text{P}^+$  ( $[\text{M-Br}]^+$ )  $m/z = 147.1298$ , found  $m/z = 147.1298$ .

### Triethylpentylphosphonium bromide

A solution of 0.801 g (5.30 mmol) of 1-bromopentane and 6.00 mL of 1.0 M triethylphosphine (6.0 mmol) in THF were stirred under argon in a pressure tube for 12 hours at room temperature, followed by a further 6 hours at 60 °C. The product was washed with ether and dried. Yield 0.244 g (0.906 mmol, 17 %). Melting point: 176-178 °C.  $^1\text{H}$  NMR ( $\text{D}_2\text{O}$ , 400 MHz):  $\delta$  2.20 (m, 2H,  $\text{H}\alpha$ ), 2.19 (dq, 6H,  $\text{P}^+\text{-CH}_2\text{CH}_3$ ,  $J_{\text{P-H}} = 18.0$  Hz,  $J = 7.8$  Hz), 1.59 (q, 2H,  $\text{H}\beta$ ,  $J_{\text{P-H}} = 23.2$  Hz,  $J = 7.2$  Hz), 1.44 (q, 2H,  $\text{H}\gamma$ ,  $J = 7.2$  Hz), 1.36 (sx, 2H,  $\text{H}\delta$ ,  $J = 7.2$  Hz), 1.22 (dt, 9H,  $\text{P}^+\text{-CH}_2\text{CH}_3$ ,  $J_{\text{P-H}} = 18.0$  Hz,  $J = 7.8$  Hz), 0.89 (t, 3H,  $\text{H}\epsilon$ ,  $J = 7.2$  Hz) ppm.  $^{13}\text{C}$  NMR ( $\text{D}_2\text{O}$ , 100 MHz):  $\delta$  32.39 (d,  $\text{C}\gamma$ ,  $J_{\text{P-C}} = 14.5$  Hz), 21.54 (s,  $\text{C}\delta$ ), 20.47 (d,  $\text{C}\alpha$ ,  $J_{\text{P-C}} = 47.8$  Hz), 16.90 (d,  $\text{C}\beta$ ,  $J_{\text{P-C}} = 4.3$  Hz), 13.28 (s,  $\text{C}\epsilon$ ), 11.24 (d,  $\text{P}^+\text{-CH}_2\text{CH}_3$ ,  $J_{\text{P-C}} = 49.3$  Hz), 4.94 (d,  $\text{P}^+\text{-CH}_2\text{CH}_3$ ,  $J_{\text{P-C}} = 5.2$  Hz) ppm.  $^{31}\text{P}$  NMR ( $\text{D}_2\text{O}$ , 133 MHz):  $\delta$  38.55 ppm. HR-ESI-MS: calc. for  $\text{C}_{11}\text{H}_{26}\text{P}^+$  ( $[\text{M-Br}]^+$ )  $m/z = 189.1766$ , found  $m/z = 189.1766$ .

### **(2-Hydroxyethyl)trimethylphosphonium bromide**

A solution of 0.618 g (5.95 mmol) of 2-bromoethanol and 5.00 mL of 1.0 M trimethylphosphine (5.0 mmol) in THF was heated at 70 °C in a pressure tube under argon for 12 hours. A precipitate was produced, which was collected and washed with ether, then dried. Yield 0.483 g (2.40 mmol, 48 %). Melting point: 290-292 °C. <sup>1</sup>H NMR (D<sub>2</sub>O, 400 MHz): δ 3.97 (dt, 2H, H $\beta$ ,  $J_{\text{P-H}} = 20.0$  Hz,  $J = 6.2$  Hz), 2.45 (dt, 2H, H $\alpha$ ,  $J_{\text{P-H}} = 13.2$  Hz,  $J = 6.2$  Hz), 1.87 (d, 9H, P<sup>+</sup>-CH<sub>3</sub>,  $J_{\text{P-H}} = 14.8$  Hz) ppm. <sup>13</sup>C NMR (D<sub>2</sub>O, 100 MHz): δ 54.88 (d, C $\beta$ ,  $J_{\text{P-C}} = 6.3$  Hz), 26.20 (d, C $\alpha$ ,  $J_{\text{P-C}} = 54.0$ ), 8.15 (d, P<sup>+</sup>-CH<sub>3</sub>,  $J_{\text{P-C}} = 54.9$  Hz) ppm. <sup>31</sup>P NMR (D<sub>2</sub>O, 133 MHz): δ 25.34 ppm. HR-ESI-MS: calc. for C<sub>5</sub>H<sub>14</sub>OP<sup>+</sup> ([M-Br]<sup>+</sup>)  $m/z = 121.0776$ , found  $m/z = 121.0772$ .

### **(2-Hydroxyethyl)triethylphosphonium bromide**

A solution of 0.800 g (6.40 mmol) of 2-bromoethanol and 7.00 mL of 1.0 M triethylphosphine (7.0 mmol) in THF was heated under argon at 70 °C for 24 hours. The product was washed with ether and dried. Yield 0.158 g (0.65 mmol, 10 %). Melting point: 221-225 °C (literature value 223 °C<sup>78</sup>). <sup>1</sup>H NMR (D<sub>2</sub>O, 400 MHz): δ 3.91 (dt, 2H, H $\beta$ ,  $J_{\text{P-H}} = 17.6$  Hz,  $J = 6.2$  Hz), 2.42 (dt, 2H, H $\alpha$ ,  $J_{\text{P-H}} = 12.4$  Hz,  $J = 6.2$  Hz), 2.21 (dq, 6H, P<sup>+</sup>-CH<sub>2</sub>CH<sub>3</sub>,  $J_{\text{P-H}} = 13.2$  Hz,  $J = 7.7$  Hz), 1.18 (dt, 9H, P<sup>+</sup>-CH<sub>2</sub>CH<sub>3</sub>,  $J_{\text{H-P}} = 18.4$  Hz,  $J = 7.7$  Hz) ppm. <sup>13</sup>C NMR (D<sub>2</sub>O, 100 MHz): δ 54.60 (d, C $\beta$ ,  $J_{\text{P-C}} = 5.0$  Hz), 20.48 (d, C $\alpha$ ,  $J_{\text{P-C}} = 49.0$  Hz), 11.60 (d, P<sup>+</sup>-CH<sub>2</sub>CH<sub>3</sub>,  $J_{\text{P-C}} = 49.4$  Hz), 4.64 (d, P<sup>+</sup>-CH<sub>2</sub>CH<sub>3</sub>,  $J_{\text{P-C}} = 5.4$  Hz) ppm. <sup>31</sup>P NMR (D<sub>2</sub>O, 133 MHz): δ 37.92 ppm. HR-ESI-MS: calc. for C<sub>8</sub>H<sub>20</sub>OP<sup>+</sup> ([M-Br]<sup>+</sup>)  $m/z = 163.1246$ , found  $m/z = 163.1246$ .

### **(2-Acetoxyethyl)trimethylphosphonium bromide**

A solution of 0.707 g (4.23 mmol) of 2-bromoethylacetate and 5.10 mL of 1.0 M trimethylphosphine (5.1 mmol) in THF was heated at 70 °C under argon for 72 hours. The hygroscopic product was washed with ether and dried, and stored under argon. Yield 0.348 g (1.43 mmol, 34 %). Melting point: 59-62 °C. <sup>1</sup>H NMR (D<sub>2</sub>O, 400 MHz): δ 4.43 ppm (dt, 2H, H<sub>β</sub>,  $J_{P-H} = 19.6$  Hz,  $J = 6.2$  Hz), 2.65 (dt, 2H, H<sub>α</sub>,  $J_{P-H} = 13.2$  Hz,  $J = 6.2$  Hz), 2.10 ppm (s, 3H, H<sub>ε</sub>), 1.91 (d, P<sup>+</sup>-CH<sub>3</sub>,  $J_{P-H} = 14.8$  Hz) ppm. <sup>13</sup>C NMR (D<sub>2</sub>O, 100 MHz): δ 173.32 (s, CO), 57.93 (d, C<sub>β</sub>,  $J_{P-C} = 6.0$  Hz), 23.04 (d, C<sub>α</sub>,  $J_{P-C} = 54.0$  Hz), 20.19 (s, CO), 7.88 (d, P<sup>+</sup>-CH<sub>3</sub>,  $J_{P-C} = 55.0$  Hz) ppm. <sup>31</sup>P (D<sub>2</sub>O, 133 MHz): δ 25.84 ppm. HR-ESI-MS: calc. for C<sub>7</sub>H<sub>16</sub>O<sub>2</sub>P<sup>+</sup> ([M-Br]<sup>+</sup>) =  $m/z$  163.0882, found  $m/z = 163.0888$ .

### **(2-Acetoxyethyl)triethylphosphonium bromide**

A solution of 0.749 g (4.48 mmol) of 2-bromoethylacetate and 5.00 mL of 1.0 M triethylphosphine (5.0 mmol) in THF was heated at 60 °C for 12 hours, with a further 12 hours at room temperature. The hygroscopic product was washed with ether, dried, and stored under argon. Yield 0.177 g (0.621 mmol, 14 %). Melting point: 58-64 °C (literature value 74.6 °C<sup>90</sup>). <sup>1</sup>H NMR (D<sub>2</sub>O, 500 MHz): δ 4.41 (dt, 2H, H<sub>β</sub>,  $J_{P-H} = 17.5$  Hz,  $J = 6.5$  Hz), 2.65 (dt, 2H, H<sub>α</sub>,  $J_{P-H} = 12.5$  Hz,  $J = 6.5$  Hz), 2.27 (dq, 6H, P<sup>+</sup>-CH<sub>2</sub>CH<sub>3</sub>,  $J_{P-H} = 12.8$  Hz,  $J = 7.6$  Hz), 2.10 (s, 3H, H<sub>ε</sub>), 1.23 (dt, 9H, P<sup>+</sup>-CH<sub>2</sub>CH<sub>3</sub>,  $J_{P-H} = 19.0$  Hz,  $J = 7.6$  Hz) ppm. <sup>13</sup>C NMR (D<sub>2</sub>O, 100 MHz): δ 173.30 (s, CO), 57.75 (d,  $J_{P-C} = 5.4$  Hz), 20.17 (s, C<sub>ε</sub>), 17.26 (d, C<sub>α</sub>,  $J_{P-C} = 49.3$  Hz), 11.51 (d, P<sup>+</sup>-CH<sub>2</sub>CH<sub>3</sub>,  $J_{P-C} = 48.8$  Hz), 4.62 (d, P<sup>+</sup>-CH<sub>2</sub>CH<sub>3</sub>,  $J_{P-C} = 5.4$  Hz) ppm. <sup>31</sup>P NMR (D<sub>2</sub>O, 133 MHz): δ 38.34 ppm. HR-ESI-MS: calc. for C<sub>10</sub>H<sub>22</sub>O<sub>2</sub>P<sup>+</sup> ([M-Br]<sup>+</sup>)  $m/z = 205.1351$ , found  $m/z = 205.1352$ .

### 5.3.2 Methods

The  $^1\text{H}$ ,  $^{13}\text{C}$ , and  $^{31}\text{P}$  NMR spectra were recorded on Bruker Avance 400 and 500 MHz spectrometers in  $\text{D}_2\text{O}$ . Assignments of the  $^{13}\text{C}$  NMR resonances were assisted by 2D NMR spectroscopy, such as HSQC and HMBC. High-resolution mass spectra were recorded on a QStar XL QqTOF instrument in the positive mode, with an ESI source. The host-guest binding affinities between CB[7] and ( $\pm$ )-carnitine and choline phosphate were determined by  $^1\text{H}$  NMR titrations, using a least-squares fitting to a 1:1 host-guest binding model, using Equations 2.2, 2.3 and 2.4. With the exception of these guests, the majority of the guests had binding constants to CB[7] ( $K_{\text{CB}[7]}$ ) that were too strong to be measured directly by titration, and instead competitive binding methods were used, as developed by Isaacs and coworkers, in a  $\text{D}_2\text{O}$  solution of 0.05 M NaOAc- $d_3$  and 0.025 M DCl at 298 K.<sup>63</sup> Competitor guests, with known CB[7] binding constants (shown in brackets) that were used in these experiments, have included *p*-xylylenediamine ( $K_{\text{CB}[7]} = (1.84 \pm 0.34) \times 10^9 \text{ M}^{-1}$ ),<sup>63</sup> 3-(trimethylsilyl)propionic-2,2,3,3- $d_4$  acid ( $K_{\text{CB}[7]} = (1.82 \pm 0.22) \times 10^7 \text{ M}^{-1}$ ),<sup>63</sup> tetramethylphosphonium bromide ( $K_{\text{CB}[7]} = (2.2 \pm 0.4) \times 10^6 \text{ M}^{-1}$ ),<sup>62</sup> 1,4-phenylenediamine ( $K_{\text{CB}[7]} = (2.07 \pm 0.33) \times 10^6 \text{ M}^{-1}$ ),<sup>63</sup> tetraethylammonium bromide ( $K_{\text{CB}[7]} = (1.0 \pm 0.2) \times 10^6 \text{ M}^{-1}$ ),<sup>62</sup> tetraethylphosphonium chloride ( $K_{\text{CB}[7]} = (1.3 \pm 0.3) \times 10^5 \text{ M}^{-1}$ ),<sup>62</sup> and 1,2-phenylenediamine ( $K_{\text{CB}[7]} = (8.04 \pm 1.28) \times 10^4 \text{ M}^{-1}$ ).<sup>63</sup> These competitors were purchased from Sigma-Aldrich and use as received.

## 5.4 Conclusions

Cucurbit[7]uril was observed to bind to a variety of choline and acetylcholine analogues, with a wide range of binding affinities being observed within the series. The binding constants are dependent upon the central atom of the quaternary head group (N or P) as well as the substituents at that head group. In addition, these binding constants are also dependent on the presence of substituents as well as charges at the opposite end of the guests, as well as along the ethylene linker. The placement of the CB[7] cavity also varies upon complexation with members of this series of guests, indicating a tendency to become more localized over the host when a head group is present to which the CB[7] has a higher affinity, which parallels results from an earlier study involving tetraalkylammonium and  $\text{-phosphonium}$  salts.<sup>62</sup> On the other hand, the presence of an extended backbone of the guest (especially a hydrophobic backbone, such as a pentyl arm) could compete with the head group for binding to the cavity, with the CB[7] becoming more localized at that arm at the expense of the head group. The presence of benzyl and quinuclidinium moieties at the head group of the guest cause the CB[7] to become localized over those respective regions, and also provide for high host-guest binding affinities.

Despite the lack of an anionic charge or aromatic units within its framework, CB[7] is able to form host-guest complexes with a variety of the choline and acetylcholine compounds, as well as their derivatives. The magnitudes of the binding affinities between CB[7] and guests such as choline, acetylcholine, and carnitine are generally in the upper range when compared to other hosts.

The encapsulation of the cationic regions of the guests by CB[7], as observed in this study with the choline guests, as well as earlier with the tetraalkylammonium and  $\text{-phosphonium}$  guests,<sup>62</sup> is somewhat unusual, with cationic components of a guest (such as a primary ammonium) normally being located on the exterior of the cavity, near the electron donating



portals, whilst the hydrophobic region of the guest (such as an aromatic group or an alkyl chain) is normally positioned within the hydrophobic cavity. The peralkylation of these nitrogen and phosphorus centers has created more charge-diffuse cations, which are more hydrophobic in nature. The research described in this chapter has been published in *Organic and Biomolecular Chemistry*.<sup>72</sup>

## References

1. I. Silman and J.L. Sussman, *Curr. Opin. Pharm.*, **2005**, *5*, 293.
2. D.A. Dougherty and D.A. Stauffer, *Science*, **1990**, *250*, 1558.
3. J.C. Ma and D.A. Dougherty, *Chem. Rev.*, **1997**, *97*, 1303.
4. N. Zacharias and D.A. Dougherty, *Trends Pharm. Sci.*, **2002**, *23*, 281.
5. M.J. Minch, J.P. Sevenair, and C. Henling, *J. Org. Chem.*, **1979**, *44*, 3247.
6. K. Ito, K. Nagase, N. Morahashi, and Y. Ohba, *Chem. Pharm. Bull.*, **2005**, *53*, 90.
7. M. Dhaenens, L. Lacombe, J.-M. Lehn, and J.-P. Vigneron, *J. Chem. Soc., Chem. Commun.*, **1984**, 1097.
8. T.H. Webb, H. Suh, and C.S. Wilcox, *J. Am. Chem. Soc.*, **1991**, *113*, 8554.
9. R. Meric, J.-P. Vigneron, and J.-M. Lehn, *J. Chem. Soc., Chem. Commun.*, **1993**, 129.
10. S.M. Ngola and D.A. Dougherty, *J. Org. Chem.*, **1998**, *63*, 4566.
11. S.M. Ngola, P.C. Kearny, S. Mecozzi, K. Russell, and D.A. Dougherty, *J. Am. Chem. Soc.*, **1999**, *121*, 1192.
12. P.C. Kearny, L.S. Mizoue, R.A. Kumpf, J.E. Forman, A. McCurdy, and D.A. Dougherty, *J. Am. Chem. Soc.*, **1993**, *115*, 9907.
13. S. Bartoli and S. Roelens, *J. Am. Chem. Soc.*, **2002**, *124*, 8307.
14. P. Sarri, F. Venturi, F. Cuda, and S. Roelens, *J. Org. Chem.*, **2004**, *69*, 3654.
15. P.T. Corbett, J.K.M. Sanders, and S. Otto, *Chem. Eur. J.*, **2008**, *14*, 2153.
16. S. Tomas, R. Prohens, M. Vega, M.C. Rotger, P.M. Deya, P. Ballester, and A. Costa, *J. Org. Chem.*, **1996**, *61*, 9394.
17. J.M. Harrowfield, W.B. Richmond, and A.N. Sobolev, *J. Incl. Phenom. Mol. Recognit. Chem.*, **1994**, *19*, 257.

18. J.-M. Lehn, R. Meric, J.-P. Vigneron, M. Cesario, J. Guilhelm, C. Pascard, Z. Asfari, and J. Vicens, *Supramol. Chem.*, **1995**, *5*, 97.
19. J.L. Atwood, L.J. Barbour, P.C. Junk, and G.W. Orr, *Supramol. Chem.*, **1995**, *5*, 105.
20. K.N. Koh, K. Araki, A. Ikeda, H. Otsuka, and S. Shinkai, *J. Am. Chem. Soc.*, **1996**, *118*, 755.
21. G. Arena, A. Casnati, L. Mirone, D. Sciotto, and R. Ungaro, *Tetrahedron Lett.*, **1997**, *38*, 1999.
22. G. Arena, A. Casnati, A. Contino, G.G. Lombardo, D. Sciotto, and R. Ungaro, *Chem. Eur. J.*, **1999**, *5*, 738.
23. G. Arena, A. Casnati, A. Contino, F.G. Gulino, D. Sciotto, and R. Ungaro, *J. Chem. Soc., Perkin Trans. 2*, **2000**, 419.
24. T. Jin, *J. Incl. Phenom. Macrocycl. Chem.*, **2003**, *45*, 195.
25. A. Specht, F. Ziarelli, P. Bernard, M. Goeldner, and L. Peng, *Helv. Chim. Acta*, **2005**, *88*, 2641.
26. H. Bakirci and W.M. Nau, *Adv. Funct. Mater.*, **2006**, *16*, 237.
27. L.-H. Wang, D.-S. Guo, Y. Chen, and Y. Liu, *Thermochim. Acta*, **2006**, *443*, 132.
28. N. Korbakov, P. Timmerman, N. Lidich, B. Urbach, A. Sa'ar, and S. Yitzchaik, *Langmuir*, **2008**, *24*, 2580.
29. V. Bohmer, A.D. Cort, and L. Mandolini, *J. Org. Chem.*, **2001**, *66*, 1900.
30. B. Masci, S.L. Mortera, D. Persiani, and P. Thuery, *J. Org. Chem.*, **2006**, *71*, 504.
31. T. Haino, H. Fukuoka, M. Katayama, and Y. Fukazawa, *Chem. Lett.*, **2007**, *36*, 1054.
32. M. Fehlinger and W. Abraham, *J. Incl. Phenom. Macrocycl. Chem.*, **2007**, *58*, 263.
33. S.-D. Tan, W.-H. Chen, A. Satake, B. Wang, Z.-L. Xu, and Y. Kobuke, *Org. Biomol. Chem.*, **2004**, *2*, 2719.
34. W.-H. Chen, Y. Wei, S.-D. Tan, B. Wang, and Z.-L. Xu, *Supramol. Chem.*, **2005**, *17*, 469.

35. H.-J. Schneider, D. Guttes, and U. Schneider, *Angew. Chem., Int. Ed. Engl.*, **1986**, *25*, 647.
36. H.-J. Schneider and U. Schneider, *J. Org. Chem.*, **1987**, *52*, 1613.
37. H.-J. Schneider, D. Guttes, and U. Schneider, *J. Am. Chem. Soc.*, **1988**, *110*, 6449.
38. H.-J. Schneider and U. Schneider, *J. Incl. Phenom. Mol. Recognit. Chem.*, **1994**, *19*, 67.
39. M. Inouye, K. Hashimoto, and K. Isagawa, *J. Am. Chem. Soc.*, **1994**, *116*, 5517.
40. S.J. Park and J.-I. Hong, *Tetrahedron Lett.*, **2000**, *41*, 8311.
41. K. Salorinne, T.-R. Tero, K. Riikonen, and M. Nissinen, *Org. Biomol. Chem.*, **2009**, *7*, 4211.
42. B. Schnatwinkel, M.V. Rekharsky, V.V. Borovkov, Y. Inoue, and J. Mattay, *Tetrahedron Lett.*, **2009**, *50*, 1374.
43. P.S. Bates, R. Katakya, and D. Parker, *J. Chem. Soc., Chem. Commun.*, **1993**, 691.
44. D. Parker, R. Katakya, P.M. Kelly, and S. Palmer, *Pure Appl. Chem.*, **1996**, *68*, 1219.
45. R.L.E. Furlan, Y.-F. Ng, G.R.L. Cousins, J.E. Redman, and J.K.M. Sanders, *Tetrahedron*, **2002**, *58*, 771.
46. M.-L. Dumartin, C. Givelet, P. Meyrand, B. Bibal, and I. Gosse, *Org. Biomol. Chem.*, **2009**, *7*, 2725.
47. J. Zhao, H.-J. Kim, J. Oh, S.-Y. Kim, J.W. Lee, S. Sakamoto, K. Yamaguchi, and K. Kim, *Angew. Chem., Int. Ed.*, **2001**, *40*, 4233.
48. P. Ballester, A. Shivanyuk, A.R. Far, and J. Rebek, Jr., *J. Am. Chem. Soc.*, **2002**, *124*, 14014.
49. F. Hof, L. Trembleau, E.C. Ullrich, and J. Rebek, Jr., *Angew. Chem., Int. Ed.*, **2003**, *42*, 3150.
50. S.M. Biros, E.C. Ullrich, F. Hof, L. Trembleau, and J. Rebek, Jr., *J. Am. Chem. Soc.*, **2004**, *126*, 2870.
51. A. Lledo, R.J. Hooley, and J. Rebek, Jr., *Org. Lett.*, **2008**, *10*, 3669.
52. F.H. Zelder and J. Rebek, Jr, *Chem. Commun.*, **2006**, 753.

53. A. Gissot and J. Rebek, Jr., *J. Am. Chem. Soc.*, **2004**, *126*, 7424.
54. S. Richeter and J. Rebek, Jr., *J. Am. Chem. Soc.*, **2004**, *126*, 16280.
55. F. Cuevas, S. Di Stefano, J.O. Magrans, P. Prados, L. Mandolini, and J. de Mendoza, *Chem. Eur. J.*, **2000**, *6*, 3228.
56. B.S. Szwegold, F. Kappler, M. Moldes, C. Shaller, and T.R. Brown, *NMR Biomed.*, **1994**, *7*, 121.
57. J.V. Jimenez, T.L. Richards, A.C. Heide, J.R. Grierson, and E.G. Shankland, *Magn. Res. Med.*, **1995**, *33*, 285.
58. J.C. Street, B.S. Szwegold, C. Matei, F. Kappler, U. Mahmoud, T.R. Brown, and J.A. Koutcher, *Magn. Res. Med.*, **1997**, *38*, 769.
59. G. Pettins, M. Potter, R.J. Leatherbarrow, and R.A. Dwek, *Biochemistry*, **1982**, *21*, 4927.
60. W.L. Mock and N.-Y. Shih, *J. Org. Chem.*, **1986**, *51*, 4440.
61. L. Isaacs, *Chem. Commun.*, **2009**, 619.
62. A.D. St-Jacques, I.W. Wyman, and D.H. Macartney, *Chem. Commun.*, **2008**, 4936.
63. S. Liu, C. Ruspic, P. Mukhopadhyay, S. Chakrabarti, P.Y. Zavalij, and L. Isaacs, *J. Am. Chem. Soc.*, **2005**, *127*, 15959.
64. F. Perret, J.-P. Morel, and N. Morel-Desrosiers, *Supramol. Chem.*, **2003**, *15*, 199.
65. H.-J. Schneider, D. Guttes, and U. Schneider, *J. Am. Chem. Soc.*, **1988**, *110*, 6449.
66. W.-H. Chen, Y. Wei, S.-D. Tan, B. Wang, and Z.-L. Xu, *Supramol. Chem.*, **2005**, *17*, 469.
67. B.-L. Poh and C.M. Teem, *Tetrahedron*, **2005**, *61*, 5123.
68. P.T. Corbett, J.K.M. Sanders, and S. Otto, *Chem. Eur. J.*, **2008**, *14*, 2153.
69. R. Meric, J.-M. Lehn, and J.-P. Vigneron, *Bull. Soc. Chim. Fr.*, **1994**, *131*, 579.
70. *Chem3D Pro 11.0*, CambridgeSoft, Cambridge, MA, 2007.
71. I.W. Wyman and D.H. Macartney, *J. Org. Chem.*, **2009**, *74*, 8031.

72. I.W. Wyman and D.H. Macartney, *Org. Biomol. Chem.*, **2010**, *8*, 253.
73. Y. H. Ko, H. Kim, Y. Kim, K. Kim, *Angew. Chem., Int. Ed.*, **2008**, *47*, 4106.
74. P. De Maria, A. Fontana, S. Frascari, G. Gargaro, D. Spinelli, and M.O. Tinti, *J. Pharm. Sci.*, **1994**, *83*, 742.
75. I.W. Wyman and D.H. Macartney, *Org. Biomol. Chem.*, **2008**, *6*, 1796.
76. W. Ong and A.E. Kaifer, *J. Org. Chem.*, **2004**, *69*, 1383.
77. C. Marquez, R.R. Hudgins, and W.M. Nau, *J. Am. Chem. Soc.*, **2004**, *126*, 5806.
78. E. Mezzina, F. Cruciani, G.F. Pedulli, and M. Lucarini, *Chem. Eur. J.*, **2007**, *13*, 7223.
79. M.V. Rekharsky, T. Mori, C. Yang, Y.H. Ko, N. Selvapalam, H. Kim, D. Sobransingh, A.E. Kaifer, S. Liu, L. Isaacs, W. Chen, S. Moghaddam, M.K. Gilson, K. Kim, and Y. Inoue, *Proc. Natl. Acad. Sci. U.S.A.*, **2007**, *104*, 20737.
80. G.A. Vincil and A.R. Urbach, *Supramol. Chem.*, **2008**, *20*, 681.
81. R. Arnecke, V. Bohmer, R. Cacciapaglia, A.D. Cort, and L. Mandolini, *Tetrahedron*, **1997**, *53*, 4901.
82. J.O. Magrans, A.R. Ortiz, M.A. Mollins, P.H.P. Lebouille, J. Sanchez-Quesada, P. Prados, M. Pons, F. Gago, and J. de Mendoza, *Angew. Chem., Int. Ed. Engl.*, **1996**, *35*, 1712.
83. A. Day, A.P. Arnold, R.J. Blanch, and B. Snushall, *J. Org. Chem.*, **2001**, *66*, 8094.
84. J.C. Kellett, Jr. and W.C. Doggett, *J. Pharm. Sci.*, **1966**, *55*, 414.
85. J.M. Orosz and J.G. Wetmur, *Biopolymers*, **1977**, *16*, 1183.
86. M.F. Shostakovskii, *Izv. Akad. Nauk SSSR, Ser. Khim.*, **1958**, 204.
87. J.J. Jaminski, K.W. Knutson, and N. Bodor, *Tetrahedron*, **1978**, *34*, 2857.
88. N.A. Horenstein, F.M. Leonik, and R.L. Papke, *Mol. Pharmacol.*, **2008**, *74*, 1496.
89. V.I. Vysochin and G.V. Shishkin, *Khimiya Geterotsiklicheskikh Soedinenii*, **1982**, *2*, 250.
90. R.R. Renshaw and R.A. Bishop, *J. Am. Chem. Soc.*, **1938**, *60*, 946.

## Chapter 6

# Host-Guest Complexes and Pseudorotaxanes of Cucurbit[7]uril with Acetylcholinesterase Inhibitors

### 6.1 Introduction

The serine hydrolase acetylcholinesterase (AChE) is an enzyme that efficiently hydrolyzes the neurotransmitter acetylcholine (Figures 6.1 and 6.2).<sup>1-3</sup> The efficiency of acetylcholinesterase is such that it hydrolyses substrates at near the diffusion control.<sup>1,2</sup> Despite its high activity, AChE's active site is located at the base of a narrow 20 Å-long gorge that is lined with aromatic residues, which is often called the *acylation site* (also called the *active site*, or sometimes simply the *A-site*).<sup>2-4</sup> A number of structural features appear to facilitate this enzyme's high activity, such as: (a) the indole ring of a nearby tryptophan (Trp) which employs cation- $\pi$  binding with the trimethylammonium group of the acetylcholine substrate, (b) a Glu-His-Ser "catalytic triad" is involved in the hydrolysis of the substrate's ester moiety, and (c) an "acyl pocket" is involved in the binding to the acetyl group of the substrate, with two Phe residues playing a prominent role in this binding subsite.<sup>2</sup> Another, more exposed, active site of acetylcholinesterase is called the *peripheral site* (sometimes abbreviated as the *P-site*), and is located near the entrance to the gorge. This site is also involved with cation- $\pi$  binding between the trimethylammonium group of a substrate and the indole ring of a tryptophan residue at this site.<sup>2</sup> This peripheral site is approximately 12-15 Å away from the receptor in the acylation site.<sup>3</sup> While some substrates will bind selectively to either the acylation or the peripheral sites, bisquaternary substrates can sometimes span the distance between the two sites, with one of its

trimethylammonium groups bound to the acylation site and the other bound to the peripheral site.<sup>2,3</sup>

Through its hydrolysis of acetylcholine, the primary role of AChE is to terminate impulse transmissions at the cholinergic synapses.<sup>2,4</sup> As a result of this key biological role carried out by this enzyme, acetylcholinesterase is the target of a variety of toxins, both natural and synthetic, in addition to drugs designed to treat neuromuscular disorders.<sup>2</sup> In addition, acetylcholinesterase is the target of neuromuscular blocking drugs, which are used to cause temporary muscle paralysis of a patient during surgical procedures such as tracheal intubation, or other procedures that require paralysis of the patient in order to facilitate the procedure.<sup>5</sup>

There has also been an interest in the roles of AChE and the related butyrylcholinesterase enzyme in Alzheimer's disease (AD).<sup>6</sup> It has been known since the mid-1970s that the pathogenesis of AD is associated with a deficiency of the enzyme that produces acetylcholine, choline acetyltransferase, and subsequently that it is also accompanied by a shortage of acetylcholine itself.<sup>6-14</sup> More recently, it has been acknowledged that butyrylcholinesterase, once thought to have no significant role in the central nervous system, is also capable of hydrolyzing acetylcholine in the brain.<sup>15</sup> In addition, while the activity of acetylcholinesterase was noted to decline in AD patients, the activity of butyrylcholinesterase has been noted to increase,<sup>16</sup> suggesting it may therefore have a greater role in the hydrolysis of acetylcholine with AD patients.<sup>15,16</sup> In order to mitigate the deficit of acetylcholine experienced by patients with mild to moderate AD, AChE inhibitors such as rivastigmine, donepezil, tacrine, or galantamine are used as standard treatment.<sup>6</sup> In cases of moderate to severe AD, the N-methyl-D-aspartate receptor antagonist memantine is used either alone, or in combination with one of the acetylcholinesterase inhibitors.<sup>6</sup> It has recently been proposed that using drugs capable of inhibiting the activities of both acetylcholinesterase and butyrylcholinesterase may be beneficial for AD patients.<sup>16</sup> In



addition to their role in preventing the hydrolysis of acetylcholine, acetylcholinesterase inhibitors, in addition to memantine, have also been found to act as anti-inflammatory agents and to enhance the production of anti-oxidants.<sup>14,17-19</sup>

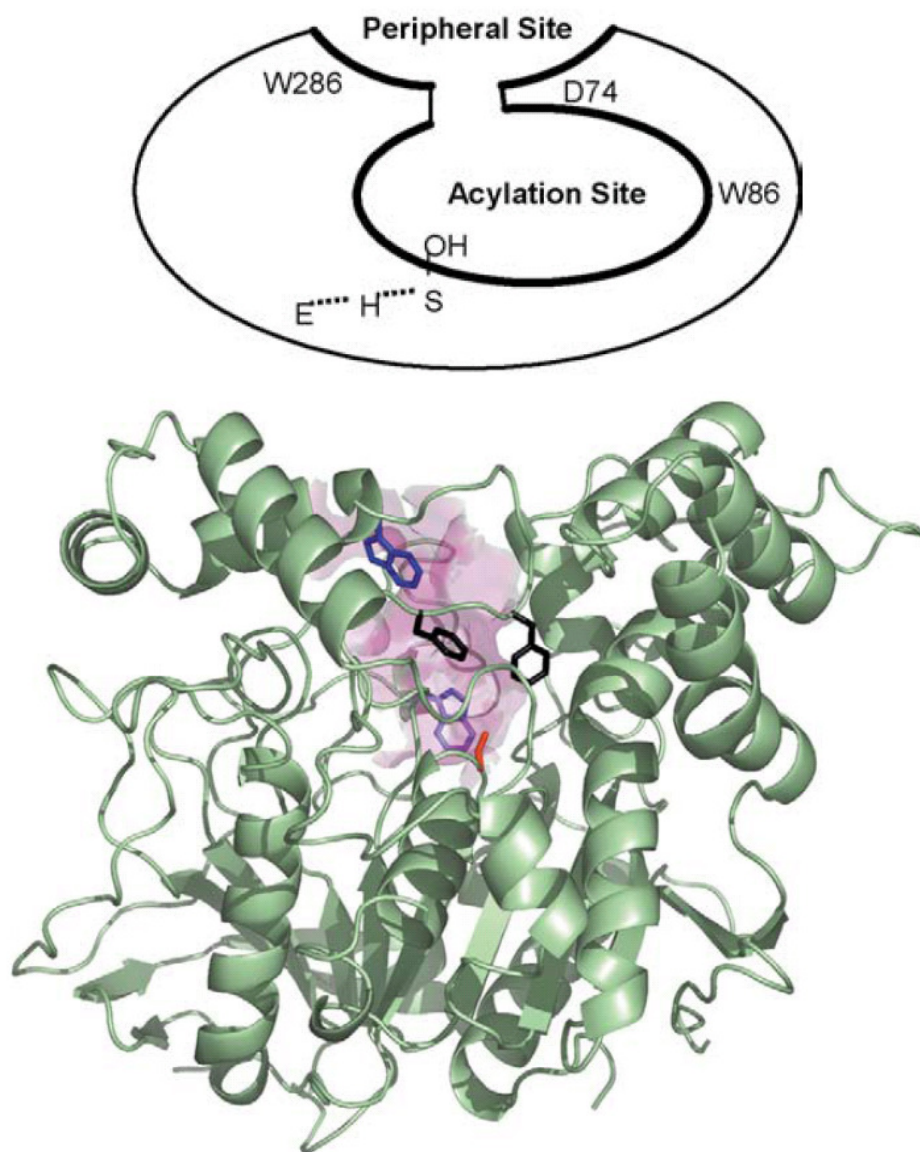


**Figure 6.1** Schematic<sup>3</sup> (above) and ribbon<sup>2</sup> (below) structures of AChE.<sup>4</sup> In the ribbon structure the  $\alpha$ -helices are represented by coils, while the  $\beta$ -sheets are represented by arrows. The shaded region represents the surface of the entrance to the gorge.<sup>4</sup>

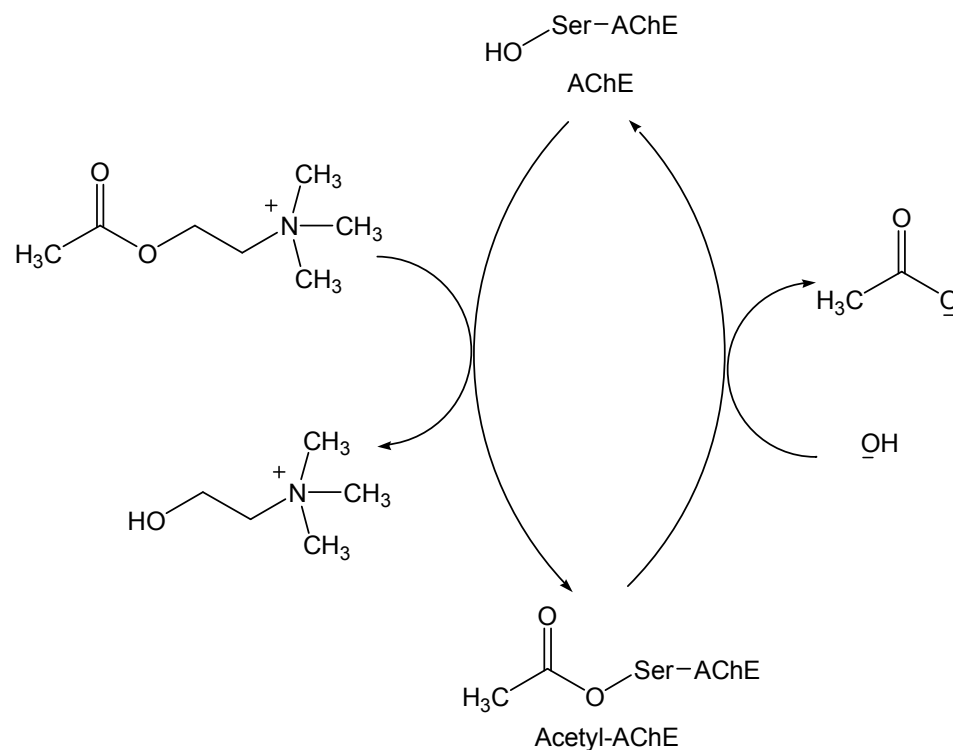


**Figure 6.2** The hydrolysis of acetylcholine by AChE, by the serine residue in the active site.<sup>58</sup> The AChE enzyme hydrolyzes acetylcholine, converting it to choline, while the enzyme forms an acetyl-bearing intermediate. This intermediate then undergoes hydrolysis, to release the acetate.<sup>58</sup>

The inhibition of AChE can be accomplished irreversibly (for example, organophosphates form a strong covalent bond with the serine residue of the catalytic triad), pseudo-irreversibly (with carbamates, as the carbamylated serine residue is slowly hydrolyzed to regenerate the active enzyme), or reversibly (involving non-covalent binding via electrostatic interactions between the inhibitor and the enzyme's active and/or peripheral site).<sup>20-22</sup> Among the reversible inhibitors, they may be classified as (a) active site inhibitors, which target the catalytic anionic subsite at the bottom of the gorge, (b) peripheral anionic site inhibitors, which bind at the entrance of the gorge, or (c) elongated gorge-spanning inhibitors that bridge the two sites.<sup>22,23</sup> The bisquaternary ligands decamethonium (1,10-bis(trimethylammonium)decane), BW284c51

(1,5-bis(4-allyldimethylammoniumphenyl)-pentan-3-one), and succinylcholine (suxemethonium), are examples of potent reversible “gorge-spanning” inhibitors which interact with both the acylation and peripheral sites.<sup>22,24</sup> Crystal structures of *Torpedo californica* AChE with BW284c51<sup>25</sup> and decamethonium<sup>26</sup> inhibitors indicate that these inhibitors both occupy similar peripheral sites. Succinylcholine has been used as a nicotinic acetylcholine receptor blocker and as a neuromuscular relaxant for over half a century, but it also has significant potential adverse effects.<sup>5,27-31</sup>

Mohanty and coworkers<sup>32</sup> have used CB[7] and CB[5] as hosts for binding the guest Thioflavin T, which has widespread use as a fluorescent dye for detecting amyloid fibrils.<sup>33-35</sup> Mohanty and coworkers note that Thioflavin T is bound internally by CB[7] and externally by the smaller CB[5] macrocycle. With CB[7], it forms a 1:1 complex with a binding constant of approximately  $10^5 \text{ M}^{-1}$ , while the binding affinity of the 2:1 complex is approximately 2 orders of magnitude weaker, with a binding constant of approximately  $10^3 \text{ M}^{-1}$ . Interestingly, Thioflavin T has also been observed recently through X-ray crystallography to bind to the peripheral site of *Torpedo californica* AChE.<sup>36</sup> As has been described in the previous chapter, we have studied the host-guest binding between CB[7] and guests such as choline and acetylcholine, as well as their derivatives.<sup>37</sup> With these choline-related guests, in addition to a series of tetralkylammonium, -phosphonium, and -sulfonium cations,<sup>38</sup> the charge-diffuse cationic regions themselves were encapsulated by the CB[7] cavity, instead of occupying the region just outside of the carbonyl-lined portals, which is the more common binding site for the cationic region of cationic guests with greater charge densities, such as such as primary ammonium<sup>39,40</sup> and methylviologen guests.<sup>41,42</sup> Macartney and coworkers have also demonstrated that upon binding between the tetracationic guest  $[\text{CH}_3\text{bpy}(\text{CH}_2)_6\text{bpyCH}_3]^{4+}$ , the first CB[7] occupies the central hexyl linker as a [2]pseudorotaxane, and when the second CB[7] is added, it binds to the methylviologen moiety

at one end of the guest, while the first CB[7] migrates to the methylviologen region at the other end.<sup>43</sup> Similar behaviour was also observed between CB[7] and a series of bis(pyridinium)alkane guests (depending on the substitution), with 1:1 and 2:1 complexes being observed, and in some cases, pseudorotaxanes being formed.<sup>44</sup> The focus of this chapter is the host-guest chemistry between CB[7] and a series of dicationic AChE inhibitors, including succinylcholine, BW284c51, decamethonium, as well as its analogues. In common with the monocationic choline and acetylcholine analogues described in the previous chapter, these AChE inhibitors have charge-diffuse, alkylated ammonium (or phosphonium) centres. Also, with their two cationic end groups, combined with their hydrophobic central linker, this series of guests have a 'bolaform',<sup>45</sup> or dumbbell, shape, which is also a feature of the bis(pyridinium)alkane guests discussed in Chapter 3. Just over a decade ago, Macartney and coworkers studied the host-guest binding of decamethonium and a series of its analogues with different aliphatic linker chain lengths (ranging between octyl and dodecyl spacer lengths) as well as the bis(trimethylphosphonium) analogue of decamethonium with the macrocyclic host  $\alpha$ -CD.<sup>46</sup> The  $\alpha$ -CD macrocycle, whose cavity size is smaller than that of CB[7] and comparable to that of CB[6], formed [2]pseudorotaxanes with members of this series, except when the trimethylammonium head groups of decamethonium each had two or more methyl groups replaced with the larger ethyl groups. When the trimethylammonium head groups were replaced with trimethylphosphonium groups, the formation of the [2]pseudorotaxane with  $\alpha$ -CD slowed by a factor of one million, and the [2]pseudorotaxane was only observed to form at elevated temperatures via the slippage mechanism.<sup>46</sup>

In this study we explored the binding between CB[7] and a series of analogues based on succinylcholine, as well as decamethonium, and its analogues (Figures 6.3 and 6.4). In the case of decamethonium, we varied its head groups between the default trimethylammonium ( $\text{NMe}_3^+$ )

head group to include trimethylammonium ( $\text{NEt}_3^+$ ), quinuclidinium ( $\text{Quin}^+$ ), trimethylphosphonium ( $\text{PMe}_3^+$ ), and triethylphosphonium ( $\text{PEt}_3^+$ ) terminal cationic groups. We observed formations of [2]pseudorotaxanes when the 1:1 complex was formed, and we also observed 2:1 complex formation when higher ratios of CB[7] were present in solution. These systems were characterized by  $^1\text{H}$  and  $^{31}\text{P}$  NMR spectroscopy, as well as by ESI mass spectrometry. Binding constants were also determined, both for the 1:1 and the 2:1 complexes. Both the binding behaviour and the binding constants within this series varied depending on the nature of the head group present on the guest, as well as its central linker. The work described in this chapter has been published.<sup>47</sup>

## 6.2 Results and Discussion

### 6.2.1 Host-Guest Complex Formation

$^1\text{H}$  and  $^{31}\text{P}$  NMR (Figures 6.5-6.16), in addition to ESI-MS (Table 6.1) were used to characterize the host-guest complexes formed within this series. While NMR titrations can provide information regarding the stoichiometry of the binding, and the binding constants, they can also provide useful information about the positions of CB[7] relative to the guests, based on the complexation-induced shifts, as represented by the  $\Delta\delta_{\text{lim}}$  values ( $\Delta\delta_{\text{lim}} = \delta_{\text{bound}} - \delta_{\text{free}}$ ). In the case of both  $^1\text{H}$  and  $^{31}\text{P}$  NMR spectroscopy, upfield shifts (with negative  $\Delta\delta_{\text{lim}}$  values) indicate that the respective proton or phosphorus centre is positioned inside the hydrophobic cucurbituril cavity, while downfield shifts (positive  $\Delta\delta_{\text{lim}}$  values) indicate that the proton (or phosphorus centre) is located outside of the cavity, and near the electron rich carbonyl portals. For all of the guests in this series, with the exception of the  $[\text{Quin}(\text{CH}_2)_{10}\text{Quin}]^{2+}$  guest, when one equivalent of CB[7] is present, the CB[7] cavity is positioned over the central linker, to form a

[2]pseudorotaxane. This is demonstrated by upfield shifts of the protons of the central linkers, indicating them to be encapsulated by the CB[7] cavity, while the protons of the terminal trialkylammonium and -phosphonium groups reveal modest downfield shifts, suggesting they are outside of the CB[7] cavity, near the portals (the corresponding  $\Delta\delta_{\text{lim}}$  values are shown in Figures 6.3 and 6.4). The  $\Delta\delta_{\text{lim}}$  values for the formation of the 1:1 complex between CB[7] and bis(trimethylammonium)octane are in reasonably good agreement with those observed previously by Bali and coworkers.<sup>47</sup> Upon 1:1 complex formation, exchange between the free and bound guest resonances is slow on the NMR timescale, with signals of both the free and bound guest being visible. With the guests containing the decyl group as the central linker, the length of the linker is longer than that required by the CB[7] guest, so that the CB[7] has a tendency to migrate back-and-forth along the [2]pseudorotaxane axle between the cationic head groups at either end of the molecule, with which it can employ ion-dipole interactions.

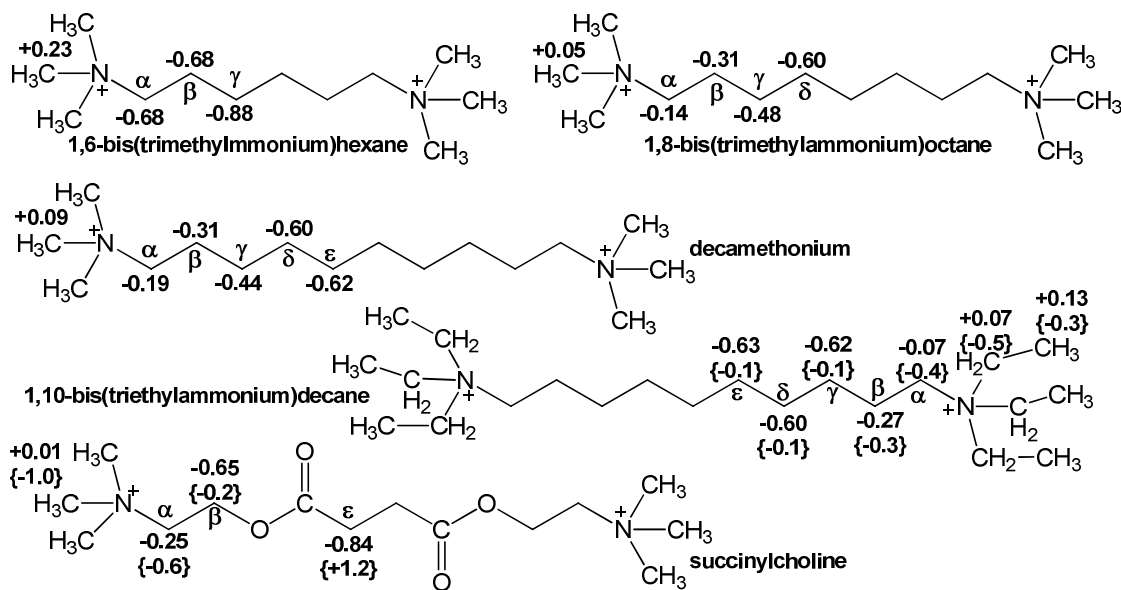


**Figure 6.3** Structures of the NMe<sub>3</sub>- and NEt<sub>3</sub>-capped guests employed in this study, along with their  $^1\text{H}$  NMR  $\Delta\delta_{\text{lim}}$  values (ppm). Upfield and downfield shifts are represented by negative and positive  $\Delta\delta_{\text{lim}}$  values, respectively. The top number is at 1 equiv. CB[7], while the lower numbers are for excess CB[7]. The numbers in round brackets represent observed values, while those in parenthesis represent extrapolated values.

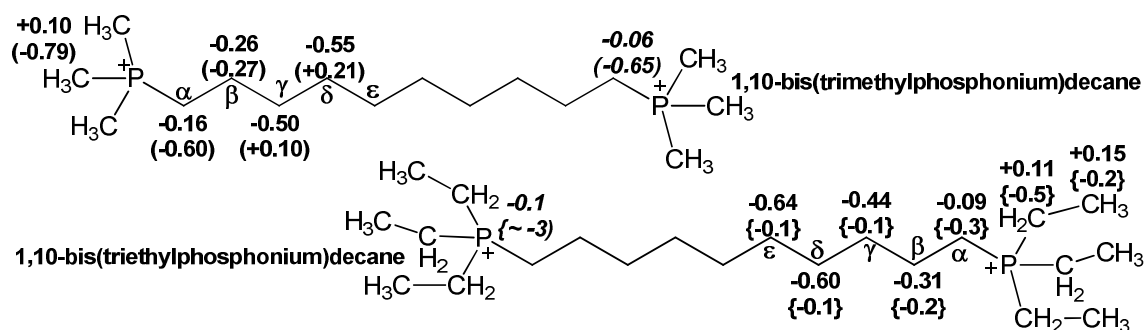


**Figure 6.4** Structures of the  $\text{PMe}_3$ - and  $\text{PEt}_3$ -capped guests employed in this study, along with their  $^1\text{H}$  NMR  $\Delta\delta_{\text{lim}}$  values. Upfield and downfield shifts are represented by negative and positive  $\Delta\delta_{\text{lim}}$  values, respectively.  $^{31}\text{P}$  NMR  $\Delta\delta_{\text{lim}}$  values are shown in italics. The numbers in round brackets represent observed values, while those in parenthesis represent extrapolated values of  $\Delta\delta_{\text{lim}}$ .

When the guests have the shorter hexyl and octyl central spacers, addition of excess CB[7] (beyond the equivalence point) results in no change to the  $^1\text{H}$  NMR spectra from those of the [2]pseudorotaxanes that are observed for the 1:1 complexes (Figures 6.5 and 6.6), while only minor changes are observed of the decamethonium guest's resonances with excess CB[7] (Figure 6.7). On the other hand, when excess CB[7] is added to the succinylcholine, as well as the bis- $\text{NEt}_3$ ,  $-\text{PMe}_3$ , and  $-\text{PEt}_3$  analogues of decamethonium, significant changes are observed from the spectra recorded at the equivalence point (Figures 6.8-6.11). For these guests, the upfield shifts of the central spacer become diminished, while the protons of the terminal quaternary head groups, experience upfield shifts as the amount of CB[7] is increased, in contrast to the mild downfield shifts occurring at the equivalence point. Thus, both the magnitude and the direction of the  $\Delta\delta_{\text{lim}}$  values reverse for the 2:1 systems as compared to the 1:1 systems, although the extent to which this occurs varies within this series. To differing degrees within this series, there appear to be two types of complexes that may be forming. In one case, upon addition of the second CB[7], the first CB[7], which is initially positioned on the central linker between the two cationic

centres, has migrated to one end of the molecule, while the second CB[7] encapsulates the cationic centre at the other end of the molecule, to give a dumbbell-shaped 2:1 complex. This binding behaviour mirrors that observed among members of the bis(pyridinium)alkane series discussed in an Chapter 3 (with the exception of the pyridinium guests bearing the bulkier *t*-butyl groups).<sup>44</sup> The tendency for the two CB[7] hosts to occupy opposing sides of the molecule arises from electrostatic repulsions between the carbonyl portals of different CB[7] macrocycles, although the extent to which this occurs is also related to the affinity of the CB[7] hosts for a particular head group. In another situation, one of the CB[7] macrocycles may be continuing to occupy the central chain, while the other CB[7] occupies one of the terminal NR<sub>3</sub><sup>+</sup> or PR<sub>3</sub><sup>+</sup> cations. With these 2:1 complexes, as observed with the tetraalkyl quaternary guests,<sup>38</sup> and with the monocationic choline series of guests,<sup>37</sup> the charge-diffuse cationic centres are encapsulated by the CB[7] cavity, as opposed to being positioned at the portals. The upfield shifts of the 2:1 complexes are generally greatest for the protons that are closest to the onium centre (that is, the nitrogen or the phosphorus atom), such as the  $\alpha$ -CH<sub>2</sub> of the central linker, and the ammonium or phosphonium protons closest to the onium. While the guest protons of this series display slow exchange behaviour on the NMR timescale below the equivalence point of CB[7], they exhibit fast exchange behaviour when the CB[7] is in excess, so that one signal, representing the average of the free and bound resonances, is visible.



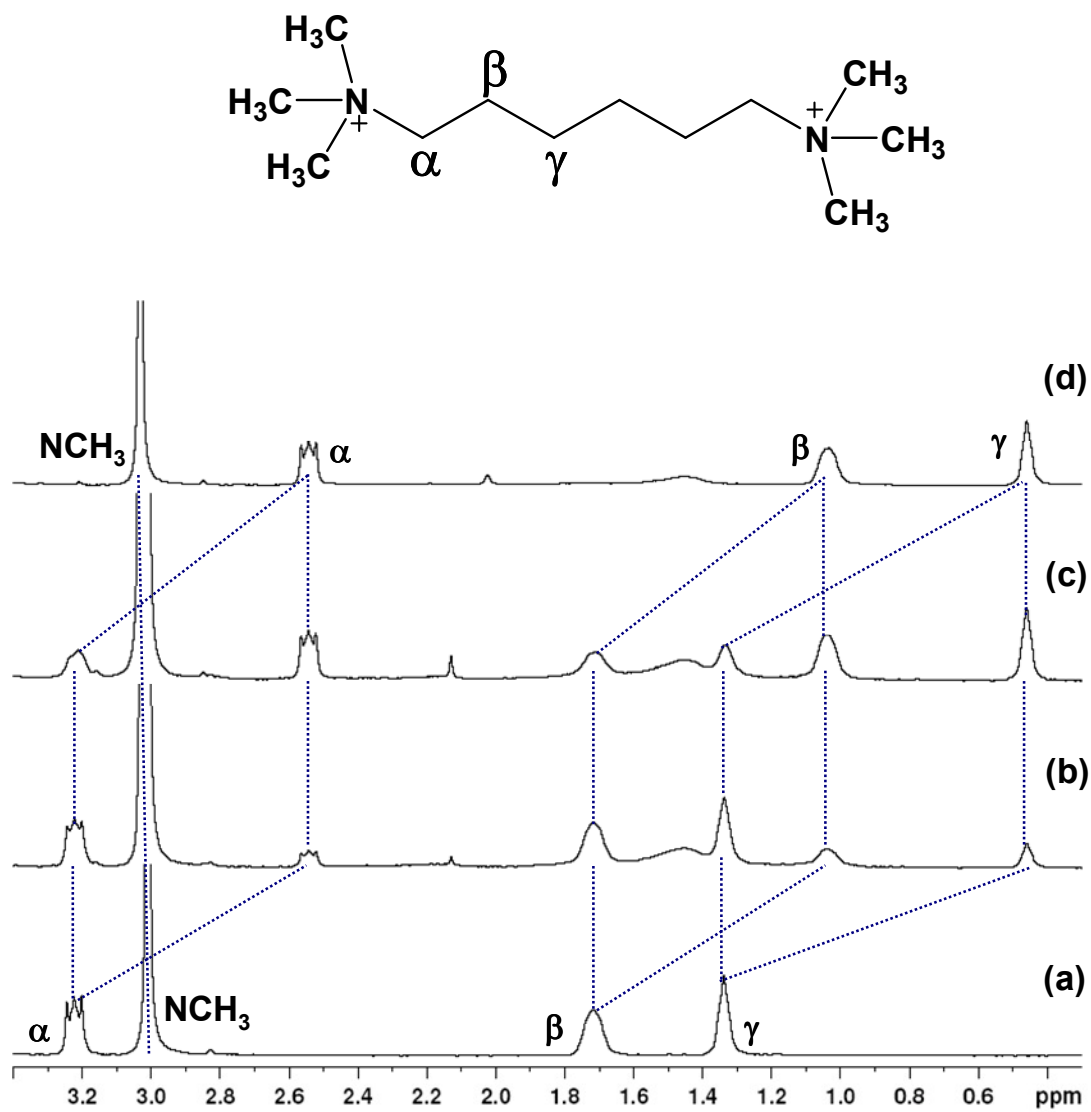


**Figure 6.5**  $^1\text{H}$  NMR titration of  $[\text{NMe}_3(\text{CH}_2)_6\text{NMe}_3]^{2+}$  (1.53 mM in  $\text{D}_2\text{O}$ ) in the presence of (a) 0.00, (b) 0.25, (c) 0.62, and (d) 1.27 equiv. of CB[7].

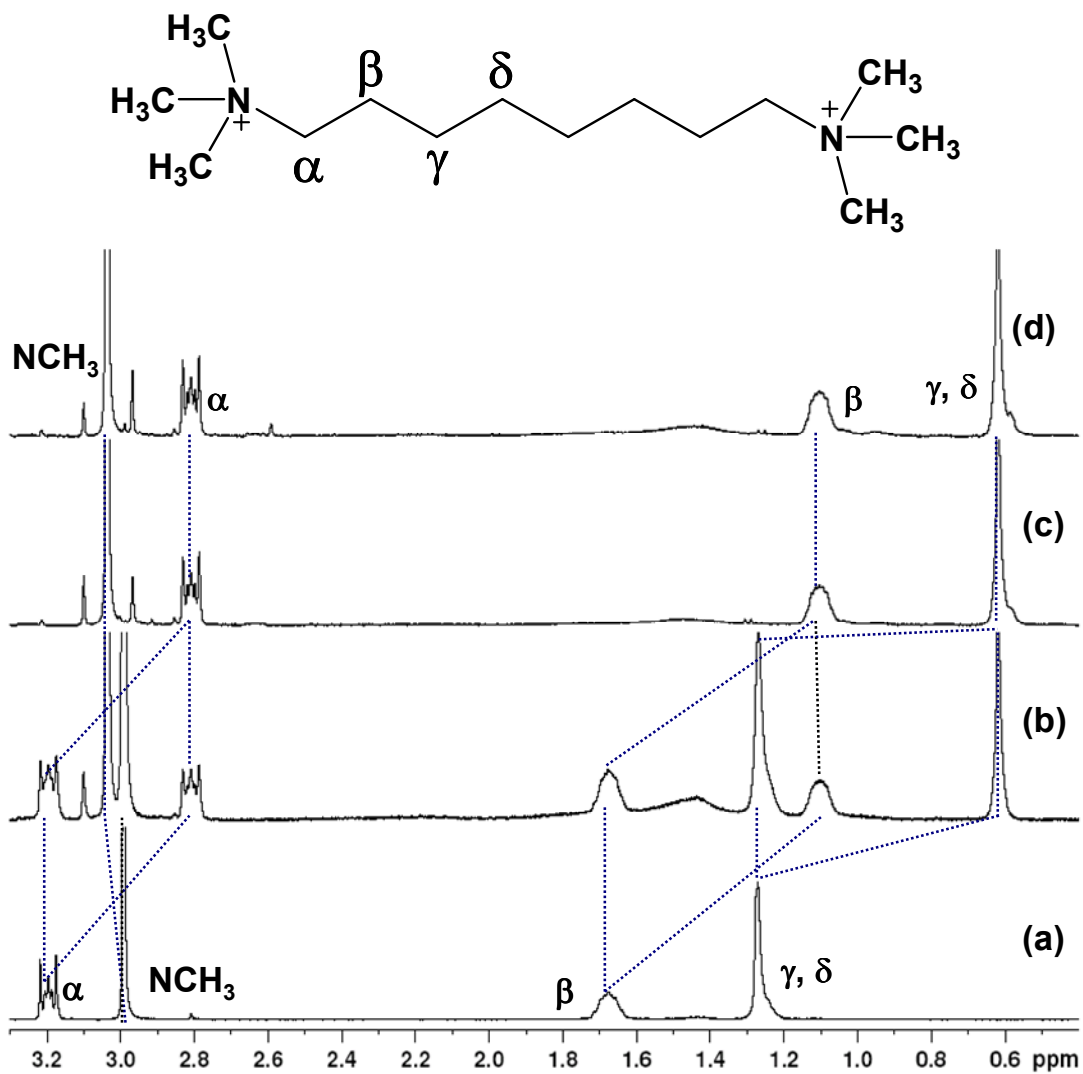


**Figure 6.6**  $^1\text{H}$  NMR titration of  $[\text{NMe}_3(\text{CH}_2)_8\text{NMe}_3]^{2+}$  (1.22 mM in  $\text{D}_2\text{O}$ ) in the presence of (a) 0.00, (b) 0.51, (c) 1.17, and (d) 2.63 equiv. of CB[7].

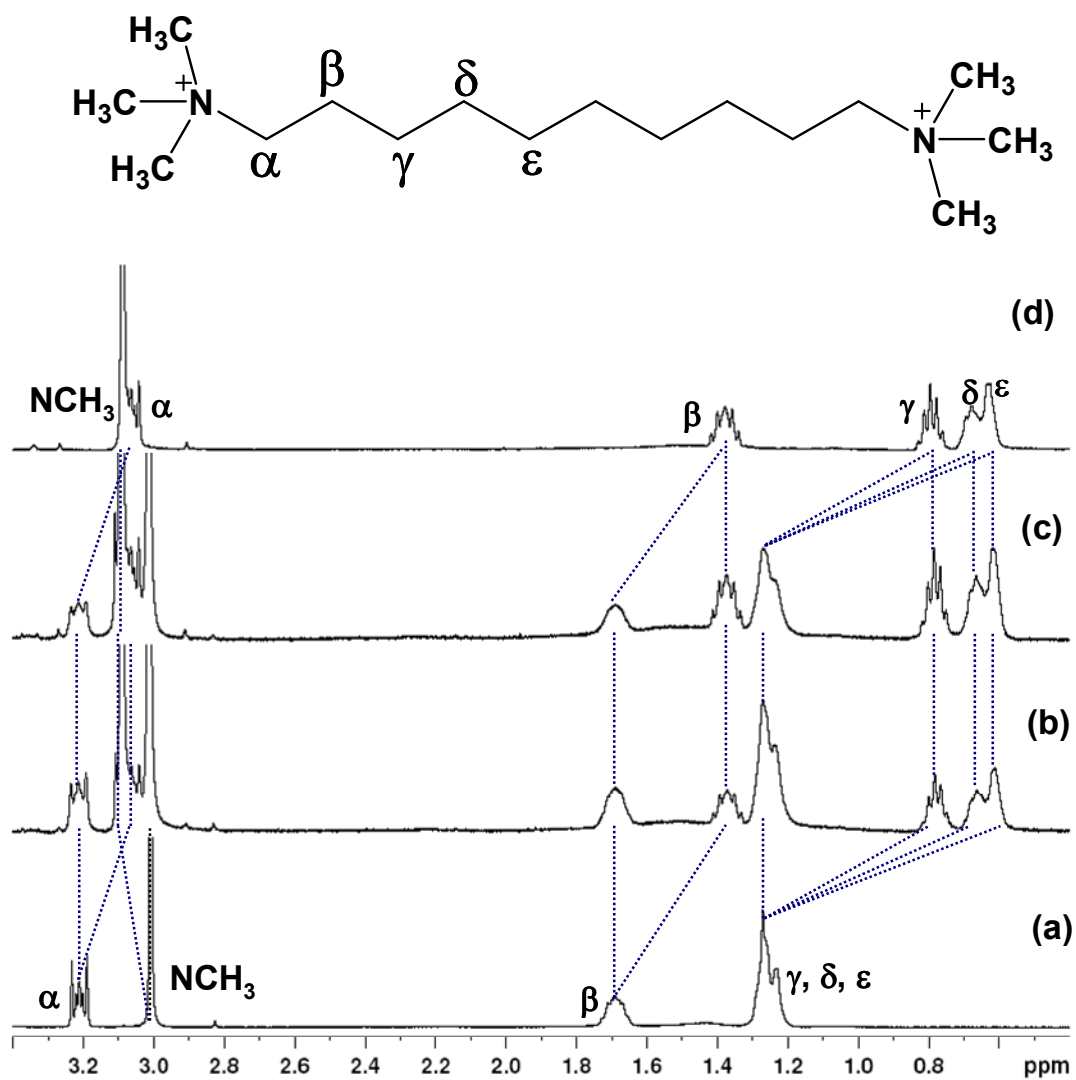


**Figure 6.7**  $^1\text{H}$  NMR titration of  $[\text{NMe}_3(\text{CH}_2)_{10}\text{NMe}_3]^{2+}$  (1.31 mM in  $\text{D}_2\text{O}$ ) in the presence of (a) 0.00, (b) 0.46, (c) 0.62, and (d) 1.57 equiv. of CB[7].

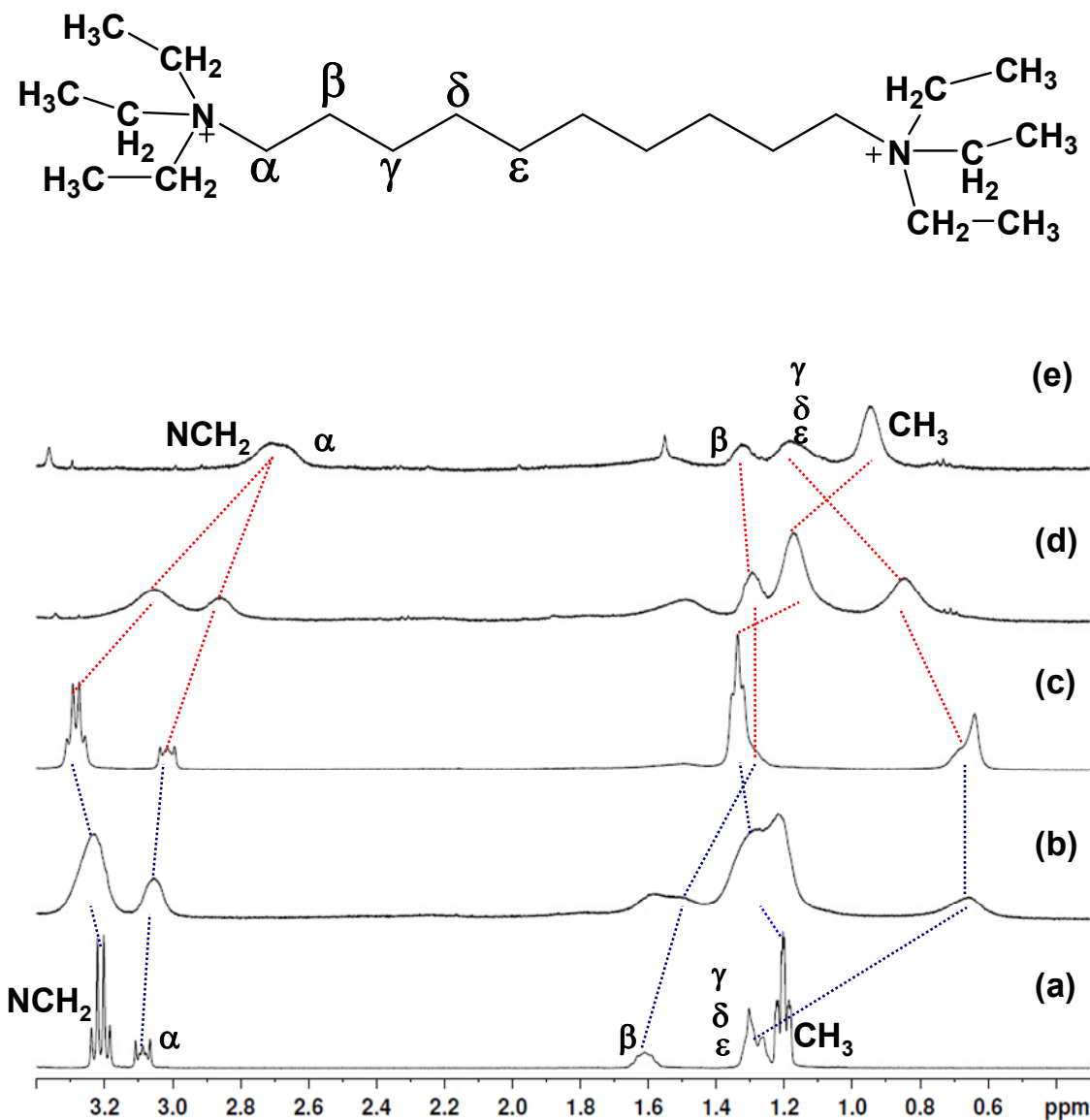


**Figure 6.8**  $^1\text{H}$  NMR titration of  $[\text{NEt}_3(\text{CH}_2)_{10}\text{NEt}_3]^{2+}$  (1.23 mM in  $\text{D}_2\text{O}$ ) in the presence of (a) 0.00, (b) 0.51, (c) 1.16, (d) 2.24, and (e) 4.93 equiv. CB[7]. Blue traces show changes prior to the equivalence point, while red lines are changes beyond the equivalence point.

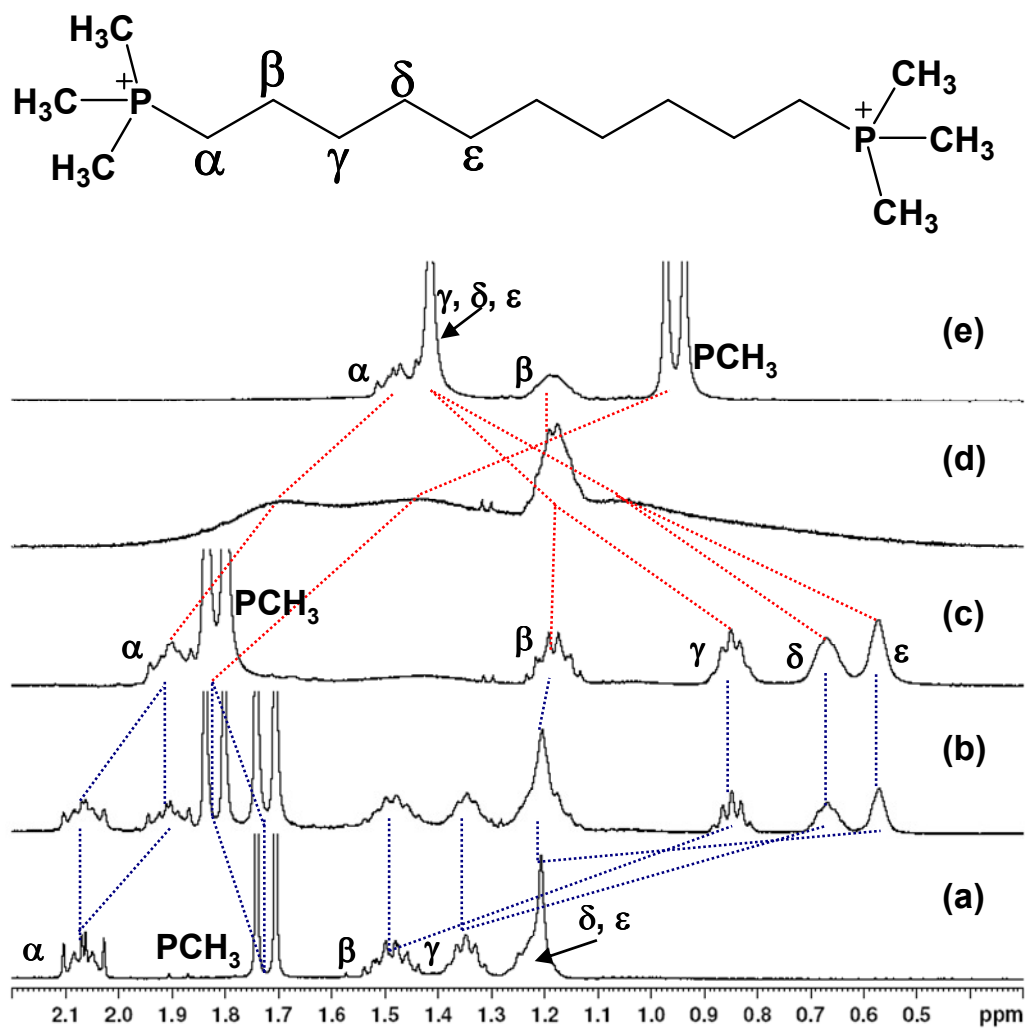


**Figure 6.9**  $^1\text{H}$  NMR titration of  $[\text{PMe}_3(\text{CH}_2)_{10}\text{PMe}_3]^{2+}$  (1.22 mM in  $\text{D}_2\text{O}$ ) in the presence of (a) 0.00, (b) 0.43, (c) 0.98, (d) 1.48, and (e) 3.08 equiv. of CB[7]. Blue traces represent changes prior to the equivalence point, and red traces show changes beyond the equivalence point.

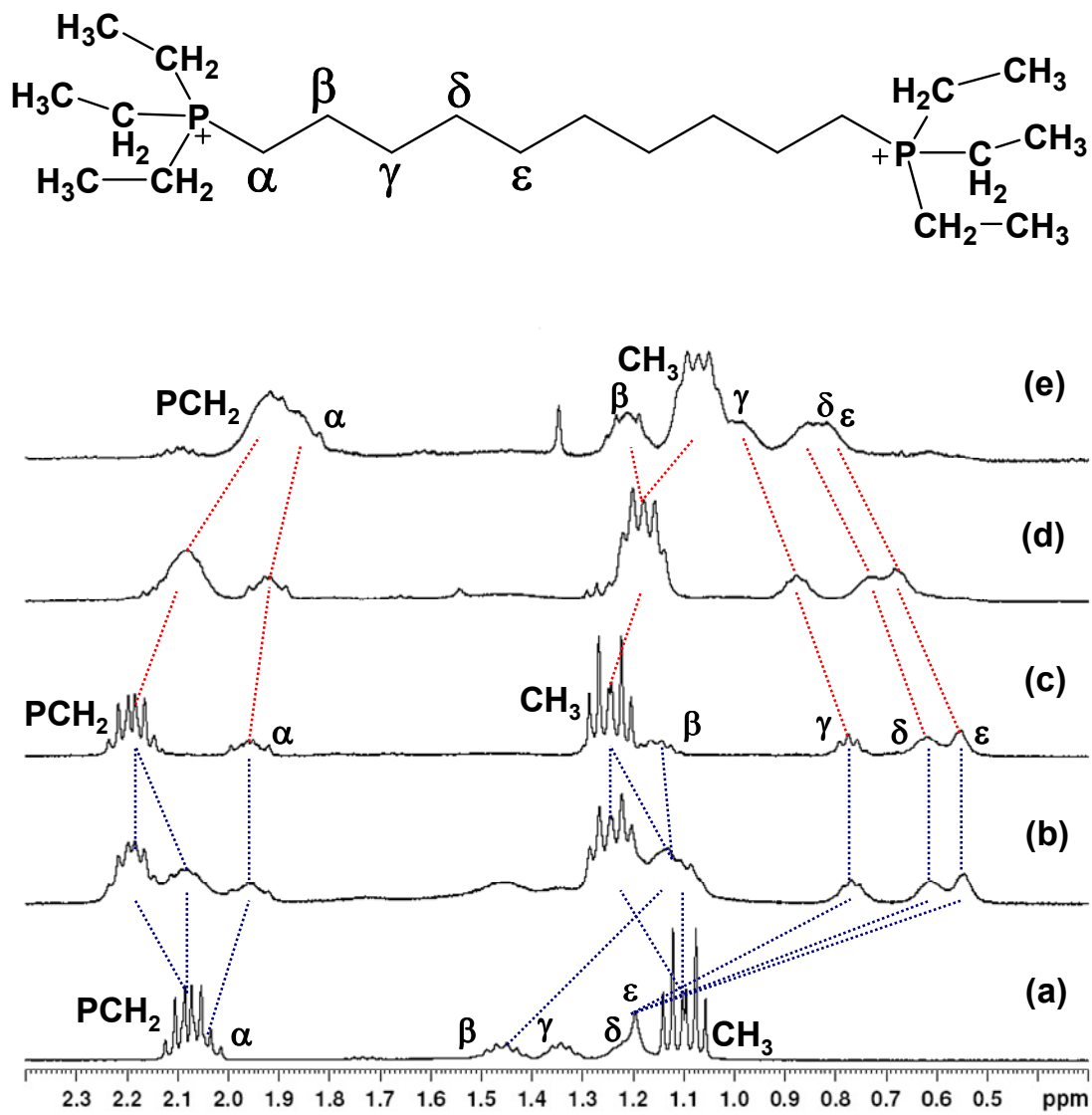


**Figure 6.10**  $^1\text{H}$  NMR titration of  $[\text{PEt}_3(\text{CH}_2)_{10}\text{PEt}_3]^{2+}$  (0.91 mM in  $\text{D}_2\text{O}$ ) in the presence of (a) 0.00, (b) 0.79, (c) 1.46, (d) 4.65, and (e) 9.63 equiv. CB[7]. Blue traces represent changes prior to the equivalence point, and red traces show changes beyond the equivalence point.

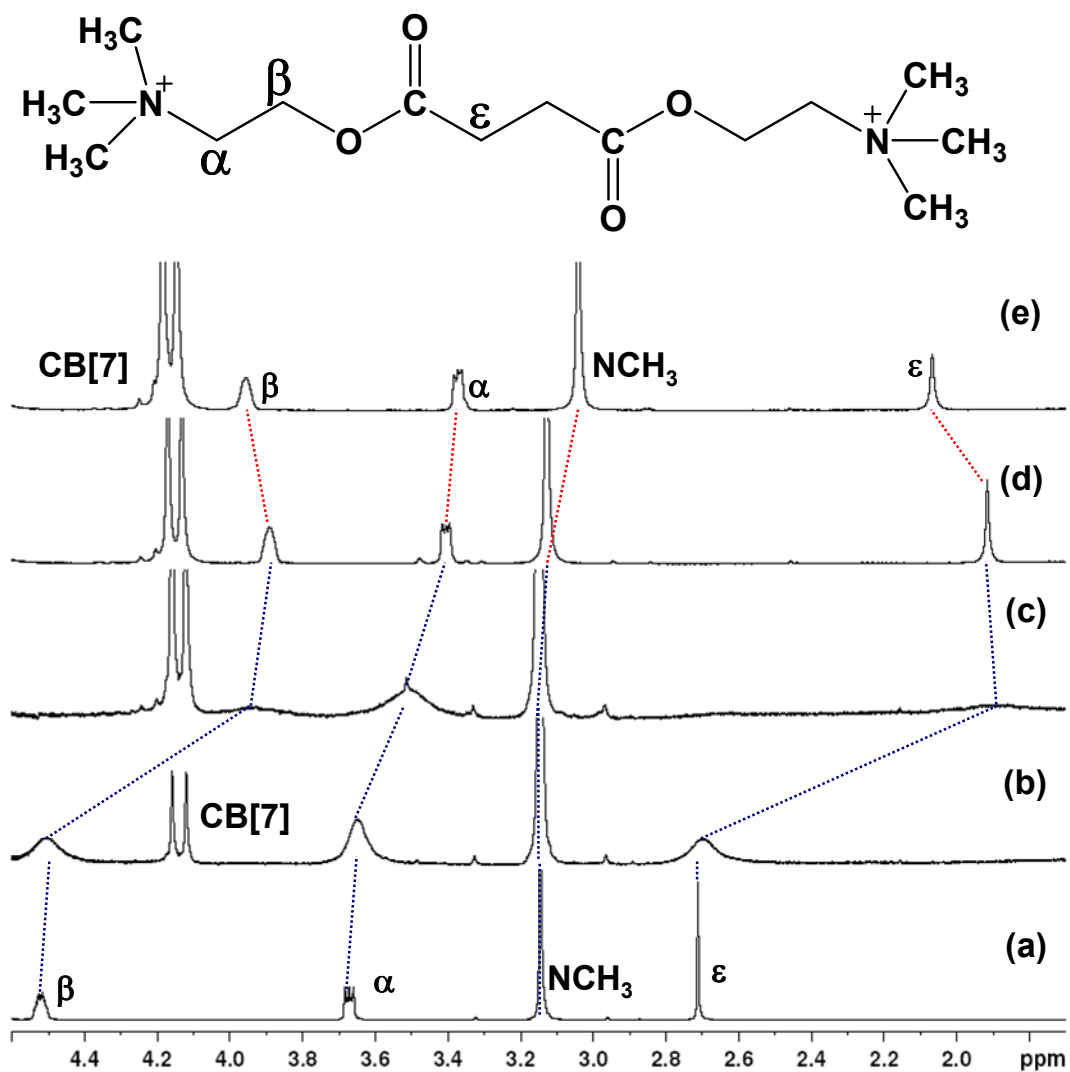


**Figure 6.11**  $^1\text{H}$  NMR titration of succinylcholine (1.31 mM in D<sub>2</sub>O) in the presence of (a) 0.00, (b) 0.14, (c) 0.59, (d) 1.45, and (e) 2.87 equiv. of CB[7]. Blue traces represent changes prior to the equivalence point, and red traces show changes beyond the equivalence point.

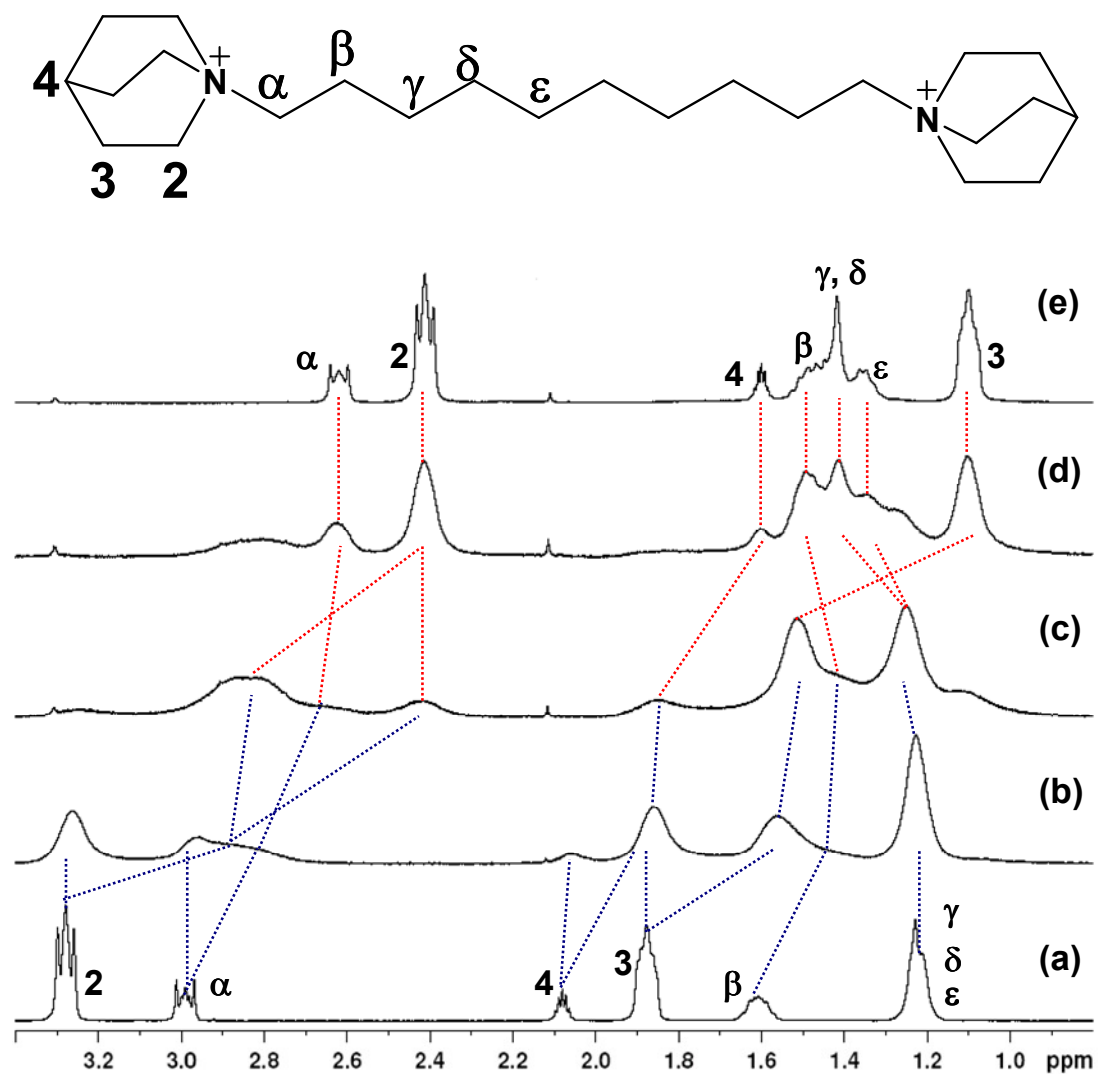


**Figure 6.12**  $^1\text{H}$  NMR titration of  $[\text{Quin}(\text{CH}_2)_{10}\text{Quin}]^{2+}$  (1.40 mM in  $\text{D}_2\text{O}$ ) in the presence of (a) 0.00, (b) 0.46, (c) 1.11, (d) 1.67, and (e) 2.10 equiv. CB[7]. Blue traces represent changes prior to the equivalence point, and red traces show changes beyond the equivalence point.



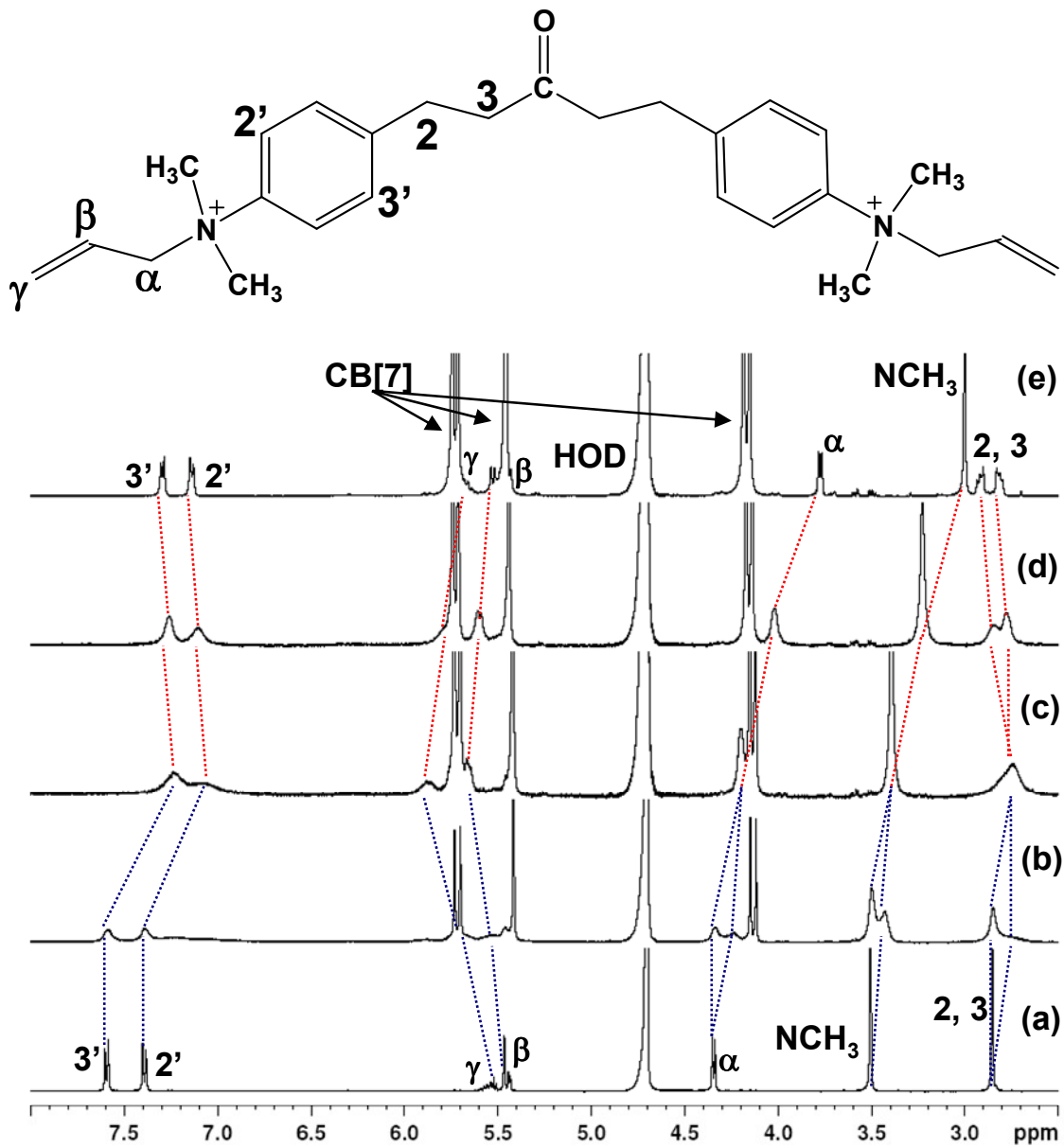


**Figure 6.13**  $^1\text{H}$  NMR titration of BW284c51 (1.03 mM in  $\text{D}_2\text{O}$ ) in the presence of (a) 0.00, (b) 0.49, (c) 1.12, (d) 1.56, and (e) 3.24 equiv. of CB[7]. The blue traces represent changes before the equivalence point, while red traces represent changes beyond the equivalence point.

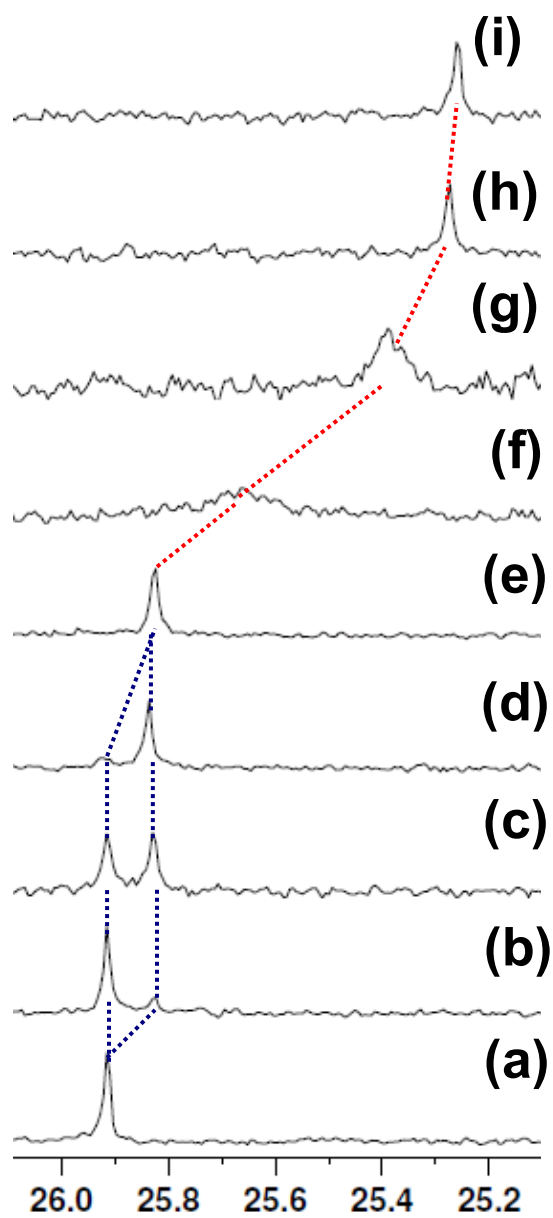


**Figure 6.14**  $^{31}\text{P}$  NMR titration of  $[\text{PMe}_3(\text{CH}_2)_{10}\text{PMe}_3]^{2+}$  (1.22 mM in  $\text{D}_2\text{O}$ ) in the presence of (a) 0.00, (b) 0.23, (c) 0.55, (d) 0.84, (e) 1.14, (f) 1.33, (g) 1.78, (h) 3.98, and (i) 4.98 equiv. of CB[7]. Blue traces represent changes before the equivalence point, while red traces represent changes beyond the equivalence point.

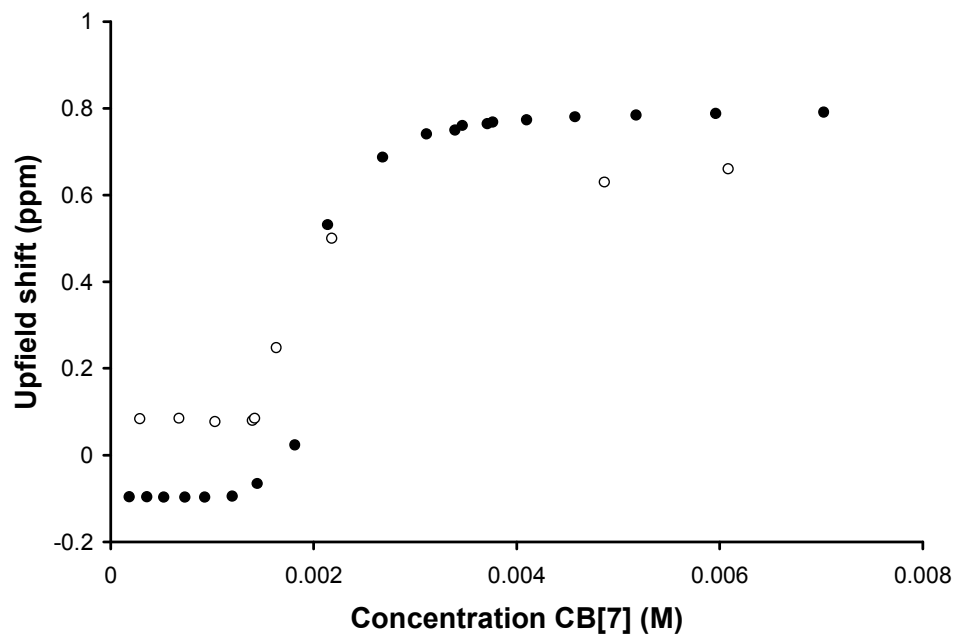


**Figure 6.15** Plot of dependence of upfield shift vs. the concentration of CB[7] for  $[\text{PMe}_3(\text{CH}_2)_{10}\text{PMe}_3]^{2+}$  (1.22 mM in  $\text{D}_2\text{O}$ ) with data for the trimethylammonium protons from  $^1\text{H}$  NMR spectra (●) and phosphorus centre from  $^{31}\text{P}$  NMR spectra (○).

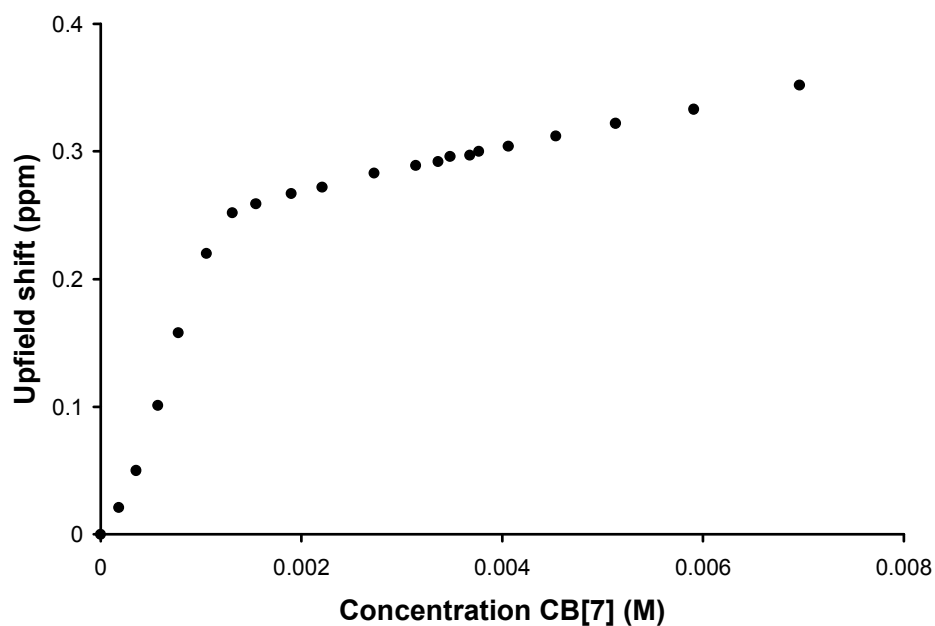


**Figure 6.16** Plot of dependence of upfield shift of  $\alpha$   $\text{CH}_2$  of succinylcholine (1.31 mM in  $\text{D}_2\text{O}$ ) vs. the concentration of CB[7] from  $^1\text{H}$  NMR spectra.

The decamethonium analogues bearing the  $\text{PMe}_3$  and  $\text{PEt}_3$  head groups allow the use of  $^{31}\text{P}$  NMR spectroscopy, and these spectra are also consistent with initial formation of a [2]pseudorotaxane, followed by formation of a 2:1 complex as the ratio of CB[7] is increased. Formation of the [2]pseudorotaxane results in small upfield shifts of -0.06 and -0.1 ppm for  $[\text{PMe}_3(\text{CH}_2)_{10}\text{PMe}_3]^{2+}$  and  $[\text{PEt}_3(\text{CH}_2)_{10}\text{PEt}_3]^{2+}$ , respectively, near the equivalence point of CB[7]. Beyond the equivalence point, much larger upfield shifts of -0.65 and approximately -3 ppm are observed when the guest is capped with  $\text{PMe}_3^+$  or  $\text{PEt}_3^+$ , respectively (Figure 6.15). These latter values can be compared to the values observed for the  $\text{PMe}_4^+$  and  $\text{PEt}_4^+$  guests, which were encapsulated by CB[7], and had  $\Delta\delta_{\text{lim}}$  values of -0.38 and -5.77 ppm, respectively.<sup>38</sup>

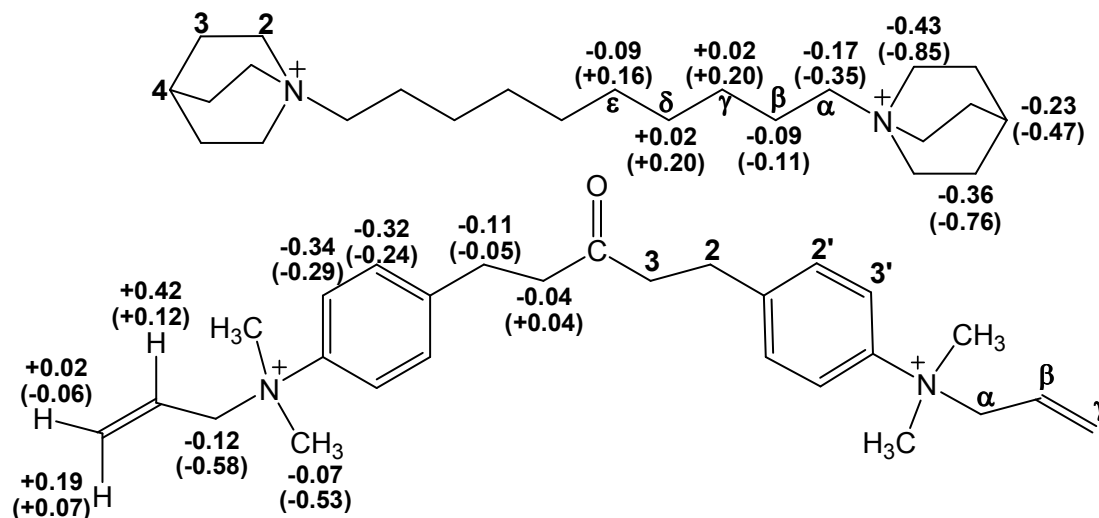


**Figure 6.17** Structures and  $^1\text{H}$  NMR  $\Delta\delta_{\text{lim}}$  values of  $[\text{Quin}(\text{CH}_2)_{10}\text{Quin}]^{2+}$  (above) and BW284c51 (below). The top number represents the 1:1  $\Delta\delta_{\text{lim}}$  value, while the bottom number represents the 2:1  $\Delta\delta_{\text{lim}}$  value, with positive numbers representing downfield shifts, and negative numbers representing upfield shifts.

When the guest is capped with quinuclidinium head groups, the 1:1 complex with CB[7] results in an asymmetrically bound complex, with the CB[7] positioned over one of the quinuclidinium head groups, instead of the central linker. This is demonstrated by upfield shifts of the quinuclidinium protons, in addition to the  $\alpha$  and  $\beta$  protons of the decyl linker, while the  $\gamma$ ,  $\delta$ , and  $\epsilon$  protons display downfield shifts (Figures 6.12 and 6.15). Both the 1:1 complex formation, as well as that of the 2:1 complex, display slow exchange behaviour on the NMR timescale. Also, the upfield shifts of the outer regions of the guest, from the  $\alpha$ -protons of the decyl linker outward through the quinuclidinium regions, approximately double in value for the 2:1 complex compared to the corresponding values for the 1:1 complex, which is also consistent with the CB[7] hosts being localized at the peripheral region of the guest throughout the titration. This behaviour is likely due to the high affinity of CB[7] for quinuclidinium-bearing guests, as observed by the binding constant between CB[7] (as described in Chapter 5, the binding constants between CB[7] and quinuclidine-bearing guests such as *N*-methylquinuclidinium and the quinuclidinium-bearing derivative of choline are  $5.7 \times 10^9$  and  $1.3 \times 10^9 \text{ M}^{-1}$ , respectively). In addition, the bulkiness of the quinuclidinium moieties may also present a steric barrier that could also be hindering the ability of CB[7] to cross over to the central aliphatic region. Similar behaviour to this was observed with members of the bis(pyridinium)alkane guests, when their pyridinium units were substituted with *t*-butyl groups.<sup>44</sup> When the 2:1 complex between CB[7] and  $[\text{Quin}(\text{CH}_2)_{10}\text{Quin}]^{2+}$  is formed, the 2:1  $\Delta\delta_{\text{lim}}$  values are almost identical to the corresponding 1:1  $\Delta\delta_{\text{lim}}$  values between CB[7] and *N*-methylquinuclidinium (whose  $\Delta\delta_{\text{lim}}$  values were -0.84, -0.69, -0.48, and -0.43 ppm for H2, H3, H4, and CH<sub>3</sub>, respectively), indicating that both CB[7] hosts are localized over the quinuclidinium moiety as it forms the 2:1 complex, further supporting the dumbbell shape of the 2:1 host-guest complex.

The AChE inhibitor BW284c51 also displays differing  $^1\text{H}$  NMR spectra for its 1:1 and 2:1 complexes with CB[7] (Figure 6.13). At the equivalence point, the upfield shifts are focused on the aromatic rings near the middle of the guest, with the H2' and H3' protons showing the larger upfield shifts. Meanwhile, the terminal allyl protons, show a downfield shift, indicating that they are initially positioned outside of the CB[7] cavity, near the portals. As excess CB[7] is added, the binding positions become focused on the cationic quaternary ammonium centre, with the largest upfield shifts being displayed by the methyl groups attached to the ammonium centre, as well as the allyl  $\alpha$  protons. The aromatic protons retain some degree of their upfield shifts, although the magnitude is diminished compared to that observed for the 1:1 complex. As is the case with the other guests in this series (except for the quinuclidinium capped guests, and those that did not participate in 2:1 binding), BW284c51 follows the trend of initial binding closer to the centre of the molecule, followed by outward migration as the second CB[7] is added, as a result of electrostatic repulsions between the cucurbiturils.

The data from high-resolution electrospray mass spectrometry are displayed in Table 6.1. In all of the guests explored in this series, peaks consistent with the formation of a 1:1 complex with CB[7] were observed. In addition, all of the guests whose binding constants indicated significant 2:1 complex formation (such as  $[\text{PMe}_3(\text{CH}_2)_{10}\text{PMe}_3]^{2+}$ ,  $[\text{Quin}(\text{CH}_2)_{10}\text{Quin}]^{2+}$ , and BW284c51) also displayed peaks in the high-resolution mass spectra that were consistent with formation of the 2:1 complex. Mass spectral evidence of 2:1 complex formation was also observed for some of the guests with weaker calculated 2:1 binding constants, such as decamethonium, and  $[\text{PEt}_3(\text{CH}_2)_{10}\text{PEt}_3]^{2+}$ .

**Table 6.1** High resolution ESI-MS data of the 1:1 and 2:1 host-guest complexes between CB[7] and the dicationic guests (The values in parenthesis represent the calculated  $m/z$  values of the peak with the corresponding formula mass).

Guest	[Guest•CB[7]-2X] <sup>2+</sup> ( $m/z$ )	[Guest•2CB[7]-2X] <sup>2+</sup> ( $m/z$ )
[NMe <sub>3</sub> (CH <sub>2</sub> ) <sub>6</sub> NMe <sub>3</sub> ] <sup>2+<sup>a</sup></sup>	682.2919 (682.2917 for [C <sub>54</sub> H <sub>72</sub> N <sub>30</sub> O <sub>14</sub> ] <sup>2+</sup> )	not observed
[NMe <sub>3</sub> (CH <sub>2</sub> ) <sub>8</sub> NMe <sub>3</sub> ] <sup>2+<sup>a</sup></sup>	696.3078 (696.3073 for [C <sub>56</sub> H <sub>76</sub> N <sub>30</sub> O <sub>14</sub> ] <sup>2+</sup> )	not observed
[NMe <sub>3</sub> (CH <sub>2</sub> ) <sub>10</sub> NMe <sub>3</sub> ] <sup>2+<sup>a</sup></sup>	710.3229 (710.3230 for [C <sub>58</sub> H <sub>80</sub> N <sub>30</sub> O <sub>14</sub> ] <sup>2+</sup> )	1291.4930 (1291.4947 for C <sub>100</sub> H <sub>122</sub> N <sub>58</sub> O <sub>28</sub> ] <sup>2+</sup> )
[NEt <sub>3</sub> (CH <sub>2</sub> ) <sub>10</sub> NEt <sub>3</sub> ] <sup>2+<sup>a</sup></sup>	752.3723 (752.3699 for C <sub>64</sub> H <sub>92</sub> N <sub>30</sub> O <sub>14</sub> ] <sup>2+</sup> )	not observed
[PMe <sub>3</sub> (CH <sub>2</sub> ) <sub>10</sub> PMe <sub>3</sub> ] <sup>2+<sup>a</sup></sup>	727.2933 (727.2936 for [C <sub>58</sub> H <sub>80</sub> N <sub>28</sub> O <sub>14</sub> P <sub>2</sub> ] <sup>2+</sup> )	1308.5332 (1308.4654 for [C <sub>100</sub> H <sub>122</sub> N <sub>56</sub> O <sub>28</sub> P <sub>2</sub> ] <sup>2+</sup> )
[PEt <sub>3</sub> (CH <sub>2</sub> ) <sub>10</sub> PEt <sub>3</sub> ] <sup>2+<sup>a</sup></sup>	769.3407 (769.3406 for [C <sub>64</sub> H <sub>92</sub> N <sub>28</sub> O <sub>14</sub> P <sub>2</sub> ] <sup>2+</sup> )	1350.5174 (1350.5124 for [C <sub>106</sub> H <sub>134</sub> N <sub>56</sub> O <sub>28</sub> P <sub>2</sub> ] <sup>2+</sup> )
[Succinylcholine] <sup>2+<sup>b</sup></sup>	726.2820 (726.2814 for [C <sub>56</sub> H <sub>72</sub> N <sub>30</sub> O <sub>14</sub> ] <sup>2+</sup> )	not observed
[Quin(CH <sub>2</sub> ) <sub>10</sub> Quin] <sup>2+<sup>a</sup></sup>	762.3630 (762.3543 for [C <sub>66</sub> H <sub>88</sub> N <sub>30</sub> O <sub>14</sub> ] <sup>2+</sup> )	1343.5748 (1343.5260 for [C <sub>108</sub> H <sub>130</sub> N <sub>58</sub> O <sub>28</sub> ] <sup>2+</sup> )
[BW284c51] <sup>2+<sup>a</sup></sup>	784.3204 (784.3204 for [C <sub>69</sub> H <sub>80</sub> N <sub>30</sub> O <sub>15</sub> ] <sup>2+</sup> )	1365.4987 (1365.4922 for [C <sub>111</sub> H <sub>122</sub> N <sub>58</sub> O <sub>29</sub> ] <sup>2+</sup> )

<sup>a</sup>X = Br<sup>-</sup>, <sup>b</sup>X = Cl<sup>-</sup>

**Table 6.2** Host-guest binding constants between CB[7] and the dicationic quaternary onium guests, for the 1:1 complexes ( $K_{CB[7]}$ ) and the 2:1 complexes ( $K_{2CB[7]}$ ), determined in aqueous solution at 298 K.

Guest	$K_{CB[7]} (M^{-1})$	$K_{2CB[7]} (M^{-1})$
$[NMe_3(CH_2)_6NMe_3]^{2+}$	$(3.9 \pm 0.9) \times 10^9{}^a$	not observed
$[NMe_3(CH_2)_8NMe_3]^{2+}$	$(2.8 \pm 0.8) \times 10^{10}{}^a$	not observed
$[NMe_3(CH_2)_{10}NMe_3]^{2+}$	$(2.6 \pm 1.3) \times 10^8{}^b$	$< 10{}^c$
$[NEt_3(CH_2)_{10}NEt_3]^{2+}$	$(1.4 \pm 0.3) \times 10^8{}^b$	$250 \pm 30{}^d$
$[PMe_3(CH_2)_{10}PMe_3]^{2+}$	$(9.0 \pm 1.5) \times 10^7{}^b$	$(6.5 \pm 0.5) \times 10^3{}^{d,e}$
$[PEt_3(CH_2)_{10}PEt_3]^{2+}$	$(6.8 \pm 1.0) \times 10^7{}^b$	$(1.1 \pm 0.2) \times 10^2{}^{c,d}$
$[Succinylcholine]^{2+}$	$(8.6 \pm 1.6) \times 10^6{}^b$ $(9.6 \pm 2.0) \times 10^6{}^f$ $(1.1 \pm 0.3) \times 10^7{}^g$	$42 \pm 5{}^c$
$[Quin(CH_2)_{10}Quin]^{2+}$	$(1.9 \pm 0.6) \times 10^{10}{}^a$ $(8.7 \pm 2.5) \times 10^9{}^g$	$(5.6 \pm 3.2) \times 10^9{}^a$ $(6.1 \pm 2.1) \times 10^8{}^g$
$[BW284c51]^{2+}$	$(1.3 \pm 0.2) \times 10^8{}^c$	$(3.5 \pm 0.5) \times 10^4{}^d$

<sup>a</sup>Determined using *p*-xylylenediamine as the competitor. <sup>b</sup>Determined using 3-(trimethylsilyl)propionic acid as the competitor. <sup>c</sup>Determined by <sup>1</sup>H NMR titration, using double-reciprocal plot for data beyond the equivalence point. <sup>d</sup>Determined by <sup>1</sup>H NMR titration, using least-squares fitting for data beyond the equivalence point. <sup>e</sup>Determined by <sup>31</sup>P NMR, using least-squares fitting for data beyond the equivalence point. <sup>f</sup>Determined using tetramethylphosphonium bromide as the competitor. <sup>g</sup>Determined using benzyltrimethylammonium as the competitor.

### 6.2.2 Host-Guest Stability Constants

The host-guest stability constants were too large for the 1:1 complexes to be measured directly by <sup>1</sup>H NMR chemical shift titration, so instead, <sup>1</sup>H NMR competitive binding methods (at pD 4.75 with 0.050 M NaOAc-*d*<sub>3</sub> and 0.025 M DCl), as developed by Isaacs and coworkers,<sup>49</sup>



were undertaken. A series of ligands with known binding affinities to CB[7] were used as competitors, and these included tetraethylphosphonium chloride ( $K_{\text{CB}[7]} = (1.3 \pm 0.3) \times 10^5 \text{ M}^{-1}$ ),<sup>38</sup> tetramethylammonium bromide ( $K_{\text{CB}[7]} = (1.2 \pm 0.4) \times 10^5 \text{ M}^{-1}$ ),<sup>38</sup> tetramethylphosphonium bromide ( $K_{\text{CB}[7]} = (2.2 \pm 0.4) \times 10^6 \text{ M}^{-1}$ ),<sup>38</sup> trimethylsilylpropionic acid ( $K_{\text{CB}[7]} = (1.82 \pm 0.22) \times 10^7 \text{ M}^{-1}$ ),<sup>49</sup> benzyltrimethylammonium bromide ( $K_{\text{CB}[7]} = (2.5 \pm 0.6) \times 10^8 \text{ M}^{-1}$ ),<sup>38</sup> or *p*-xylylenediamine ( $K_{\text{CB}[7]} = (1.84 \pm 0.34) \times 10^9 \text{ M}^{-1}$ ).<sup>49</sup> The binding affinities between CB[7] and the various guests discussed in this chapter are displayed in Table 6.2.

The 1:1 binding affinities of the trimethylammonium-capped guests were found to vary with the central alkyl chain length, reaching a maximum when the octyl spacer is present. This trend differs from that observed between hosts such as CB[6] or hexa(cyclohexyl)CB[6], and alkyl guests capped by primary ammonium cations, which have higher host-guest binding affinities when the central alkyl chain contains 6 or 5 carbon atoms, respectively.<sup>39,50</sup> With the more hydrophilic primary ammonium cations, the ion-dipole interactions between the electron rich portals are important, and they are apparently maximized when the two primary ammonium cations are separated by a pentyl or hexyl linker. When the cations are the more charge-diffuse trimethylammonium cations, however, the weaker interactions appear to afford the guest's alkyl linker some freedom to fold while inside the cucurbituril. In addition, this folding may be further facilitated by the greater width of the CB[7] cavity (although its length is the same as that of CB[6]). The measured 1:1 binding constants between CB[7] and the trimethylammonium-capped guests, which ranged between  $2.6 \times 10^8 \text{ M}^{-1}$  (for decamethonium) up to  $2.8 \times 10^{10} \text{ M}^{-1}$  (for  $[\text{NMe}_3(\text{CH}_2)_8\text{NMe}_3]^{2+}$ ), may be compared to the stability constants between these guests and  $\alpha$ -CD, which had reported values of 1360 and  $1580 \text{ M}^{-1}$ , which were both calculated values of the binding between  $\alpha$ -CD and decamethonium.<sup>46</sup> The  $\alpha$ -CD host, whose binding was driven largely by the hydrophobic effect, displayed increasing binding affinities with increasing length of the

alkyl linker, with the binding affinity ranging between  $44 \text{ M}^{-1}$  (to  $[\text{NMe}_3(\text{CH}_2)_8\text{NMe}_3]^{2+}$ ) up to values of  $6760$  and  $9170 \text{ M}^{-1}$  (with both of these calculated values representing binding to  $[\text{NMe}_3(\text{CH}_2)_{12}\text{NMe}_3]^{2+}$ ).<sup>46</sup> Meanwhile, Schneider and coworkers have observed that an anionic resorcin[4]arene formed 2:1 host-guest complexes with decamethonium, as well as its shorter hexyl-linked analogue, with binding constants of  $9.0 \times 10^4 \text{ M}^{-1}$  and  $1.0 \times 10^4 \text{ M}^{-1}$ , respectively.<sup>51,52</sup> In these systems, the resorcin[4]arene was involved in binding with the cationic head groups, through  $\pi$ -cation interactions, and not with the aliphatic linker between the cations. CB[7] is able to form [2]pseudorotaxanes with these trimethylammonium-capped guests, by employing both the hydrophobic effect as its hydrophobic cavity is localized over the guest's aliphatic linkers, as well as ion-dipole interactions between its electron rich portals and the cationic head groups of the guest.

When the trimethylammonium capping groups of decamethonium are replaced with trimethylphosphonium groups, to give  $[\text{PMe}_3(\text{CH}_2)_{10}\text{PMe}_3]^{2+}$ , the value of the 1:1 binding constant decreases by a factor of 3, suggesting that substituting the trimethylammonium cations with the more charge-diffuse trimethylphosphonium head groups has a relatively minor effect on the stability constant of the [2]pseudorotaxane. When comparing the binding affinities of decamethonium and its analogues with different capping groups, decreases in the 1:1 binding affinities are also apparent on going from the  $\text{NMe}_3$  to the  $\text{NEt}_3$  capping groups (by a factor of 19), as well as on going from the  $\text{PMe}_3$  to the  $\text{PEt}_3$  head groups (by a factor of 1.3). Throughout this series, the 1:1 binding affinities decrease somewhat as the charge density of the capping groups decrease, and the ion-dipole interactions become weaker.

Meanwhile, when some of the methylene groups of the aliphatic bridge are replaced with two esters (while the lengths of the backbones are similar), as is the case on going from decamethonium to succinylcholine, the 1:1 binding constant decreases by a factor of

approximately 25. In Chapter 2, the influence of the dipole moment on the binding between CB[7] and organic solvents, particularly those bearing carbonyl groups, was described.<sup>53</sup> It was found that some smaller solvents, such as acetone, tend to bind deeply inside the CB[7] cavity, lying flat in the middle of the cavity, with their polar carbonyl group facing the interior wall of the cucurbituril, where the carbonyl can achieve the maximum distance from either of the two electron-rich portals. The  $\Delta\delta_{\text{lim}}$  values of the 1:1 complex between succinylcholine and CB[7] are larger for the methylene protons adjacent to the ester groups (particularly for those adjacent to the carbonyls), which could suggest that the quadrupole-dipole interactions may be playing a role in the positioning of the CB[7], along the [2]pseudorotaxane, as it may attempt to position the carbonyl groups close to the centre of its cavity, away from the portals. It should be noted, however, that any enhancement of binding between CB[7] and succinylcholine as a result of quadrupole-dipole interactions has apparently been diminished by the loss of the more hydrophobic methylene groups, which were replaced by the ester groups in the succinylcholine backbone. The weaker binding affinity between CB[7] and succinylcholine, as compared to that with decamethonium, suggests that the hydrophobic effect plays a greater role in the binding affinity of the host-guest complex, although the weaker quadrupole-dipole interactions may play a role in the positioning of the CB[7] cavity relative to the carbonyl groups of the esters. It is also noteworthy that upon complexation between CB[7] and BW284c51, no significant upfield shifts were observed near the carbonyl group, as the CB[7] cavity occupied the aromatic region upon 1:1 binding, and the methylammonium and allyl regions during 2:1 complexation. This suggests that any contribution to the binding between CB[7] and BW284c51 due to quadrupole-dipole interactions was outweighed by influences of the hydrophobic effect as well as electrostatic interactions.

Among the series of guests explored in this chapter, the strongest 1:1, as well as 2:1, binding affinities with CB[7] are exhibited by [Quin(CH<sub>2</sub>)<sub>10</sub>Quin]<sup>2+</sup> and BW284c51. The 1:1 binding constant between CB[7] and [Quin(CH<sub>2</sub>)<sub>10</sub>Quin]<sup>2+</sup> is comparable to that between CB[7] and *N*-methylquinuclidinium (5.7 × 10<sup>9</sup> M<sup>-1</sup>), suggesting that the strong affinity between CB[7] and the quinuclidinium moiety plays a dominant role in contributing to the binding constant with this guest. Based on statistical grounds, it would be expected that the 2:1 binding constant should be at least 4 times weaker than that of the 1:1 binding affinity (that is  $K_{\text{CB[7]}}/K_{2\text{CB[7]}} \geq 4$ ).<sup>54</sup> The 2:1 binding affinity between CB[7] and [Quin(CH<sub>2</sub>)<sub>10</sub>Quin]<sup>2+</sup> is weaker than the corresponding 1:1 binding constant by a factor of 24. This weaker 2:1 binding affinity, which is weaker than that expected from statistical grounds, most likely arises from electrostatic repulsions between the cucurbiturils. Although diminished from the 1:1 binding constant, the 2:1 binding constant between CB[7] and [Quin(CH<sub>2</sub>)<sub>10</sub>Quin]<sup>2+</sup> is too strong to measure directly, and the binding constant was determined through competitive binding.<sup>38,49</sup> BW284c51 displays a binding affinity with CB[7] of (1.3 ± 0.2) × 10<sup>8</sup> M<sup>-1</sup>, which is comparable to that observed between CB[7] and the benzyldimethylammonium cation ((2.5 ± 0.6) × 10<sup>8</sup> M<sup>-1</sup>),<sup>38</sup> and somewhat larger than values observed between CB[7] and guests such as *p*-toluidinium ((8.38 ± 1.33) × 10<sup>6</sup> M<sup>-1</sup>),<sup>49</sup> and dimethyl(*p*-tolyl)sulfonium cations ((5.18 ± 0.83) × 10<sup>7</sup> M<sup>-1</sup>).<sup>49</sup> As is the case with the [Quin(CH<sub>2</sub>)<sub>10</sub>Quin]<sup>2+</sup> dication, the affinity of the CB[7] macrocycle for quinuclidinium or aromatic groups,<sup>49</sup> over aliphatic guests, likely contributes to the strengthened binding between CB[7] and guests such as [Quin(CH<sub>2</sub>)<sub>10</sub>Quin]<sup>2+</sup> and BW284c51. This trend is also seen with the monocationic choline derivatives, as described in Chapter 5, as the quinuclidinium- and benzyl-bearing derivatives of choline have higher binding affinities than the other derivatives in that series.<sup>37</sup> While the 2:1 binding affinity between CB[7] and [Quin(CH<sub>2</sub>)<sub>10</sub>Quin]<sup>2+</sup> shows a greater decrease, compared to its corresponding 1:1 binding constant, that exceeds that predicted from

statistical grounds, this decrease is still relatively modest compared to those observed by the other members of this series that form 2:1 complexes, which exhibit decreases reaching several orders of magnitude. This relatively modest decrease in the 2:1 binding constant observed for  $[\text{Quin}(\text{CH}_2)_{10}\text{Quin}]^{2+}$  may be due to the placement of the cucurbiturils, as when they are located over the quinuclidinium moieties, which are extended slightly when compared to the trimethyl- and triethyloxonium cations (due to the presence of the terminal carbon 4), the CB[7] units may be slightly further apart than when they are bound to other members of this series, so that the electrostatic repulsions between the two cucurbiturils may be diminished somewhat.

With the exception of the  $[\text{Quin}(\text{CH}_2)_{10}\text{Quin}]^{2+}$  guest, the 2:1 binding affinities between members of this series of guests and CB[7] were determined by  $^1\text{H}$  and  $^{31}\text{P}$  NMR titrations,<sup>55</sup> and are shown in Table 6.2. The magnitudes of the 2:1 binding affinities follow the trend observed among the tetraalkyloxonium cations<sup>38</sup> with CB[7] showing binding affinities with the various analogues  $\text{NR}_3^+$  and  $\text{PR}_3^+$  capped analogues of the decamethonium showing binding affinities that follow the order:  $\text{PMe}_3^+ > \text{NEt}_3^+ > \text{PEt}_3^+ > \text{NMe}_3^+$ . The adherence of the 2:1 binding affinities of these guests to the trend of the tetraalkyloxonium cations, which are encapsulated within the CB[7] cavity, is consistent with the CB[7] cavities being localized over the cationic head groups, as the nature of the head group appears to determine the trend of the binding affinities for these complexes. This positioning of the CB[7] cavities over the quaternary onium capping groups is also in agreement with the observations from the 2:1  $\Delta\delta_{\text{im}}$  values from the  $^1\text{H}$  and  $^{31}\text{P}$  NMR titrations.

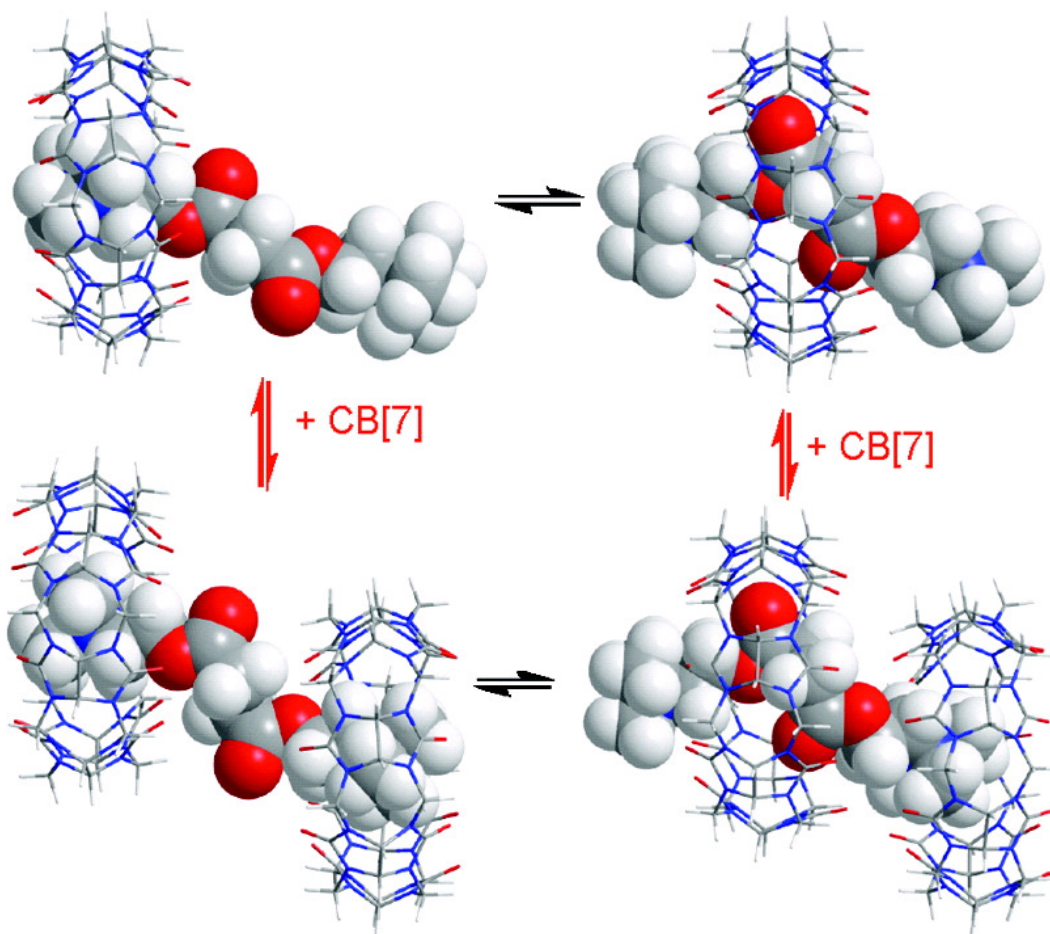


**Figure 6.18** Formation of the 1:1 [2]Pseudorotaxane and 2:1 host-guest complexes between CB[7] and succinylcholine. The red arrows indicate the effect of addition of excess (beyond 1 equiv.) CB[7].

This study has shown that it is possible to form host-guest complexes between CB[7] and a series of succinylcholine and decamethonium derivatives. The majority of the members of this series form discrete 1:1 and 2:1 complexes, depending on the ratio of CB[7] present. There are two possible placements for the binding position of CB[7] along the guest when the 1:1 complex is formed, either at the central linker of the guest, or at one of the cationic ends of the molecule. Among the majority of the guests in this study, with the exception of  $[\text{Quin}(\text{CH}_2)_{10}\text{Quin}]^{2+}$ , the

CB[7] host binds to the central linker (after initially slipping over one of the head groups) between the cationic head groups, upon formation of the 1:1 complex, in a similar manner to the structure at the top right of Figure 6.18. This placement allows both of the electron rich portals to have a cationic group nearby, while the hydrophobic linker is in the cavity. When the guests have aliphatic linkers, their 1:1  $\Delta\delta_{\text{lim}}$  values, revealing upfield shifts, suggest that the CB[7] may be moving back and forth somewhat along the linker, although the magnitude of the upfield shifts are greatest for those protons near the middle of the linker, suggesting that the CB[7] macrocycle is spending the majority of its time at or near the middle of the linker upon formation of the 1:1 complex. On the other hand, CB[7] is localized over the cationic quinuclidinium head group when it forms a 1:1 complex (similar to the top left structure of Figure 6.18), with  $[\text{Quin}(\text{CH}_2)_{10}\text{Quin}]^{2+}$ , this preference is likely related to the high affinity that exists between CB[7] and quinuclidinium guests, as suggested by the high binding constant between CB[7] and the *N*-methylquinuclidinium guest. When the 2:1 complex is formed, both CB[7] macrocycles may be bound at the quinuclidinium head groups, one at each end, similar to the bottom left of Figure 6.18, and the conversion between the 1:1 and 2:1 structures therefore follows the red arrow at the left of Figure 6.18. For the remaining guests in this series, the first CB[7] may initially remain over the central linker initially between the end groups, while the second host is located at one of the terminal cationic groups, and formation of the 2:1 complex occurs through the red arrows on the right side of Figure 6.18. Due to electrostatic repulsions between the cucurbiturils, migration of the first CB[7], either toward, or over, the other cationic group at the opposite end of the molecule will occur as the second CB[7] is added. Depending on the extent of this migration, the 2:1 complex may then exist as either a [3]semirotaxane (such as at the lower right of Figure 6.18), or form a dumbbell-shaped host-guest complex (as in lower left of Figure 6.18).

## 6.3 Experimental

### 6.3.1 Materials

Cucurbit[7]uril (CB[7]) was prepared using the method of Day and coworkers.<sup>56</sup> The 1,6-bis(trimethylammonium)hexane dibromide, 1,10-bis(trimethylammonium)decane dibromide, succinylcholine chloride, and 1,5-bis(4-allyldimethylammoniumphenyl)pentan-3-one dibromide (BW284c51 Br<sub>2</sub>) were available commercially (Sigma-Aldrich) and used as received. Quinuclidine was prepared by neutralizing quinuclidine hydrochloride with 0.10 M NaOH and subsequently extracted with chloroform, which was then removed by rotary evaporation. 1,8-bis(trimethylammonium)octane dibromide and 1,10-bis(trimethylphosphonium)decane dibromide were prepared by Macartney and coworkers a previous study.<sup>46</sup>

#### 1,10-bis(triethylammonium)decane dibromide

A solution of 0.832 g (2.77 mmol) of 1,10-dibromodecane and 1.112 g (11.09 mmol) of triethylamine in 10 mL of acetonitrile was heated at 70 °C under argon in a pressure tube for 48 hours. The white precipitate was washed with diethyl ether and dried to provide 0.712 g (1.42 mmol) of product, with a yield of 51%. Melting point: 238-240 °C (dec.). <sup>1</sup>H NMR (D<sub>2</sub>O, 400 MHz): δ 3.27 (q, 12H, N<sup>+</sup>-CH<sub>2</sub>CH<sub>3</sub>, *J* = 7.2 Hz), 3.14 (t, 4H, H<sub>α</sub>, *J* = 8.3 Hz), 1.67 (q, 4H, H<sub>β</sub>, *J* = 8.3 Hz), 1.36 (m, 8H, H<sub>γ</sub> and H<sub>δ</sub>), 1.32 (m, 2H, H<sub>ε</sub>), 1.27 (tt, 18H, N<sup>+</sup>-CH<sub>2</sub>CH<sub>3</sub>, *J* = 7.2 Hz, *J*<sub>N-H</sub> = 1.6 Hz) ppm. <sup>13</sup>C NMR (D<sub>2</sub>O, 100 MHz): δ 56.63 ppm (C<sub>α</sub>), 52.39 (N<sup>+</sup>-CH<sub>2</sub>CH<sub>3</sub>), 28.34 (C<sub>δ</sub> or C<sub>ε</sub>), 28.15 (C<sub>δ</sub> or C<sub>ε</sub>), 25.53 (C<sub>γ</sub>), 20.84 (C<sub>β</sub>), 6.60 (N<sup>+</sup>-CH<sub>2</sub>CH<sub>3</sub>) ppm. HR-ESI-MS: calc. for C<sub>22</sub>H<sub>50</sub>N<sub>2</sub><sup>2+</sup> ([M-2Br<sup>2+</sup>]) *m/z* = 171.1982, found *m/z* = 171.1985.



### 1,10-bis(trimethylphosphonium)decane dibromide

The compound was prepared in a previous study by Macartney and coworkers.<sup>46</sup> 1,10-dibromodecane was used in place of 1,10-diiododecane,<sup>46</sup> to provide 0.389 g of product. Melting point: 228-232 °C (dec.). <sup>1</sup>H NMR (D<sub>2</sub>O, 500 MHz): δ 2.16 (m, 4H, <sup>2</sup>J<sub>P-H</sub> = 13.2 Hz, J = 8.5 Hz, Hα), 1.81 (d, 18H, <sup>2</sup>J<sub>P-H</sub> = 14.5 Hz, P<sup>+</sup>-CH<sub>3</sub>), 1.57 (m, 4H, Hβ), 1.43 (qn, 4H, J = 7.0 Hz, Hγ), 1.31 (m, 4H, Hδ), 1.29 (m, 4H, Hε) ppm. <sup>13</sup>C NMR (D<sub>2</sub>O, 125 MHz): δ 30.02 (d, <sup>3</sup>J<sub>P-C</sub> = 15.6 Hz, Cγ), 28.68 (s, Cδ), 28.31 (s, Cε), 23.10 (d, <sup>1</sup>J<sub>P-C</sub> = 52.4 Hz, Cα), 21.10 (d, <sup>2</sup>J<sub>P-C</sub> = 4.2 Hz, Cβ), 7.70 (d, <sup>1</sup>J<sub>P-C</sub> = 55.2 Hz, P<sup>+</sup>-CH<sub>3</sub>) ppm. <sup>31</sup>P NMR (D<sub>2</sub>O, 133 MHz): δ 25.91 ppm. HR-ESI-MS: calc. for C<sub>16</sub>H<sub>38</sub>P<sub>2</sub><sup>2+</sup> ([M-2Br]<sup>2+</sup>) m/z = 146.1219, found m/z = 146.1219.

### 1,10-bis(triethylphosphonium)decane dibromide

A solution of 0.602 g (2.01 mmol) of 1,10-dibromodecane and 8.00 mL of 1.0 M triethylphosphine (8.00 mmol) in THF was heated at 70 °C under argon in a pressure tube for 72 hours. The hygroscopic white precipitate was washed with ether, and the ether was removed by evaporating with a stream of nitrogen gas, yielding only 0.0258 g (0.048 mmol), or about 2% of the theoretical yield (not optimized). Melting point: 222-228 °C. <sup>1</sup>H NMR (D<sub>2</sub>O, 500 MHz): δ 2.15 (dq, 12H, P<sup>+</sup>-CH<sub>2</sub>CH<sub>3</sub>, <sup>2</sup>J<sub>P-H</sub> = 13.0 Hz, J = 7.8 Hz), 2.13 (m, 4H, Hα), 1.53 (sx, 4H, Hβ, J = 7.2 Hz), 1.41 (qn, 4H, Hγ, J = 7.2 Hz), 1.28 (m, 4H, Hδ), 1.26 (m, 4H, Hε), 1.17 (dt, 18H, P<sup>+</sup>-CH<sub>2</sub>CH<sub>3</sub>, <sup>3</sup>J<sub>P-H</sub> = 18.0 Hz, J = 7.8 Hz) ppm. <sup>13</sup>C NMR (D<sub>2</sub>O, 125 MHz): δ 30.25 (d, <sup>3</sup>J<sub>P-C</sub> = 14.6 Hz, Cγ), 28.71 (s, Cδ), 28.28 (s, Cε), 20.82 (d, <sup>2</sup>J<sub>P-C</sub> = 4.5 Hz, Cβ), 16.94 (d, <sup>1</sup>J<sub>P-C</sub> = 48.1 Hz, Cα), 11.27 (d, <sup>1</sup>J<sub>P-C</sub> = 49.8 Hz, P<sup>+</sup>-CH<sub>2</sub>CH<sub>3</sub>), 5.01 (d, <sup>2</sup>J<sub>P-C</sub> = 5.5 Hz, P<sup>+</sup>-CH<sub>2</sub>CH<sub>3</sub>) ppm. <sup>31</sup>P NMR (D<sub>2</sub>O,

133 MHz):  $\delta$  38.54 ppm. HR-ESI-MS: calc. for  $C_{22}H_{50}P_2^{2+}$  ( $[M-2Br]^{2+}$ )  $m/z = 188.1688$ , found  $m/z = 188.1688$ .

### **bis(Quinuclidinium)decane dibromide**

A solution of 0.587 g (5.28 mmol) of quinuclidine in 4 mL of DMF was prepared, and to this solution was added dropwise a solution of 0.720 g (2.40 mmol) of 1,10-dibromodecane in 2 mL of DMF. The combined solution was heated at 50 °C for 5 minutes, with a white precipitate being formed. This precipitate was washed with ether and dried, to give 0.664 g (1.27 mmol) of product, with a yield of 53%. Melting point: > 300 °C.  $^1H$  NMR ( $D_2O$ , 400 MHz):  $\delta$  3.28 (t, 12H, H<sub>2</sub>,  $J = 7.8$  Hz), 3.00 (t, 4H, H $\alpha$ ,  $J = 8.4$  Hz), 2.09 (sp, 2H, H<sub>4</sub>,  $J = 3.2$  Hz), 1.88 (m, 12H, H<sub>3</sub>), 1.61 (m, 4H, H $\beta$ ), 1.23 (m, 12H, H $\gamma$ , H $\delta$ , and H $\epsilon$ ) ppm.  $^{13}C$  NMR ( $D_2O$ , 100 MHz):  $\delta$  64.37 (C $\alpha$ ), 54.55 (C<sub>2</sub>), 28.28 (C $\epsilon$ ), 28.09 (C $\delta$ ), 25.67 (C $\gamma$ ), 23.39 (C<sub>3</sub>), 21.40 (C $\beta$ ), 19.09 (C<sub>4</sub>) ppm. HR-ESI-MS: calc. for  $C_{24}H_{46}N_2^{2+}$  ( $[M-2Br]^{2+}$ )  $m/z = 181.1825$ , found  $m/z = 181.1821$ .

### **6.3.2 Methods**

$^1H$ ,  $^{13}C$ , and  $^{31}P$  NMR spectra were recorded on Bruker Avance 400 and 500 MHz NMR spectrometers, with 2D HSQC experiments conducted to confirm the assignment of the  $^1H$  and  $^{13}C$  NMR spectra. Electrospray-ionization time-of-flight high resolution mass spectra were recorded on an Applied BioSystems/MDS SciEX QStar XL QqTOF instrument. The 1:1 binding constants of all guests in this series, and the 2:1 binding constant of  $[Quin(CH_2)_{10}Quin]^{2+}$  were determined by the  $^1H$  NMR competitive binding method developed by Isaacs and coworkers, and were carried out at pD 4.75 in  $D_2O$  solution with 0.050 M NaOAc- $d_3$  and 0.025 M DCl.<sup>49</sup> The 2:1 binding constants of the rest of the compounds were determined by  $^1H$  NMR chemical shift

titration, using non-linear least squares fitting for the data beyond the equivalence point (for  $[\text{PMe}_3(\text{CH}_2)_{10}\text{PMe}_3]^{2+}$ , BW284c51,  $[\text{NEt}_3(\text{CH}_2)_{10}\text{NEt}_3]^{2+}$ , as well as  $[\text{PEt}_3(\text{CH}_2)_{10}\text{PEt}_3]^{2+}$ ), or by using double reciprocal plots (for the succinylcholine, decamethonium, and  $[\text{PEt}_3(\text{CH}_2)_{10}\text{PEt}_3]^{2+}$  dications). Equations 2.2 through 2.4 from Chapter 2 were used for the least-squares fitting to obtain the 2:1 binding constant, while Equation 2.8 was used for calculating the 2:1 binding constant through the double reciprocal plots. While plots for 1:1 binding would be plotted relative to the point at which the concentration of CB[7] was zero, the plots used to determine the 2:1 binding affinity were plotted relative to the point at which the concentration of CB[7] equaled that of the guest (the guest's concentration was kept constant throughout the titration), which is the equivalence point. The equivalence point was treated as the origin in these 2:1 titrations, with the effective concentration of CB[7] being treated as the concentration of CB[7] beyond the equivalence point. Likewise the changes in the chemical shifts (the  $\Delta\delta$  values) of the 2:1 titrations, instead of being relative to the point at which the concentration of CB[7] was zero, were relative to the equivalence point, the point at which the concentration of CB[7] equaled that of the guest.

## 6.4 Conclusions

In this chapter the host-guest binding between CB[7] and a series of dicationic guests, which have included the AChE inhibitors succinylcholine, BW284c51, decamethonium, as well as their analogues, were observed. For most members of this series, both 1:1 and 2:1 host-guest complexes were observed. The binding affinities of the guests varied with the nature of the cationic head groups, as well as the nature of the central linker between the two head groups. When the head groups were capped with trimethyl- or triethylonium cations, the 2:1 binding

constants followed the trend observed previously for the corresponding tetraalkylonium cations.<sup>38</sup> The dumbbell shape of these guests, along with the host-guest complexation behaviour observed between members of this series of guests and CB[7] approximates the general shape of the bis(pyridinium)alkane guests, as well as their complexation behaviour with CB[7], as discussed in Chapter 3.<sup>44</sup> Specifically, CB[7] is initially localized over the central linker upon formation of the 1:1 complex, and subsequently migrates towards the cationic ends of the molecule (although in some cases one CB[7] may remain near the centre, while the second CB[7] is localized over a cationic head group). Meanwhile, the [Quin(CH<sub>2</sub>)<sub>10</sub>Quin]<sup>2+</sup> guest behaves analogously to the [bis(4-*t*-butylpyridinium)alkane]<sup>2+</sup> guests, with the CB[7] binding at the cationic head groups and not over the central linkers. In both cases, an initial asymmetric host-guest complex was formed, with the CB[7] binding over one terminal cationic end, followed by addition of the second CB[7] at the other end of the guest.

A practical application of this study may be the use of cucurbiturils to reduce adverse side effects of AChE inhibitors, such as succinylcholine, through forming a host-guest complex with them. This could therefore allow CB[7] to act as a drug-reversal agent, essentially by “inhibiting the inhibitor”, and thus allowing AChE to resume its normal activity. Nau and coworkers<sup>57</sup> have reported that the activity of protease enzymes could be inhibited when CB[7] was used to bind to their substrates, such as trypsin. Similar binding could be used by analogy with the ability of CB[7] to bind to AChE substrates and products, such as acetylcholine, or choline, which could be utilized to regulate the activity of AChE. The research described in this chapter has been published in *The Journal of Organic Chemistry*.<sup>47</sup>

## References

1. D.M. Quinn, *Chem. Rev.*, **1987**, 87, 955.
2. I. Silman and J.L. Sussman, *Curr. Opin. Pharm.*, **2005**, 5, 293.
3. T.L. Rosenberry, J.L. Johnson, B. Cusack, J.L. Thomas, S. Emani, K.S. Venkatasubban, *Chem. Biol. Interact.*, **2005**, 157-158, 181.
4. J.L. Sussman, M. Harel, F. Frolow, C. Oefner, A. Goldman, L. Toker, and I. Silman, *Science*, **1991**, 253, 872.
5. R.K. Stoelting and R.D. Miller, *Basics of Anesthesia, 4<sup>th</sup> Edition*, Churchill Livingstone, A Harcourt Health Sciences Company: New York, 2000; pp. 89-106.
6. M.R. Fallow and J.R. Cummings, *Am. J. Med.*, **2007**, 120, 388.
7. P.T. Francis, A.M. Palmer, M. Schnape, and G.K. Wilcock, *J. Neurosurg. Psychiatry*, **1999**, 66, 137.
8. L.C. Walker and R.F. Rosen, *Age and Aging*, **2006**, 35, 332.
9. E.K. Perry, P.H. Gibson, G. Blessed, R.H. Perry, and B. Tomlinson, *J. Neorol. Sci.*, **1977**, 34, 247.
10. R.J. Rylett, M.J. Ball, and E.H. Colhoun, *Brain Res.*, **1983**, 289, 169.
11. P.L. McGreer, *Can. J. Physiol. Pharmacol.*, **1984**, 62, 741.
12. J. Hardy, R. Adolfsson, I. Alafuzoff, G. Bucht, J. Marcusson, P. Nyberg, E. Per Dahl, P. Wester, and B. Winblad, *Neurochem. Int.*, **1985**, 7, 545.
13. L. Nilsson, A. Nordberg, J. Hardy, P. Wester, and B. Winblad, *J. Neural Transm.*, **1986**, 67, 275.
14. N. Tabet, *Age and Aging*, **2006**, 35, 336.
15. M. Mesulam, A. Guillozet, P. Shaw, and B. Quinn, *Neurobiol. Dis.*, **2002**, 9, 88.
16. C.G. Ballard, *Eur. Neurol.*, **2002**, 47, 64.

17. H. Wang, M. Yu, M. Ochani, C.A. Amella, M. Tanovic, S. Susarla, J.H. Li, H. Wang, H. Yang, L. Ulloa, Y. Al-Abed, C.J. Czura, and K.J. Tracey, *Nature*, **2003**, *421*, 384.
18. H.Y. Zhang and X.C. Tang, *Neurosci. Lett.*, **2000**, *292*, 41.
19. R. Wang, J. Zhou, X.C. Tang, *Mol. Brain Res.*, **2002**, *107*, 1.
20. C.B. Millard and C.A. Broomfield, *J. Neurochem.*, **1995**, *64*, 1909.
21. S. Darvesh, K.V. Darvesh, R.S. McDonald, D. Mataija, R. Walsh, S. Mothana, O. Lockridge, and E. Martin, *J. Med. Chem.*, **2008**, *51*, 4200.
22. L. Weiner, V.L. Shnyrov, L. Konstantinovskii, E. Roth, Y. Ashani, and I. Silman, *Biochemistry*, **2009**, *48*, 563.
23. H.M. Greenblatt, H. Dvir, I. Silman, and J.L. Sussman, *J. Mol. Neurosci.*, **2003**, *20*, 369.
24. Y. Bourne, Z. Radic, G. Sulzenbacher, E. Kim, P. Taylor, and P. Marchot, *J. Biol. Chem.*, **2006**, *281*, 29256.
25. C.E. Felder, M. Harel, I. Silman, and J.L. Sussman, *Acta Cryst.*, **2002**, *D58*, 1765.
26. M. Harel, I. Schalk, L. Ehret-Sabatier, F. Bouet, M. Goeldner, C. Hirth, P.H. Axelsen, I. Silman, and J.L. Sussman, *Proc. Natl. Acad. Sci. USA*, **1993**, *90*, 9031.
27. J.G. Bourne, H.O.J. Collier, and G.F. Somers, *The Lancet*, **1952**, *259*, 1225.
28. A.L.W. Po and T. Girard, *J. Clin. Pharm. Ther.*, **2005**, *30*, 497.
29. M. Jonsson, M. Dabrowski, D.A. Gurley, O. Larsson, E.C. Johnson, B.B. Fredholm, and L.I. Eriksson, *Anesthesiology*, **2006**, *104*, 724.
30. C.P. Collins and O.R. Beirne, *J. Oral Maxillofac. Surg.*, **2003**, *61*, 1340.
31. M.A. Rubin and N. Sadovnikoff, *J. Emerg. Med.*, **1996**, *14*, 193.
32. S.D. Choudhury, J. Mohanty, H.P. Upadhyaya, A.C. Bhasikuttan, and H. Pal, *J. Phys. Chem. B*, **2009**, *113*, 1891.
33. H. Naiki, K. Higuchi, M. Hosokawa, and T. Takeda, *Anal. Biochem.*, **1989**, *177*, 244.

34. H. Levine III, *Methods Enzymol.*, **1999**, 309, 274.
35. T. Ban, D. Hamada, K. Hasegawa, H. Naiki, and Y. Goto, *J. Biol. Chem.*, **2003**, 278, 16462.
36. M. Harel, L.K. Sonoda, I. Silman, J.L. Sussman, and T.L. Rosenberry, *J. Am. Chem. Soc.*, **2008**, 130, 7856.
37. I.W. Wyman and D.H. Macartney, *Org. Biomol. Chem.*, **2010**, 8, 253.
38. A.D. St-Jacques, I.W. Wyman, and D.H. Macartney, *Chem. Commun.*, **2008**, 4936.
39. W.L. Mock and N.-Y. Shih, *J. Org. Chem.*, **1986**, 51, 4440.
40. L. Isaacs, *Angew. Chem., Int. Ed.*, **2005**, 44, 4844.
41. H.-J. Kim, W.S. Jeon, Y.H. Ko, and K. Kim, *Proc. Natl. Acad. Sci. U.S.A.*, **2002**, 99, 5007.
42. W. Ong, M. Gomez-Kaifer, and A.E. Kaifer, *Org. Lett.*, **2002**, 4, 1791.
43. L. Yuan, R. Wang, and D.H. Macartney, *J. Org. Chem.*, **2007**, 72, 4539.
44. I.W. Wyman and D.H. Macartney, *Org. Biomol. Chem.* **2009**, 7, 4045.
45. R.M. Fuoss and D. Edelson, *J. Am. Chem. Soc.*, **1951**, 73, 269.
46. A.P. Lyon, N.J. Banton, and D.H. Macartney, *Can. J. Chem.*, **1998**, 76, 843.
47. I.W. Wyman and D.H. Macartney, *J. Org. Chem.*, **2009**, 74, 8031.
48. M.S. Bali, D.P. Buck, A.J. Coe, A.I. Day, and J.G. Collins, *Dalton Trans.*, **2006**, 5337.
49. S. Liu, C. Ruspic, P. Mukhopadhyay, S. Chakrabarti, P.Y. Zavalij, and L. Isaacs, *J. Am. Chem. Soc.*, **2005**, 127, 15959.
50. Y. Kim, H. Kim, Y.H. Ko, N. Selvapalam, M.V. Rekharsky, Y. Inoue, and K. Kim, *Chem. Eur. J.*, **2009**, 15, 6143.
51. H.-J. Schneider and U. Schneider, *J. Org. Chem.*, **1987**, 52, 1613.
52. H.-J. Schneider, D. Guttes, and U. Schneider, *J. Am. Chem. Soc.*, **1988**, 110, 6449.
53. I.W. Wyman and D.H. Macartney, *Org. Biomol. Chem.*, **2008**, 6, 1796.
54. G. Ercolani, *J. Am. Chem. Soc.*, **2003**, 125, 16097.

55. K.A. Connors, *Binding Constants. The Measurement of Molecular Complex Stability*, John Wiley & Sons: New York: 1987; p. 197.
56. A.I. Day, A.P. Arnold, R.J. Blanch, and B. Snushall, *J. Org. Chem.*, **2001**, *66*, 8094.
57. A. Hennig, G. Ghale, and W.M. Nau, *Chem. Commun.*, **2007**, 1614.
58. H. Soreq and S. Seidman, *Nature Rev.*, **2001**, *2*, 294.



## Chapter 7

### Conclusions and Future Work

#### 7.1 Conclusions and Summary of Research

In this thesis a number of series of host-guest systems were explored, with CB[7] as the host. The guests examined in this thesis have included polar organic solvents,  $\alpha,\omega$ -bis(pyridinium)alkane guests, a series of local anaesthetics, choline and acetylcholine derivatives, and a series of acetylcholinesterase inhibitors including succinylcholine, decamethonium, as well as their analogues. Within these studies, the host-guest binding affinities were determined, and the nature of the binding behaviour (such as location of the CB[7] relative to the guest) were also explored.

##### 7.1.1 Polar Solvent Guest Complexation with CB[7]

The host-guest chemistry between CB[7] and a series of polar organic solvents has been studied and is described in Chapter 2.<sup>1</sup> One aspect of this study was to explore the potential for quadrupole-dipole interactions upon the host-guest binding between CB[7] and these polar guests, especially those containing carbonyl-groups. Due to the quadrupole moment of CB[7], it was anticipated that the carbonyl would align itself towards the interior wall of the CB[7] at the middle of the cavity, where it could obtain maximum separation from either of the electron rich portals. These neutral solvent guests provided good platforms to study influences from quadrupole-dipole interactions, as they did not have overriding ion-dipole interactions that

cationic guests would have with CB[7], which may otherwise obscure these effects. The large upfield shifts observed for acetone, were consistent with the positioning of the carbonyl inside the cavity, with the acetone lying flat and perpendicular to the channel in the CB[7] cavity. When acetophenone was explored, the bulkier aromatic group prevented the carbonyl from approaching the middle of the cavity. Also, the phenyl group was encapsulated within the cavity to a greater extent due to the higher affinity between aromatic groups and CB[7]. Noting that alkali cations can compete with a guest for binding to CB[7],<sup>2</sup> and thus lower the guest's binding affinity, the host-guest systems of acetone and acetophenone were explored in D<sub>2</sub>O solution in the presence of 0.2 M NaCl and KCl, as well as in the absence of electrolyte. The measurement of the binding constants of some of these solvents may be useful in attempts to correct for the effects of any of these solvents if they happen to be present, either as impurities, or as the solvent matrix. This is particularly relevant for DMSO, as CB[7] is moderately soluble in this solvent, and has recently been utilized by Leventis and coworkers.<sup>3</sup> With the binding affinity between this solvent and CB[7] in hand, it is now possible to account for competition that may arise from the DMSO.

### **7.1.2 $\alpha,\omega$ -Bis(pyridinium)alkane Guest Binding to CB[7]**

The binding between CB[7] and a series of  $\alpha,\omega$ -bis(pyridinium)alkane guests was explored.<sup>4</sup> In this study, the effect of the substitution of the pyridinium moiety of the guest upon the host-guest binding properties with CB[7] was examined, and also the aliphatic linker between the pyridinium units was varied. The binding position of the CB[7] macrocycle with respect to the guest could be monitored through <sup>1</sup>H NMR titrations, and the 1:1 and 2:1 binding constants were determined through competitive binding studies.<sup>5,6</sup> In most cases, 1:1 complexation resulted in formation of a [2]pseudorotaxane, with CB[7] encapsulating the aliphatic region, with each electron donating portal near one of the cationic pyridinium nitrogens. As the 2:1 complexes

were formed, the first CB[7] would tend to migrate from the central aliphatic region towards the terminal pyridinium moiety, while the second CB[7] would occupy the pyridinium unit at the other end of the guest. This migration to form the dumbbell-shaped 2:1 guest resulted from electrostatic repulsions from the portals of the two CB[7] hosts. Exceptions to this general trend occurred when the pyridinium units of the guests contained *tert*-butyl substituents. In these situations, the first CB[7] encapsulated one of the terminal *tert*-butylpyridinium units, to form an asymmetric host-guest complex, while the second CB[7] encapsulated the outer *tert*-butylpyridinium moiety at the other side of the molecule, to form the dumbbell-shaped 2:1 host-guest complex. Therefore, in these cases with the capping of the terminal regions of the guest by CB[7], migration of the first CB[7] was not required to accommodate the addition of the second CB[7], and less reorganization of the host-complexation was required to accommodate formation of the 2:1 complex. In terms of the relative strength of the 2:1 binding constant as compared to the 1:1 binding affinity, the 2:1 binding affinities were stronger when the *tert*-butyl substituents were present. Meanwhile, the 2:1 binding constants were weakest when no substituents were present on the pyridinium moiety. This is likely due to the shorter overall length of the guests which lack additional pyridinium substituents, which therefore require the CB[7] macrocycles to be closer to one another upon 2:1 binding. In addition, because the pyridinium substituents were often hydrophobic, the unsubstituted pyridinium units presented a less attractive binding site for CB[7] than their substituted analogues.

### 7.1.3 Binding between CB[7] and Local Anaesthetics

The complexation of a series of local anaesthetics by CB[7] was explored and is described in Chapter 4.<sup>7</sup> The host-guest binding constants were determined and the binding position of the CB[7] was observed using <sup>1</sup>H NMR spectroscopy. The majority of these guests

contained two protonation sites with well-separated  $pK_a$  values. As a result, in near-neutral solution, one site was protonated, while in 0.1 M HCl (or DCl) both sites were protonated. In most cases, the CB[7] occupied the site that was more readily protonated in neutral solution, while migrating from this initial position to the newly protonated site in acidic media, with the binding position therefore acting as a pH-activated switch. The complexation-induced  $pK_a$  shifts of the local anaesthetics were observed also, with  $pK_a$  increases between approximately 0.5 and 2 units being observed upon their complexation with CB[7]. These values are moderate, considering the complexation-induced  $pK_a$  increase of up to 4 units reported for thiabendazole complexation with CB[7] recently reported by Nau and coworkers.<sup>8</sup>

#### **7.1.4 Choline and Acetylcholine Guest Complexation with CB[7]**

A series of choline and acetylcholine compounds and their phosphonium analogues were bound to CB[7], and their host-guest binding affinities, as well as the positioning of CB[7] with respect to the guest were observed, as described in Chapter 5.<sup>9</sup> The guests in this series contained quaternary ammonium or phosphonium cationic centres, and in most members of this series, the CB[7] was observed to encapsulate these cationic centres of these guests, in a similar manner as that observed with charge-diffuse tetraalkylated ammonium and phosphonium salts.<sup>6</sup> In these situations, the cationic region was more hydrophobic than a primary ammonium would be, so that the cation was encapsulated inside the hydrophobic CB[7] cavity instead of near the portals, where cations normally bind to cucurbiturils. As the nature of the cation was varied, with the incorporation of larger aliphatic groups (such as ethyl groups instead of methyl groups) and a larger onium atom (such as phosphorus), the charge became softer. The positioning of the CB[7] was also affected by substitution on the guest, with extended hydrophobic guests competing with the cationic centre for encapsulation by the host.

### 7.1.5 Encapsulation of Acetylcholinesterase Inhibitors by CB[7]

The host-guest chemistry between CB[7] and a series of acetylcholinesterase (AChE) inhibitors was explored.<sup>10</sup> These guests have included succinylcholine, BW284c51, decamethonium, as well as its trimethylammonium and phosphonium analogues. In Chapter 6, the 1:1 and 2:1 binding affinities between CB[7] and these guests was described, as well as the binding behaviour. Among most of these guests, a pseudorotaxane was formed upon 1:1 host-guest formation, with the CB[7] occupying the aliphatic linker between the two onium centres. This was often followed by migration of the CB[7] towards the terminal ends of the guest as the second CB[7] was added, to form a dumbbell-shaped 2:1 host-guest system. These trends paralleled those observed with the  $\alpha,\omega$ -bis(pyridinium)alkane guests.<sup>4</sup> When the terminal trialkylammonium centres were replaced with quinuclidinium groups, the binding behaviour differed, with the CB[7] units “capping” the guest by encapsulating the quinuclidinium regions and not initially binding to the central aliphatic linker. This behaviour, with the first CB[7] occupying a quinuclidinium unit at one end of the guest, and the second CB[7] encapsulating the other end, also closely mimics the binding trends between CB[7] and  $\alpha,\omega$ -bis(pyridinium)alkane guests, specifically when the pyridinium units were substituted with *tert*-butyl groups.

The study of these AChE inhibitor guests is closely related to the study of the choline and acetylcholine guests in Chapter 5, as both of these series of guests contain charge-diffuse quaternary ammonium and phosphonium guests. The nature of the guests, such as the presence of aliphatic pentyl arms in the case of the monocationic guests of Chapter 5, or the length of the aliphatic linker between the dicationic guests of Chapter 6, had an influence on the binding behaviour. In addition, the binding behaviours in these studies were influenced by the nature of

the trialkyl ammonium or phosphonium group present, and often followed binding trends observed with the peralkylated onium salts.<sup>6</sup> Furthermore, both of these series of guests have relevance to the AChE enzyme. The dicationic guests such as succinylcholine, BW284c51, and decamethonium can act to inhibit the AChE enzyme, with succinylcholine being used as a muscle relaxant for procedures such as tracheal intubation.<sup>11</sup> Meanwhile, the neurotransmitter acetylcholine is a substrate of AChE,<sup>12</sup> with choline being produced as the enzymatic product.

#### **7.1.6 General Overview of the Research**

A major focus of this thesis was the study of how the variation of chemical structure of guests within a given series, such as their positioning, size, or functional group of the substituent, affect the host-guest binding behaviour between a particular guest and CB[7]. These changes in the host-guest binding with CB[7] could be observed through changes in position of the CB[7] cavity along the guest, as well as the orientation of the guest with respect to the CB[7] host, and the host-guest binding affinities. This thesis explored the host-guest binding between CB[7] and five different series of guests, which shared common general features within each series, but had structural variations between each series. In some cases, the conditions of the media were also varied, such as pH, or the salt content, to explore their effects on the host-guest binding.

In addition to this fundamental research, three series of medically relevant guests were also explored, including the local anaesthetics, the acetylcholine and choline analogues, as well as the dicationic AChE inhibitors. The local anaesthetics and the AChE inhibitors both have relevance towards surgical procedures, either through pain management (local anaesthetics), or muscle relaxation (AChE inhibitors). These series of guests also have in common their activity towards the nervous system. While the AChE inhibitors bind to the AChE enzyme and block

access of the acetylcholine substrate to the enzyme, local anaesthetics act by blocking ion channels.<sup>13</sup> With regard to these guests, CB[7] may have application toward drug delivery systems, or for slow-release of the drugs, as well as for drug-reversal agents. The application as drug reversal agents could be particularly relevant to the AChE inhibitors, as adverse side effects for some of these drugs, such as succinylcholine, occasionally occur.<sup>11</sup> In the event of a complication with succinylcholine, it may be possible to administer CB[7] to the patient, where it would bind the drug, and thus deactivate it. In addition to side-effects specific to succinylcholine, including, but not limited to, cardiac dysthythmias, allergic reactions, hyperthermia,<sup>11</sup> it has also been reported that up to 45 % of patients experience residual paralysis when they arrive at the post-anaesthesia care unit.<sup>14,15</sup> CB[7] may therefore be useful for emergency situations in the event of a patient experiencing a complication with the AChE inhibitor, and also in more general cases in order to accelerate a patients recovery from residual paralysis due to administration of the AChE inhibitors. In addition to improving the patient's recovery, it may also reduce demand on the hospital by reducing recovery times, and the demand for equipment, such as ventilators, in particular. The high binding affinity that is generally observed by CB[7] compared to similar families of hosts could be particularly beneficial in this regard also.

## **7.2 Suggestions for Future Work**

There are aspects of these projects that have opened doors for further exploration. This is especially true with the series of AChE inhibitors, as there are a wide variety of compounds that are either used clinically as muscle relaxants, or are not in clinical use at this time but are believed to have AChE inhibiting properties. Some examples of clinical muscle relaxants that could be studied as guests of CB[7] include rocuronium, pancuronium, neostigmine,

edrophonium, and pyridostigmine (Figure 7.1). In fact, work is currently underway in the Macartney lab, exploring the host-guest binding between CB[7] and these AChE antagonists. Adjacent to their quaternary ammonium cationic centre, the muscle relaxants neostigmine, edrophonium, and pyridostigmine contain an aromatic unit, and the binding affinity between CB[7] and these drugs would likely be strong. This may be carried even further, to explore host-guest chemistry between CB[7] and of a broad spectrum of clinical muscle relaxants. Researchers have found that the host Sugammadex, which is based on  $\gamma$ -CD and has been approved for clinical use in Europe,<sup>16</sup> has a high binding affinity for rocuronium of  $10^7 \text{ M}^{-1}$ .<sup>15-17</sup> This development demonstrates the utility of supramolecular hosts in medical systems. CB[7], with its tendency for high-selectivity, as well as high binding affinities for cationic guests, may also present an useful reversal agent for these and other AChE inhibitors.

While the work described in this thesis has been conducted completely in the absence of biological tissue, in future studies with these systems, particularly those involving a clinically utilized muscle relaxant which demonstrates a high binding affinity with CB[7], it may be beneficial to expand these studies towards *in vivo* systems, through collaboration with biologists or medical researchers. An example could include rats, to which the AChE inhibiting drug has been administered. CB[7] could then subsequently be administered to the rat, in order to determine if reversal of the muscle paralysis is achieved, and how quickly this occurs. This could be compared to the response of rats which have been administered similar doses of the muscle relaxant, but no CB[7]. Prior to these *in vivo* studies, it may also be of interest to study the effect of the presence of CB[7] upon the enzymatic activity of AChE in tissue cultures, which have an inhibitor present, in order to determine if activity of AChE is recovered more readily in the presence of CB[7].



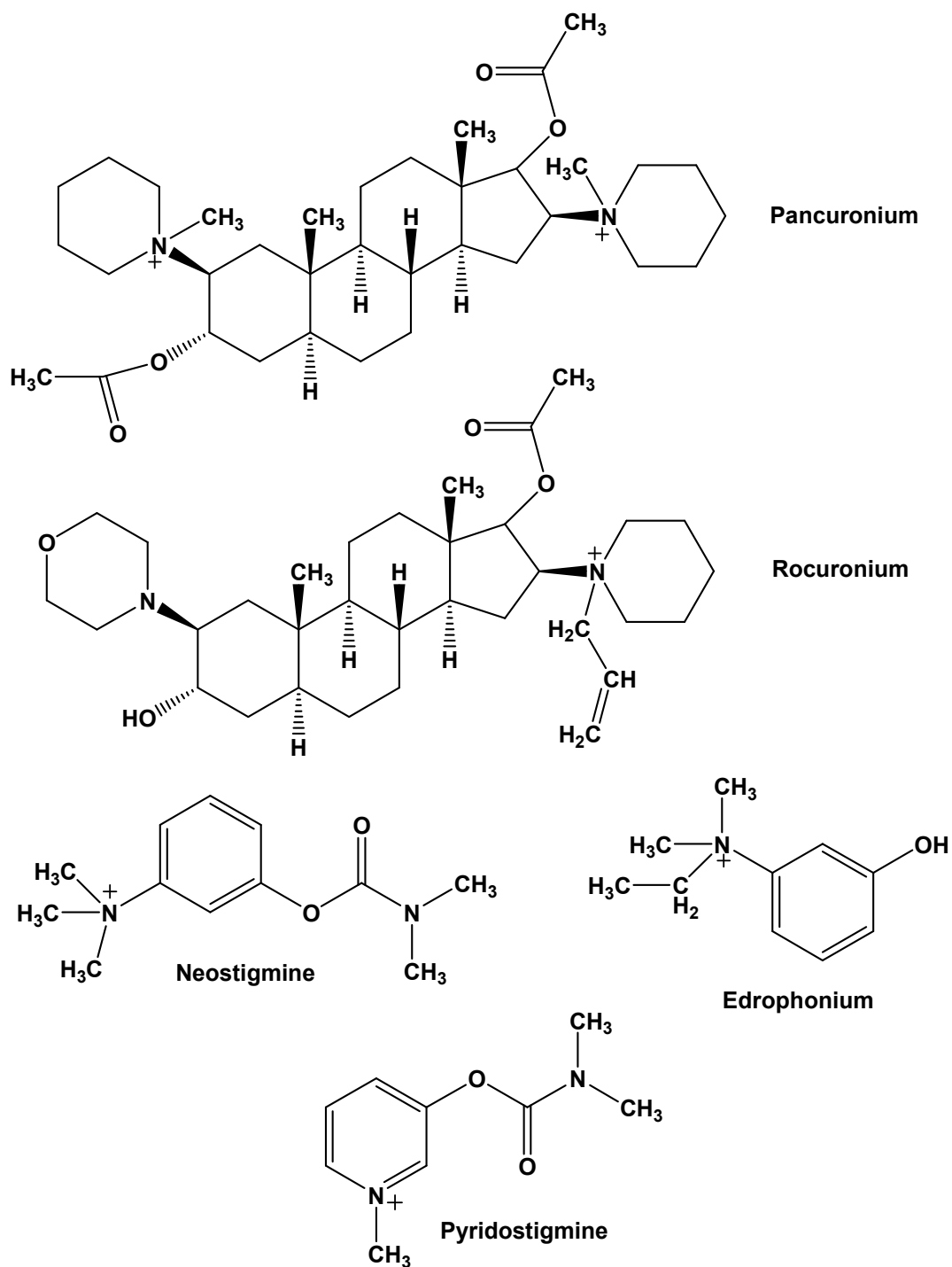


**Figure 7.1** Structures of muscle relaxants that may form suitable host-guest systems with CB[7].

While the exploration of host-guest binding between the dicationic guest 1,10-bis(quinuclidinium)decane and CB[7] has been explored, it may be of interest to carry this further, by exploring complexation with guests composed of two quaternary ammonium cations incorporated into cyclic rings that are linked by a hydrophobic unit. Work is currently underway in the Macartney lab exploring the host-guest chemistry between CB[7] and guests containing morpholinium, piperidinium, and pyrrolidinium substituents at the ends of the aliphatic linker.

The influence of host-guest binding between acetylcholine and CB[7] upon the stability of the compound would be an interesting area to pursue. While acetylcholine's conversion to choline is catalyzed by the AChE enzyme, it also can undergo ester hydrolysis in the absence of this enzyme, such as in basic solution.<sup>18,19</sup> It would be interesting, therefore, to compare the lifetime of acetylcholine in the presence and absence of CB[7], in order to see if it becomes stabilized by the host.

It may also be interesting to synthesize asymmetric dicationic hosts, either in the  $\alpha,\omega$ -bis(pyridinium)alkane form, with different substituents on either pyridinium group, or as dicationic quaternary onium guests, with different trialkylammonium or -phosphonium substituents on either end of the guest, with some examples shown in Figure 7.2. The positioning of a bulkier, high-affinity binding site at one of the molecule, and a smaller substituent at the other end of the molecule, with the aliphatic linker thus easily accessible, could present the CB[7] with two potential binding sites. Examples of these systems could include a guest containing a quinuclidinium unit at one end of an aliphatic linker, and a trimethylammonium (or even a primary ammonium) group at the other end. In a similar manner, a  $\alpha,\omega$ -bis(pyridinium)alkane guest could be prepared that consists of a 4-*tert*-butylpyridinium unit at one end of the guest, and an unsubstituted pyridinium unit at the other end of the linker. The aliphatic linker, with its hydrophobic backbone and the two cationic regions that could each be near an electron rich

portal, would present an ideal position for CB[7] to bind, as has been demonstrated by the tendency for CB[7] to position itself along this linker during 1:1 complexation with  $\alpha,\omega$ -bis(pyridinium)alkanes and dicationic quaternary onium compounds (except when both ends contain *tert*-butyl groups, or quinuclidinium groups, respectively). At the same time, if one of the cationic termini of the guest molecules contains a quinuclidinium group, or a 4-*tert*-butylpyridinium site, a high-affinity binding site for the CB[7] would become available as well, and it would be interesting to see which site the CB[7] would bind preferentially during 1:1 complexation. A series of these ligands could be prepared that would have variations in either the aliphatic chain length, or the nature of the cationic groups, in order to determine which is the threshold structure, at which the CB[7] changes from favouring one site over the other competing binding site. This could be extended further by synthesizing asymmetric dicationic guests which contain a quaternary onium site at one end of the linker, and a pyridinium unit at the other end.

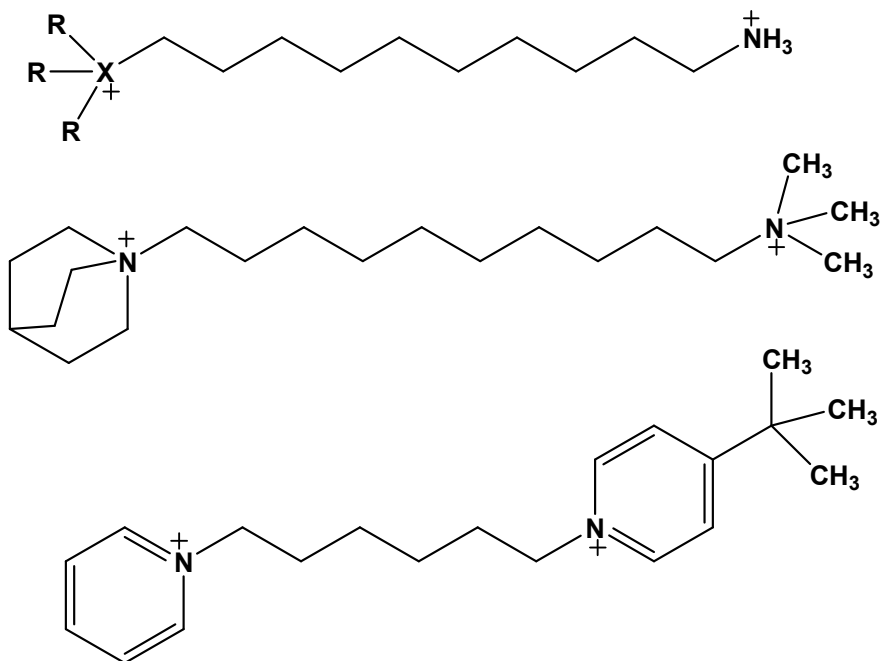


**Figure 7.2** Selected examples of asymmetric dicationic ammonium and pyridinium guests.

The study of dicationic ammonium guests which contain a quaternary ammonium (or -phosphonium) group at one end of the molecule, and a primary ammonium group at the other end could also be of interest also. The harder cationic charge of the primary cationic group could make the aliphatic linker somewhat more attractive to a nearby CB[7] portal, which could further increase the likelihood of a CB[7] unit binding to the aliphatic linker during 1:1 host-guest complexation. At the same time, the primary ammonium should not readily become encapsulated into the CB[7] cavity. This would raise the question of whether this type of host could accommodate binding to two CB[7] macrocycles. Although it may be possible for one CB[7] to occupy the quaternary ammonium site, and another CB[7] to occupy the linker, the electrostatic repulsions between the portals of the two CB[7] unit may prevent this from occurring. With these series of guests, features, such as lengths of the aliphatic linker or different quaternary ammonium or phosphonium units, could be varied to determine which substituents are necessary in order to accommodate two CB[7] units. With improved understanding of the nature of host-guest binding between CB[7] and guests due to the study of structure variation upon the binding properties, it may become possible to “tune” a guest in order to accommodate a particular mode or strength of binding between the host and the guest. This could in turn make it easier to customize features of the host-guest system (such as the binding constant, as well as the stoichiometry and mode of binding) so that it may be able to more readily meet the needs of a given application.

## References

1. I.W. Wyman and D.H. Macartney, *Org. Biomol. Chem.*, **2008**, *6*, 1796.
2. W. Ong and A.E. Kaifer, *J. Org. Chem.*, **2004**, *69*, 1383.
3. A. Thangavel, A.M.M. Rawashdeh, C. Sotiru-Leventis, and N. Leventis, *Org. Lett.*, **2009**, *11*, 1595.
4. I.W. Wyman and D.H. Macartney, *Org. Biomol. Chem.*, **2009**, *7*, 4045.
5. S. Liu, C. Ruspic, P. Mukhopadhyay, S. Chakrabarti, P.Y. Zavalij, and L. Isaacs, *J. Am. Chem. Soc.*, **2005**, *127*, 15959.
6. A.D. St-Jacques, I.W. Wyman, and D.H. Macartney, *Chem. Commun.*, **2008**, 4936.
7. I.W. Wyman and D.H. Macartney, *Org. Biomol. Chem.*, **2010**, *8*, 247.
8. N. Saleh, A.L. Koner, and W.M. Nau, *Angew. Chem., Int. Ed.*, **2008**, *47*, 5398.
9. I.W. Wyman and D.H. Macartney, *Org. Biomol. Chem.*, **2010**, *8*, 253.
10. I.W. Wyman and D.H. Macartney, *J. Org. Chem.*, **2009**, *74*, 8031.
11. R.K. Stoelting and R.D. Miller, *Basics of Anesthesia, Fourth Edition*, Churchill Livingstone: New York, 2000; pp. 89-106.
12. H. Soreq and S. Seidman, *Nature Rev.*, **2001**, *2*, 294.
13. H.B.J. Fischer and C.A. Pinnock, *Fundamentals of Regional Anaesthesia*, Cambridge University Press: Cambridge, 2004; pp. 29-31.
14. B. Debaene, B. Plaud, M.-P. Dilly, and F. Donati, *Anesthesiology*, **2003**, *98*, 1042.
15. M. Naguib, *Anesth. Analg.*, **2007**, *104*, 575.
16. A.L. Kovac, *J. Clin. Anesth.*, **2009**, *21*, 444.
17. A. Bom, M. Bradley, K. Cameron, J.K. Clark, J. van Egmond, H. Feildon, E.J. MacLean, A.W. Muir, R. Palin, D.C. Rees, and M.-Q. Zhang, *Angew. Chem., Int. Ed.*, **2002**, *41*, 265.
18. J. Butterworth, D.D. Eley, and G. Stone, *Biochem. J.*, **1953**, *53*, 30.

19. K.B. Schowen, E.S. Smissman, and W.F. Stephen, Jr., *J. Med. Chem.*, **1975**, *18*, 292.